University of Southampton

Faculty of Engineering and Physical Sciences

School of Engineering

Denitrifying enhanced biological phosphorus removal from municipal wastewater under anaerobic/anoxic conditions

by

Jialiang Xing

Thesis for the degree of DOCTOR OF PHILOSOPHY

November, 2019

University of Southampton

Abstract

Faculty of Engineering and Physical Sciences

School of Engineering

Thesis for the degree of DOCTOR OF PHILOSOPHY

Denitrifying enhanced biological phosphorus removal from municipal wastewater under anaerobic/anoxic conditions

Jialiang Xing

Conventional enhanced biological phosphorus removal is based on anaerobic phosphorus release and aerobic phosphorus uptake, which requires more energy supply and sludge production. Thus, there are growing concerns about effective phosphorus removal from wastewater with lower energy requirement.

The aim of this study was to achieve enriched sludge of denitrifying phosphorus accumulating organisms with anaerobic/anoxic conditions, especially with NO_2^--N, and explore the possibility of anoxic EBPR process with NO_2^--N as the sole electron acceptor in anaerobic/anoxic process.

This study included an extensive literature review, laboratory works involving continuous operation of biological reactors and sample analysis for data collection, data analysis and process simulation for practical phosphorus removal, to address the research questions.

The results suggested that long-period continuous NO_2^--N dosing in anoxic phase could induce faster enrichment of denitrifying phosphorus accumulating organisms and more efficient phosphorus removal than NO_3^--N at ambient temperature, without toxic inhibition of nitrite. The ratio of NO_3^--N to NO_2^--N was accorded to the amount of electron transfer of them, to remove the same amount of phosphorus. *Dechloromonas* is the functional microbial group in anoxic phosphorus uptake in both NO_2^--N and NO_3^--N based anaerobic/anoxic systems.

It was concluded that the complete phosphorus removal could be achieved with NO_2^--N as the sole electron acceptor in anaerobic/anoxic reactors, with enriched denitrifying phosphorus accumulating organisms.

Table of Contents

Table of Tables

Table of Figures

Research Thesis: Declaration of Authorship

Print name:	Jialiang Xing
Title of thesis:	Denitrifying enhanced biological phosphorus removal from municipal wastewater under anaerobic/anoxic conditions

I declare that this thesis and the work presented in it are my own and has been generated by me as the result of my own original research.

I confirm that:

1. This work was done wholly or mainly while in candidature for a research degree at this University;
2. Where any part of this thesis has previously been submitted for a degree or any other qualification at this University or any other institution, this has been clearly stated;
3. Where I have consulted the published work of others, this is always clearly attributed;
4. Where I have quoted from the work of others, the source is always given. With the exception of such quotations, this thesis is entirely my own work;
5. I have acknowledged all main sources of help;
6. Where the thesis is based on work done by myself jointly with others, I have made clear exactly what was done by others and what I have contributed myself;
7. This work has not been published.

Signature: Date:

Acknowledgements

My PhD journey has been made possible through the guidance, support, encouragement and assistance of many people. First of all, I would like to express my deepest gratitude to my PhD supervisor Dr. Yue Zhang for her invaluable guidance, constant support, kind encouragement and patience. I would not have accomplished my PhD study without her. I really appreciate everything.

I would like express appreciation to Pro. Charles Banks and Dr. Yongqiang Liu for their help in my previous reports, Dr. Bing Tao, Mrs Nopa Maulidiany and Miss Thitirat Ditkaew for their help to feed me reactors during my vacation, Mr Seongbong Heo for his help to analysis PHA contents in my samples, Pro. Sonia Heaven, Mrs Pilar Pascual-Hidalgo, Dr. Dominic Mann, Mrs Jing Lu and Miss Wei Zhang for their support in my study and lab works.

Thanks to Dr. Kui Liu, Dr. Shaopeng Chen, Mr Tao Zhu and Mr Peng Jiang for their accompanying in my PhD period.

A special thanks to my friend Dr. Yujing Lu for her persistent support and being my side along this journey,

Lastly, I would like to thank my grandparents and my parents for their never-ending love, understanding and support.

Definitions and Abbreviations

A_2N	Anaerobic/Anoxic/Nitrification
A_2O	Anaerobic/Anoxic/Aerobic
A/A	Anaerobic/Anoxic
Anammox	Anaerobic Ammonia Oxidation
A/O	Anaerobic/Aerobic
AOA	Anaerobic/Aerobic/Anoxic
ASM	Activated Sludge Model
ASM1	Activated Sludge Model NO.1
ASM2	Activated Sludge Model NO.2
ASM2d	Activated Sludge Model NO.2d
ASM3	Activated Sludge Model NO.3
AOB	Ammonia Oxidising Bacteria
ATP	Adenosine Triphosphate
Bio-P	Biological Phosphorus Removal
BNP	Biological Nutrient Removal
BOD	Biochemical Oxygen Demand
C	Carbon
C/N/P	Carbon to Nitrogen to Phosphorus Ratio
COD	Chemical Oxygen Demand
DCM	Methylene Chloride
DGAOs	Denitrifying Glycogen Accumulating Organisms

DO	Dissolved Oxygen
DPAOs	Denitrifying Phosphorus Accumulating Organisms
DPU	Denitrifying Phosphorus Uptake
e^-/P	Electron Transfer to Phosphorus Uptake Ratio
EBPR	Enhanced Biological Phosphorus Removal
FNA	Free Nitrous Acid
GAOs	Glycogen Accumulating Organisms
HAc	Acetic Acid
HRT	Hydraulic Retention Time
MAP	Magnesium Ammonium Phosphate
MLSS	Mixed Liquor Suspended Solid
MLVSS	Mixed Liquor Volatile Suspended Solid
MP	Mobile Phase
N	Nitrogen
NaAc	Sodium Acetate
NOB	Nitrite Oxidising Bacteria
P	Phosphorus
P/HAc	Phosphorus Release to Acetic acid consumption Ratio
P/N	Phosphorus Uptake to Nitrogen Consumption Ratio
PAOs	Phosphorus Accumulating Organisms
PHA	Poly-hydroxyalkanoate
PHB	Poly-hydroxybutryrate
PHV	Poly-3-hydroxyvalerate
P_i	Inorganic Phosphorus
PolyP	Polyphosphate

RAS	Recycled Activated Sludge
SBR	Sequencing Batch Reactor
SRT	Solid Retention Time
STP	Sewage Treatment Plants
TOC	Total Organic Carbon
TP	Total Phosphorus
VFA	Volatile Fatty Acid
WW	Wastewater
WWTWs	Wastewater Treatment Works

Chapter 1 Introduction

Wastewater treatment processes have been considered as one of the most important industries all over the world, due to the increasing public awareness of environmental protection and public health. Conventional municipal wastewater treatment works (WWTWs) mainly consist of primary and secondary treatment processes, although the more stringent regulations/directives (European Commission, 2019) also set upper limit on phosphorus and nitrogen removal. Enhanced biological phosphorus removal (EBPR) is an economic and ecological phosphate-phosphorus (PO_4^{3-}-P) removal approach, and has become one of the best-studied process for P treatment. Anoxic phosphorus uptake with nitrite-nitrogen (NO_2^--N) as the electron acceptor, replacing oxygen in traditional EBPR process, can potentially achieve simultaneous PO_4^{3-}-P and NO_2^--N removal and reduced energy consumption and sludge production in the wastewater treatment process.

1.1 Phosphorus and nitrogen in wastewater

Eutrophication has been recognised as one of the most common and serious environmental problem which should be reduced urgently. As the description of Ansari *et al*. (2011), eutrophication is "the enrichment of water by nutrients especially compounds of nitrogen (N) and phosphorus (P), causing an accelerated growth of algae and higher forms of plant life to produce an undesirable disturbance to the balance of organisms and the quality of the water concerned". Hence, nitrogen and phosphorus have been recognised as the two main nutrients that cause eutrophication of water bodies for decades of years (National Academy of Sciences, 1969). As essential elements for all kinds of life forms, the enrichment of nitrogen and phosphorus can lead to the excessive of production of algae and cyanobacteria, the following loss of aquatic animals and the deterioration of aquatic environments (Correll, 1998). As the basic element in DNA, RNA and ATP, phosphorus provides the important condition for algal blooms. Although eutrophication is mostly considered as the synthetical result of nutrients, based on the statement of Conley *et al*. (2009), P is the primary limiting nutrient causing the eutrophication in lakes, while N is the key influencing element for coastal area and estuaries. Hence, P suffusion is the main reason for the algal bloom and eutrophication in fresh waters.

As the main phosphorus and nitrogen pollutant sources, point sources (municipal and industrial effluents) and nonpoint sources (e.g. runoff from pastures, croplands and agriculture) are investigated to deal with, in order to find out any methods in the control of pollutants. In case of phosphorus pollutant, for instance, in the statistics of Environmental agency (EA, 2012), wastewater discharge from sewage treatment plants and agricultural land are the two primary sources in the UK, which separately contribute 60%-80% and 20%-30% of phosphorus in rivers. Hence, it is of importance to reduce the phosphorus contents from sewage effluent to decrease total P level in natural aquatic environments. Nutrients in municipal wastewater are mainly from the discharge of human waste, food, as nitrogen and phosphorus are essential elements for the cells synthesis, consisting protein, ATP, bone, DNA and RNA, *etc*. In addition, some certain soaps and detergents are also sources which contain phosphorus, discharged into the sewage in the daily life of human beings and some commercial activities. As a result, municipal wastewater consists of a mixture of domestic sewage from households and a proportion of industrial and commercial effluents (Pescod, 1992).

In order to reduce the P release in effluents and obtain the higher quality of natural aquatic environment, stricter discharge standards and requirements are developing in the recent years. In the urban waste water treatment directive (UWWTD) for Europe, lower total phosphorus (TP) concentrations in wastewater discharges were required (European Commission, 2019), with 2 mg L^{-1} (10000-100000 p. e.) and 1 mg L^{-1} (>100000 p. e.)

Since phosphorus is considered as a kind of important mineral element, it is significant to manage the footprint of phosphorus, in order to close the cycle of phosphorus, reduce waste production from phosphorus removal and save the resources. As nitrogen and phosphorus are important industrial and agricultural resources, the recovery is one of the useful methods to reduce the nutrient discharge and enhance the development of relevant economic aspects. Firstly, ammonia and phosphate are essential materials used in fertiliser, which are widely used in agriculture and horticulture. Secondly, ammonia and phosphate are both necessary materials in industries including pharmacy, chemical engineering, food industry, energy industry and so on. Due to the function of nitrogen and phosphorus in agriculture and industry and the environmental issue caused by their discharge, it is of importance to enhance sustainable development with both stable economic growth and less contaminant discharge. As a result, the recovery of nutrients, especially phosphate, can reduce the requirement of phosphorite mining to save the phosphorus resource on the earth.

1.2 Phosphorus and nitrogen removal processes

In the removal of phosphorus from wastewater, chemical and biological methods are normally considered. Nowadays, chemical precipitation is still the main treatment method in WWTWs, primarily with iron or aluminium, while EBPR process is also utilised in other treatment works (Sedlak, 1991; Tran *et al*., 2012; Attour *et al*., 2014). To achieve a higher effluent quality standard and avoid the pollutants from metal dosing, biological removal methods are being increasingly considered to utilise in treatment plants. On the contrary, chemical methods are not the most desirable selections, due to their lower cost-efficiency or inadaptability to domestic wastewater.

In addition, the recovery of phosphorus in wastewater industry is an important part of the entire phosphorus cycle and reuse. Struvite as fertiliser, for instance, has been employed to recycle phosphorus from wastewater treatment plants (Britton *et al*., 2009). In addition, other phosphorus removal methods, such as EBPR process by phosphorus accumulating organisms (PAOs), should be considered sufficiently, as an important part of the removal process.

In the aspect of nitrogen removal, biological nutrient removal (BNR) process is the main approach, with nitrification and denitrification based on the activities of microbials (Wiesman., 1994; Zhu *et al*., 2008). The process consists of the oxidisation of NH_4^+-N with ammonia oxidising bacteria (AOB), oxidisation of NO_2^--N with nitrite oxidising bacteria (NOB) in aerobic phase and denitrification from NO_3^--N to nitrogen gas in anoxic phase. In order to optimise ammonia removal, partial nitrification via nitrite is developed to save 25% oxygen demand and 60% energy consumption in aerobic phase (Peng and Zhu, 2006). Partial nitrification is a key procedure for some novel ammonia removal process, such as short-cut nitrification and denitrification, completely autotrophic N removal over nitrite (Canon), oxygen-limited autotrophic nitrification-denitrification (Oland) and anaerobic ammonia oxidation (Anammox, Verstraete and Philips, 1998).

Normally, the aerobic process, especially in conventional BNR processes, is conducted to accomplish nitrification and aerobic phosphate uptake, which has been widely used in conventional wastewater treatment process. With the development of treatment technology, more energy-efficient treatment processes with the combination of biological P and N removal is considered. These processes can develop low oxygen and energy cost ammonia removal perspective, while it is necessary to conduct extra-integrated phosphorus removal fraction in these process, in order to achieve

simultaneously N and P removal. For instance, Zeng *et al*. (2014) combined nitritation denitritation, anammox and denitrifying phosphorus removal in the treatment carbon-limited municipal wastewater, and achieved a stable phosphorus removal rate of 85%-90%.

Denitrifying phosphorus uptake combined with nitrification or partial nitrification via NO_x^--N (namely NO_3^- and/or NO_2^-) can achieve nitrogen and phosphorus simultaneously, with low oxygen and energy consumption. Meanwhile, low organic carbon in municipal wastewater cannot limit the efficiency due to the only organic material requirement of denitrifying phosphorus accumulating organisms (DPAOs), by washing out other heterotrophic denitrifying microorganisms. In addition, the amount of excess sludge can also be reduced in this system, without the existence of non-phosphorus uptake denitrifying bacteria.

Specifically, A_2N two-sludge system is one of the P and N treatment approaches which effectively combined the advantages of partial nitrification and anoxic EBPR. Firstly, the carbon consumption in anoxic P uptake is lower than aerobic P uptake. Compared with traditional treatment process where significant amount of PHB is oxidised by PAOs in aerobic period, inducing lower organic carbon used for denitrification (Kerrn-Jespersen *et al*., 1994; Kuba *et al*., 1996b), two-sludge system which separate PAOs and nitrifying bacteria, can enhance the COD usage only for P release to decrease the carbon demand.

Secondly, the oxygen demand used in the two-sludge system via nitrite can be reduced, since the oxygen is provided only for partial nitrification. Due to continuous aerobic phase for P uptake is avoided, aeration and energy demands for this progress are completely saved. In case of post aeration, it was used most of A_2 systems to improve the P removal rate, reduce the potential public health hazard and enhance the sludge settlement ability in most of the studies (Lv *et al*., 2014; Dai *et al*., 2017b). However, it will save more energy if post aeration is cancelled without any obvious hazard impacts. Thus, it is of importance to prove the P uptake ability of A_2 systems without post aeration. In addition, as discussed in above, the application of partial nitrification in ammonia oxidisation can save around 25% oxygen and 60% energy consumption. Two-sludge system, as a result, can effectively decrease the energy demand for aeration in the treatment process.

Thirdly, sludge production in the combination of partial nitrification and denitrifying phosphorus uptake can be reduced by washing out the non-functional microbial groups. The stable operation of partial nitrification can effectively wash out nitrate oxidising

bacteria (NOB, Peng and Zhu, 2006; Guo *et al*., 2009a), achieving lower sludge discharge (Tokutomi, 2004; van Kempen et al., 2001). Furthermore, denitrification P uptake was frequently reported in the previous studies (Kuba *et al*., 1996b; Dai *et al*., 2017b) for less sludge production.

The utilisation of nitrite in anoxic phosphorus uptake was discussed in some previous studies, where the feasibility of NO_2^--N for PO_4^{3-}-P uptake, while the controversial point was the threshold value of nitrogen concentration in the anoxic phase (Meinhold *et al*., 1999; Lee *et al*., 2001; Hu *et al*., 2003; Wang *et al*., 2007; Tang *et al*., 2012).

Hence, there are still limits restraining the potential of NO_2^--N based phosphorus removal in anoxic phase, including the toxicity of nitrite on microorganisms and relatively longer enrichment period of DPAOs. Due to the controversy and potential, it is significant to explore the feasibility of denitrifying phosphorus uptake (DPU) via NO_2^--N and its potential operation mode, investigate the factors influencing the treatment efficiencies of this process from the enrichment method of DPAOs to steady and effective operation, and analyse its practical value in municipal wastewater treatment. Temperature is an important factor influencing the performance of EBPR and the competition between PAOs and GAOs, while NO_2^--N based EBPR has not been comprehensively investigated at high temperature to explore the operation performance of the A_2 systems and the change of microbial communities.

In summary, if the combination of denitrifying phosphorus removal and partial nitrification can be conducted in practical, with NO_2^--N as the sole electron acceptor, the energy cost and sludge production will be significantly reduced. Even though the ratio of phosphorus to nitrogen in domestic wastewater is not constant, utilising NO_2^--N to achieve anoxic phosphorus uptake to the utmost is also important.

Chapter 2 Literature review

As an important part of the whole phosphorus cycle, phosphorus removal from wastewater is playing a necessary role after the discharge of sewage and industrial effluent, prior to the reuse of phosphorus products (Morse *et al*., 1998; Filippelli, 2008; Elser and Bennett, 2011). Hence, nutrient treatment of wastewater has been increasingly valuable in the current years. As another important nutrient element, nitrogen is normally considered and disposed with the removal of phosphorus at the same time.

Municipal wastewater is considered as one of the most important P and N pollution sources, which should be comprehensively treated to reduce the concentrations of P and N in discharge. In the development of wastewater treatment process, physical, chemical and biological methods for phosphorus and nitrogen are researched and utilised for wastewater treatment. In this review, some typical treatment processes in these method will be discussed, in which biological methods, as the most related method about this project, will be specifically evaluated.

For the biological treatment methods, the main nitrogen removal process will be discussed to declare the relationship between nitrogen and phosphorus removal. More importantly, as the core content of this study, DPU will be comprehensively reviewed, including current research about the biochemical principle of DPU, factors influencing DPU, the relationship between PAOs (DPAOs) and glycogen accumulating organisms (GAOs or DGAOs), and the enrichment of DPAOs. In addition, because of the important relativity to DPU, partial nitrification (involving the principle and main factors) and A_2N two-sludge with anaerobic - (partial) nitrification - anoxic phases (from the first finding to the later development) will be reviewed.

2.1 Physical/chemical removal of nitrogen and phosphorus

As discussed above, physical and chemical treatments are the important methods used in WWTWs to removal the nutrients and improve the quality of discharge. Even though biological treatment process of nitrogen and phosphorus is the most frequent method in

wastewater treatment process, physical and chemical approaches are still developed to adapt different treatment conditions and discharge requirements.

In some certain situations, non-biological processes of nitrogen removal, which are based on the physical or chemical properties of ammonia, may be technically and economically feasible. Some common process for nitrogen removal are breakpoint chlorination, air stripping and selective ion exchange (Atkins and Scherger, 2013).

Breakpoint chlorination, which has been utilised in practical wastewater treatment industry to achieve an additional ammonia removal, can effectively remove dissolved NH_4^+-N (Pressley *et al*., 1972). The method is based on ammonia oxidisation by the addition of chlorine into wastewater, inducing ammonia oxidisation to nitrogen gas: 1) NH_2Cl is formed from the chlorination of NH_4^+; 2) NH_2Cl is oxidised by HClO to N_2. Nonetheless, the extra HClO produced in this process should be removed by dechlorination with SO_2 or activated carbon. The main limitation of chlorination is the formation of toxic disinfections (Wang *et al*., 2007). To optimise the chlorination process, the control of undesirable by-products is necessary and important. Hence, extra treatment process should be applied to remedy the inadequacy (Zhang *et al*., 2015).

Desorption or stripping can transfer a dissolved component from a liquid to a gas phase. In the case of ammonia, it has two forms (ammonium and free ammonia) in water stream, which can convert to each other in the solutions. Hence, air stripping consists of raising the pH of the wastewater to more than 10 or 11 to increase NH_3/NH_4^+ ratio, and providing sufficient air to strop the ammonia gas from wastewater. Additionally, depending on the different conditions and requirements, some other kinds of gas can also be employed in the ammonia stripping removal, and the ammonia stripped with this method can be recovered and utilised for some other materials (Yuan *et al*., 2016). Nonetheless, the efficiency of ammonia removal by stripping is sharply influenced by temperature, and the stripping towers applied are easily affected by scaling. In addition, the process is widely used to remove high strength of ammonia, such as swine manure wastewater, landfill leachate, food waste *etc* (Liao *et al*., 1995; Kabdasli *et al*., 2000; Serna-Maza *et al*., 2014).

Ion exchange can be achieved by passing the wastewater through an ion-exchanger bed, which presents high selectivity for ammonium ion over other cations that are commonly contained in wastewater (Sedlak, 1991). Natural zeolite and its analogues are frequently used for this method, due to the highly porous alumina-silicates with the three

dimensional framework and negatively charged lattice structure. The factors influencing the NH_4^+-N exchange include the homoionic form and grain size of zeolite, HRT, initial concentration of nitrogen, competition from other cations, pH, temperature and the scaling up of the ion exchange system (Hedstrom 2011; Gupta *et al*., 2015). In recent years, some other kinds of ion exchanger such as mesolite, have also been reported in the use of ammonium with their effective adsorption performance and separation from wastewater (Thornton *et al*., 2007). As ion exchange is mainly used to optimise nitrogen efficiency in municipal wastewater treatment process, it is usually applied with the combination of other chemical or biological processes. Consequently, the application of ion exchange is normally complex, which require additional operation and management.

Chemical phosphorus removal from wastewater normally consists of the incorporation of phosphate into suspend solids (particulate form) and the removal of the formed suspend solids. Calcium, iron and aluminium are commonly used as precipitants for phosphorus removal, with the forms of $Ca_3(PO_4)_2$, $Ca_5(OH)(PO_4)_3$, $CaHPO_4$, $FePO_4$, $Fe_3(PO_4)_2$, $Fe_x(OH)_y(PO_4)_z$, $AlPO_4$ and $Al_x(OH)_y(PO_4)_z$ respectively. In these reaction processes, pH value is an important factor influencing the removal efficiency. In the previous studies, as reported by Sedlak (1991), pH values of higher than 10 are normally employed for precipitation with lime, while relative moderate pH values of lower than 7.5 are more suitable for iron salts and aluminium salts to precipitate phosphorus. Except of conventional chemical precipitation, electrocoagulation using a sacrificial anode electrode (iron or aluminium) can also be employed for phosphate removal, and increase the efficiency of chemical precipitation of phosphorus (Tran *et al*., 2012). Attour *et al*. (2014) investigated the parameters influencing on phosphate removal by electrocoagulation with aluminium electrodes, and suggested that the efficiency of this method especially depended on the electrical intensity, pH and temperature. The combination of Fe based precipitation and adsorption was also reported in the recent years (Wilfert *et al*., 2015), which indicated that a kind of iron-based particle could achieve a relatively high phosphorus adsorption capacity of 245 mg P g^{-1}. The limitations of chemical method include: a. The additional chemical dosing, which induce further metal pollutants if the dosing intensity is not controlled appropriately; b. pH adjustment, which needs extra metal (Na^+ or K^+) addition and more complicated operation and control; and c. The disposal of precipitation, which is a problem related to environmental protection and economical management (Bunce *et al*., 2018).

Anion exchange can be employed in phosphate removal and recovery (Nur *et al*., 2014), in which the recovery rate of phosphate can achieve higher than 99.5% with the iron oxide anion exchange resin and precipitation by calcium chloride. In the recent years, sorption is increasingly popular in phosphate removal and recovery from wastewater with iron oxide- or CaMg-based sorbents. For instance, Ashekuzzaman & Jiang (2014) explored the performance of Ca-, Mg- and CaMg-based sorption for PO_4^{3-}-P removal, and found that the material could remove >90% of PO_4^{3-}-P from 3.4-10.4 mg L^{-1} phosphorus containing wastewater. Lalley *et al*. (2016) compared modified and unmodified iron oxide sorbents to treat PO_4^{3-}-P in lake water directly, and found that the modified sorbents with silver had higher adsorption capacity (38.8 mg g^{-1}) than unmodified sorbents (37.7 mg g^{-1}). Membrane technologies can also be utilised for the treatment nitrogen and phosphorus in wastewater. Qiu and Ting (2014) investigated the performance of an osmotic membrane bioreactor (OMBR) to enrich phosphorus, and then recover the phosphorus supernatant within the reactor. Chon *et al*. (2013) combined different sorts of membrane methods including disk filtration, ultrafiltration and reverse osmosis to remove ammonia in municipal wastewater, and achieved a relatively high removal efficiency. However, ion exchange and membrane approaches are generally considered as improving treatment methods, which require higher investment to achieve optimised efficiency, inducing that they may not appropriate for small-scale and rural treatment plants.

Struvite or magnesium ammonium phosphate (MAP, $MgNH_4PO_4{\cdot}6H_2O$) precipitation can be used to achieve ammonia and phosphate recovery and produce an attractive fertiliser in some area of nutrient removal process (Le Corre *et al*., 2009 and Ye *et al*., 2014). In order to achieve sufficient struvite formation, suitable pH (7.6) and appropriate magnesium dosing (Jaffer *et al*., 2002) should be selected in the process. However, a large amount of chemical inputs such as $MgCl_2$, NaOH and brine solutions (Booker *et al*., 2010) need to be added into wastewater to achieve the precipitation, which is not cost-effective enough. In addition, the application of struvite recovery is more appropriate for the sewage with high-strength pollutants, such as anaerobic digestate, containing high concentration of phosphorus and nitrogen (up to hundreds mg L^{-1} of P and N), which has higher commercial value to recover.

2.2 Biological nitrogen removal

2.2.1 Conventional biological nitrogen removal

Biological treatment of nitrogen is obtained by the conversion from ammonia to nitrogen gas with the biochemical activities of microorganisms. The conventional biological oxidation of ammonia is achieved with two species of autotrophic microorganisms, which involve *Nitrosomonas* and *Nitrobacter*, via the reaction with oxygen, and accomplished in two steps which are:

$$2NH_4^+ + 3O_2 \xrightarrow{Nitrosomonas} 2NO_2^- + 2H_2O + 4H^+ \qquad (2\text{-}1)$$

$$2NO_2^- + O_2 \xrightarrow{Nitrobacter} 2NO_3^- \qquad (2\text{-}2)$$

Denitrification process is carried out by a variety of heterotrophic bacteria which utilise nitrate instead of oxygen as the electron acceptor under anoxic conditions. The stoichiometric reaction of denitrification depends on organic matter (methanol, for example), which can be expressed by the below equation (Zhu et al., 2008):

$$6NO_3^- + 5CH_3OH \rightarrow 3N_2 + 5CO_2 + 7H_2O + 6OH^- \qquad (2\text{-}3)$$

In nitrogen removal process of wastewater, nitrification and denitrification can be accomplished separate stage system (two sludge), single-sludge system with mixed liquor cycle or oxidation ditch or channel in which they occur sequentially.

However, the conventional biological nitrogen removal process has several limitations in practical treatment process, including the separation of spaces or time sequences, long retention time or large volume, higher DO requirement and organic carbon, and higher operation costs (Zhu *et al*., 2008). Hence, the substitute has been explored and designed to develop the biological nitrogen removal method, i.e. simultaneous nitrification and denitrification (SND), short-cut (or partial) nitrification and denitrification and anaerobic ammonium oxidation (ANAMMOX).

Among these approaches, partial nitrification and denitrification process, which utilises NO_2^--N as intermediate product to instead of NO_3^--N, has the advantages involving 25% lower oxygen consumption and 60% energy saving, 40% lower requirement for electron donors and 1.5-2 times denitrification rate of NO_3^--N (Turk and Mavinic, 1989; Peng *et al*., 2005; Peng and Zhu, 2006). Hence, it has been widely studied in the combination

with the other novel nitrogen removal process (Yoo *et al*., 1999; Kartal *et al*., 2007; Ma *et al*., 2016).

Since the above processes are mostly utilised in the removal of nitrogen, but very limited phosphorus removal can be achieved, effective and space-saving treatment of both nitrogen and phosphorus is needed in WWTWs, and it is of importance to combine the removal process of them, in order to remove the nutrients simultaneously. Since EBPR process can be achieved with NO_x^--N as electron acceptor (it will be discussed in nest section), the NO_2^--N production in partial nitrification is potentially become the key factor in the combination of biological phosphorus and nitrogen removal.

2.2.2 Partial nitrification

Partial nitrification for nitrite production, as one of the most important steps in BNR process, is the assistant process for NO_2^--N based A_2 phosphorus removal system, which can reduce the oxygen demand, energy requirement and sludge production. Hence, some basic knowledge about partial nitrification is discussed in this section.

2.2.2.1 Biochemical principle of partial nitrification

The oxidation process from ammonia to nitrite is achieved by ammonia oxidising bacteria (AOB) or *Nitrosomonas*, as mentioned above. Although in most equations, NH_4^+ is demonstrated as the reactant process, the actual substrate of the oxidation should be NH_3 (Suzuki *et al*., 1974 and Wood, 1988). Moreover, the reaction process consists of two steps: 1) NH_3 oxidation to NH_2OH with the function of ammonia monooxygenase (AMO); 2) NH_2OH oxidation to nitrite with the function of hydroxylamine oxidoreductase (HAO). Additionally, Andersson and Hooper (1983) considered NH_2OH oxidation also consisted two steps as shown in Table 2.1.

Table 2. 1 Reactions involved in ammonia oxidation process

Process	Reaction	ΔG^0 (kJ/mol)
NH_3 → NH_2OH	$NH_3 + O_2 + 2e \xrightarrow{AMO} NH_2OH + H_2O$	-120
NH_2OH → HNO_2	$NH_2OH + H_2O \xrightarrow{HAO} HNO_2 + 4H^+ + 4e$:	23
	① $NH_2OH \xrightarrow{HAO} [NOH] + 2H^+ + 2e$	
	② $[NOH] + H_2O \xrightarrow{HNO} HNO_2 + 2H^+ + 2e$	

2.2.2.2 Factors affecting partial nitrification

Conventional nitrification is commonly achieved by the synergic function of AOB and NOB (nitrite oxidising bacteria), which generally exist together in WWTWs. Thus, it is necessary to wash out NOB to attain the accumulation of AOB and nitrite. Compared with NOB, the factors impacting the growth of AOB include temperature, SRT, dissolved oxygen (DO) concentration, pH, operational and aeration pattern, substrate and inhibitor concentration (Peng and Zhu, 2006).

a. Temperature

In the most of research about the effect of temperature on AOB and NOB, it was found that AOB which needed more activation energy, was more sensitive to temperature changing. Thus, is was usually suggested that higher temperature was applicable, such as above 25 °C, even above 30 or 35 °C, when temperature was considered as the single parameter for nitrogen removal via nitrite (Hellinga *et al*., 1998; Yoo *et al*., 1999; Mulder *et al*., 2001; Peng and Zhu, 2006). On the other hand, low temperature below 15 °C is commonly regarded as the critical value, with which NOB activity is higher than AOB (Quinlan, 1986).

However, if temperature is not considered as the sole parameter in AOB and nitrite accumulation, relative lower value also can be applied in experiments, according to some research in recent years. Yang *et al*., (2007) have reported an above 95% average nitrite accumulation rate with low temperature (reduced from 25 °C to 11.9 °C) and normal DO concentration (≥2.5 mg/L), with which it can be observed that the nitrite accumulation rate is nearly 99% even at the lowest temperature of 11.9 °C. In other words, with appropriate conditions, AOB can also be active with a water temperature below 15 °C, which is also investigated by the results of Qiao *et al*. (2010) and Zou *et al*. (2014).

b. DO concentration

DO concentration is one of the most factor control AOB separation from NOB. In former research, the difference between oxygen affinity of AOB and NOB was investigated to enhance nitrite accumulating. Several studies on the effect of low DO concentration on partial nitrification and nitrite accumulation have been compared in Table 2.2. In the studies of Blackburne *et al*., (2008), Aslan *et al*., (2009), Guo *et al*. (2009b) and Wei *et al*. (2014), low DO concentrations of 0.4, 0.7±0.2, 0.4-0.8 and 0.5-1.0 mg L^{-1} had been analysed separately in their experiments. And relatively high nitrite accumulation rate (NAR) had been reported and suggested effective AOB accumulation and NOB wash out.

Hence, DO concentration is a key factor influencing the efficiency of the domination of AOB in partial nitrification process.

In the studies of Blackburne *et al*. (2008) and Wei *et al*. (2014), an approach of changing the DO concentration from high value to low value was employed. As reported in their articles, nitrification bacteria communities could be stable in the early phase with higher DO concentration, which caused the accumulation of nitrate. Gradually, with the decrease of DO concentration, nitrite could be accumulated and little nitrate was produced with limited DO concentration. Aslan *et al*. (2009) obtained stable ammonia oxidation and nitrite accumulation via changing SRT under low DO concentration constantly. On the contrary, Guo *et al*. (2009b) compared the effects of high and low concentrations of DO on partial nitrification after achieving stable nitrite accumulation under low DO concentration, and found that high DO concentration could not destroy the stable nitrite accumulation and nitritation culture. As a result, low DO concentration is an important condition for the accumulation and stability of AOB, in order to achieve steady partial nitrification.

Table 2. 2 Studies of effects of low DO concentration on nitrite accumulation

Research	Process	Optimal DO concentration (mg/L)	DO concentration setting	NAR
Blackburne *et al*., 2008	Continuous process	0.4	High to low	--
Aslan *et al*., 2009	SBR	0.7±0.2	Constant	80%
Guo *et al*., 2009a	SBR	0.4-0.8	Comparing high and low	96.3%, 96.6%
Wei *et al*., 2014	SBR	0.5-1.0	High to low	96.3%

c. SRT

Due to the difference of minimum doubling times of AOB and NOB, long SRT is normally suggested by researchers at relatively low temperature. For example, Peng *et al*. (2006) successfully obtained stable nitrite accumulation with the SRT of 30 days under the temperature of 13 °C. And Aslan *et al*. (2009) supported 40 days was an appropriate SRT for partial nitrification at low DO concentration under around 19 °C temperature. Additionally, some other researches also supported that SRTs of 4-8, 10-20 days were also advantageous for nitrite accumulation depending on different conditions of the experiments (Pollice *et al*., 2002; Wu *et al*., 2011; Regmi *et al*., 2014).

d. C/N ratio and substrate concentration

According to Okabe *et al*. (1996), a higher C/N ration retarded the accumulation of nitrifying bacteria, especially NOB. However, Chiu *et al*. (2007) found that a low C/N ratio at 6.3 could induce the accumulation of nitrite in SBR process, and restrained nitrate production. Additionally, a low COD can restrain the activity of denitrifying bacteria, because of the deficiency of carbon source, so it is also helpful for the separation of AOB from other bacteria culture.

According to the experimental results of Nowak *et al*. (1996) and Barack *et al*. (2000), phosphate concentration can also affect nitrite oxidation or reduction in wastewater. With the presence of phosphate, nitrite accumulation can be enhanced, with the decreased oxidation and reduction rates.

2.3 EBPR for phosphorus removal

The EBPR process is conducted based on the activities of PAOs, which are capable of assimilating excess phosphate into their cells under suitable conditions (Kerrn-Jespersen and Henze, 1993; Martin *et al*., 2006):

- In anaerobic phase, organic materials are converted to volatile fatty acids (VFAs) by fermentation organisms, and meanwhile, PAOs decompose poly-phosphate (polyP) and glycogen, in order to provide ATP and then energy, via which PAOs convert VFAs to poly-hydroxyalkanoate (PHA), e.g. poly-hydroxybutryrate (PHB) and poly-3-hydroxyvalerate (PHV). The PO_4^{3-}-P produced from the decomposition of poly-phosphate will be released in this process.
- In aerobic/anoxic phase, PAOs will decompose PHA and obtain energy to produce new cells. In the meantime, PO_4^{3-}-P in the wastewater can be absorbed into their cells and converted to ATP, phospholipid and nucleic acid, but most of the PO_4^{3-}-P will be composed as polyP. In this process, the PO_4^{3-}-Puptake amount is much larger than the release part in anaerobic phase. As a result, the phosphorus can be removed via the discharge of excess sludge.

Conventional EBPR process with nitrogen removal, which consists of nitrification, denitrification and aerobic phosphorus uptake, needs sufficient energy consumption for

aeration and carbon supply for anaerobic P release and denitrification. In comparison, the energy and carbon demands of denitrifying EBPR are relatively lower than conventional process, and the sludge production can also be decreased by anoxic P uptake (Kerrn-Jespersen *et al*., 1994; Guo *et al*., 2009a; Lv *et al*., 2014; Dai *et al*., 2017b). It has been found that the COD requirements, oxygen consumption and sludge production in denitrifying EBPR could be up to 50%, 30% and 50% less than conventional biological N and P removal, respectively (Kuba *et al*., 1996b). Hence, denitrifying phosphorus uptake with anaerobic/anoxic phases has been frequently investigated in the recent years, including P removal efficiency and microbiology of the system.

2.3.1 Background and biochemical principle of denitrifying phosphorus uptake

In the current nutrient or phosphorus removal processes, denitrifying phosphate removal has been utilised in the anoxic phase to replace a part of oxygen for energy saving. Especially, in the five-stage Bardenpho process and the Dephanox system (Bortone *et al*., 1999; Emara *et al*., 2014), the anoxic phase with NO_3^--N produced from aerobic phase provides the condition for denitrifying phosphate uptake.

The metabolic process of PAO activities is demonstrated in Fig. 2.1 and Fig. 2.2. In conventional aerobic nitrogen and phosphorus removal process, both of PAOs and denitrifiers need organic carbon to perform phosphate release and denitrification, which results in a shortage of carbon source with around 4:1-6:1 of COD/N ratio (Wachtmeister *et al*., 1997; Meinhold *et al*., 1999; Ahn *et al*., 2002; Hu *et al*., 2002). In addition, general PAOs need oxygen as electron acceptor for phosphate uptake, which lead to extensive aeration intensity and energy cost. On the contrary, DPAOs, which can accumulate phosphate with nitrate and nitrite as electron acceptor under anoxic condition, can simultaneously removal nitrogen and phosphorus in wastewater (Kuba *et al*., 1996b; Lee *et al*., 2001; Tsuneda *et al*., 2006 and Zhang *et al*., 2010).

The specific metabolism about the production of reducing equivalents in anaerobic phase is controversial. Both TCA cycle and glycolysis have been reported as the metabolic pathway in anaerobic phase to produce energy, contributing to the maintenance of PAOs and the following P uptake process. Some studies suggested both of them were involved in the anaerobic metabolism, as the sources of reducing power (Louie *et al*., 2000; Zhou *et al*., 2009; Majed *et al*., 2012; Carvalheira *et al*., 2014). In addition, the metabolic activities of PAOs in full-scale plants were investigated by Lanham *et al*. (2013), who found that

phosphate uptake would be more efficient, when the glycolysis activity of PAOs were higher than TCA cycle pathway.

Generally, at anoxic phase conventional simultaneous nitrogen and phosphorus removal is conducted with NO_3^--N as electron acceptor which is combined with comprehensive nitrification. In contrast, phosphorus uptake with nitrite by DPAOs can achieve nitrogen and phosphorus removal with partial nitrification, which can save energy for aeration, and reduce sludge production (Peng and Zhou, 2006).

According to former research about metabolic process of PAOs, phosphate removal process based on nitrate or nitrite also consists of release and uptake steps. In anaerobic phase, the organic matter is stored as PHA (PHB or PHV) (Comeau *et al*., 1986). The energy required for storage of PHB/PHV is produced by the phosphorus accumulating bacteria via decomposing polyphosphate from an intercellular store. As a result, the phosphorus accumulating bacteria will release phosphate in connection with the storage of organic matter. On the other hand, under anoxic conditions, DPAOs consume PHB/PHV. The energy produced is used by the DPAOs for growth and storage of phosphate in a polyphosphate store by nitrate or nitrite as electron acceptors (Hascoet *et al*., 1985, Comeau *et al*., 1986 and Gerber *et al*., 1987).

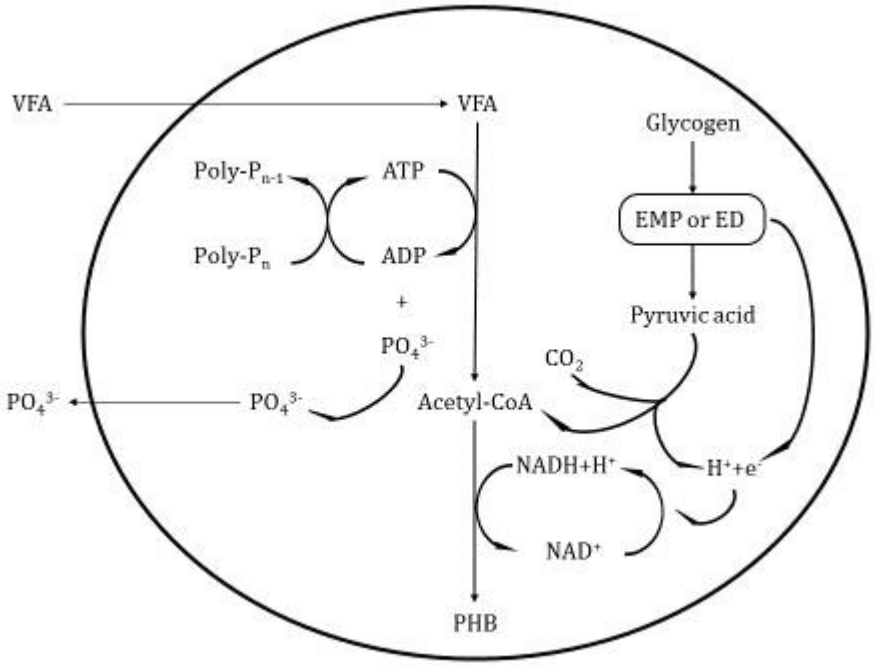

Fig. 2. 1 Anaerobic metabolism of PAOs

Source: Wentzel *et al*., 1991 and Mino *et al*., 1998

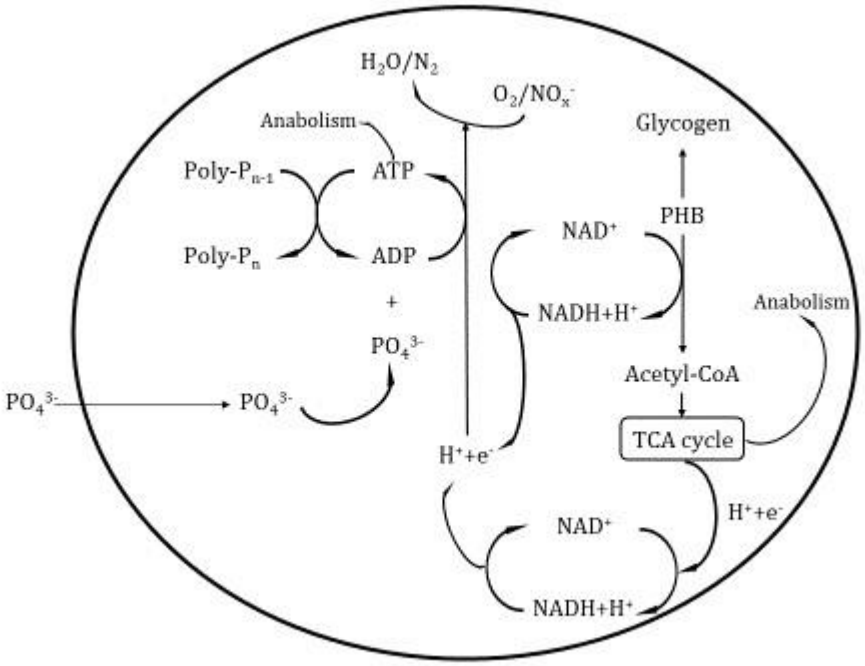

Fig. 2. 2 Aerobic or anoxic metabolism of PAOs

Source: Wentzel *et al*., 1991; Mino *et al*., 1998 ; Martin *et al*., 2006

2.3.2 Factors affecting DPU

2.3.2.1 Different electron acceptors

According to the previous studies (Ahn *et al*., 2002; Hu 2003), three types of electron acceptors (O_2, NO_3^- and NO_2^-) had been recognised to be functional in phosphorus uptake experiments, and both nitrate and nitrite can be used for anoxic P uptake to replace oxygen to achieve N and P removal simultaneously, while there are still some controversial points about the comparison between the efficiencies of PO_4^{3-}-P removal via the electron acceptors. The main debatable aspects are the limit or threshold of NO_2^--N concentration to avoid toxic inhibition in anoxic P uptake, and the difference of treatment efficiency between NO_3^--N and NO_2^--N in P removal process. Table 2.3 demonstrates the concentration of NO_2^--N in anoxic P removal process of the previous studies.

Table 2. 3 Concentration of NO_2^--N used in the previous studies

Literature	NO_2^--N Concentration (mg L^{-1})	Enrichment process	SRT (Day)	HRT (h)	Treatment efficiency	Inhibition or not
Meinhold *et al*. (1999)	8					Inhibition
Lee *et al*. (2001)	10	A/O process operated for over 10 months	12	16	100%	No inhibition
Hu *et al*. (2003)	115	A/A process with nitrate operated for 1 year and a half	20	12		No inhibition
Wang *et al*. (2007)	5.5-9.5 15	DEPHANOX operated for over 300 days	14			No inhibition Inhibition
Guisasola *et al*. (2009)	60	A/A/O process with nitrite operated for over 6 months	15	16 24	100%	No inhibition
Zhang *et al*. (2010)	5, 15, 35 & 45					No inhibition
Zhou *et al*. (2010)	4, 6, 8, 16 20, 40, 80	A/O process operated over 20 days	25	12		No inhibition Inhibition

Peng *et al*. (2011)	60	A/A process with nitrate operated for 30 days	20	8	91.33±2.38	No inhibition
Vargas *et al*. (2011)	>50	A/O process operated for over 2 years	9	12		No inhibition
Zeng *et al*., (2011)	6.2	Continuous A/A/O process operated for about 8 months	15-20	9.31-13.96	98%	No inhibition
Ma *et al*. (2013)	40-45	A/A process with nitrate			64.85%	Inhibition
Dai *et al*. (2017b)	2, 5, 8 & 11	A/O process operated for 23 days and then A/A process for 37 days A/A process operated for 28-49 days		16	87±2.3%	No inhibition

For instance, Lee *et al*. (2001) investigated the effect of different electron acceptors on phosphate uptake, and found that nitrite (up to 10 mg N L^{-1}) could be used as an electron acceptor as nitrate, and the phosphorus uptake rate was faster with the presence of NO_2^- as an electron acceptor in comparison with nitrate. On the contrary, Zhou *et al*. (2010) evaluated the effects of oxygen, nitrate and nitrite as electron acceptors, and found that anoxic phosphorus uptake could be achieved successfully both with nitrite and nitrate, but the phosphorus amount taken with nitrite was smaller than the amount with nitrate (the P/N ratios with NO_3^--N and NO_2^--N of 1.67 and 1.12). Hence, compared with NO_3^--N, which is traditional electron acceptor in anoxic phosphorus removal, NO_2^--N is always controversial in the former studies.

In case of the toxicity of NO_2^--N, some researchers considered nitrite had negative effect on phosphorus uptake, and PAOs activities would stop if nitrite concentration exceeded a critical value as the result of its toxicity. But controversial concentration values were proposed in different studies. In the opinion of Meinhold *et al*. (1999), 4-5 mg L^{-1} NO_2^--N was a suitable concentration level for anoxic phosphorus uptake, but the uptake process would be inhibited when the concentration reached around 8 mg L^{-1}. Wang *et al*. (2007) considered that when NO_2^--N concentration was between 5.5 and 9.5 mg L^{-1}, nitrite could act as electron acceptors in anoxic phosphorus uptake, but 15 mg L^{-1} would inhibit phosphate uptake process. Some research indicated that one of the reason causing phosphorus uptake inhibition of nitrite was the increasing free nitrous acid (FNA) concentration. For example, Zeng *et al*. (2011) investigated denitrifying phosphate and short-cut nitrification in an A_2O process, in which the effect of nitrite accumulation on phosphorus removal efficiency was particularly focused, and found that an FNA concentration of 0.002-0.003 HNO_2-N L^{-1} could inhibit P uptake without any extra carbon source supply in aerobic zone.

Moreover, Tang *et al*. (2012) believed 11.5 mg L^{-1} should be the highest NO_2^--N concentration for anoxic phosphorus uptake and any higher value would affect phosphorus removal rate. On the contrary, a higher nitrite concentration of 35 mg N L^{-1} was recorded by Zhang *et al*. (2010), which was an appropriate concentration for phosphorus uptake in anoxic phase. Furthermore, in the research of Zhou *et al* (2010), anoxic phosphorus uptake cannot be inhibited even when nitrite concentration reaches 80 mg N L^{-1}, and the optimal concentration is 20 mg N L^{-1}.

Additionally, some studies suggested that the A_2 systems which had been acclimated with nitrite could be adapted to higher concentration of NO_2^--N in anoxic P uptake. Guisasola *et al*. (2009) enriched nitrite-based DPAOs with anaerobic/anoxic/aerobic conditions, indicating that 30 mg L^{-1} NO_2^--N could not inhibit PO_4^{3-}-P uptake in the anoxic phase and the following aerobic phase. Besides, step-feeding strategies utilised in the study were also employed by some other researchers, who achieved anoxic P removal via NO_2^--N as the sole electron acceptor. Compared with the non-sufficient P uptake in the anoxic phase of Guisasola *et al*. (2009), in the studies by Peng *et al*. (2011) and Vargas *et al*. (2011), the anoxic P uptake via nitrite pathway was basically achieved without toxic inhibition, even though the concentration of NO_2^--N was 60 mg L^{-1}. It suggested that high concentration of NO_2^--N cannot inhibit P uptake if appropriate nitrogen feeding strategies are utilised.

Some other research also discussed the enhancement or inhibition effects of different NO_2^--N critical values on P removal. Tsuneda *et al*. (2006) used an AOA process with a SBR for simultaneous N and P removal from wastewater and achieved the efficiencies of 83% and 92% with a suitable amount of carbon substrate supplied at the start of aerobic conditions. Similar research had been conducted by Ma *et al*. (2012) who evaluated the phosphorus uptake performance of DPAOs with the nitrite concentration of 10.53, 15.82 and 21.63 mg L^{-1}, and the result demonstrated that higher denitrification rate needed less initial nitrite concentration. In comparison, the research of Hu *et al*. (2003) suggested that NO_2^--N could not inhibit P uptake if its concentration was not higher than 115 mg L^{-1}. Additionally, Zhang *et al*. (2010) evaluated the impact of NO_2^--N concentration on PO_4^{3-}-P uptake efficiency in anoxic condition and found that in the concentration range from 5 to 45 mg L^{-1}, the P removal efficiency would increase with higher NO_2^--N concentration.

Consequently, the toxic inhibition is an important issue in NO_2^--N based anoxic phosphorus uptake. As discussed above, the threshold value of NO_2^--N value causing the inhibition is controversial in the previous studies. The reasons causing the different opinions include different assessment standards of inhibition and different levels of PO_4^{3-}-P concentration. In the study of Hu *et al*. (2003), NO_2^--N concentrations of 90, 115 and 160 mg L^{-1} were investigated in batch tests of anoxic phosphorus uptake (around 100 mg L^{-1} at the beginning of anoxic phase), where the PO_4^{3-}-P concentration decreased only in the first 1.5 hour with slow rates, followed by kept stable in the later 1.5 hour. It suggested that the test with 115 mg L^{-1} NO_2^--N showed the capacity of PO_4^{3-}-P uptake, while it did not achieve effective PO_4^{3-}-P removal. Hence, it can also be recognised that that level of NO_2^--N concentration inhibit the uptake of phosphorus.

Besides, in the study of Meinhold *et al*. (1999), 10 or 15 mg L^{-1} NO_2^--N could completely inhibit anoxic PO_4^{3-}-P uptake and even the following aerobic PO_4^{3-}-P uptake, suggesting that the PAOs had totally lost the phosphorus removal capacity. An important reason causing the inhibition was the relatively low initial PO_4^{3-}-P concentration at the beginning anoxic phase, which was only around 19 mg L^{-1}, much lower than that in the test of Hu *et al*. (2003). As a result, the threshold value of NO_2^--N causing toxic inhibition is not constant in A_2 systems, while it is mostly higher than 10 mg L^{-1} in normal PO_4^{3-}-P release levels, which should be avoid in the design of experiments. Furthermore, in the report about the impacts of NO_2^--N on anoxic P efficiency by Zhang *et al*. (2010), who considered the ratio of NO_2^--N to MLSS as an importance factor influencing the effects of nitrite on the P removal performance, believed that a level of 15.2 mg NO_2^--N $gMLSS^{-1}$ was appropriate for anoxic PO_4^{3-}-P uptake, suggesting that the threshold of NO_2^--N concentration in anoxic P removal was not a constant, but related to other factors (such as MLSS). However, since the reports about the relationship between NO_2^--N and other factors were still not comprehensive, it is necessary to explore more details of it.

For the effects of NO_3^--N and NO_2^--N on anoxic P uptake efficiency, there are still some different opinions. Lv *et al*. (2014) found that the electron utilisation efficiency of denitrifying phosphorus removal sludge with NO_3^--N was higher than NO_2^--N, 2.21 and 1.51 mol P/mol e^-, respectively, which suggested that the energy generated from nitrate reduction might facilitate the DPU with nitrite, and the microbial community were similar. Similar results showed that nitrate had better DPU efficiency, compared with nitrite. Wang *et al*. (2015) investigated the starvation comparison of nitrate and nitrite-DPAOs, and found that after a long-term anaerobic starvation of 12 days, the cell decay rate in the sludge of nitrite-DPAOs was obviously lower than the sludge of nitrate DPAOs. Additionally, they found that the energy of nitrate-DPAOs during starvation was from the EPS that was mainly polysaccharides. This may suggest that the other kinds of organisms in nitrate-DPAO sludge have the synergistic effect for the activities of DPAOs and advantageous for DPR. Both of the results contribute to the viewpoints that nitrate-based DPR has more efficiency and feasibility than nitrite-based DPR. However, in the studies of Lee *et al*., (2001) and Dai *et al*., (2017b), it was found that anoxic P removal performance with the presence of NO_2^--N was better than with only NO_3^--N, suggesting the appropriate NO_2^--N adding could enhance anoxic PO_4^{3-}-P uptake efficiency, which was inconsistent with the prior viewpoint.

Consequently, compared with NO_3^--N, the effect of NO_2^--N on the anoxic PO_4^{3-}-P uptake is discrepant, described by the previous studies. Due to the unclear threshold value of NO_2^--N concentration and the contradiction between the P uptake efficiencies via NO_3^--N and NO_2^--N, it is of importance to evaluate the impacts of different NO_2^--N levels on anoxic P removal, with the comparison of NO_3^--N.

In addition, the inhibition of P uptake by nitrite is not obviously affected by the enrichment processes with oxygen or nitrate as electron acceptor. For instance, the P uptake performance with 115 mg N L^{-1} after the A_2 start-up process (nitrate based) in the study of Hu *et al*. (2003) was not more effective than the performance with 80 mg L^{-1} in the study of Zhou *et al*. (2010), who enriched PAOs with A/O conditions. Since both the NO_2^--N based P uptake suffered inhibition, it suggested that the tolerance of microbial systems to the dosing of nitrite was not affected by the enrichment process if the electron acceptor was oxygen or NO_3^--N. Although the enrichment process by Guisasola *et al*. (2009) was conducted with NO_2^--N and oxygen as the electron acceptors, the P uptake in anoxic phase with nitrite was not very efficient if the following aerobic phase was cancelled, suggesting high concentration of NO_2^--N always had the potential to induce decrease of phosphorus uptake efficiency.

2.3.2.2 PO_4^{3-}-P concentration and P/N ratio

The P/N ratio is one of the most important parameters affecting the process of anoxic phosphorus uptake, while two kinds of P/N ratio should be considered in EBPR process, namely the PO_4^{3-}-P/NH_4^+-N ratio in the influent and the PO_4^{3-}-P uptake/NO_x^--N consumption (P/N) ratio. PO_4^{3-}-P/NH_4^+-N ratio is determined by the characteristics of the influent or the synthetic wastewater, while the P/N ratio is determined by the dosing strength of external nitrogen if the NO_x^--N utilised for P uptake is not produced by ammonium oxidisation, which is decided with the experiment designs of the studies. In case of the EBPR systems with external nitrogen dosing, the NH_4^+-N in the influent is basically used for the growth of microorganisms, while it is not oxidised to NO_x^--N since the aerobic phase is replaced by the external adding of nitrate or nitrite. On the contrary, in the studies which were conducted with ammonium oxidising process, the NH_4^+-N in the influent determines the concentration of NO_x^--N and the P/N ratio. As a result, the initial PO_4^{3-}-P/NH_4^+-N ratio in the influent of these studies can directly influence the P/N ratio in the anoxic phase.

Table 2.4 shows initial PO_4^{3-}-P/NH_4^+-N ratio in the influent in some of the research about denitrifying phosphorus uptake. As can be seen in the table, the ratio of PO_4^{3-}-P/NH_4^+-N varies from < 0.1 to > 1.0, indicating that the NH_4^+-N concentration in the influent depends on the study aims. If the NO_x^--N for denitrifying P uptake was produced by nitrification, initial NH_4^+-N concentration was relatively higher to provide enough electron acceptor, and the concentration was similar with the values in practical wastewater.

Table 2. 4 PO_4^{3-}-P/NH_4^+-N ratio employed in the influent of different research and treatment performance

Research	PO_4^{3-}-P/NH_4^+-N (mg/mg)	PO_4^{3-}-P/NH_4^+-N (mmol/mmol)	COD (mg/L)	Highest P removal rate (%)	Electron acceptor
Kuba *et al*. (1996b)	0.13	0.06	400	>90	NO_3^--N
Lee et al. （2001）	0.25-0.38	0.11-0.17	300-600	96.8±1.1%	NO_3^--N & NO_2^--N
Hu et al., 2003	0.67	0.30	400		O_2, NO_3^--N & NO_2^--N
Wang *et al*. (2009)	0.34	0.15	237±58	94%	NO_3^--N
Zhang et al., 2010	0.28-0.32	0.13-0.14	200-420	78.9%	NO_2^--N
Podedworna and Zubrowska-Sudol (2012)	0.06-0.49	0.03-0.22	352-867	99.1%	NO_3^--N & NO_2^--N
Zhou *et al*. (2010)	0.33	0.15	250	92%	O_2, NO_3^--N & NO_2^--N
Peng et al., 2011	1.1	0.50	300	91.33±2.38%	NO_2^--N
Vargas et al., 2011	0.77	0.35	300		NO_2^--N & O_2
Zeng et al., 2011	0.07	0.03	177.5	98%	O_2, NO_3^--N & NO_2^--N
Ma et al., 2012	0.37	0.17	300		NO_2^--N
Dai et al., 2017b	0.75	0.34	120±15	87±2.3%	O_2, NO_3^--N & NO_2^--N

For instance, in the studies of Kuba *et al*. (1996b), an PO_4^{3-}-P/NH_4^+-N ratio of 0.13 mg/mg was chosen to provide sufficient NO_3^--N in the nitrification process, for the P uptake in the following anoxic phase. Wang *et al*. (2009) investigated a PO_4^{3-}-P/NH_4^+-N ratio of 0.34 in an anaerobic-anoxic/nitrification SBR for nitrogen and phosphorus removal with denitrifying phosphorus uptake via nitrate, and found that TN/P ratio in the influent had a positive linear correlation with phosphate removal rate, in which higher nitrate concentration was considered a key point to enhance the phosphorus uptake rate. Podedworna and Zubrowska-Sudol (2012) studied on denitrifying phosphorus removal process with a forced anoxic phase, in which a PO_4^{3-}-P/NH_4^+-N ratio from 0.06 to 0.49 was employed, and relatively high phosphorus removal rate and DPAO/PAO ratio were achieved.

On the other hand, if the NO_x^--N was provided by external chemical adding, the initial NH_4^+-N concentration in some of the studies was relatively lower, which was enough for the growth of microbial communities. As in these studies the anoxic P uptake and N consumption efficiencies are generally focused, the practical ratio of P to N in municipal wastewater is not applied for the influent (Peng *et al*., 2011; Vargas *et al*., 2011; Dai *et al*., 2017b)

In case of the anoxic P/N ratio, it is an important parameter to evaluate the efficiencies of P uptake and electron acceptor utilisation, and the activity of DPAOs in denitrifying EBPR process. The P uptake and N consumption in different studies were shown in Table 2.5. As shown in the table, the P/N ratio basically fluctuated between 0.6 and 2.0 in anoxic P uptake process. The ratio in nitrite-based EBPR process was normally lower than that in nitrate-based EBPR process, due to the higher electron accepting capacity of NO_3^--N.

Table 2. 5 Typical PO_4^{3-}-P uptake/NO_x^--N consumption (P/N) ratio in anoxic phase of the previous studies

Research	PO_4^{3-}-P/NO_x^--N (mg/mg)	PO_4^{3-}-P/N NO_x^--N (mmol/mmol)	PO_4^{3-}-P uptake (mg L^{-1})	NO_x^--N consumption (mg L^{-1})	Electron acceptor
Kuba *et al*. (1996b)	1.75	0.79	70	40	NO_3^--N
Hu *et al*. (2003)	0.57/1.2	0.26/0.54	40/42	70/35	NO_2^--N
Guisasola *et al*. (2009)	0.66	0.3			NO_2^--N
Wang *et al*. (2009)	2.00	0.90	32	16	NO_3^--N
Zhang *et al*. (2010)	0.88	0.40	29.67	33.77	NO_2^--N
Zhou *et al*. (2010)	0.89 0.60	0.40 0.27	33	30 20	NO_3^--N NO_2^--N
Lanham *et al*. (2011)	0.91-2.88 0.44-1.97	0.41-1.3 0.20-0.89			NO_3^--N NO_2^--N
Peng *et al*. (2011)	0.97	0.44	58	60	NO_2^--N
Vargas *et al*. (2011)	0.75	0.34	45	60	NO_2^--N
Ma *et al*. (2013)	0.6-1.6	0.27-0.72			NO_2^--N
Dai *et al*. (2017b)	0.6	0.27	24	40	NO_3^--N & NO_2^--N

Both of the P/N ratios in the nitrate-based and nitrite-based anoxic processes had obvious fluctuation among the previous studies, where the ratio of nitrate-based process could be up to 2.0, while the ratio of nitrite-based process was lower than 1.6. In the study of Zhou *et al*. (2010), the optimal P and N removal rates with NO_3^--N and NO_2^--N were 0.89 and 0.6, respectively, suggesting that NO_3^--N had higher electron accepting capacity per unit of nitrogen than NO_2^--N. In addition, the varying value of the ratio in nitrite-based systems indicates that the ratio was easily affected by the NO_2^--N concentration added in the anoxic phase. If the concentration causes the P uptake inhibition, the ratio will be reduced by the decreasing of P removal efficiency.

Furthermore, the P/N ratio of Hu *et al*. (2003) decreased from 1.2 to 0.57 when the N/VSS increased from 0.0215 to 0.0221, suggesting that the ratio and N consumption were not constant, but related to the biomass in the system. Besides, Lanham *et al*. (2011) found that lower pH (in the range of 7-8.2) induced higher P/N ratios in both nitrate-based and nitrite-based anoxic conditions.

Consequently, the nitrogen consumption utilised for anoxic P uptake is an important factor influencing the efficiency of P and N removal. Due to the fluctuation of N and P concentrations in municipal wastewater, the electron acceptor for anoxic P uptake can be determined with the nutrient concentrations, especially the strength of NH_4^+-N, when the other conditions are stable. If the ratio of P and N in the influent is closed to the appropriate value of PO_4^{3-}-P/NO_2^--N, partial nitrification can be conducted to produce sufficient nitrite for anoxic P uptake. In contrast, if the nitrogen loading is relatively lower, complete nitrification can be conducted to produce nitrate, or external NO_2^--N can be added into the treatment systems to provide enough electron acceptor. Additionally, the removal efficiency of nitrogen in the previous studies were normally higher than 90%, even closed to 100%, since NO_x^--N could be reduced by the microorganisms to obtain energy for anoxic maintenance.

2.3.2.3 Effects of pH

pH is an important parameter in the control of EBPR process, which can affect the P release in anaerobic phase and P uptake in anoxic phase, since it affects microbial activities, microbial community structures and nitrogen species in the treatment systems. In the previous studies, pH was commonly controlled in the stable values between 6 and 8.5, with the adjustment by dosing acid or alkali. Table 2.6 shows the P removal efficiencies with different pH levels in the previous studies.

Table 2. 6 pH control and PO_4^{3-}-P removal efficiencies in the previous studies

Research	pH	PO_4^{3-}-P removal rate	Electron acceptor
Kuba *et al*. (1996b)	7.0	Almost 100%	NO_3^--N
Serafim *et al*. (2002)	7.0	Not stable	Oxygen
	7.8-8.5	>90%	
Oehmen *et al*. (2005)	7.0	<50%	Oxygen
	8.0	>90%	
Zhang *et al*. (2010)	6.0	Around 20%	NO_2^--N
	7.0	Around 71%	
	8.0	Around 50%	
Lanham *et al*. (2011)	7.0-7.5		NO_x^--N & Oxygen
	7.0-8.2		
Peng et al. (2011)	7.2-8.2	91.33±2.38%	NO_x^--N

As can be seen in the table, although Kuba *et al*. (1996b) strictly controlled the pH at 7.0, and obtained optimised P removal result, the appropriate value of pH for efficient P uptake is still controversial. Zhang *et al*. (2010), for instance, explored the effects of pH (6, 7 or 8) on anoxic P uptake via NO_2^--N, and found that pH of 7.0 and 8.0 could get higher P removal rate (with the removal rates of around 71% and 50%), which were more appropriate for respectively P release and P uptake than pH of 6 (with the removal rate of 20%). However, Serafim *et al*. (2002) indicated that higher P removal efficiency could be achieved in the SBR without pH control (pH raised from 7.8 to 8.5), rather than the SBR with pH control (7.0), implying that the higher pH was more appropriate for P uptake than lower pH As discussed in 2.3.2.1, Lanham *et al*. (2011) investigated the effects of pH (7.0-8.2) on the ratio of P uptake to N consumption in nitrate and nitrite based anoxic EBPR process, and found that lower pH could enhance the P/N ratio with both the electron acceptors, suggesting that the P uptake efficiency could be improved with the accumulation of PAOI at the pH range of 7.0-7.5.

pH can also affect the microbial communities in EBPR systems, especially the competition between PAOs and GAOs. Serafim *et al*. (2002) found GAOs in the SBR with pH of 7.0 become the dominating microbial group in the treatment system. Similarly, Oehmen *et al*.

(2005) investigated the effect of pH on the competition between PAOs and GAOs with stable pH levels, and suggested that the pH of 8 was more attractive to PAOs, compared with GAOs.

In addition, FNA was considered as the main chemical causing the toxic inhibition in P uptake process. Based on Equation (2-4) proposed by Anthonisen *et al*. (1976), the concentration of FNA has negative relationship with pH, suggesting that higher pH could reduce the FNA amount to enhance the P uptake efficiency if the other conditions (temperature and NO_2^--N concentration) were constant.

$$C_{HNO_2-N} = \frac{C_{NO_2^--N}}{K_a \times 10^{pH}} \qquad (2\text{-}4)$$

where,

C_{HNO_2-N} is the concentration of HNO_2-N (mg L^{-1});

$C_{NO_2^--N}$ is the concentration of NO_2^--N (mg L^{-1}); and

$K_a = e^{\left(-\frac{2300}{273+℃}\right)}$ is the ionisation constant of nitrous acid equilibrium equation.

Consequently, the pH value of EBPR systems can influence the P removal efficiency under both aerobic and anoxic conditions. However, the effects of pH on nitrite-based systems have not investigated comprehensively, including the specific comparison of P/N ratio with nitrate-based systems and the long-term effects of pH change on the operation performance of treatment process. Hence, it is of importance to evaluate the P uptake and N consumption at different pH levels, in order to explore the anoxic P uptake efficiency via NO_2^--N pathway.

2.3.2.4 Different organic carbon source

As known, VFAs, especially acetate acid, is the basic carbon source for any PAOs or DPAOs in EBPR processes. Some research focused on the effects of different carbon source on EBPR processes. Zhang *et al*. (2010) investigated the difference of phosphorus release in the anaerobic phase with the organic carbon source of acetate acid, butyric acid and glucose, and suggested the anaerobic release rates decreased orderly. In order to investigate the competition between PAOs and GAOs, Wang *et al*. (2010) explored the effect of acetate, acetate/propionate, propionate and glucose as carbon source, and found that propionate was more benefit for PAOs than acetate, and glucose was the optimal carbon source for GAOs.

Coats *et al*. (2015) and Guerrero *et al*. (2015) considered glycerol as a kind of effective carbon source for anaerobic P release. As a byproduct of biodiesel manufactory and an alternate waste should be dealt with, it can be utilised as a kind of low-cost external carbon source, but the amount should be controlled to achieve efficient phosphorus removal.

Since the organic carbon source can be various for anaerobic P release, a separate fermentation step can also be added before phosphorus removal process, in order to provide abundant fermented liquor for phosphorus removal. Ji and Chen (2010) achieved denitrifying phosphorus removal via nitrite, with fermentation liquor, and found that the fraction of humic acids could increase the accumulation of nitrite and nitrite-based DPR. Similar results were found by Zhang *et al*. (2000), who believed that sufficient fulvic acids could inhibit the activities of NOB.

2.3.2.5 Duration of each phase and hydraulic retention time (HRT)

Appropriate durations of anaerobic and anoxic phase are essential for the optimised operation of P release and P uptake, which also influence the cycle time and HRT of the treatment process. In addition, the HRT is an important parameter for WWTPs, affecting the treatment efficiency and growth of microbial communities. Xu *et al*. (2014) investigated the effects of HRT (24, 12 and 6 h) on nutrient removal of municipal wastewater, and believed that shorter HRT could induce better phosphorus removal, due to the faster biomass growth.

For anaerobic P release phase, Wang *et al*. (2011b) suggested that shorter anaerobic reaction time (60 min) could enhance the formation of PHA and P removal rate, and reduce N_2O production. In the idle phase of two-sludge system, the reactor is under continuously anaerobic condition with low level of carbon source, liquor amount and high level of phosphate. On the contrary, Coats *et al*. (2011) proposed to utilise longer anaerobic HRT, in order to positively affect P removal in aerobic phase.

For two-sludge system, there must be an idle phase for A_2 reactor, because of the aerobic phase in nitrification reactor in the meantime. Hence, the stabilisation of DPAOs in this period is important, in order to avoid the decay and deterioration of P removal. Wang *et al*. (2009) compared different anoxic retention time, and found that when NO_x^- was totally consumed in longer anoxic phase, “endogenous” P release would occur, which would negatively affect P removal in the effluent. Hence, the matching between NO_x^- concentration and anoxic duration is important to achieve proper P removal efficiency in the operation of anoxic EBPR process.

2.3.2.6 Effects of SRT

As an important factor, SRT can affect the biomass culture growth rate in the reactors. Moreover, because the P removal via EBPR is achieved by the excess sludge discharge, appropriate SRT is essential to realise sufficient P removal.

Both of long and short SRT were utilised in the previous studies about EBPR process. About longer SRTs, for example, in the investigation of Lv *et al*. (2014), the SRT of the A_2 and A/O SBRs were 20 and 15 days, respectively. Dai *et al*. (2017b) kept SRT as 15 days for both of A_2 and A/O reactors. Nonetheless, as a lot of literature mentioned, longer SRT can decrease of biomass yield and excess sludge discharge, and reduce the P removed by discharging excess sludge (Kuba *et al*., 1996b; Li *et al*., 2008; Vaverde-Perez *et al*., 2016). And also shorter SRT is more helpful to wash out GAOs (Zheng *et al*., 2014), GAOs are more competitive than PAOs under a longer SRT.

Kuba *et al*. (1996b) did anoxic phosphorus uptake with SRTs of 8 d or 14 d, in which 8-d SRT had faster biomass growth, with more N requirements because of higher biomass production. Brdjanvic *et al*. (1998) analysed the optimised SRT at different temperatures with model study, and found that 8-d was most appropriate for PAOs at 20°C. With the temperature decreased to 10 °C, a 16-d SRT could be appropriate, and a 32-d SRT would be good for 5 °C. Gurtekin *et al*. (2011) evaluated the performance of an A_2 SBR with the SRT of 20, 15, 10 and 5 days. In the results, they found that the 10-d SRT was the best one, to achieve highest phosphorus removal performance. Carrera *et al* (2001) utilised a SRT of 3-5 d, and believed that SRT increase brought about a reduction in the P-removal due to the lesser purge per day of active PAOs. Additionally, in some literature, short SRT as 3.5-7 days was also suggested to employ in phosphorus removal sludge. Valverde-Perez *et al* (2016) investigated the effects of short SRTs (8, 3.5 or 3 d), and justified that such short SRT could also be utilised in EBPR process. In addition, Merzouki *et al*. (2001) suggested that P removal performance would be deceased when SRT was decreased to 7.5 days.

In the DPAO enrichment process, most of the studies utilised stable SRTs. As sludge age is an important factor to achieve stable and successful EBPR process, different SRTs will be employed to investigate their impacts on the P removal performance, PHA production and utilisation, organic carbon and electron acceptor consumptions in the enrichment process.

2.3.2.7 Effects of salinity

As there are diverse anions such as chloride and sulphate in municipal wastewater and other kinds of wastewater, which may affect the metabolic activities of DPAOs and the efficiency of P removal.

Sulphate, for instance, has been investigated in EBPR process for several years (Lu *et al*., 2012, Wu *et al*., 2013 & 2014). Wu *et al*. (2014) suggested that there was an EBPR process with a sulphur cycle-associated (SO_4^{2-} uptake and release) denitrifying P uptake, in which the DPAOs could adapt a high salinity of 20% seawater. Welles *et al*. (2014) investigated the competition of PAOs and GAOs with different level of NaCl concentrations, and found that both of the organisms were affected in a similar way by salinity.

2.3.3 The competition and cooperation between PAOs and GAOs

In the literature about EBPR processes, GAOs are widely reported, which potentially compete with PAOs, due to the metabolic similarity by consuming carbon source (VFAs) in anaerobic phase and not taking up phosphate in aerobic or anoxic phase (Mino *et al*., 1995 and 1998). In 2002, Crocetti *et al*. identified the organisms and named them as "Candidatus Competibacter phosphatis". In the review of Oehmen *et al*. (2007), two kinds of GAOs are observed in phosphorus removal works, namely *Gammaproteobacteria* GAOs which are frequently sampled in both lab-scale and full-scale EBPR processes, and *Alphaproteobateria* GAOs which are normally discovered in lab-scale process, but little in full-scale systems. Thus, the identification of PAOs (DPAOs) and GAOs, and their competition in EBPR systems will be discussed below.

2.3.3.1 The identification of PAOs and DPAOs

In 1993, Kerrn-Jespersen and Henze investigated the difference between anoxic and aerobic phosphorus uptake, and observed that a fraction of PAOs could only take up phosphate under aerobic phase and their PHA was not consumed in anoxic phase, but another PAOs (DPAOs) was able to accumulate P with either NO_3^- or oxygen. In the characteristics analysis of PAOs for the identification of the microbial group, PHB were staining positive in PAO-enriched sludge samples, while in the Gram staining analysis, both Gram negative and positive results were detected in different studies (Mino *et al*., 1998). Crocetti *et al*. (2000) investigated the EBPR sludge samples with FISH method, and found that the dominant group (>80%) in the sludge were β-2 *Proteobacteria*.

Although the complete microbial groups of PAOs are still not investigated clearly, Oehmen *et al*. (2007) concluded that *Candidatus Accumulibacter phosphatis* (*Accumulibacter*), *Rhodocyclus*-related bacteria and *Actinobacteria* are the main identified PAO communities. *Accumulibacter*, belonging to *Rhodocyclales*, is one of the main groups recognised in P removal systems. Based on the different polyphosphate kinase gene (ppk1), two clades of *Accumulibacter* were identified, namely type I and type II (Hu *et al*., 2007). Different affinities of the types could be distinguished by the probes of fluorescent *in situ* hybridisation (FISH), recognising as clade IA, IC, IIA, IIC and IID (Flowers *et al*., 2009; Saad *et al*., 2016). With the utilisation of molecular tools employed in the investigation of microorganisms, *Accumulibacter* was widely agreed as the main group that could take up phosphorus with different electron acceptors (Ahn *et al*., 2002; Zeng *et al*., 2003a; Kong *et al*., 2004; Lanham *et al*., 2011).

In the study of Carvalho *et al*. (2006), a similar result was suggested that there were two different groups of PAOs in phosphorus removal SBRs, and *Accumulibacter* was abundently observed. Moreover, the organisms with rod-type morphology had the ability to take up phosphate under anaerobic-anoxic conditions, but the organisms with cocci-type morphology would lost the capacity to take up VFA in anaerobic phase and accumulate phosphate in the anoxic phase. Based on the studies, they proposed the hypothesis that in the two groups of *Accumulibacter*, DPAOs was the rod-type organism and the cocci-type bacteria was linked to the non-DPAOs (Oehmen *et al*., 2007).

In the aspect of electron acceptor for anoxic phosphorus uptake of *Accumulibacter*, the study by Martin *et al*. (2006) suggested that nitrite was important for the P removal of DPAOs, and the reduction of nitrate was achieved by flanking species. Based on the study of Flowers *et al*. (2009 & 2013), clade IA had the capacity to couple NO_3^--N reduction and PO_4^{3-}-P uptake, and both of the clades could conduct NO_2^--N reduction, suggesting some PAOs could not use nitrate as electron acceptor, which was also demonstrated by the studies of Guisasola *et al*. (2009) and Saad *et al*. (2016). Zeng *et al*. (2018) also found the sludge with clade IA and clade IIC in WWTPs, which had denitrifying performance with nitrate. On the contrary, Rubio-Rincon *et al*. (2017) believed that enriched clade I could not achieve higher nitrate reduction without the cooperation of GAOs, suggesting clade I did not have the capacity of P uptake with nitrate as electron acceptor, which was related to clade IC, a novel PAO without denitrification capacity on nitrate (Rubio-Rincon *et al*., 2019).

Dechloromonas is also a microbial community that has been justified as a type of PAOs in EBPR processes (Goel *et al*., 2005). Terashima *et al*. (2016) investigated the community in a full-scale oxidation ditch wastewater treatment plant, and successfully isolated *Dechloromonas* that was able to take up phosphate into its cells. In the experiment of DPAO enrichment by Dai *et al*. (2017b), *Dechloromonas*-related organisms were also the most abundant culture with an alternative A_2 acclimation conditions, compared with *Accumulibacter* under alternative A/O conditions. However, as the result of Kim *et al*. (2013), who had investigated the characteristics of microbial community in a SBR with AO or A_2O conditions, the role of *Dechloromonas* was the nitrate-reducing bacteria, which produced nitrite for the anoxic P uptake of *Accumulibacter*.

Tetrasphaera was identified as another group of PAOs widely found in WWTPs, which had been discussed frequently in recent years. Based the studies of Kong *et al*. (2008), Kristansen *et al*. (2013) and Marques *et al*. (2017), the P removal capacity of *Tetrasphaera* was not only performed by their PO_4^{3-}-P uptake, but also via their fermentation capability, which could provide VFA to other kinds of PAOs. In case of denitrifying P uptake, Marques *et al*. (2018) reported that it had the capacity of denitrification, while the anoxic P uptake rate was lower than *Accumulibacter*.

2.3.3.2 The identification of GAOs

Due to the existence of GAOs in EBPR systems, the identification research of GAOs had been conducted for several years. *Candidatus Competibacter phosphatis* (*Competibacter*) and *Defluvicoccus* are the main groups of GAOs found in EBPR process (Crocetti *et al*., 2002; Wong *et al*., 2004), which can consume carbon source in the anaerobic phase, but do not have P uptake capacity.

Competibacter had been reported as the most abundant GAOs in wastewater treatment process, competing with PAOs for VFA as discussed above. However, based on the study of Rubio-Rincon *et al*. (2017) *Competibacter* could reduce nitrate to nitrite to provide electron acceptor for DPAOs. Brand *et al*. (2019) found three lineage clades of *Competibacter* from WWTPs by FISH, which still needed more exploration. In addition, two clusters of *Defluvicoccus* were identified by Wong *et al*. (2004) and Meyer *et al*. (2006), found in some P removal processes. Furthermore, Kondo et al. (2007) found there were several sub-species in *Defluvicoccus*-related GAOs, which may deteriorate P removal process.

2.3.3.3 Factors influencing the competition between PAOs and GAOs

To inhibit the activity of GAOs, the effects of carbon source, pH, and electron acceptors are mainly considered in EBPR process. Normally, it is known that the ratio of organic carbon to phosphorus (COD/P) in the influent can affect the competition between PAOs and GAOs. Compared with a high COD/P ratio, such as >50 mg COD/mg P, a low COD/P ratio as 10-20 mg COD/mg P can be more appropriate for the growth of PAOs (Mino *et al*., 1998).

Numerous studies have investigated the effects of different carbon sources on the PAOs-GAOs competition. In most of EBPR process, acetate is used as sole carbon source in the previous studies. In the recent years, other VFA carbon source and non-VFA carbon source are also considered in the studies of EBPRs and GAO competition. Propionate, for instance, is considered as a more favourable organic carbon source for successful EBPR performance, rather than acetate (Oehmen *et al*., 2005 & 2006). In the studies, propionate can provide more advantageous condition to PAOs over GAOs, via examining the microbial culture. For non-VFA carbon source, glucose was widely used for the studies about EBPR. Commonly, it is normally believed that glucose cannot be directly utilised by PAOs, but with the pervious fermentation to VFAs prior to uptake (Kong *et al*., 2004). Amino acids have also been reported that they can be taken up anaerobically by PAOs and perform aerobic phosphorus uptake (Kong *et al*., 2005).

Based on the assumption that the internal pH of the organisms is kept constant, increased pH gradient and electrical potential difference across the cell membrane exist at a high ambient pH, which will increase the energy demand for acetate transport through the membrane. Filipe *et al*. (2001) indicated that a higher pH also affected acetate uptake of GAOs. Overall, a pH of 7.25 is normally considered as the anaerobic pH critical point, below which VFA uptake by PAOs is faster than GAOs.

Although the studies on PAOs-GAOs competition have been conducted in the recent years. The competition between DPAOs and GAOs (DGAOs) has not sufficiently investigated. In some EPBR process, DGAOs was believed that they could join in the anoxic phosphorus uptake by denitrification and supply nitrite for DPAOs that could not use nitrate as electron acceptor (Lochmatter *et al*., 2009). Wang *et al*. (2011a) believed that relatively higher temperature (25-30 °C) negatively influenced the phosphorus removal rate (only 77%) in a NO_3^--N based anoxic EBPR system due to the faster growth of GAOs. However, in the comparison of Wang *et al*. (2015), the percentage of GAOs in nitrite-DPAOs sludge was lower than nitrate-DPAOs sludge, which also suggested that nitrate-based phosphorus

uptake might need the existence of DGAOs. Furthermore, as reported by Rubio-Rincon *et al*. (2017), the mixed PAO and GAO culture had more effective anoxic phosphate uptake activity via nitrate, but very negligible P uptake was conducted by an enriched PAO culture.

2.3.4 The competition between DPAOs and denitrifiers

In normal nutrient removal process, denitrifiers is a necessary heterotrophic group of microbial culture in achieving denitrification, which consume organic carbon source to reduce NO_x^- to nitrogen gas. Hence, it is a potential competitor to DPAOs in anoxic phosphorus uptake, if COD is not exhausted totally in the anaerobic phase. But few studies have been conducted to investigate the competition from denitrifiers for nitrate and nitrite.

Frison *et al*. (2016) believed that DPAOs did not compete to denitrifiers with carbon source in a short-cut SBR phosphorus removal process, as in the experiments organic carbon had been stored as PHA by DPAOs. As a result, to impede the competition of denitrifiers to DPAOs, VFAs should be consumed completely in the anaerobic phase, since thout the existence of organic carbon, denitrifiers will lose the NO_x^--reduction ability.

2.3.5 The enrichment and acclimation of DPAOs

In the sludge acclimation, the microbial communities in the raw sludge were screened with appropriate conditions to enrich the target groups (DPAOs) as the stat-up process of A_2 SBRs, in order to achieve the stable operation of the P removal systems. The enrichment of DPAOs in conventional activated sludge has been investigated in several experiments (Table 2.7). Normally, it is better to have an aerobic phase before or after anoxic phase for the fast growth of PAOs. If possible, continuous NO_x^- adding is used, for which the solution is gradually added into the reactor in the first hour of anoxic phase. For seed sludge, it is better to get from nutrient or phosphorus removal process of WWTW. Only Ong *et al*. (2010) and Zhou *et al*. (2010) collected sludge from conventional activated sludge and acclimated it under anaerobic and aerobic conditions.

Zou *et al* (2014) accumulated DPAOs with A_2 conditions, carbon source of NaAc, and a cycle of 8 hours. The phosphate removal performance was stable after 80 days. Dai *et al*. (2017b) investigated the acclimation of DPAOs with two strategies: 1) two-step strategy with A/O process and then A_2 process; 2) one step strategy with A/A/O processes. In their acclimation experiments, the shortest stable period was obtained, if nitrite/nitrate was 8/37 with one-step strategy.

NaAc is the most common carbon source in EBPR process, because PAOs can directly absorb VFAs into their cells, in order to produce PHA in anaerobic phase. With the justification of a large number of literature, NaAc is applicable as the organic carbon source in the acclimation process. In the literature above, the ratio of COD/P normally ranges from 20 to 80. In the former research (Oehmen *et al*., 2007; Dai *et al*. 2017b), lower COD can inhibit the growth of GAOs.

In PAO or DPAO acclimation process, nitrogen in ammonia is the necessary for bacteria growth, and the part in nitrite or nitrate is electron acceptor for anoxic phosphate uptake. For NH_4^+-N, COD/N ratio is lower than 20 in some literature (Ong *et al*., 2010; Zhou *et al*., 2010; Wang *et al*., 2016). However, ammonia will be oxidised to nitrite or nitrate if aerobic phase is set after anaerobic or anoxic phase, which will influence phosphate release in the next cycle. Thus, ammonia concentration should not be too high in the feedstock, only for the growth of bacteria. In the first trial, NH_4^+-N concentration in feedstock is 8 mg L^{-1} and COD/N is 37.5. In the experiments of Zhou *et al*. (2007), ammonia concentration was 5 mg N L^{-1}, with a COD of 200 mg L^{-1} in the feedstock. For magnesium and calcium, $MgSO_4 \cdot 7H_2O$ and $CaCl_2 \cdot 2H_2O$ are normally used as Mg and Ca source, but the concentrations vary depending on different authors. Mostly, the concentration of $MgSO_4 \cdot 7H_2O$ ranges from 66 to 150 mg L^{-1}, and concentration of $CaCl_2 \cdot 2H_2O$ ranges from 10-35 mg L^{-1}.

Table 2. 7 Literature on start-up of anoxic phosphate uptake

	Conditions	Substrate	Inoculum	Acclimation duration	Removal rate in stable period
Kuba *et al*., 1993	Anaerobic: 1.75-3 h, anoxic: 2.75-4.5 h (continuous adding of nitrate)	HAc, K_2HPO_4, KH_2PO_4, NH_4Cl, Ca, Mg *et al*.	Nutrient removal process	About 2 weeks	100%
Kishida *et al*., 2006	Anaerobic: 90 min, aerobic: 120 min and anoxic: 120 min	NaAc, NH_4Cl, KH_2PO_4, Ca, Mg *et al*.	Nutrient removal process	21 days	>90%
Ong *et al*., 2010	Anaerobic: 60 min, aerobic: 120 min	NaAc, Peptone, yeast extract, NH_4Cl, KH_2PO_4, Ca, Mg *et al*.	Conventional activated sludge	19 days	51.7%
Zhou *et al*., 2010	Anaerobic: 120 min, aerobic: 180 min	HAc, K_2HPO_4, KH_2PO_4, NH_4Cl, Ca, Mg *et al*.	Conventional activated sludge	9 days	90%
Dai *et al*., 2017b	a. anaerobic/aerobic - anaerobic/anoxic b.anaerobic/anoxic/aerobic	NaAc, $(NH_4)_2SO_4$, KH_2PO_4, Ca, Mg *et al*.	A_2O process	60 days 28 days	Around 87%

2.3.6 Stoichiometric yields of P/HAc, P/PHA and P/glycogen

As the main stoichiometric parameters, HAc consumption, PO_4^{3-}-P release and uptake, NO_x^--N consumption, PHA production and consumption, and glycogen production and consumption, the ratios of them were compared to characterised the P removal performance of EBPR. Table 2.8 and 2.9 separately show the stoichiometric ratios in anaerobic and anoxic phase of EBPR processes in the previous studies. The ratio of PO_4^{3-}-P release to HAc consumption (P/HAc) can reflect the P release efficiency in anaerobic phase, indicating the P accumulation and HAc uptake capacities of PAOs. As can be seen in Table 2.8, the ratio of P release to VFA uptake in anaerobic phase was relatively higher with acetate (0.35-0.62) as the carbon source, rather than propionate (0.32-0.44), suggesting the higher P release efficiency with acetate. Most of the P release/PHA production and P uptake/PHA consumption ratios were more stable, which were respectively 0.16-0.5 and 0.15-0.71 in both A_2 and A/O processes, compared with the obvious fluctuations of P release/glycogen consumption and P uptake/glycogen production ratios which were mostly <1.0 with NO_x^--N as electron acceptor and >1.0 with oxygen as the electron acceptor. It suggests that in general the amount of glycogen consumption and re-production in A_2 systems were higher than A/O systems.

Table 2. 8 Typical stoichiometric ratios in anaerobic phase of the A_2 EBPR processes in the previous studies

Research	PO_4^{3-}-P/VFA mmol P/mmol C	PO_4^{3-}P/PHA mmol P/mmol C	PO_4^{3-}P/glycogen mmol P/mmol C	Electron donor
Filipe *et al*. (2001)	0.57	0.44	1.08	Acetate
Zeng *et al*. (2003a)	0.35	0.24	0.55	Acetate
Oehmen *et al*. (2005)	0.42	0.34	1.27	Propionate
Lu *et al*. (2006)	0.62	0.49	1.35	Acetate
	0.44	0.36	1.52	Propionate
Carvalho *et al*. (2007)	0.35	0.34	0.50	Propionate
Guisasola *et al*. (2009)	0.32	0.16	0.55	Propionate
Lanham *et al*. (2011)	0.43	0.93	1.08	Propionate
Vargas *et al*. (2011)	0.38±0.08	0.40	2.53	Propionate
	0.55±0.07	0.45	6.88	Acetate

Table 2.9 Typical stoichiometric ratios in the anoxic phase of the A_2 EBPR processes in the previous studies

Research	$PO_4^{3-}P$/PHA mmol P/mmol C	$PO_4^{3-}P$/glycogen mmol P/mmol C	Electron acceptor
Filipe *et al*. (2001)	0.45	1.57	O_2
Zeng *et al*. (2003a)	0.25	0.58	NO_3^--N
Oehmen *et al*. (2005)	0.71	1.03	O_2
Lu *et al*. (2006)	0.62	1.07	O_2
	0.46	1.62	
Guisasola *et al*. (2009)	0.15	1.2	NO_2^--N
Lanham *et al*. (2011)	0.6	0.67	NO_3^--N NO_2^--N

2.4 Nutrients treatment process

Since conventional BNR process cannot achieve denitrifying P uptake with NO_2^--N as the sole electron acceptor, it is of importance to discuss about appropriate treatment process, in order to optimise the nitrite-based A_2 EBPR removal efficiency. This section reviewed some of the nutrient treatment processes, to justify the feasibility and adaptation of A_2N two-sludge process to realise P and N removal via nitrite pathway.

2.4.1 General nutrient treatment process

In these years, biological nitrogen and phosphorus removal methods including A_2/O, invert A_2/O, Bardenpho process, UCT process, SBR process and AOA process (Grady JR *et al*., 2011), have been widely used in municipal WWTPs.

A_2O process (Fig. 2.3A) and its modified method, UCT process (Fig. 2.3C) are based on pre-denitrification, in which the anoxic tank is located prior to the aerobic phase and the mixed liquor from aerobic tank is returned into the anoxic tank, in order to achieve denitrification and partial phosphate removal. In the A_2O process, high nitrate concentration liquid is returned to achieve anoxic phase, but on the other hand, the returned sludge from settling tank is also introduced into the anaerobic zone, which can inhibit the VFA uptake and PHA formation by PAOs. For the UCT process, in order to minimise nitrate concentration in anaerobic phase, mixed liquor is returned from anoxic

phase to anaerobic zone, and activated sludge is recycled instead to the anoxic zone (Metcalf and Eddy, 2003; Oehmen *et al*., 2007).

In the 5-stage Bardenpho process (Fig. 2.3B), there is an additional anoxic zone after the aerobic phase, in which the nitrate produced in the aerobic phase can be considered as electron acceptor for denitrifying uptake. Finally, the aerobic phase can promote the stripping of nitrogen gas from the wastewater and maximise phosphorus removal.

The Dephanox system (Fig. 2.3D) is based on post-denitrification, with the separation of nitrification bacteria and DPAOs, in order to enhance the efficiency of anoxic phosphorus uptake. If the phosphate removal is not sufficient, the final aerobic phase can be employed (Bortone *et al*., 1996; Bortone *et al*., 1999).

In these processes, anaerobic, anoxic and aerobic conditions are achieved regularly and sequentially in the treatment tanks, in order to induce the reactions of nitrification, denitrification and the release and uptake of phosphorus to accomplish the removal of ammonia and phosphate.

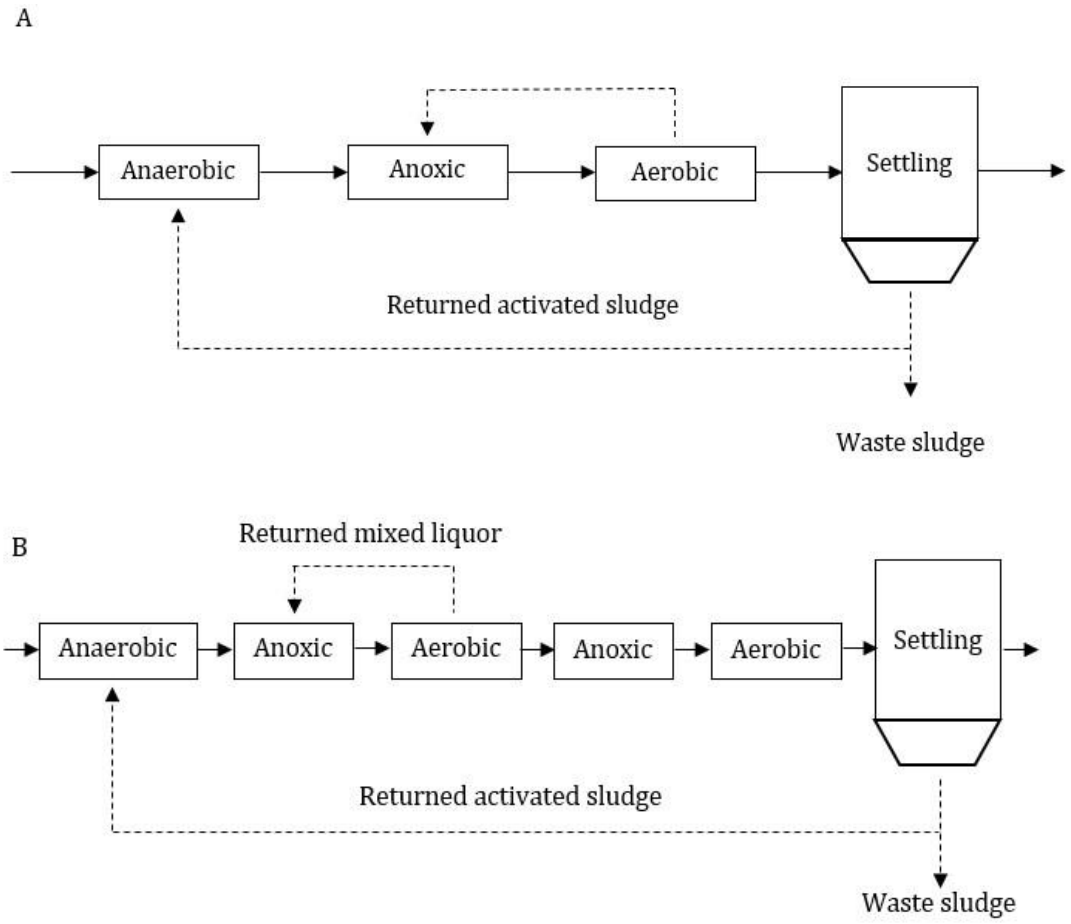

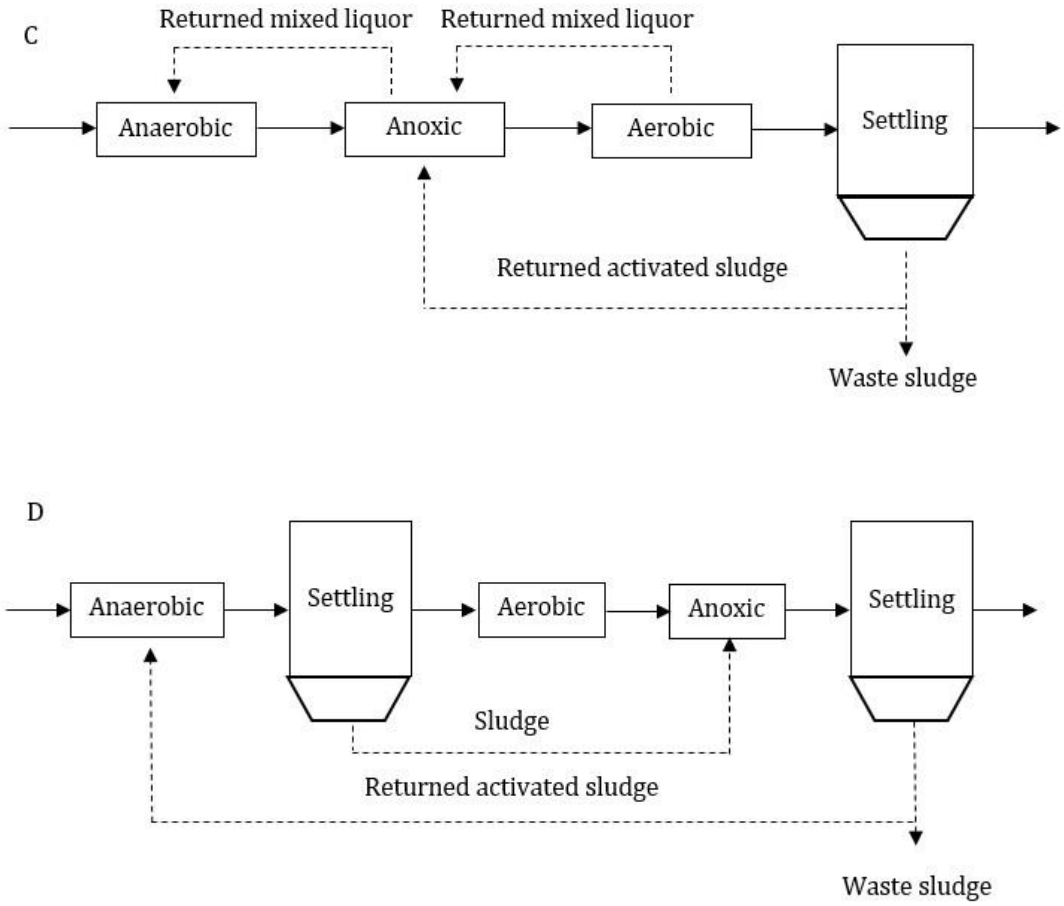

Fig. 2. 3 Process diagrams for combined biological nitrogen and phosphorus removal

A: A_2O process; B: Bardenpho process; C: UCT process; D: Dephanox process

However, the wastewater treatment processes discussed above cannot realise complete anoxic phosphorus uptake, meaning that there must be energy requirement for oxygen supply for complete nitrification and aerobic phosphorus uptake. In contrast, A_2N (anaerobic-anoxic-nitrification) two-sludge process separates the A_2 conditions and aerobic condition, which can avoid the oxygen consumption by PAOs (DPAOs) to accomplish complete denitrifying phosphorus uptake in the A_2 SBR.

2.4.2 A_2N two-sludge process and its development

The A_2N two-sludge SBR process was developed by Bortone *et al*. (1994) and Kuba *et al*. (1996b), consisting of an alternative anaerobic/anoxic SBR (A_2 SBR) and an aerobic nitrifying SBR (N-SBR). In this system, DPAOs and nitrification bacteria are strictly separated into two reactors, in which aerobic condition is only utilised for nitrification, and

the nitrate produced from nitrification is contributed for denitrifying phosphorus removal in anoxic phase, in order to maximise the efficiency of anoxic phosphate uptake.

Fig. 2.4 briefly demonstrates the process of A_2N SBR: (1) At the beginning of anaerobic phase, the wastewater is pumped into the A_2 SBR, then VFA is taken up and phosphate is released by DPAOs; (2) After the anaerobic phase and settlement, the supernatant is transferred into the N-SBR, aerobic phase is started to oxidise ammonia to nitrate, and at the end of this stage, nitrogen gas is flushed into the reactor to remove oxygen; (3) The nitrate rich supernatant is pumped back to the A_2 SBR and anoxic phase is started, in order to achieve denitrifying phosphate removal by DPAOs; (4) Finally, the effluent is pumped out from the A_2 SBR.

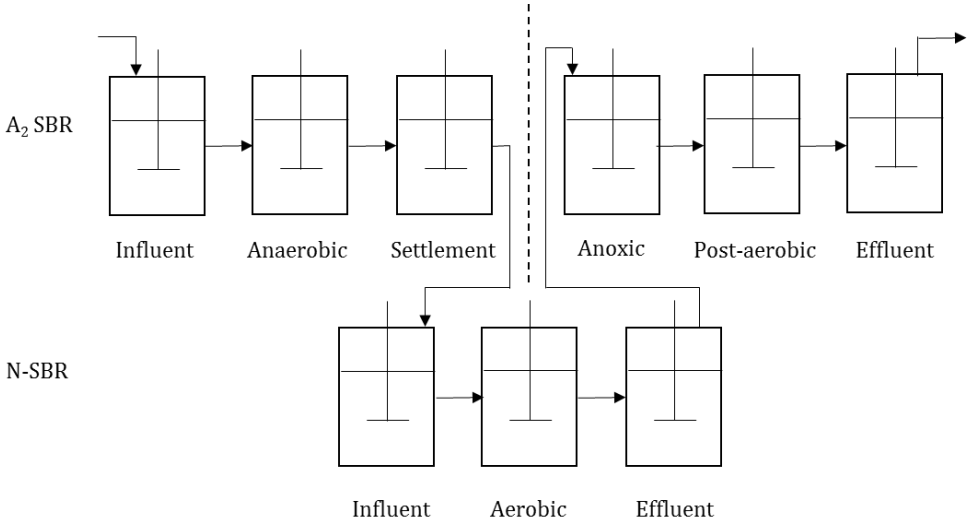

Fig. 2. 4 Brief diagram of A_2N SBR

(Kuba *et al*., 1996b)

Table 2.10 shows the operational parameters applied in the previous studies about two sludge systems. As can be seen in the table, the COD of 132-400 mg L^{-1} was selected in the influent, mostly from the synthetic wastewater with external HAc adding. The SRT of the A_2-SBR was controlled at 8-25 days, most of which were higher than 20, while the SRT of N-SBR was commonly controlled at 30-50 days. The pH values of the A_2-SBR were mostly controlled at appropriate ranges with acid or alkali adding, while the pH of N-SBR was adjusted with the supplementation of HCO_3^-.

With the development of two-sludge system, the exchange ratio of each SBR had been increased to 80%, as the higher ratio could enhance the overall P and N efficiencies. Depending on the different partial nitrification rate, the electron acceptors obtained in the

studies were separately NO_3^--N, NO_2^--N or the mixture of them. If the amount of NO_x^--N produced in aerobic phase was not sufficient, concentrated solution or post-aeration was added into the system as external electron acceptor supply.

Kuba *et al*. (1996b) justified this system can achieve efficient phosphorus removal rate with a low initial COD concentration (COD:N:P was around 400:110:15). The research of Kuba *et al*. (1996b) and Wang *et al*. (2009) were focused on the effects of influent nutrient ratios and HRT on N and P removal rate in the A_2N SBR system, and found that the ratios of COD:P and COD:N were 19.9 and 9.9, relatively optimal phosphorus and nitrogen removal rates can be achieve as 94% and 91%, respectively. Zhou *et al*. (2008) worked on two-sludge SBR which consisted of an A_2 granular sludge reactor and an aerobic biofilm reactor, in order to maximise nitrogen removal efficiency with the utilisation of biofilm. Li *et al*. (2013) proposed that two-sludge SBR process was not only improved ammonia and phosphate removal efficiency, but also reduced N_2O produced by around 31.5%. The development by Wang *et al*. (2007) and Xu *et al*. (2019) investigated the performance of an FNA-based two sludge system, and believed that the accumulation of nitrite in the N-SBR could enhance the total N and P removal efficiencies and produced high level of PHA. In addition, some variations of two-sludge system were investigated in some studies, attempting to optimise the treatment efficiency or evaluate the microbial community of the systems (Torrico *et al*., 2008; Zhao *et al*., 2019).

Table 2. 9 Operation parameters applied in A_2N two-sludge SBRs of previous studies

Research	COD ($mg\ L^{-1}$)	pH		SRT (d)		HRT (h)		Exchange ratio			N exchanging duration (min)	Electron acceptor
		A_2-SBR	N-SBR	A_2-SBR	N-SBR	A_2-SBR	N-SBR	A_2-SBR	A_2 - N	N-SBR		
Kuba *et al*. (1996b)	400	7.0	7.1	14/8	30	12	8.4	50%	71%	71%	15	NO_3^--N
Zhou *et al*. (2008)	132	7.0-7.8	7.8			8	6	75%	75%	86%	10	NO_2^--N
Wang *et al*. (2009)	237±58	7.1-8.0	7.2-7.4	18-20		9.3	7.1	75%	75%	75%		NO_3^--N
Li *et al*. (2013)	172			25	50	7.5	3.1	80%	80%	80%		NO_3^--N
Wang *et al*. (2017)	150		7.5	20	30	6.25	4.58	80%	80%	80%	5	NO_x^--N
Xu *et al*. (2019)	350			20	30	7.1	3.75	80%	80%	80%		NO_x^--N

2.5 Summary and knowledge gaps

As an important section of phosphorus cycle in the nature and wastewater treatment process, EBPR has been utilised in WWTWs in decades of years. In order to reduce aeration demand, energy consumption and sludge production, a lot of research were conducted, focusing on anoxic EBPR process. In most of combined P and N removal process, completely anoxic phosphorus removal is difficult to achieve, due to the simultaneous existence of PAOs and nitrifying bacteria, so two-sludge system that separates PAOs (DPAOs) from AOB (and NOB) is more suitable for anoxic EBPR process. In different treatment tanks, the acclimation of functional microbial communities with appropriate conditions should be conducted. For instance, DPAOs should be enriched under A_2 conditions to wash out other kinds of bacteria in the P removal tank, while nitrifying bacteria should be enriched under aerobic condition with suitable DO ranges in the N removal tank.

Although some research on the performance of anoxic phosphorus uptake with different electron acceptors (NO_3^- and NO_2^-) is conducted, the effects of NO_2^- on phosphorus removal is still controversial. Most of successful A_2 EBPR performance was achieved by NO_3^--N or mixed NO_3^--N and NO_2^--N, without enough NO_2^--N as the sole electron acceptor. As the start-up period of EBPR process, the enrichment method of DPAOs was not investigated efficient, especially the enrichment performance with NO_2^--N as the sole electron acceptor, which was always conducted with alternant anoxic and aerobic conditions to avoid the accumulation of NO_2^--N, inducing the acclimation process was more complicated. For the stable and effective operation of EBPR via only NO_2^--N pathway, rapid and easy enrichment and acclimation with nitrite is needed to achieve the fast start-up of EBPR.

In case of the stable operation of EBPR systems, suitable NO_2^- dosing strategy was not tested comprehensively to avoid toxic inhibition. Besides, based on the steady NO_2^--N based A_2 EBPR, the effects of high temperature (30 °C) on the operation performance and microbial communities were not investigated in the previous studies. As temperature is an important influencing the competition between PAOs and GAOs, it is of importance to explore the change of microorganism systems in NO_2^--N based phosphorus removal sludge reactors.

Mostly, the model development about EBPR process are based on A/O process or A/A process with NO_3^- as electron acceptor. Very few modelling and simulation studies were about NO_2^--based anoxic phosphorus uptake, even though nitrite has been an important point in biological P removal.

Overall, anoxic denitrifying EBPR process via nitrite pathway is not completely appropriate in its running and operation. There are still some unknowns, which affect the practical application of this process and need to be focused in research. Based on the summarised study gap from the literature review, according methodology was applied to develop the relative aspects of nitrite based A_2 EBPR, including the experiments of preliminary tests, enrichment of DPAOs, effects of nitrite dosing strategies, temperature and pH on operation performance and microbial communities in A_2 systems, data analysis and simulation of phosphorus removal with NO_2^--N.

2.6 Aims and objectives

As an important trend of phosphorus removal from wastewater, anoxic DPU with nitrite will be considerably developed to reduce the energy and cost demand in wastewater treatment. However, there are still some points which have not been investigated clearly or completely: 1) In the studies of DPAOs enrichment, the different levels of NO_3^--N / NO_2^--N ratio, solid retention time (SRT) was not considered as a parameter to investigate its effects on the successful achievement on the enrichment efficiency. 2) The studies about DPAOs enrichment with NO_2^--N as the sole electron acceptor were not sufficient. 3) Some studies just mentioned the existence of denitrifying glycogen accumulating organisms (DGAOs), but no point about their consumption of NO_2^-. So it is necessary to explore if DGAOs exist in NO_2^--based EBPR systems. 4) The maximum of NO_2^--N concentration in the anoxic EBPR is a controversial point, which should be justified. 5) In order to achieve effective NO_2^--based P uptake, appropriate nitrite dosing strategy should be determined.

As discussed above, some research gaps have been identified. Consequently, the aims of this research are: to achieve DPAO enriched sludge with A_2 conditions, especially with NO_2^--N, and explore the possibility of anoxic EBPR process with NO_2^--N as the sole electron acceptor to achieve complete phosphorus removal in A_2 process.

The following objectives are considered as necessary to achieve the above aims.

- To explore the effect of solid retention time (20, 15 and 10 days) on the enrichment of anoxic denitrifying phosphorus uptake via NO_x^- as electron acceptors.
- To investigate the appropriate C/P/NO_x^--N for the enrichment process and stable operation of anoxic EBPR via nitrate and nitrite pathways.
- To explore the feasibility of DPAO enrichment with NO_2^--N as the sole electron acceptor, compared with NO_3^--N, including the enrichment duration and PO_4^{3-}-P removal rates.
- To explore the effect of different dosing rate of NO_2^--N on A_2 EBPR systems.
- To explore the effect of temperature (20 and 30 °C) on NO_3^--N and NO_2^--N based A_2 EBPR systems
- To investigate the effects of different levels of pH (7 and 8) on NO_2^--based EBPR systems.
- To simulate the process of NO_2^--N based A_2N EBPR process with appropriate models

The work is carried out with laboratory-scale sequencing batch reactor (SBR) systems fed on synthetic wastewater and operated under a range of conditions. Performance and stability of the activated sludge are evaluated on the main indicators of overall COD removal and phosphorus release in anaerobic phase, and NO_x^- and PO_4^{3-} removal in anoxic phase. The synthetic wastewater used is designed to simulate the appropriate characteristics for A_2 EBPR process (with lower NH_4^+-N concentration to restrain the production of NO_3^- and NO_2^-), in order to achieve practical data on substrate degradation.

Chapter 3 Materials and methods

3.1 General experimental materials and methods

3.1.1 General materials and methods

3.1.1.1 Reagents

All chemicals used were of laboratory grade and obtained from Fisher Scientific (Loughborough, UK) or Sigma-Aldrich (Gillingham, UK).

3.1.1.2 Water

Solutions and standards used for analysis were prepared using ultra-pure deionised water obtained from a Barnstead Nanopure ultra-pure water purification system. Influents used for reactor operation were prepared using deionised water obtained from a deionised water system (Thermo Scientific, UK).

3.1.1.3 Laboratory practice

All operations in the laboratory were carried out using good laboratory practice, after having appropriate risk assessments and, where necessary COSSH assessments. All equipment, apparatus and analytical instruments in the laboratory were operated according to the instructions of manufacturers. All of the glassware was washed with washing detergent, prior to rinsing with tap water and deionised water, and all glassware and plastic ware for IC analysis was rinsed with ultra-pure deionised water.

3.1.1.4 Synthetic wastewater

The main contents of carbon, nitrogen and phosphorus in synthetic wastewater utilised for influents of the experiments were respectively from CH_3COONa & CH_3COOH, NH_4HCO_3 and KH_2PO_4, which were designed to provide appropriate conditions for EBPR systems, and adapted to the purpose of the studies to achieve the aims and objectives discussed in chapter 2. The specific ratio of C/N/P in the synthetic wastewater was not completely based on practical wastewater.

3.1.2 General conditions and parameters used in the experiments

3.1.2.1 Reactor set up

The reactors utilised in all the experiments in section 3.2 & 3.3 had 4-L working volume (Fig. 3.1), which were operated at ambient temperature (around 20 ˚C, except the temperature increase period in section 3.2.2 & 3.3.2). NO_x^--N dosing tubes were installed on the lids of the A_2 reactors, while aeration tubes were installed through the lids of A/O reactors. One-way valves were installed on the lids of the SBRs to maintain the pressure balance of the reactors. Mechanical stirrers ensured homogeneous mixing continuously with the stirring speed of 30-40 rpm during the experiment, except the settlement and discharge stages.

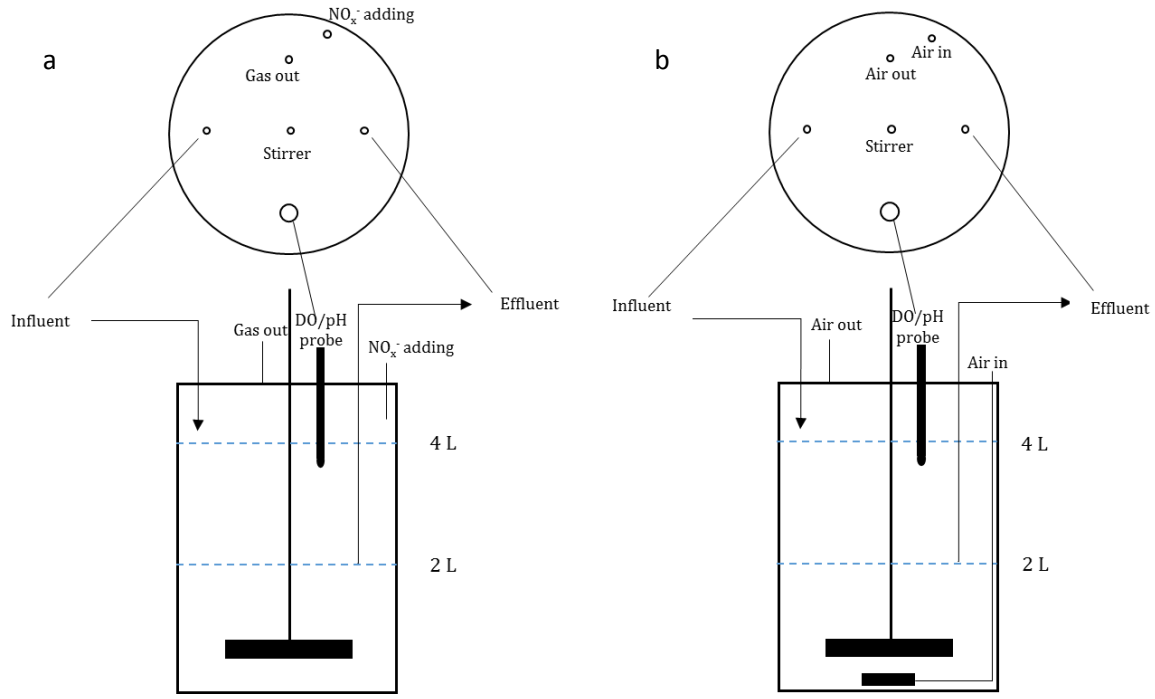

Fig. 3. 1 Diagrams of A_2 reactor (a) and A/O reactor (b) for DPAO enrichment process

3.1.2.2 Inoculum and influent

The inoculum was the recycled activated sludge (RAS) from 4-stage Bardenpho process of Millbrook WWTWs or the acclimated sludge from the previous experiment (Table 3.1). The influent contained carbon source (CH_3COONa or mixed CH_3COONa & CH_3COOH), phosphorus (KH_2PO_4), ammonia (NH_4HCO_3) and 1.25 mL L^{-1} nutrient solution. The nutrient

solution contained 22.5 g L^{-1} $MgSO_4 \cdot 6H_2O$, 3.75 g L^{-1} $CaCl_2 \cdot 2H_2O$, 1 g L^{-1} $FeCl_2 \cdot 4H_2O$, 0.5 g L^{-1} H_3BO_3, 0.5 g L^{-1} $ZnCl_2$, 0.5 g L^{-1} $MnCl_2 \cdot 4H_2O$, 0.5 g L^{-1} KI, 0.25 g L^{-1} $CoCl_2 \cdot 6H_2O$, 0.25 g L^{-1} $NiCl_2 \cdot H_2O$, 0.25 g L^{-1} $CuSO_4 \cdot 5H_2O$ and 0.25 g L^{-1} $Na_2MoO_4 \cdot 2H_2O$.

3.1.2.3 Reactor operations

1) Anaerobic phase. At the beginning of the anaerobic phase, 2-L synthetic wastewater was fed into the reactors.

2) Anoxic or aerobic phase. After the anaerobic phase, concentrated NO_x^--N solution was added into A_2 SBRs to achieve anoxic conditions, and air pump was turned on to achieve aerobic condition in A/O SBRs (the DO concentration was kept higher than 2.5 mg L^{-1}). At the end of anoxic or aerobic phase, quantitative sludge was discharged out of the SBR to achieve corresponding SRT.

3) Settlement and discharge. After the anoxic phase and the settlement, 2-L supernatant was drained out of the reactor.

Table 3.1 demonstrates the general conditions and parameters applied in the experiments of section 3.2 & 3.3. The range of each parameter was shown in the table, while the specific operation and change were stated in each section of the experiments. The pH of the systems was strictly controlled with the adjustment using acid and alkaline to achieve the values shown in the table.

3.1.2.4 Monitor and analysis

During the experiment period, pH, the concentrations of acetate, PO_4^{3-}-P, NO_x^--N in the liquid, and MLSS (MLVSS) were analysed regularly. PHA, glycogen and polyP contents were analysed after the enrichment I. Microbial communities in the sludge samples of inoculum, Enrichment I & II, before and after temperature and pH change in section 3.3.2 & 3.3.3, were analysed.

Table 3. 1 Conditions and parameters for the experiments

	Experiments	Condition	SBR	Inoculum	COD (mg L^{-1})	PO_4^{3-}-P (mg L^{-1})	NH_4^+-N (mg L^{-1})	Electron acceptor	SRT (d)	HRT (h)	pH
Enrichment process	Preliminary experiment	A_2 A/O	R1-R6 R7-R8	4-stage Bardenpho	100-300	6-15	15	NO_x^--N O_2	20	16-96	>7.0
	Enrichment I	A_2 A/O	E1-E6 E7-E8	4-stage Bardenpho	100-300	6-15	15	NO_x^--N O_2	15 or 10	16	6.8-8.0
	Enrichment II	A_2	EE1-EE8	Enrichment I or 4-stage Bardenpho	250	12	15	NO_3^--N or NO_2^--N	10	16	6.8-8.0
Optimising the process	Effect of dosing strategy	A_2	D1-D3	Enrichment II	250	12	15	NO_2^--N	10	16	6.8-8.0
	Effect of temperature	A_2	T1-T4	Enrichment II	250	12	15	NO_3^--N or NO_2^--N	10	16	6.8-8.0
	Effect of pH	A_2	H1-H2	Enrichment II	250	12	15	NO_2^--N	10	16	6.8-8.0 or 6.6.5-7.5

*NO_x^--N was added into the reactors as electron acceptor, with the concentration of 20-40 mg L^{-1} in section 3.2.1 (Table 3.2), 20-30 mg L^{-1} in section 3.2.2 (Table 3.4), and 27-48 mg L^{-1} in 3.2.3 and 3.3 (Table 3.5)

3.2 DPAOs enrichment from 4-stage Bardenpho process sludge

Since the enrichment of DPAOs is an essential procedure for the start-up of A_2 EBPR process, for both lab-scale experiments and practice WWTPs, the first step of this study is the investigation of the rapid enrichment of DPAOs. After a series of pre-test, the RAS from 4-stage Bardenpho process was justified that it had P removal capacity in A/O conditions. Thus, several studies including preliminary experiments, Enrichment I and Enrichment II, were conducted to explore the acclimation of the sludge with A_2 conditions.

3.2.1 Preliminary experiments

In the preliminary experiments, NO_x^--N dosing strength, cycle duration and HRT, COD and P concentrations were trialled to provide useful information for the following long-term enrichment experiments. The preliminary experiments included 6 stages with different conditions. Depending on the P removal performance in the previous stage, the conditions were adjusted in the following stage in order to obtain better performance to prove the possibility of successful enrichment of DPAOs from the inoculum. The SRT of the SBRs was controlled at 20 days. The specific parameters are shown in Table 3.2 & 3.3. pH was only controlled with the the ratio of NaAc to HAc in the influent. In the general operation, after the 2-h anaerobic phase, electron acceptor was dosed into the A_2 SBRs in the first 60 min of anoxic phase, while the air pump was turned on to achieve aerobic phase of A/O SBRs.

During the preliminary experiments, two cycle studies of PO_4^{3-}-P concentration were separately conducted during Stage 4 & 5. For the study in Stage 4, wastewater samples for PO_4^{3-}-P were collected every 30 min in the 3.5-h anaerobic phase and 3.5-h anoxic or aerobic phase. In case of the study in Stage 5, hourly samples of PO_4^{3-}-P were collected in the 2-h anaerobic phase and 9-h anoxic phase of A_2 SBRs, and in the 3-h anaerobic phase and 8-h aerobic phase in the A/O SBRs. The anoxic phase in the A_2 SBRs was longer than the normal operation of Stage 5, in order to try to achieve better P uptake.

Table 3. 2 Summary of the operation of R1-R8 in the preliminary experiments

Stage	Period (days)	Cycles	HAc (mg L^{-1})	PO_4^{3-}-P (mg L^{-1})	NO_x^--N (mg L^{-1})	N Dosing period (h)	HRT (h)	Cycle (h)	Anaerobic phase (h)	Anoxic/aerobic phase (h)
*	0~7	7	250-300	12-15	40	1	96	24	8	15
1	8~15	8	250-300	12-15	40	1	48	24	8	15
2	16~32	17	250-300	12-15	20	0.5	48	24	8	15
3	33~39	7	250-300	12-15	40	1	48	24	8	15
	40~53	14	Unexpected operation due to shortage of DI water							
4	54~67	42	200-250	12-15	20	0.5	16	8	2	5
	68~71	8	No discharge and feeding, kinetics analysis							
5	72~95	48	200-250	12-15	40	1	24	12	4	7
6	96~137	126	100-120	6-7.5	20	0.5	16	8	2	5

*As the pumping system had not been assembled completely, the feeding and discharge volume (around 1 L).

Table 3. 3 Electron acceptors for the SBRs

Reactors	Electron acceptor
R1&R2	only NO_3^--N
R3&R4	NO_3^--N:NO_2^--N=3:1
R5&R6	NO_3^--N:NO_2^--N=1:1
R7&R8	Only O_2

3.2.2 DPAO Enrichment I: Start-up with different SRTs and different NO_3^--N/NO_2^--N ratios

SRT is an important factor influencing the growth and activity of microbial groups, while the P removal was not successful in the preliminary experiments with the SRT of 20 days which was relatively long in the SRT range based on the previous studies. Hence, shorter SRT (15 days and 10 days) was utilised from this section. In this DPAO enrichment process, the effects of SRT and NO_3^--N/NO_2^--N ratio on the enrichment performance would be investigated. From day 0 to day 19, a 15-day SRT was kept in the stage 1, and then it was changed to 10 days from day 19 to day 194 (stage 2 &3), to explore the efficiency of DPAO enrichment with the different growth rate of microbial culture caused by different sludge age. In the general operation, after the 2-h anaerobic phase, electron acceptor was dosed into the A_2 SBRs in the first 45 min of anoxic phase, while the air pump was turned on to achieve aerobic phase of A/O SBRs.

Overall, the operational strategy and parameters during Enrichment I process is shown in Table 3.4. The ratio of COD to PO_4^{3-}-P was based on the appropriate range obtained from the literature review. However, due to the decrease of SRT from Stage 2, the initial concentrations of COD and PO_4^{3-}-P were increased to maintain enough biomass in the SBRs. In case of NO_x^--N, the initial concentration was 20 mg L^{-1} to avoid nitrogen accumulation as preliminary experiments, while the value was increased to 30 mg L^{-1} in Stage 3 due to the increasing nitrogen requirement after SRT reduction. The proportion of NO_2^--N in electron acceptor was lower than preliminary experiments, to avoid toxic inhibition.

Table 3. 4 Important initial parameters in the Enrichment I

	Reactors	COD (mg L^{-1})	P (mg L^{-1})	Electron acceptor	SRT (Day)
Stage 1 (Day 0 - Day 19)	E1 & E2	150	6	20 mg NO_3^--N L^{-1}	15
	E3 & E4	150	6	17.5 mg NO_3^--N L^{-1} and 2.5 mg NO_2^--N L^{-1}	15
	E5 & E6	150	6	15 mg NO_3^--N L^{-1} and 5.0 mg NO_2^--N L^{-1}	15
	E7 & E8	150	6	O_2	15
Stage 2 (Day 20 - Day 37)	E1 & E2	250	12	20 mg NO_3^--N L^{-1}	10
	E3 & E4	250	12	17.5 mg NO_3^--N L^{-1} and 2.5 mg NO_2^--N L^{-1}	10
	E5 & E6	250	12	15 mg NO_3^--N L^{-1} and 5.0 mg NO_2^--N L^{-1}	10
	E7 & E8	250	12	O_2	10
Stage 3	E1 & E2	250	12	30 mg NO_3^--N L^{-1}	10

(Day 38 - Day 216)	E3 & E4	250	12	26.3 mg NO_3^--N L^{-1} and 3.7 mg NO_2^--N L^{-1}	10
	E5 & E6	250	12	22.5 mg NO_3^--N L^{-1} and 7.5 mg NO_2^--N L^{-1}	10
	E7 & E8	250	12	O_2	10

Cycle studies were conducted before and after the stable performance was achieved, separately on Day 18 (Stage 1), Day 35 (Stage 2) and Day 124 (Stage 3). For the cycle studies in Stage 1 & 2, the concentrations of HAc, PO_4^{3-}-P and NO_x^--N at the beginning of anaerobic phase, the end of anaerobic phase and the end of the cycle in E1-E8 were analysed to investigate the concentration change in the SBRs and compare the difference between A_2 and A/O SBRs. For the cycle study of the stable operation in Stage 3, the concentrations of HAc, PO_4^{3-}-P and NO_x^--N in E3 & E4 were analysed every 30 minutes from the beginning to the end of the cycle, in order to investigate the P uptake and N consumption performance in anoxic phase.

At the end of Enrichment I, two tests for P uptake potential with NO_2^--N as sole electron acceptor were conducted:

1. NO_2^--N based anoxic P uptake without pH adjustment:
   40 mg NO_2^--N L^{-1} was continuously added into E3 & E4 during the 5-h anoxic phase on Day 120 without pH control.
2. Comparison of NO_2^--N and NO_3^--N based anoxic P uptake
   40 mg L^{-1} of NO_2^--N and NO_3^--N were continuously added into E3 during the 5-h anoxic phase on Day 125 & 127, with anoxic pH of <8.0.

3.2.3 DPAO Enrichment II: Start-up with different electron acceptor via long-period dosing

Based on the literature review and the experiments in section 3.2.2, NO_2^--N can be used as electron acceptor with controlled dosing strength or appropriate dosing strategy to avoid inhibition. This DPAO enrichment process investigated the effects of different electron acceptors and their impacts of long-period dosing on A_2 enrichment performance of the SBRs (NO_3^--N for EE1&EE2 and EE7&EE8; NO_2^--N for EE3-EE6).

The inoculum for EE1-EE4 was from the acclimated sludge of E1 & E2 in Enrichment I (acclimated inoculum), while the inoculum for EE5-EE8 was new RAS from 4-stage Bardenpho process of Millbrook WWTWs (as shown in Table 3.5). The concentration of

NO_3^--N applied in anoxic phase was 27-30 mg L^{-1}, closed to the value in Enrichment I, while the concentration of NO_2^--N was 45-48 mg L^{-1}. In the general operation, concentrated NO_x^--N solution was constantly added into EE1-EE8 in the first 4 hours of anoxic phase (Fig. 3.2) to achieve continuous dosing of electron acceptor and avoid toxic inhibition caused by nitrite.

An analysis of anoxic concentration changes of PO_4^{3-}-P and NO_2^--N was conducted in EE3 on Day 13, to investigate P uptake and N consumption before the stable period of nitrite based SBRs.

Table 3. 5 Electron acceptors for EE1-EE8

Reactors	EE1&EE2	EE3&EE4	EE5&EE6	EE7&EE8
Electron acceptor	27-30 mg NO_3^--N L^{-1}	45-48 mg NO_2^--N L^{-1}	45-48 mg NO_2^--N L^{-1}	27-30 mg NO_3^--N L^{-1}
Inoculum	Acclimated	Acclimated	New RAS	New RAS

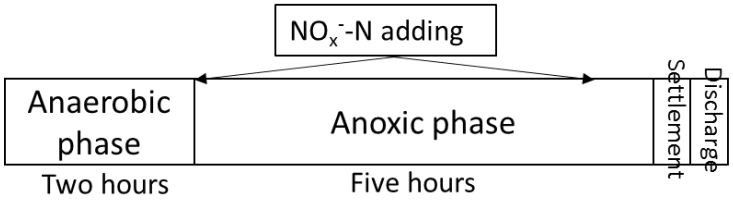

Fig. 3. 2 Cycle procedure of A_2 SBR operation

3.3 Experimental studies of the effects of NO_2^--N dosing strategies, temperature and pH on A_2 EBPR systems

3.3.1 The investigation of the effects of NO_2^--N dosing strategies on A_2 EBPR systems

This section was designed to investigate the effect of different dosing rate of NO_2^--N on A_2 EBPR systems, explore the most appropriate dosing rate of NO_2^--N to optimise the simulation of A_2N two-sludge system for P and N removal, and investigate the relationship of PO_4^{3-}-P uptake, NO_2^--N consumption and PO_4^{3-}-P concentration in the systems.

After the Enrichment II process, EE3-EE6 had achieved >95% phosphorus removal rate, and were run continuously for 50 days when different NO_2^--N dosing strategies were

tested in EE6 (renamed as D1) at ambient temperature (around 20 °C). For comparison, R5 (renamed as D2) was run as the same operation conditions as Enrichment II (except the pH changing period in 3.3.3), while single-pulse test was conducted in it. In addition, one test with 4-h dosing strategy was conducted in EE3, as the normal operation during Enrichment II, and one test with 5-h dosing strategy of E3 in Enrichment I was compared with the short duration strategies.

In the tests of different strategies, concentrated NO_2^--N solution was added into the SBRs with three dosing methods to achieve anoxic phase:

- Constant rate dosing during the first 5, 4, 3, 2 and 1 hours of anoxic phase:
  After the 2-h anaerobic phase, NO_2^--N solution was added into the reactor with constant flow rate during 5h, 4h, 3h, 2h and 1h of anoxic phase. The flow rates are shown in Table 3.6.

- Reducing dosing over the anoxic phase:
  T_a. After the 2-h anaerobic phase, 30 mL NO_2^--N solution with the concentration of 6 g L^{-1} was added into the reactor with controlled flow rates of 16, 16, 8, 8, 8 and 4 mL h^{-1} in the first six 30 minutes (3 hours) separately, to achieve 45 mg L^{-1} of NO_2^--N in the reactor.
  T_b. After the 2-h anaerobic phase, 32 mL NO_2^--N solution with the concentration of 6 g L^{-1} was added into the reactor with controlled flow rates of 16, 16, 16, 8, 4 and 4 mL h^{-1} in the first six 30 minutes (3 hours) separately, to achieve 48 mg L^{-1} of NO_2^--N in the reactor.

- Single pulse addition at the beginning of anoxic phase:
  After the 2-h anaerobic phase, 10 mL NO_2^--N solution with the concentration of 19.2 g L^{-1} was added into the reactor in a single pulse to achieve 48 mg L^{-1} of NO_2^--N in the reactor.

Among the tests, 5-h test was conducted in E3 after the Enrichment I (Day 159 in section 4.2). 4-h test, which was run as general operation of the reactors from Enrichment II, was conducted in EE3 after the enrichment (Day 64 in section 4.3) and before the temperature increase (in 3.3.2), as the performance of EE3, EE5 and EE6 was basically the same at that time. 3-h, 2-h and 1-h constant rate dosing tests and reducing tests were conducted in D1 on Day 15, Day 48, Day 49, Day 41 and Day 43 (in section 5.1). single-pulse test was conducted in D2 on Day 49 (in section 5.1). Fig.3.3 demonstrates the timeline of the processes of enrichments and their following periods when the P release, uptake and

removal efficiencies were basically stable. The performance of the SBRs for Enrichment I was stable when the 5-h dosing test was conducted in E3. Furthermore, the MLSS in the SBRs used for the dosing tests was normally kept between 1000 and 1300 mg L^{-1}. In other words, the performance of the dosing tests should not be affected by other factors.

Table 3. 6 Operation design of dosing strategies

Strategy	Test	Day	Reactor	Dosing concentration (mg L^{-1})	Dosing Volume (mL)	Solution concentration (g L^{-1})
Constant rate	5 hour	Enrichment I: 159	E3	45.0	50.0	3.6
	4 hour	Enrichment II: 64	EE3	47.5	48.0	4.0
	3 hour	Day 15	D1	51.6	34.4	6.0
	2 hour	Day 48	D1	48.0	22.9	8.4
	1 hour	Day 49	D1	48.0	11.5	16.7
Reducing rate	T_a	Day 41	D1	45.0	30.0	6.0
	T_b	Day 43	D1	48.0	32.0	6.0
Single-pulse		Day 49	D2	48.0	10.0	19.2

<table>
<tr><td colspan="2">Enrichment I and the following stable period</td><td></td><td rowspan="2"></td></tr>
<tr><td rowspan="2"></td><td>Enrichment II</td></tr>
<tr><td></td><td>Stable period after Enrichment II</td></tr>
<tr><td colspan="2">216 Days</td><td>75 Days</td><td>73 Days</td></tr>
</table>

Fig. 3. 3 Timeline of Enrichment I&II and the periods after the enrichment processes

3.3.2 The investigation of the effects of temperature on nitrite-based A_2 EBPR systems

Since temperature was an important factor influencing the performance of EBPR process and the competition of the microbial communities, the effects of different temperature levels on nitrate and nitrite based EBPR systems were investigated. Due to the decrease of P removal performance of E1-E2 in enrichment I when temperature was increased from around 20 ˚C to up to 30 ˚C, the operation of the SBRs was conducted with the temperature levels of 20 ˚C and 30 ˚C. Overall, from the start-up Enrichment II, EE1-EE4 (renamed as T1-T4) were continued to be operated at ambient temperature (around 20 °C) for 75 days, and then increased to 30 °C for 51 days. The other conditions and parameters were the same as Enrichment II.

3.3.3 The investigation of the effects of pH on NO_2^--N based A_2 EBPR systems

Since pH is also an important factor influencing the toxicity of nitrogen and the performance of anoxic P uptake, the effects of different pH levels on nitrite-based EBPR process were investigated in this section. The studies included a cycle test without pH control, compared with a cycle test with pH control, and the long-term operation of DPAO systems at low pH level.

3.3.3.1 Uncontrolled pH test

PO_4^{3-}-P and NO_2^--N concentration changes in the whole cycle with and without pH control were investigated in the later period of Enrichment I. The tests were conducted with the same initial pH level (around 6.9) at the beginning of anaerobic phase and with 5-hour constant-rate dosing of NO_2^--N, while one of the test was operated without any pH control in anoxic phase and the other test was operated with the pH of <8.0.

3.3.3.2 Lower pH operation

In this section, R5 (H1) was continuously operated at ambient temperature (around 20 °C) at different pH levels, while R6 (H2) was run for comparison after Enrichment II. The operation of H1 consisted of three stages.

Stage 1 (Day 0 ~ Day 27): pH of H1 in anaerobic phase was controlled at 6.8~7.5 by the HAc content in the influent. In anoxic phase the pH was kept at 7.5~8.0 with concentrated HCl.

Stage 2 (Day 28 ~ Day 42): pH of H1 in anaerobic phase was controlled at 6.5~7.0 by the HAc content in the influent. In the anoxic phase, the pH was kept at 7.0~7.5 with concentrated HCl.

Stage 3 (Day 43 ~ Day 92): pH was controlled as same as Stage 1.

In comparison, the pH of H2 was kept 6.8-7.5 in anaerobic phase, and 7.5-8.0 in anoxic phase, without any changes during the three stages.

3.4 Analytical methods

3.4.1 Nitrite, nitrate and phosphate

Important anions in liquid samples (i.e., NO_2^-, NO_3^- and PO_4^{3-}) were measured via ion chromatographic (IC) determination method, by a set of Metrohm IC 882 analyser with Metrosep A sup 5-150/4.0 column. All samples were diluted by Mobile phase (MP) to obtain the concentrations that were lower than the maximums of the standards, and then filtered by membrane with 0.45-μm pore size.

Within the auto-sampler, samples and standards were injected by a peristaltic pump, into a sample loop. MP (a buffered aqueous solution consisted with Na_2CO_3 and $NaHCO_3$) carried the samples from the loop onto the column that contained some form of stationary phase material, and the sample ions were then attracted to the charged stationary phase of the column. The charged eluent eluted the retained ions which then went through the conductivity detector and were depicted as peaks on a chromatogram. Finally, the graphs were demonstrated into the software.

The standards of NO_2^--N and NO_3^--N used in IC were respectively prepared from $NaNO_2$ and $NaNO_3$ (concentrations: 5 mg L^{-1}, 10 mg L^{-1} and 15 mg L^{-1}), while standards of PO_4^{3-}-P were prepared from KH_2PO_4 (concentrations: 10 mg L^{-1}, 20 mg L^{-1} and 30 mg L^{-1}) and MP was used for blank samples. The standards of NO_2^-, NO_3^- and PO_4^{3-} were calculated to NO_2^--N, NO_3^--N and PO_4^{3-}-P, and then used for standard curve.

The relationship between peak area and concentration is linear. Calibration curve of peak area against the NO_2^--N, NO_3^--N and PO_4^{3-}-P contents in mg L^{-1} of the calibration solutions (including blanks and standards) was constructed using linear regression analysis. The concentrations in samples were calculated by the determined slope and intercept of the calibration curve in Excel (Equation (3-1)).

$$C = \frac{(PA - i) \times DF}{s} \quad (3\text{- }1)$$

Where

C is the concentration of NO_2^--N, NO_3^--N or PO_4^{3-}-P (mg L^{-1});

PA is the peak area of the samples;

i is the intercept of the calibration graph;

DF is the dilution factor; and

s is the slope of the calibration graph (1 L mg^{-1}).

3.4.2 Acetic acid

Acetic acid was analysed by Gas chromatographic (GC) determination method. Samples were prepared by analysis by centrifugation at 13,500 rpm (micro-centrifuge, various manufacturers) for 15 minutes. The supernatants diluted with formic acid composition was adjusted to 10 % vol. The diluted sample was centrifuged 15 minutes at 13,500 to obtain a clearer supernatant. The supernatants after acidification and centrifugation was transferred into the vials and loaded onto the GC auto-sampler ready for the VFA measurement.

A standard solution containing acetic, propionic, iso-butyric, n-butyric, iso-valeric, valeric, hexanoic and heptanoic acids, at three dilutions to give individual acid concentrations of 50, 250 and 500 mg l^{-1} respectively, was used for calibration and also loaded onto the GC.

Quantification of the acetic acid was by a Shimazdu GC-2010 gas chromatograph (Shimadzu, Milton Keynes, UK), using a flame ionization detector and a capillary column type SGE BP-21. The carrier gas was helium at a flow of 190.8 ml min^{-1} and a split ratio of 100 to give a flow rate of 1.86 ml min^{-1} in the column and a 3.0 ml min^{-1} purge. The GC oven temperature was programmed to increase from 60 to 210 ^{0}C in 15 minutes with a final hold time of 3 minutes. The temperatures of injector and detector were 200 and 250 ^{0}C, respectively.

The relationship between peak area and concentration is linear. Calibration curve of peak area against the acetic acid content in mg L^{-1} of the calibration solutions (including blanks and standards) was constructed using linear regression analysis. The concentrations in

samples were calculated by the determined slope and intercept of the calibration curve in Excel (Equation (3-2)).

$$C = \frac{(PA-i)\times DF}{s} \quad (3\text{-}2)$$

Where

C is the concentration of acetic acid (mg L^{-1});

PA is the peak area of the samples;

i is the intercept of the calibration graph;

DF is the dilution factor; and

s is the slope of the calibration graph (1 L mg^{-1}).

3.4.3 Ammonia

Ammonia in liquid samples was analysed by spectrophotometric method (Ceceil 3000 series, UK). Samples were prepared by analysis by centrifugation at 13,500 rpm (micro-centrifuge, various manufacturers) for 15 minutes. The supernatants were put into glass tubes and diluted with deionised water to 8 mL. An NH_4Cl stock solution was diluted to give ammonium concentrations of 0.5, 1.0, 1.5 and 2.0 mg L^{-1}, and pipetted 8 mL of the standard solutions into glass tubes. Salicylate reagent and sodium dichloroisocyanurate reagent were added into the samples, standard solutions and an 8-mL blank sample, and mixed well, prior to colour development for at least 1 hour.

The absorbance of the solutions was measured at 655 nm in a cuvette with 10 mm path length. The relationship between absorbance and concentration is linear. Calibration curve of absorbance against the ammonia content in mg N L^{-1} of the calibration solutions (including blanks and standards) was constructed using linear regression analysis. The ammonia concentrations in samples were calculated by the determined slope and intercept of the calibration curve in Excel (Equation (3-3)).

$$C_N = \frac{(A-i)\times DF}{s} \quad (3\text{-}3)$$

Where

C_N is the concentration of NH_4^+-N (mg N L^{-1});

A is the absorbance of the samples;

i is the intercept of the calibration graph;

DF is the dilution factor; and

s is the slope of the calibration graph (1 L mg^{-1}).

3.4.4 pH and DO

pH and DO were measured using a IP67 COMBO water quality meter (AZ Instrument Corp., China). pH was calibrated in buffers at pH 4, 7 and 9.2. The pH meter was temperature compensated and had a sensitivity of ± 0.01 pH unit and accuracy of 0.01 ± 0.005 pH units. Buffer solution used for calibration was prepared from buffer tablets (Fisher Scientific, UK). DO probe was calibrated by saturation calibration before the measurements. During measurements, either of the probes was immerged in the mixed sludge of the reactors to determine the real-time values. In addition, the probes were rinsed with deionised water between measurements to avoid cross-contamination.

3.4.5 Solid contents

Mixed liquor suspended solid (MLSS) and mixed liquor volatile suspended solid (MLVSS) of the EBPR sludge were determined by weight method (APHA, 2005). 47-mm glass fibre filter papers (with aluminium foil plates) were placed in the muffle furnace at 550 °C for 30 minutes to burn off any organic residues, prior to cool the filter papers in the desiccator and then weighed (W_0) using a balance with accuracy of at least 0.1 mg. To do the filtration, a certain amount (V) of mixed sludge was sucked through the filter paper by vacuum pump. After filtration, filter papers were placed in the oven at 105 °C for 2 hours, and then they were weighed (W_1) again. The MLSS was calculated by Equation (3-4).

$$MLSS = \frac{W_1 - W_0}{V} \qquad (3\text{-}4)$$

After recording W_1, the filter papers were placed in the muffle furnace for 2 hours at 550 °C, and then cooled in the desiccator. Finally, the papers with ash residue were weighed (W_2) and recorded to calculate MLVSS by Equation (3-5).

$$MLVSS = \frac{W_1 - W_2}{V} \qquad (3\text{-}5)$$

The volatile ratio (R_V) and ash ratio (R_A) of the solid contents were calculated by Equation (3-6) and (3-7).

$$R_V = \frac{MLVSS}{MLSS} \times 100\% \quad (3\text{-}6)$$

$$R_A = \frac{MLSS - MLVSS}{MLSS} \times 100\% \quad (3\text{-}7)$$

3.4.6 polyP

PolyP in DPAOs was released by thermal method and measured by spectrophotometric method Mixed activated sludge were put in 10-mL test tubes. The tubes containing 6-mL sludge samples were incubated at 70°C by using temperature-controlled water baths to release polyP. After 60 min, the heated samples were centrifuged for 15 min at 8000 g. The supernatants were placed to new tubes and mixed with hydrochloride acid to achieve the concentration of 1M HCl, before heating them at 100°C for 7 min for the acid hydrolysis of polyP to PO_4^{3-}-P (Kuroda *et al*., 2002). After the heat treatment, the solution was centrifuged at 13,500 rpm for 15 min and a certain amount of supernatant was transferred to a glass tube and diluted to 10 mL to ensure the resulting phosphate concentration was within the calibration range. This centrifugation and following supernatant dilution process were also applied to original mixed activated sludge sample to eliminate the effect of free phosphate on polyP determination.

A KH_2PO_4 stock solution was diluted to give P concentrations of 0.25, 0.5, 0.75 and 1.00 mg L^{-1}, and pipetted 10 mL of the standard solutions into glass tubes. Acidic colour reagents containing ammonium molybdate, potassium antimonyl tartrate and ascorbic acid were added into the samples, standard solutions and a 10-mL blank sample (for free PO_4^{3-}-P determination, the above process was not needed), and mixed well, prior to colour development for 10 minutes.

The absorbance of the solutions was measured at 880 nm in a cuvette with 10 mm path length. The relationship between absorbance and concentration is linear. Calibration curve of absorbance against the phosphate content in mg P L^{-1} of the calibration solutions (including blanks and standards) was constructed using linear regression analysis. The phosphorus concentrations in samples were calculated by the determined slope and intercept of the calibration curve in Excel (Equation (3-8)).

$$C_P = \frac{(A - i) \times DF}{s} \quad (3\text{-}8)$$

where

C_P is the concentration of PO_4^{3-}-P (mg P L^{-1});

A is the absorbance of the samples;

i is the intercept of the calibration graph;

DF is the dilution factor; and

s is the slope of the calibration graph (1 L mg^{-1}).

The polyP content was calculated by Equation (3-9).

$$C_{polyP} = C_1 - C_0 \qquad (3\text{-}9)$$

where

C_1 is the concentration of treated samples (total phosphorus, mg P L^{-1});

C_0 is the concentration of untreated samples (soluble phosphorus, mg P L^{-1}).

3.4.7 PHA

PHA was quantified according to the method described by Furrer *et al*. (2007), with transesterification and analysed by GC. Fresh samples were taken and placed into centrifuged tubes, and 5 drops of formaldehyde were added to stop all biological activities. These samples were subsequently washed with KP-buffer solution and then centrifuged at 13000 g for 5 min, and the remaining pellets were freeze-dried and stored at -20 °C until analysis. Ethyl (R)-3-hydroxybutyrate was used as a standard in the analysis and treated alongside with the samples. An accurately weight 20 mg of freeze-dried cell mass was placed in a PTFE-lined screw-cap test tube. Methylene chloride (DCM) which resulted in freeze-dried cell mass concentration of 3-4 mg mL^{-1} was added into the samples and completely sealed the tubes to prevent DCM evaporation. The resulting suspension was sonicated for ca. 30 min until the suspension was completely homogenised. 1 mL of this suspension was added 0.85 mL of propanol containing ca. 0.5 mg of benzoic acid per mL as an internal standard and 0.15 mL of concentrated HCl. The closed tubes were vortexed and then heated for 2 h at 100 °C in the heating block. During this period, tubes were shaken every 15 min to allow good contact between biomass and products. After cooling down to room temperature rapidly, organic phase was extracted with 1 mL deionised water by shaking vigorously to remove the cell debris. The organic phase was separated

from the water phase by simple vigorous shaking of tubes or by applying vortex or by centrifugation. The two liquids were allowed to separate, during which cell debris gathered at the interface. Finally, 10 to 100 mg of Na_2CO_3 powder was added into the vail of organic phase, followed by shaking for 1 min to neutralise remaining acid or dry the water, and then DCM phase with Na_2CO_3 was filtered through 0.45 µm membrane filter for GC analysis.

Varian CP-3800 with flame ionisation detector (FID) with Aglient DB-FFAP 0.53 mm capillary column with 0.25 µm of thickness and 30 m length was used in the determination. Split inject with ratio of 100:1, injector temperature was 250 °C and detector temperature was 300 °C. Carrier gas was helium with a flow rate of 1.5 mL min^{-1}. Oven temperature had the following profile: initially at 80 °C and temperature was raised with a rate of 10 °C min^{-1} to 250 °C and held for 3 munutes. The injection volume was 1 µL (Tao et al., 2016).

3.4.8 Glycogen

Mixed sludge samples were mixed with hydrochloride acid to a final concentration of 0.6 M HCl. The mixed samples were placed in waterbath at 100 °C for 1 h for the hydrolysis of glycogen to glucose (Smolders *et al*., 1994a). After cooling and centrifugation, the glucose concentration of the supernatant was measured with spectrophotometric machine.

A glucose stock solution prepared from dried anhydrous glucose was diluted to give glucose concentrations of 40, 80, 120 and 160 mg L^{-1}, and pipetted 1 mL of the standard solutions into glass tubes. 1 mL of 5% w/w phenol and 5 mL concentrated sulphuric acid were added into the samples, standard solutions and a 1-mL blank sample, and mixed well, prior to colour development for 30 minutes at 25-30 °C (Dubois *et al*., 1956; Myklestad *et al*., 1997).

The absorbance of the solutions was measured at 485 nm in a cuvette with 10 mm path length. The relationship between absorbance and concentration is linear. Calibration curve of absorbance against the glucose content in mg L^{-1} of the calibration solutions (including blanks and standards) was constructed using linear regression analysis. The glucose concentrations in samples were calculated by the determined slope and intercept of the calibration curve in Excel (Equation (3-10)).

$$C_{glucose} = \frac{(A-i)\times DF}{s} \qquad (3\text{-}10)$$

Where

$C_{glucose}$ is the concentration of glucose (mg L^{-1});

A is the absorbance of the samples;

i is the intercept of the calibration graph;

DF is the dilution factor; and

s is the slope of the calibration graph (1 L mg^{-1}).

3.4.9 DNA analysis

Samples were thawed at 4 °C overnight then at room temperature to fully defrost. Tubes were centrifuged at 5000rpm for 10mins, the supernatant was removed, and lysis buffer (approximately 5mL) was added to the pellet. This was incubated in a shaking incubator for 1 hour at 37 °C. Samples were shaken to homogenise, and then 200 µL was removed and processed following the Qiagen DNA mini kit protocol (Qiagen, UK).

Data was imported into the platform of Qiime2 workflow system, and primers were trimmed from the sequences with Cutadapt. Following this, read pairs were joined with Vsearch before being quality filtered with the Qiime2 quality-filter tool. Deblur was then used to denoise the data, which was followed by chimera checking again with Vsearch. A classifier trained on the Silva database was provided to the classify sklearn feature classifier, which was responsible for making taxonomic assignments (Martin *et al*., 2011; Pedregosa *et al*., 2011; Bokulich *et al*., 2013; Mandal *et al*., 2015; Callahan *et al*., 2016; Rognes *et al*., 2016; Bokulich *et al*., 2018).

3.5 Calculation methods

3.5.1 P removal efficiency

P removal efficiency was one of the most important parameters, which directly demonstrated the P removal capacity of EBPR systems. The calculation of P removal rate was based on the P concentrations at cycle beginning and cycle end, as Equation (3-11):

$$r_E = \frac{C_B - C_E}{C_B} \times 100\% \qquad (3\text{-}11)$$

where

r_E is the P removal efficiency;

C_B is the P concentration at cycle beginning (mg P L^{-1}); and

C_E is the P concentration in the effluent (mg P L^{-1}).

3.5.2 P release and P uptake

Anaerobic P release (ΔP_I) and anoxic or aerobic P uptake (ΔP_D) were directly calculated by the P concentration change in different conditions in mg L^{-1}, as Equation (3-12) and (3-13). Anaerobic P release and anoxic uptake rate (r) were calculated by the ratio of P change to time (mg L^{-1} h^{-1}), as Equation (3-14) and (3-15).

$$\Delta P_I = C_A - C_B \quad (3\text{-}12)$$

$$\Delta P_D = C_A - C_E \quad (3\text{-}13)$$

$$r_{release} = \frac{\Delta P_I}{t_{an}} \quad (3\text{-}14)$$

$$r_{uptake} = \frac{\Delta P_D}{t_a} \quad (3\text{-}15)$$

where

C_A is the P concentration at the end of anaerobic phase;

t_{an} is anaerobic duration; and

t_a is anoxic or aerobic duration.

Furthermore, the specific P release and uptake with regard to MLVSS (mg g^{-1}) can be calculated as Equation (3-16) and (3-17). Hence, hourly specific P release and uptake rates (mg g^{-1} h^{-1}) could also be calculated as Equation (3-18) and (3-19).

$$\Delta P_I' = \frac{\Delta P_I}{MLVSS} \quad (3\text{-}16)$$

$$\Delta P_D' = \frac{\Delta P_D}{MLVSS} \quad (3\text{-}17)$$

$$r_{release}' = \frac{\Delta P_I'}{t_{an}} \quad (3\text{-}18)$$

$$r_{uptake}' = \frac{\Delta P_D'}{t_a} \quad (3\text{-}19)$$

The ratio of P release to acetate consumption in anaerobic phase and P uptake to NO_x^--N consumption in anoxic phase was calculated as $\Delta P_I/\Delta A$ and $\Delta P_D/\Delta N$ in mmol $mmol^{-1}$, where acetate amount was conversed as carbon content.

In addition, with the consumption of NO_x^--N in anoxic phase, the amount of transferred electron was calculated in mmol L^{-1}, as Equation (3-20) and (3-21),

$$e_{NO_3^-} = \frac{5 \times \Delta NO_3^- - N}{14} \quad (3\text{-}20)$$

$$e_{NO_2^-} = \frac{3 \times \Delta NO_2^- - N}{14} \quad (3\text{-}21)$$

where

$e_{NO_3^-}$ is the amount of transferred electron by nitrate consumption (mmol L^{-1});

$e_{NO_2^-}$ is the amount of transferred electron by nitrite consumption (mmol L^{-1});

$\Delta NO_3^- - N$ is the amount of consumed nitrate (mg L^{-1}); and

$\Delta NO_2^- - N$ is the amount of consumed nitrite (mg L^{-1}).

3.5.3 Ratio of P/HAc

The ratio of P/HAc (mg/mg) during anaerobic phase was calculated by Equation (3-22):

$$P/HAc = \frac{\Delta P_I}{\Delta HAc_P} \quad (3\text{-}22)$$

where

ΔHAc_P is the concentration of HAc utilised in phosphorus release (mg L^{-1}).

3.5.4 Ratio of PO_4^{3-}-P uptake to NO_x^--N consumption (P/N)

The overall P/N ratio (mg/mg) during the anoxic phase was calculated by Equation (3-23):

$$P/N = \frac{\Delta P_D}{N_A - N_E} \quad (3\text{-}23)$$

where

N_A is the NO_x^--N concentration added into the reactor during anoxic phase (mg L^{-1});

N_E is the NO_x^--N concentration at the end of anoxic (mg L^{-1}).

For the short-time P/N ratio (mg/mg) in anoxic phase of single-pulse and continuous dosing strategy tests, the below equations were separately utilised:

$$P/N = \frac{P_1 - P_0}{N_1 - N_0} \quad (3\text{-}24)$$

$$P/N = \frac{P_1 - P_0}{N_1 + N_a - N_0} \quad (3\text{-}25)$$

where

P_0 is the PO_4^{3-}-P concentration at the beginning of the time slot (mg L^{-1});

P_1 is the PO_4^{3-}-P concentration at the end of the time slot (mg L^{-1});

N_0 is the NO_2^--N concentration at the beginning of the time slot (mg L^{-1});

N_1 is the NO_2^--N concentration at the end of the time slot (mg L^{-1});

N_a is the NO_2^--N addition in the time slot (mg L^{-1}).

3.5.5 Ratio of electron transfer to PO_4^{3-}-P uptake (e^-/P)

The e^-/P ratio (mmol/mmol) during anoxic phase was calculated by Equation (3-26):

$$e^-/P = \frac{e_{NO_x^- - N}}{\Delta P_D/31} \qquad (3\text{-}26)$$

where

$e_{NO_x^- - N}$ is the electron transfer in anoxic phase (mmol L^{-1}), calculated by Equation (3-20) or (3-21).

3.6 Anova and Venn diagram analysis of microbial communities

One-way Anova analysis via SPSS was conducted to compare the microbial communities of the seeds and the SBRs after DPAO Enrichment I & II. The analysis was based on the number of genus level in each sludge samples, and the influencing factor was the condition of SBRs. The significance level was 0.05 in the analysis.

Venn diagram was applied for the comparison of the microbial communities in different samples, including the inoculum from 4-stage Bardenpho, acclimated sludge in EBPR systems, and the sludge after condition changes (temperature and pH).

3.7 Modelling and the simulation of two-sludge process

3.7.1 Model description

The model developed in this study was based on the measured data of experiments and calculation, with several assumptions: 1) accumulation of $NADH_2$ and ATP does not occur in EBPR biomass; 2) the required ATP for polyP synthesis (α_3) and the polymerisation

constant in biomass synthesis (κ) in anoxic phase equal to the figure in aerobic phase. Both of anaerobic and anoxic metabolisms were combined experimental measurement of PO_4^{3-}-P, NO_2^--N, HAc, polyP, PHB and glycogen, and the development of the models by Smolders *et al*. (1994a & 1994b) and Kuba *et al*. (1996).

In anaerobic phase, there are three essential reactions involved: 1) Organic substrate (acetic acid) uptake and PHB production; 2) PolyP degradation for ATP production; and 3) NADH production from TCA cycle and glycogen degradation.

In anoxic phase, five essential reactions are involved: 1) PHB catabolism; 2) oxidative phosphorylation; 3) biomass synthesis from PHB; 4) phosphate transport and polyP synthesis; and 5) glycogen production. Based on the theory by Smolder *et al*. (1994b) and Kuba *et al*. (1996a), the only difference between aerobic and nitrite-based anoxic metabolism is oxidative phosphorylation and phosphate transport with oxygen or nitrite.

Anaerobic and anoxic stoichiometric coefficients were obtained from the data of experimental results in the tests of NO_2^--N dosing strategies and the enrichment processes, or from the values selected in the previous studies. The kinetics of the reactions in anaerobic and anoxic conditions was determined based on the measured results of MLSS, HAc, PO_4^{3-}-P, and NO_2^--N concentrations in the NO_2^--N dosing strategy tests (2-h, 3-h and 4-h constant-rate dosing strategies). All the kinetics and stoichiometric coefficients and parameter values are shown in Appendix C.

3.7.2 Model calibration and sensitivity analysis

The model was firstly calibrated with the results of experiments:

a. The kinetics of 2-h dosing tests was calibrated with T_a and T_b, since all of them were conducted with sufficient NO_2^--N adding;
b. The kinetics of 3-h and 4-h dosing tests was calibrated with 5-h test, since all of them were conducted with non-sufficient NO_2^--N adding.

Sensitivity analysis was then conducted to assess whether the parameters significantly affected the output, namely the concentrations of HAc, PO_4^{3-}-P and NO_2^--N in the effluent. RSF is an important method which can be utilised for sensitivity analysis. The RSF of output *Y* (HAc, PO_4^{3-}-P and NO_2^--N concentrations) with respect to parameter *x* was calculated with Equation (3-27)

$$RSF_{x_0} = \left| \frac{Y_{x_1} - Y_{x_0}}{Y_{x_0}} \Big/ \frac{x_1 - x_0}{x_0} \right| \qquad (3\text{-}27)$$

where

RSF_{x_0} is the relative sensitivity factor of parameter x_0;

Y_{x_1}, Y_{x_0} are the output values with parameters x_1 and x_0;

$x_1 = (1 + 10\%) \times x_0$ in this study;

The parameters (x) used for sensitivity analysis included the main stoichiometric and kinetics coefficients, which were assessed to calibrate the model and then conduct the simulation.

3.7.3 Simulation of two-sludge systems

The simulation of A_2 SBR in two-sludge process was based on Excel, with the developed models including kinetics and stoichiometry of anaerobic and anoxic metabolisms of DPAOs.

Chapter 4 Enrichment of DPAOs under anaerobic/anoxic conditions

4.1 Preliminary experiments

In order to investigate the characteristics of the RAS collected from the 4-stage Bardenpho process and determine the appropriate conditions for A_2 EBPR systems, the preliminary experiments were conducted before the enrichment operations. Since the results of some pre-tests had proved that the RAS had P uptake capacity under A/O condition, the hypothesis of the preliminary experiments was the sludge of the 4-stage Bardenpho process had P removal potential at A_2 conditions, and could be used for rapid DPAO enrichment.

4.1.1 Performance of the SBRs in the preliminary experiments

The preliminary experiment was conducted for 137 days at ambient temperature (around 20 °C). Some operational parameters and N & P dosing strength were altered during the experiment in response to experimental observations, as shown in Table 3.1, in order to enhance phosphorus removal rate.

4.1.1.1 Overview of the preliminary experiments

The experiments totally included six stages. Before Stage 1, the pumping system had not been assembled completely, inducing the smaller feeding and discharge volume (around 1 L). Hence, it was not considered as a stage due to the incomplete system. From Stage 1 to Stage 3, the HRT was kept at 48 h. As Stage 1 suffered NO_x^--N accumulation caused by the incomplete consumption of electron acceptor, nitrogen addition was decreased from 40 to 20 mg L^{-1} in Stage 2 after washing out the excess NO_x^--N. However, the phosphorus removal performance was not enhanced with 20 mg N L^{-1} electron acceptor, while NO_x^--N could not be detected at the end of the cycles, suggesting 20 mg N L^{-1} was not enough for PO_4^{3-}-P uptake in the systems. After 17 days of Stage 2, NO_x^--N addition for Stage 3 was increased back from 20 to 40 mg L^{-1}, to prevent the shortage of electron acceptor in anoxic phase. However, the phosphorus removal efficiency in Stage 3 was not obviously enhanced, with similar anaerobic phosphorus release and anoxic phosphorus uptake amounts in the A_2 SBRs. Between Stage 3 and Stage 4, there was an unexpected period, when the DI water utilised for influent was used up, the influent solution could be only

made with tap water. From the start of Stage 4, the cycle duration was decreased to 8 h with the 16-h HRT, as 48-h HRT was not appropriate for practical wastewater treatment process. Meanwhile, the acetate and NO_x^--N loadings were lower than Stage 3 to avoid incomplete carbon and nitrogen consumption in the cycles, and HAc was mixed with NaAc (with CH_3COONa-CH_3COOH mole ratio of 3:1) in the influent to adjust the pH (6.8-7.0 at the beginning of cycles) at the same time. In Stage 5, HRT was extended to 24 h, with 40 mg L^{-1} NO_x^--N for the anoxic phase. Finally, HRT was shortened to 16 h, and all of acetate, P and N concentrations were decreased in Stage 6.

In summary, the operational parameters in the preliminary experiments is shown in Table 3.1. Between the stages, there were some operations for removing the excess NO_x^--N and adjusting the conditions of the reactors to keep the activities of the microbial groups for the conduction of the experiments in the following stages. Hence, the total duration of the preliminary experiments was longer the sum of stage durations.

During the 137-day SBR operation of the preliminary experiments, the results of pH, acetate concentration, PO_4^{3-}-P concentration and NO_x^--N concentrations were mainly monitored to demonstrate the performance of the SBRs. In addition, the ratios of anaerobic PO_4^{3-}-P release/HAc consumption, anoxic PO_4^{3-}-P uptake/ NO_x^--N consumption and e^- transfer/P uptake were calculated for the analysis of phosphorus removal level.

4.1.1.2 The adjustment of pH in preliminary experiments

As one of the most important operational parameters for the experiment, pH should be adjusted during the operation of the SBRs, in order to attain the most appropriate range to buffer the impact of the OH^- production from NO_x^--N consumption and PO_4^{3-}-P decrease. However, pH was not controlled strictly before Stage 4. As a result, the effluent pH during the period of preliminary experiments in all the A_2 reactors achieved a peak on day 32, due to the continuous increase of anoxic phosphorus uptake and nitrogen consumption in Stage 2 & 3, especially the increase of NO_x^--N dosing at the beginning of Stage 3. While due to the high NO_x^--N dosing in the anoxic phase of Stage 3, the nitrogen, which could not be consumed completely in the cycle with the 20-days SRT, caused the decrease of pH in the following days of Stage 3.

After Stage 3, because of the decrease of NO_x^--N consumption, effluent pH also reduced but it was still in a high range between 8.0 and 9.0. To decrease pH and keep it in a stable level, organic carbon source from Stage 4 was exchanged to the combination of sodium

acetate and acetic acid with a ratio of 3:1. Consequently, the effluent pH was controlled at around 7.5-8.0.

4.1.1.3 HAc uptake in anaerobic phase of preliminary experiments

Fig. 4.1 shows the HAc change in the cycles during the preliminary experiments. As can be seen in the graphs, compared with the concentration at the beginning of the cycle, the HAc concentration at the end of anaerobic phase decreased to different levels in different stages. The organic carbon content could not be removed completely with 250-300 mg L^{-1} acetate in the influent except in Stage 3, Stage 5 and Stage 6. The higher anaerobic acetate consumption in Stage 3 and 5 was not only caused by the HAc accumulation via DPAOs, but also by the consumption via denitrifiers, due to the higher level of NO_x^--N residual if the N addition for anoxic phase was 40 mg L^{-1}. In case of the other stages, since the NO_x^--N addition was 20 mg L^{-1}, inducing little N residual at the beginning of the cycles, the acetate consumption in anaerobic phase was not effective, which suggested that the microbial groups in the SBRs could not produce enough PHA for the P uptake in anoxic phase. In anoxic or aerobic phase, the acetate remained in the systems could be exhausted by the adding of NO_x^--N or the beginning of aeration. For Stage 6, as the influent acetate concentration was decreased, it could be completely consumed by the sludge systems during the anaerobic period.

As discussed above, the utilisation of HAc by PAOs was not sufficient during anaerobic phase in the stages of the preliminary experiments. The main reason was the existence of NO_x^--N at the beginning of the cycles. Fig. 4.2 shows the concentration of HAc consumed by NO_x^--N anaerobic phase (Equation (4-1) and (4-2)) in the SBRs during the preliminary experiments, which suggests that the majority of HAc consumption is caused by denitrification in this period. The concentration levels of NO_x^--N in the reactors were increased with high nitrogen dosing (40 mg L^{-1}) at the beginning of anoxic phase, which induced the higher HAc consumption. The concentration of HAc consumed by denitrification achieved two peaks in stage 3 and 5, for instance.

$$5CH_3COOH + 8NO_3^- \rightarrow 10CO_2 + 6H_2O + 4N_2 + 8OH^- \qquad (4\text{-}1)$$

$$3CH_3COOH + 8NO_2^- \rightarrow 6CO_2 + 6H_2O + 4N_2 + 8OH^- \qquad (4\text{-}2)$$

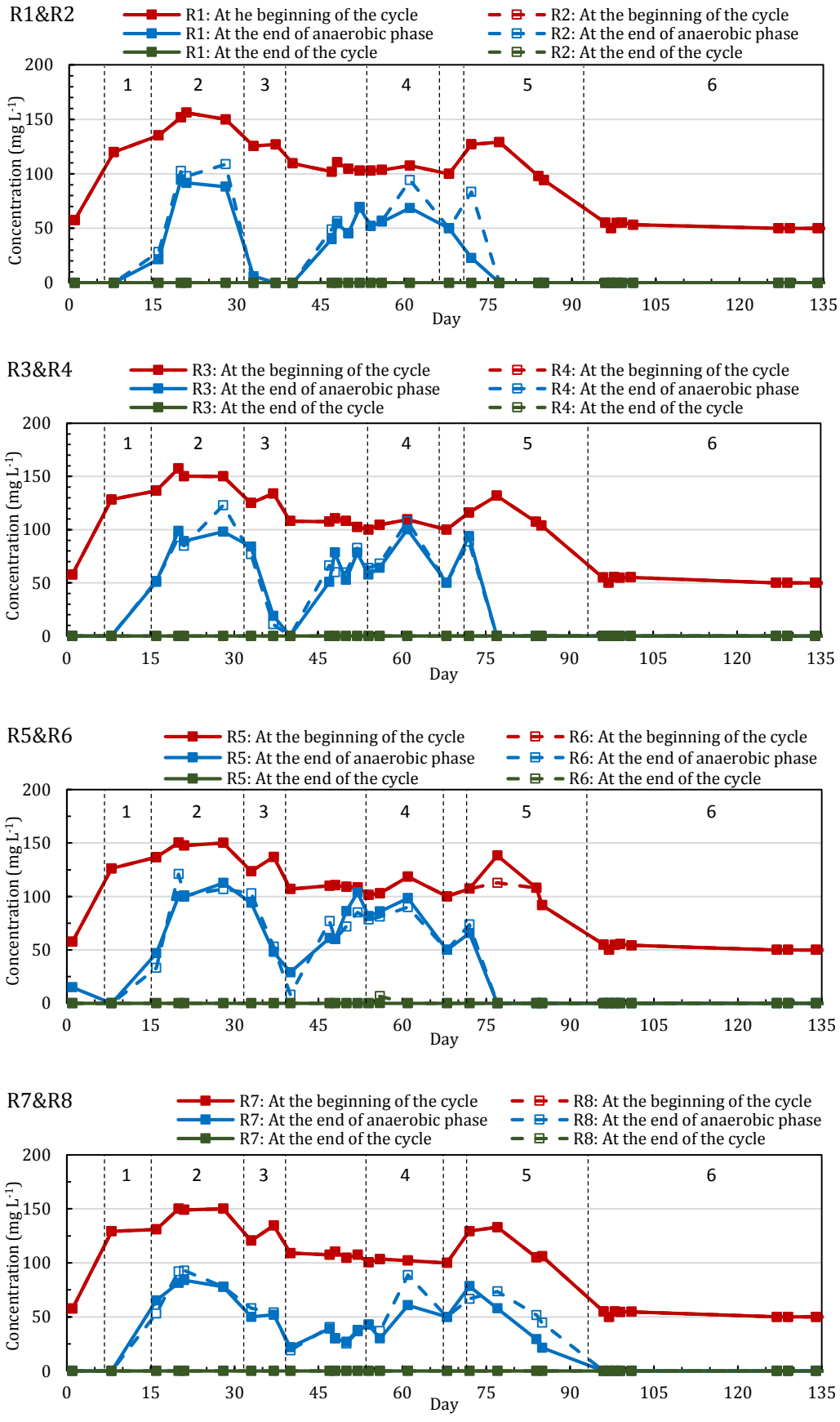

Fig. 4. 1 Acetate concentration change during the preliminary experiment (R1&R2: only NO_3^--N; R3&R4: NO_3^--N/NO_2^--N=3/1; R5&R6: NO_3^--N/NO_2^--N=1:1; R7&R8: only O_2)

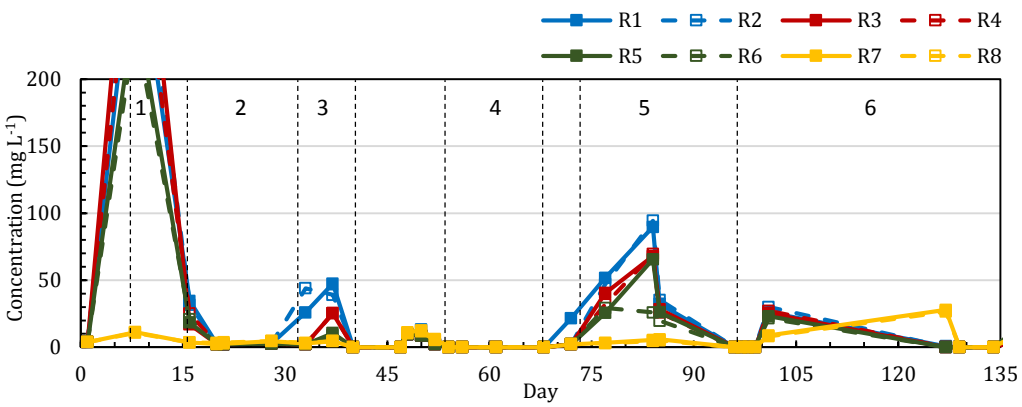

Fig. 4. 2 Acetate consumption by denitrification in anaerobic phase (R1&R2: only NO_3^--N; R3&R4: NO_3^--N/NO_2^--N=3/1; R5&R6: NO_3^--N/NO_2^--N=1:1; R7&R8: only O_2)

4.1.1.4 P release and uptake efficiencies in the preliminary experiments

PO_4^{3-}-P concentration was the most important parameter in the preliminary experiments, which could directly reflect the performance of the SBRs. Nonetheless, the overall phosphorus removal performance of the reactors was not successful during the preliminary experiment. As can be seen in Fig. 4.3, before reducing the cycle duration from 24 h to 8 h, most of the SBRs had obvious anaerobic P release in Stage 2&3, which was stopped after the influent was made with tap water inducing the P settlement between the period of Stage 3 and Stage 4. The A_2 SBRs that had the best P release and uptake trends were R1 and R2, where NO_3^--N was utilised as the sole electron acceptor in anoxic phase. The PO_4^{3-}-P concentration at the end of anaerobic phase in R1&R2 increased from only 14.4 and 15.4 mg L^{-1} to around 27.0 and 25.2 mg L^{-1} during the period of Stage 1, 2 and 3. The fastest increase occurred in Stage 3, when NO_3^--N adding was increased from 20 to 40 mg L^{-1}, suggesting the 20-mg N L^{-1} was not sufficient for A_2 systems with 24-h cycles. Compared with R1 & R2, the P release in other A_2 SBRs was lower, and the P release amount decreased with the ratio increase of NO_2^--N in electron acceptor. The main reason causing the results should be that there was not enough polyP produced in the DPAOs, especially in the sludge of R5&R6, as the amount of NO_2^--N added in anoxic phase was higher than the threshold value, and induced the toxic inhibition of P uptake.

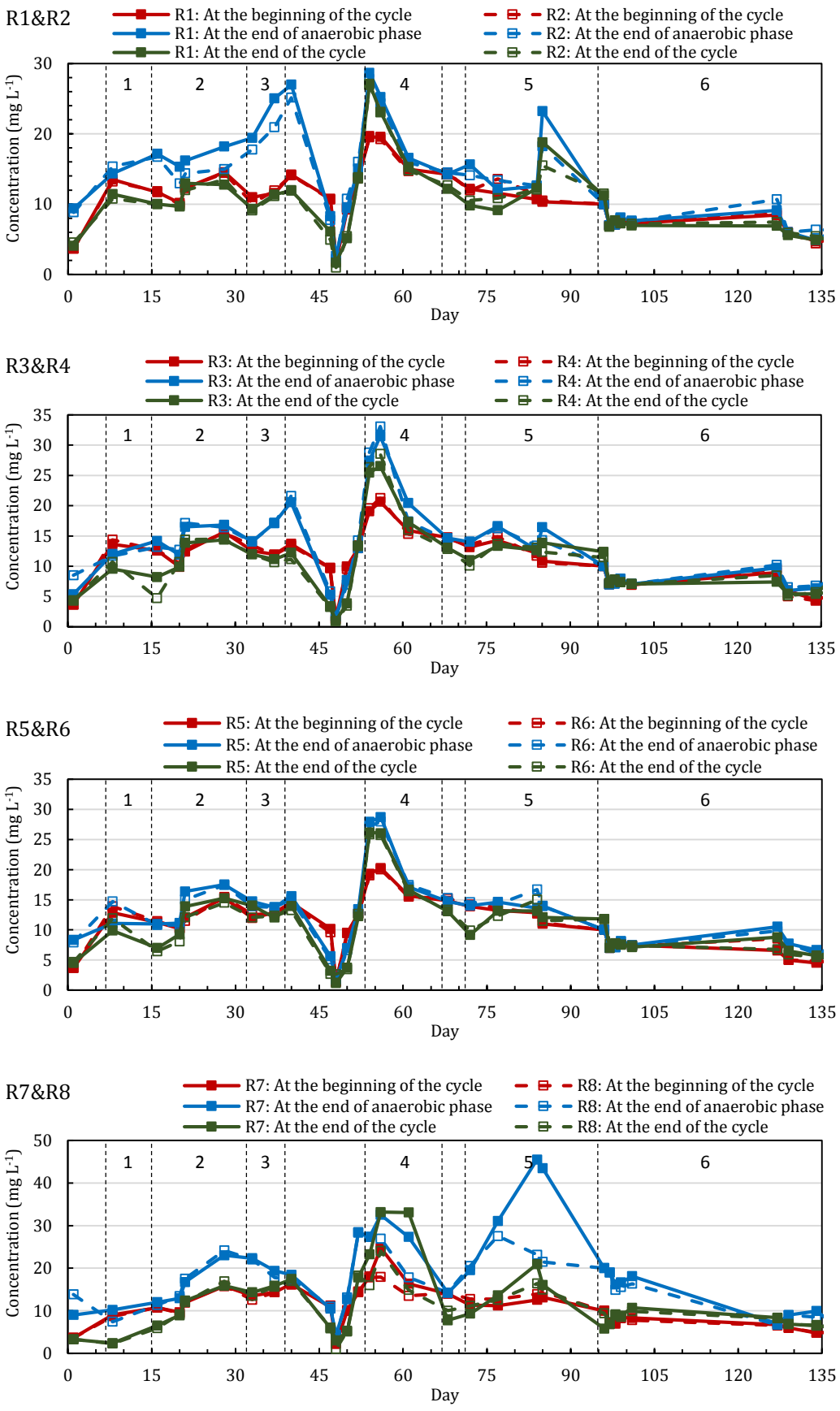

Fig. 4. 3 PO_4^{3-}-P concentration change in the stages of preliminary experiments (R1&R2: only NO_3^--N; R3&R4: NO_3^--N/NO_2^--N=3/1; R5&R6: NO_3^--N/NO_2^--N=1:1; R7&R8: only O_2)

As mentioned above, there was a period after Stage 3 when the influent was made with tap water (the HRT had been reduced to 16 h from this period), the phosphorus settlement with calcium caused that the detected values were not correct, making the drops in the graphs of all the reactors on Day 48. After the DI water system was recovered, Stage 4 was started with 8-h cycles. Since the high NO_x^--N residual in the effluent might affect the acetate utilisation in anaerobic phase, the N adding was decreased to 20 mg L^{-1}. However, the P release and uptake performance were not enhanced in Stage 4. The peaks of P release in A_2 SBRs on day 54 should be caused by the P accumulation before Stage 4 when N adding in anoxic phase was still 40 mg L^{-1}. With the development of Stage 4, the P release amount decreased sharply from the peak to relatively low level. The reason causing the consequence was suspected that the residual acetate at the end of anaerobic phase restrain the P uptake in anoxic phase, which induced the decrease of P accumulation in DPAOs and reduced the following P release and uptake. Thus, the cycle duration was prolonged to 12 h to provide enough anaerobic duration to consume acetate and anoxic duration to accumulate PO_4^{3-}-P in Stage 5. The P release in R1&2 had an obvious increase on Day 85, which was higher than the other A_2 SBRs. On the contrary, the P release in A/O SBRs was more efficient than all A_2 SBRs in this period. However, the P removal in anoxic or aerobic phase was not effective even the period had been prolonged to 7 hours.

Finally, the cycle duration was shortened back to 8 h in Stage 6. In addition, as it was considered that PO_4^{3-}-P after P release might be too high to remove with 20 mg N L^{-1} in anoxic phase, P and acetate concentrations in the influent were both decreased to avoid acetate residual after anaerobic phase and reduce the P concentration at the beginning of anoxic phase. However, the P release and uptake in all the A_2 SBRs were not enhanced, which were similar with the performance in Stage 4. There were small peaks of P release on Day 127, due to the new sludge inoculum, while the P removal performance in all the SBRs were not enhanced after the day.

As a result of the unstable P release and uptake in the preliminary experiments, P removal rates in all the SBRs were extremely fluctuated during the stages. Since in many cases the anaerobic P release was always higher than anoxic or aerobic P uptake, P removal rates were usually lower than zero. Although sometimes there was slight enhanced P uptake during the stages, the removal rate did never achieve 80% or higher.

Fig. 4.4 shows the change of P/HAc consumption ratio during the preliminary experiments. Mostly, the ratios in A_2 SBRs were relatively small, lower than 0.2, compared with the peaks in Stage 4. The ratios in most of the SBRs achieved a peak in Stage 4, mainly caused by the high amount of P release with the low acetate consumption in anaerobic phase of that period. The other higher values were found in A/O SBRs in Stage 5 and 6, because of more effective P release than A_2 SBRs. However, the low acetate loading was not sufficient for the operation of the SBRs, inducing the gradual decrease of the ratios.

In case of the performance of P uptake and N consumption in anoxic phase of A_2 SBRs, the ratios of P/N in the A_2 SBRs were below 2.6 (mostly lower than 0.5), while some peaks were found in Stage 3, as shown in Fig. 4.5. The maximums of R1&R2 on Day 37 were induced by the relatively high P uptake. In comparison, the ratios of R3&4 were much lower than R1&R2, while they were still higher than figures of R5&R6, due to the decrease of P uptake rate in anoxic phase. Additionally, the fluctuations of R2 and R6 in Stage 6 were produced by the unstable and slight changes of the P concentration in anoxic phase.

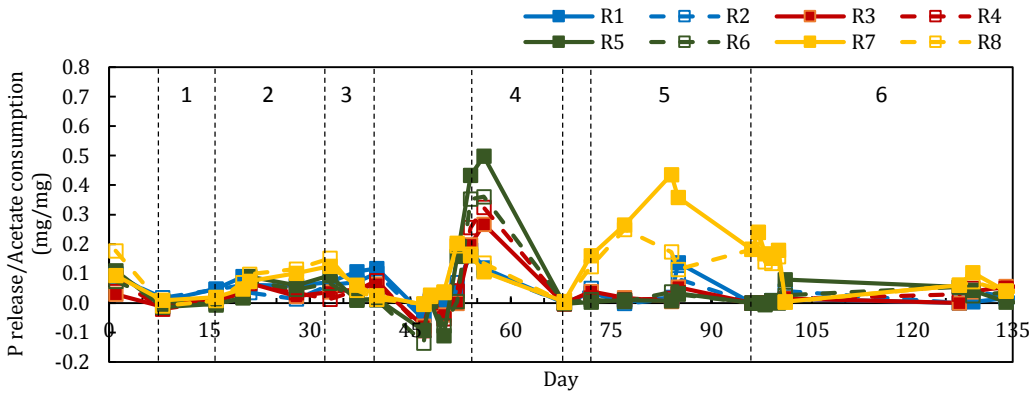

Fig. 4.4 Anaerobic PO_4^{3-}-P release/acetate consumption in the stages of preliminary experiments (R1&R2: only NO_3^--N; R3&R4: NO_3^--N/NO_2^--N=3/1; R5&R6: NO_3^--N/NO_2^--N=1:1; R7&R8: only O_2)

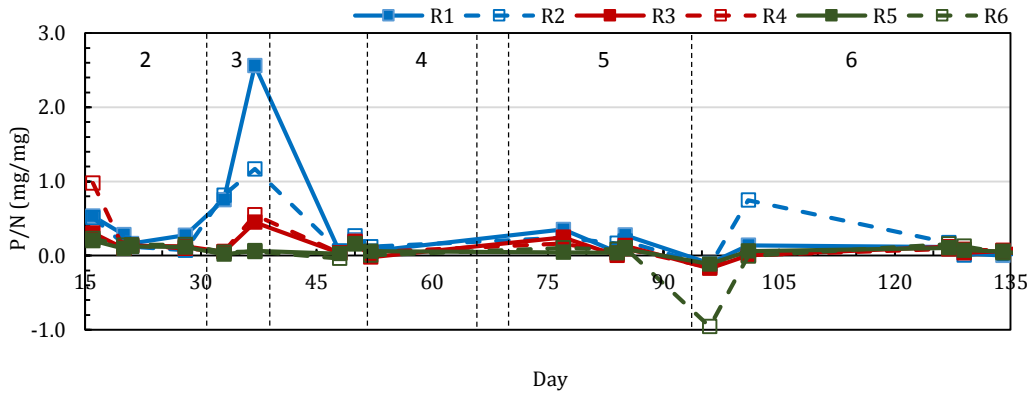

Fig. 4.5 Anoxic PO_4^{3-}-P uptake/NO_x^--N consumption in the A_2 SBRs of preliminary experiments (R1&R2: only NO_3^--N; R3&R4: NO_3^--N/NO_2^--N=3/1; R5&R6: NO_3^--N/NO_2^--N=1:1)

4.1.1.5 Hourly analysis of P release and uptake in Stage 4&5 of preliminary experiments

As discussed above, the P removal performance in both A_2 SBRs and A/O SBRs did not achieved an optimised condition during the period of preliminary experiments. In order to understand the change of P concentration in one cycle, hourly or half-hourly samples were analysed. Some points in Stage 4 and 5 were selected in this analysis, as shown in Fig. 4.6. In both of the results in Stage 4 and Stage 5, the hourly performance of P release and uptake had the similar trends, namely the little changes in A_2 SBRs and continuous change in A/O SBRs.

Fig. 4.6a and Fig. 4.6b demonstrate the examples about the PO_4^{3-}-P concentration changes in anaerobic phase and anoxic (aerobic) phase in Stage 4, separately. As can be seen in the graphs, both of the anaerobic P release and anoxic P uptake in A_2 SBRs were very slight, compared with the P release and uptake in the A/O SBR (R7). Fig. 4.6c demonstrates the hourly change of P concentration in Stage 5 of preliminary experiments, when the cycles of A_2 SBRs consist of a 2-h anaerobic phase and a 9-h anoxic phase (since the longer anoxic phase was designed to achieve better P uptake). On the contrary, the cycle of A/O SBRs consisted of a 3-h anaerobic phase and an 8-hour aerobic phase. As can be seen in the graph, the P release in the first hour of anaerobic phase had basically achieved the maximums in the A_2 SBRs, while there was not continuous increase of PO_4^{3-}-P concentration in the second hour. In contrast, the P release continued during the first 5 hours of the cycle of A/O reactors, even though aeration had been started from the 4th hour. The reason causing the difference should be that: 1) A_2 SBRs did not accumulate enough polyP in the sludge, so they could only release that amount of phosphate, while A/O SBRs had more effective P accumulation in the previous period, which could induce higher amount of P release; 2) as there was still acetate residual at the end of anaerobic phase, which was immediately consumed when NO_x^--N solution was added into the systems of A_2 SBRs, but the aeration of A/O SBRs could not instantly remove the acetate that induced the continuous P release until it was totally consumed by the PAOs and other aerobic bacteria.

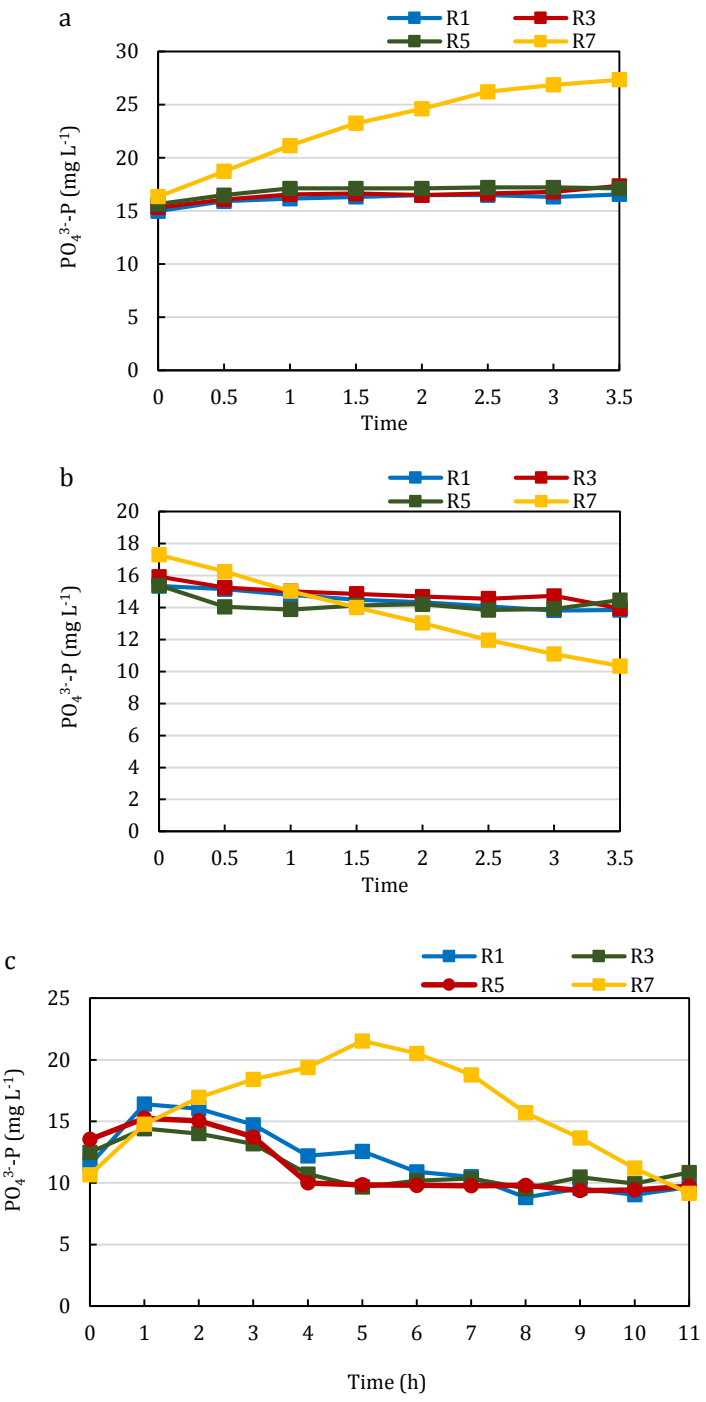

Fig. 4. 6 Hourly PO_4^{3-}-P changes of the SBRs in Stage 4 and Stage 5

As discussed above, the P removal performance of A_2 SBRs, including the anaerobic P release and anoxic P uptake, was mostly not effective in the preliminary experiments based on Fig. 4.6, with lower than 2.0 mg L^{-1} concentration increase and decrease of PO_4^{3-}-P in the 7-h cycle, and lower than 8.0 L^{-1} concentration increase and decrease of PO_4^{3-}-P in the 11-h cycle. However, in some stages the PO_4^{3-}-P concentration some changed more

efficiently with the ratio increase of NO_3^--N in electron acceptors, which suggested that the DPAOs enrichment with NO_3^- as the sole electron acceptor was more effective than with the existence of NO_2^-, which was different from the results of Dai *et al*. (2017b). The reason causing the results may be the amount of NO_2^--N added into the reactors was excess, inducing the toxic inhibition of P uptake, or the operational condition parameters (such as SRT) had not been adjusted to the optimised values, which did not provide the most appropriate environment for the growth and activities of DPAOs.

For A/O reactors, the DO concentration during aerobic phase is an important parameter to achieve stable and effective aerobic P uptake. In the operation of R7 and R8, the DO concentration fluctuated between 2.0 and 5.7 mg L^{-1} (except the period when the aeration tube of R7 was broken in Stage 4). Nittami *et al*. (2011) suggested that a DO concentration of 2.0 mg L^{-1} was appropriate to achieve effective P removal. To achieve a relatively stable DO environment for R7 & R8, the fluctuation would be controlled properly. Nonetheless, the P removal performance in the stages of R7&R8 was not effective, although they mostly had better P accumulation than A_2 SBRs. Thus, there must be some reasons causing the fails of the PAOs (DPAOs) enrichment and P removal in the preliminary experiments.

4.1.2 Discussion and summary

The results of preliminary experiments demonstrated that the PAOs (DPAOs) enrichment did not achieved due to the improper experimental conditions. Compared with phosphorus release and uptake by PAOs, the activities of denitrifiers were more positive in the A_2 systems, which indicated that PAOs were not be accumulated in this stage of reactor operation.

However, although the current results suggest that PAOs (DPAOs) have not dominate the microbial group in the reactors, the obvious P release and uptake in some stages prove the existence of PAOs (DPAOs) in the activated sludge. Hence, if the denitrifers can be successfully restrained by avoiding the simultaneous existence of organic carbon and NO_x^--N, PAOs (DPAOs) will be enriched gradually with these conditions. Additionally, as in the period of these stages, the C/P ratio was kept as 5.3/1 - 6.7/1, which was absolutely lower than normal wastewater substrate ratio for conventional activated sludge. Liu *et al*. (1997) believed that PAO could accumulated a high amount of polyphosphate with more effective acetate uptake, with a C/P ratio of 100/20 (namely 5/1). However, in most of research on EBPR process (Kuba *et al*., 1996b; Wang *et al*., 2009; Chuang *et al*., 2011), the

C/P ratio was normally around or higher than 10/1, which suggested that the phosphorus concentration in the feedstock was relatively high, compared with the COD level. Hence, the lower C/P ratio is not appropriate for the PAO enrichment process, and it should be adjusted in the next step of experiments. Additionally, it had been proved that P removal performance could not be changed or enhanced only by changing the amounts of organic carbon, PO_4^{3-}-P and NO_x^--N in the synthetic wastewater. Consequently, a higher C/P ratio should be utilised in the next experiment, while the optimised PO_4^{3-}-P/NO_x^--N ratio should be explored to achieve successful phosphorus uptake.

Since the removal of P from wastewater with EBPR process should be achieved via the discharge of excess sludge, sludge discharge rate which is determined by SRT, can affect the performance of EBPR process. As discussed above, SRT of 20 days was utilised in the experimental process with the 16-h and 48-h HRT. Compared with the SRT setting in other research, the 20-day SRT was selected as the longest one in the literature, which may not be appropriate for growth of bacteria in the stages. Hence, to enhance the growth of biomass and discharge enough PO_4^{3-}-P, shorter SRTs of 10-15 days should be employed in the following experiments.

A similar result suggesting that biomass growth was not properly during the experiment period, was that the increasing percentage of inorganic content in the activated sludge, based on the measurement and calculation, in which the MLVSS/MLSS ratio reduced from around 90% to around 60%, with the enrichment process after inoculation. The decrease of MLVSS/MLSS ration was discussed by Kuba *et al.* (1996b) and Brdjanovic *et al.* (1998), who believed that the enhanced inorganic content was the produced polyP in the bacteria cell. But the current phosphorus removal results cannot support the same deduction that polyP is produced properly in the biomass cells.

From the results of the preliminary experiments, several deductions can be summarised, which can be utilised in the next stage of experiments.

- One of the most important deductions was that the SRT of 20 days was not an appropriate solid age for the enrichment DPAOs in both A_2 and A/O SBRs in this experiment. Therefore, shorter SRT would be employed in next stage of enrichment, to explore an optimised value for the operation of the reactors.
- Secondly, the amount changes of substrates in synthetic wastewater (i.e. organic carbon and PO_4^{3-}-P) could not enhance the P removal performance of A_2 SBRs, if the SRT was not change in the operation.

- Thirdly, the amount of NO_x^--N added in the anoxic phase should be explored, combined with the initial concentration of PO_4^{3-}-P in the influent, to make sure the appropriate ratio of P uptake/N consumption.
- As NO_2^--N had not detected in the preliminary experiment, its potential in anoxic PO_4^{3-}-P uptake should be investigated, with its portion accounted in the total amount of NO_x^--N.
- The effluent pH of the SBRs was kept at 7.5-8.0 in the preliminary experiments, which could be maintained and utilised for the anoxic P uptake in the next experiments.

4.2 DPAO Enrichment I

From the results of preliminary experiments, RAS from 4-stage Bardenpho process was justified that it could be used for PAOs enrichment due to the phosphorus release and uptake performance in different phases, while the operational conditions should be modified due to the unsuccessful P removal in all the stages of preliminary experiments. Moreover, the parameters including pH, HRT, cycle duration and period of anaerobic and anoxic phases, were optimised in preliminary experiments, which could be utilised in the following experiments. Since 20-day SRT did not achieve successful P removal performance in preliminary experiments, the hypothesis in this section was that the enrichment of DPAOs could be more effective with shorter SRT. Furthermore, higher proportion of NO_2^--N in electron acceptor should be more appropriate for the enrichment process, based on the result of literature review.

In this sludge acclimation process, SRT was an important factor, which was adjusted to improve the DPAOs enrichment. The process of Enrichment I included three stages: The operational parameters (temperature, HRT and cycle time, COD, PO_4^{3-}-P and NO_x^--N loading, and pH) in the first stage (Stage 1) were similar with the Stage 6 of preliminary experiments, except the SRT (15 days). In Stage 2, SRT was decreased to 10 days, and the COD and PO_4^{3-}-P concentrations in the influent were increased to avoid the excess washing out of sludge from the SBRs. While for Stage 3, the NO_x^--N adding for A_2 SBRs was increased to 30 mg L^{-1}. In addition, the performance of the SBRs (especially E1&E2 and E7&E8) was influenced by the temperature increased from Day 110 to Day 165 when the

P release was suddenly decreased, followed by gradually increasing. The comprehensive description of parameters had been shown in Table 3.2.

4.2.1 The performance of P removal sludge acclimation

Compared with change of PO_4^{3-}-P concentration in preliminary experiments, performance of the reactors in Enrichment I was much more effective. The trends of the accumulation of PAOs (DPAOs) can be found in the operation process, especially in Stage 3, by the increasing phosphorus release during the anaerobic phase. The continuous rising of the P concentration at the end of anaerobic phase from Day 37 to the stable period suggested that the experimental conditions of Enrichment I was obviously enhanced, rather than preliminary experiments.

In the whole process, the EBPR systems in all reactors with 15-days SRT had lower performance than that with 10-days SRT, especially in A_2 SBRs (as shown in Fig. 4.7). During the complete enrichment process, the P removal performance in A_2 SBRs was hardly enhanced in Stage 1 and 2, while it was enhanced in Stage 3 when the SRT, COD, P and NO_x^--N concentrations were adjusted to appropriate values.

In order to enhance the enrichment performance, NO_x^--N amount for A_2 reactors was increased to 30 mg L^{-1} from day 37 (Stage 3). After the adjustment, the PO_4^{3-}-P release performance during the anaerobic phase had been gradually increased. In the A_2 reactors, the obvious change happed from around day 40, then the growth level became increasingly higher until day 96 (E1 & E2, the 61st day of Stage 3), day 106 (E3 & E4, the 71st day of Stage 3) and day 110 (E5 & E6, the 75th day of Stage 3), when the P release level would become stable with some fluctuation. In contrast, Stage 2 and 3 are actually the same stage for the operation of A/O SBRs, where P removal performance was continuously increasing, with higher anaerobic P release and aerobic P uptake by day 42 (the 23rd day after SRT decrease) when they achieved the maximum and kept stable with small fluctuations.

The relatively stable operation of SBRs was destroyed by the gradual increase of temperature (from around 20 °C to 27 °C) from Day 110, which decreased back on Day 165. The unexpected temperature change induced the different extents decline of anaerobic P release in the SBRs. In the A_2 reactors, the extent of decline was increased with the ratio of NO_3^--N accounting in the electron acceptors. In case of E1&E2, for instance, the PO_4^{3-}-P concentrations at the end of anaerobic phase on Day 142 had been

decreased from normal values (40-45 mg L^{-1}) to the minimums (22.1 and 25.6 mg L^{-1}, separately). On the contrary, the minimums of other A_2 SBRs were still higher than 40 mg L^{-1}, with much lower decline extent than E1&E2.

Overall, all the SBRs used in PAO enrichment had been more efficient after SRT decrease and C, P & N adjustment, especially in A_2 SBRs where anaerobic P release and anoxic P uptake were enhanced positively. The PO_4^{3-}-P concentration in the effluent was mostly lower than the concentration at the beginning of the cycle, with different removal rate up to 92% in A_2 reactors and 99% in A/O reactors, even though the removal rate was not stable at high values in the A_2 SBRs.

Except the fluctuation period with temperature change, the accumulating trends of the A_2 systems were slower than the performance of the of Dai *et al*. (2017b), who acclimated DPAO sludge with two-step and one-step strategies. On the other hand, the anaerobic phosphorus release levels of 30-55 mg L^{-1} were higher than the figures (around 25 mg L^{-1}) of Dai *et al*. (2017b), due to the higher COD loading and lower NO_x^--N residue (for E3-E6).

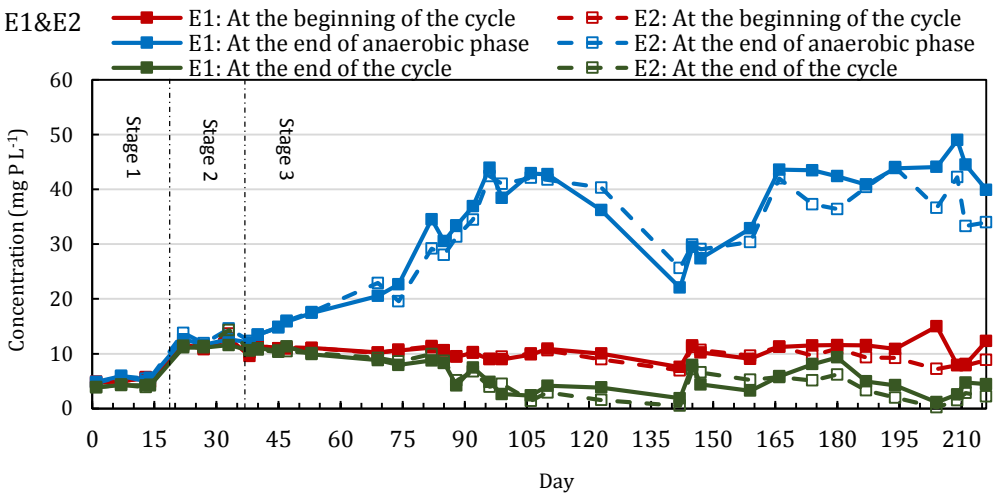

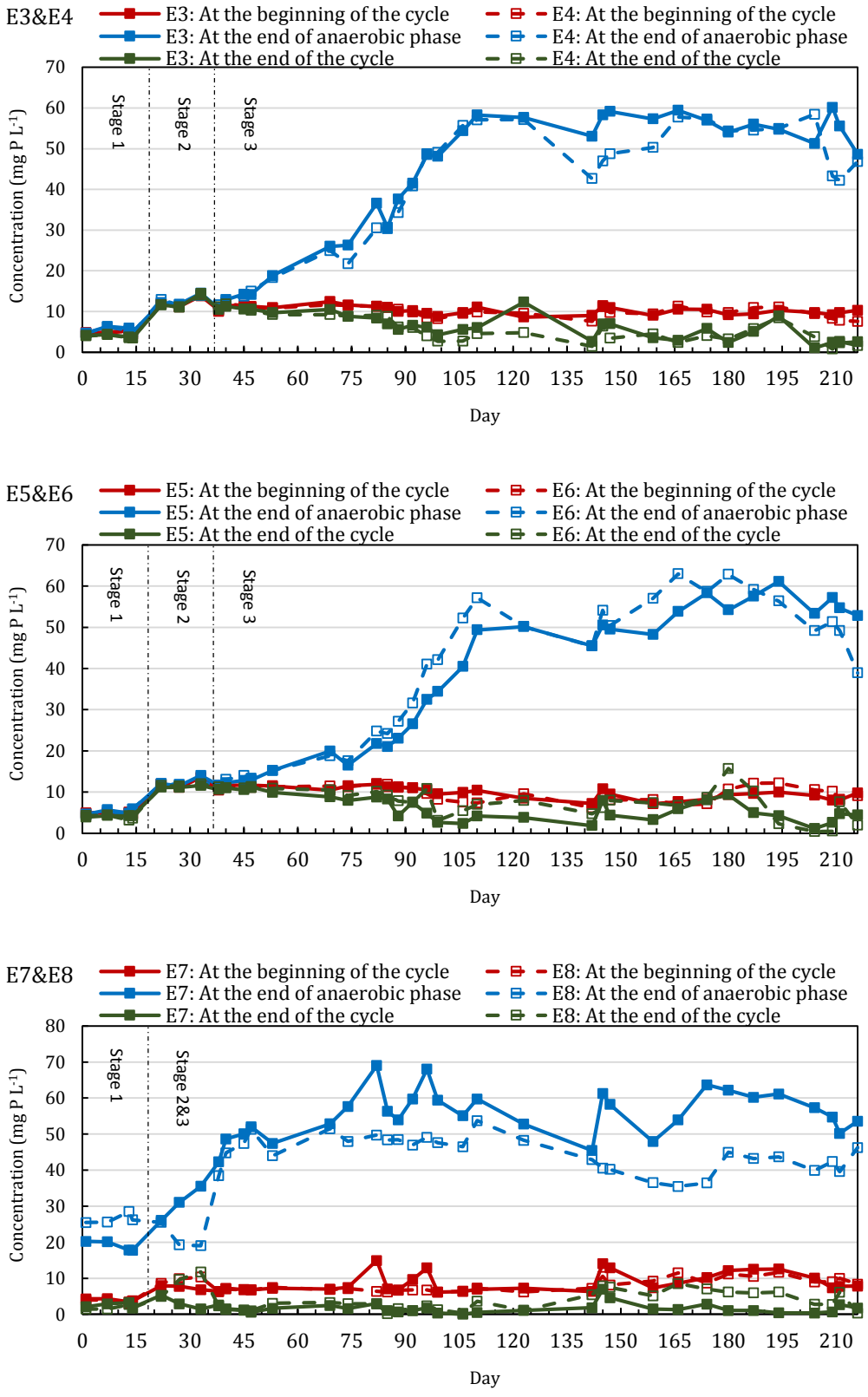

Fig. 4. 7 Operation performance of A_2 and A/O SBRs in DPAO enrichment I (E1&E2: only NO_3^--N; E3&E4: NO_3^--N/NO_2^--N=7/1; E5&R6: NO_3^--N/NO_2^--N=3:1; E7&E8: only O_2)

As can be seen in Fig. 4.7, PO_4^{3-}-P concentration at the end of anaerobic phase of E1&E2 after the increasing period were respectively 40-50 mg L^{-1}, while the value of E3−E6 was around 50-65 mg L^{-1}. The main factor causing the difference should be the higher NO_x^--N residual. Since sole NO_3^--N dosing systems (E1&E2) could accept larger amount of electrons with the same amount of nitrogen adding, less nitrogen was consumed by DPAOs during anoxic phase. As a result, higher initial NO_x^--N concentration at next cycle beginning (Fig. 4.8 a) would be utilised by denitrifiers to grab VFA from DPAOs (Fig. 4.8 b), which induced lower P release. The data in Fig 4.8b was calculated with the initial NO_x^--N concentration, with the assumptions that denitrifiers could use all the NO_x^--N in anaerobic phase to consume HAc, and the reactions were as Equation (4-1) and (4-2). It can be found that with the decrease of NO_3^--N ratio, initial NO_x^--N concentration in E5&E6 systems was lower than that in E3&E4 systems, while more acetic acid could be utilised by DPAOs. Nevertheless, although the PO_4^{3-}-P release and NO_x^--N utilisation were increased with the higher NO_2^--N ratio in electron acceptor, E5 & E6 did not have higher and more stable P removal performance than E3 & E4, and all of them were less efficient than E1&E2 and E7&E8 systems, if the plots of them in Fig. 4.8 were compared with each other. It also indicated that due to the increase of NO_2^--N/NO_3^--N ratio, its electron acceptor capacity was lower than sole NO_3^--N, if the same amount of NO_x^--N was provided into the reactors. As a result, higher NO_x^--N amount should be added for denitrifying P uptake, if NO_2^--N was considered as electron acceptor.

Fig. 4.8c shows the change of the P release/HAc consumption ratio in anaerobic phase of A_2 SBRs, compared with A/O SBRs in the enrichment process. As can be seen, the ratio of A/O SBRs had become relatively stable after Day 45, while the ratios in A_2 SBRs were still increasing from very low level. The main reason causing the difference should be that the PAOs enrichment of A/O SBRs had started to be enhanced from Stage 2, and the enrichment efficiency of A/O condition was mostly higher than A_2 conditions.

In addition, it can be found that the performance of E1&E2 was influenced by the temperature increase, from both Fig. 4.8a and Fig. 4.8b, where the higher N residual at the beginning of the cycles caused the decrease of P release, and then the decrease of P release/HAc consumption ratio.

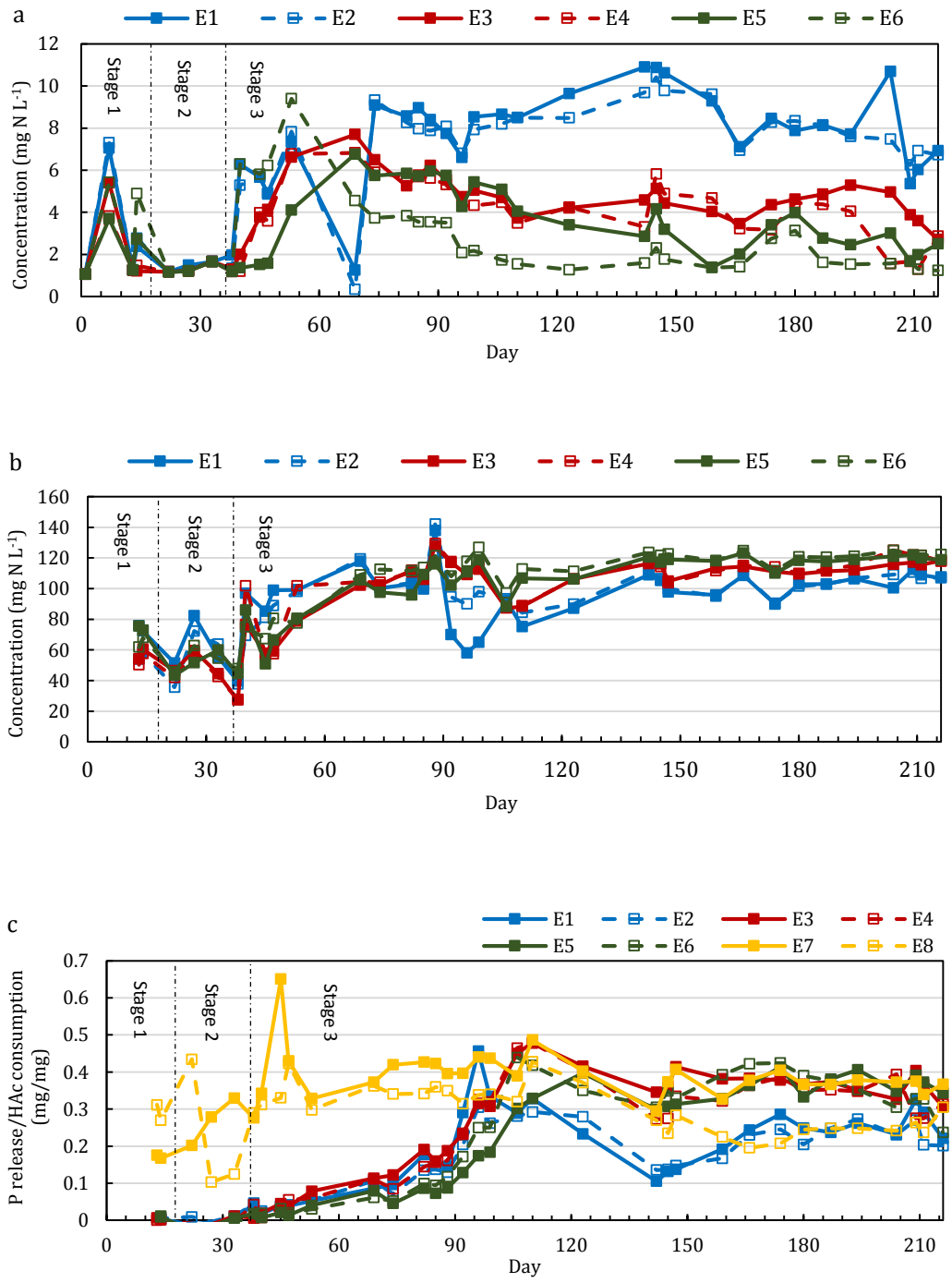

Fig. 4. 8 Average NO_x^--N concentration at cycle beginnings (a), HAc amount consumed by DPAOs during anaerobic phase (b) and the P release/HAc consumption ratio (c) in Enrichment I (E1&E2: only NO_3^--N; E3&E4: NO_3^--N/NO_2^--N=7/1; E5&E6: NO_3^--N/NO_2^--N=3:1; E7&E8: only O_2)

The similar changes occurred in anoxic phase, the ratios of P uptake/N consumption and e^- transfer/P uptake of the E1&E2 both changed obviously during the period of temperature increase (shown in Fig. 4.9). In Stage 3, P/N ratios in the A_2 SBRs gradually increased from very low level to 1.2-2.4. The value of E1&E2 was higher than E3&E4 and

E5&E6 at the beginning, but declined after the temperature increase. In contrast, the e^- transfer/P uptake ratio decreased from thousand level (due to the non-sufficient P uptake) to 5-10, while the ratio in E1&E2 had an obvious peak during the temperature increase period, compared with other A_2 SBRs.

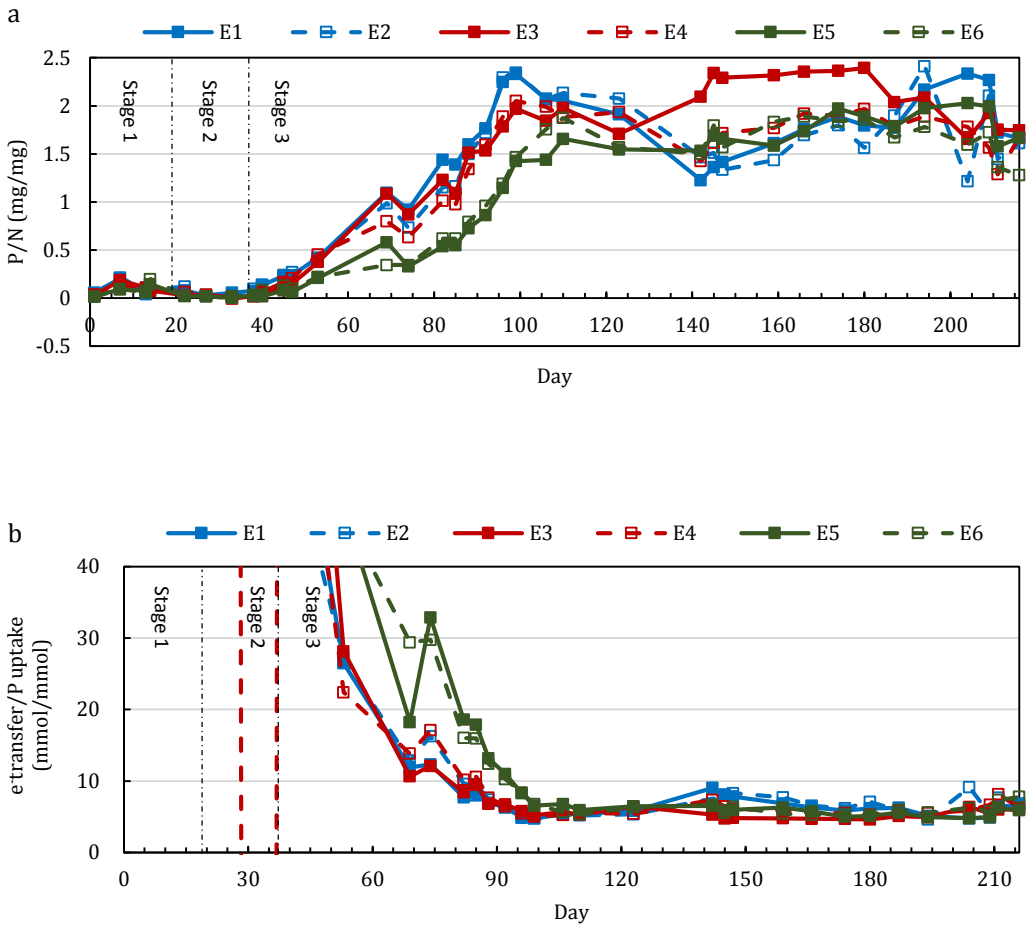

Fig. 4. 9 The ratios of P uptake/N consumption (a) and e- transfer/P uptake (b) in anoxic phase of A_2 SBRs (E1&E2: only NO_3^--N; E3&E4: NO_3^--N/NO_2^--N=7/1; E5&E6: NO_3^--N/NO_2^--N=3:1)

Fig. 4.10 demonstrates the PO_4^{3-}-P, HAc and NO_x^--N concentration changes in one cycle with 15-day SRT. The initial HAc of around 75 mg L^{-1} was obviously consumed during the anaerobic phase, basically exhausted at the beginning of anoxic or aerobic phase in all the reactors. However, very slight anaerobic P release (only around 1.0 mg L^{-1}) in A_2 reactors was detected in the anaerobic phase, while the P release had achieved proximately 14 mg L^{-1} in A/O SBRs. In anoxic phase, the PO_4^{3-}-P uptake amount of around 1.5 mg L^{-1} in all the A_2 reactors was relatively minor, compared with the consumption of NO_x^--N, which

indicated the ineffective P uptake performance. On the contrary, the aerobic P uptake efficiency in A/O reactors was much higher than A_2 reactors, with the PO_4^{3-}-P removal rate of around 70%. As the P release and uptake in both A_2 and A/O SBRs were not enhanced in this stage, the operation period was transferred into the second stage.

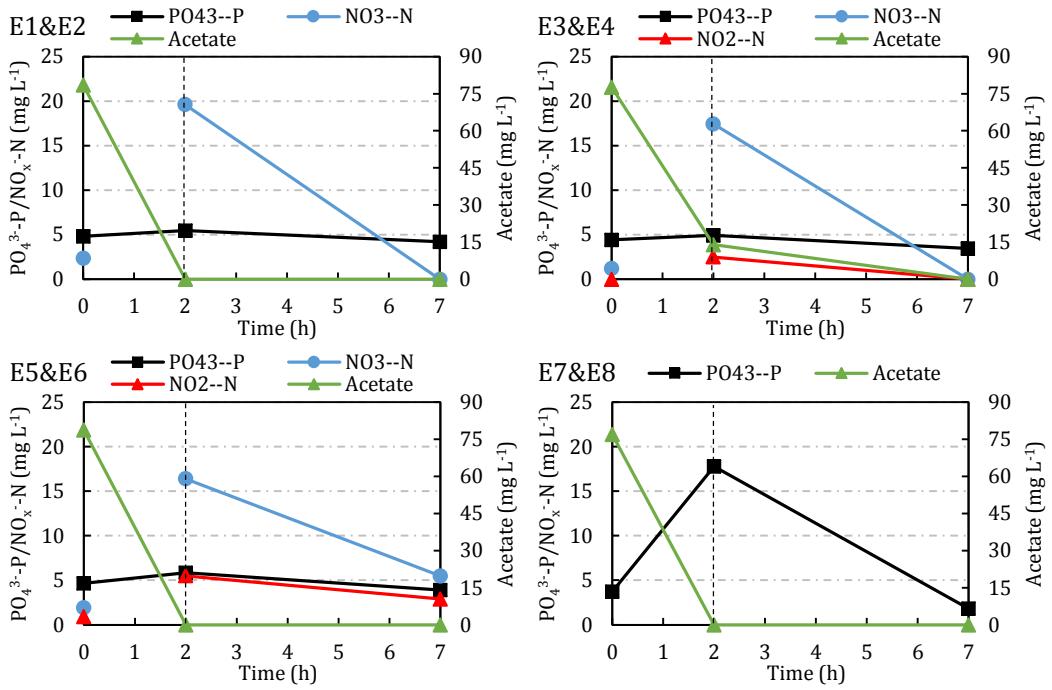

Fig. 4. 10 Typical HAc, PO_4^{3-}-P and NO_x^--N concentration change in a cycle of DPAO Enrichment I: Stage 1 (E1&E2: only NO_3^--N; E3&E4: NO_3^--N/NO_2^--N=7/1; E5&E6: NO_3^--N/NO_2^--N=3:1; E7&E8: only O_2)

From day 19 of Enrichment I process, Stage 2 was started when the SRT was decreased to 10 days in order to enhance the enrichment efficiency. Meanwhile, higher acetate and P were added into the feedstock to avoid the washing out of microbial communities. However, the P release and uptake in different phases of A_2 SBRs did have any obvious change, and HAc could not be completely exhausted at the end of anaerobic phase, while the 20 mg N L^{-1} was basically used out at the cycle end in all A_2 reactors (Fig. 4.11). The reason causing the result is that with the faster growth with shorter SRT, microorganisms in the SBRs needed more electron acceptors to maintain their faster metabolic process and growth, but NO_x^--N provided in A_2 SBRs was not enough. Due to the shortage of electron acceptor, DPAOs could not accumulate enough polyP, accordingly, P release and uptake could not be enhanced during the cycles. In addition, without enough stored polyP, DPAOs did not have sufficient energy to produce PHA, inhibiting the consumption of acetic acid.

On the contrary, P removal performance in A/O SBR in this stage was much better than that in Stage 1, with more obvious anaerobic release and aerobic uptake during this period, based on the continuous air supply in aerobic phase. In the anaerobic phase, acetic acid was consumed completely, and P concentration was increased from 6.8 to 35.5 mg L^{-1}, followed by decreasing to 1.5 mg L^{-1} (with removal rate of 78%) during the aerobic phase.

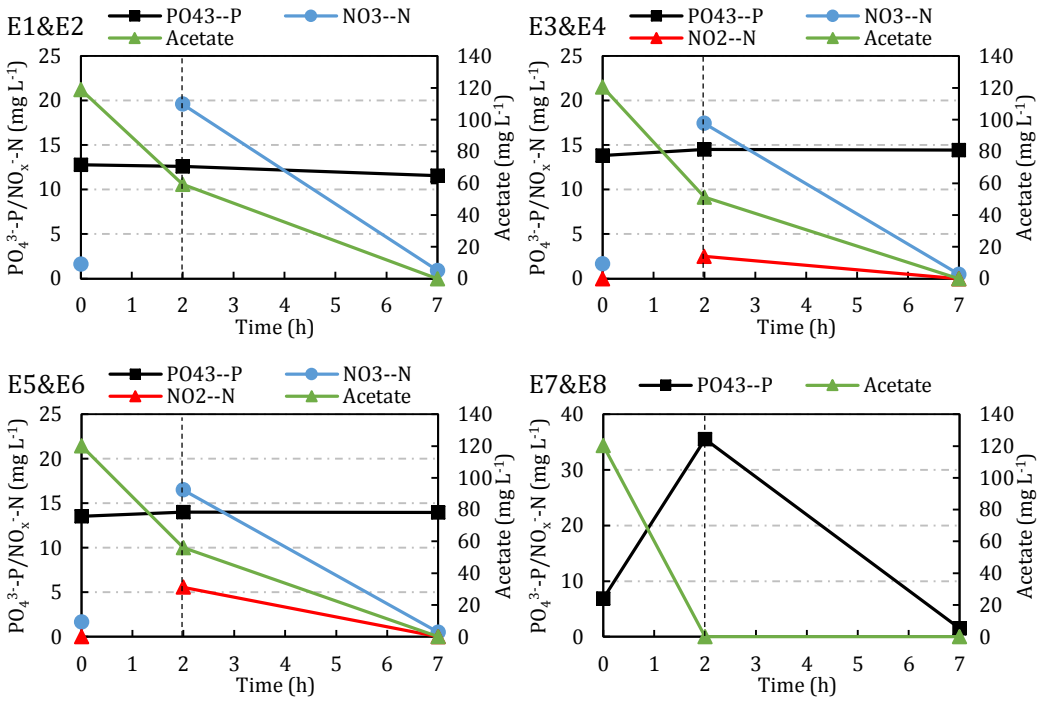

Fig. 4. 11 Typical acetate, PO_4^{3-}-P and NO_x^--N concentration change in a cycle of DPAO enrichment I: Stage 2 (E1&E2: only NO_3^--N; E3&E4: NO_3^--N/NO_2^--N=7/1; E5&E6: NO_3^--N/NO_2^--N=3:1; E7&E8: only O_2)

With the increase of nitrogen dosing from 20 to 30 mg L^{-1} in Stage 3, the performance of the A_2 reactors was enhanced obviously, as discussed above. In order to understand the change process of PO_4^{3-}-P and NO_x^--N concentration during a whole cycle in this stage, cycle analysis of A_2 SBRs was conducted (Fig. 4.12). In the cycle of E3&E4, for instance, acetic acid could be consumed completely in the first 1.5 hour of anaerobic phase, it suggested with the growth of DPAOs in the systems in Stage 3, the anaerobic HAc consumption was enhanced, inducing complete carbon removal with the enrichment process. The reason causing the enhancement should be that with the growth of DPAOs in the systems in stage 3, the anaerobic HAc demand was also increased to produce more PHB, inducing complete carbon removal with the enrichment process. Moreover, PO_4^{3-}-P concentration increased sharply from around 9 mg L^{-1} to 50 mg L^{-1} in the first 1.5 hour. In

the last 30 minutes of anaerobic phase, PO_4^{3-}-P concentration only changed slightly and achieved the maximum at the end of this phase.

In anoxic phase, PO_4^{3-}-P concentration gradually decreased to around 5 mg L^{-1}, with the NO_x^--N solution dosing. The concentration of NO_3^--N increased from 0 to above 20 mg L^{-1} in the first hour of this period, due to the continuous concentrated solution adding, while decreased from the second hour. In contrast, NO_2^--N was hardly detected during the complete cycle, which suggested that the low concentration of nitrite could be consumed immediately after adding into the SBRs. Because it was hard to decide if the P decrease in the first hour of anoxic phase was caused by nitrate or nitrite, the ratio of PO_4^{3-}-P uptake/NO_3^--N consumption was calculated from the second to the last hour of anoxic phase (Fig. 4.13). The main trend of the ratio was decrease as time passes, from averagely 2.4 to 1.1, while the PO_4^{3-}-P uptake/NO_3^--N consumption ratio was globally around 1.9 during this period.

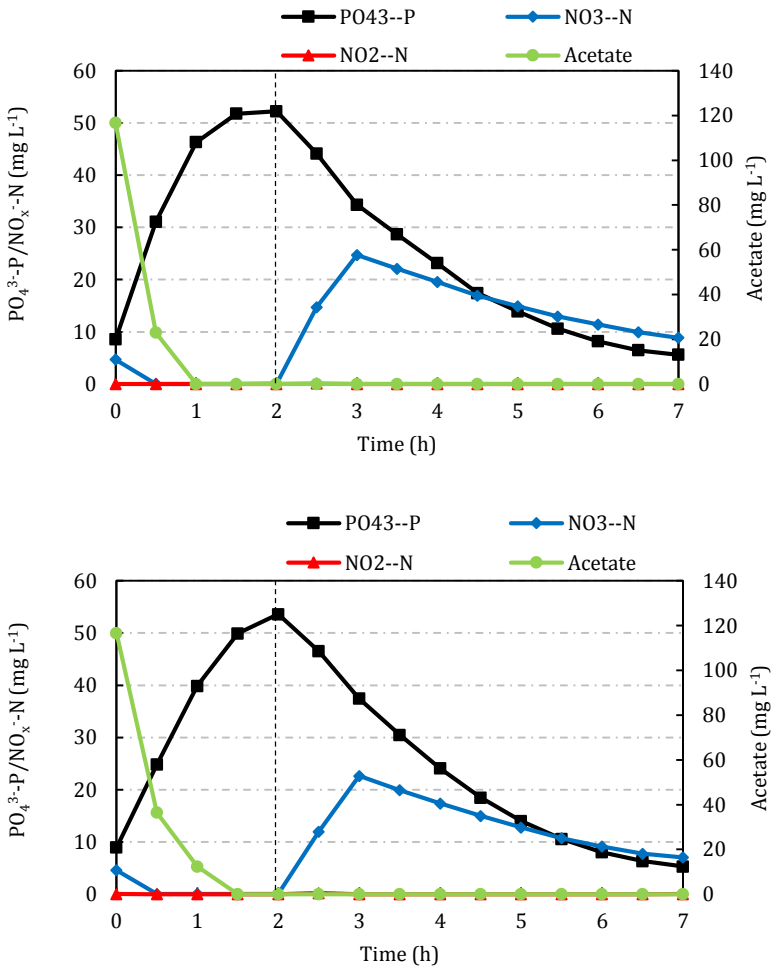

Fig. 4. 12 Cycle performance of E3 and E4 in stable period of Enrichment I

NH_4^+-N was a special element contained in the influent of the enrichment process, only participating the growth of microbial communities. Hence, lower concentration (around 12.5 mg L^{-1}) was applied to avoid any other conversion of ammonia (e.g. nitrification) that may influence the concentration of NO_3^--N and NO_2^--N. During the complete cycle of SBR operation, NH_4^+-N concentration decreased gradually in both anaerobic and anoxic (aerobic) phases, with approximate linear trend. It indicated that the NH_4^+-N absorption of the P removal sludge was conducted continuously under different conditions. In all the A_2 SBRs, there was still around 2 mg N L^{-1} ammonia remained at the cycle end, which suggested that the NH_4^+-N amount provided for the SBRs was enough, even though it was much lower than the actual concentration of practical municipal wastewater. In comparison, the consumption rate in A/O SBRs was higher than that of A_2 SBRs, which should be caused by the higher bacteria growth rate in A/O sludge. The NO_x^--N concentration at the end of the cycle in A/O SBRs was mostly lower than 0.4 mg L^{-1}, similar as the figure at the end of anaerobic phase, indicating that reactions of nitrification did not occur during the aerobic phase and ammonia in the reactor was mainly used for PAO absorption and growth.

In the enrichment process, MLSS of A_2 and A/O SBRs decreased from around 2800 mg L^{-1} to 500 and 800 mg L^{-1} in the duration of Stage 1 and Stage 2, and then increased to around 1000 and 1500 mg L^{-1} during Stage 3. At the beginning of the enrichment process, the MLVSS/MLSS ratio of the new inoculum was around 88%, which increased to higher than 90% in A_2 SBRs during Stage 1 and 2, followed by decreasing to around 60%-70% in Stage 3. In case of A/O SBRs, it gradually reduced from 88% to 50%-60% during the whole enrichment process. The reason causing the difference is that in Stage 1 and 2, the enrichment process in A_2 SBRs was not successful enough, inducing little reproduction of DPAOs and slight polyP production in the sludge. With the development of enrichment in Stage 3, the amount of DPAOs increased, enhancing the generation of polyP and improving the proportion of non-volatile content in the activated sludge. On the contrary, the enrichment performance in A/O systems was better than A_2 systems during whole process, inducing lower MLVSS/MLSS ratio in the samples of activated sludge.

4.2.2 Tests for P uptake potential with NO_2^--N as sole electron acceptor

Because NO_3^--N contributed to the majority of electron acceptors in all of the A_2 SBRs of Enrichment I, and Fig. 4.12 showed that small amount of NO_2^--N was easily to be

consumed by DPAOs in anoxic phase, it was necessary to investigate the role of NO_2^--N in anoxic P uptake, in order to explore the possibility of P removal with high level of nitrite. Thus, some duplicated tests were conducted in enriched A_2 SBRs with only NO_2^--N (40 mg N L^{-1}) as electron acceptor, compared with NO_3^--N (same N concentration). In the tests, the concentrated solution was pumped into the reactors gradually during the whole anoxic phase (namely 8 mg N L^{-1} per hour), in order to induce toxic inhibition.

4.2.2.1 NO_2^--N based anoxic P uptake without pH adjustment

Fig. 4.13 shows the change of PO_4^{3-}-P, NO_2^--N and pH during the 5-h anoxic phase in the tests (averagely figures) without pH control. As can be seen in the plot, pH increased from 7.2 to 9.0, due to the production of OH^- from denitrification and the absorption of PO_4^{3-}-P, which weakened the buffering capacity of the activated sludge. As a result, the P uptake ability of the sludge was decreased gradually after pH increased to 8.5.

In the complete anoxic period, 43.1 mg L^{-1} PO_4^{3-}-P was removed by A_2 SBR via 36.5 mg L^{-1} NO_2^--N, with the P/N ratio of 1.2. PO_4^{3-}-P concentration decreased 13.8, 10.7, 9.2, 6.2 and 3.1 mg L^{-1} in every hour, while the consumption of NO_2^--N was steadier between 6.5 and 7.9 mg L^{-1}. Consequently, the hourly P/N ratio decreased from 1.8 to 0.5 during the anoxic phase. It suggested that DPAOs could still consume NO_2^--N at very high level of pH, but their capacity of PO_4^{3-}-P accumulation could not maintain at this pH level simultaneously. Thus, pH should be controlled properly during NO_2^--N based SBR operation, in order to sustain effective anoxic P uptake.

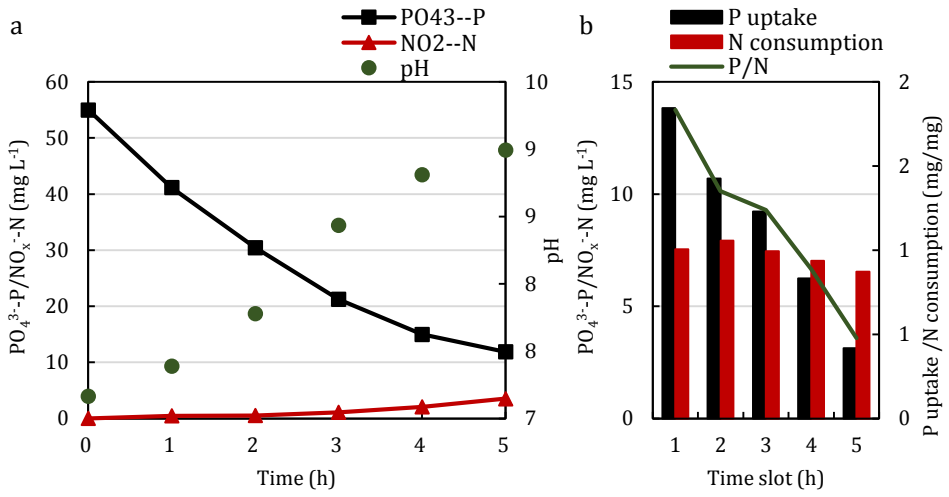

Fig. 4. 13 NO_2^--N based anoxic P uptake tests without pH adjustment: a. PO_4^{3-}-P, NO_2^--N concentration and pH; b. P uptake, N consumption and P/N ratio

4.2.2.2 Comparison of NO_2^--N and NO_3^--N based anoxic P uptake

In the following tests, pH was control under 8.0 during the cycles in both NO_2^--N and NO_3^--N SBRs. As shown in Fig. 4.14, P concentration in both reactors decreased from around 50 mg L^{-1} to quite low level, 2.2 mg L^{-1} in NO_2^--N based SBR and 0.6 mg L^{-1} in NO_3^--N based SBR, respectively. 50.6 mg L^{-1} and 53.9 mg L^{-1} PO_4^{3-}-P were separately removed by 38.6 mg NO_2^--N L^{-1} and 31.2 mg NO_3^--N L^{-1}, with the P/N ratio of 1.3 and 1.7.

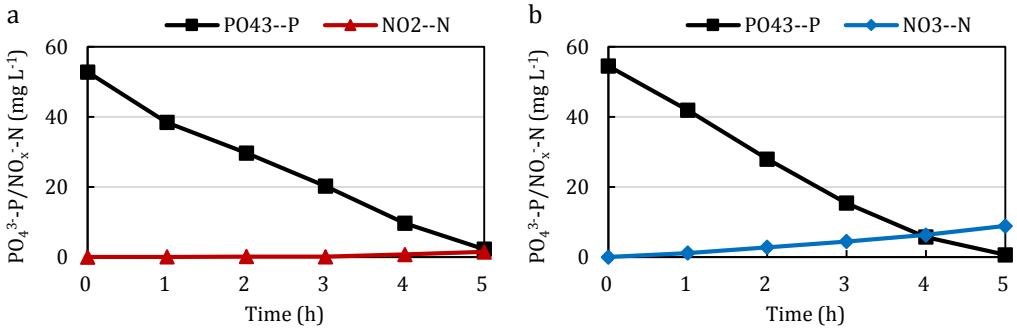

Fig. 4. 14 NO_2^--N (a) and NO_3^--N (b) based anoxic P uptake with pH control

In the hourly determination (Fig. 4.15), NO_2^--N based SBR had higher P uptake rate in the last two hours, which achieved more efficient total P removal, compared the test without pH adjustment. Both of hourly consumption of NO_2^--N and NO_3^--N did not changed sharply, with decrease of 7.3-8.0 mg L^{-1} and 5.5-6.9 mg L^{-1}, respectively. The P/N ratio of NO_2^--N based SBR, which fluctuated between 1.0 and 1.8, was lower than that of NO_3^--N based SBR (from 0.9 to 2.2). It justified that compared with NO_3^--N, higher amount of NO_2^--N was required in anoxic P uptake, to remove the same quantity of PO_4^{3-}-P.

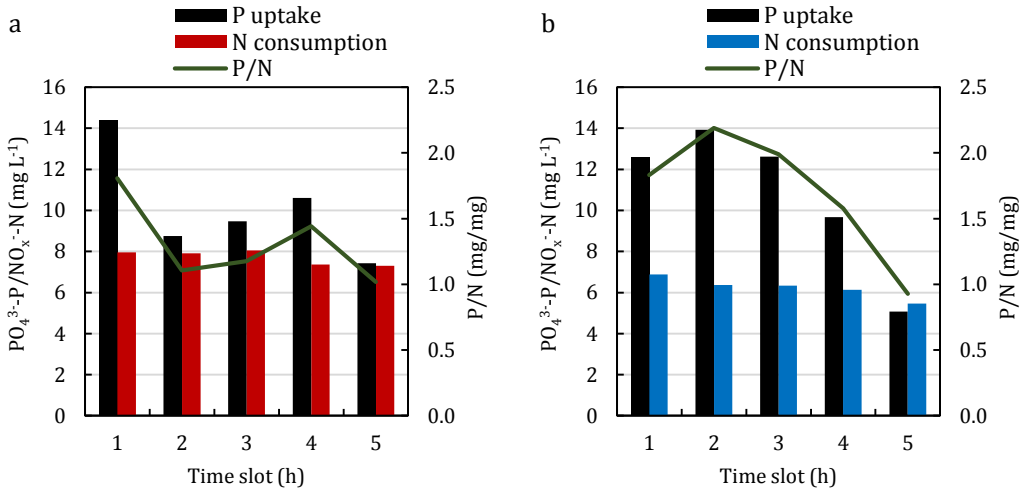

Fig. 4. 15 P uptake, N consumption and P/N ratio in NO_2^--N based and NO_3^--N based P removal SBRs

In summary, the results from the NO_2^--N tests could provide some necessary evidence for the next enrichment experiments of DPAOs, such as the possibility of P uptake in A_2 systems with NO_2^--N as the sole electron acceptor, the potential amount of NO_2^--N required in the anoxic phase, the adjustment of pH in SBR operation, *etc*.

4.2.3 Microbial community analysis of Enrichment I

Five sludge samples, including inoculum (Seed), E1&E2, E3&E4, E5&E6 and E7&E8, were selected in microbial community analysis for this PAOs enrichment process. For the five sludge samples 188986, 398009, 489238, 486567 and 555775 effective reads were separately detected, mostly belonging to the phyla of *Proteobacteria*, *Bacteroidetes*, *Planctomycetes*, *Chloroflexi*, *WPS-2*, *Actinobacteria*, *Acidobacteria*, *Patescibacteria*, *Verrucomicrobia*, *Spirochaetes*, *Cyanobacteria*, *Armatimonadetes*, *Firmicutes*, *Chlamydiae*, *Lentisphaerae*, *etc*.

4.2.3.1 Microbial community similarity

630 genera were effectively detected among the five samples, totally, while the numbers in each sample were 462, 153, 174, 190 and 179, respectively. It indicated that most non-functional genera in the inoculum were washed out during the enrichment process. A Venn diagram (Fig. 4.16) was adopted in the similarity comparison of genus among the four enriched sludge samples (E1&E2, E3&E4, E5&E6 and E7&E8). The common genera among the four samples was 63, accounting for 18.4% of the total 343 genera. In the A/O sample, the genus number unique to individual community was 63, higher than all the A_2 samples. It suggested the similarity of microbial community tend to be changed from A/O to A_2 acclimation conditions. Table 4.1 shows the common genera number among the samples with paired comparison, where it was found that the number of common genera among A_2 reactors was relatively higher than that between A_2 and A/O reactors. Especially, the highest number was 121, found among E3&E4 and E5&E6, which suggested the addition of NO_2^--N in A_2 reactors caused more similar microbial communities.

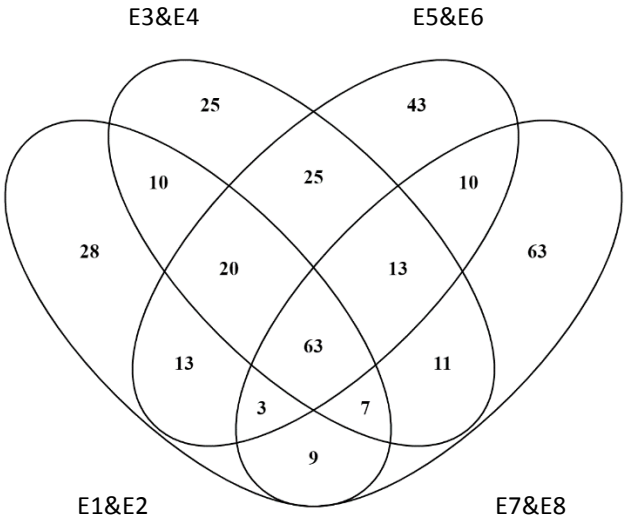

Fig. 4. 16 Venn diagram based on genus of different enriched P removal sludge in Enrichment I (E1&E2: only NO_3^--N; E3&E4: NO_3^--N/NO_2^--N=7/1; E5&E6: NO_3^--N/NO_2^--N=3:1; E7&E8: only O_2)

Table 4. 1 Number of common genera between samples based on Venn diagram (E1&E2: only NO_3^--N; E3&E4: NO_3^--N/NO_2^--N=7/1; E5&E6: NO_3^--N/NO_2^--N=3:1; E7&E8: only O_2)

	E3&E4	E5&E6	E7&E8
E1&E2	100	99	82
E3&E4	--	121	94
E5&E6	--	--	89

In the one-way Anova analysis, 630 (the total genus number detected among the five sludge samples) was adopted as the general sample size, in order to compare them globally, although the effective reads in each sludge sample were different. The results indicated that the similarity of microbial communities in the enriched sludge samples was much higher than that between enriched samples and the inoculum.

4.2.3.2 Microbial community structure and functional populations

Based on the results, in both of A_2 and A/O reactors, *Proteobacteria* was the most abundant phylum (76.2%-79.0%, average value was 77.3%), where the classes of *γ-proteobacteria* and *α-proteobacteria* occupied a large ratio in the population (75.7%-78.6% in total, average value was 76.9%) in all acclimated EBPR systems from E1 to E8, much higher than that in the inoculum (only 22.4% in total). As shown in Fig 4.17, *Bacteroidia*,

the most abundant class in inoculum (27.8%), was decreased to 9.1%, 8.6%, 13.6% and 16.4% in E1&E2, E3&E4, E5&E6 and E7&E8, separately. On the contrary, *γ-proteobacteria* was increased from 10.4% to 43.2%, 36.6%, 42.6% and 38.2%, and *α-proteobacteria* was increased from 11.9% to 34.1%, 42.0%, 33.1% and 37.7%, respectively. In addition, the other frequent classes in acclimated sludge were separately *Planctomycetacia* (0.1%-7.3%, average value was 2.5%), *Anaerolineae* (1.5%-4.8%, average value was 2.9%), *Metagenome* (0.2%-1.9%, average value was 1.3%), *Actinobacteria* (0.2%-0.5%, average value was 0.3%), *δ-proteobacteria* (0.4%-0.5%, average value was 0.5%), *Verrucomicrobiae* (0.3%-1.1%, average value was 0.7%) and *Ignavibacteria* (0.03%-4.0%, average value was 1.2%). Except the dominated classes, other classes accounted 0.9%-2.5% in the microbial population in E1-E8, decreased from 22.7% in the inoculum, which suggested that some microbial classes were washed out from the sludge during the acclimation process.

In the class of *γ-proteobacteria*, *β-proteobacteriales* was the dominant order (In most of literature, *β-proteobacteria* was a class collocated with *γ-proteobacteria* and *α-proteobacteria*, based on the old database. While in the new SILVA database, it was rearranged as an order in class of *γ-proteobacteria*, namely *β-proteobacteriales*.), which accounted for 99.8%, 99.8%, 99.6% and 98.6% of *γ-proteobacteria* in the four enriched EBPR systems, obviously higher than 68.9% in the seed. In the A/O SBR (E7&E8), the ratio was relatively lower than the A_2 SBRs (E1-E6), which was mainly caused by the more frequent existence of *Pseudomonadales* (a marginal order in aerobic EBPR process, Tarayre *et al*., 2017).

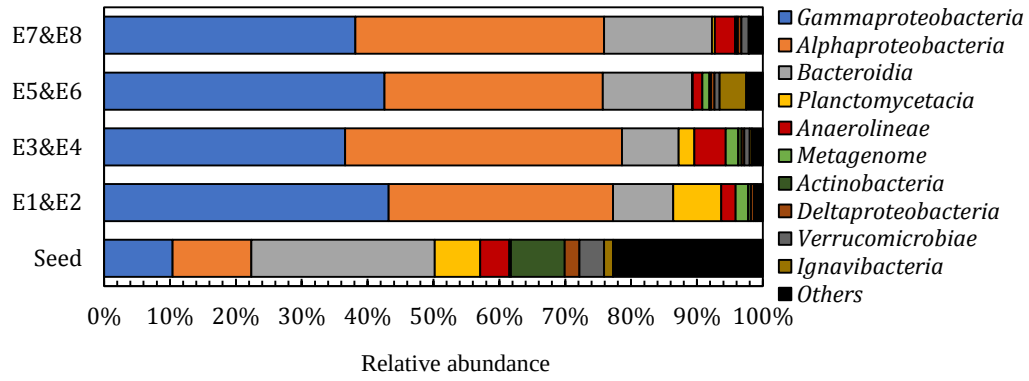

Fig. 4. 17 The relative abundances of classes in the five sludge samples (E1&E2: only NO_3^--N; E3&E4: NO_3^--N/NO_2^--N=7/1; E5&E6: NO_3^--N/NO_2^--N=3:1; E7&E8: only O_2)

Fig. 4.18 shows the most abundant 20 genera detected in the four sample of enriched sludge, compared with the inoculum. The 20 genera separately belonged to *Proteobacteria* (including 7 genera in *β-proteobacteriales* and 6 genera in *α-proteobacteria*), *Bacteroidetes* (3 genera), *Planctomycetes* (1 genus), *Chloroflexi* (2 genera) and WPS-2 undescribed phyla (1 genus).

In both A_2 and A/O SBRs, an unknown group of *Rhodocyclaceae* (represented by dark red bars in picture b) in *β-proteobacteriales* was the most plentiful genus in the communities, respectively accounting for 23.5%, 24.4%, 23.9% and 22.2% (average value was 23.5%), increasing from only 0.1% in the inoculum. The second and third genera were separately *Phreatobacter* (*α-proteobacteria*) and a *Rhodobacteraceae*-related genus (*α-proteobacteria*), accounting for 11.5% and 10.17%, averagely. On the contrary, *Candidatus Accumulibacter*, another *Rhodocyclaceae*-related genus which was most frequently reported PAO in EBPR process (Ahn *et al*., 2001; Zeng *et al*., 2003a; Kong *et al*., 2004; Carvalho *et al*., 2006; Martin *et al*., 2006; Oehmen *et al*., 2007), only accounted for 0.6%, 2.9%, 2.7% and 1.7% (average value was 2.0%), even lower than *Sulfuritalea* (also a genus in *Rhodocyclaceae)*. It suggested that a *Rhodocyclaceae*-related genus was most responsible in P removal in enriched EBPR sludge, while *Candidatus Accumulibacter* was not the frequent group in the samples.

As the most abundant family in all acclimated systems, *Rhodocyclaceae* (including *Candidatus Accumulibacter*, *Sulfuritalea* and other genera) accounted for 42.8%, 36.2%, 41.9% and 32.0% in the total microbial communities, much higher than 1.8% in the microbial community of the inoculum. Table 4.2 shows relative abundance of *Rhodocyclaceae*-related genera found in E1-E8, compared with the inoculum sample. As discussed above, the unknown *Rhodocylaceae*-related genus was the most responsible for P removal in the enriched sludge systems, much more abundant than the other *Rhodocylaceae*-related genera. In addition, *Dechlorosoma* was reported as the most abundant microbial population by Dai *et al*. (2017), was only detected in E3&E4 (0.2%) and E5&E6 (0.01%), which were operated under A_2 conditions with both NO_3^--N and NO_2^--N.

The second abundant microbial group is *α-proteobacteria*, including *Rhizobiales* (*e.g. Phreatobacter*) and *Rhodobacterales* (e.g. *Gemmobacter*), which were both regular orders in WWTPs (Zielińska *et al*., 2016). *Rhizobiales* was reported by Martin *et al*. (2006), as a common functional flanking population in EBPR communities. Following

Proteobacteria, *Bacteroidetes* (another dominant microbial group in normal WWTPs reported by Hu *et al*., 2012) was the second abundant phylum (13.1 %, averagely) in all the acclimated sludge samples, which was the most dominant group in the inoculum (accounting for 29.2%). The predominant genera of *Bacteroidetes* in E1-E8 were *Flavobacterium* (3.1%, averagely), *Sediminibacterium* (3.0%, averagely) and *Terrimonas* (0.4%), which were obviously different from the structure in the inoculum. The most abundant *Bacteroidetes* in the inoculum was *Saprospiraceae*-related groups (14.9%, totally), while they only accounted for 0.3%, 0.03%, 0.002% and 0.003% in the enriched samples, respectively.

Another frequent group in E1&E2 and E3&E4 was a *Planctomycetales*_uncultured genus, accounting for 6.9% and 2.1%, respectively. On the contrary, it was very rare in the other reactors and inoculum, which suggested the *Planctomycetales*_uncultured genus might be related to NO_3^--N based anoxic P uptake, similar to the report by Chouari *et al*. (2010).

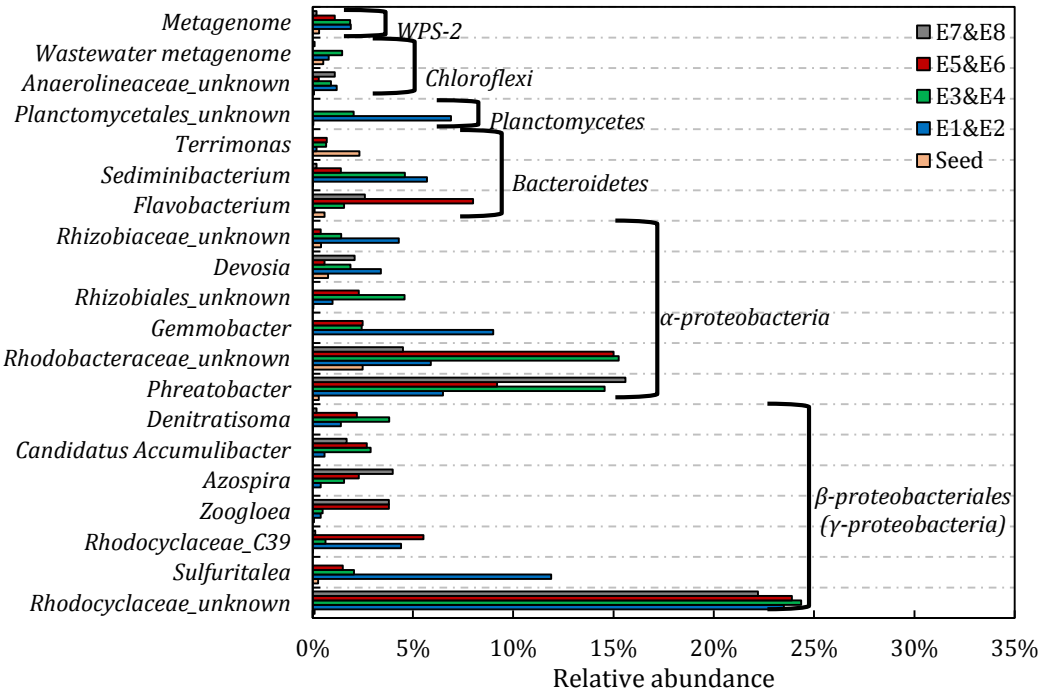

(a)

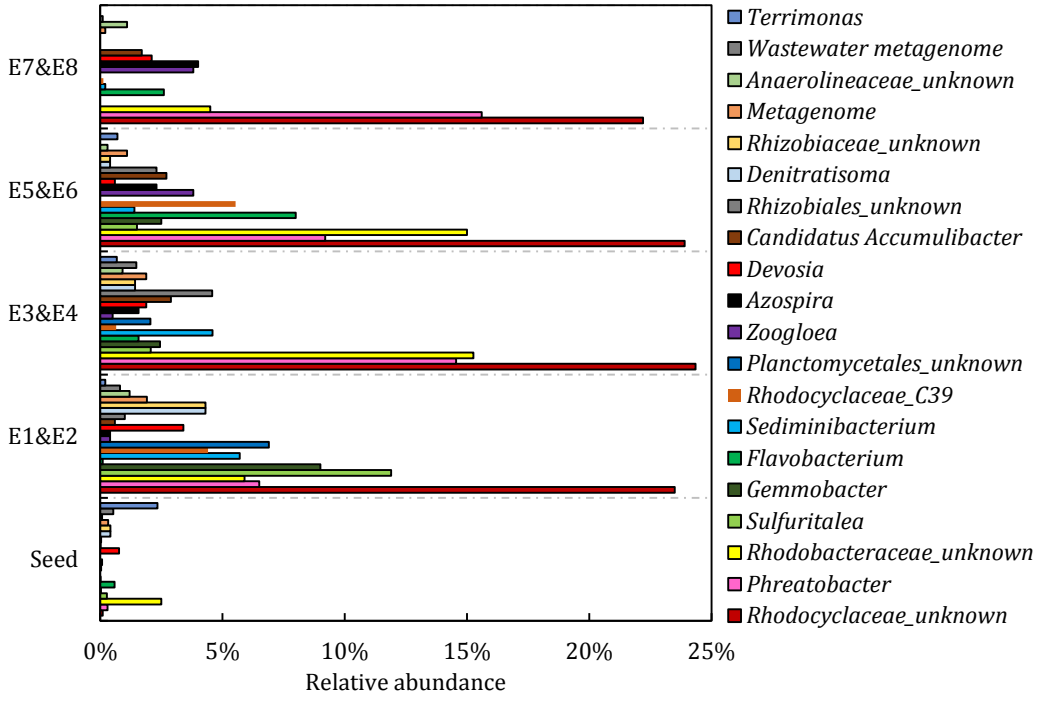

(b)

Fig. 4. 18 The relative abundances of the dominant groups (> 0.4% averagely) in enriched sludge samples compared with the inoculum sample at genus level (E1&E2: only NO_3^--N; E3&E4: NO_3^--N/NO_2^--N=7/1; E5&E6: NO_3^--N/NO_2^--N=3:1; E7&E8: only O_2)

Table 4. 2 The relative abundance of *Rhodocyclaceae*-related genera in the samples (detected in all of E1-E8)

	Seed	**E1&E2**	**E3&E4**	**E5&E6**	**E7&E8**
Rhodocyclaceae_unknown	0.1%	23.5%	24.4%	23.9%	22.2%
Sulfuritalea	0.3%	11.9%	2.1%	1.5%	0.04%
Rhodocyclaceae_C39	0.005%	4.4%	0.6%	5.5%	0.1%
Zoogloea	0.1%	0.4%	0.5%	3.8%	3.8%
Azospira	--	0.4%	1.6%	2.3%	4.0%
Candidatus Accumulibacter	0.005%	0.6%	2.9%	2.7%	1.7%
Denitratisoma	0.001%	1.4%	3.8%	2.2%	0.2%

4.3 DPAO Enrichment II

Due to the efficient P uptake via NO_2^--N in the final tests of Enrichment I, it indicated that proper nitrite dosing strategies could achieve P removal, which could effectively avoid toxic inhibition in the reactors. Hence, in the process of Enrichment II, long-period dosing strategy (4-hour) was employed in NO_2^--N based SBRs. While to compare the performance of DPAOs enrichment with different electron acceptors in A_2 conditions, the NO_3^--N based SBRs were also operated with long-period dosing strategy. Based on the discussion in Chapter 2, NO_2^--N can be used as electron acceptor in DPAO enrichment process, which can reduce the enrichment duration (Dai *et al*., 2017b). In addition, the different P/N ratios in the tests with NO_2^--N and NO_3^--N as the sole electron acceptor in section 4.2.2.2 suggested that anoxic P uptake efficiency should be influenced by the nitrous species. Thus, the hypothesis of this section was that the enrichment of DPAOs could be achieved with NO_2^--N as the sole electron acceptor to achieve complete PO_4^{3-}-P removal via long period dosing strategy, while the ratio of NO_3^--N to NO_2^--N was around 3:5 to remove the same concentration of phosphorus due to the difference of their electron accepting capacities based on their valence states of nitrogen.

In this experiment, nitrite-based DPAO enrichment with raw sludge from WWTP was compared with the sludge which had been acclimated with NO_3^--N as the sole electron acceptor in the enrichment process. The inoculum for EE1-EE4 was the acclimated sludge from Enrichment I, while the inoculum for EE5-EE8 was new RAS of 4-stage Bardenpho process from WWTW. The electron acceptor used for the SBRs have been shown in Table 3.3.

In addition, the enrichment process was re-started on day 22, as an unexpected excess acid pumping deteriorated the NO_2^--N based activated sludge (the results before restart would not be demonstrated). In the second star-up operation, half of the sludge in EE1&EE2 and EE7&EE8 was inoculated into EE3&EE4 and EE5&EE6, separately. Hence, the results in this section were all based on the experiments after the re-startup of the SBRs.

4.3.1 The performance of P removal sludge acclimation

In the Enrichment II process of DPAOs with acclimated inoculum, P removal performance of both NO_3^--N (EE1&EE2) and NO_2^--N (EE3&EE4) SBRs began to be steady by day 43, approximately, with the relatively stable anaerobic P release level. However, after achieving the steady period, the PO_4^{3-}-P concentration in the effluent and P removal rate

in NO_3^--N based SBRs were not stable as NO_2^--N based SBRs. As can be seen in Fig. 4.19, P concentration at the end of cycle in EE1&EE2 always fluctuated between 0.1 and 5.0 mg L^{-1}, with removal rate of 40%-99% (standard deviation of 0.15). On the contrary, the effluent concentration of PO_4^{3-}-P in EE3&EE4 was mostly lower than 1.0 mg L^{-1} (even achieving 0 mg L^{-1} sometimes), with removal rate of 85%-100% (standard deviation of 0.06), except the data of EE4 on day 50 and 54 when some disorder occurred and affected the P removal performance. The result comparison of the SBRs with different electron acceptors indicated that if the amount of nitrogen was provided sufficiently, NO_2^--N was more attractive to DPAOs, even though both of the sludge in the SBRs were inoculated from Enrichment I, which was acclimated mainly with NO_3^--N.

In case of the enrichment process with new RAS (EE5-EE8), more obvious difference was found in the results of P removal performance. Both of NO_2^--N based SBRs (EE5-EE6) achieved completely P removal on day 25, and then gradually kept stable with high P removal efficiency (mostly between 90%-100%, with standard deviation of 0.1). In contrast, NO_3^--N based SBRs did not achieve effective P uptake during the complete enrichment process, although the sludge could release sufficient PO_4^{3-}-P at the end of anaerobic phase from day 50 approximately. In conclusion, long-period NO_2^--N based DPAOs enrichment was obviously faster and more effective than NO_3^--N based enrichment process. It suggested that nitrite was an effective electron acceptor for DPAOs enrichment and anoxic P removal, if appropriate dosing strategy was utilised, which can avoid toxic inhibition and achieve completely P removal.

No matter acclimated inoculum or new inoculum, complete PO_4^{3-}-P removal was achieved in NO_2^--N based A_2 enrichment, which had more positive performance than NO_3^--N based operation. Mostly, in the steady period of acclimation process, PO_4^{3-}-P concentration could increase to around 50 mg L^{-1} during the anaerobic phase in all SBRs, but only EE3-EE6 could always decrease the concentration to lower than 1 mg L^{-1}, even 0 mg L^{-1}. In addition, NO_2^--N based EBPR with new inoculum needed a quite short enrichment period, even shorter than acclimated inoculum, which also suggested that the long-period NO_2^--N dosing strategy (4 hour) was an appropriate method to enrich DPAOs from raw activated sludge of 4-stage Bardenpho process. The performance of A_2 SBRs with NO_2^--N proved that if the N concentration was controlled properly in anoxic phase, nitrite was an effective electron acceptor for DPAOs in denitrifying P uptake, enhancing P removal sludge enrichment and P removal rate.

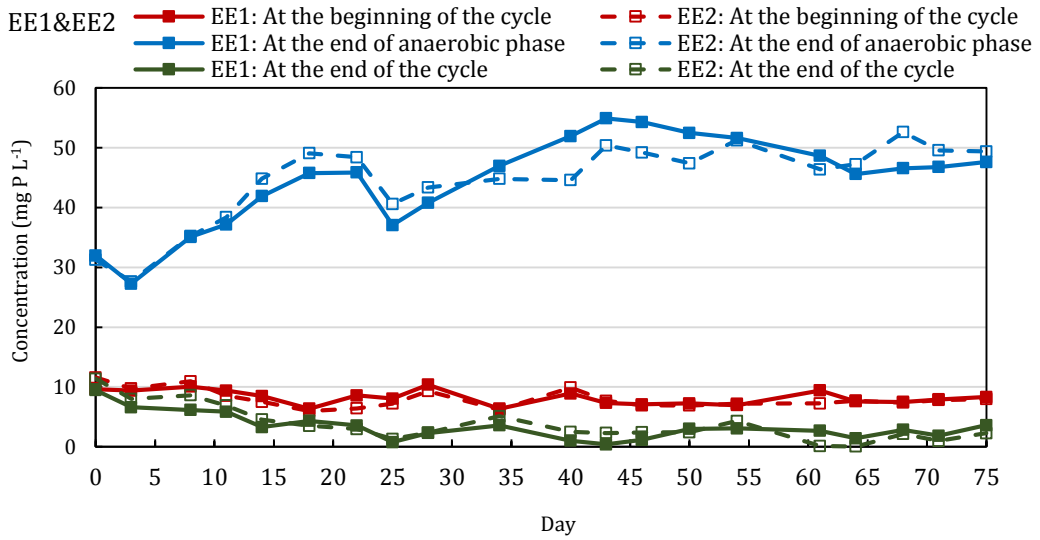
EE1&EE2
EE1: At the beginning of the cycle
EE1: At the end of anaerobic phase
EE1: At the end of the cycle
EE2: At the beginning of the cycle
EE2: At the end of anaerobic phase
EE2: At the end of the cycle
Concentration (mg P L-1)
Day

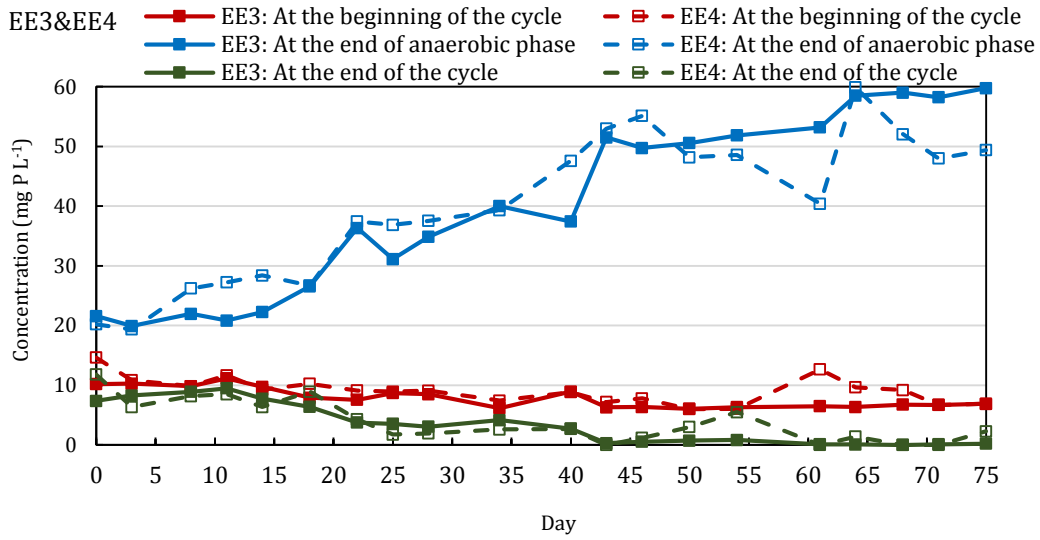
EE3&EE4
EE3: At the beginning of the cycle
EE3: At the end of anaerobic phase
EE3: At the end of the cycle
EE4: At the beginning of the cycle
EE4: At the end of anaerobic phase
EE4: At the end of the cycle
Concentration (mg P L-1)
Day

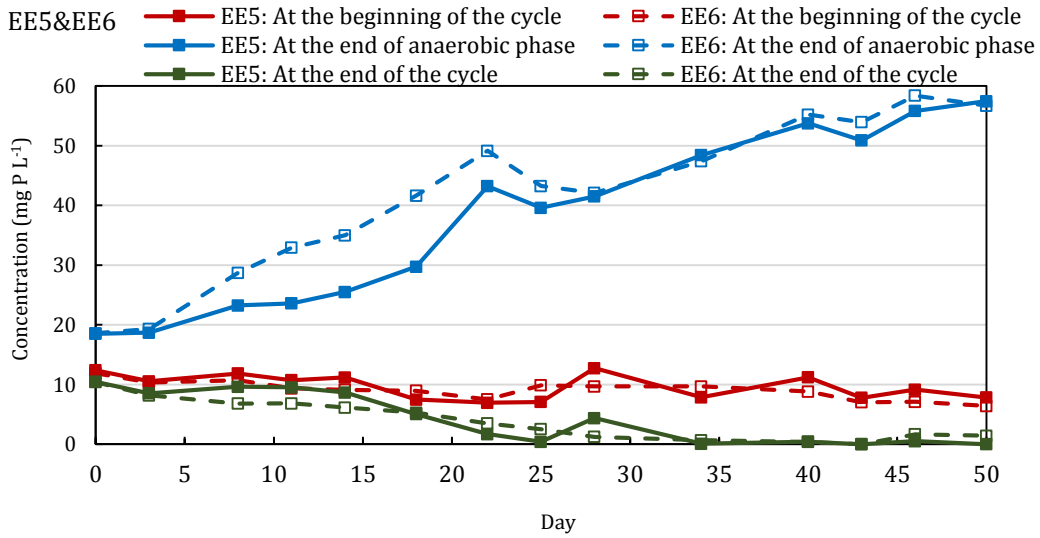
EE5&EE6
EE5: At the beginning of the cycle
EE5: At the end of anaerobic phase
EE5: At the end of the cycle
EE6: At the beginning of the cycle
EE6: At the end of anaerobic phase
EE6: At the end of the cycle
Concentration (mg P L-1)
Day

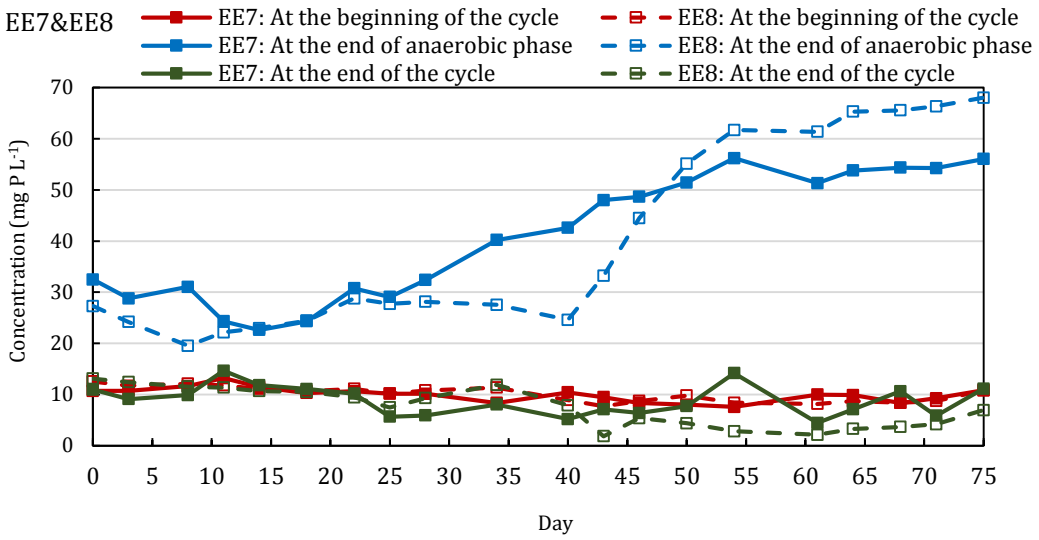

Fig. 4. 19 P removal performance of A_2 SBRs during Enrichment II process (EE1&EE2: only NO_3^--N with acclimated inoculum; EE3&EE4: only NO_2^--N with acclimated inoculum; EE5&EE6: only NO_2^--N with new inoculum; EE7&EE8: only NO_3^--N with new inoculum)

Fig. 4.20 shows the results about the performance of anaerobic P release in the A_2 systems. As can be seen in Fig. 4.20a, the initial NO_x^--N concentration in all SBRs became gradually stable between 2 and 8 mg L^{-1} after they achieved steady operation (only one exceptional point of EE4 on day 61), due to the stable N consumption in the cycles. The small and stable initial NO_x^--N concentration decreased the consumption of HAc by denitrifiers but helped the stable and effective HAc utilisation by DPAOs. Fig. 4.20b demonstrates that HAc consumption by DPAOs is gradually raised with the continuous operation of SBRs, and the amount in all systems becomes increasingly closed. Both the graphs suggested that with the development of enrichment process, HAc was mainly consumed and utilised by DPAOs in the 2-hour anaerobic phase, compared with the low efficiency at the beginning after the inoculation.

As shown in Fig. 4.20c, at the beginning of the enrichment, the ratio of P/HAc by DPAOs in both of NO_3^--N based A_2 SBRs (0.18 in EE1&EE2 and 0.16 in EE7&EE8) was higher than that in NO_2^--N based SBRs (0.07 EE3&EE4 and 0.06 EE5&EE6), suggesting that in this period nitrate was more attractive to the sludge systems in the SBRs. However, in the following days the ratio in all A_2 reactors increased gradually to around 0.4-0.5, which implied that during the enrichment process DPAOs in the A_2 systems obtained higher P release capacity from enhanced polyP storage.

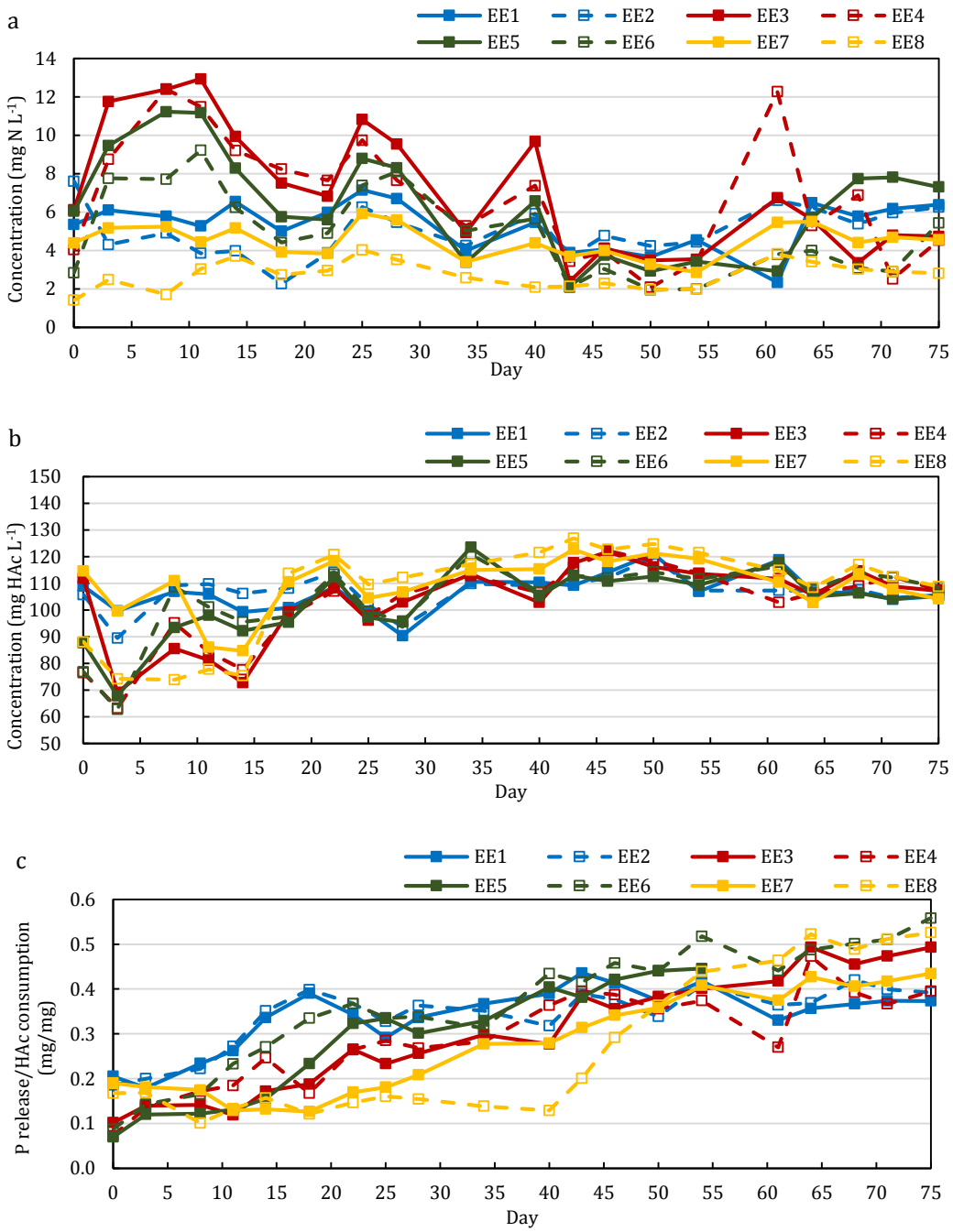

Fig. 4. 20 Average NO_x^--N concentration at cycle beginnings (a), acetic acid amount consumed by DPAOs during anaerobic phase (b) and the ratio of P/HAc by DPAOs (c) in Enrichment II (EE1&EE2: only NO_3^--N with acclimated inoculum; EE3&EE4: only NO_2^--N with acclimated inoculum; EE5&EE6: only NO_2^--N with new inoculum; EE7&EE8: only NO_3^--N with new inoculum)

The P/N ratio in all SBRs during the enrichment process is shown in Fig. 4.21. It revealed that at the beginning of the enrichment, the ratio in all A_2 SBRs was relatively low, at 0.98, 0.26, 0.65 and 0.71 in EE1&EE2, EE3&EE4, EE5&EE6 and EE7&EE8, respectively. With the development of enrichment process, the ratio in the SBRs gradually increased to around

2.00-2.26 in NO_3^--N SBRs and 1.00-1.30 in NO_2^--N SBRs, when the SBRs achieved steady conditions.

In case of the reduction of electron acceptor, 10 mol electrons is accepted by 2 mol NO_3^--N to produce 1 mol gas of N_2. On the contrary, 6 mol electrons is accepted by 2 mol NO_2^--N to produce the same amount of N_2 (with similar principle of Equation (4-1) and (4-2)), inducing that the electron accepting capacity of per mol NO_3^--N is higher than that of per mole NO_2^--N, with the ratio of 5:3. Hence, if the same amount of electron should be obtained by NO_x^--N to accumulate the same amount of PO_4^{3-}-P, lower NO_3^--N amount will be consumed compared with NO_2^--N, which causes higher P/N ratio. In the steady period of the enrichment, the ratio of PO_4^{3-}-P uptake/NO_3^--N consumption was truly higher than the PO_4^{3-}-P uptake/NO_2^--N ratio, closed to 5:3, which suggested that the P uptake in all SBRs was relatively effective and N consumption (especially NO_3^--N) was mostly triggered by DPAOs, without other microbial communities. Namely, the DPAOs in NO_3^--N based SBRs could directly utilise NO_3^--N, without the cooperation of other microorganisms.

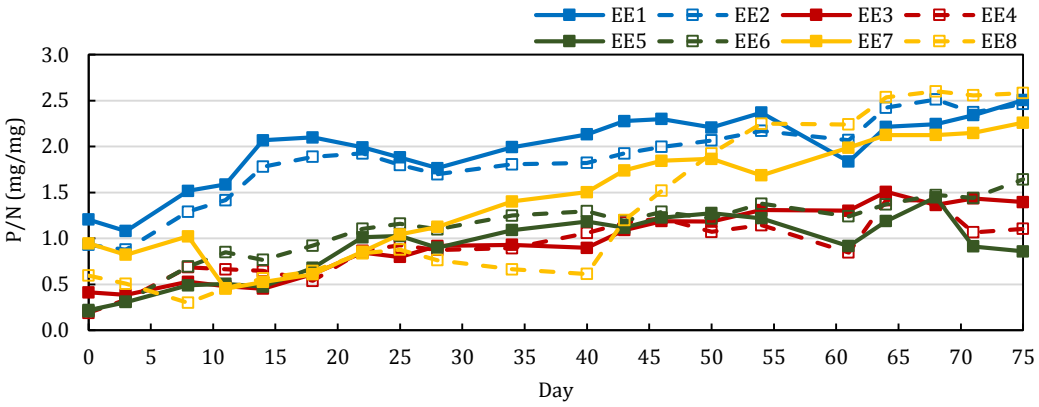

Fig. 4. 21 PO_4^{3-}-P uptake/NO_x^--N consumption ratio in anoxic phase of all SBRs during the Enrichment process II (EE1&EE2: only NO_3^--N with acclimated inoculum; EE3&EE4: only NO_2^--N with acclimated inoculum; EE5&EE6: only NO_2^--N with new inoculum; EE7&EE8: only NO_3^--N with new inoculum)

The data in Fig. 4.22 proves the hypothesis above, presenting the ratio of electron transfer to PO_4^{3-}-P uptake in the anoxic phase of the SBRs during the enrichment process. At the beginning of the acclimation, the ratio in all SBRs was relatively high, up to respectively 11.5, 29.5, 37.4 and 16.6 in EE1&EE2, EE3&EE4, EE5&EE6 and EE7&EE8, due to the ineffective phosphorus accumulation. With the development of the enrichment, the ratio in all SBRs decreased gradually, and finally achieved a comparatively stable range between 4.9 and 6.0. The faster decrease in EE3-EE6 suggested that the status in NO_2^--N based SBRs changed more than NO_3^--N based SBRs, basically caused by the increasing adoption of NO_2^--N by the sludge systems in the SBRs. On the contrary, the decrease of the ratio in

NO_3^--N based SBRs was smoother (especially EE1&EE2, which had been acclimated with NO_3^--N in A_2 conditions in Enrichment process I), indicating that NO_3^--N was more acceptable for both acclimated and new inoculums at the beginning of the enrichment. Nevertheless, both of the inoculums could accept NO_2^--N with the long-period dosing in the enrichment process. Finally, the values in both NO_3^--N and NO_2^--N based systems became approximate with more efficient anoxic P uptake, which also suggested that the acceptance of electron induced the effective P uptake, with very little activities of other microbial groups. As reported by Lochmatter *et al*. (2009), some kinds of DPAOs could only accumulate PO_4^{3-}-P via NO_2^--N, which needed other functional microorganisms (DGAOs) to transfer NO_3^--N to NO_2^--N, inducing useless electron acceptance. Hence, the DPAOs in both of EE1&EE2 and EE7&EE8, which should not be the kind reported by Lochmatter *et al*. (2009), could directly utilise NO_3^--N as electron acceptor, due to the similar e^- transfer/P uptake ratios as EE3-EE6.

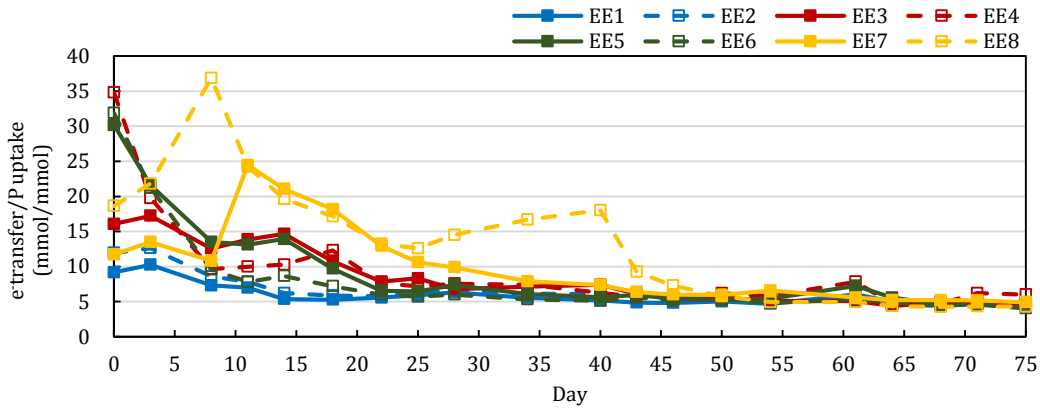

Fig. 4. 22 The ratio of electron transfer to P uptake in anoxic phase of all A_2 SBRs during Enrichment II (EE1&EE2: only NO_3^--N with acclimated inoculum; EE3&EE4: only NO_2^--N with acclimated inoculum; EE5&EE6: only NO_2^--N with new inoculum; EE7&EE8: only NO_3^--N with new inoculum)

In the early period of this enrichment process when P removal performance was not optimistic enough, the utilisation of HAc in NO_2^--N based SBRs was lower than NO_3^--N based SBRs, causing the acetate residual at the beginning of anoxic phase. Fig. 4.23 shows the anoxic P and N concentration change with HAc residual of around 20 mg L^{-1} at the end of anaerobic phase. It indicated that in the first 30 min of anoxic phase, P concentration was still increased from 26.6 mg L^{-1} to 28.5 mg L^{-1}, although NO_2^--N as electron acceptor had started to add into the reactor. As a result, DPAOs would tend to release P and store acetate, rather than accumulate P, if both acetate and electron acceptor existed in the systems. After HAc was consumed completely, DPAOs started to utilise electron acceptor and to accumulate phosphate.

Additionally, as in the early period, DPAOs did not account a large ratio in the activated sludge, the consumption rate of NO_2^--N was not as high as that in the steady period, causing the accumulation of nitrite. In the first 30 min of anoxic phase, due to the existence of HAc, the fast consumption of NO_2^--N should be triggered by the denitrifiers. In conclusion, the P/N ratio consumption was very low, only 0.7 in this cycle.

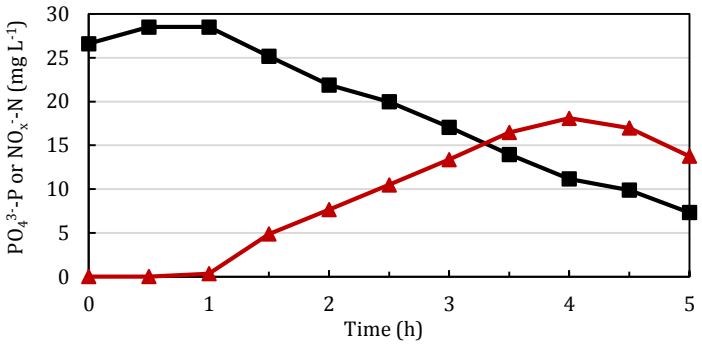

Fig. 4. 23 Typical PO_4^{3-}-P and NO_2^--N concentration change in anoxic phase of NO_2^--N based SBRs in early period of enrichment
(Black circle: PO_4^{3-}-P; Red rhombus: NO_2^--N)

On the contrary, cycle performance of NO_3^--N based and NO_2^--N based SBRs in stable period of Enrichment II is shown in Fig. 4.24, which was more effective. As can be seen in the graphs, HAc could be consumed completely in the first 30 min of anaerobic phase, which was more efficient than the beginning stage and the performance in Enrichment I. On the contrary, the increase of PO_4^{3-}-P concentration was not completed in the first 30 min, but continued in the second 30 min. In other words, P release, which was not completely synchronous with HAc consumption, basically finished in the first hour of anaerobic phase, and there was little change in the second hour.

In anoxic phase when NO_3^--N and NO_2^--N solutions were pumped into the SBRs, PO_4^{3-}-P concentration in both reactors gradually decreased to very low level. In contrast, due to the continuous adding of the solution, the concentration of NO_x^--N in the first four hours of anoxic phase increased slowly, followed by the smooth decrease in the last hour. It suggested that with the decrease of PO_4^{3-}-P concentration, the electron acceptor consumption rate and P uptake rate were reduced gradually, but P removal could also be achieved in the 5-hour anoxic phase.

With the 4-hour dosing, NO_2^--N concentration achieved the maximum at the end of the 4th hour, while the maximum of 12.3 mg L^{-1} was lower than the peak in Fig. 4.23, and did

not induce the toxic inhibition for P uptake. It suggested that with the development of enrichment process, NO_2^--N consumption rate was enhanced, which could avoid abundant nitrite accumulation and toxic inhibition to P uptake, with the employed dosing strength.

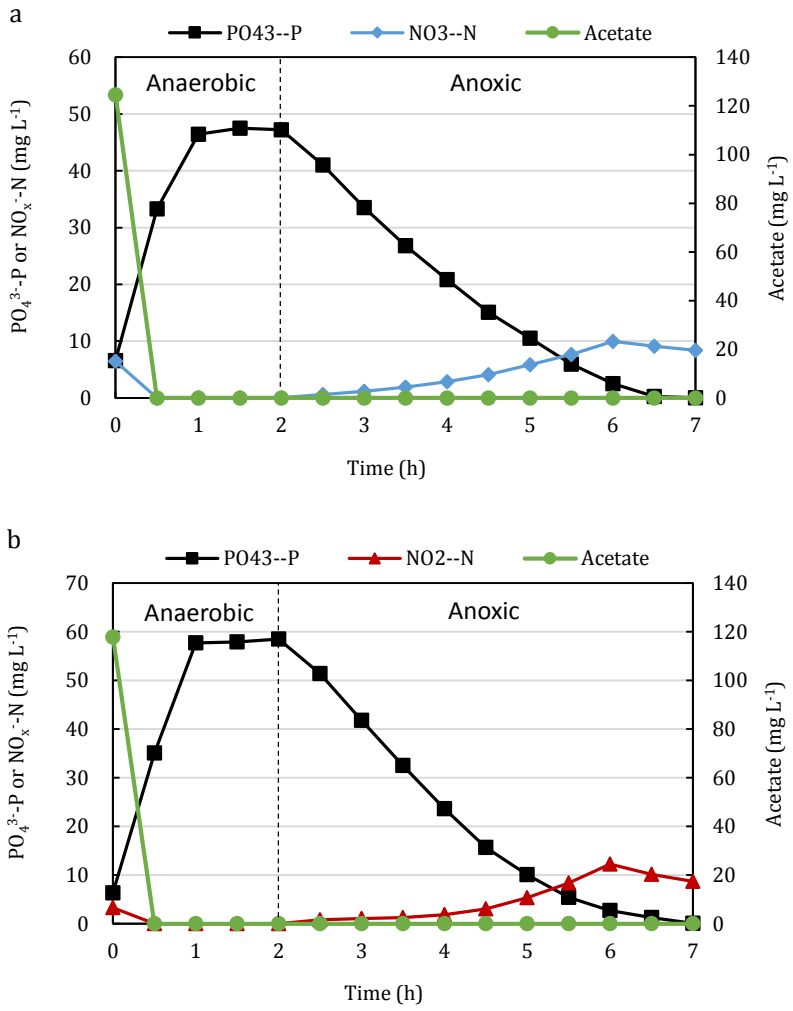

Fig. 4. 24 Cycle performance of NO_3^--N based (a) and NO_2^--N based (b) SBRs in the stable period of Enrichment II process

Fig. 4.25 demonstrates the amount P and N decrease and their ratio in the anoxic phase. As can be seen in the Fig. 4.25a and Fig. 4.25b, there was an increase of P uptake between the first and the second 30 min in both NO_3^--N and NO_2^--N based SBRs, which suggested that DPAOs in both systems needed an adaptation process to change from P release to P uptake process. In the following hour, P uptake rate could achieve a high level, prior to decreasing gradually. In case of NO_x^--N consumption, the rate kept relatively stable in the

early hours, and then reduced smoothly with the decrease of P concentration in the wastewater.

The P/N ratio in NO_3^--N based system kept > 2.0 before the last 30 min, while it was sharply decreased to around 0.3 in the last 30 min due to the tiny amount of PO_4^{3-}-P in the wastewater. The figure of NO_2^--N based system had a similar trend, which was kept between 1.3 and 1.7 in the earlier period, followed by decreasing to lower than 1.0 in the last 1.5 hours. Fig. 4.25c shows the linear trend lines of P/N ratio, with N consumption as x axis and P uptake as y axis. It indicated that the average P/N ratio in the SBRs were around 2.3 and 1.7 separately, which were similar as the ratio of total P uptake to N consumption during the complete anoxic phase (2.10 and 1.50). It implied that there was a proximate linear relationship between P uptake and N consumption during the anoxic phase in both NO_3^--N and NO_2^--N based systems, whether in the complete anoxic phase or most of small time slots.

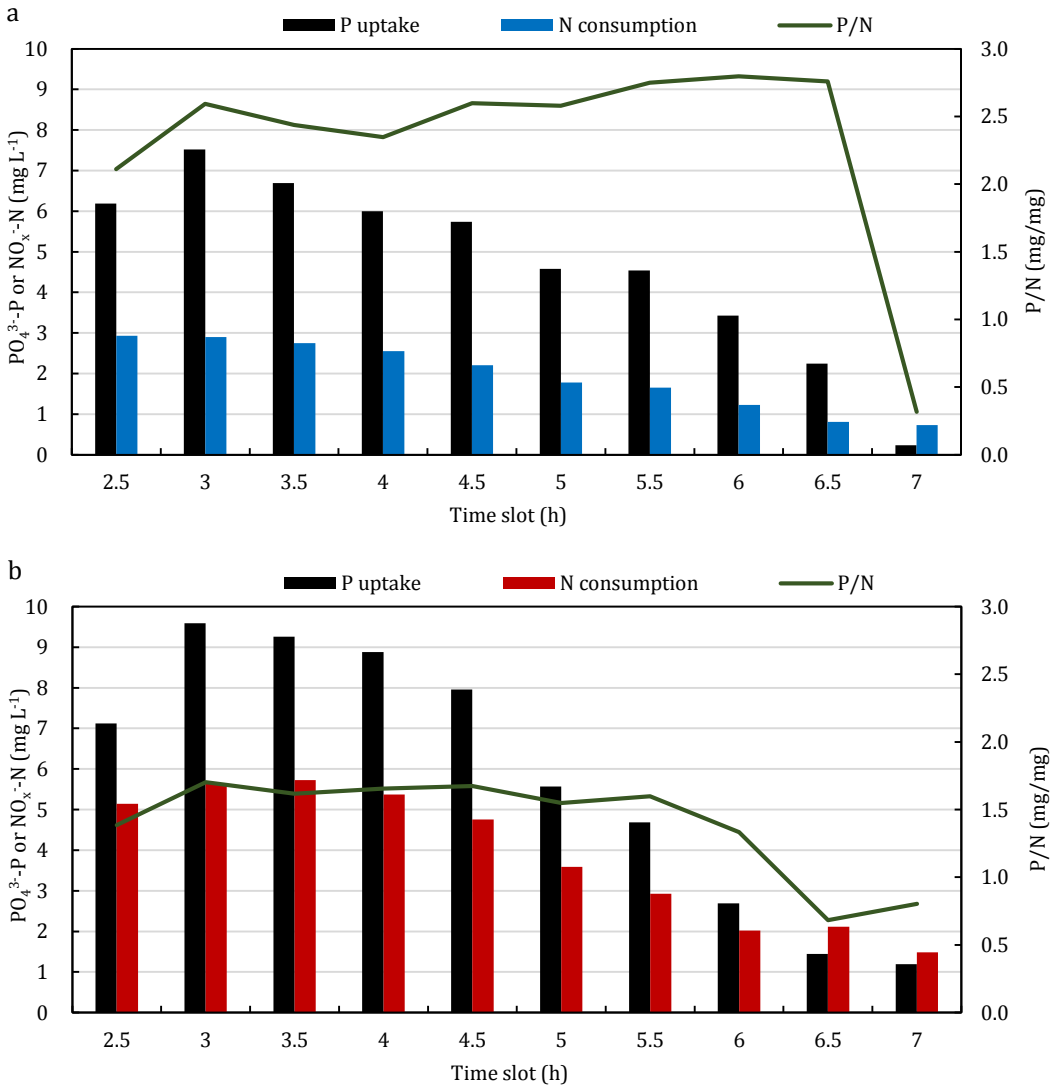

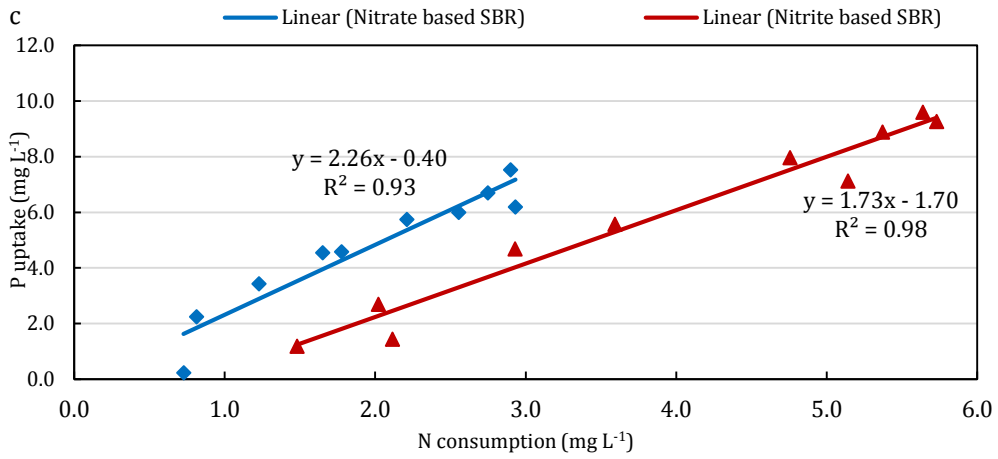

Fig. 4. 25 The comparison of relationship of P uptake and N consumption during anoxic phase of NO_3^--N and NO_2^--N based SBRs in steady period of Enrichment II

In the comparison of the changes of NH_4^+-N concentration in the SBRs between Enrichment I and II, similar trends could be found in the A_2 systems, gradually decreasing from the beginning of anaerobic phase to the end of anoxic phase. At the end of the cycle, there was still NH_4^+-N residual of around 2 mg L^{-1} in the samples of Enrichment I and 5-7 mg L^{-1} in the samples of Enrichment II, indicating that the NH_4^+-N amounts provided in the feedstock of both the enrichment processes were adequate for the growth of the activated sludge, which would not restrain the activities of DPAOs in A_2 SBRs.

During the period of Enrichment II process, the change of MLSS and MLVSS in EE1&EE2, which increased gradually with small fluctuations, was different from the other SBRs, which decreased in the early period and then increased in the middle period, followed by keeping relatively stable in the later period. The reason causing the difference should be that the conditions in Enrichment I and II was similar for EE1&EE2 and E1&E2, where the only change was the dosing rate of NO_3^--N, while the activated sludge in other SBRs experienced more condition alteration. Hence, the increase of solids in EE1&EE2 were smoother, compared with the other SBRs where the sludge systems needed to adapt the variation of acclimation conditions. Finally, the MLSS and MLVSS in all SBRs fluctuated at 1200-1400 mg L^{-1} and 800-1000 mg L^{-1}, separately.

For the percentage of MLVSS accounting for the total MLSS, the ratios in all SBRs were around 85% at the beginning of the enrichment process, decreasing to around 60-70% in the later period (closed to the ratio in the A_2 SBRs in Enrichment I), as shown in Fig. 4.26. Hence, the ash content ratios in the samples increased from around 15% to 35%,

suggesting the accumulation of polyP and DPAOs in the sludge, which was similar with the results in section 4.2.1.

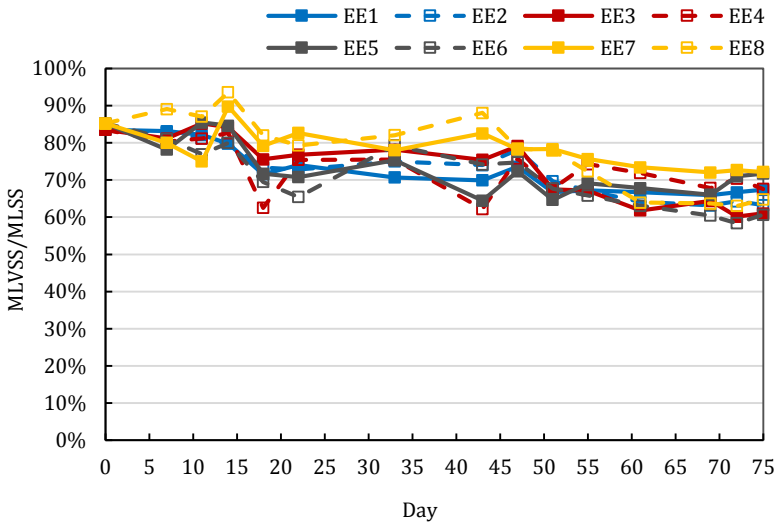

Fig. 4. 26 MLVSS/MLSS ratio in all A_2 SBRs during the Enrichment II (EE1&EE2: only NO_3^--N with acclimated inoculum; EE3&EE4: only NO_2^--N with acclimated inoculum; EE5&EE6: only NO_2^--N with new inoculum; EE7&EE8: only NO_3^--N with new inoculum)

4.3.2 Microbial community analysis of Enrichment II

Sludge samples of EE1&EE2, EE3&EE4, EE5&EE6 and EE7&EE8 were detected for microbial community analysis for the Enrichment II process. 360423, 402413, 266725 and 462217 effective reads were detected in the samples, where *Proteobacteria* was still the most dominating phylum, followed by *Bacteroidetes*, *Planctomycetes*, *Chloroflexi*, *WPS-2*, *Acidobacteria*, *Verrucomicrobia*, *Patescibacteria*, *Firmicutes*, *Actinobacteria*, *Chlamydiae*, *Spirochaetes*, *Cyanobacteria*, *Gemmatimonadetes*, *Armatimonadetes*, *Nanoarchaeaeota*, *Deinococcus-Thermus*, *etc*.

4.3.2.1 Microbial community similarity

390 genera were effectively detected among the four samples, and the numbers in each sample were 228, 185, 246 and 250, respectively. A Venn diagram (Fig. 4.27) was adopted in the similarity comparison of genus among the four enriched sludge samples. The common genera among the four samples was 100, accounting for 25.6% of the total 390 genera. In the samples of EE5&EE6 and EE7&EE8, the genus number unique to individual community were 43 and 52, higher than that in EE1&EE2 and EE3&EE4 samples, due to the shorter acclimation duration of new inoculum. As can be seen in Table 4.3, the

common genera among EE3&EE4 and other sludge samples were relatively smaller, suggesting that with the long acclimation period with different operation conditions, the microbial community in EE3&EE4 became more concentrated. However, compared with other SBRs, they still had more common genera (149) with EE5&EE6, which were also NO_2^--N based SBRs. On the contrary, EE1&EE2 had the most common genera (169) with EE7&EE8, because of their mutual acclimation conditions.

Based on the Anova test, the similarity of sludge with same electron acceptors were higher than that among different electron acceptors. Additionally, the sample from EE7&EE8 had the more similarity with the seed, which was from the inoculum from 4-stage Bardenpho process.

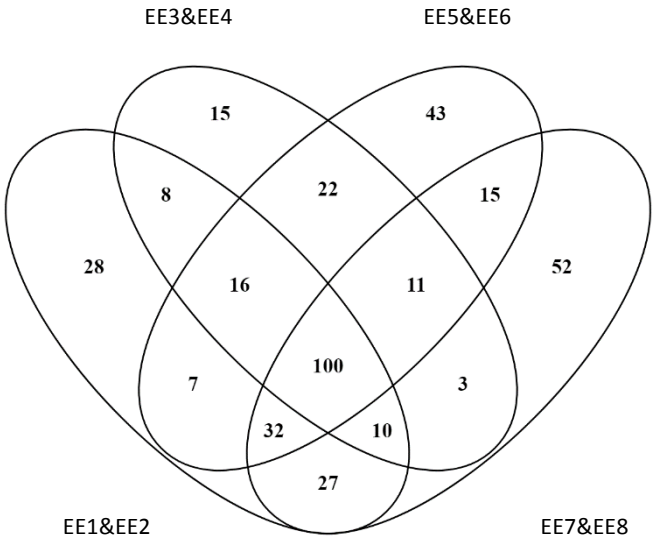

Fig. 4. 27 Venn diagram based on genus of different P removal sludge in Enrichment II (EE1&EE2: only NO_3^--N with acclimated inoculum; EE3&EE4: only NO_2^--N with acclimated inoculum; EE5&EE6: only NO_2^--N with new inoculum; EE7&EE8: only NO_3^--N with new inoculum)

Table 4. 3 Number of common genera between samples based on Venn diagram (EE1&EE2: only NO_3^--N with acclimated inoculum; EE3&EE4: only NO_2^--N with acclimated inoculum; EE5&EE6: only NO_2^--N with new inoculum; EE7&EE8: only NO_3^--N with new inoculum)

	EE3&EE4	**EE5&EE6**	**EE7&EE8**
EE1&EE2	134	155	169
EE3&EE4	--	149	124
EE5&EE6	--	--	158

4.3.2.2 Microbial community structure and functional populations

Similar acclimation results with Enrichment I were found in all A_2 SBRs, where *Proteobacteria* was the most abundant phylum. Due to the long term of enrichment of EE1-EE4, the ratio of *Proteobacteria* achieved 78.5% and 82.9% in EE1&EE2 and EE3&EE4, respectively, while the ratio in EE5&EE6 and EE7&EE8 were relatively lower, increasing to 69.0% and 69.1%, from 24.6% in the inoculum. The classes of *γ-proteobacteria* and *α-proteobacteria* in *Proteobacteria* accounted the majority in the whole population (totally 77.1%, 82.6%, 68.0% and 68.8%, separately) in all acclimated P removal sludge among EE1-EE8, much higher than that in the inoculum (only 22.4% in total). As can be seen in Fig 4.28, except *Proteobacteria related classes, Bacteroidia*, the most abundant class in inoculum (27.8%), was decreased to 2.4%, 10.4%, 24.7% and 10.4% in EE1&EE2, EE3&EE4, EE5&EE6 and EE7&EE8, separately. On the contrary, *γ-proteobacteria* was increased from 10.4% to 50.1%, 52.5%, 39.1% and 30.6%, and *α-proteobacteria* was increased from 11.9% to 27.1%, 30.1%, 28.9% and 38.3%, respectively. In addition, the following frequent classes in acclimated sludge were separately *Metagenome* (2.3%-7.4%, average value was 3.7%), *Planctomycetacia* (0.6%-6.2%, average value was 2.0%), *Verrucomicrobiae* (0.3%-6.5%, average value was 2.0%), *Anaerolineae* (0.6%-3.2%, average value was 1.9%), *δ-proteobacteria* (0.3%-1.0%, average value was 0.6%), *Ignavibacteria* (0.1%-0.8%, average value was 0.4%) and *Actinobacteria* (0.1%-0.2%, average value was 0.1%). Except the dominated classes, other classes accounted 0.9%-7.0% in the microbial population in EE1-EE8, decreased from 22.7% in the inoculum, which suggested that some microbial classes were washed out from the sludge during the acclimation process.

In the class of *γ-proteobacteria*, *β-proteobacteriales* was the dominant order, which accounted for 99.7%, 93.9%, 71.1% and 96.9% of *γ-proteobacteria* in the four enriched EBPR systems, higher than 68.9% in the seed. In NO_2^--N based SBRs, the ratio was relatively lower than the NO_3^--N based SBRs, which was mainly caused by the frequent existence of *Xanthomonadales* (very common in wastewater treatment works, reported by Lim *et al*., 2012 and Atashgahi *et al*., 2015), another order belonging to *γ-proteobacteria*. In the inoculum, *Xanthomonadales* was a kind of abundant order, accounting for 14.6% in *γ-proteobacteria*. After the acclimation process, the ratio in the four sets of SBRs were 0.1%, 5.9%, 28.7% and 2.4%, while the higher ratio in NO_2^--N based SBRs did not negatively influence the anoxic P removal performance.

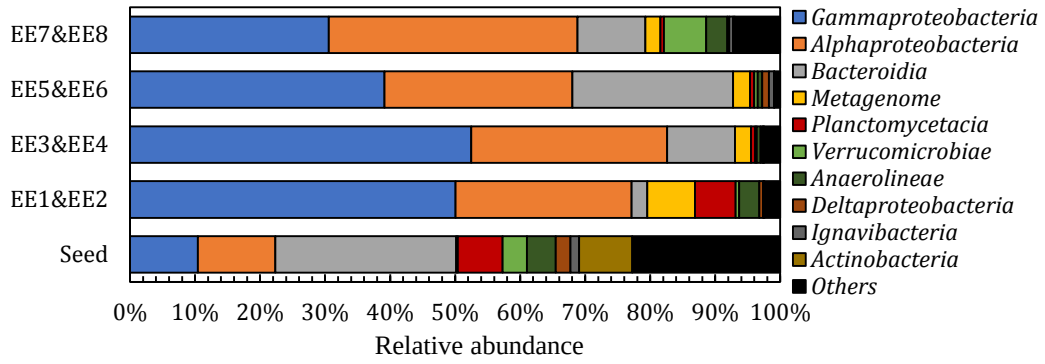

Fig. 4. 28 The relative abundances of classes in the acclimated sludge samples in Enrichment II compared with inoculum (EE1&EE2: only NO_3^--N with acclimated inoculum; EE3&EE4: only NO_2^--N with acclimated inoculum; EE5&EE6: only NO_2^--N with new inoculum; EE7&EE8: only NO_3^--N with new inoculum)

Fig. 4.29 shows the most abundant 16 genera detected in the sludge sample of the four pairs of A_2 SBRs, compared with the inoculum. The 16 genera belonged to *Proteobacteria* (including 6 genera in *β-proteobacteriales* and 5 genera in *α-proteobacteria*), *Bacteroidetes* (3 genera), *Chloroflexi* (1 genus) and WPS-2 undescribed phyla (1 genus), respectively.

Among the *β-proteobacteriales* in all SBRs, the majority genera were *Rhodocyclaceae* related, except *Simplicispira* (a kind of *Burkholderiaceae*) found in all NO_2^--N SBRs. The most abundant *Rhodocyclaceae* related genus was *Rhodocyclaceae*_unknown (the same one as that in Enrichment I), accounting for 14.7%, 5.0%, 4.8% and 12.9% (averagely 9.3%) in the samples of enriched DPAO sludge. The ratios were obviously lower than that in Enrichment I, due to the increase of other *Rhodocyclaceae* related genera and *Simplicispira*. The second and third enriched *β-proteobacteriales* genera among the samples were *Dechloromonas* and *Sulfuritalea*, accounting for 7.9% and 7.0%, separately, while they were respectively the predominate genera in EE3&EE4 and EE1&EE2. It suggested that with the change of A_2 conditions and continuous acclimation, the acclimated inoculum experienced some alternation of microbial communities. *Simplicispira* was the fourth frequent genus among *β-proteobacteriales* in the samples, which was only found in NO_2^--N based SBRs (12.9% in EE3&EE4 and 5.3% in EE5&EE6). The last two abundant *β-proteobacteriales* were *Denitratisoma* and *Candidatus Accumulibacter*, which occupied 2.2% and 0.3%, averagely among the acclimated samples.

The second abundant microbial group was *α-proteobacteria*, including *Rhizobiales* (*e.g. Phreatobacter*) and *Rhodobacterales* (e.g. *Gemmobacter*), similar with the results in the

Enrichment I. *Phreatobacter* was one the most abundant *α-proteobacteria* among the acclimated sludge samples, while the ratio in NO_3^--N based SBRs (averagely 15.8%) was much higher than that in NO_2^--N based SBRs (averagely 1.8%), suggesting that it was more adaptable in nitrate dominating environment.

Bacteroidetes was the most dominant group in the inoculum (accounting for 29.2%), decreasing to the second abundant phylum in all the acclimated sludge samples after the enrichment process. The predominant genera of *Bacteroidetes* in EE1-EE8 were *Flavobacterium* (3.8%, averagely), *Sediminibacterium* (1.8%, averagely) and *Saprospiraceae_uncultured* (0.7%), respectively. The other two relatively abundant microbial groups in the enriched samples were *WPS2*-related *metagenome* and *Chloroflexi*-related *wastewater metagenome*, accouting for 2.6% and 0.6% averagely.

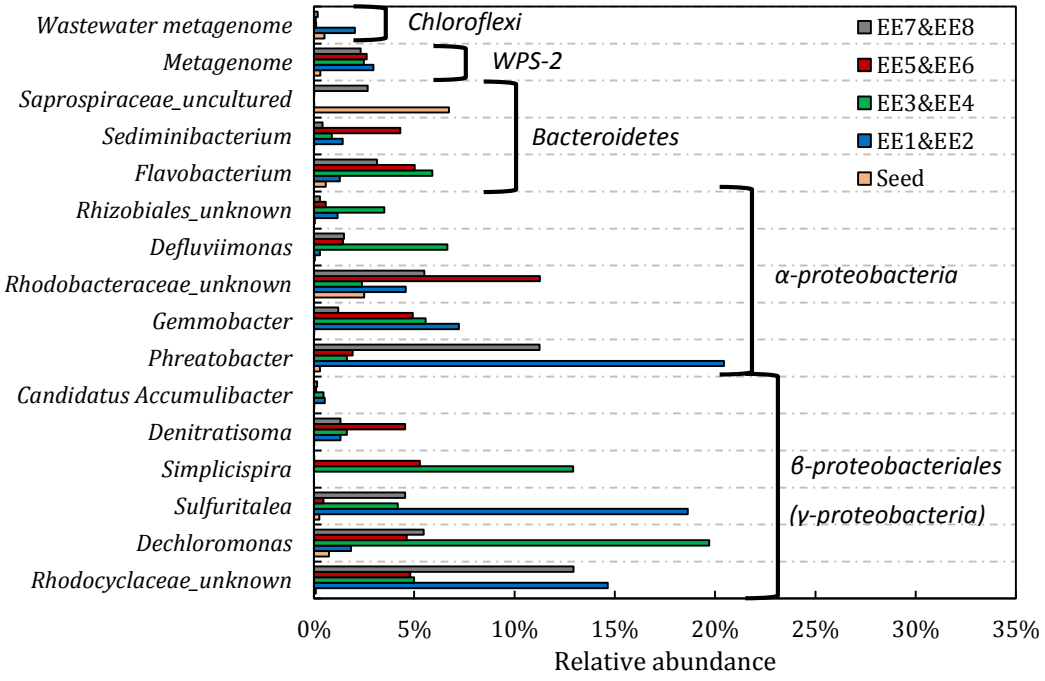

(a)

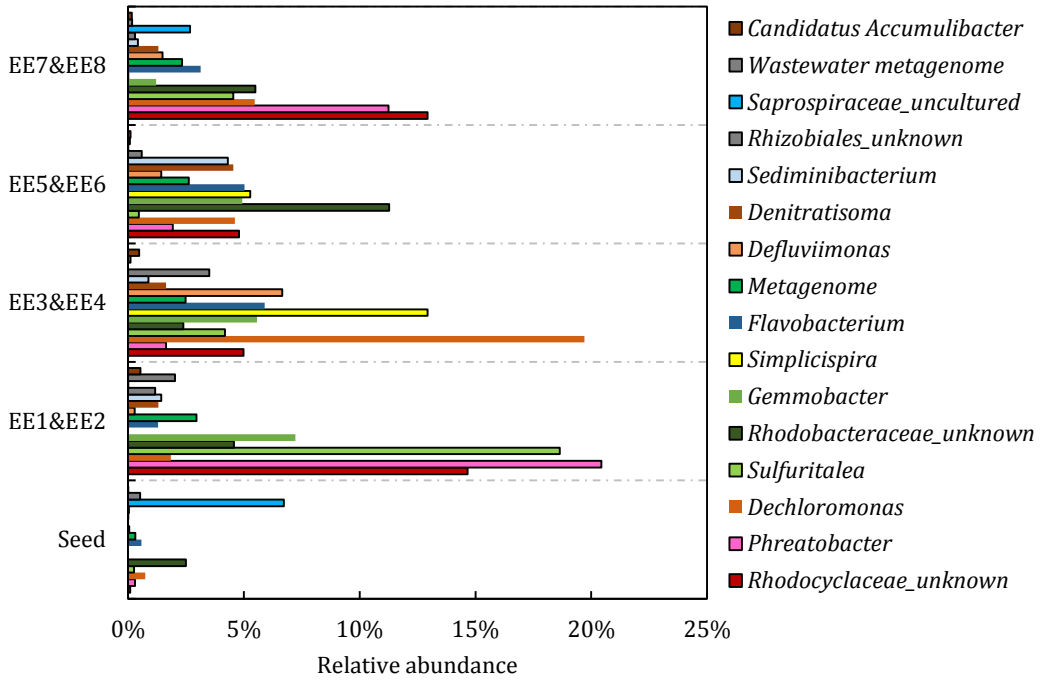

(b)

Fig. 4. 29 The relative abundances of the dominant groups in enriched sludge samples compared with the inoculum sample at genus level (EE1&EE2: only NO_3^--N with acclimated inoculum; EE3&EE4: only NO_2^--N with acclimated inoculum; EE5&EE6: only NO_2^--N with new inoculum; EE7&EE8: only NO_3^--N with new inoculum)

As recognised as the main functional groups in denitrifying P uptake in EBPR systems, Table 4.4 listed the ratios of detected *Rhodocyclaceae*-related genera in all A_2 SBRs in Enrichment II. As can be seen, except the genera discussed above, there were still the little existence of *Azospira, Candidatus Accumulibacter and C39- Rhodocyclaceae* in the sludge samples. However, they were not abundance enough to support for P removal, especially *Candidatus Accumulibacter*, the most frequently reported PAOs in EBPR systems.

Table 4. 4 The relative abundance of *Rhodocyclaceae*-related genera in the samples (detected in all of EE1-EE8) of Enrichment II

	Seed	**EE1&EE2**	**EE3&EE4**	**EE5&EE6**	**EE7&EE8**
Rhodocyclaceae_unknown	0.1%	14.7%	5.0%	4.8%	12.9%
Dechloromonas	0.7%	1.9%	19.7%	4.6%	5.5%
Sulfuritalea	0.3%	18.6	4.2%	0.5%	4.5%
Denitratisoma	0.001%	1.3%	1.6%	4.5%	1.3%
Azospira	--	0.1%	3.9%	1.7%	0.9%
Candidatus Accumulibacter	0.005%	0.5%	0.5%	0.1%	1.9%

C39	0.005%	0.7%	0.1%	0.8%	--

4.4 Discussion

An important point should be discussed is the synthetic wastewater (influent) applied in this study. The components in the synthetic wastewater were not completely designed to simulate practical municipal wastewater. Firstly, the carbon source applied in the synthetic wastewater was acetate (NaAc and HAc), which was not the main carbon content in actual municipal wastewater. However, since acetate is the most common carbon source selected for EBPR systems, it is also utilised in this study to achieve effective treatment performance. Secondly, the concentration of NH_4^+-N in the influents (around 12-15 mg L^{-1}) was lower than the actual values in municipal wastewater, as the NH_4^+-N in the influent was only used for the growth of microbial communities and NO_x^--N used for P uptake was from the external dosing. As a result, the COD: N: P ratio was depended on the performance of the EBPR systems in the experiments, while it could be adjusted with extra acetate or NO_x^--N dosing, if the ratio in actual municipal wastewater was not consistent with the values in the experimental studies. Specifically, the relatively low COD (around 250 mg L^{-1}) in the synthetic wastewater of main sections was determined to inhibit GAOs, 12 mg L^{-1} PO_4^{3-}-P was applied to achieve similar phosphorus concentration in practical wastewater (Metcalf and Eddy, 2003).

As the start-up stage of wastewater treatment process, the enrichment of functional microbial communities was an essential and important step. In case of A_2 EBPR systems, DPAOs are the mainly purposeful organisms, utilised for anoxic PO_4^{3-}-P and NO_x^--N removal. Since the preliminary experiments had verified that the RAS from 4-stage Bardenpho process could be used in DPAO enrichment, the operation of Enrichment I was the following process, to explore the appropriate SRT, C/P/N ratio, the possibility of acclimation with only A_2 conditions and the influence of the existence of NO_2^--N on the enrichment , in order to achieve the successful P removal in Enrichment II.

SRT was a basic factor influencing the growth rate of microbial groups in the systems, which affected anaerobic P release and anoxic P uptake efficiency. After experiencing the reduction of SRT from 15 days to 10 days, the HAc and NO_x^--N consumption was increased immediately, inducing the improvement of electron acceptor adding. Even though the SRT

strategies in the previous studies ranged from 3.8 days to 20 days, 10 days was the optimised period for these studies, which was also used in Enrichment II. As it had been discussed in Chapter 2, the SRT utilised in the previous studies varied from 3 to 20 days, and longer SRT was suggested for the operation of A_2 EBPR process, 20-day SRT was selected in the preliminary experiments. However, effective phosphorus removal was not achieved with SRT of 20 days or 15 days, while the 10-day SRT was appropriate in the P removal system enrichment and stable operation processes. Compared with the performance of A_2 SBRs in Enrichment I Stage 1, the performance in Stage 3 was enhanced obviously, with rapid increase of P release and uptake, even though there were also slight P release and uptake in Stage 1. The COD and PO_4^{3-}-P concentrations in the influent were similar to the values of Dai *et al*. (2017b), only the concentration of NO_x^--N was lower, while the residuals of NO_x^--N in Fig 4.8a suggested that the nitrogen level was enough for the operation of the system. Hence, it indicated that the enrichment performance in this study was much lower than the performance of Dai *et al*. (2017b) with the same conditions of SRT, COD and PO_4^{3-}-P concentrations, *etc*. The reason causing the difference may be the different inoculum used for the acclimation. The most abundant microbial groups in the seed sludge of Dai *et al*. (2017b) were *β-proteobacteria* and *Bacteroidetes*, accounting for around 30% and 26%, while the percentages of *β-proteobacteria* and *Bacteroidetes* were separately lower than 10% and around 30%. Consequently, shorter SRT was more effective for the enrichment to induce the faster growth of functional microbial groups in the systems. Although it suggested that longer SRT was more appropriate for A_2 EBPR, the 10-day SRT was proved that it was optimised for the operations in this study, which was the same as the study of Gurtekin *et al*. (2011).

Electron acceptor was another key factor that directly participated in P removal. As demonstrated in Fig. 4.7, the P removal performance in A_2 SBRs reduced with the ratio increase of NO_2^--N portion in dosed electron acceptors. The cycle analysis (Fig. 4.16) and the tests in section 4.2.2 suggested that the reason causing the result in Fig. 4.7 was not the inhibition form nitrite, but the amount shortage of electron acceptor in E4-E6. Thus, the tests in section 4.2.2 explored the potential of the feasibility of P uptake via NO_2^--N pathway, determined the proper amount of electron acceptors added into the SBRs and confirmed the importance of pH control.

The C/P/N ratio can be separated to COD/PO_4^{3-}-P ratio and P /N ratio. The COD/PO_4^{3-}-P ratio utilised in the enrichment processes and stable operation period was around 20, which was closed to the figure of Dai *et al*. (2017b). As discussed in Chapter 2, relatively

low C/P ratio was more appropriate for the inhibition of growth of GAOs to promote the enrichment of PAOs. In the analysis of P release, the initial HAc content could induce around 40-55 mg L^{-1} of PO_4^{3-}-P increase, which affected the adding amount of NO_x^--N for P uptake. Based on the results of the Enrichment I and II, the ratios of PO_4^{3-}-P/NO_3^--N and PO_4^{3-}-P/NO_2^--N were respectively around 2.0 mg/mg (0.90 mmol/mmol) and 1.2 mg/mg (0.54 mmol/mmol), with the initial concentrations of PO_4^{3-}-P, NO_3^--N and NO_2^--N were around 6, 27-30 and 45-48 mg L^{-1}. Hence, it proved that the nitrogen dosing for the A_2 SBRs in Enrichment I was not enough for E3-E6, inducing the worse performance than E1 & E2. However, in the study of Dai *et al*. (2017b), the nitrogen dosing concentration for each A_2 SBRs was the same (45 mg L^{-1}), which removed around 25 mg L^{-1} PO_4^{3-}-P with around 40 mg L^{-1} NO_x^--N. The P/N ratio of 0.63 was much lower than the ratios in this study, suggesting the P uptake efficiency was relatively higher. In the research of Peng *et al*. (2011), 60 mg L^{-1} PO_4^{3-}-P was removed by 60 mg L^{-1} NO_2^--N, which was closed to the ratio in this study. Compared with nitrite based P uptake in the study of Peng *et al*. (2011), the less PO_4^{3-}-P and NO_2^--N were consumed in Enrichment II inducing lower P and N decrease rate in the later period of the cycle. As a result, combined with the other conditions (HRT, SR, pH and so on), the appropriate ratios of COD/PO_4^{3-}-P/NO_3^--N and COD/PO_4^{3-}-P/NO_2^--N were around 125/6/27 and 125/6/45, where the ratio of NO_3^--N to NO_2^--N was around 3/5.

In case of temperature, it had been reported that high-temperature environment was more suitable for the growth of GAOs, which would be restrain the activities of PAOs (Carlos *et al*., 2009). In the results of Enrichment I, the P removal performance of NO_3^--N based and A/O SBRs was more seriously affected by temperature increase than others. Hence, the decline might be influenced by the higher growth of GAOs in the SBRs, since GAOs were more attractive to NO_3^--N and oxygen as electron acceptor, rather than NO_2^--N.

Duration the process of Enrichment II, sufficient amount of nitrogen was dosed into the SBRs of NO_2^--N based systems. Based on the performance of the tests in 4.2.2, long-period dosing was adopted to avoid toxic inhibition of nitrite. As a result, the P removal performance in A_2 SBRs in Enrichment II was generally better than that in Enrichment I, especially for the NO_2^--N based systems that had faster enrichment period and more effective P removal. Furthermore, based on the comparison between nitrate and nitrite based DPAOs enrichment, the process with NO_2^--N as the electron acceptor new inoculum was faster and more effective than NO_3^--N, suggesting nitrite was more appropriate for

the acclimation of DPAOs if the dosing strength was lower than the threshold. The outcome was similar with the result of Dai *et al*. (2017b), in which the enrichment process with highest NO_2^--N/NO_3^--N ratio (0.3) could achieve the stable condition in the shortest period.

One common result of both Enrichment I and II was that the ratio of MLVSS/MLVSS in A_2 systems decreased to 60%-70%, suggesting the P accumulation was achieved in all of the DPAO sludge. The discharged sludge with P accumulation could be utilised in other process to achieve phosphorus recycling.

The long-period dosing of electron acceptor was a smooth way to avoid nitrite or FNA accumulation and toxic inhibition of P uptake. Compared with other approach, such as real-time pulse-dosing (reported by Peng *et al*., 2011), it was more appropriate in continuous flow of practice WWPT operation.

As discussed above, it suggested the microorganisms could directly utilise NO_3^--N as electron acceptor in the relevant SBRs, due to the relationship of P /N ratios in NO_3^--N and NO_2^--N based systems. Based on the results of microbial community analysis, the main biological groups in the EBPR systems belonged to *β-proteobacteriales* and *α-proteobacteria*, while *Candidatus Competibacter*, which was mostly reported as common GAOs, was hardly detected in all enriched EBPR sludge.

In the analysis of microbial communities, the quantification was based on the relative abundances of DNA sequences of bacteria in the sludge samples combined with high-throughput sequencing (HTS), QIIME 2 package and Silva database, which induced some limitation in the analysis. Compared with biovolume analysis via FISH, relative abundances of DNA sequences cannot detect visual distribution of DPAOs in the sludge. Furthermore, the result of HTS is easily influenced by the biases during DNA extraction (Guo and Zhang, 2013), error rate of enzymatic amplification, and insufficient chemical reactions. For instance, the accuracy of taxonomic classification may be influenced by the short-length 16S rRNA amplicons (Liu *et al*., 2016), which will affect the calculation of relative abundance and the analysis result of DPAO communities. Hence, based on the limitation of the DNA analysis, some biases may be induced. The unknown *Rhodocyclaceae*-related genera had been found that it was the most abundant group in the sludge systems of Enrichment I, while it was not clear that whether it belonged to any other genera (i.e. *Dechloromonas*, *Accumulibacter*, *etc*). As a result, although the result

of DNA analysis did not find *Accumulibacter*, there might be the existence of *Accumulibacter* in the A_2 systems.

Within *Accumulibacter*, two types (I and II) had been recognised in EBPR processes (He *et al*., 2007; Peterson *et al*., 2008), while both of them were not obviously detected in the enriched phosphorus removal systems. As discussed above, there was little *Accumulibacter* detected in the sludge samples of Enrichment II, but the sequencing method did not recognise which clade they are. Based on the reports by Flowers *et al*. (2009), clade IA had the capacity to couple NO_3^--N reduction and PO_4^{3-}-P uptake, and both of them could conduct NO_2^--N reduction (Flowers *et al*., 2013). Hence, it was probable that unrecognised *Rhodocyclaceae*-related genera in Enrichment I was a clade of *Accumulibacter* IA, while it was gradually replaced by *Dechloromonas* during Enrichment II.

The SILVA database is a comprehensive resource of rRNA gene sequences, while there are still some limitations which influenced the analysis results of the microbial communities. Firstly, the taxonomic changes of SILVA can be proposed with the development of studies, which may induce that the target microbial groups are classified into different ranks. *Betaproteobacteria*, for instance, was a class in the old databases, while now an order of *Gammaproteobacteia*. Secondly, the classification of the database is mainly based on some authoritative resources, there are some deviations existing from the original classifications (Quast *et al*., 2013).

Hence, it suggested that the majority of dominating microbial groups in the enriched sludge systems were functional organisms, mostly including *Rhodocyclaceae*-related genera (e.g. the unknown *Rhodocyclaceae* genus or *Accumulibacter*, *Dechloromonas*, *Sulfuritalea*, *etc*.), *Rhodobacterales*- and *Rhizobiales*-related genera (e.g. *Phreatobacter*, *Gemmobacter*, the unknown *Rhodobacterales* genus, *etc.*). More discussion about the microbial communities of acclimated sludge in A_2 systems was conducted in next chapter, where the effects of temperature and pH on A_2 systems were investigated.

4.5 Summary

With the successful enrichment of DPAO sludge for A_2 EBPR systems without any aerobic phases, especially in Enrichment II, P removal from the synthetic wastewater was

achieved, with the appropriate factors and optimised conditions. Overall, the below points of conclusion could be summarised:

- The A_2 EBPR systems with a 10-day SRT can achieve successful DPAO enrichment, rather than longer SRTs.
- The appropriate HAc/PO_4^{3-}-P/NO_x^--N ratios for A_2 sludge via nitrate and nitrite pathways are different, separately around 125/6/27 and 125/6/45, with the ratio of NO_3^--N:NO_2^--N of 3:5.
- With the same conditions, NO_2^--N based DPAO enrichment can be achieved faster than that based NO_3^--N.
- After achieving the stable stage, NO_2^--N based A_2 SBRs have more successful and stable P removal performance than NO_3^--N based SBRs.

The main functional microbial groups in these A_2 EBPRs were some *Rhodocyclaceae*-related genera, including *Dechloromonas*.

Chapter 5 Effects of dosing strategy, temperature and pH on the process performance of NO_2^--N based denitrifying P removal

Based on the successful enrichment of DPAOs in A_2 SBRs, it is of importance to conduct specific investigations about anoxic phosphorus removal via NO_2^--N pathway, especially exploring the threshold value of NO_2^--N concentration and the maximum of NO_2^--N dosing rate, in order to avoid the possibility of toxic inhibition, explore the P uptake and N consumption efficiencies and optimise the practical operation process of EBPR systems.

In addition, the impacts of temperature and pH on the process performance of NO_2^--N based A_2 SBRs, which were both important environmental factors, were investigated to explore the appropriate operation condition for the P removal systems in practice. As discussed in Chapter 2, there are research gaps in these aspects.

In summary, the studies in this chapter will be discussed the appropriate conditions including the feeding approach of NO_2^--N, temperature and pH in nitrite-based EBPR systems, to provide the optimised operation control for practical treatment process.

5.1 Effects of NO_2^--N doing strategy on phosphorus removal performance of A_2 SBRs

As demonstrated in Chapter 4, denitrifying phosphorus removal in A_2 SBRs achieved high phosphorus removal efficiency of >95% when nitrite was used as sole electron acceptor, with the DPAOs enriched reactors. More strategies could be developed to explore more effective phosphorus uptake performance, detect the toxicity effects of excess NO_2^--N, and optimise SBR operation design. According to the Monod-type equation, the consumption rate of phosphorus should be related to the concentration of PO_4^{3-}-P. In addition, due to the potential of nitrite based anoxic P uptake in the previous results of Enrichment I&II and literature review, appropriate NO_2^--N dosing strategies should be applied to achieve efficient P removal. Thus, an important hypothesis of this section was that the P uptake efficiency was related to the P concentration in the wastewater, which could induce the change of the threshold of NO_2^--N concentration, if MLSS was relatively stable in the EBPR system. Hence, different dosing strategies (constant-rate dosing,

reducing-rate dosing and single pulse dosing) were conducted in the acclimated A_2 EBPR systems.

In this section, the experiments were operated in the SBRs with enriched DPAOs. NO_2^--N solution dosing was conducted with different strategies in anoxic phase, namely constant-rate dosing with 5h, 4h, 3h, 2h and 1h, reducing-rate dosing and single-pulse addition at the beginning of anoxic phase. Among the tests, 4-h test, which was run as general operation of the reactors from Enrichment II, was conducted in EE3 after the enrichment (Day 64 in section 4.3), before the temperature increase (3.3.2), as the performance of EE3, EE5 (renamed as D2) and EE6 (renamed as D1) was basically the same at that time. 3-h, 2-h and 1-h constant rate dosing tests and reducing tests (T_a & T_b) were conducted in D1 on Day 15, Day 48, Day 49, Day 41 and Day 43. 5-h test was conducted in E3 after the Enrichment I (Day 159 in section 4.2), as a comparison to the tests with shorter duration tests (1-4 h tests). Single-pulse test was conducted in D2 on Day 49.

Fig. 5.1 shows the P release and uptake performances of D1 and D2 during the period of the dosing strategy tests. As can be seen in the figure, the PO_4^{3-}-P concentration results at the beginning of the cycles, the end of anaerobic phases and the end of the cycles had some fluctuation in the stable period, where some of them were from the accidental operation (due to the fails of pH control in some cycles) or the change of pH value, and some were from the results of the dosing tests. However, both of D1 and D2 kept relatively high PO_4^{3-}-P removal performance (>90%) in the duration of the testing period.

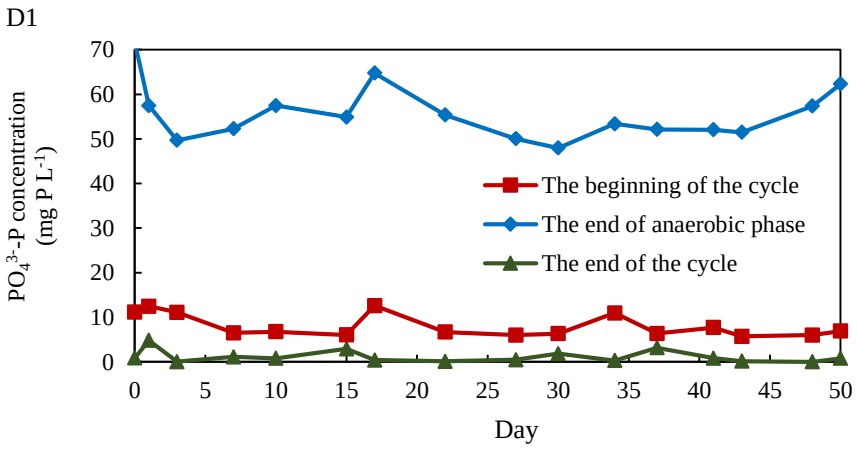

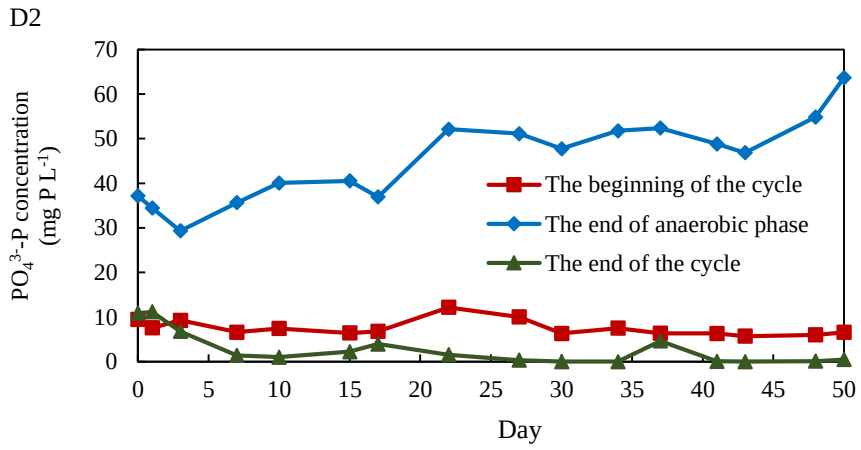

Fig. 5. 1 PO_4^{3-}-P release and uptake performance of D1 and D2 in the experimental period

5.1.1 Phosphorus removal performance with different NO_2^--N dosing strategies

5.1.1.1 Constant-rate dosing strategies

Since constant-rate dosing strategy that had been used in the enrichment process, was easier to control in experimental operation, it was firstly selected in the study. 4-hour dosing was utilised in the enrichment process, constant-dosing tests with other dosing rates were conducted to compare with the enrichment performance. Fig. 5.2 demonstrates the performance of PO_4^{3-}-P release, uptake and NO_2^--N consumption with 5-h (Fig. 5.2a), 4-h (Fig. 5.2b), 3-h (Fig. 5.2c), 2-h (Fig. 5.2d) and 1-h (Fig. 5.2e) constant-rate dosing for anoxic phase of A_2 SBRs.

Anoxic phosphorus uptake with 5-h NO_2^--N dosing could achieve efficient phosphorus removal, where 49.3 mg P L^{-1} was decreased with 38.7 mg N L^{-1}. It also suggested that the NO_2^--N based anoxic phosphorus uptake could be also achieved with the EBPR sludge that was mainly acclimated with NO_3^--N (the ratio of NO_3^--N to NO_2^--N in that enrichment process was around 7:1). 4-h NO_2^--N dosing was the general operation of the SBRs, which had been discussed in section 4.3.1. On the contrary, effective phosphorus removal with 3-h dosing was not achieved, due to the decrease of PO_4^{3-}-P uptake rate in last 2 hours of anoxic phase, while it still removed 52.0 mg P L^{-1} with 42.6 mg N L^{-1} (duplicated test was conducted with closed results). If only the first 3 hours were considered, both Fig. 5.2b and Fig. 5.2c had faster phosphorus uptake rate than that in Fig. 5.2a, because of the higher NO_2^--N adding rate before nitrogen accumulation. However, due to the fast

decrease of PO_4^{3-}-P concentration and gradual nitrogen accumulation, P uptake in Fig. 5.2c reduced in the last 2 hours of anoxic phase.

In case of 2-hour dosing test, even though the test shown in Fig. 5.2d had faster NO_2^--N dosing rate than that in Fig. 5.2c, it still achieved completely P removal in the first 3.5 hours of anoxic phase. At the end of N dosing, the maximum of NO_2^--N concentration in Fig. 5.2d was 13.0 mg L^{-1}, only 1.9 mg L^{-1} lower than that in Fig. 5.2c. It suggested that in the later hours of anoxic phase in Fig. 5.2d, similar N concentration level did not restrain P uptake, due to the higher initial P concentration of 13.2 mg L^{-1} after N dosing, which was much higher than 6.5 mg L^{-1} in Fig. 5.2c. Hence, the comparison indicated that the toxic inhibition of P uptake in the A_2 system was not only based on the concentration of NO_2^--N, but also the concentration of PO_4^{3-}-P, when MLSS in the system was stable.

However, the result in Fig. 5.2e, where NO_2^--N was added in the first hour of anoxic phase, suggested PO_4^{3-}-P uptake would be nearly deteriorated if the NO_2^--N concentration achieved a relative high level (26.5 mg L^{-1} in the figure). Although the P uptake in the first hour of anoxic phase was relatively high, it was limited after NO_2^--N achieved the maximum and did not recover with the decrease of NO_2^--N concentration. Compared with the other constant-rate dosing strategies, the P removal performance basically failed.

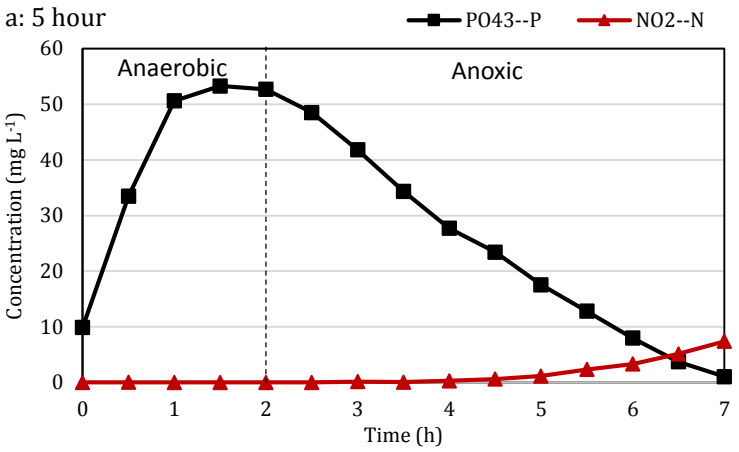
a: 5 hour
PO43--P
NO2--N
Anaerobic
Anoxic
Concentration (mg L-1)
Time (h)

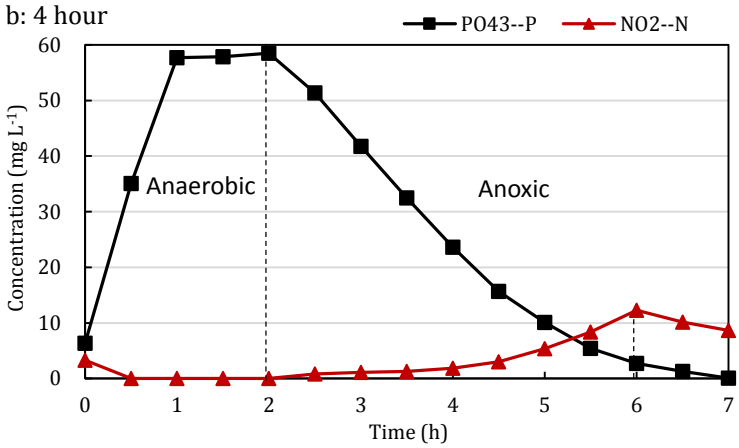
b: 4 hour
PO43--P
NO2--N
Anaerobic
Anoxic
Concentration (mg L-1)
Time (h)

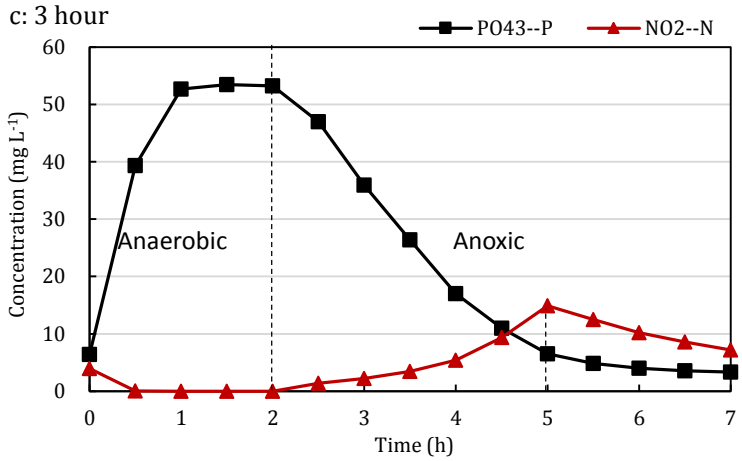
c: 3 hour
PO43--P
NO2--N
Anaerobic
Anoxic
Concentration (mg L-1)
Time (h)

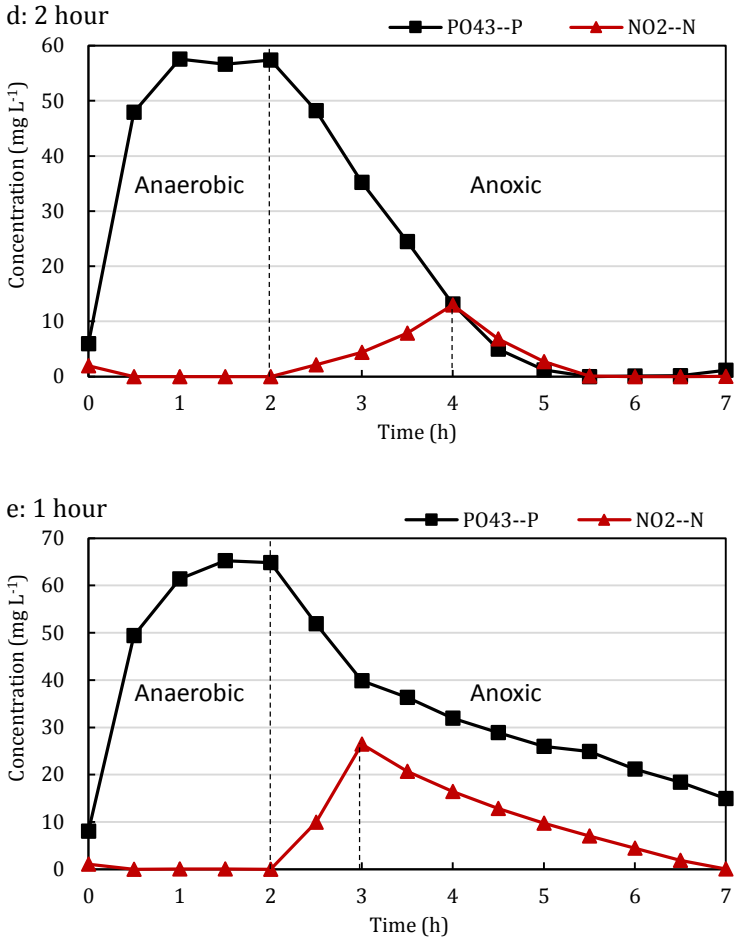

Fig. 5. 2 PO_4^{3-}-P and NO_2^--N change in one cycle of constant rate dosing strategies

To compare the difference of phosphorus removal efficiencies among the dosing strategies, the PO_4^{3-}-P uptake, NO_2^--N consumption and P/N ratio were calculated for the performance analysis of the tests. As can be seen in Fig. 5.3, during the anoxic phase, the consumption of NO_2^--N changed smoother than PO_4^{3-}-P uptake, which induced the change of P/N ratio in every time slots. The maximum of PO_4^{3-}-P uptake in 30 min among the tests was increased with the NO_2^--N dosing rate enhancement, which were separately 7.5, 9.6, 10.8, 13.0 and 12.9 mg L^{-1}. Meanwhile, the efficiencies of P uptake and N consumption were smoother and more stable with lower NO_2^--N dosing rate, while the changes of P and N concentration were weakened with the enhancement of N dosing rate. Except Fig. 5.3e, the maximums of P uptake in the other graphs occurred in the second or third 30-min of anoxic phase as discussed in the last chapter, while the maximum in Fig. 5.3e was in the first 30-min, due to the most intense N dosing in the half an hour, which stimulated the fastest P accumulation.

The overall P uptake/N consumption ratio in the tests were 1.34, 1.50, 1.24, 1.17 and 1.04, respectively, which suggested that the slower N dosing rate could enhance the P efficiency while consuming the same amount of NO_2^--N. Specifically, in the majority of the tests, the P/N ratios had a reducing trend with the continue of anoxic phase, because of the gradual decrease of PO_4^{3-}-P concentration in the wastewater. The reducing trend was increasingly obvious from Fig. 5.3a to Fig. 5.3d, with the slopes of 0.0090, -0.0803, -0.1280 and -0.1679, due to the deceasing P concentration in the wastewater. In case of Fig. 5.3e, even there was no stable trend, due to the inhibition of P uptake causing the irregular concentration decreasing, the NO_2^--N was still consumed gradually and smoothly without the instability like PO_4^{3-}-P.

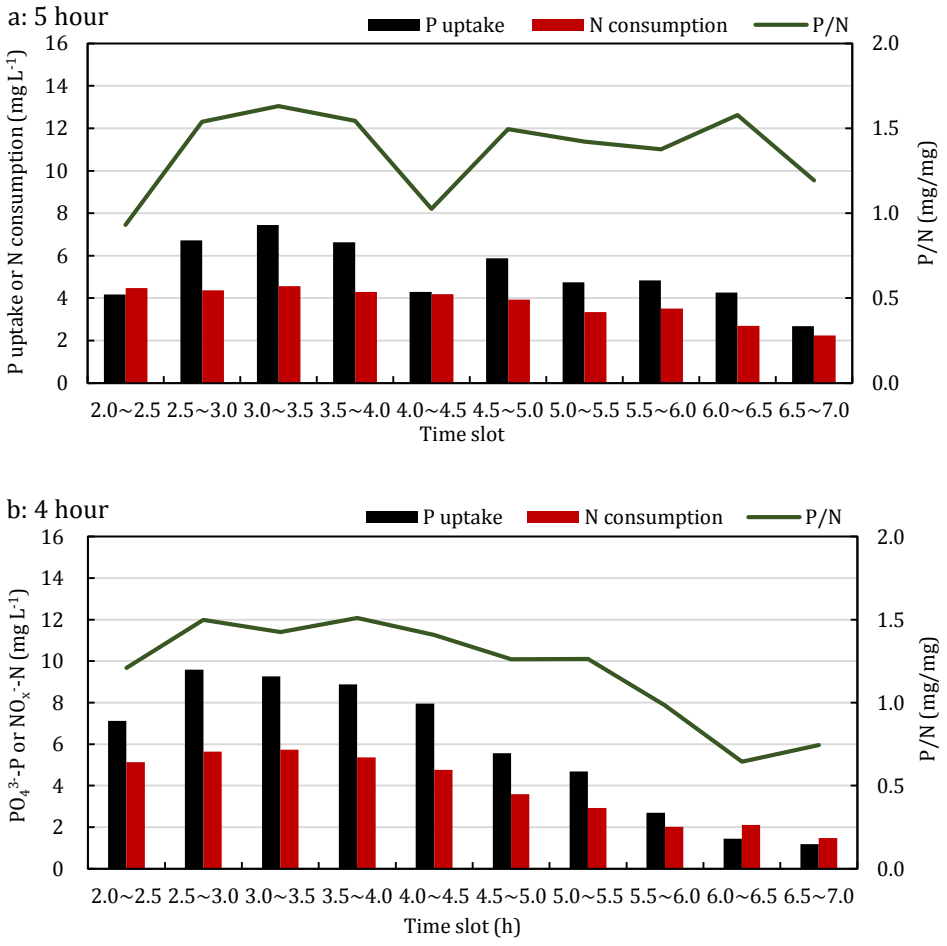

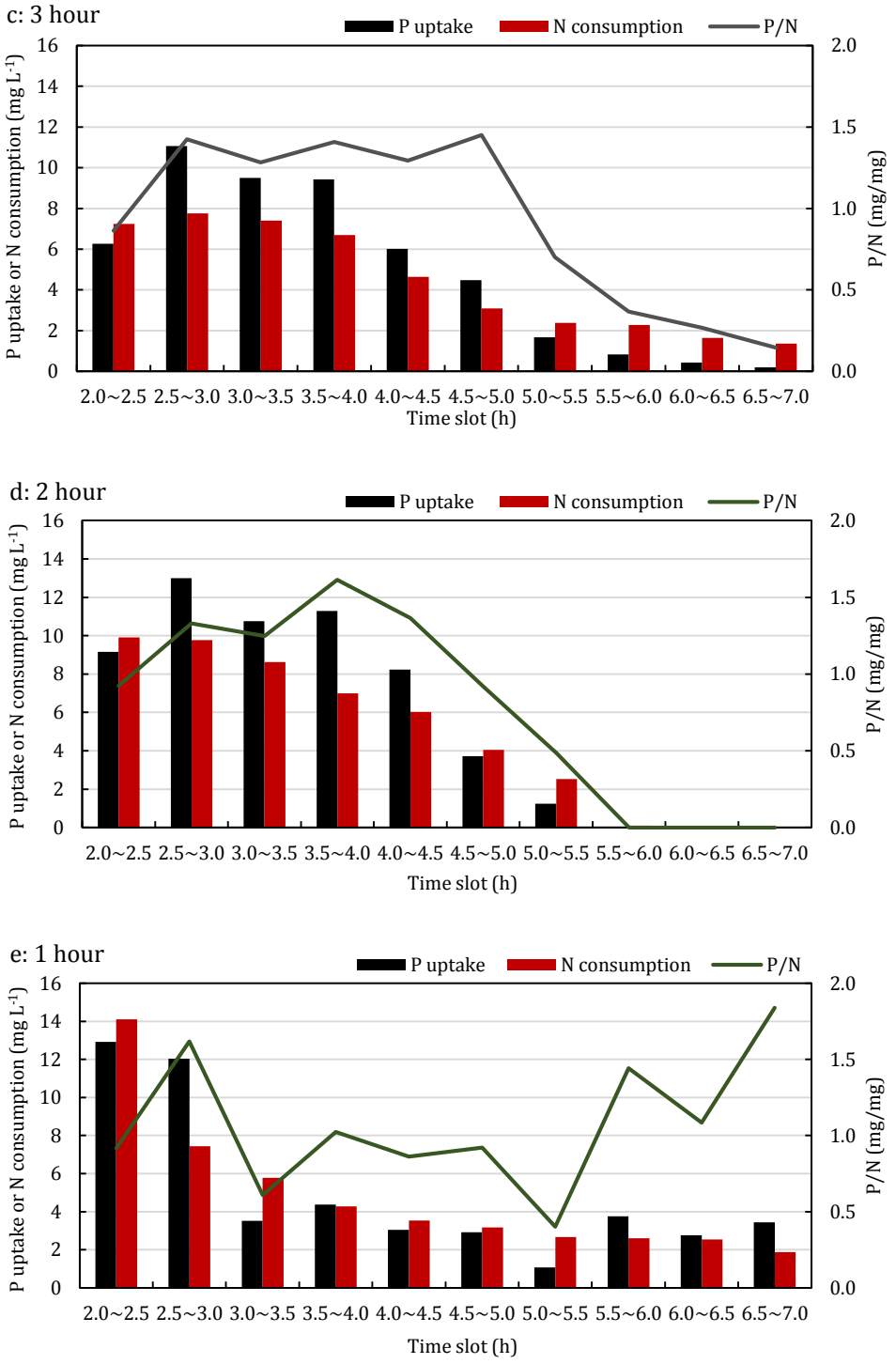

Fig. 5. 3 PO_4^{3-}-P uptake, NO_2^--N consumption and P/N ratio in anoxic phase of constant-rate dosing strategies

Fig. 5.4a-e demonstrates the linear relationship between PO_4^{3-}-P uptake (*y* axis) and NO_2^--N consumption (*x* axis), which indicates that the linear trend is more obvious in 4-h, 3-h and 2-h dosing tests with higher R-squared values. The slopes of the linear plots among the tests were separately 1.33, 1.92, 1.49, 1.34 and 0.96, which were higher than their

overall P/N ratio during the anoxic phase. It was caused by the relatively lower phosphorus uptake with relatively higher nitrogen consumption, namely lower P/N ratio, suggesting that the NO_2^--N consumption in the later period of anoxic phase was not only used for phosphorus uptake, while there should be other reaction pathway in the DPAOs. The overall relationship of P uptake and N consumption among all the tests was also approximately linear (shown in Fig. 5.4f) with the slope of 1.19. In contrast, it was found that if only the tests of 2-h to 4-h were included, the P/N would be higher (1.35) with more proximately linear relationship, due to the exclusion of 1-h dosing test, which experienced toxic inhibition of P uptake.

a: 5-h

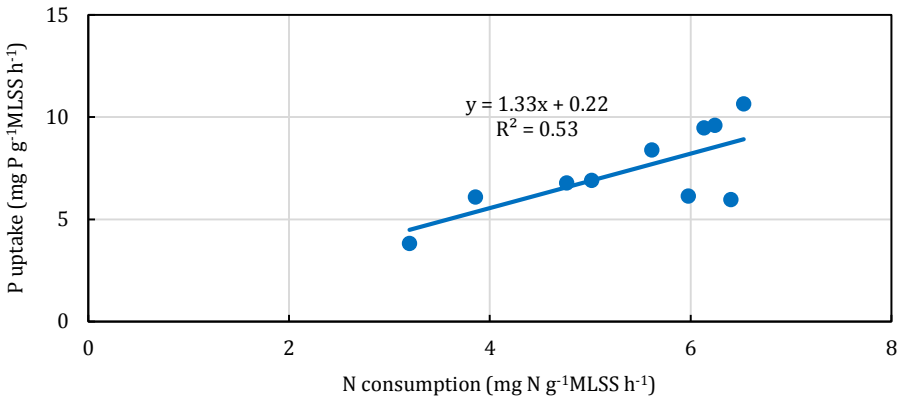

b: 4-h

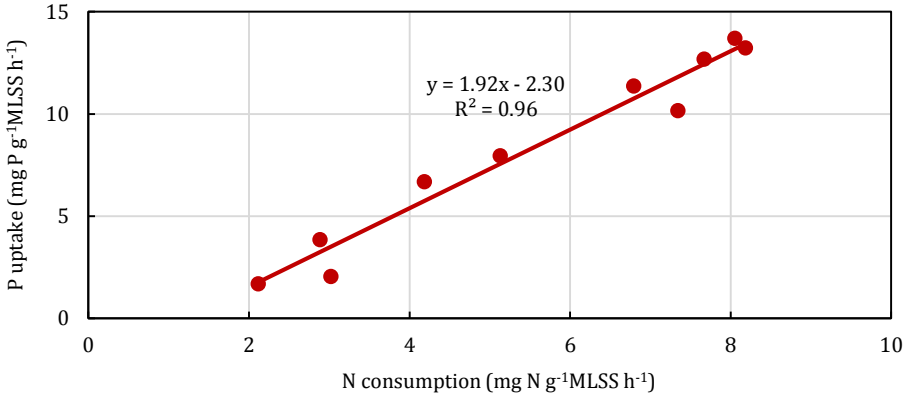

c: 3-h

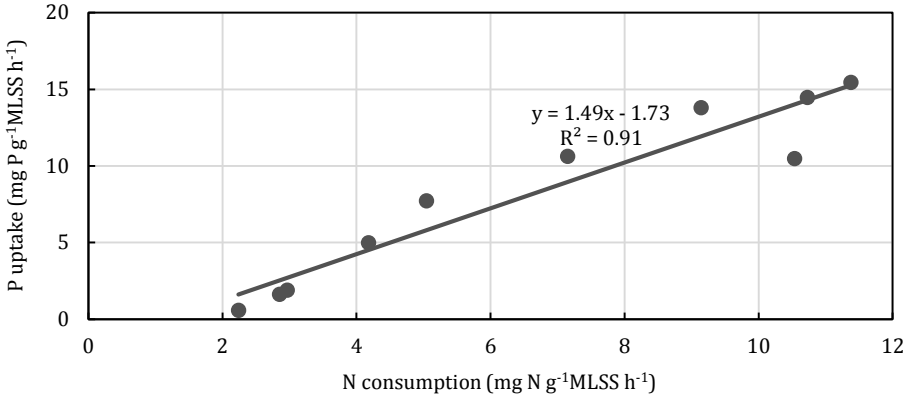
y = 1.49x - 1.73
R² = 0.91
P uptake (mg P g-1MLSS h-1)
N consumption (mg N g-1MLSS h-1)
0
5
10
15
20
0
2
4
6
8
10
12

d: 2-h

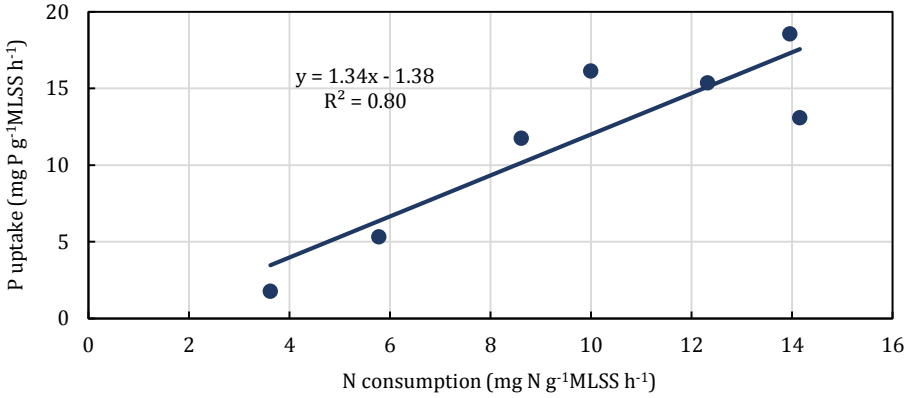
y = 1.34x - 1.38
R² = 0.80
P uptake (mg P g-1MLSS h-1)
N consumption (mg N g-1MLSS h-1)
0
5
10
15
20
0
2
4
6
8
10
12
14
16

e: 1-h

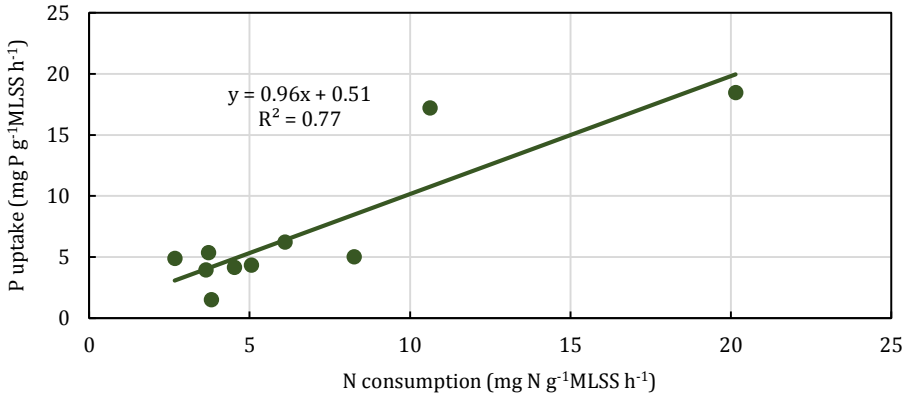
y = 0.96x + 0.51
R² = 0.77
P uptake (mg P g-1MLSS h-1)
N consumption (mg N g-1MLSS h-1)
0
5
10
15
20
25
0
5
10
15
20
25

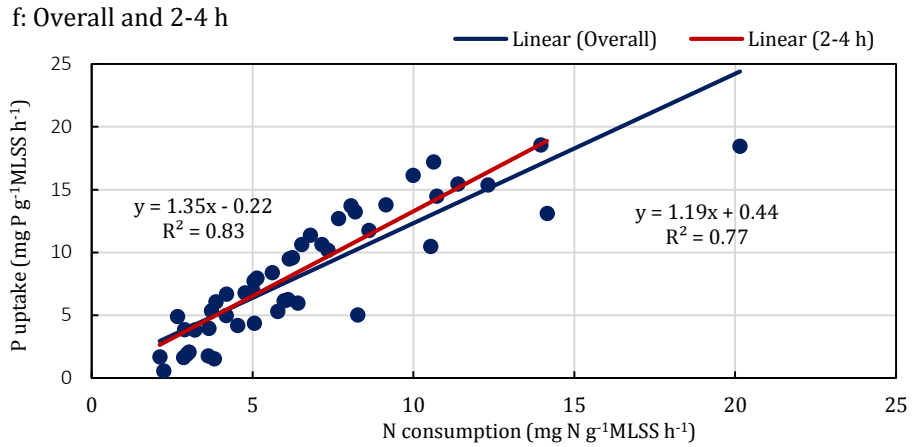

Fig. 5. 4 The comparison of relationship of P uptake and N consumption in anoxic phase among the tests with different NO_2^--N dosing rate

5.1.1.2 Reducing-rate dosing strategy

Due to the fails of phosphorus removal with 3-hour NO_2^--N dosing (on Day 15), more tests were conducted to explain this occurrence. Because in the 3-hour dosing test, NO_2^--N dosing rate was around 17.2 mg L^{-1} h^{-1}, it was presumed that the NO_2^--N utilisation potential in the earlier period of anoxic phase was higher than dosing rate in the 3-hour test, while the potential in the later period was lower than the dosing rate. Based on the assumption, it suggested that the NO_2^--N input rate could be reduced with decreasing of P concentration in the wastewater. Hence, two reducing-rate NO_2^--N dosing strategies (T_a and T_b) were conducted (on Day 41 and 43) as Table 5.1, where the concentrated NO_2^--N solutions were pumped into the SBRs with decreasing rates from 12.0 to 3.0 mg L^{-1} per 30 min (totally 45.0 and 48.0 mg N L^{-1}).

Table 5. 1 Two reducing-rate dosing strategies for NO_2^--N based A_2 SBRs (mg N L^{-1})

Time slot (h)	2.0-2.5	2.5-3.0	3.0-3.5	3.5-4.0	4.0-4.5	4.5-5.0
T_a	12.0	12.0	6.0	6.0	6.0	3.0
T_b	12.0	12.0	12.0	6.0	3.0	3.0

The results of PO_4^{3-}-P and NO_2^--N concentration change were demonstrated in Fig. 5.5, which indicated that both of tests achieved efficient P removal in the 5-hour anoxic phase. Compare with 3-hour constant rate dosing, NO_2^--N accumulation was not induced with reducing-rate N input, while PO_4^{3-}-P concentration was decreased to the minimum at the 3.5 hour of anoxic phase, similar with the test of 2-hour constant-rate dosing test. It

suggested that the failure of 3-hour constant rate dosing test was caused by the inconformity among constant N input rate, input duration and ambient P concentration. As can be seen in the Fig. 5.5a and Fig. 5.5b, with the decrease of P concentration in the SBR, lower N input rate induced continuous P uptake without any obvious growth of N concentration.

Among the two reducing-rate dosing strategies of NO_2^--N, the N input rate in T_a decreased earlier, which caused more placid alteration of N concentration. On the contrary, the plot of N concentration in the first three 30 mins of anoxic phase in T_b was similar with that in 2-h constant rate dosing strategy, which had a peak of N concentration at 8.6 mg L^{-1}, while the different points between 2-h dosing test and T_b was that due to the decrease of N adding rate, the concentration reduced gradually with the process of P uptake.

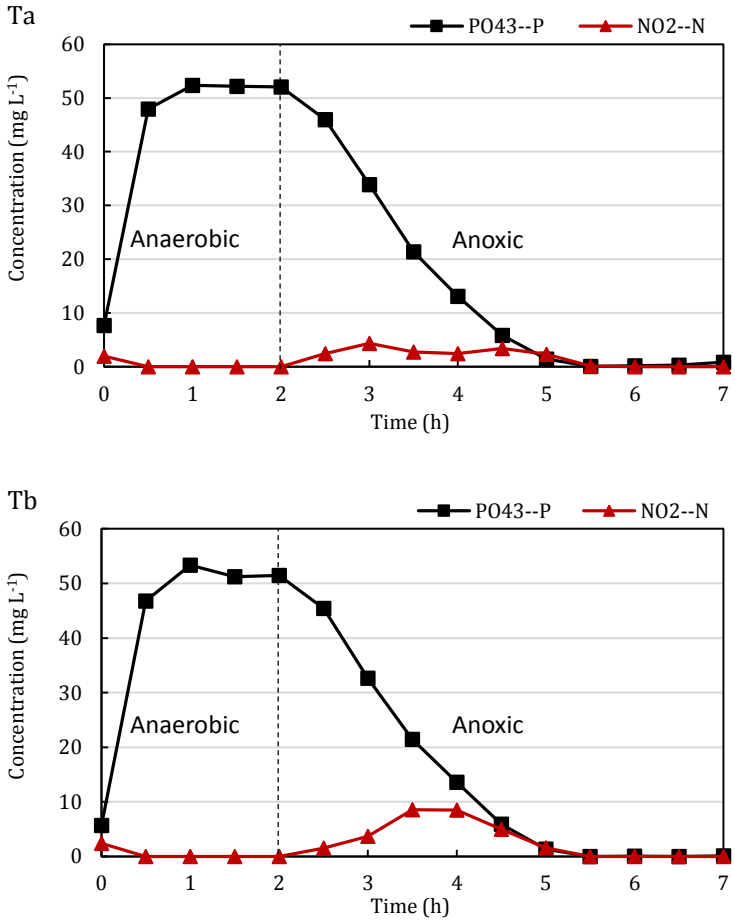

Fig. 5. 5 PO_4^{3-}-P and NO_2^--N change in the cycle of reducing rate dosing strategies

As can be seen in Fig. 5.6, the trends of PO_4^{3-}-P uptake, NO_2^--N consumption and P/N ratio in the reducing-rate dosing tests were all similar, which were also comparable to the 2-

hour constant rate dosing experiment. Both of P/N ratios in the tests experienced an increase in the early period of anoxic phase, followed by the decrease in the later period, until PO_4^{3-}-P concentration was reduced to the minimum.

The reducing-rate N dosing was finished in the first 3 hours of anoxic phase in the tests, while compared with the result of 3-hour dosing, they achieved compete P removal in the anoxic phase. Hence, it suggested that the more intensified NO_2^--N dosing into wastewater with high PO_4^{3-}-P concentration would not induce toxic inhibition, and P uptake rate could be enhanced in the meantime. Correspondingly, with the decrease of ambient P concentration, the reduced N dosing rate effectively avoided N accumulation and triggered entire P removal.

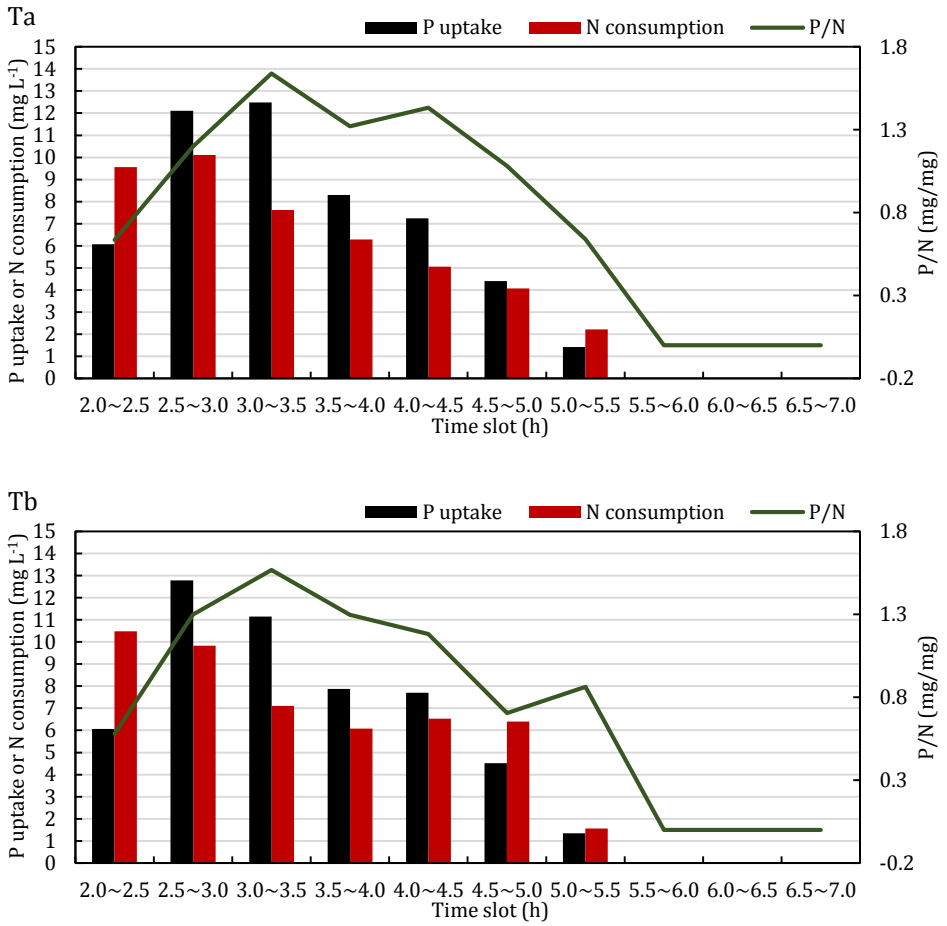

Fig. 5. 6 PO_4^{3-}-P uptake, NO_2^--N consumption and the ratio of P/N in anoxic phase of reducing-rate dosing strategies

The linear relationship between PO_4^{3-}-P uptake and NO_2^--N consumption in T_a and T_b was not ideal as constant-rate N dosing strategies, mainly due to the disproportion of P uptake and N consumption in the first 30 min, when the P/N ratios in the strategies were only 0.63 and 0.58, respectively (Fig. 5.6). If the data in the first 30 min of anoxic phase was removed, the R-squared values would be 0.89 and 0.81, apparently higher than the values in the chart (0.56 and 0.44). Additionally, the slopes would be increased from 1.03 and 0.88 to 1.47 and 1.41. The reason causing this was that as discussed above, after the 2-h anaerobic phase the DPAO system needed an adaptive phase when the P uptake was relatively low, although the N input was sufficient. Overall, the strategies of reducing-rate NO_2^--N dosing in anoxic phase achieved complete P removal performance, which had similar result and P/N ratio with 2-hour dosing strategy, meaning that this kind of operation modes could be utilised in A_2 SBRs via NO_2^--N pathway, to adapt in appropriate cycle duration and arrangement.

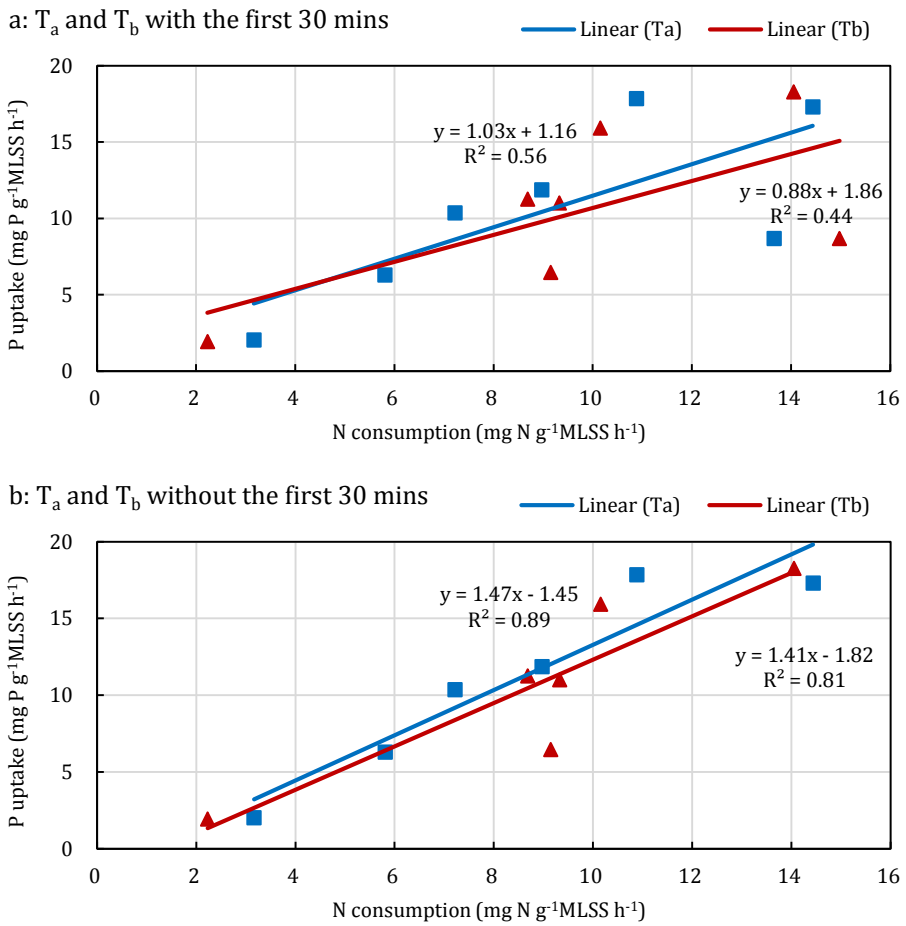

Fig. 5. 7 P uptake and N consumption in anoxic phase in the tests with reducing NO_2^--N dosing rate strategies

In the comparison between 3-h constant-rate dosing and reducing-rate dosing strategies, the overall advantage of reducing-rate dosing strategies was reflected from the higher

phosphorus uptake rate in the earlier stage of anoxic phase. In the 3-hour dosing test, NO_2^--N dosing rate was around 17.2 mg L^{-1} h^{-1}, namely 8.6 mg L^{-1} per 30 min, with the maximum of NO_2^--N concentration of 14.9 mg L^{-1}, causing the decrease of phosphorus uptake in the later hours. If it is considered that similar N amount is added into the SBR, the higher dosing rate in the earlier hours of enhanced the phosphorus uptake rate in the time slots. In the first 1.5 hours of anoxic phase, for instance, the PO_4^{3-}-P concentrations of reducing-rate dosing tests were decreased to 21.4 and 21.5 mg L^{-1}, relatively lower than 26.4 mg L^{-1}, the value in constant-rate dosing test. The concentrations were decreased to 1.5, 1.4 and 6.5 mg L^{-1} at the end of dosing, prior to being declined to 0.0, 0.0 and 4.8 mg L^{-1} in the later 30 min. In addition, as the expectation for reducing-rate dosing tests, there was not obvious NO_2^--N accumulation in the anoxic phase, with the maximums of NO_2^--N concentration of 4.3 and 8.6 mg L^{-1}, lower than 14.9 mg L^{-1}, which caused the slight phosphorus uptake inhibition in the 3-h constant-rate dosing test. Even though the overall NO_2^--N dosing strength in the 3-h constant-rate dosing test was a little higher than T_a and T_b and the general operation, it should not be the reason causing the slight inhibition. Because with the lower NO_2^--N dosing rate in the first 3 hours, the PO_4^{3-}-P uptake rate would also be lower, causing higher PO_4^{3-}-P concentration with the peak of NO_2^--N at the end of third hour of anoxic phase, which must be higher than the nitrogen peak in 4-h dosing strategy (normal operation). The peak should be around 13-15 mg L^{-1} and would inhibit the final phosphorus uptake in the last two hours. Furthermore, compared 3-h constant-rate dosing test with the reducing-rate dosing tests, it suggested that in the earlier period of anoxic phase, the phosphorus uptake was more potentially, while the dosing strength in 3-h constant rate test was not enough. The phosphorus uptake potential decreased in the third hour of anoxic phase, inducing the faster NO_2^--N accumulation and the slight inhibition. Hence, the ineffective phosphorus removal in 3-h constant-rate test was not induced by the higher total NO_2^--N dosing concentration, but the relatively lower dosing strength in the first two hours and relatively high dosing strength in the third hour of anoxic phase.

The reducing-rate doing tests suggested that phosphorus removal in A_2 systems with NO_2^--N as the sole electron acceptor could be achieved with shorter period of anoxic phase than 4-h NO_2^--N dosing operation, avoiding the toxic inhibition from FNA, and lower NO_2^--N requirement than the study of Peng *et al*. (2011). In comparison, 3-h constant-rate dosing test revealed that phosphorus uptake was inhibited after the end of NO_2^--N dosing when NO_2^--N concentration achieved 14.9 mg L^{-1}. The maximum of NO_2^--N was similar as

the result of Wang *et al*. (2007) and Tang *et al*. (2012), higher than the threshold value reported by Meinhold *et al*. (1999). It suggested that threshold value of NO_2^--N was not constant to avoid toxic inhibition of phosphorus uptake. In the study of Meinhold *et al*. (1999), the initial PO_4^{3-}-P concentration of anoxic phase was lower than 20 mg L^{-1}, 10 mg L^{-1} initial NO_2^--N inhibited phosphorus uptake from the beginning of anoxic phase. On the contrary, 12 mg L^{-1} initial NO_2^--N in each pulse of dosing realised efficient phosphorus uptake with initial PO_4^{3-}-P concentration of around 60 mg L^{-1}, in the study of Peng *et al*. (2011). In this study, the phosphorus uptake from the third hour of anoxic phase was obviously lower than the earlier period, when the PO_4^{3-}-P concentration was lower than 20 mg L^{-1}, suggesting the threshold value of NO_2^--N was related to the concentration of PO_4^{3-}-P.

5.1.1.3 Single-pulse dosing strategy

Single-pulse dosing strategy, which was done with the immediate adding of concentrated NO_2^--N solution into A_2 SBR achieving 48 mg N L^{-1} as the beginning of anoxic phase, was conducted to compare with long-period dosing of nitrite, in order to explore the P uptake performance after high strength of NO_2^--N dosing.

Fig. 5.8 demonstrates the concentration change of PO_4^{3-}-P and NO_2^--N in the cycle of single-pulse dosing strategy. As can be seen in the Fig. 5.8a, after the 48.0 mg NO_2^--N L^{-1} was dosed into the SBR, both P and N concentration decreased slowly, from 55.6 and 48.0 mg L^{-1} at the beginning of anoxic phase to 27.1 and 16.0 mg L^{-1} at the end of anoxic phase. The PO_4^{3-}-P concentration was only reduced around 50% during the anoxic phase, and the final concentration was around 4.3 times of the initial figure at the beginning of the cycle, which indicated that the P removal was absolutely deteriorated in this test. Compared with one-hour constant-dosing test, the consumption of NO_2^--N was also non-sufficient, only decreased 66.7% during the anoxic phase, suggesting that the DPAO system in SBR was completely restrained by the intensive nitrite dosing.

Fig. 5.8b demonstrates the decrease amount of P and N, and P/N ratio in each 30 min of anoxic phase, indicating that after the inhibition, the concentration reduction of PO_4^{3-}-P and NO_2^--N are both lower than 6 mg L^{-1} in each 30 min, and still diminish during the anoxic phase. In addition, due to the toxic inhibition, the P/N ratio fluctuated frequently between 0.41 and 1.29 without any stable trend.

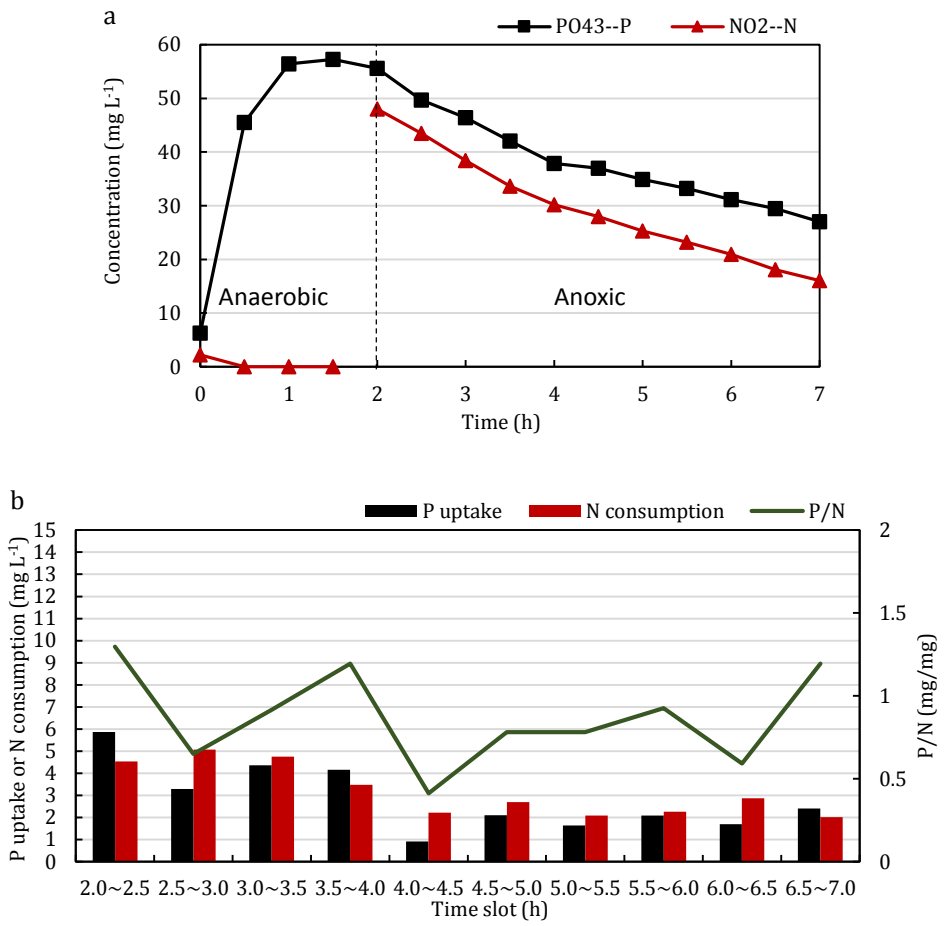

Fig. 5. 8 Performance of P uptake in sing-pulse dosing strategy: a. PO_4^{3-}-P and NO_2^--N change in the cycle; b. P uptake, N consumption and P/N ratio during anoxic phase

5.1.2 The derivation of HAc, PO_4^{3-}-P and NO_2^--N in one cycle with long-period NO_2^--N dosing

In order to explore the anoxic P uptake efficiency in A_2 SBRs via NO_2^--N pathway, the relationship between P uptake and real-time P concentration in the wastewater was explored. As in the long-period dosing strategies, some tests (e.g. 5-hour and 4-hour dosing) were conducted with very limited N input, while some tests (e.g. 2-hour and reducing rate dosing) were conducted with relatively sufficient N input, P uptake derivations were different in these two kinds of tests.

5.1.2.1 Anaerobic HAc consumption and PO_4^{3-}-P release

The HAc changes in the 4-h dosing, reducing rate dosing strategies is shown in Fig. 5.9. The consumption of HAc was more closed to a zero order reaction in the first hour of

anaerobic phase before its exhausting, with the averagely reaction rate of 3.79 mg L^{-1} min^{-1} (with standard deviation of 0.1).

Meanwhile, if a 1st order reaction was considered for the uptake of HAc, a constant coefficient of 0.0885±0.0007 (min^{-1}) was calculated with the two reducing rate dosing strategies (T_a and T_b), as Equation (5-1),

$$r_{HAc} = 0.0885 \times C_{HAc} \qquad (5\text{-}1)$$

where

r_{HAc} is the uptake rate of HAc (mg L^{-1} min^{-1});

C_{HAc} is the concentration of HAc (mg L^{-1}).

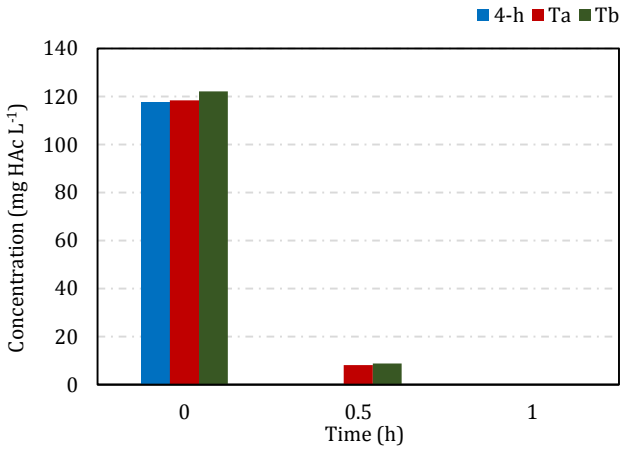

Fig. 5. 9 HAc consumption in the first hour of anaerobic phase of 4-h constant rate and reducing-rate NO_2^--N dosing strategies

The kinetics of PO_4^{3-}-P concentration in Fig. 5.2 indicated that the release in all the operation was generally similar, namely fast in the first hour of anaerobic phase, and stopped in the second hour. Thus, in order to fit the PO_4^{3-}-P increase in anaerobic phase, the concentration change in the first hour should be ensured. The simulated P concentrations at 0.5 and 1 hour in the model were calculated by averaging the average concentrations in the three dosing tests (as shown in Table 5.2) at these time points, respectively. Consequently, the values, which are shown in Table 5.2, are utilised in the regression of Fig. 6.2. As can be seen in the graphs, both polynomial and linear regression was attempted to fit the P concentration change in the first hour of anaerobic phase. As the R^2 value in Fig. 5.10a is higher than Fig. 5.10b, the Equation (5-2) of the polynomial trend line could be more appropriate to deduce the phosphorus release in the anaerobic

phase. In case of the later period of anaerobic phase, the concentration will be equal to the value at hour 1, and kept constant to the end of anaerobic phase.

$$C_{PO_4^{3-}-P} = -32.73t^2 + 81.97t + 6 \qquad (5\text{-}2)$$

, where

t is between 0 and 1.

Table 5. 2 Values of PO_4^{3-}-P concentration in the first hour of anaerobic phase for simulation

Time	0 h	0.5 h	1.0 h
5-h dosing test	9.9	33.5	50.6
4-h dosing test	6.4	35.0	57.7
2-h dosing test	6.0	47.9	57.4
Simulation	6.0	38.8	55.2

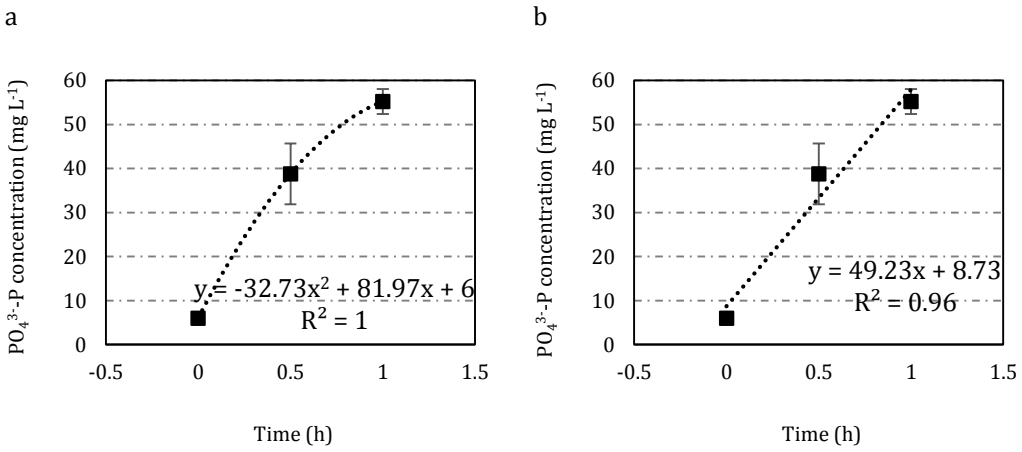

Fig. 5. 10 Trend lines of PO_4^{3-}-P concentration change in the first hour of anaerobic phase in A_2 SBRs

There was another possibility that the increase of PO_4^{3-}-P was similar as decrease of HAc, with constant rate of around 1 mg L^{-1} min^{-1}, to the limit of phosphorus release capacity of DPAOs with the corresponding HAc uptake, namely approximately 120 mg L^{-1} HAc uptake with 45 mg L^{-1} PO_4^{3-}-P release.

The HAc decrease and PO_4^{3-}-P increase trends in the steady period of the EBPR systems in this study was similar with most of previous studies (Kuba *et al.*, 1996b; Zhang *et al.*, 2010; Peng *et al.*, 2011).

5.1.2.2 PO_4^{3-}-P uptake with limited NO_2^--N input

With slower N input (9 or 11.2 mg L^{-1} h^{-1}) of 5-hour and 4-hour constant rate dosing tests, P uptake rate basically had linear relationship with N input rate, especially in the early period of anoxic phase. As demonstrated in 5.1.1, the average P/N ratio was around 1.1-1.3. Thus, the P uptake rate could be calculated as Equation (5-3):

$$-r_{PO_4^{3-}-P} = a * r_{NO_2^--N} \qquad (5\text{-}3)$$

where

$-r_{PO_4^{3-}-P}$ is P uptake rate (mg L^{-1} h^{-1});

a is P uptake constant (1.1-1.3); and

$r_{NO_2^--N}$ is N input rate (mg L^{-1} h^{-1}).

Based on the NO_2^--N dosing and consumption rates, Fig. 5.11 was made for the regression of NO_2^--N accumulation in the anoxic phase. As can be seen in the graphs, the exponential trend lines of the nitrogen concentration change in the anoxic phase of 5-h and 4-h dosing can simulate the NO_2^--N accumulation with R^2 values of 0.94 and 0.98. While the NO_2^--N decrease in the last hour of 4-h dosing test can be simulated with the equation of trend line in Fig. 5.11b-2.

$$C_{NO_2^--N} = 1.27t^2 - 15.02t + 52.04 \qquad (5\text{-}4)$$

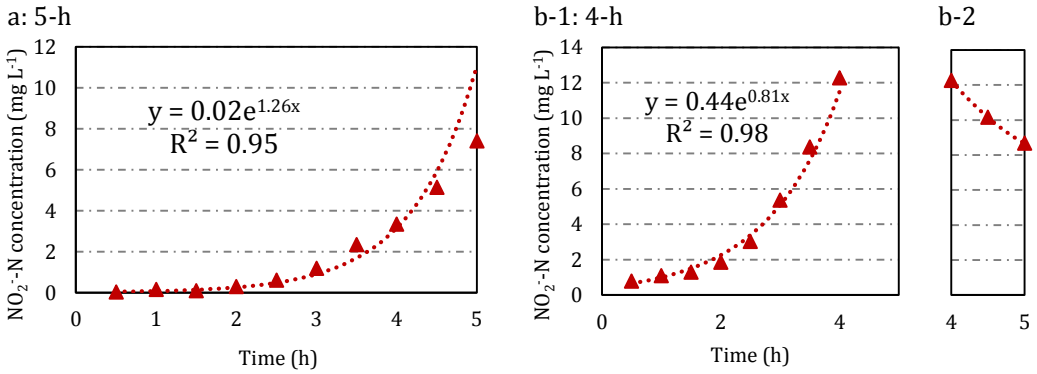

Fig. 5. 11 The trend lines of anoxic NO_2^--N accumulation in 5-h and 4-h dosing tests

As a result, the NO_2^--N consumption in the anoxic phase can be simulated by the difference between N dosing amount and the simulated N concentration in the dosing period. Hence, the P uptake rate can be calculated, and the PO_4^{3-}-P concentrations can also be deduced. In 5-h test, the calculation of PO_4^{3-}-P is:

$$C_{t_1} = C_{t_0} - 1.287 \times (0.02e^{1.2571t_0} - 0.02e^{1.2571t_1}) \quad (5\text{-}5)$$

where:

t_0 is the previous time point;

t_1 is the current time point; and

t_1 - t_0 is equal to 0.5 h.

In 4-h test, the calculation of PO_4^{3-}-P in the first 4 hours is:

$$C_{t_1} = C_{t_0} - 1.287 \times (0.44e^{0.814t_0} - 0.44e^{0.814t_1}) \quad (5\text{-}6)$$

, while calculation in the last hour of anoxic phase is:

$$C_{t_1} = C_{t_0} - 1.287 \times [1.27 \times (t_1^2 - t_0^2) - 15.02 \times (t_0 - t_1)] \quad (5\text{-}7)$$

where:

t_0 is the previous time point;

t_1 is the current time point; and

t_1 - t_0 is equal to 0.5 h.

5.1.2.3 PO_4^{3-}-P uptake with sufficient NO_2^--N input

Compared with 4-h and 5-h constant-rate dosing tests, NO_2^--N adding in 2-h constant-rate dosing test, T_a and T_b provided an anoxic condition with sufficient electron acceptor providing. In general, substrate consumption follows Monod equation, while PO_4^{3-}-P uptake and NO_2^--N consumption with limited nitrite input were both relatively smooth in

anoxic phase without any obvious regulation of P and N removal following Monod equation. On the contrary, the reducing-rate strategies and 2-h constant-rate strategy had more intensive nitrite input, suggesting the faster P and N consumption should be related to Monad equation. Hence, the hypothesis of this section is that PO_4^{3-}-P uptake and NO_2^--N consumption can be more effective and follow Monod equation with appropriate nitrite dosing strategy (efficient nitrite input), if toxic inhibition is avoided. In this deduction, the optimised P uptake rate was aimed to be utilised with each point of P concentration in the anoxic phase. Thus, most of data was selected from 2-hour test, T_a and T_b, which achieved successful P removal and adequate NO_2^--N input in each time slots. The range of the data was firstly based on the P concentration and P uptake in the cycle duration from 2.5-3.0 h to 5.0-5.5 h of each test when there was efficient P uptake. However, as the P uptake in 2.5-3.0 h was not effective enough in all the three tests, the data in 2.5-3.0 h was all replaced by the figures of 1-hour test due to the highest P uptake rate in this time slot.

In Fig. 5.12, the x axles represent the mean of PO_4^{3-}-P concentration (mg g^{-1}MLSS, $C_P = (C_0 - C_1)/2$) between each time point in wastewater, and the y axles represent the P uptake rate per hour (mg g^{-1}MLSS h^{-1}, $= 2 \times \text{P uptake per } 30 \text{ min}$). Fig. 5.12a, Fig. 5.12b and Fig. 5.12c separately represented reducing-rate dosing tests (T_a and T_b) and 2-hour constant rate dosing test. As can be seen in the graphs, the trend lines of the plots in the tests were basically logarithmic with the R^2 of 0.94, 0.94 and 0.96, and the PO_4^{3-}-P uptake rate could be represented as:

$$-r_{PO_4^{3-}-P} = 4.05 \times ln(C_P) + 3.49 \qquad (5\text{-}8)$$

$$-r_{PO_4^{3-}-P} = 3.91 \times ln(C_P) + 3.61 \qquad (5\text{-}9)$$

$$-r_{PO_4^{3-}-P} = 4.08 \times ln(C_P) + 4.07 \qquad (5\text{-}10)$$

where

$r_{PO_4^{3-}-P}$ is the rate of P uptake (mg g^{-1}MLSS h^{-1});

C_P is the real time P concentration in the wastewater (mg g^{-1}MLSS).

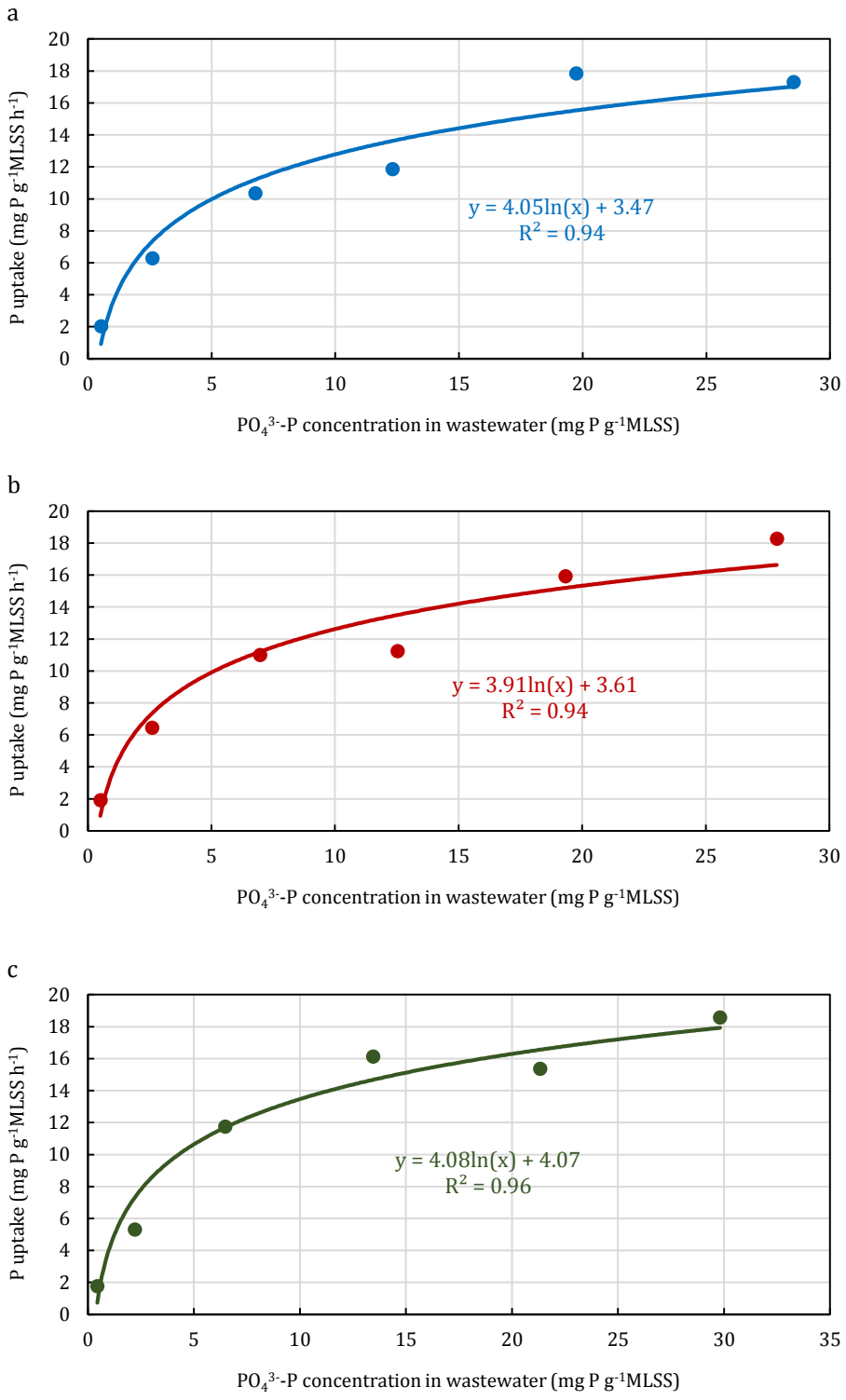

Fig. 5. 12 Relationship between P uptake rate and P concentration in wastewater

As P uptake (mg g^{-1}MLSS h^{-1}) had proximately linear relationship with the natural logarithm of P concentration in wastewater, Fig. 5.13 was made with the ln(C_P) as x axis

and P uptake rate as y axis. Based on the graph, P uptake rates could also be calculated as:

$$-r_{PO_4^{3-}-P} = 4.97 \times ln(C_P) + 1.07 \quad (5\text{- }11)$$

$$-r_{PO_4^{3-}-P} = 4.77 \times ln(C_P) + 1.41 \quad (5\text{- }12)$$

$$-r_{PO_4^{3-}-P} = 4.84 \times ln(C_P) + 2.10 \quad (5\text{- }13)$$

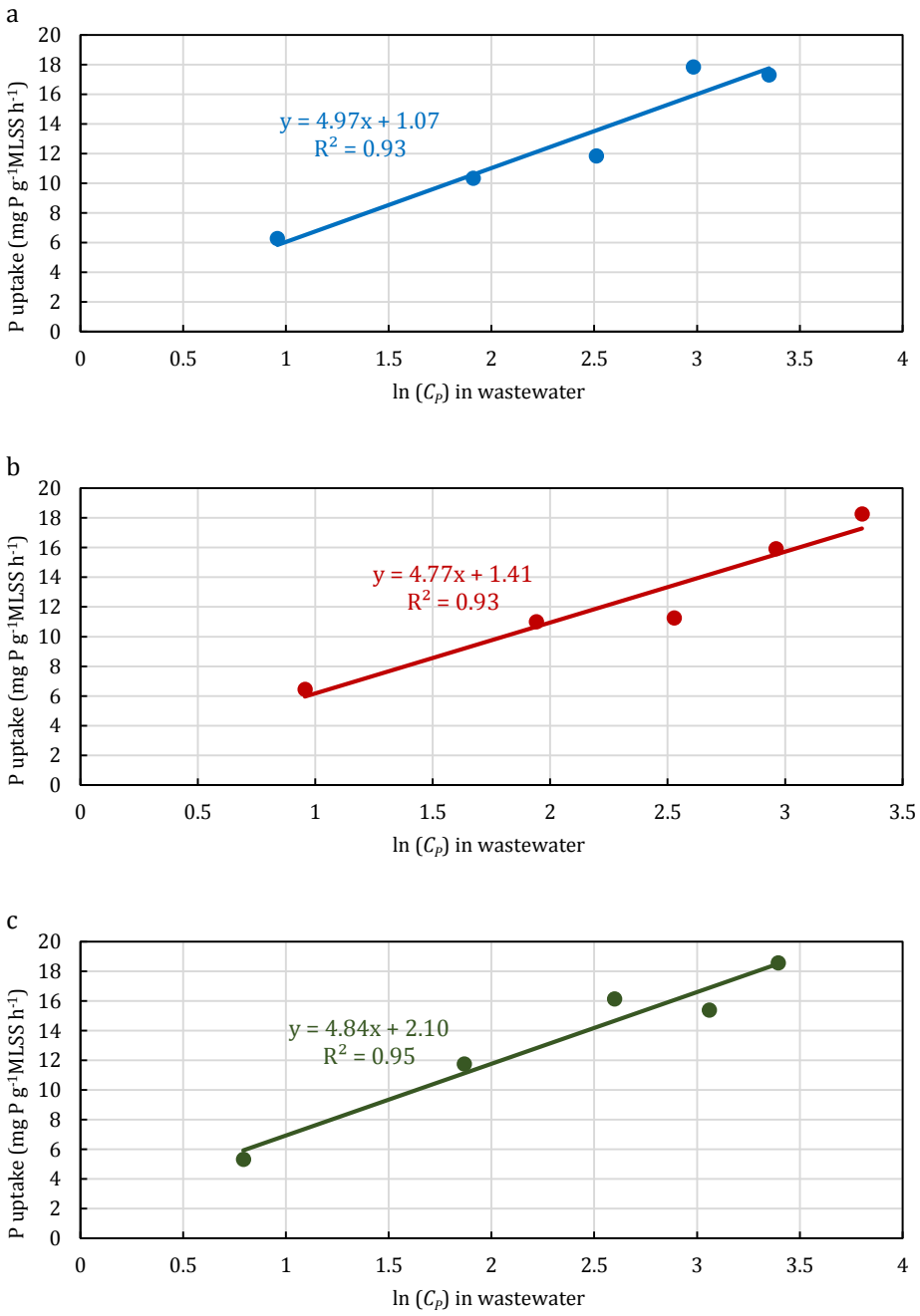

Fig. 5. 13 Relationship between P uptake rate and the logarithm of P concentration in wastewater

If all the data in the three tests was combined in one plot (Fig. 5.14), the linear relationship between P uptake rate and ln(C_P) in the A_2 SBR was still apparent, with R^2 value of 0.93 and the equation below:

$$-r_{PO_4^{3-}-P} = 4.86 \times ln(C_P) + 1.53 \qquad (5\text{-}14)$$

The combined equation should be more appropriate than the separate ones of the tests, due to the more comprehensive data collection and homogeneous slope and R^2 value, which can be used in the deduction of PO_4^{3-}-P uptake rate in A_2 SBR system via NO_2^--N pathway. In this calculation, the equation would not be changed, if the point from 1-hour dosing test was removed.

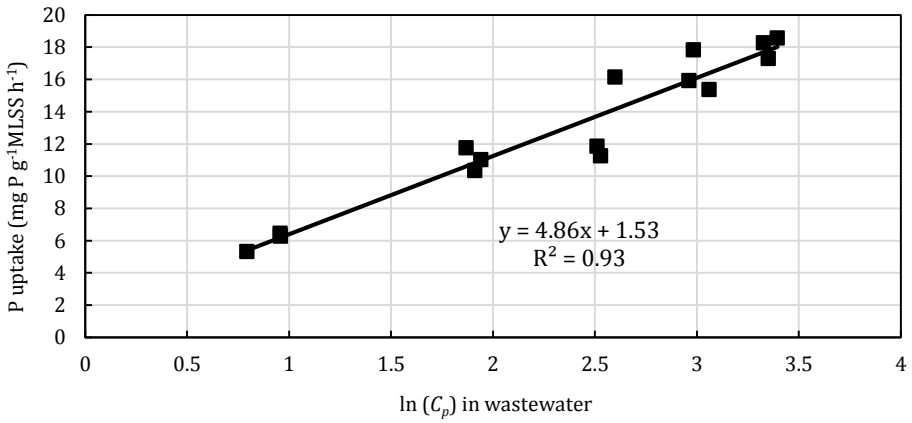

Fig. 5. 14 Combined relationship between P uptake rate and *ln*(C_P) in wastewater among test a, b and c

If the PO_4^{3-}-P uptake in anoxic phase with the efficient NO_2^--N dosing is a 1st order reaction, the k value can be calculated with the three tests, at 0.031±0.008 (min^{-1}). $r_{PO_4^{3-}-P}$ (mg g^{-1}MLSS min^{-1}), as a result, can be also calculated by Equation (5-15).

$$-r_{PO_4^{3-}-P} = 0.031 \times C_P \qquad (5\text{-}15)$$

On the aspect of NO_2^--N consumption, it was highly related to P uptake amount with the P/N ratio of 1.1-1.3 as discussed above. The relationship between N consumption and P concentration in wastewater with the assumption that N input was sufficient for P uptake. Especially in the 2-hour constant rate dosing test, it achieved most optimised degree of fitting in the trend lines. As can be seen in Fig. 5.15a, the relationship between N consumption and ambient P concentration was also logarithmic, with the equation:

$$-r_{NO_2^- - N} = 3.02 \times ln(C_P) + 3.06 \quad (5\text{-}16)$$

where

$-r_{NO_2^- - N}$ is N consumption rate (mg g^{-1}MLSS h^{-1}).

If ln(C_P) was directly used as axis, their linear relationship was shown as Fig. 5.15 b, the equation was the same as Equation (5-16).

The ratios of the slopes in Fig. 5.12 to the slope in 5.15 could be calculated, and the value was around 1.35, which was just proximately similar with optimised ratio of P/N in NO_2^--N based A_2 SBRs.

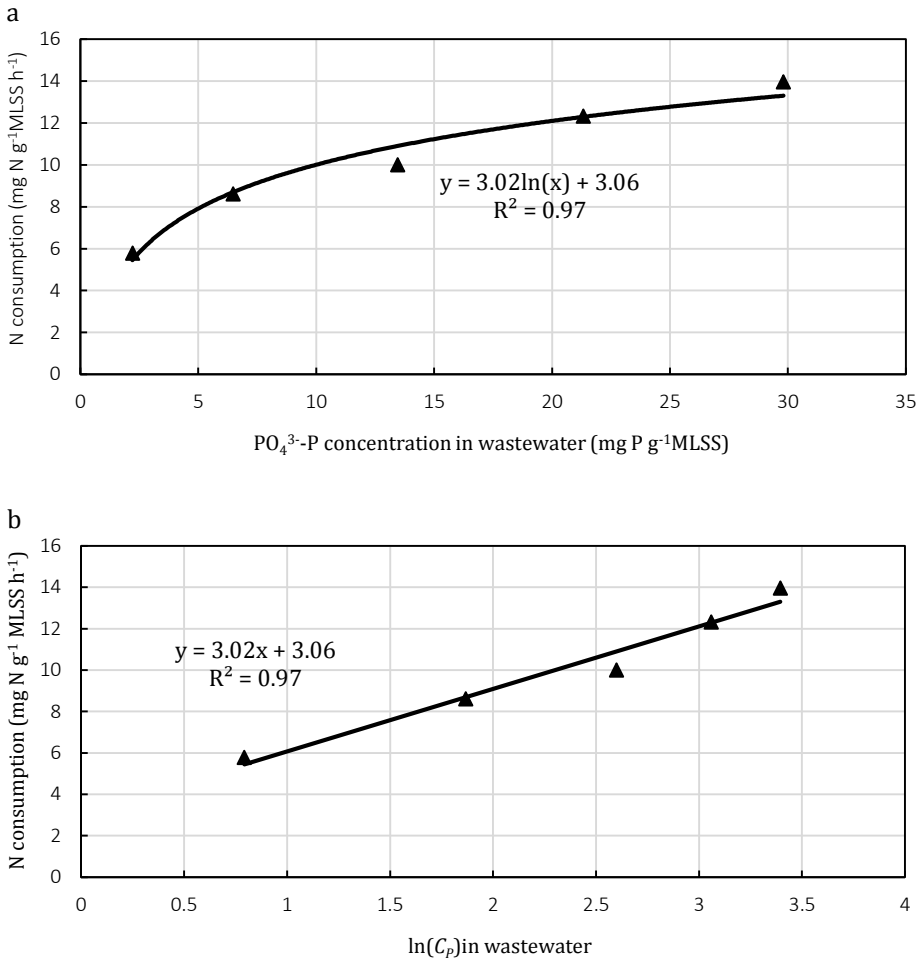

Fig. 5. 15 Relationship between NO_2^--N consumption and PO_4^{3-}-P concentration in wastewater in 2-hour dosing test

If it was assumed that sing-pulse dosing strategy could not induce toxic inhibition, the optimised NO_2^--N consumption in A_2 SBR could be deduced, combined with the performance of 2-hour dosing test. In this assumption, as the N concentration in each

time point could be calculated with the N consumption in each period, the graphs can be plotted as Fig. 5.16. In Fig. 5.16a, where x axis was the mean value of assumed N concentration in each time, the N consumption rate had obvious logarithmic relationship with the assumed N concentration in wastewater, with the equation below:

$$-r_{NO_2^- - N} = 4.66 \times ln(C_N) - 2.62 \qquad (5\text{-}17)$$

If *ln* (C_N) was considered as x axis, there would be the linear trend line of the plot to represent the correlation between N consumption and N concentration in Fig. 5.16b, the same equation could be obtained.

Hence, with this assumption the NO_2^--N consumption rate also had evident trend with the supposed theoretical values of N concentration in the wastewater, compared with the slow and inhibited N consumption rate in single-pulse test, which reflected the performance of N consumption with high ambient N concentration in practice.

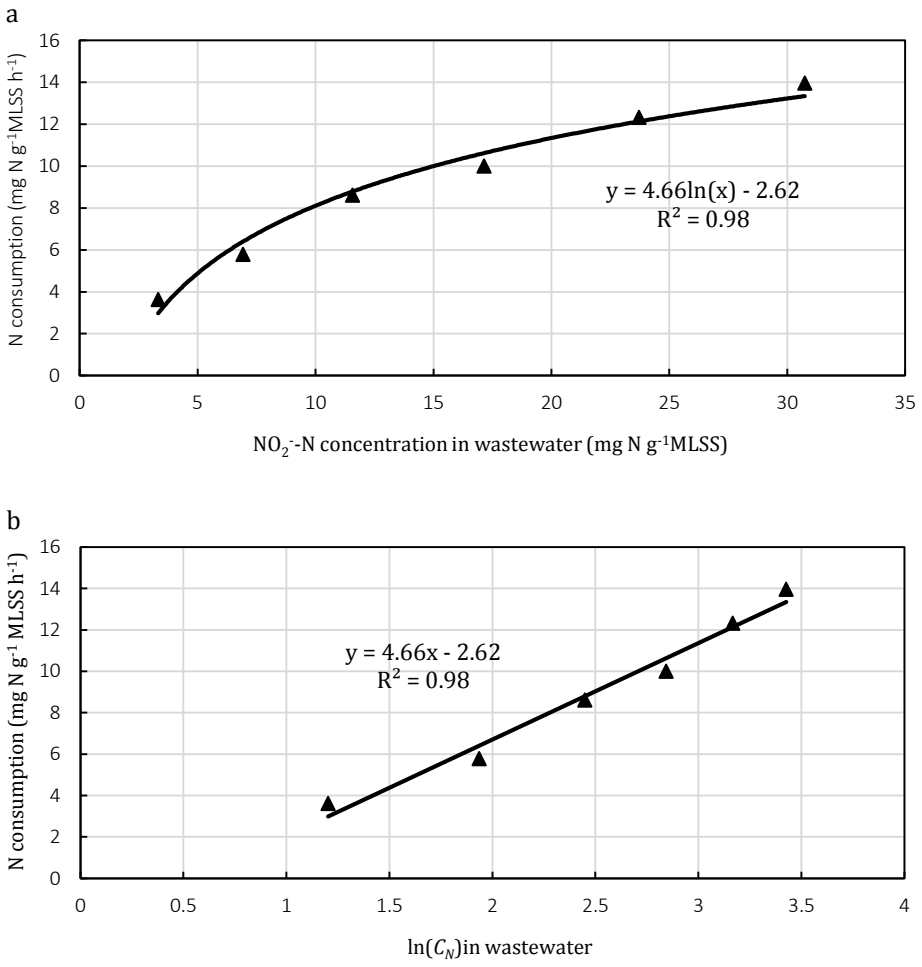

Fig. 5. 16 Relationship between NO_2^--N consumption and NO_2^--N concentration in wastewater in 2-hour dosing test (assumed)

For NO_2^--N accumulation and consumption in 2-h dosing test, two stages were separated, as 4-h dosing test, including the accumulation stage (0-2 h) and decreasing stage (2-3.5 h). In both of the stages, the polynomial trend lines could simulate the concentration change with higher R^2 values of 0.9977 and 0.9999 (Fig. 5.17).

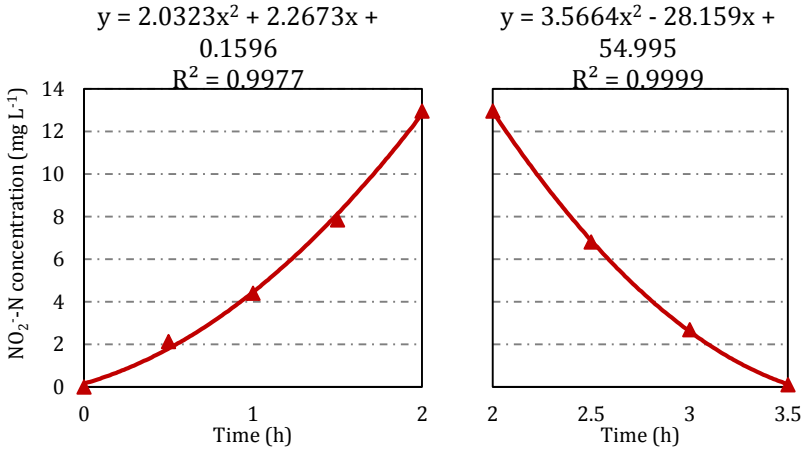

Fig. 5. 17 The trend lines of anoxic NO_2^--N accumulation in 2-h dosing tests

Hence, the NO_2^--N concentration in the two stages of anoxic phase in 2-h N dosing test can be calculated as the equations of the trend lines, as below:

$$C_{NO_2^-} = 2.03t^2 + 2.2673t + 0.1596 \qquad (5\text{-}18)$$

, where

t is between 0 and 2, and

$$C_{NO_2^-} = 3.5664t^2 - 28.159t + 54.995 \qquad (5\text{-}19)$$

, where

t is between 2 and 3.5.

On the contrary, if it presumed that the dosing was single-pulsed, the k value of 1st-order reaction of NO_2^--N consumption in the anoxic phase could be calculated with the experimental data in the three tests, at 0.036±0.005 (min^{-1}). Thus, the NO_2^--N consumption rate (mg g^{-1}MLSS min^{-1}) can be calculated as Equation (5-22).

$$r_{NO_2^-} = 0.036 \times C_{NO_2^-} \qquad (5\text{-}20)$$

5.1.3 Discussion

As discussed in chapter 2, the threshold of NO_2^--N concentration was related to MLSS. With the level of MLSS in the A_2 systems, the nitrite levels in the tests were shown in Table 5.3. Based on the result of Zhang *et al*. (2010), the nitrite level of 15.2 mg N g^{-1}MLSS was appropriate for anoxic P uptake to avoid inhibition. The nitrite levels shown in the table were mostly lower than 15.2, while the lower values in 3-hour constant rate tests did not achieve complete P removal. Besides, the difference between 2-h and 3-h dosing tests were very small, which indicated that NO_2^--N/MLSS was not the only factor influencing anoxic P uptake efficiency, if the other conditions were kept stable (including pH, temperature duration of anoxic phase and so on). In the 3-h and 2-h constant-rate dosing tests, the PO_4^{3-}-P concentration at the end of nitrogen doing were separately 8.5 and 12.3 mg L^{-1}, suggesting that the toxic impact of nitrite was related to PO_4^{3-}-P concentration. As discussed above, the anoxic P uptake followed Monod-type equation with sufficient NO_2^--N supply, inducing faster PO_4^{3-}-P removal, compared with 4-h and 5-h dosing strategies. Hence, in order to achieve most effective P and N removal, efficient NO_2^--N dosing, especially at the earlier period of anoxic phase, should be conducted.

Table 5. 3 Highest nitrite level in the tests of different strategies

Strategy	Test	Highest nitrite level (mg N g^{-1}MLSS)
Constant-rate	5-h	5.3
	4-h	8.8
	3-h	10.6
	2-h	9.3
	1-h	18.9
Reducing-rate	T_a	3.1
	T_b	6.1
Single-pulse		34.3

The consumption trend of NO_2^--N inducing complete PO_4^{3-}-P removal was hardly analysed in the previous studies, since toxic inhibition always occurred with higher concentration of nitrite feeding, while with step-feed strategy it can only analyse the NO_2^--N consumption trend in one single feed. Compared with step-pulse feeding of nitrite (Peng *et al*., 2011; Vargas *et al*., 2011), continuous feeding was more suitable for practical operation of WWTWs. As a result, the kinetics analysis of NO_2^--N consumption in these continuous feeding studies indicates the NO_2^--N utilisation characteristics in order to direct the operation of nitrite feeding in WWTWs.

The PO_4^{3-}-P uptake and NO_2^--N consumption rates were preliminarily developed in section 5.1.2. While based on ASM2d (Henze *et al*., 1999), both P concentration and DO are responsible to the aerobic phosphorus uptake in EBPR systems. Hence, as the activities of DPAOs, both P and N concentration in the wastewater should influence the reaction rates in anoxic phase. Consequently, the specific analysis of kinetics of phosphorus uptake and nitrogen consumption in anoxic phase will be conducted in Chapter 6, in order to modify the model development and simulation process.

5.2 Effects of temperature on P removal performance of A_2 SBRs

As temperature change in different seasons was an important environmental factor influencing the performance of P removal in practical WWTW operation, and few studies were focused on the effects of temperature change on NO_2^--N based anoxic P uptake, the impacts of temperature on anoxic P uptake in A_2 SBRs were explored in this section. In addition, as discussed in Chapter 4, the impact of temperature on NO_3^--N based SBRs (E1&E2) was the most serious among the A_2 systems. Hence, the hypothesis in this section is the performance and microbial communities in nitrate-based SBRs would be obviously changed, while nitrite-based SBRs should be relatively stable. In this experiment, the A_2 systems with NO_2^--N (T3&T4), which were compared with NO_3^--N based systems (T1&T2), were operated at 20 °C for 75 days (namely Enrichment II), and then 30 °C for 51 days.

5.2.1 The PO_4^{3-}-P removal performance in A_2 SBRs with different temperature levels

The PO_4^{3-}-P concentration change during the period of experimental operation was shown in Fig. 5.18. As can be seen in the figure, the P removal performance in T3&T4 was similar with the result in Chapter 4, higher and more stable than NO_3^--N based SBRs (T1&T2) at ambient temperature (20°C). Nevertheless, after experiencing the sudden temperature increase, totally different trends occurred in these two sets of SBRs. The performance in NO_3^--N based SBRs did not changed obviously, with non-complete P removal, where there were no large changes in the PO_4^{3-}-P concentrations at the end of anaerobic phase and the end of anoxic phase before and after the temperature increase.

On the contrary, the sludge system in NO_2^--N based SBRs was basically deteriorated by the sudden increase of temperature. In the first seven days after temperature increase, the operation performance in both T3 and T4 became worsened, with the excess PO_4^{3-}-P

amount at the end of anoxic phase. From the 8th day after temperature increase, the PO_4^{3-}-P concentration at the end of anaerobic phase was decreased to only around 16.0-18.0 mg L^{-1}, much lower than the concentration in the previous stable period. Meanwhile, the anaerobic P release and anoxic P uptake amount became approximate, followed by gradual enhancement of the performance in the following 42 days, when the recovery trend of the sludge was similar with the enrichment process of DPAOs, However, in this recovery period, P removal performance did not achieve the optimised condition before temperature increase, achieving the P removal rate of around 60-70%, which should be caused by the higher temperature.

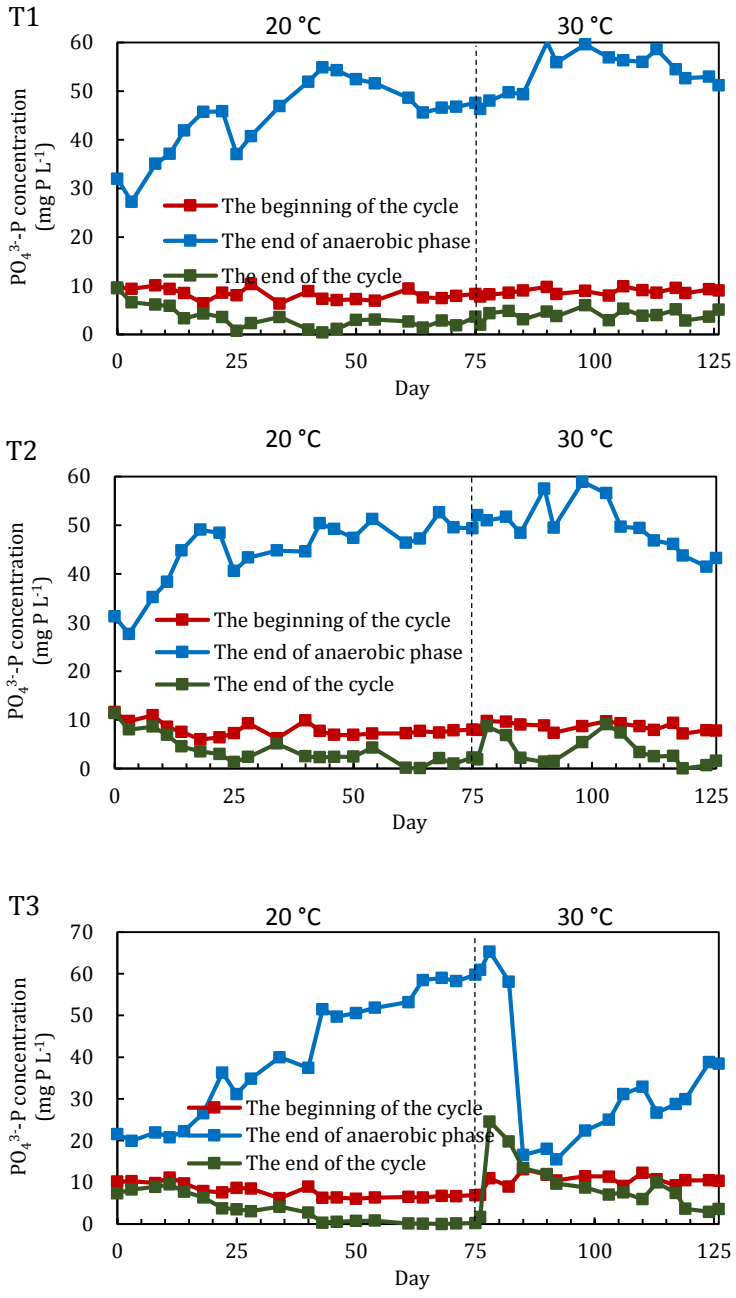

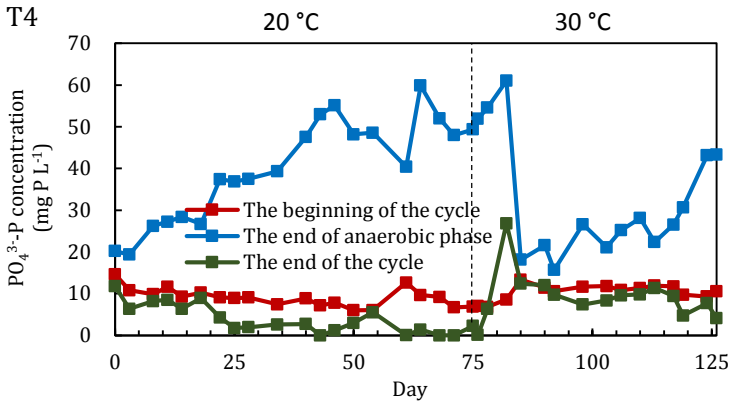

Fig. 5. 18 Performance of A_2 SBRs at different operational temperature

Fig. 5.19 demonstrates the P release performance of the A_2 SBRs with different temperature. As an important factor of the initial condition in anaerobic phase, the NO_x^--N concentration at the beginning of the cycle, which was shown in Fig. 5.19a, influenced the HAc consumption efficiency during the anaerobic phase. It suggested that during the stable period at ambient temperature (20 °C), the initial N concentration in NO_2^--N based SBRs was lower than that in NO_3^--N based SBRs, while after the temperature increase, the figure in NO_2^--N based SBRs grew suddenly and fluctuated around 12 mg L^{-1}, compared with the proximately steady values in NO_3^--N based SBRs. During the last 13 days of the experiment operation, initial N concentration in NO_2^--N based SBRs decreased from 13.7 to 6.1 mg L^{-1}, due to the gradual recovery of efficient anoxic P uptake.

The trends of DPAOs-based HAc consumption (Fig. 5.19b) and P release/HAc consumption ratio (Fig. 5.19c) were opposite with initial N concentration in NO_2^--N based SBRs, as the deterioration of DPAOs caused the insufficient HAc consumption and P release. Compared with steady period, the HAc consumption by DPAOs in T3&T4 was not adequate, commonly causing the acetate residual at the end of anaerobic phase, due to the wash out of functional microbial communities.

In Fig. 5.19c, the ratio of P/HAc in the anaerobic phase of T3&T4 experienced a sharp decrease from 0.42 to 0.04, suggesting the large amount of DPAO wash out. In the following days, with the recovery of the A_2 systems, the ratio was gradually increased to 0.34, which was similar with the value in NO_3^--N based SBRs.

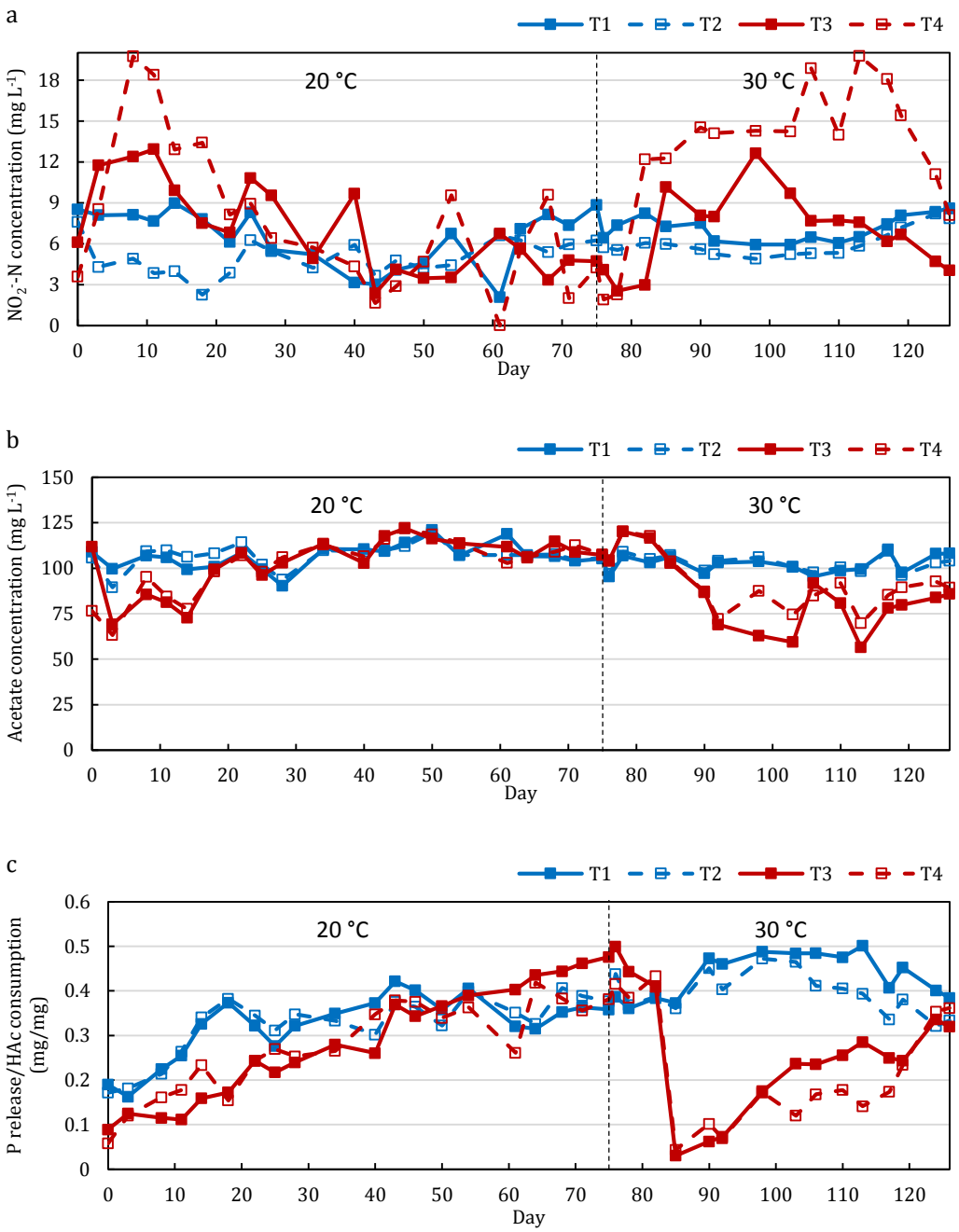

Fig. 5. 19 P release performance in T1-T4 at different temperature
Average NO_x^--N concentration at cycle beginnings (a), acetic acid amount consumed by DPAOs during anaerobic phase (b) and the ratio of P release/HAc consumption by DPAOs (c) in NO_3^--N and NO_2^--N based SBRs at different temperature

In case of anoxic phase P uptake, Fig. 5.20 demonstrates the change of P/N and e^-/P ratios during the experiment period. Due to the deterioration of NO_2^--N based A_2 systems, P uptake efficiency decreased observably, with the reduction of P/N ratio from 1.0 to 0.1 and the sudden increase of e^-/P ratio from 6.6 to 51.2. In contrast, the ratios in NO_3^--N based systems were more stable, fluctuating in 2.1-2.7 and 4.1-5.5, separately.

The main reason causing the ratio changes in NO_2^--N based A_2 systems was the fast reduction of PO_4^{3-}-P uptake rate due to the wash out of DPAOs, compared with relatively lower decrease of NO_2^--N consumption. For instance, on the 85th day of the experiment, the average anoxic P uptake in T3 and T4 was only 4.5 mg L^{-1} (45-60 mg L^{-1} at 20 °C), while the average N consumption still achieved 32.2 mg L^{-1} (40-47 mg L^{-1} at 20 °C). The slighter reduction in N consumption was mostly caused by the HAc residual at the beginning of anoxic phase, which induced the N consumption by denitrifiers in the system. In addition, as discussed in Chapter 4, in the early period of anoxic phase, PO_4^{3-}-P was still released into the systems due to the existence of HAc, although NO_2^--N dosing had been started, indicating that the values of PO_4^{3-}-P concentration at the end of anaerobic phase were not the maximums in the cycles. Hence, the actual P uptake amount in the anoxic phase should be a little higher than the measured values.

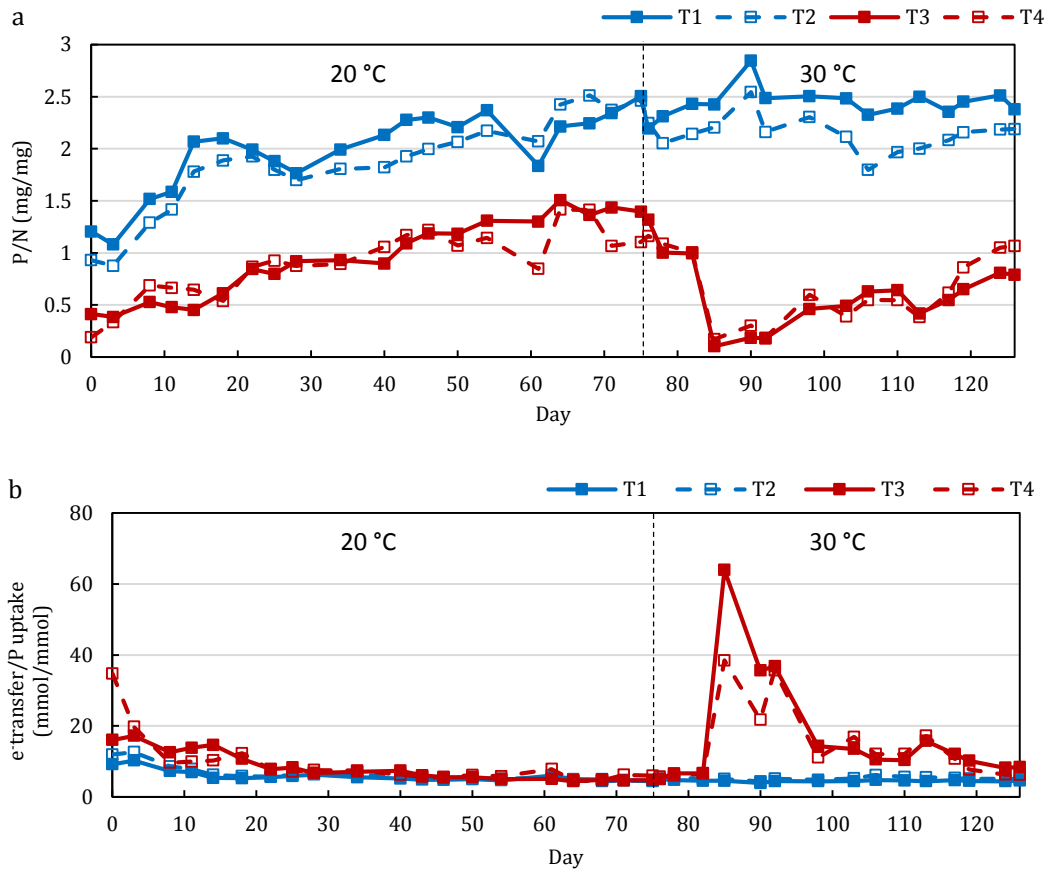

Fig. 5. 20 Ratios of P/N (a) and e^-/P (b) in anoxic phase at the different temperature

Additionally, in the first seven days after the temperature increase, the average MLSS in T3&T4 decreased from around 1400 to 800 mg L^{-1}, and the ratio of MLVSS/MLSS was increased from 67% to 89%. It was another evidence suggesting that DPAOs, the functional microbial community in A_2 P removal systems, had been washed out after the sudden temperature increase. According to the FNA calculation equation by Anthonisen *et al*. (1976), FNA concentration was decreased with the increase of temperature. It decreased from 0.26 to 0.20 μm L^{-1}, for instance, if temperature was increased from 20 to 30 °C, and NO_2^--N concentration was 10 mg L^{-1} with a pH level of 8.0. The level of FNA was much lower than that in the study of Wang *et al*. (2017), who investigated FNA based anoxic phosphorus removal. Hence, it suggested that the deterioration of the nitrite based SBRs before and after temperature increase was not caused by the change of FNA concentration.

In summary, it was concluded that at ambient temperature (20 °C) NO_2^--N based SBRs could achieve more efficient P removal, compared with NO_3^--N based systems, while anoxic P uptake with NO_3^--N were more resistant to sudden temperature increase than NO_2^--N. The result suggests that the hypothesis of this section is denied, while the opposite outcome is created. Therefore, the decline of treatment efficiencies of the SBRs in Enrichment I should be caused some other reason.

5.2.2 Microbial community analysis of A_2 SBRs with different temperature

As discussed in Chapter 4, in all the enriched P removal sludge, *Proteobacteria* was the most dominating group, replacing *Bacteroidetes* in the inoculum from WWPWs. In order to explore the change of microbial communities in the SBRs after temperature increase, the sludge samples from the reactors were analysed and compared. Two groups of samples from T1&T2 and T3&T4 were separately selected to analyse, in which 418063 and 420447 effective reads were detected. The groups in sample from T1&T2 were similar with that at ambient temperature, where *Proteobacteria* was the most frequent phylum, accounting for 45.8% of the total effective reads, followed by *Bacteroidetes*, *Planctomycetes*, *Chloroflexi*, *Acidobacteria*, *WPS*-2, *Verrucomicrobia*, *Actinobacteria*, *etc*. In comparison, the predominate group in NO_2^--N based systems was substituted by *Bacteroidetes*, accounting for 53.6%, followed by *Proteobacteria* and other groups, suggesting the wash out of DPAOs after the sudden temperature increase.

Fig. 5.21 demonstrates the common genera contained in A_2 SBRs before and after temperature increase. As can be seen in the graphs, there were 153 common genera

among NO_3^--N based systems, accounting for 50.8% in the total detected genera, while the number of the common genera between NO_2^--N based systems was only 98, accounting for 41.9% in the total detected genera. Hence, it suggested that the microbial communities in NO_2^--N based systems changed more than that in NO_3^--N based systems.

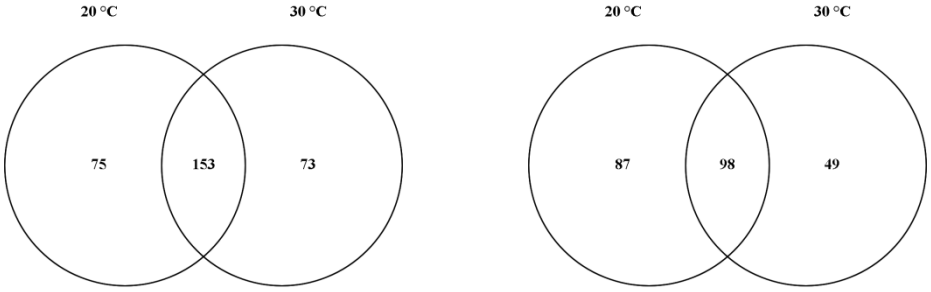

Fig. 5. 21 Venn diagrams based on genus of NO_3^--N (left) and NO_2^--N (right) based A_2 systems before and after temperature increase

After the temperature increase, the percentages of *Proteobacteria* related classes were relatively decreased, while the rate of *Bacteroidia* was increased in both A_2 systems (shown in Fig. 5.22). However, the increased percentage of *Bacteroidia* in NO_2^--N based systems was 52.5%, much higher than NO_3^--N systems (29%). In other words, *Bacteroidia* had become the dominating class in NO_2^--N based systems after the temperature increase, affecting the P removal rate of the SBRs. It also suggested that in the later period after temperature increase, P removal rate was increasing slowly, as the ratios of *Proteobacteria related classes* did not recover to initial level. On the contrary, *Bacteroidia* in T1&T2 at 30 °C was not the predominate class, which could not consume more resources for activities of DPAOs.

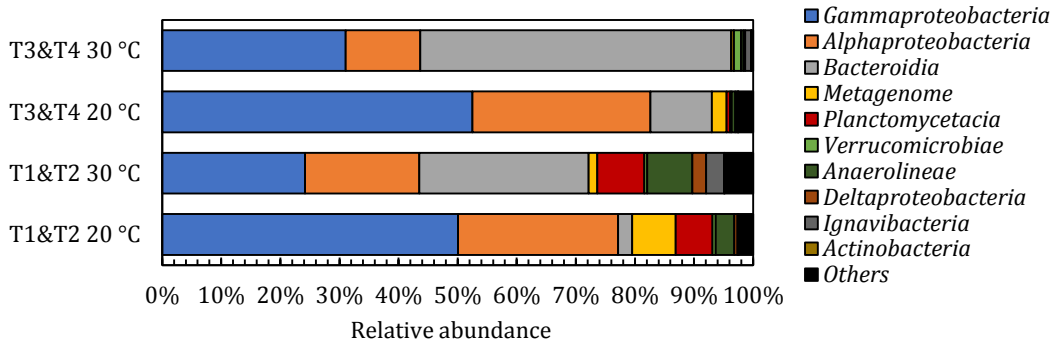

Fig. 5. 22 The relative abundances of classes in A_2 systems at different temperature

Fig. 5.23 shows the most abundant genera detected in the sludge samples of NO_3^--N and NO_2^--N based SBRs at 30 °C, compared with 20 °C. As can be seen in Fig. 5.23a, *β-proteobacteriales* related genera were still the most abundant groups in the NO_3^--N systems at 30 °C. However, the most frequent genus after temperature increase was *Dechloromonas* (the ratio increased from 1.9% to 15.0%), which replaced the unknown *Rhodocyclaceae*-related genus at 20 °C. It suggested that with the long-period continuous operation of the NO_3^--N systems, *Dechloromonas* which had been the most abundant *Rhodocyclaceae*-related group in EE3&EE4 in Enrichment II, gradually became the functional microbial group in T1&T2. In case of *α-proteobacteria*, similar genera were detected at different temperature, while all the ratios of them were basically decreased after temperature increase. In the addition, the percentages of *Terrimonas*, *Saprospiraceae*_OLB8, *Ferruginibacter* and *Microscillaceae*_OLB12, which belonged to *Bacteroidetes*, were all higher at 30 °C than 20 °C.

In comparison, the enhancing abundance of *Saprospiraceae*_OLB8 from nearly 0 to 44.4% in T3&T4 after temperature growth induced the overall rise of *Bacteroidetes*, which was the main factor causing the deterioration of P removal in the A_2 systems. *Saprospiraceae*_OLB8 was one of the most abundant microbial group in the inoculum sample from 4-stage Bardenpho process, indicating that the most frequent genus in the inoculum had recovered in the NO_2^--N based SBRs after the temperature increase. On the contrary, the ratio of *Dechloromonas* in NO_2^--N based SBRs decreased from 19.7 to 2.0% after the temperature increase, suggesting the wash out of DPAOs from the sludge. Among *Rhodocyclaceae*-related groups, the ratio of *Azospira* increased from 3.9 to 22.2%, which indicated that it might be the functional genus for P removal at the high temperature.

The results in this study suggested that the *Dechloromonas* was the functional phosphorus removal organisms in both NO_2^--N and NO_3^--N based A_2 EBPR systems in stable operation period. However, both of *Candidatus Competibacter* and *α-proteobacteria*-related GAOs reported in the previous studies (Crocetti *et al*., 2002; Beer *et al*., 2004; Wong *et al*., 2004; Oehmen *et al.*, 2005) were still hardly detected in the A_2 systems of this study. The organisms with relative high frequency, *i.e. Phreatobacter, Azospira and Saprospiraceae*, were not recognised as GAOs. Hence, it suggested that in both of NO_3^--N and NO_2^--N based A_2 EBPR systems in this study, the growth of GAOs was not enhanced by the temperature increase from 20 to 30 °C.

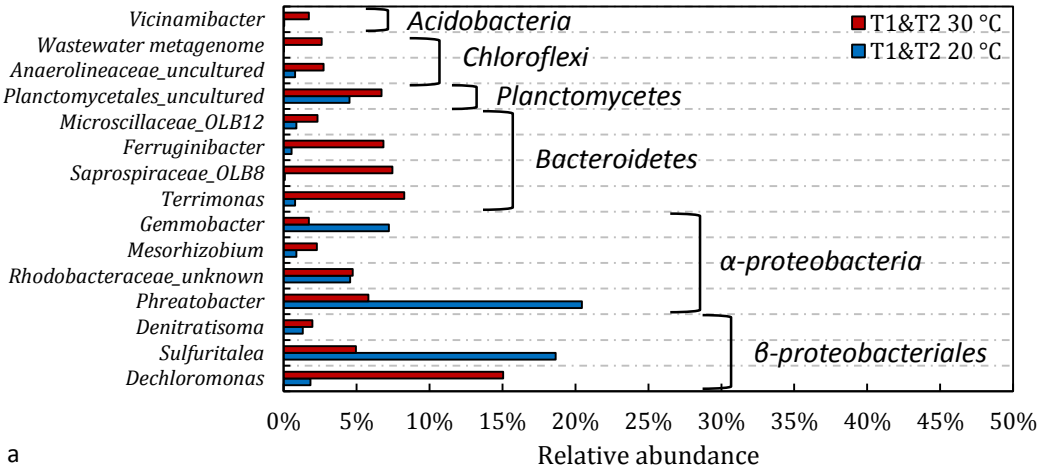

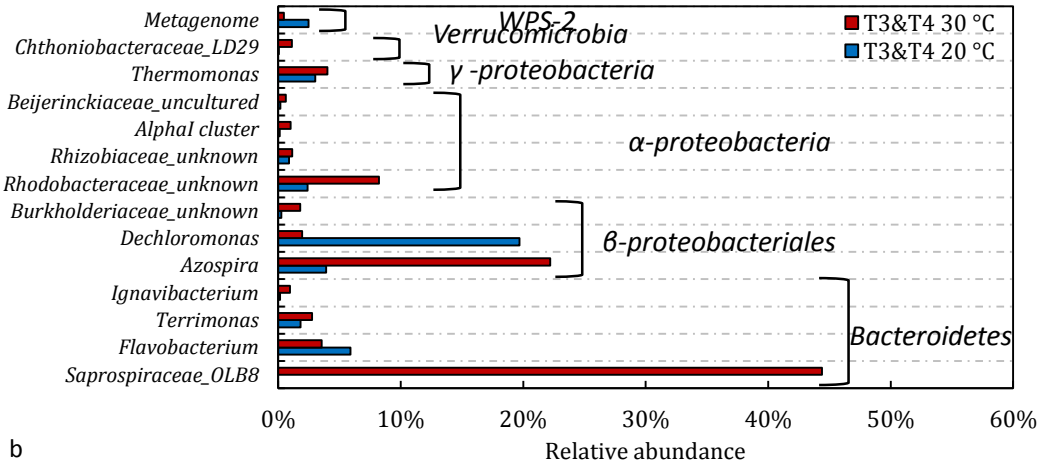

Fig. 5. 23 The relative abundance comparison of the dominant groups in NO_3^--N and NO_2^--N based SBRs at 20 °C and 30 °C

5.3 Effects of pH on P removal performance of A_2 SBRs via NO_2^--N pathway

An appropriate pH value is one of the basic factors influencing the performance of wastewater treatment process. In A_2 P removal process, 1 mol OH^- can be produced with the reduction of 1 mol NO_3^- or NO_2^-, and PO_4^{3-}-P is gradually accumulated into the sludge, which will weaken the buffer capacity of the wastewater, so pH will be increased during anoxic phase without acid addition. As more amount of NO_2^--N was consumed by the systems than NO_3^--N, pH in NO_2^--N based systems would increase more seriously.

In this session, the performances of NO_2^--N based A_2 SBR with and without anoxic pH adjustment were compared, to explore the importance of pH control in the system. In addition, the P removal performance with different pH levels (8.0 and 7.0) was evaluated, in order to justify the optimised pH was selected in the operation of the SBRs.

5.3.1 Performance comparison of NO_2^--N based A_2 SBR with and without anoxic pH adjustment

In the comparison, 5-hour N dosing was utilised for the anoxic P uptake tests, in order to achieve continuous N adding during anoxic phase to compare the change of pH and N consumption. As can be seen in Fig. 5.24, the anaerobic P release amount in both tests were at the similar level, between 50.0 and 55.0 mg L^{-1}, due to the same condition in the SBR, while the anoxic P uptake without pH control experienced lower accumulation rate in the later period. In the anaerobic phase with consumption of HAc, the pH was slightly increased from 6.85 to 7.21, due to the increase of buffer capacity of the system caused by the PO_4^{3-}-P release. In the anoxic phase, pH in Fig. 5.26a gradually increased from 7.21 to 9.45, inducing the slower P uptake, especially after the 4th hour, when pH increased to higher than 8.5.

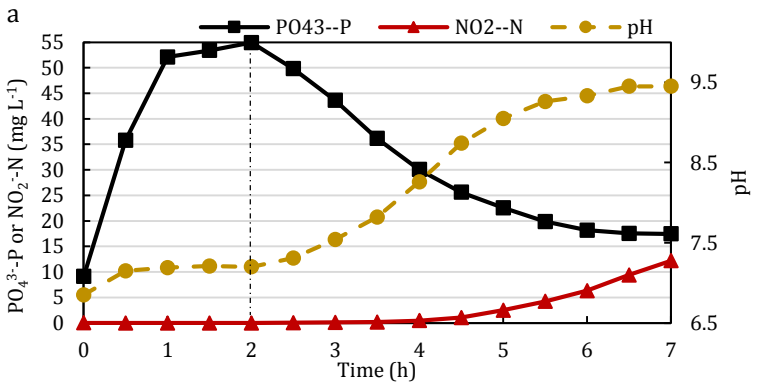

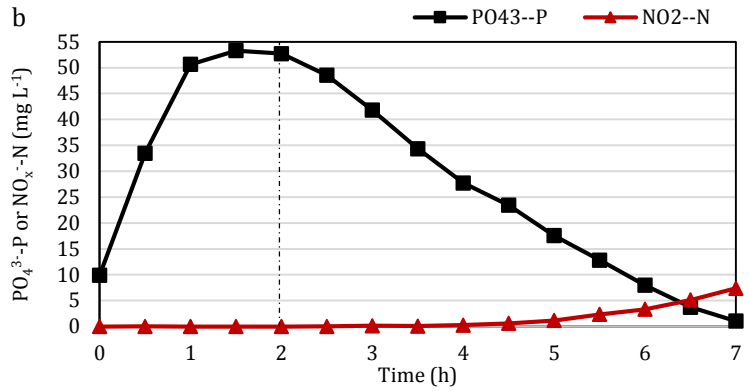

Fig. 5. 24 Cycle performance of NO_2^--N based SBR without (a) and with (b) pH adjustment

Fig. 5.25 compared the difference of PO_4^{3-}-P uptake and NO_2^--N consumption and their ratio in the A_2 SBR without and with pH adjustment. Contrasted with the stable and smooth change of P uptake rate in each time slot with pH control, only the trends of P uptake in the first five 30 min without pH control were similar when pH was lower than 8.75, while after that period the P uptake efficiency became obviously lower than the efficiency in the corresponding time of test with pH control. From the 6th 30 min of the anoxic phase without pH control, the PO_4^{3-}-P decreasing levels were always lower than 3.0 mg L^{-1}, especially in the last 30 min when the pH had been 9.45, PO_4^{3-}-P concentration was only decreased 0.1 mg L^{-1}.

In addition, N consumption efficiency without pH control were also lower than that with pH control, but the weakened extent was smaller than PO_4^{3-}-P uptake. In Fig. 5.25a, the N consumption levels in the first six 30 min were all higher than 4.0 mg L^{-1}, followed by decreasing to 2.6-3.5 mg L^{-1} per 30min. On the contrary, N consumption amounts in the first five 30 min in Fig. 5.25b were closed to or higher than 4 mg L^{-1}, while from the 6th 30 min, the rates became lower than 3.0 mg L^{-1}. As a result, the P/N ratio in the test without pH control reduced to only 0.006 in the final 30 min.

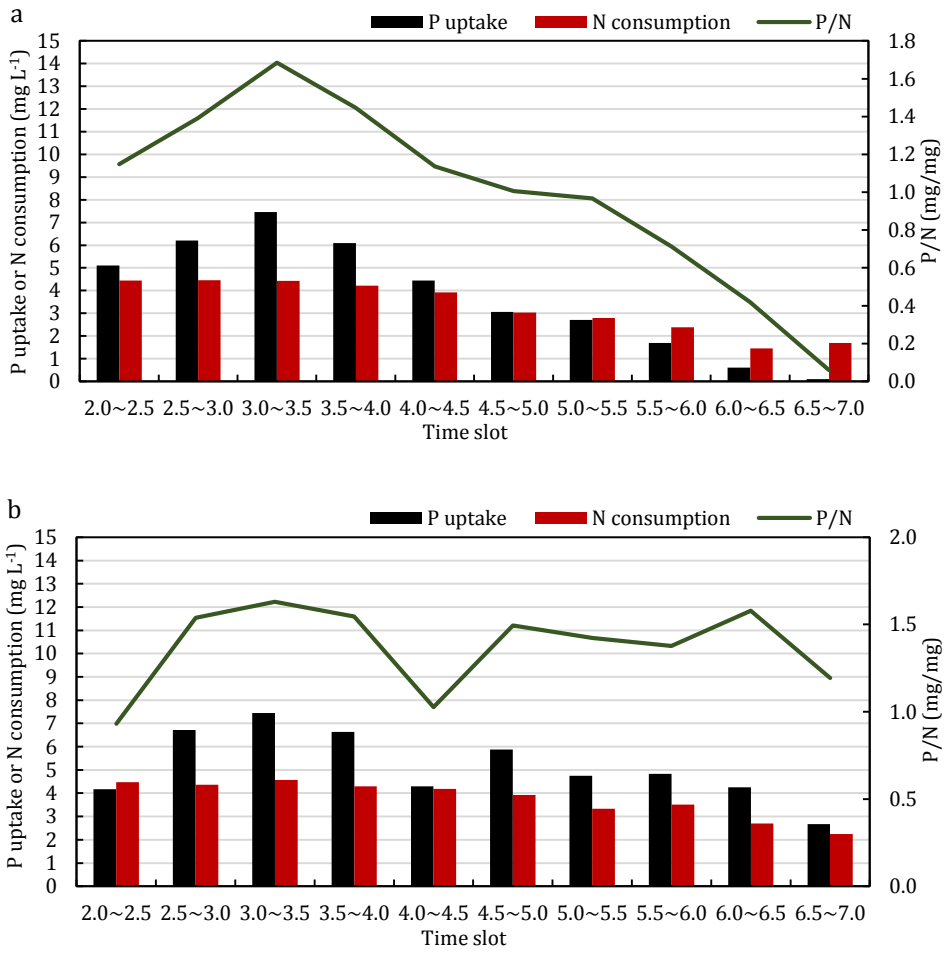

Fig. 5. 25 P uptake, N consumption and P/N ratio during anoxic phase without and with pH control

5.3.2 Effects of lower pH on the process performance and microbial communities of A_2 SBR via NO_2^--N pathway

Since pH can affect the performance of P removal and microbial communities in EBPR systems, nitrite-based EBPR with lower pH level was conducted with the comparison of normal pH level in this section. The hypothesis of this section was that lower pH level could deteriorate P removal performance in the nitrite-based EBPR system, based on the literature review of the previous studies and the successful enrichment of DPAOs in Enrichment II with the anoxic pH level of 7.5-8.0. It had been justified that 7.5-8.0 was an appropriate pH range for anoxic P removal, while P uptake would be obviously restrained if pH was higher than 8.5. In this session, anoxic pH value range between 7.0 and 7.5 was investigated in an A_2 SBR (H1) where contained enriched DPAO sludge via NO_2^--N, to explore its impacts of pH on PO_4^{3-}-P removal. In the experiment, the anoxic pH of the SBR

was kept at 7.5-8.0 for 27 days after the successful enrichment of DPAOs, and then decreased to 7.0-7.5 for 17 days, followed by being increased back to 7.5-8.0 for 48 days. The other operation factors were kept as the same as that in Enrichment process II.

5.3.2.1 The effects of pH change on P removal performance of NO_2^--N based SBR

The PO_4^{3-}-P changes in H1 during the period were shown in Fig. 5.26. As can be seen in the graph, the PO_4^{3-}-P concentration in the effluent was increased gradually and became higher than the value at the beginning of the cycles during the period of pH reduction, while the P concentration at the end of anaerobic phase was not stable and decreased, which suggested that the DPAO system in the SBR was becoming deteriorated after experiencing the pH decrease. On the 44th day of the experiment, the pH in anoxic phase was adjusted back to 7.5-8.0 to recover the P removal system, PO_4^{3-}-P concentration in the effluent was decreased to below 1.0 mg L^{-1} after one week, and then gradually reduced to below 0.5 mg L^{-1} after 25 days, suggesting the P removal capacity of the system was completely recovered.

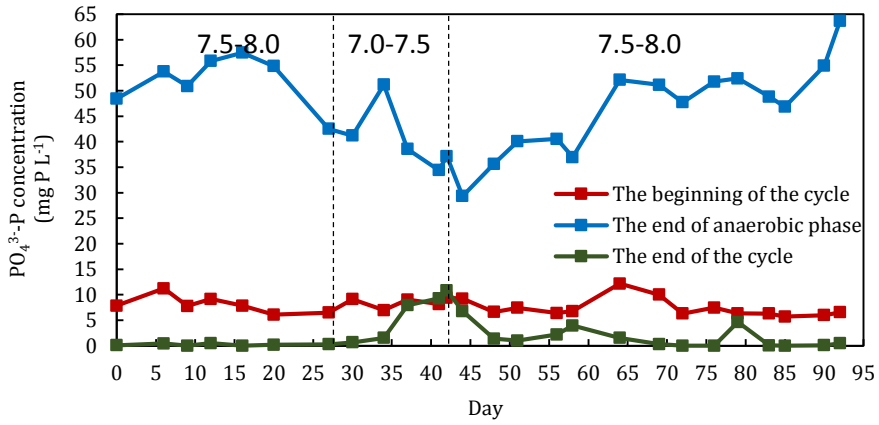

Fig. 5. 26 Performance of H1 with different anoxic pH value ranges

The anaerobic P release and HAc uptake performance during the period of experiment was shown in Fig. 5.27, with the comparison of H2, which was operated under the same conditions but stable anoxic pH (7.5-8.0). It suggested that duration of pH decrease in the experiment, the amount of acetate consumption in H1 was only slightly lower than H2, without any obvious difference from the period with normal pH, suggesting that the sludge system in H1 could also consume sufficient HAc when anoxic pH was reduced.

However, even though there was fluctuating difference between the ratios of P/HAc in H1 and H2, it became very notable on the 41st day of the experiment (0.27 in H1 and 0.55 in H2, respectively), when the pH had been reduced for 15 days. After adjusting the pH back, the ratio in H1 gradually increased and narrowed the gap, prior to the elimination of the difference after around 10 days.

Consequently, P release in anaerobic phase was also affected by the decrease of pH, possibly caused by the nonsufficient P uptake and the change of microbial communities in the reactor, which had been proved in analysis of microbial groups in the next session.

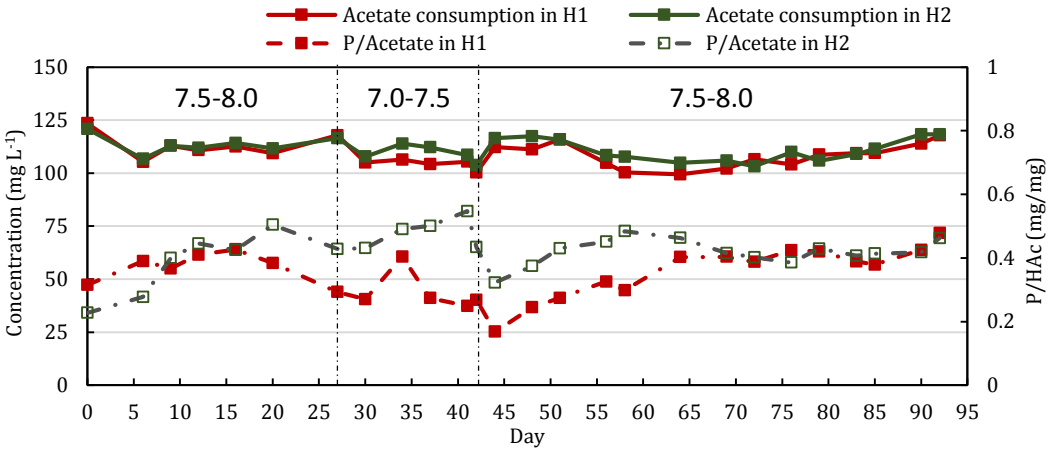

Fig. 5. 27 Performance comparison of anaerobic P release and HAc consumption in H1 and H2

In case of anoxic P uptake and N consumption (Fig. 5.28a), the P/N ratios in both reactors were between 1.0 and 1.5 in the stable period with normal pH (7.5-8.0), while the ratio in H1 was decreasing to around 0.7, from the period of pH decrease to the early period after pH rising back. In the following days, the ratio in H1 gradually increased back to the similar level as H2, when the P removal rate recovered as well. Similar result was found in the ratio of e^-/P, as shown in Fig. 5.28b, where there was an obvious peak at 9.7 in the beginning period after pH was adjusted back in H1. It suggested the weaken P uptake capacity of the system at that time, before the gradual recovery in the following duration when the rate reduced to normal level.

The results indicated that with the anoxic pH of 7.0-7.5, the activated sludge system in H1 gradually lost the capacity of PO_4^{3-}-P removal, while this capacity could be easily recovered after a period (around 25 days) if the pH was adjusted back to 7.5-8.0.

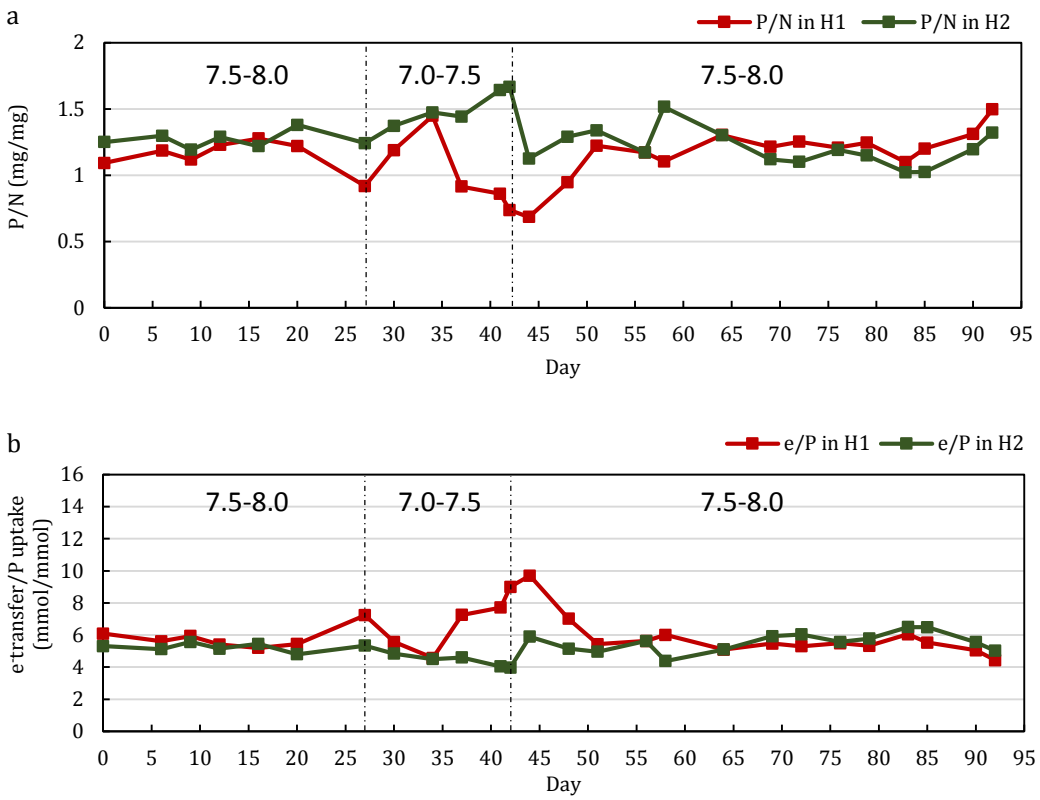

Fig. 5. 28 P uptake performance with different anoxic pH level in H1, compared with H2 (a: P/N; b: e^- /P)

Additionally, the MLSS and MLVSS in H1 were decreasing during the period with pH of 7.0-7.5, respectively declining to 900 and 660 mg L^{-1} (with the ratio of MLVSS/MLSS of 73%) at the beginning of the period when pH increased back, which also suggested the wash out of a part of activated sludge in the system. With the changing back of anoxic phase, the solids were still decreasing in the first two weeks, to 680 and 410 mg L^{-1}, while the MLVSS/MLSS ratio was decreased to 60%, which suggested that in this period the inoperative organisms were gradually washed out of the system, and phosphorus was gradually accumulated in the sludge. By the end of the experiment, the MLSS and MLVSS were increased back to 1200 and 760 mg L^{-1} (with the ratio of MLVSS/MLSS of 63%), respectively, due to the complete recovery of the DPAOs.

5.3.2.2 Microbial community analysis after pH decrease in H1

As discussed above, *Rhodocyclaceae*-related genera in *Proteobacteria* was the main functional group of DPAOs in the enriched P removal sludge. The sludge sample in H1 after pH decrease was analysed, which justified that the reduction of pH induced the change of microbial communities in the reactor. The sludge sample in H1 on the last day of pH

decrease was selected to analyse, where *Proteobacteria* and *Bacteroidetes* were still the most phyla in the sample, accounting for 98.2% (50.5% and 47.7, separately) of the detected effective reads.

As can be seen in Fig. 5.29, after the change of anoxic pH change, the most abundant groups, namely *Bacteroidia*, *γ-proteobacteria* and *α-proteobacteria*, had totally accounted for 98.1% of the microbial system in the sludge sample, and the percentages of all the other groups were below 0.5%. The percentages of *γ-proteobacteria* and *α-proteobacteria* in the SBR decreased from 39.1% and 28.9% to 29.4% and 21.0%, while the rate of *Bacteroidia* increased from 24.7% to 47.7%. Since the majority of DPAOs belonged to *γ-proteobacteria* as discussed above, the comparison of its wash out and the growth of *Bacteroidia* suggested the decline of P removal performance in the SBR.

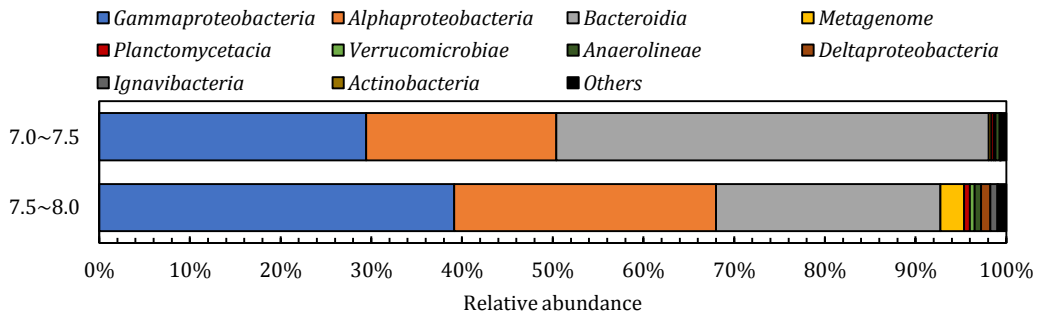

Fig. 5. 29 The relative abundances of classes in sludge samples before and after anoxic pH decrease

The most abundant genera in the sludge sample after pH decreased was shown in Fig. 5.30, compared with the sample with normal pH. It indicated that *Chryseobacterium*, a kind of bacteria related to nitrification and denitrification in wastewater (Kundu *et al*., 2014), contributed the most ratio of the increase of *Bacteroidetes*, increased from 6.7% to 46.3% of the total effective reads in the sample, which was much higher than the other groups. On the contrary, the functional DPAOs did not account for a relatively large ratio in the sludge, inducing the decline of P removal performance.

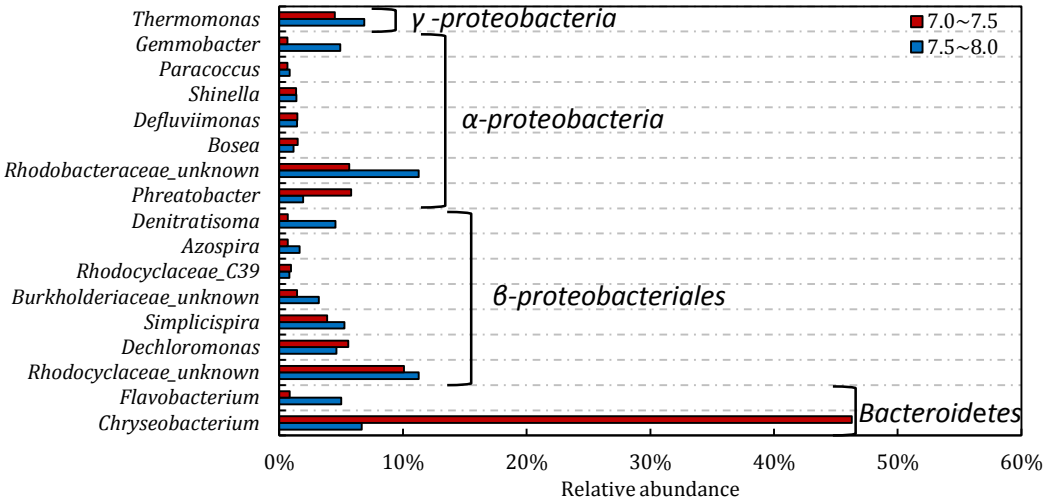

Fig. 5. 30 The relative abundances of the dominant groups in the sludge sample after pH decrease compared with the sample at normal pH

5.4 Discussion and summary

Based on the successful enrichment of DPAOs with 4-hour constant-rate dosing of NO_2^--N, more anoxic dosing strategies for A_2 SBRs were analysed to explore the characteristics and potential of P uptake via NO_2^--N pathway. The results indicated that efficient P removal (50.0-55.0 mg L^{-1}) could be achieved with constant-rates of 5-hour, 4-hour 2-hour, and reducing-rates of 3-hour with 45-48 mg L^{-1} NO_2^--N in the 5-hour anoxic phase. 3-hour constant-rate dosing did not accomplish optimised anoxic P uptake, since its dosing rate was relatively slow in the early period of anoxic phase, while relatively fast in the late period, causing the slight NO_2^--N accumulation. Compared with 3-hour constant-rate dosing, the reducing rate dosing strategies effectively enhanced the P uptake and N consumption in the early period and avoid the N accumulation in the late period of anoxic phase. The overall P uptake rate in the tests could averagely achieve 15.7 mg L^{-1} h^{-1} or 11.2 mg g^{-1}MLSS h^{-1}, if the MLSS in the SBR was recognised as 1.4 g L^{-1}.

The different performance of 3-h and 2-h dosing tests showed that the threshold value of NO_2^--N was not constant, which should be related to the PO_4^{3-}-P concentration in the EBPR system. Compared with step-feeding strategy (Peng *et al*., 2011; Vargas *et al*., 2011), continuous dosing of NO_2^--N is more appropriate for the practical treatment in WWTPs, with more convenient operation and easier determination equipment.

A stable temperature was a key factor which could support the stable P removal in A_2 SBRs via NO_2^--N pathway. As stated in section 5.2, the sudden temperature increased could deteriorate the P removal system with NO_2^--N, which needed to recover the microbial communities and P removal capacity slowly with high temperature. However, the results in section 5.2 were inconsistent with the P removal performance change in the period of temperature increase in Enrichment I (in section 4.2). Based on the previous suggestion in section 4.2, the growth of GAOs might be enhanced after temperature increase (Oehmen *et al*., 2005 and Lopez-Vazquez *et al*., 2009). Nonetheless, it was found that in section 5.2, the ratio of *Dechloromonas*, one of the abundant genera in the enriched P removal sludge in T3&T4, was decreased from 19.7% to 2.0% after the temperature increase, while the ratio in T1&T2 was increased from 1.9% to 15.0%. It suggested that the growth of the effective PAO in NO_3^--N based A_2 SBRs was enhanced after temperature increase, while it was not found the ratio of GAOs was obviously increased in this process. Hence, it would indicate that the performance decline of E1&E2 in Enrichment I was caused some other unexpected reasons, not only the temperature increase. On the contrary, the deterioration of P removal in NO_2^--N based SBRs after the sudden temperature increase in section 5.2 should be caused by the inadaptability of microbial groups to the temperature rise, or that the NO_2^--N concentration threshold value of the sludge systems was changed after the temperature rise, which needed the DPAOs to adapt gradually. Overall, NO_2^--N based SBRs were more appropriate to operate at more stable temperature.

In case of pH, the optimised anoxic pH range was 7.5-8.0, which could enhance P uptake in anoxic phase and the growth of DPAOs (PAOs), with the similar result of Serafil *et al*. (2002), Oehmen *et al*. (2005), Zhang *et al*. (2010) and Peng *et al*. (2011). The pH decrease could decline the P removal and induce the growth of non-DPAOs in the system, while they could be recovered if the pH was adjusted back to the appropriate level.

In summary, with the exploration of this session, it can be concluded that:

- A_2 SBRs with NO_2^--N pathway could be achieved with several N dosing strategies, including long-term constant-rate dosing and reducing-rate dosing, which can effectively avoid toxic inhibition from N accumulation and realise complete PO_4^{3-}-P removal

- The anoxic P uptake and N consumption efficiencies were related to the real-time P concentration in the wastewater if NO_2^--N dosing rate was sufficient in each unit of time
- Anoxic PO_4^{3-}-P uptake with NO_2^--N can achieve better efficiency than NO_3^--N at ambient temperature.
- Anoxic PO_4^{3-}-P uptake with NO_3^--N is more resistant to sudden temperature increase than NO_2^--N.
- pH range of 7.0-7.5 in anoxic phase was not appropriate for A_2 P removal via NO_2^--N pathway, while if the anoxic pH was increased to higher than 8.5, it will also restrain the P uptake.

Chapter 6 Model development and simulation for A_2 EBPR system in two-sludge process

6.1 Model development

6.1.1 Data collection

The experimental results including MLSS, HAc, PO_4^{3-}-P and NO_2^--N concentrations in 2-h, 3-h, 4-h constant-rate NO_2^--N dosing strategies were mainly utilised in the model development. In addition, the results of polyP, PHB and glycogen analysis, and basic HAc and PO_4^{3-}-P changes in the enrichment processes were also applied in this section to describe the model.

6.1.1.1 Data collection of MLSS, HAc, PO_4^{3-}-P and NO_2^--N concentrations

The concentrations of HAc, PO_4^{3-}-P and NO_2^--N in the constant-rate dosing tests were the essential information used for the model development, including the determination of the coefficients of kinetics and stoichiometry.

Since the MLSS in the systems was kept at 1200-1400 mg L^{-1} during the test period, 1.4 g L^{-1} was utilised for the calculation of PO_4^{3-}-P uptake and NO_2^--N consumption rates. Hence, the HAc and PO_4^{3-}-P concentrations in the influent were 2.64 mmol C g^{-1}MLSS and 0.14 mmol P g^{-1}MLSS. In addition, the PO_4^{3-}-P concentration was 1.25 mmol g^{-1}MLSS at the end of anaerobic phase (1.11 mmol P g^{-1}MLSS released, the average phosphorus release level in the stable period of EE6 and D1 in Enrichment II and the test period, since the P release level from the successful enrichment and test period were stable). In anoxic phase, the total NO_2^--N dosing strength in 2-h, 3-h and 4-h were separately 2.45, 2.64 and 2.42 mmol g^{-1}MLSS.

6.1.1.2 Estimation of polyP, PHA and glycogen changes during the cycle

a. polyP

The PO_4^{3-}-P release was induced by the hydrolysis of polyP, while the analysis of polyP had relatively obvious error, so the fraction of polyP was determined by estimation. If the conversion is assumed to be complete, the estimation of polyP-P can be conducted via the combination of the measured results of released phosphorus and the concentration of PO_4^{3-}-P in the wastewater.

The measured values (Table 6.1) of polyP in E3&E4 on Day 106, 147 and 180 of Enrichment I, were selected in the estimation. Since the phosphorus release level of E3&E4 in the stable period of Enrichment I was basically as the same as EE3 &EE4 in Enrichment II and D1&D2 in the period of dosing-strategy tests, the polyP storage level should be similar in the three process.

Table 6. 1 Selected values of polyP for the estimation (mg P L^{-1})

Sample		The beginning of anaerobic phase	The end of anaerobic phase	The end of anoxic phase
Day 106	**E3**	50.3	24.4	58.8
	E4	50.7	0.0%	31.6
Day 147	**E3**	63.6	0.0%	22.7
	E4	55.9	0.0%	16.4
Day 166	**E3**	68.2	0.5%	34.5
	E4	67.7	0.5%	27.2
Average		59.4±7.5	26.0±5.8	68.4±7.3

Based on the measurement, the estimation was conducted, where 59.4 mg L^{-1} was selected as the concentration of polyP at the beginning of the anaerobic phase, and the concentration of polyP at H 0.5 and H 1.0 would be calculated with the same sum of PO_4^{3-}-P and polyP (59.4 + 6 = 65.4 mg L^{-1}, where 6 mg L^{-1} is the initial PO_4^{3-}-P concentration at the beginning of anaerobic phase), as 26.6 and 10.2 mg L^{-1}. Consequently, a profile of polyP change in the first hour of anaerobic phase can be made, as Fig. 6.1. It can be seen that the polynomial trend line of the points has higher R^2 value than the linear one, similar with the change of PO_4^{3-}-P concentration change.

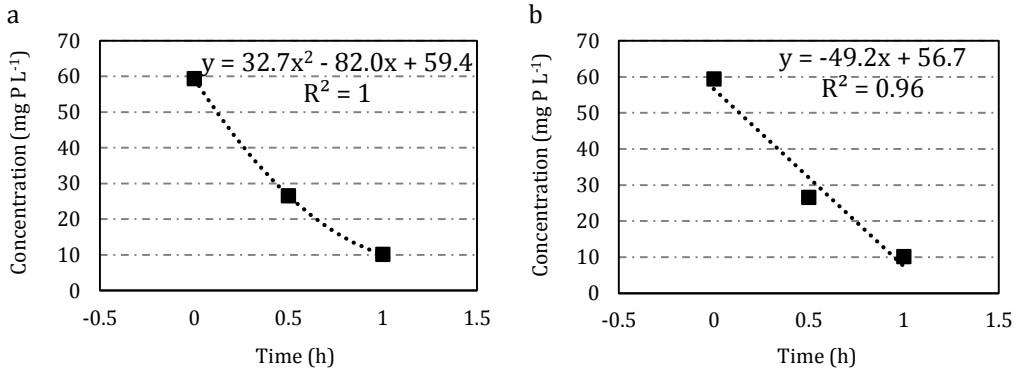

Fig. 6. 1 Trend lines of polyP concentration change in the first hour of anaerobic phase in A_2 SBRs

Hence, Equation (6-1) determined by polynomial trend line can be utilised to calculate the polyP amounts in the first hour of anaerobic phase.

$$C_{polyP-P} = 32.7t^2 - 82.0t + 59.4 \quad (6\text{-}1)$$

where

t is between 0 and 1.

For the estimation of anoxic phase, polyP increased with the uptake of PO_4^{3-}-P. If the phosphorus utilisation in biomass growth is ignored, the accumulated PO_4^{3-}-P will be used in polyP production. Hence, the polyP change in anoxic phases of 5-h, 4-h and 2-h can be estimated with the difference between 65.4 mg L^{-1} (the same sum value as anaerobic estimation) and PO_4^{3-}-P concentration in the wastewater, as Fig. 6.2, suggesting that polynomial trend lines can fit the polyP increase in the anoxic phase of constant NO_2^--N dosing rate dosing strategies, with highest R^2 values of 0.9979, 0.996 and 0.993.

a: 5-h

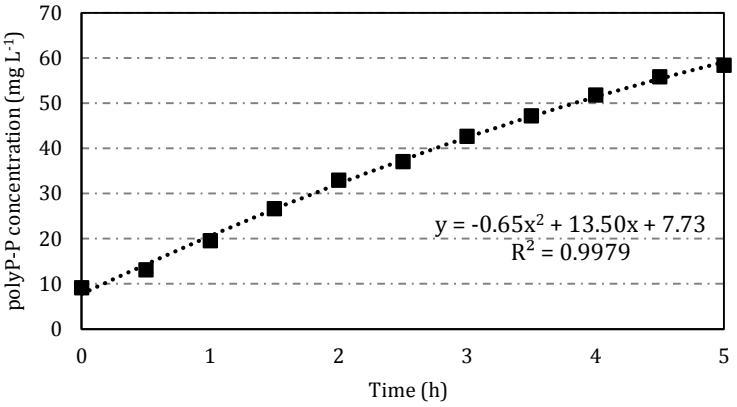

b: 4-h

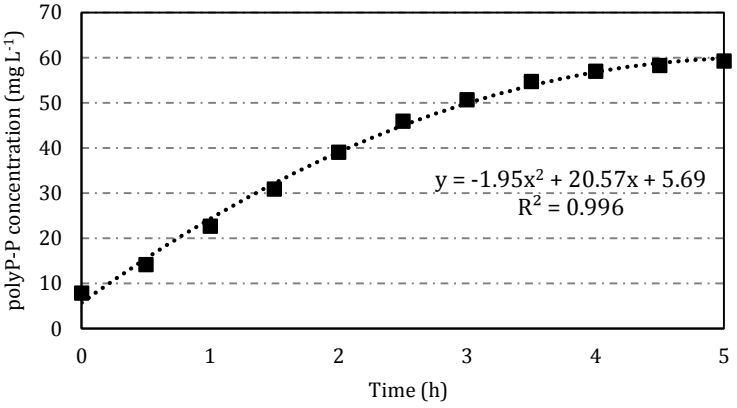

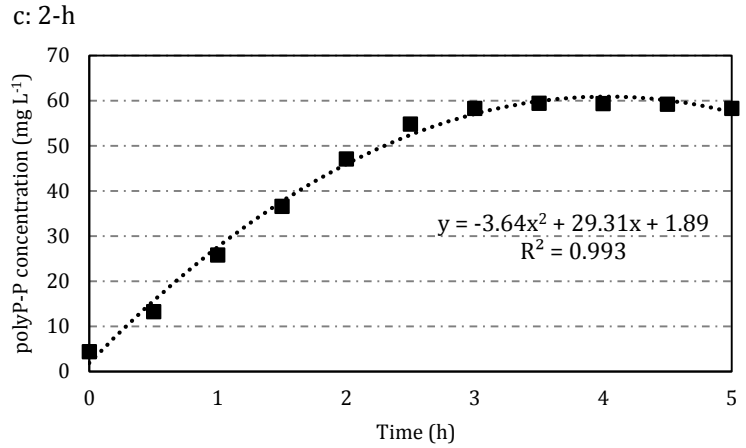

Fig. 6. 2 Trend lines of polyP concentration change in anoxic phase of A_2 SBRs

b. PHA and Glycogen

Since PHB is the main product of PHA in acetate based EBPR process, this section will only focus the estimation of PHB. Based on the measurement of PHB of EE1 and EE5 in the stable period of Enrichment II, the content at the end of anaerobic phase was around 55.0-66.1 mg g^{-1}MLSS (Table 6.2), while no PHB content could be detected at the beginning of anaerobic phase and the end of anoxic phase.. If MLSS was controlled at 1400 mg L^{-1}, PHB content at the end of anaerobic phase was in the range of 77.0-92.5 mg L^{-1} (averagely 85.4 mg L^{-1}, or 2.79 mmol C g^{-1}MLSS).

Table 6. 2 Detected PHB content in the A_2 systems (mg g^{-1}MLSS)

Sample		At the beginning of anaerobic phase	At the end of anaerobic phase	At the end of anoxic phase
Day 48	**EE1**	0	66.1 & 62.0	0
Day 78	**EE5**	0	55.0	0
Average		0	61.0±4.6	0

The measurement of glycogen had relatively high error in the analysis. The detected results on the selected 5 days from Day 88 to Day 166 in Enrichment I were applied for the estimation of glycogen change. The range of glycogen at the beginning of anaerobic phase, the end of anaerobic phase and the end of anoxic phase in the measurement period (in A_2 SBRs in Enrichment I, as shown in Table 6.3) was separately 4.7-9.2, 4.0-7.9 and 5.0-8.5 mmol C L^{-1}. Thus, the anaerobic consumption range was 0-3.4 mmol C L^{-1} (averagely 1.4±0.8 mmol C L^{-1}) and the anoxic storage range was 0.1-4.1 mmol C L^{-1} (averagely 1.3±0.9 mmol C L^{-1}).

Table 6. 3 Detected glycogen content in the A_2 systems (mmol C L^{-1})

Sample		At the beginning of anaerobic phase	At the end of anaerobic phase	At the end of anoxic phase
Day 88	E1&E2	7.2 & 7.7	6.2 & 6.4	6.6 & 7.1
	E3&E4	5.9 & 5.7	5.3 & 5.2	5.7 & 5.6
	E5&E6	5.9 & 7.4	5.5 & 6.4	5.7 & 6.5
Day 96	E1&E2	8.1 & 6.1	4.7 & 4.8	7.5 & 6.2
	E3&E4	6.6 & 6.9	4.4 & 4.2	6.4 & 5.8
	E5&E6	6.7 & 6.6	4.2 & 4.1	6.4 & 6.3
Day 106	E1&E2	7.0 & 6.9	5.5 & 5.5	7.0 & 7.3
	E3&E4	5.4 & 5.3	4.1 & 4.7	6.2 & 5.5
	E5&E6	6.0 & 5.7	5.2 & 4.8	6.3 & 6.4
Day 147	E1&E2	5.9 & 4.7	5.1 & 3.9	5.4 & 4.9
	E3&E4	6.0 & 5.6	4.5 & 4.3	6.1 & 5.7
	E5&E6	7.8 & 7.1	6.5 & 5.1	7.0 & 6.3
Day 166	E1&E2	9.2 & 8.5	7.9 & 7.1	8.2 & 7.8
	E3&E4	7.1 & 7.5	4.1 & 5.1	8.1 & 8.5
	E5&E6	8.7 & 7.5	7.0 & 4.4	7.4 & 6.6
Average		6.7±1.0	5.2±1.0	6.4±0.9

In the anaerobic phase of this study, the PHB production is induced via the HAc uptake and degradation of glycogen. The general HAc consumption in anaerobic phase is 3.7 mmol C L^{-1} (2.64 mmol C g^{-1}MLSS), with glycogen degradation (1.4 mmol C L^{-1} or 1.0 mmol C g^{-1}MLSS), which should produce around 3.9 mmol C L^{-1} PHB (2.79 mmol C g^{-1}MLSS).

In case of anoxic phase, the consumption of PHB contributes to the PO_4^{3-}-P transport, polyP synthesis, glycogen production and biomass growth. Thus, the relationship of PHB and glycogen can also be analysed with carbon mass balance, which can be basically presented by the below equation (Smolders *et al*., 1994b).

$$3.6CH_{1.5}O_{0.5}(PHB) \rightarrow CH_{2.09}O_{0.54}N_{0.2}P_{0.015}(biomass) + CH_{\frac{10}{6}}O_{\frac{5}{6}}(Glycogen) + 1.6CO_2 \quad (6\text{-}2)$$

If the MLVSS of the SBR was 850 mg L^{-1} (general level during the stable period in Chapter 4&5), the biomass growth amount was 85 mg L^{-1} d^{-1}, as the SRT was 10 days. Accordingly, the growth amount per cycle (anoxic phase) 28.3 mg L^{-1}, namely 1.1 mmol C L^{-1}. As a result, in order to produce 1.1 mmol C L^{-1} biomass, around 4.0 mmol C L^{-1} PHB would be degraded (closed to the measurement value of 3.9 mmol C L^{-1}), while 1.1 mmol C L^{-1} (also in the measurement range of 0.1-4.1) glycogen would be produced as well.

The general ratios of P/VFA and P release/PHA production in anaerobic phase were respectively around 0.43 and 0.41 (mg/mg), which were in the ranges of 0.35-0.62 and 0.24-0.49 in the HAc-based P release among the previous studies, suggesting the P release and PHA production in anaerobic phase were at the normal level of EBPR process. While compared with the oxygen based EBPR process (Filipe *et al*., 2001; Oehmen *et al*., 2005; Lu *et al*., 2006), the ratio of P/VFA was relatively lower, implying that NO_2^--N based EBPR could achieve P removal even though anoxic P storage capacity of DPAOs was lower than aerobic PAOs. The ratio of P release/glycogen consumption was 1.14, which was also in the normal range in the previous studies.

In anoxic phase, the ratio of P uptake/PHA consumption was 0.43, which was higher than the values of Guisasola *et al*. (2009) and Lanham *et al*. (2011) in anoxic P uptake process, suggesting the P uptake efficiency was relatively higher with nitrite in this study. The ratio of P uptake/glycogen production was 1.55, higher than most ratios of previous studies, which indicated more effective PHA and electron acceptor consumption was used for P uptake rather than glycogen replenishment.

6.1.2 Metabolisms in anaerobic phase

The kinetics of HAc uptake in anaerobic phase was developed with determined HAc concentration, which could be demonstrated as Equation (5-1). As discussed in Chapter 3, the anaerobic metabolisms include polyP hydrolysis, glycogen degradation, HAc uptake and PHB production. With the HAc consumption of 2.64 mmol C g^{-1}MLSS by DPAOs, PHB of 2.79 mmol C g^{-1}MLSS was produced. In addition, the released PO_4^{3-}-P was around 1.11 mmol g^{-1}MLSS. The averagely value of glycogen consumption of 1.0 mmol C g^{-1}MLSS was applied.

Based on the metabolic model of Kuba *et al*. (1996a), the energy for PAOs maintenance was from the degradation of polyP. However, it was found that the anaerobic maintenance of PAOs was not only supported by polyP but also by glycolysis (Zhou *et al*., 2009; Lanham *et al*., 2014). Hence, the anaerobic metabolism including maintenance should consist of polyP hydrolysis and glycolysis. Based on the results of experiments in Chapter 4 & 5, the stoichiometric equations in anaerobic phase of A_2 process can be determined. The overall metabolism is shown as Equation (6.3), and the yield coefficients were also demonstrated in Appendix C.

$$-CH_2O - 0.38CH_{\frac{10}{6}}O_{\frac{5}{6}} - 0.42HPO_3 + 1.05CH_{1.5}O_{0.5} + 0.33CO_2 + 0.42H_3PO_4 + 0.63H_2O = 0 \quad (6\text{-}3)$$

6.1.3 Metabolisms in anoxic phase

The relationship among P uptake, N consumption and the P concentration was pre-discussed in last chapter, and it will be investigated more specifically in this section. The kinetics of P uptake and N consumption in anoxic phase was depended on the NO_2^--N dosing strength, as mentioned in section 5.1. Hence, the model development should be conducted with different cases, including sufficient N dosing (2-h test) and non-sufficient N dosing (3-h and 4-h test), in order to distinguish the reaction rates under altered conditions.

6.1.3.1 PO_4^{3-}-P uptake rate

In 3-h and 3-4 constant-rate dosing tests (nitrogen input <4.6 mmol g^{-1}MLSS h^{-1}), P uptake rate was related to both PO_4^{3-}-P and NO_2^--N concentrations in the wastewater, since it was influenced by the low nitrogen feeding in the anoxic phase. Consequently, if the inhibition caused by FNA was avoided, the P uptake reaction rate can be calculated by Equation (6-4), which was derived from ASM2d (Henze *et al*., 1999).

$$r_P = r_{Pmax} \cdot \frac{S_{NO_2}}{K_{P-NO_2}+S_{NO_2}} \cdot \frac{S_{PO_4}}{K_{P-PO_4}+S_{PO_4}} \cdot \frac{X_{PHA}/X_{PAO}}{K_{PHA}+X_{PHA}/X_{PAO}} \quad (6\text{-}4)$$

While if the anoxic P uptake is inhibited like 3-h test when NO_2^--N and PO_4^{3-}-P concentrations are respectively lower than 0.7 and 0.2 mmol g^{-1}MLSS, the inhibition coefficient (K_{PI}) should be applied to modify the equation, as shown below.

$$r_P = r_{Pmax} \cdot \frac{S_{NO_2}}{K_{P-NO_2}+S_{NO_2}+S_{NO_2}^2/K_{PI}} \cdot \frac{S_{PO_4}}{K_{P-PO_4}+S_{PO_4}} \cdot \frac{X_{PHA}/X_{PAO}}{K_{PHA}+X_{PHA}/X_{PAO}} \quad (6\text{-}5)$$

On the contrary, 2-h constant-rate dosing test represents the P uptake with sufficient electron acceptor feeding (nitrogen input >4.6 mmol g^{-1}MLSS h^{-1}), in which NO_2^--N cannot restrain the rate of P uptake. Hence, there is no the nitrogen term in the equation in this condition (Equation (6-6)).

$$r_P = r_{Pmax} \cdot \frac{S_{PO_4}}{K_{P-PO_4}+S_{PO_4}} \cdot \frac{X_{PHA}/X_{PAO}}{K_{PHA}+X_{PHA}/X_{PAO}} \quad (6\text{-}6)$$

6.1.3.2 NO_2^--N consumption rate

In case of NO_2^--N consumption rate, PO_4^{3-}-P in the wastewater of 3-h and 4-h tests is more sufficient than NO_2^--N. Thus, phosphorus concentration does not influence the NO_2^--N consumption rate at the beginning of the reaction, and only nitrogen is considered in the equation, as below:

$$r_N = r_{Nmax} \cdot \frac{S_{NO_2}}{K_{N-NO_2}+S_{NO_2}} \quad (6\text{-}7)$$

With the decrease of PO_4^{3-}-P concentration, phosphorus will not be sufficient (<0.9 mmol g^{-1}MLSS), then NO_2^--N consumption rate will be influenced by both phosphorus and nitrogen concentrations, as below:

$$r_N = r_{Nmax} \cdot \frac{S_{NO_2}}{K_{N-NO_2}+S_{NO_2}} \cdot \frac{S_{PO_4}}{K_{N-PO_4}+S_{PO_4}} \quad (6\text{-}8)$$

In addition, if the P uptake efficiency is inhibited by the excess NO_2^--N (3-h test), nitrogen consumption rate will also be restrained. Hence, the equation is modified with inhibition coefficient (K_{NI}) as well.

$$r_N = r_{Nmax} \cdot \frac{S_{NO_2}}{K_{N-NO_2}+S_{NO_2}+S_{NO_2}^2/K_{NI}} \cdot \frac{S_{PO_4}}{K_{N-PO_4}+S_{PO_4}} \quad (6\text{-}9)$$

Furthermore, the NO_2^--N consumption rate with sufficient nitrogen dosing is also different from 3-h and 4-h test. Only phosphorus influences the reaction rate when PO_4^{3-}-P concentration is adequate (>0.1 mmol g^{-1}MLSS):

$$r_N = r_{Nmax} \cdot \frac{S_{PO_4}}{K_{N-PO_4}+S_{PO_4}} \quad (6\text{-}10)$$

In contrast, when PO_4^{3-}-P concentration is decreased to lower than 0.1 mmol g^{-1}MLSS, nitrogen consumption rate is only related to NO_2^--N concentration. The equation is shown as below:

$$r_N = r_{Nmax} \cdot \frac{S_{NO_2}}{K_{N-NO_2}+S_{NO_2}} \quad (6\text{-}11)$$

For all the equations discussed above, the maximums of reaction rates (r_{Pmax} and r_{Nmax}) were obtained from 1-h constant-rate dosing test, which achieved fastest P and N decrease rates (in the first 30 min) observed among the tests of nitrite dosing strategies. The values of all the parameters and coefficients are shown in Appendix C.

In all the NO_2^--N dosing tests of 5-h, 4-h, 2-h constant rates and reducing rates in section 5.1, the maximums of P/N ratio (mg/mg) were separately 1.6, 1.5, 1.5, 1.6 and 1.6, with

the mole ratio of 0.7. Based on the data collection in section 6.1.1.2, 2.79 mmol C g^{-1}MLSS of PHB was consumed and 0.9 mmol C g^{-1} MLSS of glycogen was produced in anoxic phase. The stoichiometric coefficients in anoxic phase are also shown Appendix C.

6.1.4 Discussion and summary

As mentioned above, the fractions of PHB, glycogen and polyP were not measured regularly during the experimental period, which could not be applied for more comprehensive kinetic and stoichiometric modelling. Hence, the reaction rates of them were totally based on the change of HAc uptake in anaerobic phase and PO_4^{3-}-P uptake in anoxic phase.

The kinetics of P uptake in ASM2d (Henze *et al*., 1999) also included the impacts of alkalinity, polyP fraction and biomass, while these factors in this study were considered as constant, which determined the values of r_{Pmax} and r_{Nmax} together. In addition, since the modelling study about nitrite-based anoxic EBPR was not widely conducted, the information about inhibition coefficient of NO_2^--N was not mentioned frequently in the literature. Thus, the values of K_{PI} and K_{NI} need more investigation in the future research.

To summarise, the developed model in this study, which investigated the kinetic change of P uptake and N consumption in anoxic phase with different NO_2^--N dosing strength in the provided tests, should be calibrated with other similar tests for the validation.

6.2 Modelling calibration and validation

The modelling calibration was only focused on the anoxic P uptake and N consumption, since anaerobic HAc uptake and P release in all the tests and common operation had the same trends. Hence, the calibration of kinetics in anoxic phase with experiments and sensitivity analysis were conducted to validate the model.

6.2.1 Calibration with experimental results

6.2.1.1 Calibration of sufficient nitrogen dosing test

Fig 6.3 demonstrates the comparison between simulation results and experimental results of 2-h constant-rate dosing test and the calibration with T_a and T_b. As can be seen in the figure, the P uptake, N accumulation and consumption during the anoxic phase in

the simulation were closed to the experimental results of 2-h test. In the results of T_a and T_b, the concentrations of PO_4^{3-}-P and NO_2^--N at the end of anoxic phase in the simulation were also similar to the experimental results, suggesting that the kinetics model obtained from 2-h constant-rate test could simulate the P uptake and N consumption of the other tests with sufficient nitrogen dosing.

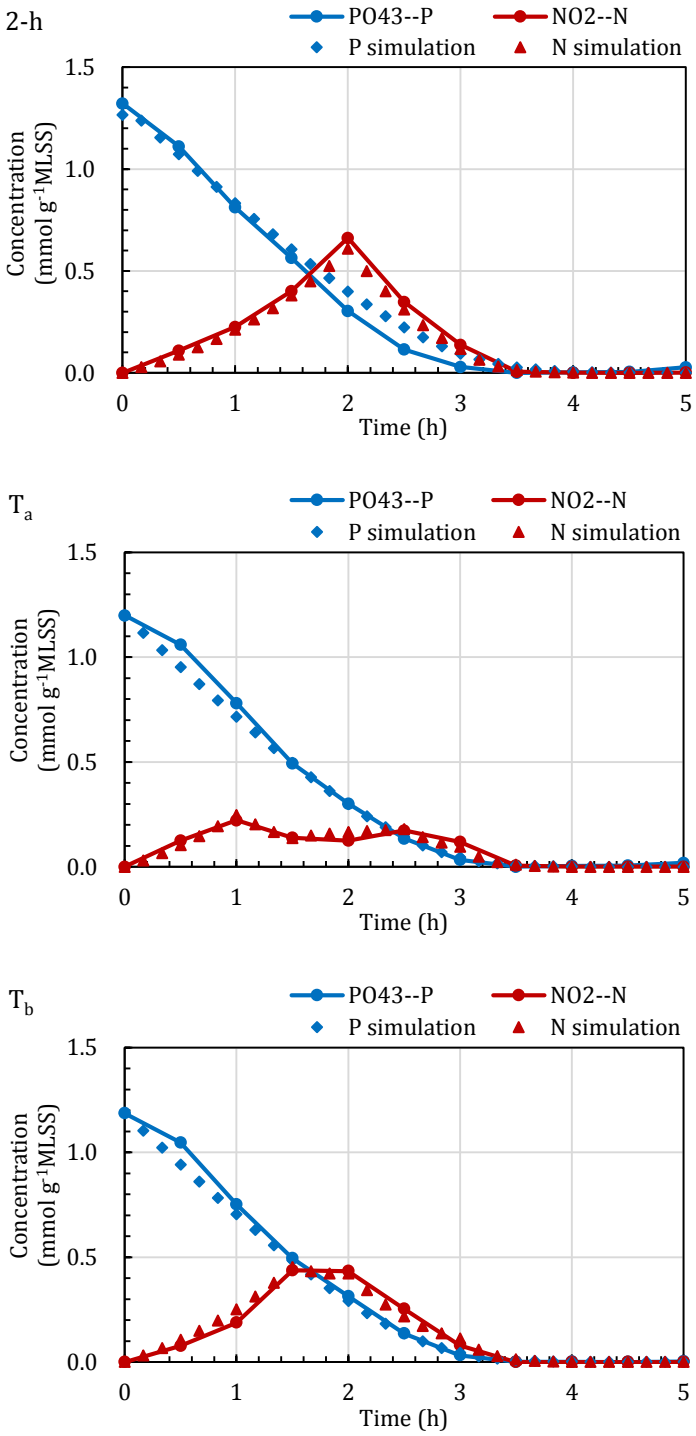

Fig. 6. 3 The comparison of simulation results and experimental results of 2-h test, T_a and T_b

6.2.1.2 Calibration with non-sufficient nitrogen dosing test

The results of simulation and experiments in 3-h and 4-h tests are shown in Fig. 6.4, which are compared with 5-h test for calibration. It can be seen that the simulation concentrations of PO_4^{3-}-P and NO_2^--N at the end of anoxic are closed to the experimental figures, while the accumulation trends of NO_2^--N in all the three tests are not very fitting to the lines of experimental results. It suggests that the N consumption rates simulated in these periods are lower than the experiments, especially in the 5-h test, which indicates that the when NO_2^--N dosing rate is in such a lower level, the consumption is relatively high to satisfy the requirement of DPAOs.

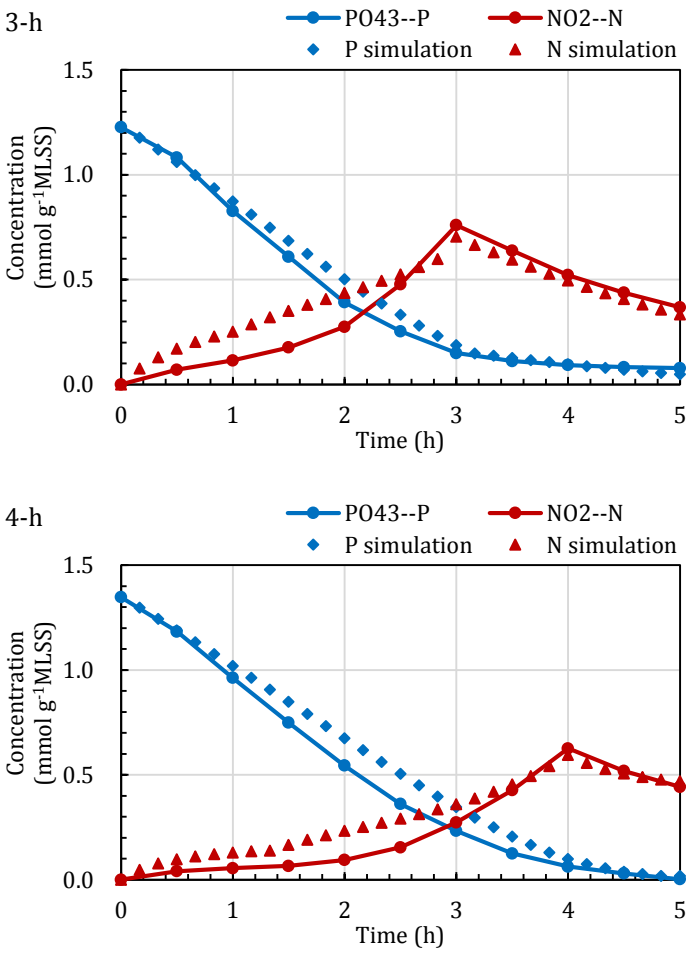

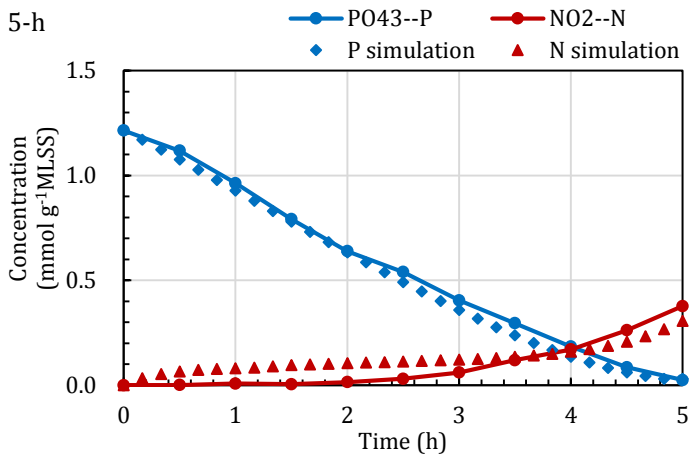

Fig. 6. 4 The comparison of simulation results and experimental results of 3-h, 4-h and 5-h tests

6.2.2 Sensitivity analysis

The relative sensitivity factors of the main parameters applied in the kinetics used in the modelling are listed in Table 6.4 to analyse the important variables of outputs (HAc, PO_4^{3-}-P and NO_2^--N). It was found that all the parameters did not influence the HAc concentration in the effluent due to the fast and complete consumption in anaerobic phase, while most of the parameters could affect P and N outputs. Specifically, K_{P-PO_4} (saturation coefficient of PO_4^{3-}-P for P uptake) and r_{Pmax} (maximum of P uptake rate) are the most important for anoxic P uptake, while K_{N-NO_2} (saturation coefficient of NO_2^--N for N consumption) and r_{Nmax} (maximum of N consumption rate) are the most influential parameters for the N consumption.

Table 6. 4 Values of RSF_x for the main parameters in different tests

Parameters	HAc			PO_4^{3-}-P			NO_2^--N		
	2-h	3-h	4-h	2-h	3-h	4-h	2-h	3-h	4-h
r_{Pmax}	0	0	0	9.0	5.0	8.1	2.5	6.1	5.0
r_{Nmax}	0	0	0	0	1.1	7.1	10	5.6	3.4
K_{P-PO_4}	0	0	0	20.7	2.2	8.3	2.7	1.4	1.7
K_{P-NO_2}	0	0	0	0	0.4	0.9	13.8	1.6	1.0
K_{N-PO_4}	0	0	0	0	1.1	5.0	0	1.0	1.4

K_{N-NO_2}	0	0	0	0	0.3	2.2	64.0	2.4	1.7
K_{PHA}	0	0	0	1.1	0.2	0.7	0.2	0.1	0.1
K_{PI}	--	0	--	--	0.7	--	--	0.2	--
K_{NI}	--	0	--	--	0.2	--	--	0.7	--

6.2.3 Discussion and Summary

The values of the common parameters applied in previous studies were generally different due to the different conditions, including the scale of the plants, treatment process, electron acceptor, *etc* (Smolders *et al*, 1994b; Gujer *et al*., 1995; Kuba *et al*., 1996a; Henze *et al*., 1999; Hao *et al*., 2001; Dai *et al*., 2017a). The values in this study were mostly attained by the mathematical optimisation with the measured data in the tests, combined with the values in the literature, which cannot be obtained from the experiments.

In order to simulate the practical treatment process, the process with relatively higher P uptake and N consumption rates should be applied in the following sections to enhance the treatment efficiency and decrease the retention time. Hence, the model with sufficient NO_2^--N dosing was utilised for the simulation. Although the values of most RSFs are higher than 0.25, which is the limit deciding if the parameter is influential to the outputs (Petersen *et al*., 2002; Dai *et al* 2017a), the calibration with T_a and T_b achieved very closed results to 2-h dosing strategy. Therefore, most of the parameters in the 2-h test model did not need to change. However, K_{P-PO_4} and K_{N-NO_2} are better to change the value from 8.5 and 7.0 to 9.0 and 8.0, respectively, to make the model more suitable for all three tests. Although the RSFs of K_{P-PO_4} and K_{N-NO_2} on P and N outputs in the effluent are relatively high, the actual concentration values are not changed obviously. As the kinetic and stoichiometric parameters in nitrite-based EBPR were not investigated frequently in the previous studies, most of parameters were not calibrated to any verifiable values.

6.3 Simulation of A_2N two-sludge process

6.3.1 Cycle simulation of A_2N two-sludge system

The two-sludge system proposed for the modelling study and simulation consisted an A_2 SBR and an N SBR, while the N SBR was designed for partial nitrification. Mathematic calculations were conducted in Excel to simulate the operation process of two sludge systems (Appendix B). Both the SBRs had a 5-L working volume, and the flowrate of the system for influent, effluent and the flows between the SBRs was 20 L h^{-1}, causing the duration of wastewater flow was 12 min.

It was assumed that partial nitrification was ideal in the aerobic SBR, where NH_4^+-N could be oxidised to NO_2^--N completely. The operation of two-sludge system with 8-h cycles can be conducted as below:

- Stage 1: 1.5-h anaerobic phase (including a 12-min feeding);
- Stage 2: 0.5-h settlement period of A_2 SBR;
- Stage 3: 1.5-h aerobic phase (including a 12-min pumping period of wastewater exchange from A_2 SBR to N SBR);
- Stage 4: 2-h pumping period of wastewater exchange from N SBR to A_2 SBR;
- Stage 5: 1.5-h mixed anoxic phase;
- Stage 6: 0.5-h settlement period of A_2 SBR; and
- Stage 7: 12-min discharge period.

In order to simulate the operation of two-sludge systems, the exchange rate should be ensured. The exchange rate applied in the experiment of A_2 SBRs in Chapter 4&5 was 50%, while it was not appropriate in two-sludge systems. The comparison between wastewater exchange rates of 50% and 80% in A_2N two-sludge process was conducted (Appendix B), which suggested that 80% exchange rate can be much faster to achieve stable and efficient phosphorus removal than 50% exchange rate, with the same phosphorus and nitrogen loading strength. If the wastewater contains 75 mg NH_4^+-N L^{-1} and 8 mg PO_4^{3-}-P L^{-1}, Table 6.5 demonstrates the calculated parameters in the simulation. In the simulation, the reactions during wastewater exchanges (Stage 3&4) were ignored to facilitate the calculation.

As can be seen in the table, all the parameters in the simulated operation can achieve stable in different cycles. The ratio of P/N at the beginning of anoxic phase was 1.124 in the first cycle, prior to decreasing to 1.028 in the sixth cycle and keeping stable in the following cycles. Since the ratio is closed to the appropriate ratios in the enrichment and the dosing tests experiments, anoxic PO_4^{3-}-P uptake should be efficient and successful. In this operation, the concentration of NH_4^+-N in A_2 SBR became 12.5 mg L^{-1} from stage 5 to the effluent from the 5th cycle, suggesting that there should be an ammonia removal process in or after the anoxic phase, via oxidation by oxygen of aerobic phase, or NO_2^--N residual after P uptake.

Table 6. 5 Simulation of important parameters in the two-sludge system in different stages

Stage	SBR	Parameter	Value in the first cycle	Equation	Stable value
After feeding	A_2	NH_4^+-N① (mg L^{-1})	60.0	$C_{①_1} = \frac{75 \times 3.2 + C_{⑥_0} \times 0.8}{4}$	62.5
After pumping from A_2 to N	N	PO_4^{3-}-P② (mg L^{-1})	41.1	$C_{②_1} = \frac{51.4 \times 3.2 + C_{②_0} \times 0.8}{4}$	51.4
		NH_4^+-N③ (mg L^{-1})	48.0	$C_{③_1} = \frac{C_{①_1} \times 3.2}{4}$	50.0
After aerobic	N	NO_2^--N④ (mg L^{-1})	48.0	$C_{④_1} = C_{③_1} + \frac{C_{④_0} \times 0.8}{4}$	62.5
After pumping from N back to A_2 *	A_2	PO_4^{3-}-P⑤ (mg L^{-1})	43.2	$C_{⑤_1} = \frac{C_{②_1} \times 3.2 + 51.4 \times 0.8}{4}$	51.4
		NH_4^+-N⑥ (mg L^{-1})	12.0	$C_{⑥_1} = \frac{C_{①_1} \times 0.8}{4}$	12.5
		NO_2^--N⑦ (mg L^{-1})	38.4	$C_{⑦_1} = \frac{C_{④_1} \times 3.2}{4}$	50.0
		P/N (mg/mg)	1.124	$R_1 = \frac{C_{⑤_1}}{C_{⑦_1}}$	1.028

where $C_{②_0}$, $C_{④_0}$ and $C_{⑥_0}$ were the values before the first cycle, all of which should be 0 mg L^{-1}; *ignore the P uptake and N consumption during the pumping for simplified calculation.

As a result, the proposed process can be employed for operation of practical A_2N treatment process, and the operation mode can be selected for the following modelling study and simulation.

6.3.2 Simulation results

The simulation results of PO_4^{3-}-P, NO_2^--N, HAc, polyP, PHB and glycogen in A_2 EBPR system are shown in Fig. 6.5. As can be seen in the graphs, the change of all the factors were basically accorded to the results of experiments, especially HAc, PO_4^{3-}-P and NO_2^--N, which

were determined regularly during the experimental period. P release and HAc uptake were both finished in the 1.5-h anaerobic phase, and with the dosing back of wastewater with accumulated PO_4^{3-}-P and NO_2^--N, both P and N concentrations were decreased nearly 0 at 7.5 h.

As a result, the simulation of A_2 EBPR process in two-sludge systems implied that phosphorus and nitrogen could be completely removed by this method, if the conditions of the operation were followed to the lab-scale experiment. The P and N removal could be achieved in 7.5 hours, suggesting that around 3 cycles could be conducted in 24 hours.

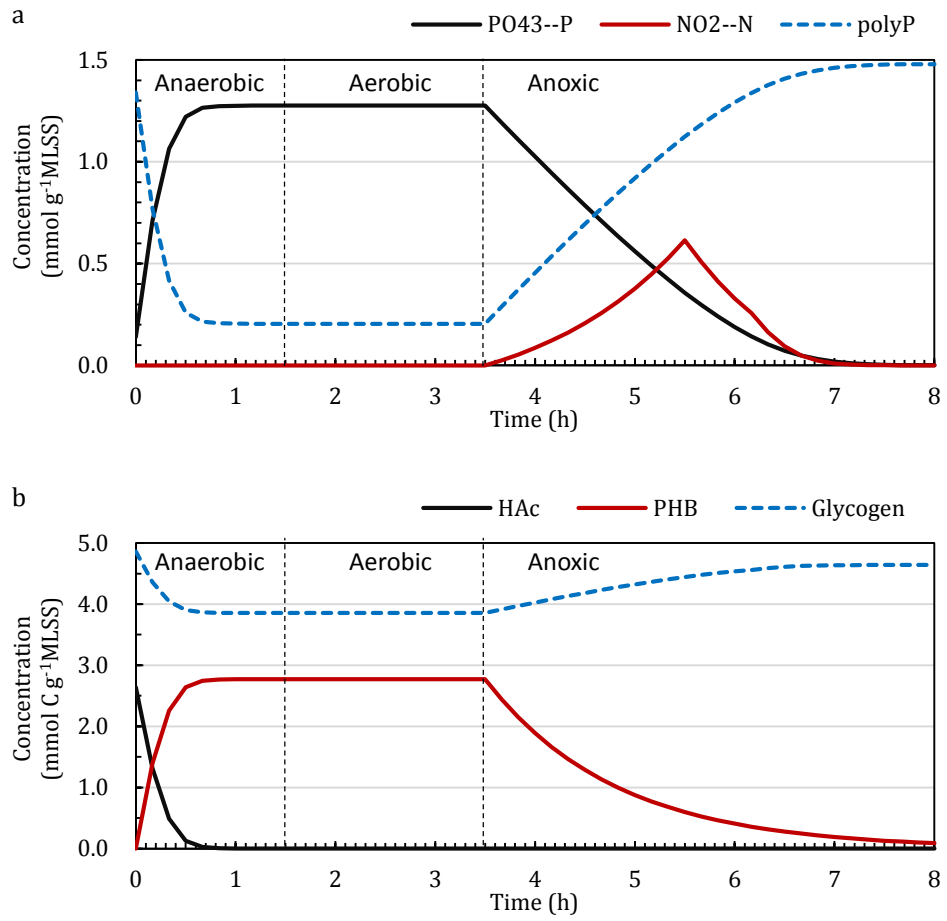

Fig. 6. 5 Simulation results of PO_4^{3-}-P, NO_2^--N, HAc, polyP, PHB and glycogen in A_2 SBR of two-sludge system

6.4 Discussion and summary

A_2N two-sludge system had been proposed for longer than 20 years, achieving simultaneous PO_4^{3-}-P uptake and denitrification, in order to save carbon consumption,

energy requirement and reduce sludge production, which had been discussed in chapter 2. However, there are still some aspects which can be developed to optimise two-sludge systems, especially for nitrite based process.

One of the points is the approach to obtain high efficiency of nitrite accumulation in the N-SBR, although partial nitrification had been studied decades of years. Partial nitrification can be achieved under appropriate conditions, such as temperature, DO concentration, SRT and so on. In order to enhance the nitrite production ratio in the nitrification process of two-sludge system, Wang *et al*. (2017) and Xu *et al*. (2019) utilised pre-treated nitrifying sludge with FNA to enhance the accumulation of AOB and reduce the abundance of NOB.

Another issue of the utilisation of A_2N two-sludge process was the operation mode to achieve the stable work in practical wastewater treatment (Fig. 6.6). The most important point of SBR process is that both of A_2 SBR and N-SBR may have an idle period in one cycle, when the other SBR is in operation. In the experimental studies about two-sludge SBR systems, the idle periods were not discussed specifically. In the A_2 SBR, for instance, which generally had a 3-6 h idle stage, there was no statements about any deterioration of P uptake after the idle periods, suggesting the idle condition did not affect the treatment efficiency of the systems. Furthermore, based on the research on the anaerobic starvation of P removal sludge of Wang *et al*. (2012 & 2015), nitrite based DPAOs can obtain high resistance to starvation of 3 days, and can recover after 12 days. Thus, it suggested that the idle phases in two-sludge SBR systems should not induce any negatively effects on nutrient removal efficiency.

Moreover, continuous flow A_2N system (Hao et al., 2001; Shi *et al*., 2012; Dai *et al*., 2017a) which separates the A_2 SBR to two tanks of respective anaerobic and anoxic phase with the same sludge (via sludge bypass), avoids the idle period in the SBR system. According to the experiment results in section 5.1.1, P and N can be removed completely without post-aerobic phase, while due to the concentration change of C, N and P in practical wastewater, if necessary post-aerobic condition or external NO_2^--N feeding should be conducted to achieve higher treatment efficiency and stricter treatment standards.

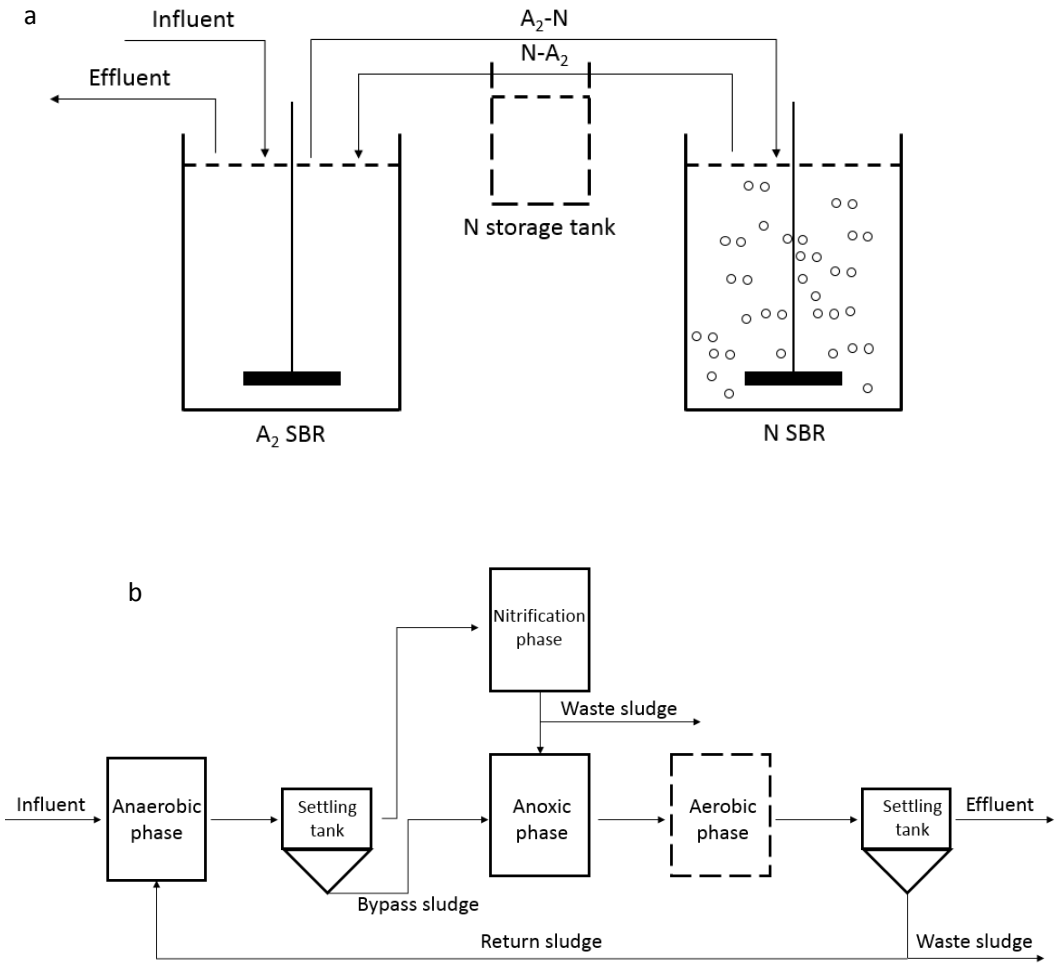

Fig. 6. 6 Diagrams of A_2N two-sludge systems: a SBR process; b continuous process (Kuba *et al*., 1996; Hao *et al*., 2001)

An important point of the operation of A_2 EBPR system is the method of carbon feeding. Since P release needs VFA as the carbon source, the COD in practical wastewater should be reacted to VFA before the wastewater is pumped into EBPR systems. Consequently, between the processes of pre-treatment (including screening and primary clarifier) and EBPR system, a fermentation process should be added to produce VFA (Skalsky and Daigger, 1995; Choi *et al*., 1996). In addition, depending on the remained VFA concentration, external supplement may be fed into the anaerobic phase to achieve sufficient P release and PHA production.

Developing models for NO_2^--N based anoxic phosphorus uptake process is a useful method to understand the metabolisms of DPAOs, simulate the treatment process of A_2N two-sludge systems, and optimise the operation process of the systems. In this study, the main aim of the simulation via the combination of experimental data and developed models was to successfully simulate NO_2^--N based A_2N two-sludge phosphorus removal

system with continuous dosing of electron acceptor, as well as compare the process performance of the A_2 SBR with other studies via the difference of the models.

Compared with the metabolic models of DPAOs with NO_3^--N, reported by Kuba *et al*., (1996a), there were lower PHB production, glycogen consumption and maintenance if the HAc uptake and PO_4^{3-}-P release were at the same ratio in the anaerobic phase. Meanwhile, there were lower PHB consumption, glycogen synthesis and maintenance, but higher nitrogen consumption in the anoxic phase. The reason causing the difference should be the lower initial HAc concentration at the beginning of anaerobic phase and the function of NO_2^--N as the sole electron acceptor, which restrained the activities of GAOs in the A_2 system, and kept lower MLSS in the SBRs inducing lower energy requirement for maintenance of biomass.

Based on the successful and effective anoxic phosphorus uptake via NO_2^--N as the sole electron acceptor in the 2-h constant-rate dosing strategy, anoxic duration in the A_2 process can be shortened, which could reduce the cycle period with the combination of aerobic SBR for nitrite production via short-cut nitrification. This study positively simulated the process of two-sludge system, with appropriate effluent condition of PO_4^{3-}-P and NO_2^--N concentrations.

In addition, since the data in the simulation was based on the constant MLSS, the biomass should be kept stable in the EBPR process. The MLSS value in the simulation was 1.4 g L^{-1}, while the figure in actual WWTPs should kept at around 2.5 g L^{-1} after calculation, because the exchange ratio between the reactors was 80%, which would enhance the NO_2^--N dosing strength in unit volume.

In summary, based on the modelling development and simulation results, it indicates that if the partial nitrification process can be controlled successfully, phosphorus removal with two-sludge SBR system can be achieved with stable PO_4^{3-}-P removal rate, and toxic inhibition can be effectively avoided. Hence, with the development of model study on A_2N process, it will be increasingly feasible in the practical wastewater treatment process (Dai *et al*., 2017a; Dai *et al*., 2019).

Chapter 7 Conclusions and further work

7.1 Conclusions

From the studies carried out, it had been proved that: a. the faster and easier enrichment of DPAOs in A_2 systems could be achieved via NO_2^--N as the sole electron acceptor, obtaining more effective P removal results than NO_3^--N in the stable operation period. According to the aim of this study, the specific conclusions can be obtained:

- SRT is an important parameter influencing the enrichment of DPAOs and stable operation of phosphorus removal process in A_2 systems. In the comparison among 20-days, 15-days and 10-days of SRT, the acclimation process of the A_2 activated sludge with 10-days SRT achieved successful enrichment of DPAOs, inducing the obvious anaerobic PO_4^{3-}-P release and anoxic PO_4^{3-}-P uptake.
- Initial HAc concentration as around 125 mg L^{-1} can achieve 40-50 mg L^{-1} of PO_4^{3-}-P release, with little NO_x^--N residual at the beginning of the anaerobic phase, if the initial PO_4^{3-}-P concentration is kept as around 6 mg L^{-1}. Accordingly, the electron acceptor amount added into the systems need to achieve 27-30 mg NO_3^--N L^{-1} or 45~50 mg NO_2^--N L^{-1}. The ratios of PO_4^{3-}-P uptake/NO_3^--N consumption and PO_4^{3-}-P uptake/NO_2^--N consumption in anoxic phase are separately 2.0 mg/mg (0.90 mmol/mmol) and 1.2 mg/mg (0.54 mmol/mmol) in stable and ideal operation process, deducing the 5:3 of NO_3^--N:NO_2^--N utilised to accumulate the same amount of PO_4^{3-}-P.
- Long-period dosing strategy of appropriate NO_2^--N amount, as sole electron acceptor, can achieve DPAO enrichment in A_2 systems more rapidly and effectively, rather than NO_3^--N as the electron acceptor. In the stable operation period, the NO_2^--N based A_2 system can realise phosphorus removal rate of >95% or 100%, generally higher than NO_3^--N based system at ambient temperature (around 20 °C).
- Long-period dosing strategies of NO_2^--N, including 5-h, 4-h, 3-h (reducing-rate) and 2-h dosing, can achieve successful PO_4^{3-}-P removal, avoiding the toxic inhibition from NO_2^--N or FNA. Among the process, 3-h and 2-h dosing strategies can attain faster anoxic PO_4^{3-}-P uptake to shorten the cycle period.

- The threshold value of NO_2^--N in the experimental system was not constant, which varies depending the PO_4^{3-}-P concentration if MLSS of the system is stable.
- Anoxic P uptake with NO_3^--N is more resistant to sudden temperature increase from 20 to 30 °C, rather than NO_2^--N. Sudden temperature increase can deteriorate the NO_2^--N based system with the wash-out of responsible microbial of DPAOs, which need to recover gradually during the operation.
- Low pH value <7.5 or high pH value > 8.6 in anoxic phase are not appropriate for PO_4^{3-}-P uptake. The operation of NO_2^--N based A_2 system with lower pH in long-period can induce the destroy of the P removal efficiency, while it can be rapidly recover after the adjustment back of pH value.
- The functional microbial group in the DPAOs of A_2 EBPR system was *Rhodocyclaceae*-related genera in the class of *β-proteobacteriales*. For instance, *Dechloromonas* is the most frequent genera in the activated sludge of enriched DPAO systems after long-period operation.
- The PO_4^{3-}-P uptake and NO_2^--N consumption rates in the anoxic phase are both accorded with Monod-type equation, while they are influenced by the dosing strength of NO_2^--N.

The study justified that nitrite based denitrifying P removal could be applied in practical wastewater treatment with appropriate nitrite feed strategy, temperature and pH, combined with A_2N two-sludge systems where the nitrification could be replaced by short-cut nitrification as far as possible, depending on the seasonal change of temperature. Besides, Continuous feeding of nitrite can simplify the enrichment process of DPAOs, and the post-aerobic phase could be selected to utilise or cancel to save more energy.

Furthermore, based on the relationship between PO_4^{3-}-P uptake, NO_2^--N consumption and P concentration in the wastewater, appropriate dosing strength of nitrite is suggested in practical wastewater treatment process.

7.2 Future work

Since the complete A_2N two-sludge systems were not conducted in this study, the experimental and pilot scale operations of two-sludge systems with the connection of A_2 tank and aerobic tank (SBR process and continuous flow process) should be focused for

the practical phosphorus and nitrogen removal from municipal wastewater. Batch tests can be employed to explore the specific NO_2^--N or FNA threshold value inducing PO_4^{3-}-P uptake inhibition with different levels of PO_4^{3-}-P concentration and MLSS, as well as optimise the models of NO_2^--N based anoxic phosphorus uptake in A_2N two-sludge systems, combined with more comprehensive analysis of polyP, PHA and glycogen which did not measured frequently due to time limitations. In addition, more microbial community analysis should be conducted with different method (e.g. FISH) to compare with the results of HTS.

Based on the efficient treatment of domestic wastewater via anoxic PO_4^{3-}-P removal, phosphorus is accumulated in the activated sludge, producing polyP. As a kind of macromolecule chemical, polyP can achieve potential utilisation in agricultural and industrial areas to achieve phosphorus recycling. Due to the special structure and characteristics, polyP has the potential applications in the aspects including antibacterial action, ATP regeneration, insulating fibres and so on. Hence, recycling phosphorus and polyP is another direction of future work.

References

Ahn, J., Daidou, T., Tsuneda, S. and Hirata, A. (2001). Metabolic behavior of denitrifying phosphate-accumulating organisms under nitrate and nitrite electron acceptor conditions. *Journal of bioscience and bioengineering,* 92 (5), 442-446.

Ahn, J., Daidou, T., Tsuneda, S. and Hirata, A. (2002). Characterization of denitrifying phosphate accumulating organisms cultivated under different electron acceptor conditions using polymerase chain reaction-denaturing gradient gel electrophoresis assay. *Water research,* 36**,** 403-412.

Andersson, K. K., & Hooper, A. B. (1983). O2 and H2O are each the source of one O in NO− 2 produced from NH3 by Nitrosomonas: 15N-NMR evidence. *Febs Letters*, *164*(2), 236-240.

Ansari, A. A., Singh, G. S., Lanza, G. R., & Rast, W. (Eds.). (2010). *Eutrophication: causes, consequences and control* (Vol. 1). Springer Science & Business Media.

Anthonisen, A.C., Loehr, R.C., Prakasam, T.B.S. and Srinath, E.G. (1976). Inhibition of nitrification by ammonia and nitrous acid. *Journal (Water Pollution Control Federation)*, pp.835-852.

APHA (2005). *Standard Methods for the Examination of Water and Wastewater (2710 D - Sludge Volume Index)*, Washington, USA, American Public Health Association, American Water Works Association, Water Environment Federation

Ashekuzzaman, S. M., & Jiang, J. Q. (2014). Study on the sorption–desorption–regeneration performance of Ca-, Mg-and CaMg-based layered double hydroxides for removing phosphate from water. *Chemical Engineering Journal*, *246*, 97-105.

Aslan, S., Miller, L., & Dahab, M. (2009). Ammonium oxidation via nitrite accumulation under limited oxygen concentration in sequencing batch reactors. *Bioresource technology*, *100*(2), 659-664.

Atashgahi, S., Aydin, R., Dimitrov, M.R., Sipkema, D., Hamonts, K., Lahti, L., Maphosa, F., Kruse, T., Saccenti, E., Springael, D. and Dejonghe, W. (2015). Impact of a wastewater treatment plant on microbial community composition and function in a hyporheic zone of a eutrophic river. *Scientific reports*, *5*, p.17284.

References

Attour, A., Touati, M., Tlili, M., Amor, M. B., Lapicque, F., & Leclerc, J. P. (2014). Influence of operating parameters on phosphate removal from water by electrocoagulation using aluminum electrodes. *Separation and Purification Technology*, *123*, 124-129.

Barak, Y., & van Rijn, J. (2000). Relationship between Nitrite Reduction and Active Phosphate Uptake in the Phosphate-Accumulating DenitrifierPseudomonas sp. Strain JR 12. *Appl. Environ. Microbiol.*, *66*(12), 5236-5240.

Blackburne, R., Yuan, Z., & Keller, J. (2008). Partial nitrification to nitrite using low dissolved oxygen concentration as the main selection factor. *Biodegradation*, *19*(2), 303-312.

Bokulich, N.A., Dillon, M.R., Bolyen, E., Kaehler, B.D., Huttley, G.A. and Caporaso, J.G. (2018). q2-sample-classifier: machine-learning tools for microbiome classification and regression. *Journal of open research software*, *3*(30).

Bokulich, N.A., Subramanian, S., Faith, J.J., Gevers, D., Gordon, J.I., Knight, R., Mills, D.A. and Caporaso, J.G. (2013). Quality-filtering vastly improves diversity estimates from Illumina amplicon sequencing. *Nature methods*, *10*(1), pp.57-59.

Booker, N. A., Priestley, A. J., & Fraser, I. H. (1999). Struvite formation in wastewater treatment plants: opportunities for nutrient recovery. *Environmental Technology*, *20*(7), 777-782.

Bortone, G., Libelli, S. M., Tilche, A., & Wanner, J. (1999). Anoxic phosphate uptake in the DEPHANOX process. *Water science and technology*, *40*(4-5), 177-185.

Bortone, G., Malaspina, F., Stante, L. and Tilche, A. (1994). Biological nitrogen and phosphorus removal in an anaerobic/anoxic sequencing batch reactor with separated biofilm nitrification. *Water Science and Technology*, *30*(6), p.303.

Bortone, G., Saltarelli, R., Alonso, V., Sorm, R., Wanner, J., & Tilche, A. (1996). Biological anoxic phosphorus removal-the dephanox process. *Water Science and Technology*, *34*(1-2), 119-128.

Brdjanovic, D., Slamet, A., Van Loosdrecht, M. C. M., Hooijmans, C. M., Alaerts, G. J., & Heijnen, J. J. (1998). Impact of excessive aeration on biological phosphorus removal from wastewater. *Water Research*, *32*(1), 200-208.

Brdjanovic, D., Van Loosdrecht, M.C.M., Versteeg, P., Hooijmans, C.M., Alaerts, G.J., Heijnen, J.J. (2000). Modeling COD, N and P removal in a full-scale wwtp Haarlem Waarderpolder. *Water Res*. 34 (3), 846–858.

Bunce, J.T., Ndam, E., Ofiteru, I.D., Moore, A. and Graham, D.W. (2018). A review of phosphorus removal technologies and their applicability to small-scale domestic wastewater treatment systems. *Frontiers in Environmental Science*, *6*, p.8.

Callahan, B.J., McMurdie, P.J., Rosen, M.J., Han, A.W., Johnson, A.J.A. and Holmes, S.P. (2016). DADA2: high-resolution sample inference from Illumina amplicon data. *Nature methods*, *13*(7), pp.581-583.

Carrera, J., Sarra, M., Lafuente, F. J., & Vicent, T. (2001). Effect of different operational parameters in the enhanced biological phosphorus removal process. Experimental design and results. *Environmental technology*, *22*(12), 1439-1446.

Carvalheira, M., Oehmen, A., Carvalho, G. and Reis, M.A. (2014). The effect of substrate competition on the metabolism of polyphosphate accumulating organisms (PAOs). *water research*, *64*, pp.149-159.

Carvalho, G., Lemos, P., Oehmen, A., Crespo, M. & Reis, M. Microbial diversity of the Candidatus Accumulibacter phosphatis clade in denitrifying phosphorus removal systems. Proceedings of the 11th International Symposium on Microbial Ecology—ISME, 2006. 20-25.

Carvalho, G., Lemos, P.C., Oehmen, A. and Reis, M.A. (2007). Denitrifying phosphorus removal: linking the process performance with the microbial community structure. *Water research*, *41*(19), pp.4383-4396.

Chiu, Y. C., Lee, L. L., Chang, C. N., & Chao, A. C. (2007). Control of carbon and ammonium ratio for simultaneous nitrification and denitrification in a sequencing batch bioreactor. *International biodeterioration & biodegradation*, *59*(1), 1-7.

Choi, Y.S., Shin, E.B. and Lee, Y.D. (1996). Biological phosphorus removal from w astew ater in a single reactor combining anaerobic and aerobic conditions. *Water Science and Technology*, *34*(1-2), pp.179-186.

Chon, K., Cho, J., & Shon, H. K. (2013). A pilot-scale hybrid municipal wastewater reclamation system using combined coagulation and disk filtration, ultrafiltration, and reverse osmosis: removal of nutrients and micropollutants, and characterization of membrane foulants. *Bioresource technology*, *141*, 109-116.

Chouari, R., Le Paslier, D., Daegelen, P., Dauga, C., Weissenbach, J. and Sghir, A. (2010) Molecular analyses of the microbial community composition of an anoxic basin of a municipal wastewater treatment plant reveal a novel lineage of proteobacteria. *Microbial ecology,* 60 (2), 272-281.

Chuang, S. H., Chang, W. C., Huang, Y. H., Tseng, C. C., & Tai, C. C. (2011). Effects of different carbon supplements on phosphorus removal in low C/P ratio industrial wastewater. *Bioresource technology*, *102*(9), 5461-5465.

Coats, E. R., Dobroth, Z. T., & Brinkman, C. K. (2015). EBPR using crude glycerol: assessing process resiliency and exploring metabolic anomalies. *Water Environment Research*, *87*(1), 68-79.

Comeau, Y., Hall, K. J., Hancock, R. E. W., & Oldham, W. K. (1986). Biochemical model for enhanced biological phosphorus removal. *Water Research*, *20*(12), 1511-1521.

Conley, D.J., Paerl, H.W., Howarth, R.W., Boesch, D.F., Seitzinger, S.P., Havens, K.E., Lancelot, C. and Likens, G.E. (2009). Controlling eutrophication: nitrogen and phosphorus. *Science*, *323*(5917), pp.1014-1015.

Correll, D. L. (1998). The role of phosphorus in the eutrophication of receiving waters: A review. *Journal of environmental quality*, *27*(2), 261-266.

Crocetti, G. R., Banfield, J. F., Keller, J., Bond, P. L., & Blackall, L. L. (2002). Glycogen-accumulating organisms in laboratory-scale and full-scale wastewater treatment processesb. *Microbiology*, *148*(11), 3353-3364.

Crocetti, G.R., Hugenholtz, P., Bond, P.L., Schuler, A., Keller, J., Jenkins, D. and Blackall, L.L. (2000). Identification of polyphosphate-accumulating organisms and design of 16S rRNA-directed probes for their detection and quantitation. *Appl. Environ. Microbiol.*, *66*(3), pp.1175-1182.

Dai, H., Chen, W., Dai, Z., Li, X. and Lu, X. (2017a) Efficient model calibration method based on phase experiments for anaerobic–anoxic/nitrifying (A2N) two-sludge process. *Environmental Science and Pollution Research,* 24 (23), 19211-19222.

Dai, H., Chen, W., Peng, L., Wang, X. and Lu, X. (2019). Modeling and performance improvement of an anaerobic–anoxic/nitrifying-induced crystallization process via the multi-objective optimization method. *Environmental Science and Pollution Research*, *26*(5), pp.5083-5093.

Dai, H., Lu, X., Peng, L., Li, X. and Dai, Z. (2017b) Enrichment culture of denitrifying phosphorus removal sludge and its microbial community analysis. *Environmental technology,* 38 (22), 2800-2810.

Elser, J., & Bennett, E. (2011). Phosphorus cycle: a broken biogeochemical cycle. *Nature*, *478*(7367), 29.

Environment Agency (2012). *Freshwater Eutrophication Briefing Note*

European Commission (2019). *Evaluation of the Council Directive 91/271/EEC of 21 May 1991, concerning urban waste-water treatment*.

Filipe, C. D., Daigger, G. T., & Grady, C. P. (2001a). pH as a key factor in the competition between glycogen-accumulating organisms and phosphorus-accumulating organisms. *Water Environment Research*, *73*(2), 223-232.

Filipe, C.D., Daigger, G.T. and Grady Jr, C.L. (2001b). Stoichiometry and kinetics of acetate uptake under anaerobic conditions by an enriched culture of phosphorus-accumulating organisms at different pHs. *Biotechnology and bioengineering*, *76*(1), pp.32-43.

Filippelli, G. M. (2008). The global phosphorus cycle: past, present, and future. *Elements*, *4*(2), 89-95.

Flowers, J.J., He, S., Yilmaz, S., Noguera, D.R. and McMahon, K.D. (2009). Denitrification capabilities of two biological phosphorus removal sludges dominated by different 'Candidatus Accumulibacter'clades. *Environmental microbiology reports*, *1*(6), pp.583-588.

Frison, N., Katsou, E., Malamis, S., & Fatone, F. (2016). A novel scheme for denitrifying biological phosphorus removal via nitrite from nutrient-rich anaerobic effluents in a short-cut sequencing batch reactor. *Journal of Chemical Technology & Biotechnology*, *91*(1), 190-197.

Furrer, P., Hany, R., Rentsch, D., Grubelnik, A., Ruth, K., Panke, S. and Zinn, M. (2007). Quantitative analysis of bacterial medium-chain-length poly ([R]-3-hydroxyalkanoates) by gas chromatography. *Journal of Chromatography A*, *1143*(1-2), pp.199-206.

Gerber, A., De Villiers, R. H., Mostert, E. S., & Van Riet, C. J. J. (1987). The phenomenon of simultaneous phosphate uptake and release, and its importance in biological nutrient removal. In *Biological phosphate removal from wastewaters* (pp. 123-134). Pergamon.

Goel, R. K., Sanhueza, P., & Noguera, D. R. (2005). Evidence of Dechloromonas sp. participating in enhanced biological phosphorus removal (EBPR) in a bench-scale aerated-anoxic reactor. *Proceedings of the Water Environment Federation*, *2005*(12), 3864-3871.

Grady Jr, C. L., Daigger, G. T., Love, N. G., & Filipe, C. D. (2011). *Biological wastewater treatment*. CRC press.

Guerrero, J., Guisasola, A., & Baeza, J. A. (2015). Controlled crude glycerol dosage to prevent EBPR failures in C/N/P removal WWTPs. *Chemical Engineering Journal*, *271*, 114-127.

Guisasola, A., Qurie, M., del Mar Vargas, M., Casas, C. and Baeza, J.A. (2009). Failure of an enriched nitrite-DPAO population to use nitrate as an electron acceptor. *Process Biochemistry*, *44*(7), pp.689-695.

Gujer,W., Henze, M., Mino, T., van Loosdrecht, M. (1999). Activated sludge model no. 3. Water Sci. Technol. 39 (1), 183–193.

Guo, J. H., Peng, Y. Z., Wang, S. Y., Zheng, Y. N., Huang, H. J., & Ge, S. J. (2009a). Effective and robust partial nitrification to nitrite by real-time aeration duration control in an SBR treating domestic wastewater. *Process Biochemistry*, *44*(9), 979-985.

Guo, J., Peng, Y., Wang, S., Zheng, Y., Huang, H. and Wang, Z. (2009b). Long-term effect of dissolved oxygen on partial nitrification performance and microbial community structure. *Bioresource technology*, *100*(11), pp.2796-2802.

Guo, F., & Zhang, T. (2013). Biases during DNA extraction of activated sludge samples revealed by high throughput sequencing. *Applied microbiology and biotechnology*, *97*(10), 4607-4616.

Gupta, V. K., Sadegh, H., Yari, M., Shahryari Ghoshekandi, R., Maazinejad, B., & Chahardori, M. (2015). Removal of ammonium ions from wastewater: A short review in development of efficient methods. *Global Journal of Environmental Science and Management*, *1*(2), 149-158.

Gürtekin, E. (2011). The effect of sludge retention time and hydraulic retention time on biological phosphorus removal performance in anaerobic/anoxic sequencing batch reactor. *International Journal of Academic Research*, *3*(3).

Hao, X., Van Loosdrecht, M. C., Meijer, S. C. F., & Qian, Y. (2001). Model-based evaluation of two BNR processes—UCT and A2N. *Water Research*, *35*(12), 2851-2860.

Hascoet, M. C., Florentz, M., & Granger, P. (1985). Biochemical aspects of enhanced biological phosphorus removal from wastewater. *Water science and technology*, *17*(11-12), 23-41.

He, S., Gall, D.L. and McMahon, K.D. (2007). "Candidatus Accumulibacter" population structure in enhanced biological phosphorus removal sludges as revealed by polyphosphate kinase genes. *Appl. Environ. Microbiol.*, *73*(18), pp.5865-5874.

Hedström, A. (2001). Ion exchange of ammonium in zeolites: a literature review. *Journal of environmental engineering*, *127*(8), pp.673-681.

Hellinga, C. S. A. A. J. C., Schellen, A. A. J. C., Mulder, J. W., van Loosdrecht, M. V., & Heijnen, J. J. (1998). The SHARON process: an innovative method for nitrogen removal from ammonium-rich waste water. *Water science and technology*, *37*(9), 135-142.

Henze, M., Grady, C.P.L., Gujer,W., Marais, G.v.R., Matsuo, T. (1987). Activated Sludge Model No. 1. IAWPRC Scientific and Technical Report No. 1., London, UK.

Henze, M., Gujer, W., Mino, T., Matsuo, T., Wentzel, M.C., Marais, G.v.R. (1995). Activated Sludge Model. No. 2. IAWQ Scientific and Technical Report No. 3., London, UK.

Henze, M., Gujer, W., Mino, T., Matsuo, T., Wentzel, M.C., Marais, G.v.R., Van Loosdrecht, M.C.M. (1999). Activated sludge model no.2d, ASM2d. Water Sci. Technol. 39 (1), 165–182.

Hirota, R., Kuroda, A., Kato, J., & Ohtake, H. (2010). Bacterial phosphate metabolism and its application to phosphorus recovery and industrial bioprocesses. *Journal of bioscience and bioengineering*, *109*(5), 423-432.

Holenda, B. (2007). Development of modelling, control and optimization tools for the activated sludge process. *Doctorate School of Chemical Engineering, University of Pannonia*, *155*.

Hu, J. Y., Ong, S. L., Ng, W. J., Lu, F., & Fan, X. J. (2003). A new method for characterizing denitrifying phosphorus removal bacteria by using three different types of electron acceptors. *Water Research*, *37*(14), 3463-3471.

Hu, Z. R., Wentzel, M. C., & Ekama, G. A. (2002). Anoxic growth of phosphate-accumulating organisms (PAOs) in biological nutrient removal activated sludge systems. *Water Research*, *36*(19), 4927-4937.

Jaffer, Y., Clark, T.A., Pearce, P. and Parsons, S.A. (2002). Potential phosphorus recovery by struvite formation. *Water research*, *36*(7), pp.1834-1842.

Ji, Z., & Chen, Y. (2010). Using sludge fermentation liquid to improve wastewater short-cut nitrification-denitrification and denitrifying phosphorus removal via nitrite. *Environmental science & technology*, *44*(23), 8957-8963.

Jin, R. C., Yang, G. F., Yu, J. J., & Zheng, P. (2012). The inhibition of the Anammox process: a review. *Chemical Engineering Journal*, *197*, 67-79.

Kabdaslı, I., Tünay, O., Öztürk, I., Yılmaz, S. and Arıkan, O. (2000). Ammonia removal from young landfill leachate by magnesium ammonium phosphate precipitation and air stripping. *Water science and technology*, *41*(1), pp.237-240.

Kerrn-Jespersen, J. P., & Henze, M. (1993). Biological phosphorus uptake under anoxic and aerobic conditions. *Water Research*, *27*(4), 617-624.

Kerrn-Jespersen, J.P., Henze, M. and Strube, R. (1994). Biological phosphorus release and uptake under alternating anaerobic and anoxic conditions in a fixed-film reactor. *Water Research*, *28*(5), pp.1253-1255.

Kim, J. M., Lee, H. J., Lee, D. S., & Jeon, C. O. (2013). Characterization of the denitrification-associated phosphorus uptake properties of "Candidatus Accumulibacter phosphatis" clades in sludge subjected to enhanced biological phosphorus removal. *Appl. Environ. Microbiol.*, *79*(6), 1969-1979.

Kishida, N., Kim, J., Tsuneda, S., & Sudo, R. (2006). Anaerobic/oxic/anoxic granular sludge process as an effective nutrient removal process utilizing denitrifying polyphosphate-accumulating organisms. *Water Research*, *40*(12), 2303-2310.

Kondo, T., Ebie, Y., Tsuneda, S. and Inamori, Y. (2007). Detection of Defluvicoccus-related glycogen-accumulating organisms in enhanced biological phosphorus removal processes. *Microbes and Environments*, *22*(2), pp.190-195.

Kong, Y., Nielsen, J. L., & Nielsen, P. H. (2004). Microautoradiographic study of Rhodocyclus-related polyphosphate-accumulating bacteria in full-scale enhanced biological phosphorus removal plants. *Appl. Environ. Microbiol.*, *70*(9), 5383-5390.

Kong, Y., Nielsen, J. L., & Nielsen, P. H. (2005). Identity and ecophysiology of uncultured actinobacterial polyphosphate-accumulating organisms in full-scale enhanced biological phosphorus removal plants. *Appl. Environ. Microbiol.*, *71*(7), 4076-4085.

Kong, Y., Xia, Y. and Nielsen, P.H. (2008). Activity and identity of fermenting microorganisms in full-scale biological nutrient removing wastewater treatment plants. *Environmental microbiology*, *10*(8), pp.2008-2019.

Kristiansen, R., Nguyen, H.T.T., Saunders, A.M., Nielsen, J.L., Wimmer, R., Le, V.Q., McIlroy, S.J., Petrovski, S., Seviour, R.J., Calteau, A. and Nielsen, K.L. (2013). A metabolic model for members of the genus Tetrasphaera involved in enhanced biological phosphorus removal. *The ISME journal*, *7*(3), pp.543-554.

Kuba, T., Smolders, G., Van Loosdrecht, M. C. M., & Heijnen, J. J. (1993). Biological phosphorus removal from wastewater by anaerobic-anoxic sequencing batch reactor. *Water Science and Technology*, *27*(5-6), 241-252.

Kuba, T., Murnleitner, E., Van Loosdrecht, M. C. M., & Heijnen, J. J. (1996a). A metabolic model for biological phosphorus removal by denitrifying organisms. *Biotechnology and Bioengineering*, *52*(6), 685-695.

Kuba, T. M. C. M., Van Loosdrecht, M. C. M., & Heijnen, J. J. (1996b). Phosphorus and nitrogen removal with minimal COD requirement by integration of denitrifying dephosphatation and nitrification in a two-sludge system. *Water research*, *30*(7), 1702-1710.

Kundu, P., Pramanik, A., Dasgupta, A., Mukherjee, S. and Mukherjee, J. (2014). Simultaneous heterotrophic nitrification and aerobic denitrification by Chryseobacterium sp. R31 isolated from abattoir wastewater. *BioMed research international*, *2014*.

Kuroda, A., Takiguchi, N., Gotanda, T., Nomura, K., Kato, J., Ikeda, T., & Ohtake, H. (2002). A simple method to release polyphosphate from activated sludge for phosphorus reuse and recycling. *Biotechnology and Bioengineering*, *78*(3), 333-338.

Lalley, J., Han, C., Li, X., Dionysiou, D. D., & Nadagouda, M. N. (2016). Phosphate adsorption using modified iron oxide-based sorbents in lake water: kinetics, equilibrium, and column tests. *Chemical Engineering Journal*, *284*, 1386-1396.

Lanham, A. B., Moita, R., Lemos, P. C., Reis, M. A. M. (2011). Long-term operation of a reactor enriched in accumulibacter clade i dpaos: performance with nitrate, nitrite and oxygen. *Water Science & Technology, 63*(2), p.352-359.

Lanham, A. B., Oehmen, A., Saunders, A. M., Carvalho, G., Nielsen, P. H., & Reis, M. A. (2013). Metabolic versatility in full-scale wastewater treatment plants performing enhanced biological phosphorus removal. *Water research*, *47*(19), 7032-7041.

Le Corre, K. S., Valsami-Jones, E., Hobbs, P., & Parsons, S. A. (2009). Phosphorus recovery from wastewater by struvite crystallization: A review. *Critical Reviews in Environmental Science and Technology*, *39*(6), 433-477.

Lee, D. S., Jeon, C. O., & Park, J. M. (2001). Biological nitrogen removal with enhanced phosphate uptake in a sequencing batch reactor using single sludge system. *Water Research*, *35*(16), 3968-3976.

Li, C., Liang, S., Zhang, J., Ngo, H. H., Guo, W., Zheng, N., & Zou, Y. (2013). N2O reduction during municipal wastewater treatment using a two-sludge SBR system acclimatized with propionate. *Chemical engineering journal*, *222*, 353-360.

Li, N., Wang, X., Ren, N., Zhang, K., Kang, H., & You, S. (2008). Effects of solid retention time (SRT) on sludge characteristics in enhanced biological phosphorus removal (EBPR) reactor. *Chemical and biochemical engineering quarterly*, *22*(4), 453-458.

Liao, P.H., Chen, A. and Lo, K.V. (1995). Removal of nitrogen from swine manure wastewaters by ammonia stripping. *Bioresource Technology*, *54*(1), pp.17-20.

Lim, S., Kim, S., Yeon, K.M., Sang, B.I., Chun, J. and Lee, C.H., (2012). Correlation between microbial community structure and biofouling in a laboratory scale membrane bioreactor with synthetic wastewater. *Desalination*, *287*, pp.209-215.

Liu, T., Liu, S., Zheng, M., Chen, Q., & Ni, J. (2016). Performance assessment of full-scale wastewater treatment plants based on seasonal variability of microbial communities via high-throughput sequencing. PloS one, 11(4), e0152998.

Liu, W. T., Nakamura, K., Matsuo, T., & Mino, T. (1997). Internal energy-based competition between polyphosphate-and glycogen-accumulating bacteria in biological phosphorus removal reactors—Effect of PC feeding ratio. *Water Research*, *31*(6), 1430-1438.

Lochmatter, S., Weissbrodt, D., Gonzalez-Gil, G., & Holliger, C. (2009). *DENITRIFYING PAO AND GAO IN AEROBIC GRANULAR BIOFILM CULTIVATED WITH ACETATE AND PROPIONATE* (No. POST_TALK).

Louie, T.M., Mah, T.J., Oldham, W. and Ramey, W.D. (2000). Use of metabolic inhibitors and gas chromatography/mass spectrometry to study poly-β-hydroxyalkanoates

metabolism involving cryptic nutrients in enhanced biological phosphorus removal systems. *Water Research*, *34*(5), pp.1507-1514.

Lv, X., Shao, M., Li, C., Li, J., Liu, D., Gao, X., & Xia, X. (2014). Operation performance and microbial community dynamics of phosphorus removal sludge with different electron acceptors. *Journal of industrial microbiology & biotechnology*, *41*(7), 1099-1108.

Lu, H., Oehmen, A., Virdis, B., Keller, J. and Yuan, Z. (2006). Obtaining highly enriched cultures of Candidatus Accumulibacter phosphates through alternating carbon sources. *Water Research*, *40*(20), pp.3838-3848.

Lu, H., Wu, D., Jiang, F., Ekama, G. A., van Loosdrecht, M. C., & Chen, G. H. (2012). The demonstration of a novel sulfur cycle-based wastewater treatment process: Sulfate reduction, autotrophic denitrification, and nitrification integrated (SANI®) biological nitrogen removal process. *Biotechnology and bioengineering*, *109*(11), 2778-2789.

Ma, B., Wang, S., Zhu, G., Ge, S., Wang, J., Ren, N., & Peng, Y. (2013). Denitrification and phosphorus uptake by DPAOs using nitrite as an electron acceptor by step-feed strategies. *Frontiers of Environmental Science & Engineering*, *7*(2), 267-272.

Majed, N., Chernenko, T., Diem, M. and Gu, A.Z. (2012). Identification of functionally relevant populations in enhanced biological phosphorus removal processes based on intracellular polymers profiles and insights into the metabolic diversity and heterogeneity. *Environmental science & technology*, *46*(9), pp.5010-5017.

Mandal, S., Van Treuren, W., White, R.A., Eggesbø, M., Knight, R. and Peddada, S.D. (2015). Analysis of composition of microbiomes: a novel method for studying microbial composition. *Microbial ecology in health and disease*, *26*(1), p.27663.

Marques, R., Ribera-Guardia, A., Santos, J., Carvalho, G., Reis, M.A.M., Pijuan, M., Oehmen, A., (2018). Denitrifying capabilities of Tetrasphaera and their contribution towards nitrous oxide production in enhanced biological phosphorus removal processes. Water Res. 137, 262-272.

Marques, R., Santos, J., Nguyen, H., Carvalho, G., Noronha, J.P., Nielsen, P.H., Reis, M.A. and Oehmen, A. (2017). Metabolism and ecological niche of Tetrasphaera and Ca. Accumulibacter in enhanced biological phosphorus removal. *Water research*, *122*, pp.159-171.

Martin, M. (2011). Cutadapt removes adapter sequences from high-throughput sequencing reads. *EMBnet. journal*, *17*(1), pp.10-12.

Martin, H. G., Ivanova, N., Kunin, V., Warnecke, F., Barry, K. W., McHardy, A. C., ... & Dalin, E. (2006). Metagenomic analysis of two enhanced biological phosphorus removal (EBPR) sludge communities. *Nature biotechnology*, *24*(10), 1263.

Meinhold, J., Arnold, E., & Isaacs, S. (1999). Effect of nitrite on anoxic phosphate uptake in biological phosphorus removal activated sludge. *Water Research*, *33*(8), 1871-1883.

Merzouki, M., Bernet, N., Deigenès, J. P., Moletta, R., & Benlemlih, M. (2001). Biological denitrifying phosphorus removal in SBR: effect of added nitrate concentration and sludge retention time. *Water Science and Technology*, *43*(3), 191-194.

Metcalf & Eddy (2003). *Wastewater engineering: Treatment and reuse (4th ed.*).Ed. G. Tchobanoglous, F.L. Burton, H. D. Stensel. Boston, McGraw-Hill.

Meyer, R.L., Saunders, A.M. and Blackall, L.L. (2006). Putative glycogen-accumulating organisms belonging to the Alphaproteobacteria identified through rRNA-based stable isotope probing. *Microbiology*, *152*(2), pp.419-429.

Mino, T., Liu, W. T., Kurisu, F., & Matsuo, T. (1995). Modelling glycogen storage and denitrification capability of microorganisms in enhanced biological phosphate removal processes. *Water Science and Technology*, *31*(2), 25-34.

Mino, T. V., Van Loosdrecht, M. C. M., & Heijnen, J. J. (1998). Microbiology and biochemistry of the enhanced biological phosphate removal process. *Water research*, *32*(11), 3193-3207.

Morse, G. K., Brett, S. W., Guy, J. A., & Lester, J. N. (1998). Phosphorus removal and recovery technologies. *Science of the total environment*, *212*(1), 69-81.

Mulder, J. W., Van Loosdrecht, M. C. M., Hellinga, C., & Van Kempen, R. (2001). Full-scale application of the SHARON process for treatment of rejection water of digested sludge dewatering. *Water science and technology*, *43*(11), 127-134.

Murnleitner, E., Kuba, T., Van Loosdrecht, M. C. M., & Heijnen, J. J. (1997). An integrated metabolic model for the aerobic and denitrifying biological phosphorus removal. *Biotechnology and Bioengineering*, *54*(5), 434-450.

National Academy of Sciences (1969). Eutrophication: causes, consequences, correctives. Printing and Publishing office, National Academy of Sciences, Washington, DC. ISBN: 0-309-01700-9.

Nittami, T., Oi, H., Matsumoto, K., & Seviour, R. J. (2011). Influence of temperature, pH and dissolved oxygen concentration on enhanced biological phosphorus removal under strictly aerobic conditions. *New biotechnology*, *29*(1), 2-8.

Nowak, O., Svardal, K., & Kroiss, H. (1996). The impact of phosphorus deficiency on nitrification-case study of a biological pretreatment plant for rendering plant effluent. *Water Science and Technology*, *34*(1-2), 229-236.

Nur, T., Johir, M. A. H., Loganathan, P., Nguyen, T., Vigneswaran, S., & Kandasamy, J. (2014). Phosphate removal from water using an iron oxide impregnated strong base anion exchange resin. *Journal of Industrial and Engineering Chemistry*, *20*(4), 1301-1307.

Oehmen, A., Lemos, P. C., Carvalho, G., Yuan, Z., Keller, J., Blackall, L. L., & Reis, M. A. (2007). Advances in enhanced biological phosphorus removal: from micro to macro scale. *Water research*, *41*(11), 2271-2300.

Oehmen, A., Lopez-Vazquez, C. M., Carvalho, G., Reis, M. A. M., & Van Loosdrecht, M. C. M. (2010). Modelling the population dynamics and metabolic diversity of organisms relevant in anaerobic/anoxic/aerobic enhanced biological phosphorus removal processes. *Water research*, *44*(15), 4473-4486.

Oehmen, A., Saunders, A. M., Vives, M. T., Yuan, Z., & Keller, J. (2006). Competition between polyphosphate and glycogen accumulating organisms in enhanced biological phosphorus removal systems with acetate and propionate as carbon sources. *Journal of Biotechnology*, *123*(1), 22-32.

Oehmen, A., Vives, M. T., Lu, H., Yuan, Z., & Keller, J. (2005). The effect of pH on the competition between polyphosphate-accumulating organisms and glycogen-accumulating organisms. *Water Research*, *39*(15), 3727-3737.

Okabe, S., Oozawa, Y., Hirata, K., & Watanabe, Y. (1996). Relationship between population dynamics of nitrifiers in biofilms and reactor performance at various C: N ratios. *Water Research*, *30*(7), 1563-1572.

Ong, Y. H., Chua, A. S. M., & Ngoh, G. C. (2010). Establishment of enhanced biological phosphorus removal in a sequencing batch reactor by using seed sludge from a

conventional activated sludge wastewater treatment process. *Journal of Applied Sciences(Faisalabad)*, *10*(21), 2643-2647.

Pedregosa, F., Varoquaux, G., Gramfort, A., Michel, V., Thirion, B., Grisel, O., Blondel, M., Prettenhofer, P., Weiss, R., Dubourg, V. and Vanderplas, J. (2011). Scikit-learn: Machine learning in Python. *the Journal of machine Learning research*, *12*, pp.2825-2830.

Peng, Y. Z., Wang, X. L., & Li, B. K. (2006). Anoxic biological phosphorus uptake and the effect of excessive aeration on biological phosphorus removal in the A2O process. *Desalination*, *189*(1-3), 155-164.

Peng, Y.Z., Wu, C.Y., Wang, R.D. and Li, X.L. (2011). Denitrifying phosphorus removal with nitrite by a real-time step feed sequencing batch reactor. *Journal of Chemical Technology & Biotechnology*, *86*(4), pp.541-546.

Peng, Y., & Zhu, G. (2006). Biological nitrogen removal with nitrification and denitrification via nitrite pathway. *Applied microbiology and biotechnology*, *73*(1), 15-26.

Pescod, M. (1992). *Wastewater treatment and use in agriculture-FAO irrigation and drainage paper 47*. Food and Agriculture Organization, Rome.

Petersen B, Gernaey K, Henze M et al (2002) Evaluation of an ASM1 model calibration procedure on a municipal–industrial wastewater treatment plant. J Hydroinf 4:15–38.

Peterson, S.B., Warnecke, F., Madejska, J., McMahon, K.D. and Hugenholtz, P. (2008). Environmental distribution and population biology of Candidatus Accumulibacter, a primary agent of biological phosphorus removal. *Environmental microbiology*, *10*(10), pp.2692-2703.

Podedworna, J., & Żubrowska-Sudoł, M. (2012). Nitrogen and phosphorus removal in a denitrifying phosphorus removal process in a sequencing batch reactor with a forced anoxic phase. *Environmental technology*, *33*(2), 237-245.

Pollice, A., Tandoi, V., & Lestingi, C. (2002). Influence of aeration and sludge retention time on ammonium oxidation to nitrite and nitrate. *Water research*, *36*(10), 2541-2546.

Pressley, T.A., Bishop, D.F. and Roan, S.G. (1972). Ammonia-nitrogen removal by breakpoint chlorination. *Environmental Science & Technology*, *6*(7), pp.622-628.

Qiao, S., Matsumoto, N., Shinohara, T., Nishiyama, T., Fujii, T., Bhatti, Z., & Furukawa, K. (2010). High-rate partial nitrification performance of high ammonium containing wastewater under low temperatures. *Bioresource technology*, *101*(1), 111-117.

Qiu, G., & Ting, Y. P. (2014). Direct phosphorus recovery from municipal wastewater via osmotic membrane bioreactor (OMBR) for wastewater treatment. *Bioresource technology*, *170*, 221-229.

Quast, C., Pruesse, E., Yilmaz, P., Gerken, J., Schweer, T., Yarza, P., Peplies, J. and Glöckner, F.O. (2012). The SILVA ribosomal RNA gene database project: improved data processing and web-based tools. *Nucleic acids research*, *41*(D1), pp.D590-D596.

Quinlan, A. V. (1986). Optimum temperature shift for Nitrobacter winogradskyi: Effect of dissolve oxygen and nitrate concentrations. *Water Research*, *20*(5), 611-617.

Reichert, P. (1998). Aquasim 2.0-user manual. *Swiss Federal Institute for Environmental Science and Technology. Dubendorf, Switzerland*.

Reichert, P.: Concepts underlying a computer program for the identification and simulation of aquatic systems. Swiss Federal Institute for Environmental Science and Technology (EAWAG), Dübendorf (1994).

Regmi, P., Miller, M. W., Holgate, B., Bunce, R., Park, H., Chandran, K., ... & Bott, C. B. (2014). Control of aeration, aerobic SRT and COD input for mainstream nitritation/denitritation. *Water research*, *57*, 162-171.

Rieger, L., Koch, G., Kuhni, M., Gujer, W., Siegrist, H., (2001). The EAWAG bio-P module for activated sludge model no. 3. Water Res. 35 (16), 3887–3903.

Regmi, P., Miller, M. W., Holgate, B., Bunce, R., Park, H., Chandran, K., & Bott, C. B. (2014). Control of aeration, aerobic SRT and COD input for mainstream nitritation/denitritation. *Water research*, *57*, 162-171.

Rognes, T., Flouri, T., Nichols, B., Quince, C. and Mahé, F., 2016. VSEARCH: a versatile open source tool for metagenomics. *PeerJ*, *4*, p.e2584.

Rubio-Rincón, F.J., Weissbrodt, D.G., Lopez-Vazquez, C.M., Welles, L., Abbas, B., Albertsen, M., Nielsen, P.H., van Loosdrecht, M.C.M. and Brdjanovic, D. (2019). "Candidatus Accumulibacter delftensis": A clade IC novel polyphosphate-accumulating organism without denitrifying activity on nitrate. *Water research*, *161*, pp.136-151.

Saad, S.A., Welles, L., Abbas, B., Lopez-Vazquez, C.M., van Loosdrecht, M.C. and Brdjanovic, D. (2016). Denitrification of nitrate and nitrite by 'Candidatus Accumulibacter phosphatis' clade IC. *Water research*, *105*, pp.97-109.

Sedlak. R.I. (1991). *Phosphorus and nitrogen removal from municipal wastewater: Principles and practice, second edition*, New York, CRC Press.

Serafim, L.S., Lemos, P.C. and Reis, M.A.M. (2002). Effect of pH control on EBPR stability and efficiency. *Water science and technology*, *46*(4-5), pp.179-184.

Serna-Maza, A., Heaven, S. and Banks, C.J. (2014). Ammonia removal in food waste anaerobic digestion using a side-stream stripping process. *Bioresource technology*, *152*, pp.307-315.

Shi, J., Lu, X., Yu, R. and Zhu, W. (2012). Nutrient removal and phosphorus recovery performances of a novel anaerobic-anoxic/nitrifying/induced crystallization process. *Bioresource technology*, *121*, pp.183-189.

Skalsky, D.S. and Daigger, G.T. (1995). Wastewater solids fermentation for volatile acid production and enhanced biological phosphorus removal. *Water Environment Research*, *67*(2), pp.230-237.

Smolders, G. J. F., van der Meij, J., van Loosdrecht, M. C. M., Heijnen, J. J. (1994a). Model of the anaerobic metabolism of the biological phosphorus removal process: Stoichiometry and pH influence. Biotechnol. Bioeng. 43: 461470.

Smolders, G. J. F., Van der Meij, J., Van Loosdrecht, M. C. M., & Heijnen, J. J. (1994b). Stoichiometric model of the aerobic metabolism of the biological phosphorus removal process. *Biotechnology and bioengineering*, *44*(7), 837-848.

Strous, M., Van Gerven, E., Zheng, P., Kuenen, J. G., & Jetten, M. S. (1997). Ammonium removal from concentrated waste streams with the anaerobic ammonium oxidation (anammox) process in different reactor configurations. *Water Research*, *31*(8), 1955-1962.

Suzuki, I., Dular, U., & Kwok, S. C. (1974). Ammonia or ammonium ion as substrate for oxidation by Nitrosomonas europaea cells and extracts. *Journal of Bacteriology*, *120*(1), 556-558.

Tang, Y. C., Tang, L. H., Wu, C. N., Pan, F. K., Tao, Y., Xue, L. P., ... & Nie, H. Y. (2012). Effect of Electron Acceptors and Carbon Resources on De-nitrification Phosphorus Removal from Wastewater. *Sustainable Development-Special track within SCET2012*, 368.

Tao, B., Passanha, P., Kumi, P., Wilson, V., Jones, D. and Esteves, S. (2016). Recovery and concentration of thermally hydrolysed waste activated sludge derived volatile fatty acids and nutrients by microfiltration, electrodialysis and struvite precipitation for polyhydroxyalkanoates production. *Chemical Engineering Journal*, *295*, pp.11-19.

Tarayre, C., Charlier, R., Delepierre, A., Brognaux, A., Bauwens, J., Francis, F., Dermience, M., Lognay, G., Taminiau, B. and Daube, G. (2017) Looking for phosphate-accumulating bacteria in activated sludge processes: a multidisciplinary approach. *Environmental Science and Pollution Research,* 24 (9), 8017-8032.

Terashima, M., Yama, A., Sato, M., Yumoto, I., Kamagata, Y., & Kato, S. (2016). Culture-dependent and-independent identification of polyphosphate-accumulating Dechloromonas spp. predominating in a full-scale oxidation ditch wastewater treatment plant. *Microbes and environments*, ME16097.

Thornton, A., Pearce, P., & Parsons, S. A. (2007). Ammonium removal from digested sludge liquors using ion exchange. *Water research*, *41*(2), 433-439.

Tokutomi, T. (2004). Operation of a nitrite-type airlift reactor at low DO concentration. *Water Science and Technology*, *49*(5-6), pp.81-88.

Torrico, V., Kuba, T. and Kusuda, T. (2008). Optimization of internal bypass ratio for complete ammonium and phosphate removal in a dephanox-type two-sludge denitrification system. *Journal of Environmental Engineering*, *134*(7), pp.536-542.

Tran, N., Drogui, P., Blais, J. F., & Mercier, G. (2012). Phosphorus removal from spiked municipal wastewater using either electrochemical coagulation or chemical coagulation as tertiary treatment. *Separation and Purification Technology*, *95*, 16-25.

Tsuneda, S., Ohno, T., Soejima, K., & Hirata, A. (2006). Simultaneous nitrogen and phosphorus removal using denitrifying phosphate-accumulating organisms in a sequencing batch reactor. *Biochemical Engineering Journal*, *27*(3), 191-196.

Valverde-Pérez, B., Ramin, E., Smets, B. F., & Plósz, B. G. (2015). EBP2R–an innovative enhanced biological nutrient recovery activated sludge system to produce growth medium for green microalgae cultivation. *water research*, *68*, 821-830.

Valverde-Pérez, B., Wágner, D. S., Lóránt, B., Gülay, A., Smets, B. F., & Plosz, B. G. (2016). Short-sludge age EBPR process–Microbial and biochemical process characterisation during reactor start-up and operation. *Water research*, *104*, 320-329.

Van de Graaf, A. A., Mulder, A. R. N. O. L. D., de Bruijn, P. E. T. E. R., Jetten, M. S., Robertson, L. A., & Kuenen, J. G. (1995). Anaerobic oxidation of ammonium is a biologically mediated process. *Appl. Environ. Microbiol.*, *61*(4), 1246-1251.

Van Kempen, R., Mulder, J.W., Uijterlinde, C.A. and Loosdrecht, M.C.M.V. (2001). Overview: full scale experience of the SHARON® process for treatment of rejection water of digested sludge dewatering. *Water science and technology*, *44*(1), pp.145-152.

Van Veldhuizen, H., van Loosdrecht, M. C., & Heijnen, J. J. (1999). Modelling biological phosphorus and nitrogen removal in a full scale activated sludge process. *Water Research*, *33*(16), 3459-3468.

Vargas, M., Guisasola, A., Artigues, A., Casas, C. and Baeza, J.A. (2011). Comparison of a nitrite-based anaerobic–anoxic EBPR system with propionate or acetate as electron donors. *Process Biochemistry*, *46*(3), pp.714-720.

Verstraete, W., & Philips, S. (1998). Nitrification-denitrification processes and technologies in new contexts. *Environmental pollution*, *102*(1), 717-726.

Wachtmeister, A., Kuba, T., Van Loosdrecht, M. C. M., & Heijnen, J. J. (1997). A sludge characterization assay for aerobic and denitrifying phosphorus removing sludge. *Water Research*, *31*(3), 471-478.

Wang, D., Fu, Q., Xu, Q., Liu, Y., Ngo, H.H., Yang, Q., Zeng, G., Li, X. and Ni, B.-J. (2017) Free nitrous acid-based nitrifying sludge treatment in a two-sludge system enhances nutrient removal from low-carbon wastewater. *Bioresource technology,* 244, 920-928.

Wang, Y., Geng, J., Peng, Y., Wang, C., Guo, G. and Liu, S. (2012). A comparison of endogenous processes during anaerobic starvation in anaerobic end sludge and aerobic end sludge from an anaerobic/anoxic/oxic sequencing batch reactor performing denitrifying phosphorus removal. *Bioresource technology*, *104*, pp.19-27.

Wang, Y., Geng, J., Ren, Z., He, W., Xing, M., Wu, M., & Chen, S. (2011). Effect of anaerobic reaction time on denitrifying phosphorus removal and N2O production. *Bioresource Technology*, *102*(10), 5674-5684.

Wang, L.S., Hu, H.Y. and Wang, C. (2007). Effect of ammonia nitrogen and dissolved organic matter fractions on the genotoxicity of wastewater effluent during chlorine disinfection. *Environmental science & technology*, *41*(1), pp.160-165.

Wang, Y., Jiang, F., Zhang, Z., Xing, M., Lu, Z., Wu, M., ... & Peng, Y. (2010). The long-term effect of carbon source on the competition between polyphosphorus accumulating organisms and glycogen accumulating organism in a continuous plug-flow anaerobic/aerobic (A/O) process. *Bioresource technology*, *101*(1), 98-104.

Wang, Y. Y., Pan, M. L., Min, Y., Peng, Y. Z., & Wang, S. Y. (2007). Characteristics of anoxic phosphors removal in sequence batch reactor. *Journal of Environmental Sciences*, *19*(7), 776-782.

Wang, Y., Peng, Y., & Stephenson, T. (2009). Effect of influent nutrient ratios and hydraulic retention time (HRT) on simultaneous phosphorus and nitrogen removal in a two-sludge sequencing batch reactor process. *Bioresource Technology*, *100*(14), 3506-3512.

Wang, M. X., Zhao, W. H., & Wang, S. Y. (2016). Startup and stability of A 2 N 2 double sludge system denitrifying phosphorus removal process. *CIESC Journal*, *67*(7), 2987-2997.

Wang, Y., Zhou, S., Ye, L., Wang, H., Stephenson, T., & Jiang, X. (2014). Nitrite survival and nitrous oxide production of denitrifying phosphorus removal sludges in long-term nitrite/nitrate-fed sequencing batch reactors. *Water research*, *67*, 33-45.

Wang, Y., Zhou, S., Wang, H., Ye, L., Qin, J., & Lin, X. (2015). Comparison of endogenous metabolism during long-term anaerobic starvation of nitrite/nitrate cultivated denitrifying phosphorus removal sludges. *water research*, *68*, 374-386.

Wong, M.T., Tan, F.M., Ng, W.J. and Liu, W.T. (2004). Identification and occurrence of tetrad-forming *Alphaproteobacteria* in anaerobic–aerobic activated sludge processes. *Microbiology*, 150(11), pp.3741-3748.

Wei, D., Du, B., Xue, X., Dai, P., & Zhang, J. (2014). Analysis of factors affecting the performance of partial nitrification in a sequencing batch reactor. *Applied microbiology and biotechnology*, *98*(4), 1863-1870.

Welles, L., Lopez-Vazquez, C. M., Hooijmans, C. M., Van Loosdrecht, M. C. M., & Brdjanovic, D. (2014). Impact of salinity on the anaerobic metabolism of phosphate-accumulating organisms (PAO) and glycogen-accumulating organisms (GAO). *Applied microbiology and biotechnology*, *98*(17), 7609-7622.

Wentzel, M. C., Lötter, L. H., Ekama, G. A., Loewenthal, R. E., & Marais, G. V. R. (1991). Evaluation of biochemical models for biological excess phosphorus removal. *Water Science and Technology*, *23*(4-6), 567-576.

Wiesmann, U. (1994). Biological nitrogen removal from wastewater. In *Biotechnics/wastewater* (pp. 113-154). Springer, Berlin, Heidelberg.

Wilfert, P., Kumar, P.S., Korving, L., Witkamp, G.J. and van Loosdrecht, M.C. (2015). The relevance of phosphorus and iron chemistry to the recovery of phosphorus from wastewater: a review. *Environmental science & technology*, *49*(16), pp.9400-9414.

Wood, P. Monooxygenase and free radical mechanisms for biological ammonia oxidation. The Nitrogen and Sulfur Cycles Soc. Gen. Micro. Symp, 1988. 65-98.

Wu, D., Ekama, G. A., Lu, H., Chui, H. K., Liu, W. T., Brdjanovic, D., ... & Chen, G. H. (2013). A new biological phosphorus removal process in association with sulfur cycle. *Water research*, *47*(9), 3057-3069.

Wu, D., Ekama, G. A., Wang, H. G., Wei, L., Lu, H., Chui, H. K., ... & Chen, G. H. (2014). Simultaneous nitrogen and phosphorus removal in the sulfur cycle-associated Enhanced Biological Phosphorus Removal (EBPR) process. *Water research*, *49*, 251-264.

Wu, C., Peng, Y., Wang, S., Li, X. & Wang, R. (2011). Effect of sludge retention time on nitrite accumulation in real-time control biological nitrogen removal sequencing batch reactor. *Chinese Journal of Chemical Engineering,* 19**,** 512-517.

Xu, Q., Liu, X., Yang, G., Wang, D., Wang, Q., Liu, Y., Li, X. and Yang, Q. (2019). Free nitrous acid-based nitrifying sludge treatment in a two-sludge system obtains high polyhydroxyalkanoates accumulation and satisfied biological nutrients removal. *Bioresource technology*, *284*, pp.16-24.

Xu, S., Wu, D., & Hu, Z. (2014). Impact of hydraulic retention time on organic and nutrient removal in a membrane coupled sequencing batch reactor. *Water research*, *55*, 12-20.

Yagci, N., Artan, N., Çokgör, E. U., Randall, C. W., & Orhon, D. (2003). Metabolic model for acetate uptake by a mixed culture of phosphate-and glycogen-accumulating organisms under anaerobic conditions. *Biotechnology and bioengineering*, *84*(3), 359-373.

Yang, Q., Peng, Y., Liu, X., Zeng, W., Mino, T., & Satoh, H. (2007). Nitrogen removal via nitrite from municipal wastewater at low temperatures using real-time control to optimize nitrifying communities. *Environmental science & technology*, *41*(23), 8159-8164.

Ye, Z., Shen, Y., Ye, X., Zhang, Z., Chen, S., & Shi, J. (2014). Phosphorus recovery from wastewater by struvite crystallization: property of aggregates. *Journal of Environmental Sciences*, *26*(5), 991-1000.

Yoo, H., Ahn, K. H., Lee, H. J., Lee, K. H., Kwak, Y. J., & Song, K. G. (1999). Nitrogen removal from synthetic wastewater by simultaneous nitrification and denitrification (SND) via nitrite in an intermittently-aerated reactor. *Water research*, *33*(1), 145-154.

Yuan, M. H., Chen, Y. H., Tsai, J. Y., & Chang, C. Y. (2016). Removal of ammonia from wastewater by air stripping process in laboratory and pilot scales using a rotating packed bed at ambient temperature. *Journal of the Taiwan Institute of Chemical Engineers*, *60*, 488-495.

Zeng, W., Li, B., Wang, X., Bai, X., & Peng, Y. (2014). Integration of denitrifying phosphorus removal via nitrite pathway, simultaneous nitritation–denitritation and anammox treating carbon-limited municipal sewage. *Bioresource technology*, *172*, 356-364.

Zeng, W., Li, L., Yang, Y. Y., Wang, X. D., & Peng, Y. Z. (2011). Denitrifying phosphorus removal and impact of nitrite accumulation on phosphorus removal in a continuous anaerobic–anoxic–aerobic (A2O) process treating domestic wastewater. *Enzyme and microbial technology*, *48*(2), 134-142.

Zeng, R. J., Saunders, A. M., Yuan, Z., Blackall, L. L., & Keller, J. (2003a). Identification and comparison of aerobic and denitrifying polyphosphate-accumulating organisms. *Biotechnology and Bioengineering*, *83*(2), 140-148.

Zeng, R. J., Van Loosdrecht, M. C., Yuan, Z., & Keller, J. (2003b). Metabolic model for glycogen-accumulating organisms in anaerobic/aerobic activated sludge systems. *Biotechnology and Bioengineering*, *81*(1), 92-105.

Zeng, R. J., Yuan, Z., & Keller, J. (2003c). Enrichment of denitrifying glycogen-accumulating organisms in anaerobic/anoxic activated sludge system. *Biotechnology and Bioengineering*, *81*(4), 397-404.

Zeng, W., Zhang, L., Fan, P., Guo, J. and Peng, Y. (2018). Community structures and population dynamics of “Candidatus Accumulibacter” in activated sludges of wastewater treatment plants using ppk1 as phylogenetic marker. *Journal of Environmental Sciences*, *67*, pp.237-248.

Zhang, X., Li, W., Blatchley III., Wang, X. & Ren, P. (2015). UV/chlorine process for ammonia removal and disinfection by-product reduction: comparison with chlorination. *Water Research*, 68, 804811.

Zhang, S. H., Huang, Y., & Hua, Y. M. (2010). Denitrifying dephosphatation over nitrite: effects of nitrite concentration, organic carbon, and pH. *Bioresource technology*, *101*(11), 3870-3875.

Zhang, S. Y., Wang, J. S., Jiang, Z. C., & Chen, M. X. (2000). Nitrite accumulation in an attapulgas clay biofilm reactor by fulvic acids. *Bioresource technology*, *73*(1), 91-93.

Zhao, W., Peng, Y., Wang, M., Huang, Y. and Li, X. (2019). Nutrient removal and microbial community structure variation in the two-sludge system treating low carbon/nitrogen domestic wastewater. *Bioresource Technology*, *294*, p.122161.

Zheng, X., Sun, P., Han, J., Song, Y., Hu, Z., Fan, H., & Lv, S. (2014). Inhibitory factors affecting the process of enhanced biological phosphorus removal (EBPR)–a mini-review. *Process Biochemistry*, *49*(12), 2207-2213.

Zhou, Y., Pijuan, M., & Yuan, Z. (2007). Free nitrous acid inhibition on anoxic phosphorus uptake and denitrification by poly-phosphate accumulating organisms. *Biotechnology and Bioengineering*, *98*(4), 903-912.

Zhou, Y., Pijuan, M., & Yuan, Z. (2008). Development of a 2-sludge, 3-stage system for nitrogen and phosphorous removal from nutrient-rich wastewater using granular sludge and biofilms. *Water research*, *42*(12), 3207-3217.

Zhou, Y., Pijuan, M., Zeng, R.J. and Yuan, Z. (2009). Involvement of the TCA cycle in the anaerobic metabolism of polyphosphate accumulating organisms (PAOs). *Water research*, *43*(5), pp.1330-1340.

Zhou, S., Zhang, X., & Feng, L. (2010). Effect of different types of electron acceptors on the anoxic phosphorus uptake activity of denitrifying phosphorus removing bacteria. *Bioresource technology*, *101*(6), 1603-1610.

Zhu, G., Peng, Y., Li, B., Guo, J., Yang, Q. and Wang, S. (2008). Biological removal of nitrogen from wastewater *Reviews of environmental contamination and toxicology*. Springer, 159-195.

Zielińska, M., Rusanowska, P., Jarząbek, J. and Nielsen, J.L. (2016) Community dynamics of denitrifying bacteria in full-scale wastewater treatment plants. *Environmental technology,* 37 (18), 2358-2367.

References

Zou, S., Yao, S., & Ni, J. (2014). High-efficient nitrogen removal by coupling enriched autotrophic-nitrification and aerobic-denitrification consortiums at cold temperature. *Bioresource technology*, *161*, 288-296.

Appendix A: Data from experiments

a. Performance of preliminary experiments

R1		HAc (mg L^{-1})					PO_4^{3-}-P (mg L^{-1})			Removal rate	NO_3^--N (mg L^{-1})			NO_2^--N (mg L^{-1})					
Date	Day	feedstock	Ana	Ano	E	feedstock	Ana	Ano	E		Ana	Ano	E	Ana	Ano	E	pH	MLSS&MLVSS (mg L^{-1})	
2017/8/4	1	250.0	57.6	0.0	0.0	16.2	3.7	9.4	4.1	-11%	1.4	7.2	28.0	0.0	5.0	0.0	7.8	1806.7	1640.0
2017/8/11	8	240.1	120.0	0.0	0.0	15.2	13.5	14.4	11.4	15%	116.3	172.9	288.2	1.4	15.6	9.2	7.8	1726.7	1346.7
2017/8/19	16	270.37	135.2	21.6	0.0	16.1	11.7	17.2	10.0	14.5%	10.1	20.0	1.3	4.6	0.1	5.3	7.8	1500.0	1353.3
2017/8/23	20	303.6	151.8	94.4	0.0	13.1	10.2	15.3	9.7	5.0%	0.9	20.0	0.0	0.0	0.0	0.0	8.3		
2017/8/24	21	312.3	156.1	91.6	0.0	14.9	12.3	16.2	13.0	-5.5%	0.9	20.0	0.2	0.0	0.0	0.0	8.2	1713.3	1540.0
2017/8/31	28	300.0	150.0	88.2	0.0	15.0	14.6	18.2	12.8	12.2%	1.0	20.0	0.3	0.0	0.0	0.0	8.0	1633.3	1560.0
2017/9/5	33	251.0	125.5	6.0	0.0	12.8	11.0	19.4	9.3	15.1%	7.7	40.0	22.6	3.4	0.0	4.0	8.7	1326.7	1253.3
2017/9/9	37	254.0	127.0	0.0	0.0	13.6	11.6	25.0	11.4	1.7%	17.1	40.0	32.2	1.1	0.0	2.5	8.5	1526.7	1406.7
2017/9/12	40	219.0	109.5	0.0	0.0	15.3	14.2	27.0	11.9	16.1%							8.5	1495.0	1395.0
2017/9/19	47	204.0	102.0	40.0	0.0	16.3	10.8	8.3	6.1	43.5%							8.6	1680.0	1445.0
2017/9/20	48	221.0	110.5	54.4	0.0	1.1	1.8	2.6	1.7	8.4%	3.6	20.0	0.0	0.0	0.0	0.0	8.5		
2017/9/22	50	209.0	104.5	45.5	0.0	14.2	9.2	9.4	5.1	44.3%	4.9	20.0	0.0	0.0	0.0	0.0	8.5		
2017/9/24	52	206.0	103.0	68.8	0.0	14.7	13.8	15.1	13.8	-0.5%	1.0	20.0	0.0	0.0	0.0	0.0	8.7	3566.7	2666.7
2017/9/26	54	206.0	103.0	51.9	0.0	14.6	19.5	28.7	27.1	-39.0%							7.6	2540.0	1585.0
2017/9/28	56	207.0	103.5	56.0	0.0	14.9	19.6	25.2	23.1	-17.7%							7.6		
2017/10/3	61	214.9	107.4	68.6	0.0	14.7	15.0	16.6	15.3	-2.0%							7.4	2020.0	1470.0
2017/10/10	68	200.0	100.0	50.0	0.0	15.0	14.3	14.3	12.2	14.6%							7.3	1826.7	1325.0
2017/10/14	72	254.2	127.1	22.7	0.0	13.2	12.2	15.6	9.8	19.4%	8.1	40.0	372.3	0.0	0.1	0.0	7.2		
2017/10/19	77	258.2	129.1	0.0	0.0	15.0	11.6	12.0	9.1	21.0%	19.3	40.0	31.7	0.0	0.0	0.0	7.4	1653.3	1150.0
2017/10/26	84	195.8	97.9	0.0	0.0	12.0	10.7	12.5	12.3	-14.8%	33.5	40.0	34.5	0.0	0.0	0.0	7.6		
2017/10/27	85	188.4	94.2	0.0	0.0	14.2	10.3	23.2	18.8	-82.0%	12.0	40.0	24.0	0.0	0.0	0.0	7.6		

Appendix A

2017/11/7	96	110.0	55.0	0.0	0.0	7.5	10.0	10.0	11.2	-12.3%		20.0	8.2		0.0	0.0	7.6		
2017/11/8	97	100.0	50.0	0.0	0.0	7.3	7.0	7.0	6.8	2.2%							7.6	1380.0	1253.3
2017/11/9	98	109.8	54.9	0.0	0.0	7.5	7.1	7.1	7.7	-8.2%							7.5		
2017/11/10	99	110.3	55.2	0.0	0.0	7.8	7.6	8.1	7.3	4.7%							7.5		
2017/11/12	101	106.6	53.3	0.0	0.0	7.9	7.3	7.6	7.0	4.2%	9.5	20.0	15.0	0.3	0.0	0.0	7.4		
2017/12/8	127	100.0	50.0	0.0	0.0	6.0	8.4	9.1	6.9	18.2%	0.3	20.0	0.8	0.0	0.0	0.0	7.5	2273.3	2053.3
2017/12/10	129	100.0	50.0	0.0	0.0	6.0	6.0	6.0	5.6	7.3%	0.0	20.0	7.4	0.0	0.0	0.0	7.4		
2017/12/15	134	100.0	50.0	0.0	0.0	5.9	4.7	4.9	4.9	-3.9%	0.0	20.0	4.3	0.0	0.0	0.0	7.4		
2017/12/18	137	100.0	50.0	0.0	0.0	6.0	5.3	6.2	5.4	-0.8%	3.9	20.0	4.7	0.0	0.0	0.0			
R2		HAc (mg L^{-1})					PO_4^{3-}-P (mg L^{-1})				NO_3^--N (mg L^{-1})			NO_2^--N (mg L^{-1})					
Date	Day	feedstock	Ana	Ano	E	feedstock	Ana	Ano	E		Ana	Ano	E	Ana	Ano	E	pH	MLSS&MLVSS (mg L^{-1})	
2017/8/4	1	250.0	57.6	0.0	0.0	15.0	3.7	8.8	4.5	-23.8%	1.4	9.0	26.6	0.0	3.7	0.0	7.7	2046.7	1820.0
2017/8/11	8	240.1	120.0	0.0	0.0	15.2	13.2	15.4	10.8	18.5%	132.7	174.9	281.3	1.6	12.5	2.9	7.7	1693.3	1293.3
2017/8/19	16	270.37	135.2	28.4	0.0	16.1	11.8	16.7	10.0	15.7%	8.5	20.0	2.7	5.6	0.1	4.2	8.0	1500.0	1333.3
2017/8/23	20	303.6	151.8	102.6	0.0	13.1	9.9	12.9	9.7	1.9%	0.9	20.0	0.0	0.0	0.0	0.0	8.4		
2017/8/24	21	312.3	156.1	97.8	0.0	14.9	12.3	14.4	12.0	2.8%	0.9	20.0	0.0	0.0	0.0	0.0	8.3	1666.7	1486.7
2017/8/31	28	300.0	150.0	108.9	0.0	15.0	14.4	15.0	13.5	6.1%	1.0	20.0	0.1	0.0	0.0	0.0	8.3	1740.0	1620.0
2017/9/5	33	251.0	125.5	0.0	0.0	12.8	10.1	17.8	9.1	10.0%	15.7	40.0	25.3	1.1	0.0	4.1	8.6	1246.7	1180.0
2017/9/9	37	254.0	127.0	0.0	0.0	13.6	11.9	21.0	11.1	6.7%	13.1	40.0	27.1	2.4	0.0	4.4	8.2	1493.3	1380.0
2017/9/12	40	219.0	109.5	0.0	0.0	15.3	14.1	25.2	12.0	15.1%							8.3	1470.0	1365.0
2017/9/19	47	204.0	102.0	49.0	0.0	16.3	10.7	7.7	4.9	54.0%							8.5	1450.0	1260.0
2017/9/20	48	221.0	110.5	56.7	0.0	1.1	1.8	2.2	1.0	47.0%	3.6	20.0	0.0	0.0	0.0	0.0	8.5		
2017/9/22	50	209.0	104.5	45.3	0.0	14.2	9.5	10.8	5.4	43.2%	3.3	20.0	0.0	0.0	0.0	0.0	8.6		
2017/9/24	52	206.0	103.0	69.5	0.0	14.7	13.7	16.0	13.6	0.7%	0.9	20.0	0.0	0.0	0.0	0.0	8.5	3480.0	2606.7
2017/9/26	54	206.0	103.0	52.4	0.0	14.6	19.7	27.8	26.9	-36.7%							7.5	2440.0	1535.0
2017/9/28	56	207.0	103.5	57.0	0.0	14.9	19.2	24.4	23.1	-20.4%							7.5		
2017/10/3	61	214.9	107.4	94.2	0.0	14.7	14.7	15.9	14.8	-0.7%							7.3	1773.3	1310.0

2017/10/10	68	200.0	100.0	50.0	0.0	15.0	14.5	14.5	12.7	12.5%							7.3	1586.7	1170.0
2017/10/14	72	254.2	127.1	83.4	0.0	13.2	11.9	14.1	10.5	11.9%	0.8	40.0	72.7	0.1	0.2	0.9	7.1		
2017/10/19	77	258.2	129.1	0.0	0.0	15.0	13.6	13.4	10.8	20.2%	17.6	40.0	29.4	0.0	0.0	0.0	7.4	1686.7	1170.0
2017/10/26	84	195.8	97.9	0.0	0.0	12.0	11.4	12.6	12.1	-6.1%	35.2	40.0	36.6	0.0	0.0	0.0	7.5		
2017/10/27	85	188.4	94.2	0.0	0.0	14.2	10.5	18.2	15.5	-47.4%	13.2	40.0	25.8	0.0	0.0	0.0	7.5		
2017/11/7	96	110.0	55.0	0.0	0.0	7.5	10.0	10.0	11.5	-15.2%		20.0	9.2		0.0	0.0	7.6		
2017/11/8	97	100.0	50.0	0.0	0.0	7.3	7.0	7.0	6.8	3.2%							7.6	1306.7	1180.0
2017/11/9	98	109.8	54.9	0.0	0.0	7.5	7.1	7.1	7.6	-8.3%							7.5		
2017/11/10	99	110.3	55.2	0.0	0.0	7.8	7.6	7.9	7.2	4.9%							7.5		
2017/11/12	101	106.6	53.3	0.0	0.0	7.9	7.4	7.5	7.2	2.4%	11.2	20.0	19.6	0.0	0.0	0.0	7.4		
2017/12/8	127	100.0	50.0	0.0	0.0	6.0	8.6	10.7	7.4	13.8%	0.1	20.0	1.3	0.0	0.0	0.0	7.5	2253.3	1980.0
2017/12/10	129	100.0	50.0	0.0	0.0	6.0	6.0	6.0	5.9	1.2%	0.0	20.0	5.0	0.0	0.0	0.0	7.4		
2017/12/15	134	100.0	50.0	0.0	0.0	5.9	4.4	6.4	5.4	-23.0%	0.0	20.0	4.5	0.0	0.0	0.0	7.4		
2017/12/18	137	100.0	50.0	0.0	0.0	6.0	5.3	6.3	5.2	1.6%	2.9	20.0	3.3	0.0	0.0	0.0			
R3		HAc (mg L^{-1})					PO_4^{3-}-P (mg L^{-1})				NO_3^--N (mg L^{-1})			NO_2^--N (mg L^{-1})					
Date	Day	feedstock	Ana	Ano	E	feedstock	Ana	Ano	E		Ana	Ano	E	Ana	Ano	E	pH	MLSS&MLVSS (mg L^{-1})	
2017/8/4	1	250.0	57.6	0.0	0.0	15.6	3.7	5.4	4.4	-19.2%	1.4	21.5	19.7	0.0	1.2	3.7	7.7	2053.3	1813.3
2017/8/11	8	256.6	128.3	0.0	0.0	15.2	13.6	12.0	9.6	29.9%	130.8	167.0	264.7	29.2	54.0	55.3	8.0	1666.7	1173.3
2017/8/19	16	273.1	136.5	50.8	0.0	19.9	12.6	14.2	8.2	34.8%	2.7	15.0	0.2	6.0	5.0	0.2	7.8	1546.7	1360.0
2017/8/23	20	315.2	157.6	98.7	0.0	15.1	9.9	11.9	9.9	-0.3%	0.9	15.0	0.0	0.0	5.0	0.0	8.1		
2017/8/24	21	300.5	150.2	89.2	0.0	15.8	12.4	16.5	13.8	-11.6%	0.9	15.0	0.0	0.0	5.0	0.0	8.1	1766.7	1540.0
2017/8/31	28	300.0	150.0	98.1	0.0	15.0	15.6	16.8	14.4	8.2%	1.0	15.0	0.1	0.0	5.0	0.0	8.3	1533.3	1433.3
2017/9/5	33	250.0	125.0	84.0	0.0	12.0	12.5	14.1	12.0	4.6%	0.8	30.0	0.0	0.0	10.0	0.0	9.2	1013.3	1000.0
2017/9/9	37	268.0	134.0	19.0	0.0	14.3	11.9	17.2	11.2	6.6%	4.3	30.0	9.1	8.5	10.0	17.5	8.7	1333.3	1246.7
2017/9/12	40	216.0	108.0	0.0	0.0	15.1	13.7	20.6	12.2	10.6%							8.2	1360.0	1275.0
2017/9/19	47	215.0	107.5	50.8	0.0	16.4	9.8	5.3	3.4	65.4%							8.8	1515.0	1295.0
2017/9/20	48	221.0	110.5	78.5	0.0	1.1	1.3	1.6	0.9	24.9%	3.6	15.0	0.0	0.0	5.0	0.0	8.7		

2017/9/22	50	216.0	108.0	52.8	0.0	15.2	9.9	7.7	3.9	61.1%	3.3	15.0	0.0	0.0	5.0	0.0	8.7		
2017/9/24	52	205.0	102.5	78.5	0.0	14.8	13.0	13.0	13.4	-3.2%	0.9	15.0	0.0	0.0	5.0	0.0	8.7	3653.3	2626.7
2017/9/26	54	200.0	100.0	57.7	0.0	15.2	19.1	27.4	25.5	-33.5%							7.5	3040.0	1760.0
2017/9/28	56	209.0	104.5	64.0	0.0	14.6	20.6	31.5	26.5	-28.5%							7.6		
2017/10/3	61	219.0	109.5	100.2	0.0	14.6	15.9	20.4	17.3	-8.8%							7.3	2086.7	1475.0
2017/10/10	68	200.0	100.0	50.0	0.0	15.0	14.7	14.6	13.1	11.4%							7.4	1800.0	1305.0
2017/10/14	72	232.0	116.0	93.7	0.0	14.8	13.1	14.0	11.0	16.3%	0.8	30.0	413.7	0.0	10.0	78.8	7.1		
2017/10/19	77	263.7	131.9	0.0	0.0	17.7	14.3	16.6	13.3	6.6%	14.8	30.0	25.1	0.4	10.0	1.7	7.6	1593.3	1095.0
2017/10/26	84	214.5	107.3	0.0	0.0	12.6	12.1	12.7	12.7	-4.3%	24.8	30.0	27.7	0.9	10.0	0.7	7.7		
2017/10/27	85	208.0	104.0	0.0	0.0	14.2	10.8	16.4	13.9	-27.9%	10.0	30.0	20.2	0.9	10.0	0.6	7.7		
2017/11/7	96	110.0	55.0	0.0	0.0	7.5	10.0	10.0	12.4	-23.6%		15.0	6.3		5.0	0.0	7.7		
2017/11/8	97	100.0	50.0	0.0	0.0	7.1	7.0	7.0	7.2	-3.2%							7.7	1286.7	1146.7
2017/11/9	98	110.8	55.4	0.0	0.0	7.5	7.2	7.1	7.8	-8.4%							7.7		
2017/11/10	99	109.5	54.7	0.0	0.0	7.1	7.7	7.9	7.3	5.0%							7.6		
2017/11/12	101	110.4	55.2	0.0	0.0	7.2	7.0	7.1	7.1	-1.1%	9.5	15.0	16.9	0.0	5.0	0.0	7.6		
2017/12/8	127	100.0	50.0	0.0	0.0	6.0	8.9	9.7	7.4	17.2%	0.0	15.0	0.2	0.0	5.0	0.0	7.6	2340.0	2066.7
2017/12/10	129	100.0	50.0	0.0	0.0	6.0	6.0	6.0	5.4	9.3%	0.0	15.0	4.9	0.0	5.0	0.0	7.6		
2017/12/15	134	100.0	50.0	0.0	0.0	5.9	4.4	6.4	5.4	-22.0%	0.0	15.0	4.1	0.0	5.0	0.0	7.6		
2017/12/18	137	100.0	50.0	0.0	0.0	6.0	5.3	8.1	7.9	-50.6%	1.5	15.0	2.6	0.0	5.0	0.0			
R4		HAc (mg L^{-1})					PO_4^{3-}-P (mg L^{-1})				NO_3^--N (mg L^{-1})			NO_2^--N (mg L^{-1})					
Date	Day	feedstock	Ana	Ano	E	feedstock	Ana	Ano	E		Ana	Ano	E	Ana	Ano	E	pH	MLSS&MLVSS (mg L^{-1})	
2017/8/4	1	250.0	57.6	0.0	0.0	15.6	3.7	8.5	4.3	-17.5%	1.4	5.2	21.7	0.0	5.4	2.5	7.8	1740.0	1566.7
2017/8/11	8	256.6	128.3	0.0	0.0	15.2	14.4	11.7	10.7	25.6%	110.7	154.0	269.9	23.1	45.5	56.6	8.0	1446.7	1240.0
2017/8/19	16	273.1	136.5	51.6	0.0	19.9	12.7	13.2	4.7	62.7%	6.3	15.0	8.6	5.1	5.0	2.8	7.9	1460.0	1273.3
2017/8/23	20	315.2	157.6	92.7	0.0	15.1	10.4	12.7	10.7	-2.5%	0.9	15.0	0.0	0.0	5.0	0.0	8.2		
2017/8/24	21	300.5	150.2	84.8	0.0	15.8	12.8	17.1	14.4	-12.4%	0.9	15.0	0.0	0.0	5.0	0.0	8.2	1566.7	1413.3
2017/8/31	28	300.0	150.0	122.9	0.0	15.0	15.5	16.4	14.5	6.6%	1.0	15.0	0.1	0.0	5.0	0.0	8.6	1660.0	1540.0

Appendix A

2017/9/5	33	250.0	125.0	77.0	0.0	12.0	13.4	14.1	12.0	11.0%	0.8	30.0	0.0	0.0	10.0	0.0	9.1	940.0	926.7
2017/9/9	37	268.0	134.0	11.0	0.0	14.3	11.8	17.1	10.7	10.1%	4.5	30.0	13.5	8.2	10.0	14.7	8.6	1326.7	1260.0
2017/9/12	40	216.0	108.0	0.0	0.0	15.1	13.4	21.6	11.1	16.8%							8.2	1305.0	1200.0
2017/9/19	47	215.0	107.5	66.4	0.0	16.4	9.7	5.8	3.2	66.5%							8.8	1130.0	1005.0
2017/9/20	48	221.0	110.5	60.0	0.0	1.1	1.2	1.6	0.9	25.6%	3.6	15.0	0.0	0.0	5.0	0.0	8.6		
2017/9/22	50	216.0	108.0	59.8	0.0	15.2	9.5	7.0	3.5	63.8%	3.3	15.0	0.0	0.0	5.0	0.0	8.8		
2017/9/24	52	205.0	102.5	82.8	0.0	14.8	13.4	14.2	13.3	1.0%	0.9	15.0	0.0	0.0	5.0	0.0	8.7	3660.0	2566.7
2017/9/26	54	200.0	100.0	64.0	0.0	15.2	19.6	28.8	26.4	-34.8%							7.6	2960.0	1700.0
2017/9/28	56	209.0	104.5	68.0	0.0	14.6	21.3	33.1	28.6	-34.4%							7.7		
2017/10/3	61	219.0	109.5	107.9	0.0	14.6	15.3	17.4	16.0	-4.4%							7.4	1893.3	1365.0
2017/10/10	68	200.0	100.0	50.0	0.0	15.0	14.5	14.4	12.8	11.6%							7.4	1720.0	1250.0
2017/10/14	72	232.0	116.0	88.7	0.0	14.8	13.6	14.0	10.1	25.6%	0.8	30.0	449.2	0.0	10.0	61.8	7.2		
2017/10/19	77	263.7	131.9	0.0	0.0	17.7	14.9	16.3	13.7	7.8%	11.9	30.0	24.3	0.0	10.0	0.0	7.5	1373.3	955.0
2017/10/26	84	214.5	107.3	0.0	0.0	12.6	11.7	13.4	13.1	-11.4%	26.0	30.0	28.4	0.0	10.0	0.0	7.8		
2017/10/27	85	208.0	104.0	0.0	0.0	14.2	10.6	14.3	12.4	-17.1%	9.6	30.0	19.1	0.0	10.0	0.0	7.7		
2017/11/7	96	110.0	55.0	0.0	0.0	7.5	10.0	10.0	11.4	-14.5%		15.0	11.0		5.0	0.0	7.7		
2017/11/8	97	100.0	50.0	0.0	0.0	7.1	7.0	7.0	7.2	-2.6%							7.7	1340.0	1213.3
2017/11/9	98	110.8	55.4	0.0	0.0	7.5	7.2	7.1	7.7	-7.0%							7.7		
2017/11/10	99	109.5	54.7	0.0	0.0	7.1	7.6	7.9	7.3	4.2%							7.7		
2017/11/12	101	110.4	55.2	0.0	0.0	7.2	6.9	7.1	7.1	-2.6%	10.1	15.0	17.5	0.0	5.0	0.0	7.7		
2017/12/8	127	100.0	50.0	0.0	0.0	6.0	9.5	10.2	8.5	11.3%	0.0	15.0	0.1	0.0	5.0	0.0	7.6	2400.0	2133.3
2017/12/10	129	100.0	50.0	0.0	0.0	6.0	5.0	6.5	5.1	-2.8%	0.0	15.0	3.6	0.0	5.0	0.0	7.5		
2017/12/15	134	100.0	50.0	0.0	0.0	5.8	4.3	6.8	5.7	-32.3%	0.0	15.0	4.6	0.0	5.0	0.0	7.5		
2017/12/18	137	100.0	50.0	0.0	0.0	6.0	5.0	7.5	5.4	-7.9%	3.0	15.0	3.2	0.0	5.0	0.0			
R5		HAc (mg L^{-1})					PO_4^{3-}-P (mg L^{-1})				NO_3^--N (mg L^{-1})			NO_2^--N (mg L^{-1})					
Date	Day	feedstock	Ana	Ano	E	feedstock	Ana	Ano	E		Ana	Ano	E	Ana	Ano	E	pH	MLSS&MLVSS (mg L^{-1})	
2017/8/4	1	250.0	57.6	15.0	0.0	15.6	3.7	8.3	4.5	-22.9%	1.4	0.7	13.9	0.0	6.0	9.8	7.8	1780.0	1613.3

2017/8/11	8	252.4	126.2	0.0	0.0	15.2	12.8	11.1	9.9	23.2%	61.0	73.5	129.0	58.2	101.4	123.8	8.1	1566.7	1320.0
2017/8/19	16	273.4	136.7	46.8	0.0	16.9	11.2	11.0	7.0	37.8%	1.6	10.0	0.1	8.7	10.0	0.0	8.1	1626.7	1353.3
2017/8/23	20	300.5	150.3	100.1	0.0	16.6	10.2	11.1	9.2	9.6%	0.9	10.0	0.0	0.0	10.0	0.0	8.3		
2017/8/24	21	295.4	147.7	99.7	0.0	17.9	12.1	16.4	13.9	-15.1%	0.9	10.0	0.0	0.0	10.0	0.0	8.3	1713.3	1293.3
2017/8/31	28	300.0	150.0	112.6	0.0	15.0	15.3	17.5	15.3	0.2%	1.0	10.0	0.0	0.0	10.0	0.0	8.2	1326.7	1233.3
2017/9/5	33	247.0	123.5	94.0	0.0	11.2	12.0	14.7	14.0	-17.3%	0.8	20.0	0.0	0.0	20.0	0.0	9.6	800.0	780.0
2017/9/9	37	274.0	137.0	48.0	0.0	14.1	12.9	13.8	12.0	6.5%	1.4	20.0	2.8	4.2	20.0	11.1	9.0	1046.7	953.3
2017/9/12	40	214.0	107.0	29.0	0.0	14.9	14.5	15.6	13.9	3.9%							8.9	1035.0	890.0
2017/9/19	47	220.0	110.0	61.1	0.0	16.3	10.1	5.6	3.2	68.4%							8.9	1670.0	1480.0
2017/9/20	48	221.0	110.5	60.0	0.0	1.1	1.3	1.7	1.2	12.5%	3.6	10.0	0.0	0.0	10.0	0.0	8.6		
2017/9/22	50	218.0	109.0	86.2	0.0	14.9	9.5	6.9	3.7	60.7%	3.3	10.0	0.0	0.0	10.0	0.0	8.6		
2017/9/24	52	217.0	108.5	103.9	0.0	14.4	12.7	13.4	12.3	3.4%	0.9	10.0	0.0	0.0	10.0	0.0	8.7	4260.0	3060.0
2017/9/26	54	203.0	101.5	81.5	0.0	14.9	19.3	27.9	26.2	-35.7%							7.5	3620.0	2090.0
2017/9/28	56	206.0	103.0	86.0	0.0	14.7	20.3	28.7	26.0	-28.6%							7.6		
2017/10/3	61	237.0	118.5	98.5	0.0	14.5	15.6	17.1	16.6	-6.4%							7.4	2226.7	1535.0
2017/10/10	68	200.0	100.0	50.0	0.0	15.0	14.8	14.7	13.1	11.8%							7.4	2013.3	1420.0
2017/10/14	72	214.6	107.3	65.7	0.0	14.9	13.9	14.0	9.2	34.0%	0.8	20.0	476.9	0.0	20.0	138.1	7.3		
2017/10/19	77	276.5	138.3	0.0	0.0	13.9	13.2	14.6	13.1	0.8%	9.5	20.0	5.7	0.1	20.0	0.1	7.7	1566.7	1080.0
2017/10/26	84	216.0	108.0	0.0	0.0	13.6	12.9	13.6	13.1	-2.2%	24.3	20.0	25.3	0.3	20.0	1.9	8.0		
2017/10/27	85	183.7	91.8	0.0	0.0	14.6	11.0	14.0	12.1	-9.9%	9.7	20.0	19.0	0.0	20.0	0.0	7.7		
2017/11/7	96	110.0	55.0	0.0	0.0	7.5	10.0	10.0	11.8	-18.0%		10.0	4.2		10.0	0.0	7.8		
2017/11/8	97	100.0	50.0	0.0	0.0	7.3	7.0	7.0	7.0	0.4%							7.7	1766.7	1560.0
2017/11/9	98	109.6	54.8	0.0	0.0	7.5	7.2	7.1	7.7	-7.4%							7.7		
2017/11/10	99	110.8	55.4	0.0	0.0	7.6	7.6	8.1	7.5	2.1%							7.7		
2017/11/12	101	108.6	54.3	0.0	0.0	7.6	7.4	7.5	7.1	4.0%	8.6	10.0	14.6	0.0	10.0	0.0	7.7		
2017/12/8	127	100.0	50.0	0.0	0.0	6.0	6.6	10.5	8.8	-33.8%	0.0	10.0	3.0	0.0	10.0	0.0	7.7	2320.0	2000.0
2017/12/10	129	100.0	50.0	0.0	0.0	6.0	5.0	7.7	6.5	-30.1%	0.0	10.0	3.1	0.0	10.0	0.0	7.6		
2017/12/15	134	100.0	50.0	0.0	0.0	5.7	4.5	6.7	5.7	-26.8%	0.0	10.0	3.6	0.0	10.0	0.0	7.7		

Appendix A

2017/12/18	137	100.0	50.0	0.0	0.0	6.0	5.1	5.2	4.9	3.5%	4.5	10.0	4.3	0.0	10.0	0.0			
R6		HAc (mg L^{-1})					PO_4^{3-}-P (mg L^{-1})				NO_3^--N (mg L^{-1})			NO_2^--N (mg L^{-1})					
Date	Day	feedstock	Ana	Ano	E	feedstock	Ana	Ano	E		Ana	Ano	E	Ana	Ano	E	pH	MLSS&MLVSS (mg L^{-1})	
2017/8/4	1	250.0	57.6	0.0	0.0	15.6	3.7	7.9	4.6	-27.0%	1.4	0.7	14.0	0.0	4.9	9.3	7.8	1993.3	1780.0
2017/8/11	8	252.4	126.2	0.0	0.0	15.2	13.9	14.7	11.9	14.4%	53.2	65.5	112.1	60.1	105.8	123.4	7.8	1693.3	1273.3
2017/8/19	16	273.4	136.7	33.2	0.0	16.9	11.4	10.8	6.4	43.8%	2.4	10.0	0.6	8.8	10.0	0.5	8.1	1726.7	1473.3
2017/8/23	20	300.5	150.3	121.0	0.0	16.6	10.3	10.8	8.1	21.5%	0.9	10.0	0.0	0.0	10.0	0.0	8.8		
2017/8/24	21	295.4	147.7	101.0	0.0	17.9	11.5	15.0	12.1	-5.4%	0.9	10.0	0.0	0.0	10.0	0.0	8.4	2660.0	1953.3
2017/8/31	28	300.0	150.0	106.9	0.0	15.0	15.4	17.4	14.5	6.2%	1.0	10.0	0.0	0.0	10.0	0.0	8.7	1146.7	1066.7
2017/9/5	33	247.0	123.5	103.0	0.0	11.2	12.5	13.9	12.1	3.7%	0.8	20.0	0.0	0.0	20.0	0.0	9.6	680.0	653.3
2017/9/9	37	274.0	137.0	53.0	0.0	14.1	12.7	13.7	12.3	2.8%	1.0	20.0	1.5	3.8	20.0	12.6	8.9	980.0	893.3
2017/9/12	40	214.0	107.0	8.0	0.0	14.9	14.1	15.1	13.2	6.0%							8.8	1045.0	840.0
2017/9/19	47	220.0	110.0	76.9	0.0	16.3	9.6	5.1	2.7	71.9%							9.0	1655.0	1460.0
2017/9/20	48	221.0	110.5	60.0	0.0	1.1	1.4	1.9	2.6	-87.3%	3.6	10.0	0.0	0.0	10.0	0.0	8.4		
2017/9/22	50	218.0	109.0	71.8	0.0	14.9	9.5	6.6	3.4	63.6%	3.3	10.0	0.0	0.0	10.0	0.0	8.6		
2017/9/24	52	217.0	108.5	85.0	0.0	14.4	12.6	12.8	12.7	0.0%	0.9	10.0	0.0	0.0	10.0	0.0	8.7	4140.0	2986.7
2017/9/26	54	203.0	101.5	78.3	0.0	14.9	19.0	27.2	25.9	-35.9%							7.6	3373.3	1950.0
2017/9/28	56	206.0	103.0	81.0	6.7	14.7	20.1	28.0	25.7	-28.3%							7.6		
2017/10/3	61	237.0	118.5	90.0	0.0	14.5	15.5	17.4	16.4	-5.9%							7.5	2313.3	1580.0
2017/10/10	68	200.0	100.0	50.0	0.0	15.0	15.2	15.3	13.3	12.4%							7.5	2213.3	1540.0
2017/10/14	72	214.6	107.3	73.7	0.0	14.9	14.2	14.6	9.9	30.5%	0.8	20.0	352.0	0.0	20.0	100.6	7.3		
2017/10/19	77	225.5	112.7	0.0	0.0	15.9	13.7	14.2	12.3	10.2%	10.9	20.0	21.1	0.0	20.0	0.3	7.6	1886.7	1270.0
2017/10/26	84	216.0	108.0	0.0	0.0	13.6	12.7	16.7	15.0	-18.4%	9.7	20.0	19.7	0.0	20.0	0.0	7.7		
2017/10/27	85	183.7	91.8	0.0	0.0	14.6	11.2	13.9	11.5	-2.9%	7.4	20.0	17.1	0.0	20.0	0.0	7.7		
2017/11/7	96	110.0	55.0	0.0	0.0	7.5	10.0	10.0	11.8	-18.0%		10.0	8.1		0.0	0.0	7.7		
2017/11/8	97	100.0	50.0	0.0	0.0	7.3	7.0	7.0	7.7	-9.4%							7.7	1726.7	1500.0
2017/11/9	98	109.6	54.8	0.0	0.0	7.5	7.5	7.2	7.8	-3.3%							7.7		

Appendix A

2017/11/10	99	110.8	55.4	0.0	0.0	7.6	7.7	8.1	7.5	1.9%							7.7		
2017/11/12	101	108.6	54.3	0.0	0.0	7.6	7.3	7.3	7.4	-1.0%	8.0	10.0	14.9	0.0	10.0	0.0	7.7		
2017/12/8	127	100.0	50.0	0.0	0.0	6.0	8.5	9.8	6.8	20.7%	0.0	10.0	0.3	0.0	10.0	0.0	7.6	2333.3	2040.0
2017/12/10	129	100.0	50.0	0.0	0.0	6.0	5.0	7.7	5.9	-18.4%	0.0	10.0	5.9	0.0	10.0	0.0	7.7		
2017/12/15	134	100.0	50.0	0.0	0.0	5.7	4.8	6.0	5.5	-14.1%	0.0	10.0	4.2	0.0	10.0	0.0	7.6		
2017/12/18	137	100.0	50.0	0.0	0.0	6.0	5.3	7.1	6.6	-24.4%	3.1	10.0	3.5	0.0	10.0	0.0			
R7		HAc (mg L^{-1})					PO_4^{3-}-P (mg L^{-1})				NO_3^--N (mg L^{-1})			NO_2^--N (mg L^{-1})					
Date	Day	feedstock	Ana	Ano	E	feedstock	Ana	Ano	E		Ana	Ano	E	Ana	Ano	E	pH	MLSS&MLVSS (mg L^{-1})	
2017/8/4	1	250.0	57.6	0.0	0.0	15.6	3.7	9.0	3.3	10.5%	1.4	0.2	8.2	0.0	0.1	0.0	7.4	2226.7	1826.7
2017/8/11	8	258.5	129.2	0.0	0.0	15.2	9.1	10.2	2.4	73.7%	4.0	0.2	2.2	0.3	0.1	0.0	7.9	1960.0	1280.0
2017/8/19	16	261.9	131.0	65.2	0.0	15.3	10.7	12.0	6.5	39.0%	1.3	0.1	0.8	0.0	0.0	0.0	8.1	1893.3	1326.7
2017/8/23	20	300.0	150.0	81.5	0.0	13.7	9.7	12.9	8.9	7.6%	0.9	0.1	0.3	0.0	0.0	0.0	7.9		
2017/8/24	21	298.1	149.1	83.9	0.0	14.2	11.9	16.7	12.4	-3.8%	1.0	0.1	0.8	0.0	0.0	0.0	7.9	1826.7	1286.7
2017/8/31	28	300.0	150.0	77.8	0.0	15.0	15.8	23.0	15.9	-0.9%	1.7	0.0	0.7	0.0	0.0	0.0	8.3	613.3	573.3
2017/9/5	33	241.0	120.5	50.0	0.0	11.9	13.5	22.3	14.3	-5.8%	1.0	0.0	1.0	0.0	0.0	0.0	8.7	453.3	426.7
2017/9/9	37	269.0	134.5	52.0	0.0	14.2	14.4	19.4	15.9	-10.3%	1.7	0.1	1.7	0.0	0.0	0.0	8.5	560.0	540.0
2017/9/12	40	218.0	109.0	22.0	0.0	15.2	16.3	18.5	17.5	-7.1%							8.8	360.0	293.3
2017/9/19	47	215.0	107.5	39.1	0.0	16.3	10.8	10.5	5.9	45.6%							8.6	1455.0	1320.0
2017/9/20	48	221.0	110.5	30.0	0.0	1.1	2.2	4.4	3.0	-39.0%	4.2	0.0	0.1	0.0	0.0	0.0	8.2		
2017/9/22	50	209.0	104.5	26.9	0.0	14.5	10.0	12.7	5.1	48.7%	4.7	0.0	2.0	0.0	0.0	0.0	8.6		
2017/9/24	52	215.0	107.5	37.8	0.0	14.7	14.3	28.5	17.9	-24.4%	2.3	0.1	2.4	0.0	0.0	0.0	8.5	3540.0	2766.7
2017/9/26	54	201.0	100.5	42.6	0.0	15.1	18.1	27.3	23.3	-28.8%							7.5	3146.7	1965.0
2017/9/28	56	207.0	103.5	30.0	0.0	15.0	24.7	32.5	33.2	-34.1%							7.2		
2017/10/3	61	204.2	102.1	60.8	0.0	14.5	16.4	27.4	33.1	-102.2%							7.4	2066.7	1425.0
2017/10/10	68	200.0	100.0	50.0	0.0	15.0	14.0	14.2	7.8	44.6%							7.4	1640.0	1190.0
2017/10/14	72	258.7	129.4	78.4	0.0	15.3	11.3	19.5	9.3	17.9%	0.8	0.0	0.1	0.0	0.0	0.0	7.5		
2017/10/19	77	266.0	133.0	57.9	0.0	13.9	11.2	31.1	13.6	-21.4%	1.2	0.0	0.8	0.0	0.0	0.0	7.5	1620.0	1045.0

Appendix A

2017/10/26	84	210.0	105.0	29.3	0.0	12.8	12.5	45.5	21.0	-67.1%	2.0	0.1	3.1	0.0	0.0	0.0	7.5		
2017/10/27	85	212.2	106.1	21.5	0.0	14.3	13.1	43.5	16.1	-22.4%	2.2	3.3	2.0	0.0	0.0	0.0	7.5		
2017/11/7	96	110.0	55.0	0.0	0.0	7.5	10.0	20.0	5.8	41.9%			4.0			0.0	7.5		
2017/11/8	97	100.0	50.0	0.0	0.0	7.1	7.0	19.0	6.8	2.5%							7.5	1513.3	1180.0
2017/11/9	98	110.0	55.0	0.0	0.0	7.5	7.0	16.2	9.2	-31.5%							7.5		
2017/11/10	99	109.1	54.6	0.0	0.0	7.1	8.4	16.6	8.9	-5.9%							7.4		
2017/11/12	101	109.4	54.7	0.0	0.0	7.2	8.3	18.1	10.7	-28.7%	3.2	0.1	4.6	0.0	0.0	0.0	7.3		
2017/12/8	127	100.0	50.0	0.0	0.0	6.0	6.8	7.0	8.4	-23.8%	10.4	1.4	5.9	0.0	0.0	0.0	7.5	2086.7	1780.0
2017/12/10	129	100.0	50.0	0.0	0.0	6.0	6.0	9.0	6.9	-14.7%	0.0	0.0	3.2	0.0	0.0	0.0	7.4		
2017/12/15	134	100.0	50.0	0.0	0.0	5.7	4.8	9.9	6.5	-35.2%	0.0	0.0	4.3	0.0	0.0	0.0	7.5		
2017/12/18	137	100.0	50.0	0.0	0.0	6.0	5.0	7.0	6.0	-20.1%	3.1	0.0	3.5	0.0	0.0	0.0			
R8		HAc (mg L^{-1})					PO_4^{3-}-P (mg L^{-1})				NO_3^--N (mg L^{-1})			NO_2^--N (mg L^{-1})					
Date	Day	feedstock	Ana	Ano	E	feedstock	Ana	Ano	E		Ana	Ano	E	Ana	Ano	E	pH	MLSS&MLVSS (mg L^{-1})	
2017/8/4	1	250.0	57.6	0.0	0.0	15.6	3.7	13.9	3.3	9.7%	1.4	2.2	7.7	0.0	0.2	0.0	8.0	2453.3	1980.0
2017/8/11	8	258.5	129.2	0.0	0.0	15.2	8.7	7.4	2.3	73.7%	3.8	0.1	2.4	0.3	0.0	0.0	8.2	2100.0	1233.3
2017/8/19	16	261.9	131.0	53.2	0.0	15.3	10.8	11.4	5.9	44.9%	1.3	0.2	0.6	0.0	0.0	0.0	8.1	1806.7	1286.7
2017/8/23	20	300.0	150.0	92.1	0.0	13.7	9.4	13.4	9.2	2.6%	1.2	0.1	0.1	0.0	0.0	0.0	7.9		
2017/8/24	21	298.1	149.1	92.8	0.0	14.2	12.0	17.5	12.0	0.3%	1.3	0.0	1.2	0.0	0.0	0.0	7.9	2120.0	1466.7
2017/8/31	28	300.0	150.0	77.8	0.0	15.0	15.9	24.2	16.9	-6.7%	1.7	0.0	0.7	0.0	0.0	0.0	8.2	993.3	906.7
2017/9/5	33	241.0	120.5	58.0	0.0	11.9	12.6	22.1	13.5	-7.3%	1.2	0.1	1.1	0.0	0.0	0.0	8.7	586.7	566.7
2017/9/9	37	269.0	134.5	54.0	0.0	14.2	14.3	17.8	15.6	-9.3%	1.7	0.1	1.8	0.0	0.0	0.1	8.6	573.3	553.3
2017/9/12	40	218.0	109.0	19.0	0.0	15.2	16.1	17.3	17.0	-5.2%							8.6	406.7	333.3
2017/9/19	47	215.0	107.5	40.5	0.0	16.3	11.2	11.0	6.0	46.3%							8.3	1660.0	1490.0
2017/9/20	48	221.0	110.5	30.0	0.0	1.1	2.4	4.2	1.0	57.6%	3.9	0.0	0.0	0.0	0.0	0.0	8.3		
2017/9/22	50	209.0	104.5	25.2	0.0	14.5	10.1	13.1	5.3	47.8%	4.4	0.0	1.6	0.0	0.0	0.0	8.2		
2017/9/24	52	215.0	107.5	36.6	0.0	14.7	14.5	28.3	18.3	-25.7%	2.0	0.1	2.0	0.0	0.0	0.0	8.2	3480.0	2726.7
2017/9/26	54	201.0	100.5	42.9	0.0	15.1	17.8	27.3	16.0	10.2%							7.5	2586.7	1690.0

2017/9/28	56	207.0	103.5	37.0	0.0	15.0	17.9	26.9	24.0	-34.0%							7.2		
2017/10/3	61	204.2	102.1	88.7	0.0	14.5	13.5	17.9	14.9	-10.2%							7.1	1953.3	1415.0
2017/10/10	68	200.0	100.0	50.0	0.0	15.0	14.2	14.3	10.0	29.1%							7.4	1373.3	900.0
2017/10/14	72	258.7	129.4	66.7	0.0	15.3	12.8	20.5	11.1	12.7%	0.9		0.5	0.0	0.0	0.0	7.4		
2017/10/19	77	266.0	133.0	73.6	0.0	13.9	12.7	27.6	12.6	1.1%	1.1	0.0	0.9	0.0	0.0	0.0	7.5	1220.0	850.0
2017/10/26	84	210.0	105.0	51.7	0.0	12.8	13.9	23.2	16.4	-17.8%	1.7	0.1	2.9	0.0	0.0	0.0	7.5		
2017/10/27	85	212.2	106.1	44.5	0.0	14.3	14.5	21.5	15.0	-3.7%	1.9	0.1	1.4	0.0	0.0	0.0	7.6		
2017/11/7	96	110.0	55.0	0.0	0.0	7.5	10.0	20.0	9.4	6.0%			2.9			0.0	7.6		
2017/11/8	97	100.0	50.0	0.0	0.0	7.1	7.0	19.0	7.3	-4.8%							7.6	986.7	826.7
2017/11/9	98	110.0	55.0	0.0	0.0	7.5	7.2	14.9	8.9	-23.3%							7.5		
2017/11/10	99	109.1	54.6	0.0	0.0	7.1	8.3	15.6	8.6	-3.7%							7.5		
2017/11/12	101	109.4	54.7	0.0	0.0	7.2	7.8	16.4	9.9	-26.9%	3.0	0.1	4.3	0.0	0.0	0.0	7.5		
2017/12/8	127	100.0	50.0	0.0	0.0	6.0	6.5	6.7	8.2	-25.7%	9.9	1.0	5.5	0.0	0.0	0.0	7.4	2066.7	1766.7
2017/12/10	129	100.0	50.0	0.0	0.0	6.0	6.0	9.0	6.8	-13.5%	0.0	0.0	3.0	0.0	0.0	0.0	7.4		
2017/12/15	134	100.0	50.0	0.0	0.0	5.7	4.9	8.5	6.6	-34.7%	0.0	0.0	4.3	0.0	0.0	0.0	7.5		
2017/12/18	137	100.0	50.0	0.0	0.0	6.0	5.3	7.4	6.5	-22.4%	3.0	0.4	2.3	0.0	0.0	0.0			

b. Performance of Enrichment I

E1		HAc (mg L^{-1})					PO_4^{3-}-P (mg L^{-1})			Removal rate	NO_3^--N (mg L^{-1})			NO_2^--N (mg L^{-1})					
Date	Day	feedstock	Ana	Ano	E	feedstock	Ana	Ano	E		Ana	Ano	E	Ana	Ano	E	pH	MLSS&MLVSS (mg L^{-1})	
2018/2/1	1					5.6	4.9	4.9	3.9	20.4%	1.1	17.9	0.3	0.0	0.0	0.0	7.4	1880	1700

2018/2/7	7					5.6	4.9	5.9	4.3	12.6%	7.0	18.3	10.3	0.0	0.0	0.0	7.4	1226.7	1140.0
2018/2/13	13	157.9	79.0	0.0	0.0	5.7	5.7	5.0	4.2	26.5%	1.2	19.6	0.1	0.0	0.0	0.0	7.4	1025.0	930.0
2018/2/14	14	157.1	78.5	0.0	0.0	5.7	4.8	5.5	4.2	12.9%	2.4	23.3	8.5	0.0	0.0	0.0	7.4	940.0	885.0
2018/2/22	22	230.0	115.0	62.1	0.0	12.4	11.8	12.6	11.1	5.3%	1.2	19.4	0.8	0.0	0.0	0.0	7.6	960.0	890.0
2018/2/27	27	247.3	123.6	36.2	0.0	11.8	10.8	11.6	11.1	-2.9%	1.5	17.8	0.1	0.0	0.0	0.1	7.64	1025.0	985.0
2018/3/5	33	238.0	119.0	59.3	0.0	13.0	12.8	12.6	11.6	9.6%	1.7	19.6	0.9	0.0	0.0	0.0	7.68	1055.0	1015.0
2018/3/10	38	225.7	112.8	68.5	0.0	12.1	9.6	12.0	10.6	-10.7%	2.0	20.0	0.4	0.0	0.0	0.0	7.78	800.0	780.0
2018/3/12	40	225.5	112.7	0.0	0.0	12.4	11.4	13.4	11.0	3.7%	6.3	27.9	9.4	0.0	0.0	0.0	8.02	730	705
2018/3/17	45	250.9	125.4	26.5	0.0	12.1	11.0	14.9	10.5	4.2%	5.6	27.7	8.9	0.1	0.0	0.0	7.76	610.0	600.0
2018/3/19	47	259.8	129.9	19.9	0.0	12.4	10.9	15.9	11.3	-3.7%	4.9	26.5	7.2	0.1	0.0	0.0	7.64	735.0	705.0
2018/3/25	53	237.3	118.7	0.0	0.0	12.2	11.1	17.4	9.9	10.5%	7.0	31.3	13.1	0.4	0.0	0.2	7.8	560.0	545.0
2018/4/10	69	240.0	120.0	0.0	0.0	10.4	10.2	20.6	8.8	13.7%	0.2	30.0	14.5	1.1	0.0	4.8	7.77	765.0	675.0
vacation																			
2018/5/7	74	242.1	121.1	0.0	0.0	12.7	10.6	22.7	7.9	24.8%	8.8	30.2	13.2	0.3	0.0	1.0	7.68	650.0	580.0
2018/5/15	82	244.1	122.0	0.0	0.0	13.3	11.1	34.5	8.8	21.4%	8.5	30.2	12.2	0.0	0.0	0.1	7.62	970.0	685.0
2018/5/18	85	241.1	120.6	0.0	0.0	12.5	10.6	30.5	8.3	22.0%	9.0	30.2	14.2	0.0	0.0	0.0	7.68	915.0	670.0
2018/5/21	88	323.3	161.7	2.8	0.0	12.8	9.5	33.4	4.2	55.8%	8.4	30.1	11.7	0.0	0.0	0.1	7.66	1090.0	810.0
2018/5/25	92	240.2	120.1	36.3	0.0	12.5	10.1	36.9	7.5	26.4%	7.7	30.5	13.8	0.0	0.0	0.0	7.68	1120.0	830.0
2018/5/29	96	214.3	107.2	32.3	0.0	12.4	9.0	44.0	4.8	46.7%	6.6	32.4	15.0	0.0	0.0	0.0	7.74		
2018/6/1	99	235.8	117.9	31.6	0.0	11.7	9.0	38.5	2.6	70.8%	8.5	32.9	17.3	0.0	0.0	0.2	7.76	910.0	730.0
2018/6/8	106	229.7	114.9	0.0	0.0	12.5	9.9	42.9	2.3	76.2%	8.6	30.0	10.4	0.0	0.0	0.0	7.72		
2018/6/12	110	210.0	105.0	9.6	0.0	12.9	10.9	42.8	4.2	61.8%	8.5	30.3	11.5	0.0	0.0	0.0	7.62		
2018/6/25	123	215.7	107.8	0.0	0.0	12.7	10.0	36.2	3.8	61.9%	9.6	30.3	13.4	0.0	0.0	0.0	7.68	1070.0	810.0
2018/7/14	142	264.6	132.3	0.0	0.0	11.9	7.6	22.1	1.9	75.5%	10.9	31.9	15.4	0.0	0.0	0.0			
2018/7/17	145	261.3	130.7	0.0	0.0	13.2	11.5	29.5	7.9	31.3%	10.9	31.6	15.7	0.0	0.0	0.0	7.72	706.2	620.6
2018/7/19	147	244.8	122.4	0.0	0.0	13.0	10.2	27.4	4.4	57.2%	10.6	31.8	15.5	0.0	0.0	0.0	7.62	790.0	680.0
2018/7/31	159	236.7	118.4	0.0	0.0	13.3	9.1	32.9	3.2	64.2%	9.3	31.8	13.4	0.0	0.0	0.0	7.68	1300.0	810.0
2018/8/7	166	251.4	125.7	0.0	0.0	12.6	11.3	43.6	5.9	47.8%	7.1	29.7	8.2	0.0	0.0	0.0	7.85	930.0	730.0

Appendix A

2018/8/15	174	221.7	110.9	0.0	0.0	13.4	11.5	43.5	8.1	29.7%	8.5	29.7	10.9	0.0	0.0	0.0	7.98	1110.0	840.0
2018/8/21	180	241.2	120.6	0.0	0.0	13.0	11.6	42.4	9.3	19.6%	7.9	30.4	12.0	0.0	0.0	0.0	7.99	990.0	770.0
2018/8/28	187	245.0	122.5	0.0	0.0	13.9	11.5	40.9	4.9	57.2%	8.1	30.4	10.1	0.0	0.0	0.0	7.85	1240.0	910.0
2018/9/4	194	227.9	113.9	0.0	0.0	14.7	10.9	43.9	4.2	61.0%	7.7	30.4	12.1	0.0	0.0	0.0	7.98		
2018/9/14	204	236.3	118.2	0.0	0.0	12.3	15.0	44.1	1.1	92.4%	10.7	30.4	11.9	0.0	0.0	0.1	7.99	1310.0	900.0
2018/9/19	209	250.0	125.0	0.0	0.0	12.3	7.9	49.0	2.6	67.7%	5.1	30.4	9.9	0.3	0.0	0.0	8.41		
2018/9/21	211	250.0	125.0	0.0	0.0	11.8	8.1	44.5	4.7	41.8%	6.0	30.4	7.3	0.0	0.0	0.0	7.96		
2018/9/26	216	250.0	125.0	0.0	0.0	13.6	12.3	39.9	4.4	63.9%	6.9	29.4	8.1	0.0	0.0	0.0	8.05		
E2		HAc (mg L^{-1})					PO_4^{3-}-P (mg L^{-1})			Removal rate	NO_3^--N (mg L^{-1})			NO_2^--N (mg L^{-1})					
Date	Day	feedstock	Ana	Ano	E	feedstock	Ana	Ano	E		Ana	Ano	E	Ana	Ano	E	pH	MLSS&MLVSS (mg L^{-1})	
2018/2/1	1					5.6	4.7	4.6	3.9	17.1%	1.1	18.4	0.0	0.0	0.0	0.0	7.4	1780	1620
2018/2/7	7					5.6	5.1	5.9	4.3	14.4%	7.3	19.0	11.6	0.0	0.0	0.0	7.4	1266.7	1166.7
2018/2/13	13	157.9	79.0	22.0	0.0	5.7	5.5	5.4	3.9	29.6%	1.2	20.4	0.0	0.0	0.0	0.0	7.4	1160.0	1065.0
2018/2/14	14	157.1	78.5	12.9	0.0	5.7	4.8	5.6	4.3	10.8%	2.8	24.1	10.1	0.0	0.0	0.0	7.7	1105.0	1005.0
2018/2/22	22	230.0	115.0	78.0	0.0	12.4	11.9	13.8	11.4	3.9%	1.2	20.1	0.1	0.0	0.0	0.0	7.9	965.0	890.0
2018/2/27	27	247.3	123.6	46.8	0.0	11.8	10.9	11.9	11.4	-3.9%	1.2	18.5	0.2	0.0	0.0	0.2	7.73	960.0	915.0
2018/3/5	33	238.0	119.0	51.2	0.0	13.0	13.6	14.6	14.3	-4.9%	1.7	20.4	0.5	0.0	0.0	0.0	7.76	850.0	820.0
2018/3/10	38	225.7	112.8	71.9	0.0	12.1	10.2	12.3	10.6	-3.9%	1.3	20.0	1.9	0.0	0.0	0.0	8.01	860.0	825.0
2018/3/12	40	225.5	112.7	28.9	0.0	12.4	11.5	13.5	10.7	6.6%	5.3	29.2	9.7	0.0	0.0	0.0	7.86	685	655
2018/3/17	45	247.0	123.5	30.5	0.0	12.1	11.0	14.8	10.3	6.1%	5.6	29.1	10.5	0.0	0.0	0.0	7.67	705.0	685.0
2018/3/19	47	259.8	129.9	30.0	0.0	12.4	11.2	16.0	10.4	6.7%	4.8	28.7	7.8	0.0	0.0	0.0	7.91	800.0	765.0
2018/3/25	53	237.3	118.7	0.0	0.0	12.2	11.0	17.6	10.1	8.5%	7.3	33.9	15.6	0.5	0.0	0.0	7.79	475.0	455.0
2018/4/10	69	240.0	120.0	0.0	0.0	10.4	10.1	22.9	9.2	9.1%	0.1	30.0	11.1	0.2	0.0	5.0	7.7	795.0	700.0
vacation																			
2018/5/7	74	242.1	121.1	0.0	0.0	12.7	10.7	19.6	8.5	20.3%	8.0	30.2	12.3	1.3	0.0	2.8	7.61	605.0	555.0
2018/5/15	82	244.1	122.0	0.0	0.0	13.3	11.4	29.2	9.9	12.7%	8.2	30.2	13.5	0.0	0.0	0.0	7.7	890.0	650.0
2018/5/18	85	241.1	120.6	50.9	0.0	12.5	10.6	28.1	8.7	17.8%	8.0	30.2	13.6	0.0	0.0	0.0	7.77	950.0	715.0

Appendix A

2018/5/21	88	323.3	161.7	0.0	0.0	12.8	9.5	31.4	5.1	46.5%	7.9	30.2	12.7	0.0	0.0	0.0	7.66	1130.0	860.0
2018/5/25	92	240.2	120.1	12.6	0.0	12.5	10.2	34.5	6.7	34.1%	8.1	30.7	14.5	0.0	0.0	0.1	7.75		
2018/5/29	96	214.3	107.2	0.0	0.0	12.4	9.0	42.4	4.0	56.0%	6.7	32.4	15.6	0.1	0.0	0.0	7.89	1020.0	820.0
2018/6/1	99	235.8	117.9	0.0	0.0	11.7	9.4	41.0	4.5	52.6%	7.9	32.7	17.0	0.0	0.0	0.1	7.74		
2018/6/8	106	229.7	114.9	0.0	0.0	12.5	10.0	42.1	1.4	86.1%	8.2	29.9	10.2	0.0	0.0	0.0	7.44		
2018/5/12	110	210.0	105.0	0.0	0.0	12.9	10.6	41.8	2.9	72.6%	8.5	30.3	12.0	0.0	0.0	0.0	7.52		
2018/6/25	123	215.7	107.8	0.0	0.0	12.7	9.0	40.3	1.5	82.8%	8.5	30.3	11.6	0.0	0.0	0.0	7.42	1070.0	750.0
2018/7/14	142	264.6	132.3	0.0	0.0	11.9	6.9	25.6	0.5	92.9%	9.6	31.0	13.8	0.1	0.0	0.0			
2018/7/17	145	261.3	130.7	0.0	0.0	13.2	11.2	29.9	7.1	36.2%	10.4	30.7	15.6	0.0	0.0	0.0	7.44	651.6	556.0
2018/7/19	147	244.8	122.4	0.0	0.0	13.0	10.6	29.1	6.6	38.4%	9.8	31.0	14.1	0.0	0.0	0.0	7.52	640.0	510.0
2018/7/31	159	236.7	118.4	0.0	0.0	13.3	9.6	30.4	5.2	45.8%	9.6	31.0	13.4	0.0	0.0	0.0	7.42	1210.0	750.0
2018/8/7	166	251.4	125.7	0.0	0.0	12.6	11.3	42.0	5.7	49.2%	6.9	29.5	8.0	0.0	0.0	0.1	7.78	800.0	650.0
2018/8/15	174	221.7	110.9	0.0	0.0	13.4	9.6	37.3	5.1	47.1%	8.3	29.5	11.6	0.0	0.0	0.0	7.83	1040.0	760.0
2018/8/21	180	241.2	120.6	0.0	0.0	13.0	10.9	36.4	6.2	43.4%	8.3	30.2	10.9	0.0	0.0	0.0	7.72	1140.0	820.0
2018/8/28	187	245.0	122.5	0.0	0.0	13.9	9.3	40.4	3.3	64.7%	8.1	30.2	10.7	0.0	0.0	0.0	7.78	1070.0	740.0
2018/9/4	194	227.9	113.9	0.0	0.0	14.7	9.2	44.0	2.0	78.5%	7.6	30.2	12.8	0.0	0.0	0.0	7.83		
2018/9/14	204	236.3	118.2	0.0	0.0	12.3	7.2	36.7	0.2	97.2%	7.5	30.2	0.2	0.0	0.0	0.0	7.72	1130.0	820.0
2018/9/19	209	250.0	125.0	0.0	0.0	12.3	7.9	42.2	1.5	80.8%	5.9	30.2	10.9	0.4	0.0	0.0	7.91		
2018/9/21	211	250.0	125.0	0.0	0.0	11.8	7.8	33.3	2.8	63.9%	6.9	30.2	9.2	0.0	0.0	0.0	7.85		
2018/9/26	216	250.0	125.0	0.0	0.0	13.6	8.8	34.0	2.2	75.4%	6.7	29.2	9.5	0.0	0.0	0.0	7.88		
E3		HAc (mg L^{-1})					PO_4^{3-}-P (mg L^{-1})			Removal rate	NO_3^--N (mg L^{-1})			NO_2^--N (mg L^{-1})					
Date	Day	feedstock	Ana	Ano	E	feedstock	Ana	Ano	E		Ana	Ano	E	Ana	Ano	E	pH	MLSS&MLVSS (mg L^{-1})	
2018/2/1	1					5.5	4.7	4.6	4.1	12.5%	1.1	15.7	0.0	0.0	2.2	0.0	7.5	1773.33	1626.667
2018/2/7	7					5.6	4.9	6.3	4.3	11.9%	5.4	16.2	7.7	0.0	2.3	0.0	7.4	1340.0	1240.0
2018/2/13	13	157.6	78.8	21.5	0.0	5.6	5.3	5.9	3.7	29.8%	1.2	17.4	0.1	0.0	2.5	0.0	7.4	925.0	855.0
2018/2/14	14	155.2	77.6	14.2	0.0	5.4	4.4	4.9	3.4	21.8%	1.2	20.6	4.8	0.0	2.9	0.0	7.9	1080.0	990.0
2018/2/22	22	239.7	119.9	71.9	0.0	12.3	11.9	12.2	11.6	2.7%	1.2	17.2	0.0	0.0	2.4	0.0	7.8	945.0	845.0

2018/2/27	27	251.8	125.9	61.8	0.0	11.9	11.2	11.8	11.1	0.5%	1.2	15.8	0.1	0.0	2.2	0.0	7.65	810.0	780.0
2018/3/5	33	241.2	120.6	72.0	0.0	13.0	13.8	14.5	14.4	-4.4%	1.7	17.4	0.5	0.0	2.5	0.0	8.02	900.0	825.0
2018/3/10	38	232.4	116.2	85.9	0.0	11.4	10.3	10.8	10.5	-1.6%	1.3	17.5	0.1	0.0	2.5	0.0	7.97	680.0	650.0
2018/3/12	40	208.3	104.1	21.9	0.0	12.7	11.6	12.9	11.2	3.3%	2.0	24.9	1.1	0.0	3.6	0.0	7.88	600	570
2018/3/17	45	247.0	123.5	57.2	0.0	12.6	11.2	14.2	10.6	5.1%	3.6	24.8	6.5	0.1	3.5	0.0	8.34	765.0	730.0
2018/3/19	47	227.5	113.7	45.9	0.0	12.0	11.2	14.1	10.6	5.7%	3.8	24.5	4.5	0.3	3.5	0.0	8.05	790.0	755.0
2018/3/25	53	238.9	119.4	27.1	0.0	12.7	10.9	18.8	9.7	11.3%	5.5	28.1	6.7	1.1	4.0	1.1	7.95	930.0	895.0
2018/4/10	69	240.0	120.0	0.0	0.0	10.9	12.4	26.0	10.5	15.5%	5.1	26.2	10.3	2.6	3.8	5.4	7.73	465.0	450.0
vacation																			
2018/5/7	74	232.5	116.3	0.0	0.0	12.8	11.6	26.3	8.8	24.1%	5.7	26.2	8.5	0.8	3.8	1.3	7.92	595.0	510.0
2018/5/15	82	245.9	122.9	0.0	0.0	12.7	11.2	36.6	8.4	25.0%	5.3	26.2	7.1	0.0	3.8	0.0	7.99	765.0	595.0
2018/5/18	85	238.8	119.4	0.0	0.0	11.9	11.0	30.7	6.9	37.1%	5.8	26.2	8.2	0.0	3.8	0.1	7.91	755.0	595.0
2018/5/21	88	285.9	143.0	0.0	0.0	12.6	10.0	37.7	5.6	44.4%	6.2	26.3	8.8	0.0	3.8	0.1	8.11	750.0	570.0
2018/5/25	92	243.6	121.8	0.0	0.0	12.2	10.2	41.5	6.6	35.2%	5.5	26.5	7.5	0.0	3.8	0.0	7.5		
2018/5/29	96	241.8	120.9	0.0	0.0	12.0	9.5	48.5	6.1	36.1%	4.5	28.2	8.4	0.2	4.0	0.0	8	790.0	590.0
2018/6/1	99	250.5	125.3	0.0	0.0	11.4	8.8	48.1	4.3	51.3%	5.0	28.4	10.0	0.0	4.1	0.2	8.08		
2018/6/8	106	199.3	99.6	0.0	0.0	12.5	9.7	54.4	5.6	42.7%	4.7	25.9	3.2	0.0	3.7	0.0	8.03		
2018/5/12	110	199.3	99.6	29.5	0.0	13.2	11.1	58.3	6.0	45.7%	3.7	25.9	3.2	0.0	3.7	0.0	8.15		
2018/6/25	123	228.2	114.1	0.0	0.0	12.2	8.6	57.7	12.3	-42.9%	4.2	26.1	0.2	0.0	3.8	3.2	8.16	930.0	700.0
2018/7/14	142	249.2	124.6	0.0	0.0	11.6	9.0	53.1	2.7	70.6%	4.6	26.8	2.7	0.0	0.0	0.0		898.0	744.9
2018/7/17	145	254.5	127.3	0.0	0.0	13.2	11.4	58.3	7.0	38.9%	5.1	26.6	4.6	0.0	0.0	0.0	8.03	939.0	742.4
2018/7/19	147	228.5	114.3	0.0	0.0	13.3	11.0	59.2	7.0	36.4%	4.4	26.6	3.9	0.0	0.0	0.0	8.15	980.0	740.0
2018/7/31	159	245.6	122.8	0.0	0.0	13.8	9.0	57.3	3.5	60.9%	4.0	26.6	3.4	0.0	0.0	0.0	8.16	1420.0	850.0
2018/8/7	166	244.2	122.1	0.0	0.0	12.8	10.6	59.4	2.9	72.7%	3.5	26.2	2.2	0.0	0.0	0.0	7.75	840.0	650.0
2018/8/15	174	244.0	122.0	0.0	0.0	14.0	10.5	57.0	5.8	44.6%	4.4	26.2	4.6	0.0	0.0	0.0	7.68	940.0	650.0
2018/8/21	180	237.2	118.6	0.0	0.0	14.1	9.2	54.0	2.4	74.0%	4.6	26.7	5.1	0.0	0.0	0.0	7.68	930.0	690.0
2018/8/28	187	246.0	123.0	0.0	0.0	14.0	9.4	56.0	5.1	46.2%	4.8	26.7	5.5	0.0	3.8	0.0	7.75	990.0	710.0

Appendix A

2018/9/4	194	236.4	118.2	0.0	0.0	15.0	10.3	54.8	8.9	13.8%	5.3	26.7	8.5	0.0	3.8	0.0	7.68		
2018/9/14	204	230.9	115.5	0.0	0.0	12.7	9.8	51.3	1.0	89.2%	4.9	26.7	0.1	0.0	3.8	0.0	7.68	870.0	610.0
2018/9/19	209	250.0	125.0	0.0	0.0	13.0	9.2	60.1	2.4	73.6%	3.4	26.7	0.5	0.4	3.8	0.0	9.45		
2018/9/21	211	250.0	125.0	0.0	0.0	12.4	9.7	55.6	2.3	76.4%	3.6	26.7	0.1	0.0	3.8	0.0	8.11		
2018/9/26	216	250.0	125.0	0.0	0.0	13.7	10.3	48.6	2.6	75.1%	2.7	25.7	3.0	0.0	3.7	0.0	7.88		
E4		HAc (mg L^{-1})					PO_4^{3-}-P (mg L^{-1})			Removal rate	NO_3^--N (mg L^{-1})			NO_2^--N (mg L^{-1})					
Date	Day	feedstock	Ana	Ano	E	feedstock	Ana	Ano	E		Ana	Ano	E	Ana	Ano	E	pH	MLSS&MLVSS (mg L^{-1})	
2018/2/1	1					5.5	4.9	4.7	4.0	17.6%	1.1	15.9	0.0	0.0	2.3	0.0	7.4	1533.33	1420
2018/2/7	7					5.6	4.8	6.2	4.3	10.1%	3.7	16.1	4.5	0.1	2.3	0.0	7.4	1126.7	1060.0
2018/2/13	13	157.6	78.8	25.5	0.0	5.6	5.2	5.3	3.5	31.7%	1.2	17.2	0.0	0.0	2.4	0.0	7.4	1080.0	995.0
2018/2/14	14	155.2	77.6	16.4	0.0	5.4	4.3	4.7	3.5	18.9%	1.5	20.4	6.6	0.0	2.9	0.0	7.4	1046.7	966.7
2018/2/22	22	239.7	119.9	76.6	0.0	12.3	11.8	12.9	11.7	1.2%	1.2	17.1	0.0	0.0	2.4	0.0	7.7	985.0	900.0
2018/2/27	27	251.8	125.9	62.8	0.0	11.9	11.1	11.5	11.1	0.4%	1.2	15.7	0.0	0.0	2.2	0.0	7.79	890.0	850.0
2018/3/5	33	241.2	120.6	74.0	0.0	13.0	14.1	13.9	14.0	0.3%	1.7	17.3	0.5	0.0	2.5	0.0	7.5	690.0	675.0
2018/3/10	38	232.4	116.2	85.5	0.0	11.4	10.0	11.7	11.2	-11.6%	1.2	17.5	0.0	0.0	2.5	0.0	8.16	645.0	615.0
2018/3/12	40	208.3	104.1	0.0	0.0	12.7	11.8	12.3	11.8	-0.2%	1.2	24.6	0.3	0.0	3.5	0.0	7.85	565	540
2018/3/17	45	247.0	123.5	58.7	0.0	12.6	11.5	13.7	10.6	7.6%	3.1	24.6	5.1	0.9	3.5	0.0	7.76	660.0	640.0
2018/3/19	47	227.5	113.7	48.8	0.0	12.0	11.0	15.0	10.3	6.3%	3.5	24.2	5.0	0.0	3.5	0.0	8.03	855.0	820.0
2018/3/25	53	238.9	119.4	0.0	0.0	12.7	10.8	18.3	9.2	14.7%	6.2	27.8	11.9	0.6	4.0	0.0	7.95	1065.0	1025.0
2018/4/10	69	240.0	120.0	0.0	0.0	10.9	11.7	25.0	9.3	20.7%	4.3	26.2	6.7	2.5	3.8	3.6	7.81	560.0	530.0
vacation																			
2018/5/7	74	232.5	116.3	0.0	0.0	12.8	11.5	21.7	8.9	22.9%	4.7	26.2	7.1	1.2	3.7	2.5	7.74	640.0	550.0
2018/5/15	82	245.9	122.9	0.0	0.0	12.7	11.3	30.5	9.1	19.8%	5.7	26.2	8.7	0.0	3.7	0.0	7.79	885.0	720.0
2018/5/18	85	238.8	119.4	0.0	0.0	11.9	11.0	30.3	8.8	20.7%	5.7	26.2	7.8	0.0	3.7	0.0	7.88	865.0	675.0
2018/5/21	88	285.9	143.0	0.0	0.0	12.6	10.6	34.3	6.2	41.8%	5.6	26.1	8.8	0.0	3.7	0.0	7.81	830.0	620.0
2018/5/25	92	243.6	121.8	0.0	0.0	12.2	9.9	40.8	6.0	39.1%	5.3	26.4	8.4	0.0	3.8	0.0	7.97		
2018/5/29	96	241.8	120.9	0.0	0.0	12.0	8.5	48.8	4.0	52.8%	4.3	28.3	8.6	0.0	4.0	0.0	7.94	800.0	630.0

Appendix A

2018/6/1	99	250.5	125.3	0.0	0.0	11.4	8.3	49.1	2.7	67.4%	4.3	28.6	10.0	0.0	4.1	0.1	7.85		
2018/6/8	106	199.3	99.6	0.0	0.0	12.5	9.5	55.7	2.7	71.1%	4.5	26.1	3.2	0.0	3.7	0.0	8.18		
2018/5/12	110	199.3	99.6	0.0	0.0	13.2	9.9	57.1	4.6	53.9%	3.5	26.3	2.2	0.0	3.8	0.0	8.23	1070.0	720.0
2018/6/25	123	228.2	114.1	0.0	0.0	12.2	9.5	57.2	4.8	49.6%	4.2	26.3	3.0	0.0	3.8	0.0	8.12	1020.0	820.0
2018/7/14	142	249.2	124.6	0.0	0.0	11.6	7.6	42.7	1.4	81.3%	3.3	26.3	1.3	0.0	3.9	0.0		898.0	744.9
2018/7/17	145	254.5	127.3	0.0	0.0	13.2	11.1	47.0	6.4	42.4%	5.8	27.0	5.8	0.0	3.9	0.0	8.18	939.0	742.4
2018/7/19	147	228.5	114.3	0.0	0.0	13.3	9.7	48.8	3.5	64.5%	4.9	27.2	4.7	0.0	3.9	0.0	8.23	980.0	740.0
2018/7/31	159	245.6	122.8	0.0	0.0	13.8	9.4	50.3	4.5	52.3%	4.7	27.2	5.2	0.0	3.9	0.0	8.12	1420.0	850.0
2018/8/7	166	244.2	122.1	0.0	0.0	12.8	11.3	57.8	2.4	78.8%	3.2	26.2	1.1	0.0	3.7	0.0	7.63	840.0	650.0
2018/8/15	174	244.0	122.0	0.0	0.0	14.0	9.9	57.3	4.1	58.8%	3.2	26.2	1.9	0.0	3.7	0.0	7.64	940.0	650.0
2018/8/21	180	237.2	118.6	0.0	0.0	14.1	9.7	54.4	3.2	66.7%	4.4	27.0	4.8	0.0	3.9	0.0	7.52	930.0	690.0
2018/8/28	187	246.0	123.0	0.0	0.0	14.0	10.9	54.6	5.8	47.0%	4.4	27.0	3.5	0.0	3.9	0.0	7.63		
2018/9/4	194	236.4	118.2	0.0	0.0	15.0	11.1	55.0	8.5	23.8%	4.0	27.0	6.2	0.0	3.9	0.0	7.64	1450.0	1070.0
2018/9/14	204	230.9	115.5	0.0	0.0	12.7	9.4	58.4	3.8	59.9%	1.6	27.0	0.1	0.0	3.9	0.0	7.52		
2018/9/19	209	250.0	125.0	0.0	0.0	13.0	8.3	43.3	0.8	90.5%	1.7	27.0	3.7	0.0	3.9	0.0	8.79		
2018/9/21	211	250.0	125.0	0.0	0.0	12.4	7.8	42.2	2.6	66.3%	1.3	27.0	0.1	0.0	3.9	0.0	8.03		
2018/9/26	216	250.0	125.0	0.0	0.0	13.7	7.6	46.9	1.6	78.6%	2.9	25.9	2.5	0.0	3.7	0.0	7.96		
E5		HAc (mg L^{-1})					PO_4^{3-}-P (mg L^{-1})			Removal rate	NO_3^--N (mg L^{-1})			NO_2^--N (mg L^{-1})					
Date	Day	feedstock	Ana	Ano	E	feedstock	Ana	Ano	E		Ana	Ano	E	Ana	Ano	E	pH	MLSS&MLVSS (mg L^{-1})	
2018/2/1	1					5.6	4.8	4.6	4.3	10.8%	1.1	13.1	0.0	0.0	4.4	0.0	7.5	1686.67	1526.667
2018/2/7	7					5.7	5.0	5.7	4.4	11.8%	2.7	13.3	2.4	1.0	4.5	1.0	7.5	1400.0	1280.0
2018/2/13	13	157.5	78.8	0.0	0.0	5.5	5.1	4.9	3.5	32.0%	1.2	14.2	0.1	0.0	4.8	0.1	7.4	1185.0	1065.0
2018/2/14	14	157.6	78.8	0.0	0.0	5.6	4.7	5.8	3.9	16.3%	1.8	16.4	5.6	1.0	5.5	2.9	7.5	930.0	845.0
2018/2/22	22	233.8	116.9	72.0	0.0	12.5	11.9	12.0	11.6	2.1%	1.2	14.0	0.0	0.0	4.7	0.0	7.9	605.0	580.0
2018/2/27	27	245.5	122.7	66.5	0.0	12.0	11.1	11.5	11.2	-1.5%	1.2	12.8	0.0	0.0	4.3	0.0	7.76	670.0	655.0
2018/3/5	33	240.2	120.1	56.1	0.0	12.9	13.5	14.0	14.0	-3.1%	1.7	13.9	0.0	0.0	4.7	0.0	7.72	490.0	485.0
2018/3/10	38	224.3	112.1	64.7	0.0	11.8	10.4	11.6	11.0	-5.2%	1.2	15.0	0.0	0.0	5.0	0.0	8.3	555.0	540.0

2018/3/12	40	245.7	122.9	32.9	0.0	12.4	11.7	12.2	11.7	-0.7%	1.4	19.9	0.2	0.0	6.7	0.0	8.02	560	550
2018/3/17	45	242.8	121.4	68.2	0.0	12.3	11.7	12.8	10.7	8.2%	1.3	19.9	0.0	0.3	6.7	0.2	7.95	605.0	595.0
2018/3/19	47	245.8	122.9	54.4	0.0	12.3	11.7	12.9	11.3	3.2%	1.4	19.4	0.6	0.1	6.5	0.0	8.4	715.0	705.0
2018/3/25	53	235.1	117.5	30.4	0.0	12.1	11.5	15.2	10.5	8.8%	2.5	22.1	4.2	1.6	7.5	2.7	8.33	605.0	545.0
2018/4/10	69	240.0	120.0	0.0	0.0	10.9	10.4	19.9	8.7	16.5%	3.2	22.5	5.3	3.5	7.5	5.3	8.05	620.0	560.0
vacation																			
2018/5/7	74	236.4	118.2	9.0	0.0	12.2	11.5	16.5	9.5	17.3%	1.8	22.1	2.1	3.9	7.3	6.0	7.98	595.0	535.0
2018/5/15	82	237.7	118.8	9.6	0.0	12.2	11.8	21.8	10.3	12.7%	4.3	22.1	6.0	1.6	7.3	2.2	8.04	520.0	430.0
2018/5/18	85	243.2	121.6	0.0	0.0	12.7	11.2	21.0	9.5	15.5%	4.8	22.1	7.1	0.9	7.3	1.3	8.07	660.0	550.0
2018/5/21	88	260.1	130.0	0.0	0.0	12.6	11.1	23.0	8.2	26.5%	5.6	22.3	8.9	0.3	7.3	0.2	8	730.0	620.0
2018/5/25	92	216.8	108.4	0.0	0.0	12.5	11.0	26.5	8.8	19.7%	5.7	22.4	9.2	0.0	7.4	0.1	8.07		
2018/5/29	96	246.3	123.2	0.0	0.0	12.2	10.5	32.5	7.6	28.3%	4.3	23.8	9.9	0.0	7.8	0.0	8.15	990.0	770.0
2018/6/1	99	264.6	132.3	0.0	0.0	11.6	9.5	34.4	5.9	38.5%	5.4	24.0	11.9	0.0	7.9	0.0	7.88		
2018/6/8	106	203.4	101.7	0.0	0.0	11.7	9.9	40.4	6.5	34.3%	5.1	22.0	5.6	0.0	7.2	0.0	8.3		
2018/5/12	110	194.7	97.3	0.0	0.0	13.4	10.4	49.4	7.7	26.1%	4.0	22.0	4.1	0.0	7.2	0.0	8.32	1170.0	840.0
2018/6/25	123	224.2	112.1	0.0	0.0	12.5	8.5	50.2	5.0	41.3%	3.4	22.0	0.0	0.0	7.2	0.0	8.54	1100.0	820.0
2018/7/14	142	249.5	124.8	0.0	0.0	10.9	7.2	45.5	2.8	60.7%	2.8	21.6	0.9	0.0	7.1	0.0		714.3	561.2
2018/7/17	145	251.8	125.9	0.0	0.0	13.4	10.8	50.5	6.6	39.0%	4.2	21.5	2.5	0.0	7.1	0.0	8.3	812.1	620.6
2018/7/19	147	250.6	125.3	0.0	0.0	13.2	9.5	49.5	5.3	43.9%	3.2	21.6	2.1	0.0	7.1	0.0	8.32	910.0	680.0
2018/7/31	159	242.2	121.1	0.0	0.0	13.4	7.1	48.2	2.7	61.8%	1.4	21.6	0.1	0.0	7.1	0.0	8.54	1540.0	1040.0
2018/8/7	166	254.4	127.2	0.0	0.0	12.2	7.6	53.8	2.2	71.0%	2.0	22.3	0.0	0.0	7.4	0.0	7.59	1070.0	820.0
2018/8/15	174	236.9	118.5	0.0	0.0	13.3	8.2	58.3	5.9	27.9%	3.4	22.3	3.2	0.0	7.4	0.0	7.3	1220.0	810.0
2018/8/21	180	251.5	125.7	0.0	0.0	13.6	9.4	54.2	7.7	17.4%	4.0	22.6	5.6	0.0	7.5	0.0	7.54	1210.0	810.0
2018/8/28	187	248.8	124.4	0.0	0.0	14.1	9.6	57.6	6.7	30.1%	2.8	22.6	1.7	0.0	7.5	0.0	7.59		
2018/9/4	194	220.8	110.4	0.0	0.0	14.4	10.0	61.1	11.9	-19.8%	2.5	22.6	5.3	0.0	7.5	0.0	7.3	1100.0	790.0
2018/9/14	204	230.2	115.1	0.0	0.0	12.5	9.2	53.3	3.5	61.4%	3.0	22.6	5.6	0.0	7.5	0.0	7.54		
2018/9/19	209	250.0	125.0	0.0	0.0	12.6	8.0	57.2	2.4	70.6%	1.7	22.6	2.7	0.0	7.5	0.0	8.8		

Appendix A

2018/9/21	211	250.0	125.0	0.0	0.0	12.0	8.1	54.7	7.3	9.9%	2.0	22.6	0.2	0.0	7.5	0.0	7.97		
2018/9/26	216	250.0	125.0	0.0	0.0	13.9	9.7	52.8	9.4	3.6%	2.5	22.0	3.3	0.0	7.3	0.0	8.05		
E6		HAc (mg L^{-1})					PO_4^{3-}-P (mg L^{-1})			Removal rate	NO_3^--N (mg L^{-1})			NO_2^--N (mg L^{-1})					
Date	Day	feedstock	Ana	Ano	E	feedstock	Ana	Ano	E		Ana	Ano	E	Ana	Ano	E	pH	MLSS&MLVSS (mg L^{-1})	
2018/2/1	1					5.6	4.9	4.5	4.3	13.4%	1.1	13.5	0.0	0.0	5.5	0.0	7.5	1680	1533.333
2018/2/7	7					5.7	4.9	5.5	4.4	10.1%	3.9	13.7	4.8	1.5	4.6	2.1	7.5	1186.7	1106.7
2018/2/13	13	157.5	78.8	13.9	0.0	5.5	4.9	4.3	3.2	35.8%	1.2	16.4	0.6	0.0	5.5	0.8	7.5	1070.0	960.0
2018/2/14	14	157.6	78.8	0.0	0.0	5.6	4.5	5.8	3.6	20.0%	3.0	21.1	11.6	1.9	7.1	5.3	7.5	835.0	760.0
2018/2/22	22	233.8	116.9	69.8	0.0	12.5	11.9	12.0	11.5	2.8%	1.2	15.7	0.0	0.0	5.3	0.0	7.5	780.0	710.0
2018/2/27	27	245.5	122.7	55.4	0.0	12.0	11.3	11.8	11.4	-0.8%	1.2	14.0	0.1	0.0	4.7	0.0	8.09	710.0	670.0
2018/3/5	33	240.2	120.1	61.6	0.0	12.9	12.4	12.4	11.9	3.9%	1.6	18.6	0.5	0.0	6.2	0.0	7.9	535.0	530.0
2018/3/10	38	224.3	112.1	61.4	0.0	11.8	11.4	11.6	11.2	1.3%	1.2	15.0	0.1	0.0	5.0	0.0	7.34	540.0	530.0
2018/3/12	40	245.7	122.9	31.7	0.0	12.4	11.4	13.0	11.0	3.6%	5.2	25.1	8.2	1.1	8.4	1.2	8.18	450	440
2018/3/17	45	242.8	121.4	42.7	0.0	12.3	11.4	14.0	10.9	4.4%	3.4	25.3	6.7	2.4	8.5	4.1	8.04	505.0	490.0
2018/3/19	47	245.8	122.9	30.3	0.0	12.3	11.1	13.3	11.0	0.8%	3.9	24.7	5.8	2.4	8.3	3.3	7.95	545.0	535.0
2018/3/25	53	235.1	117.5	22.1	0.0	12.1	11.3	15.2	10.9	3.5%	5.9	27.2	10.2	3.5	9.2	6.4	8.29	555.0	550.0
2018/4/10	69	240.0	120.0	0.0	0.0	10.9	11.4	18.8	10.5	8.1%	3.5	22.5	3.7	1.0	7.5	2.2	8.18	545.0	505.0
vacation																			
2018/5/7	74	236.4	118.2	0.0	0.0	12.2	11.2	17.6	9.1	18.6%	1.4	20.5	0.7	2.3	6.8	2.0	8	795.0	715.0
2018/5/15	82	237.7	118.8	0.0	0.0	11.0	12.1	24.7	10.1	15.9%	3.4	20.5	3.1	0.5	6.8	0.6	7.86	1010.0	915.0
2018/5/18	85	243.2	121.6	0.0	0.0	12.7	11.8	24.2	9.2	21.9%	3.3	20.5	2.9	0.3	6.8	0.3	7.96	695.0	580.0
2018/5/21	88	260.1	130.0	0.0	0.0	12.6	11.2	27.1	7.8	30.4%	3.5	20.5	2.9	0.0	6.8	0.1	7.98	840.0	690.0
2018/5/25	92	216.8	108.4	0.0	0.0	12.5	11.0	31.6	7.5	31.7%	3.5	20.8	2.6	0.0	6.9	0.0	7.82		
2018/5/29	96	246.3	123.2	0.0	0.0	12.2	9.6	41.0	10.8	-12.6%	2.1	19.1	0.0	0.0	6.3	0.0	7.96	900.0	700.0
2018/6/1	99	264.6	132.3	0.0	0.0	11.6	8.2	42.1	3.1	62.3%	2.2	21.9	2.5	0.0	7.2	0.0	8.15		
2018/6/8	106	203.4	101.7	0.0	0.0	11.7	7.5	52.2	5.5	27.6%	1.7	20.0	0.0	0.0	6.6	0.0	7.97		
2018/5/12	110	194.7	97.3	0.0	0.0	13.4	7.3	57.1	7.0	4.9%	1.5	20.2	0.1	0.0	6.7	0.0	8.23		

Appendix A

2018/6/25	123	224.2	112.1	0.0	0.0	12.5	9.5	50.2	8.0	16.6%	1.3	20.2	0.0	0.0	6.7	0.0	8.12	1080.0	770.0
2018/7/14	142	249.5	124.8	0.0	0.0	10.9	6.2	45.4	4.7	23.9%	1.6	20.4	0.0	0.0	6.7	0.0		714.3	561.2
2018/7/17	145	251.8	125.9	0.0	0.0	13.4	9.0	54.1	6.2	31.2%	2.3	20.3	0.3	0.0	6.7	0.0	8.23	812.1	620.6
2018/7/19	147	250.6	125.3	0.0	0.0	13.2	8.1	50.4	8.0	1.0%	1.8	20.4	0.0	0.0	6.7	0.0	8.12	910.0	680.0
2018/7/31	159	242.2	121.1	0.0	0.0	13.4	8.2	57.0	7.4	9.8%	1.4	20.4	0.0	0.0	6.7	0.0	8.13	1540.0	1040.0
2018/8/7	166	254.4	127.2	0.0	0.0	12.2	6.9	63.0	6.7	2.1%	1.4	22.4	0.0	0.0	7.5	0.0	7.57	1070.0	820.0
2018/8/15	174	236.9	118.5	0.0	0.0	13.3	7.1	58.7	8.6	-21.7%	2.7	22.4	2.6	0.0	7.5	0.0	7.25	1220.0	810.0
2018/8/21	180	251.5	125.7	0.0	0.0	13.6	10.7	62.8	15.7	-47.3%	3.1	23.0	5.3	0.0	7.7	0.0	7.57	1210.0	810.0
2018/8/28	187	248.8	124.4	0.0	0.0	14.1	12.1	59.1	10.2	15.8%	1.6	23.0	1.4	0.0	7.7	0.0	7.57	970.0	820.0
2018/9/4	194	220.8	110.4	0.0	0.0	14.4	12.2	56.4	2.3	81.3%	1.5	23.0	0.3	0.0	7.7	0.0	7.25		
2018/9/14	204	230.2	115.1	0.0	0.0	12.5	10.5	49.2	0.4	96.3%	1.6	23.0	0.1	0.0	7.7	0.0	7.57	740.0	530.0
2018/9/19	209	250.0	125.0	0.0	0.0	12.6	10.1	51.3	0.5	95.0%	1.7	23.0	1.2	0.0	7.7	0.0	8.68		
2018/9/21	211	250.0	125.0	0.0	0.0	12.0	8.2	49.2	7.6	7.5%	1.3	23.0	0.1	0.0	7.7	0.0	7.9		
2018/9/26	216	250.0	125.0	0.0	0.0	13.9	9.0	38.9	1.9	78.7%	1.2	22.0	0.4	0.0	7.3	0.0	7.89		
E7		HAc (mg L^{-1})					PO_4^{3-}-P (mg L^{-1})			Removal rate	NO_3^--N (mg L^{-1})			NO_2^--N (mg L^{-1})					
Date	Day	feedstock	Ana	Ano	E	feedstock	Ana	Ano	E		Ana	Ano	E	Ana	Ano	E	pH	MLSS&MLVSS (mg L^{-1})	
2018/2/1	1					5.6	4.3	20.2	2.1	51.4%	1.8	0.1	1.6	0.0	0.0	0.0	7.5	1926.67	1666.667
2018/2/7	7					5.6	4.3	20.1	2.9	32.5%	1.6	0.1	1.0	0.0	0.0	0.0	7.5	1346.7	1153.3
2018/2/13	13	155.4	77.7	0.0	0.0	5.6	3.4	17.8	3.3	5.1%	1.9	0.0	1.4	0.0	0.0	0.0	7.5	1005.0	840.0
2018/2/14	14	153.8	76.9	0.0	0.0	5.5	3.7	17.8	1.8	50.6%	1.8	0.1	1.3	0.0	0.0	0.0	7.5	835.0	690.0
2018/2/22	22	236.0	118.0	36.4	0.0	12.2	7.9	26.0	5.3	33.5%	1.3	0.1	0.8	0.0	0.0	0.0	7.5	900.0	695.0
2018/2/27	27	242.3	121.2	0.0	0.0	12.0	7.7	31.1	2.9	62.4%	1.3	0.1	0.3	0.0	0.0	0.0	7.7	855.0	630.0
2018/3/5	33	240.6	120.3	0.0	0.0	12.7	6.8	35.5	1.5	78.2%	1.7	0.1	0.7	0.0	0.0	0.0	7.77	1190.0	780.0
2018/3/10	38	246.5	123.2	56.9	0.0	11.4	6.4	42.3	2.6	59.0%	1.2	0.1	0.2	0.0	0.1	0.0	8.13	945.0	635.0
2018/3/12	40	207.2	103.6	0.0	0.0	12.5	7.2	48.6	1.5	78.8%	1.5	0.1	0.5	0.0	0.0	0.0	8.1	1000	665
2018/3/17	45	240.8	120.4	0.0	0.0	12.6	6.9	50.1	1.2	82.2%	1.3	0.1	0.4	0.0	0.0	0.0	8.04	785.0	515.0
2018/3/19	47	248.7	124.3	0.0	0.0	12.1	6.7	52.0	0.5	91.9%	1.4	0.0	0.8	0.0	0.0	0.1	8.12	1200.0	710.0

2018/3/25	53	241.7	120.9	0.0	0.0	12.9	7.2	47.4	1.7	77.0%	1.4	0.1	0.5	0.2	0.0	0.3	8.08	1345.0	795.0
2018/4/10	69	246.2	123.1	0.0	0.0	11.2	7.0	52.9	2.5	64.9%	0.3	0.2	0.4	0.2	4.2	0.5	8.09	890.0	490.0
vacation																			
2018/5/7	74	234.3	117.2	0.0	0.0	12.4	7.5	57.7	1.6	78.4%	0.3	0.0	0.3	0.0	1.0	0.0	8.18	1055.0	585.0
2018/5/15	82	225.3	112.6	0.0	0.0	11.7	14.9	69.0	3.0	79.9%	1.6	0.1	0.2	0.3	0.1	0.0	8.15	1235.0	660.0
2018/5/18	85	231.6	115.8	0.0	0.0	12.4	7.1	56.3	1.0	85.7%	1.2	0.1	0.0	0.0	0.0	0.1	8.11	1320.0	720.0
2018/5/21	88	233.3	116.6	0.0	0.0	12.4	6.8	53.9	0.7	90.0%	1.4	0.1	0.2	0.0	0.1	0.1	8.15	1345.0	755.0
2018/5/25	92	227.9	113.9	0.0	0.0	12.2	9.7	59.7	1.0	89.2%	1.3	0.0	0.1	0.3	0.1	0.1	8.07		
2018/5/29	96	245.0	122.5	0.0	0.0	12.3	12.9	68.0	1.8	86.3%	1.4	0.1	0.1	0.3	0.1	0.1	8.01	1430.0	1010.0
2018/6/1	99	238.3	119.2	0.0	0.0	11.5	6.1	59.4	0.4	93.8%	1.4	0.1	0.2	0.0	0.1	0.0	8.13		
2018/6/8	106	213.4	106.7	0.0	0.0	12.5	6.3	55.1	0.0	99.5%	1.5	0.1	0.1	0.0	0.1	0.0	8.27		
2018/5/12	110	230.0	115.0	0.0	0.0	12.9	6.9	59.8	0.5	92.4%	1.6	0.1	0.3	0.0	0.1	0.0	8.12	1370.0	980.0
2018/6/25	123	251.4	125.7	0.0	0.0	12.1	7.2	52.8	1.1	84.7%	1.4	0.1	0.2	0.1	0.0	0.2	7.69	1360.0	780.0
2018/7/14	142	256.8	128.4	0.0	0.0	11.6	6.3	45.4	1.8	71.2%	1.4	0.1	0.2	0.2	0.1	0.3		1306.1	938.8
2018/7/17	145	249.5	124.8	0.0	0.0	12.9	14.0	61.3	6.9	50.5%	1.6	0.0	0.3	0.0	0.0	0.9	7.69	1308.1	914.4
2018/7/19	147	219.5	109.7	0.0	0.0	13.2	12.9	58.2	4.6	64.4%	1.5	0.0	0.3	0.0	0.0	0.7	7.68	1310.0	890.0
2018/7/31	159	232.7	116.4	0.0	0.0	12.0	7.3	47.9	1.5	79.9%	1.9	0.1	1.2	0.2	0.1	0.5	8.12	1170.0	750.0
2018/8/7	166	228.3	114.1	0.0	0.0	12.6	8.6	53.9	1.3	84.5%	2.6	0.0	2.2	0.1	0.0	0.1	7.68	1490.0	1000.0
2018/8/15	174	260.0	130.0	0.0	0.0	10.7	10.2	63.7	2.8	72.4%	1.9	0.1	2.7	0.4	0.1	0.1	7.96	1290.0	830.0
2018/8/21	180	256.2	128.1	0.0	0.0	14.4	12.1	62.2	1.1	91.3%	2.9	0.1	2.9	0.2	0.1	0.0	7.92	1520.0	920.0
2018/8/28	187	254.9	127.5	0.0	0.0	14.9	12.5	60.2	1.1	91.6%	2.7	0.2	2.5	0.2	0.4	0.0	7.68		
2018/9/4	194	239.2	119.6	0.0	0.0	15.3	12.6	61.1	0.4	96.8%	2.6	0.1	2.0	0.1	0.1	0.0	8.12	1450.0	850.0
2018/9/14	204	245.6	122.8	0.0	0.0	12.7	10.1	57.3	0.4	96.5%	3.0	0.1	2.1	0.1	0.0	0.0	7.68		
2018/9/19	209	250.0	125.0	0.0	0.0	12.9	7.4	54.7	0.7	90.9%	2.6	0.0	2.4	0.0	0.1	0.0	7.96		
2018/9/21	211	250.0	125.0	0.0	0.0	12.8	7.8	50.2	2.7	65.8%	2.3	0.0	2.3	0.0	0.0	0.0	7.92		
2018/9/26	216	250.0	125.0	0.0	0.0	13.2	7.8	53.6	1.7	77.8%	2.2	0.0	2.1	0.0	0.0	0.0	8.46		
E8		HAc (mg L^{-1})					PO_4^{3-}-P (mg L^{-1})				NO_3^--N (mg L^{-1})			NO_2^--N (mg L^{-1})					

Appendix A

Date	Day	feedstock	Ana	Ano	E	feedstock	Ana	Ano	E	Removal rate	Ana	Ano	E	Ana	Ano	E	pH	MLSS&MLVSS (mg L^{-1})	
2018/2/1	1					5.6	4.0	25.5	1.5	63.0%	1.5	0.1	1.3	0.0	0.0	0.0	7.5	1720	1473.333
2018/2/7	7					5.6	3.9	25.6	1.5	62.5%	1.5	0.1	1.4	0.0	0.0	0.0	7.5	1453.3	1226.7
2018/2/13	13	155.4	77.7	0.0	0.0	5.6	3.0	28.5	2.7	9.4%	1.9	0.0	1.4	0.0	0.0	0.0	7.5	1225.0	1000.0
2018/2/14	14	153.8	76.9	0.0	0.0	5.5	3.7	26.2	1.7	53.3%	1.7	0.0	1.3	0.0	0.0	0.0	7.4	1035.0	835.0
2018/2/22	22	236.0	118.0	47.0	0.0	12.2	8.6	25.5	5.0	42.5%	1.3	0.1	0.5	0.0	0.0	0.0	7.5	945.0	710.0
2018/2/27	27	242.3	121.2	0.0	0.0	12.0	9.9	19.3	9.6	2.5%	1.2	0.1	0.0	0.0	0.0	0.0	7.52	450.0	385.0
2018/3/5	33	240.6	120.3	46.5	0.0	12.7	10.4	19.0	11.8	-13.5%	1.7	0.1	0.5	0.0	0.0	0.0	7.74	680.0	590.0
2018/3/10	38	246.5	123.2	18.3	0.0	11.4	6.3	38.4	2.3	63.1%	1.2	0.1	0.2	0.0	0.0	0.1	8.02	1130.0	760.0
2018/3/12	40	207.2	103.6	0.0	0.0	12.5	7.0	44.8	1.4	80.7%	1.4	0.1	0.4	0.0	0.0	0.1	7.98	800	570
2018/3/17	45	240.8	120.4	0.0	0.0	12.6	6.8	47.4	1.1	83.6%	1.2	0.2	0.3	0.0	0.0	0.0	7.56	850.0	550.0
2018/3/19	47	248.7	124.3	0.0	0.0	12.1	6.8	51.4	1.0	85.7%	1.4	0.0	0.8	0.0	0.0	0.2	7.99	1290.0	765.0
2018/3/25	53	241.7	120.9	0.0	0.0	12.9	7.5	44.0	3.1	59.1%	1.3	0.1	0.2	0.2	0.1	0.3	7.98	1375.0	820.0
2018/4/10	69	246.2	123.1	0.0	0.0	11.2	6.9	51.5	3.3	51.8%	0.2	0.1	0.2	0.3	4.3	0.7	8.09	775.0	470.0
vacation																			
2018/5/7	74	234.3	117.2	0.0	0.0	12.4	7.1	47.9	2.9	58.7%	0.3	0.0	0.1	0.0	1.0	0.0	8.04	970.0	510.0
2018/5/15	82	225.3	112.6	0.0	0.0	11.7	6.4	49.7	2.9	54.5%	1.5	0.1	0.2	0.0	0.0	0.0	8.14	1385.0	730.0
2018/5/18	85	231.6	115.8	0.0	0.0	12.4	6.2	48.4	0.2	96.3%	1.2	0.1	0.0	0.0	0.0	0.1	8.1	1180.0	620.0
2018/5/21	88	233.3	116.6	0.0	0.0	12.4	6.7	48.4	1.6	76.6%	1.4	0.1	0.1	0.1	0.0	0.1	7.98	1295.0	890.0
2018/5/25	92	227.9	113.9	0.0	0.0	12.2	6.8	47.0	1.0	85.2%	1.3	0.1	0.1	0.1	0.0	0.2	7.98		
2018/5/29	96	245.0	122.5	0.0	0.0	12.3	6.7	49.1	2.4	65.0%	1.4	0.1	0.1	0.5	0.1	0.9	8	1140.0	860.0
2018/6/1	99	238.3	119.2	0.0	0.0	11.5	6.2	47.6	1.3	79.0%	1.3	0.1	0.1	0.8	0.1	1.7	8.03		
2018/6/8	106	213.4	106.7	0.0	0.0	12.5	6.4	46.5	0.3	95.5%	1.4	0.1	0.1	0.3	0.2	0.6	8.17		
2018/5/12	110	230.0	115.0	0.0	0.0	12.9	7.3	53.7	3.6	49.9%	1.4	0.1	0.1	0.1	0.1	0.1	7.99	1160.0	830.0
2018/6/25	123	251.4	125.7	0.0	0.0	12.1	6.2	48.3	1.1	82.6%	1.2	0.1	0.0	0.1	0.0	0.3	7.77	1240.0	850.0
2018/7/14	142	256.8	128.4	0.0	0.0	11.6	7.2	42.9	5.5	24.5%	1.3	0.1	0.0	0.0	0.0	0.0		1193.9	1000.0
2018/7/17	145	249.5	124.8	0.0	0.0	12.9	10.5	40.6	7.9	25.0%	1.6	0.0	0.2	0.0	0.0	0.0	7.77	1266.9	1050.0

Appendix A

2018/7/19	147	219.5	109.7	0.0	0.0	13.2	8.1	40.2	7.5	8.1%	1.5	0.0	0.2	0.0	0.0	0.0	7.61	1340.0	1100.0
2018/7/31	159	232.7	116.4	0.0	0.0	13.5	9.2	36.5	5.1	44.1%	1.5	0.1	0.4	0.6	0.0	1.4	8.09	1530.0	1140.0
2018/8/7	166	228.3	114.1	0.0	0.0	12.6	11.5	35.5	8.5	25.6%	2.2	0.8	1.7	0.9	0.1	2.2	7.69	1230.0	1090.0
2018/8/15	174	260.0	130.0	0.0	0.0	10.7	8.7	36.4	7.0	19.1%	2.4	0.1	2.8	0.1	0.1	0.6	7.94	890.0	670.0
2018/8/21	180	256.2	128.1	0.0	0.0	14.4	11.2	45.0	6.2	44.5%	3.0	0.0	2.9	0.0	0.0	0.1	7.92	640.0	490.0
2018/8/28	187	254.9	127.5	0.0	0.0	14.9	10.5	43.2	5.9	43.6%	2.8	0.1	2.5	0.0	0.0	0.0	7.61		
2018/9/4	194	239.2	119.6	0.0	0.0	15.3	11.6	43.7	6.2	46.8%	2.8	0.1	2.8	0.0	0.0	0.0	8.09	1050.0	740.0
2018/9/14	204	245.6	122.8	0.0	0.0	12.7	9.0	39.9	2.8	69.1%	2.8	0.1	2.4	0.0	0.0	0.0	7.69		
2018/9/19	209	250.0	125.0	0.0	0.0	12.9	9.0	42.4	2.8	69.5%	2.5	0.0	2.3	0.0	0.1	0.0	7.94		
2018/9/21	211	250.0	125.0	0.0	0.0	12.8	10.0	39.6	6.2	38.3%	2.2	0.0	2.3	0.0	0.0	0.0	7.92		
2018/9/26	216	250.0	125.0	0.0	0.0	13.2	8.4	46.3	0.4	95.6%	2.0	0.0	1.8	0.0	0.0	0.0	8.47		

c. Performance of Enrichment II

EE1		HAc (mg L^{-1})					PO_4^{3-}-P (mg L^{-1})			Removal rate	NO_3^--N (mg L^{-1})			NO_2^--N (mg L^{-1})					
Date	Day	feedstock	Ana	Ano	E	feedstock	Ana	Ano	E		Ana	Ano	E	Ana	Ano	E	pH	MLSS&MLVSS (mg L^{-1})	
2018/11/1	0	246.4	123.2	0.0	0.0	12.7	9.6	32.0	9.5	1.9%	5.3	27.6	8.9	0.0	0.0	0.0		637.5	532.5
2018/11/4	3	232.0	116.0	0.0	0.0	12.8	9.4	27.3	6.6	29.6%	6.1	27.6	8.4	0.0	0.0	0.1			
2018/11/9	8	244.7	122.3	0.0	0.0	13.2	10.1	35.1	6.1	39.0%	5.8	27.6	8.5	0.0	0.0	0.0	7.8	830.0	690.0
2018/11/12	11	240.1	120.0	0.0	0.0	13.3	9.4	37.2	5.9	37.6%	5.3	27.9	8.2	0.0	0.0	0.0	7.9	950.0	780.0
2018/11/15	14	233.6	116.8	0.0	0.0	12.8	8.5	41.9	3.3	61.1%	6.5	28.0	9.3	0.0	0.0	0.1	8.0	1040.0	830.0
2018/11/19	18	228.4	114.2	0.0	0.0	11.5	6.4	45.8	4.3	32.1%	5.0	27.9	8.1	0.0	0.0	0.1	8.0	1020.0	730.0
2018/11/23	22	249.1	124.5	0.0	0.0	12.9	8.6	45.9	3.6	58.7%	6.0	27.8	6.5	0.0	0.0	0.0	8.0	1000.0	740.0
2018/11/26	25	237.2	118.6	0.0	0.0	12.3	8.0	37.1	0.8	90.5%	7.1	28.0	8.6	0.1	0.0	0.0	8.1		
2018/11/29	28	216.5	108.2	0.0	0.0	11.4	10.4	40.8	2.3	77.7%	6.6	27.9	5.8	0.1	0.0	0.3	8.1	900.0	670.0

Appendix A

2018/12/5	34	242.4	121.2	0.0	0.0	11.6	6.4	47.0	3.6	43.6%	3.9	27.5	5.7	0.0	0.0	0.1	8.2	990.0	700.0
2018/12/11	40	250.0	125.0	0.0	0.0	13.3	8.9	51.9	1.0	88.4%	5.4	27.3	3.4	0.0	0.0	0.0	8.4		
2018/12/14	43	239.2	119.6	0.0	0.0	12.6	7.3	54.9	0.4	94.6%	3.9	27.2	3.3	0.0	0.0	0.0	7.8	1530	1070
2018/12/17	46	249.9	124.9	0.0	0.0	12.3	7.1	54.3	1.1	83.9%	4.0	27.5	4.3	0.0	0.0	0.0	8.0	1400.0	1030.0
2018/12/21	50	261.6	130.8	0.0	0.0	12.5	7.3	52.5	3.0	58.8%	3.6	27.3	4.9	0.0	0.0	0.0	7.9	1140.0	760.0
2018/12/25	54	238.2	119.1	0.0	0.0	11.9	7.0	51.6	3.1	55.8%	4.5	27.3	6.7	0.0	0.0	0.1		1160.0	780.0
2019/1/1	61	250.0	125.0	0.0	0.0	13.5	9.4	48.6	2.7	71.6%	2.3	27.3	2.2	0.0	0.0	0.0		960.0	640.0
2019/1/4	64	247.8	123.9	0.0	0.0	13.4	7.6	45.6	1.4	81.2%	6.5	27.6	7.6	0.0	0.0	0.0	7.9		
2019/1/8	68	244.0	122.0	0.0	0.0	14.0	7.5	46.6	2.8	62.1%	5.8	28.3	8.8	0.0	0.0	0.0		940.0	620.0
2019/1/11	71	241.0	120.5	0.0	0.0	13.4	7.9	46.8	1.9	76.5%	6.2	27.3	8.1	0.0	0.0	0.0	8.2	1080.0	720.0
2019/1/15	75	244.6	122.3	0.0	0.0	13.7	8.3	47.6	3.6	56.6%	6.4	27.2	9.6	0.0	0.0	0.0	8.0	920.0	620.0
EE2		HAc (mg L^{-1})					PO_4^{3-}-P (mg L^{-1})			Removal rate	NO_3^--N (mg L^{-1})			NO_2^--N (mg L^{-1})					
Date	Day	feedstock	Ana	Ano	E	feedstock	Ana	Ano	E		Ana	Ano	E	Ana	Ano	E	pH	MLSS&MLVSS (mg L^{-1})	
2018/11/1	0	246.4	123.2	0.0	0.0	12.7	11.6	31.2	11.4	1.8%	4.9	27.6	6.1	2.7	0.0	0.1		637.5	532.5
2018/11/4	3	232.7	116.4	0.0	0.0	12.8	9.7	27.7	8.0	17.8%	4.2	27.6	5.1	0.1	0.0	0.1			
2018/11/9	8	244.7	122.3	0.0	0.0	13.2	10.9	35.2	8.6	21.3%	4.9	27.3	6.6	0.0	0.0	0.1	7.8	870.0	720.0
2018/11/12	11	240.1	120.0	0.0	0.0	13.3	8.5	38.4	6.9	19.3%	3.8	27.6	5.4	0.0	0.0	0.0	7.9	320.0	260.0
2018/11/15	14	233.6	116.8	0.0	0.0	12.8	7.5	44.8	4.5	39.7%	4.0	27.7	5.0	0.0	0.0	0.0	8.0	1140.0	910.0
2018/11/19	18	228.4	114.2	0.0	0.0	11.5	6.0	49.1	3.5	41.5%	2.3	27.5	3.3	0.0	0.0	0.0	8.2	1200.0	880.0
2018/11/23	22	249.1	124.5	0.0	0.0	12.9	6.4	48.4	3.0	53.8%	3.8	27.5	3.8	0.0	0.0	0.1	7.9	1250.0	910.0
2018/11/26	25	237.2	118.6	0.0	0.0	12.3	7.2	40.6	1.3	81.8%	6.2	27.8	5.9	0.0	0.0	0.0	8.1		
2018/11/29	28	216.5	108.2	0.0	0.0	11.4	9.3	43.3	2.4	74.6%	5.4	27.9	3.3	0.1	0.0	0.5	8.1	1110	850
2018/12/5	34	242.4	121.2	0.0	0.0	11.6	6.2	44.8	5.1	17.4%	4.2	27.6	5.6	0.0	0.0	0.1	7.9	1160.0	870.0
2018/12/11	40	250.0	125.0	0.0	0.0	13.3	9.9	44.6	2.5	74.9%	5.9	27.6	4.4	0.0	0.0	0.1	8.2		
2018/12/14	43	239.2	119.6	0.0	0.0	12.6	7.7	50.4	2.3	69.9%	3.6	27.6	2.6	0.0	0.0	0.0	7.7	1540.0	1140.0
2018/12/17	46	249.9	124.9	0.0	0.0	12.3	6.9	49.2	2.4	65.1%	4.7	27.8	4.3	0.0	0.0	0.1	8.0	1280.0	1000.0
2018/12/21	50	261.6	130.8	0.0	0.0	12.5	6.9	47.4	2.4	64.9%	4.2	27.7	5.9	0.0	0.0	0.0	7.8	1120.0	780.0
2018/12/25	54	238.2	119.1	0.0	0.0	11.9	7.2	51.2	4.3	40.0%	4.4	27.7	6.0	0.0	0.0	0.0		1400.0	940.0

Appendix A

2019/1/1	61	250.0	125.0	0.0	0.0	13.5	7.3	46.4	0.1	98.3%	6.6	27.7	5.3	0.0	0.0	0.0		1420.0	910.0
2019/1/4	64	247.8	123.9	0.0	0.0	13.4	7.7	47.2	0.1	99.2%	6.2	27.9	8.4	0.0	0.0	0.0	7.9		
2019/1/8	68	244.0	122.0	0.0	0.0	14.0	7.4	52.6	2.1	71.1%	5.3	27.9	7.8	0.0	0.0	0.0		1520.0	960.0
2019/1/11	71	241.0	120.5	0.0	0.0	13.4	7.8	49.6	1.0	87.1%	6.0	27.9	7.4	0.0	0.0	0.0	8.2	1540.0	990.0
2019/1/15	75	244.6	122.3	0.0	0.0	13.7	8.0	49.4	2.3	71.6%	6.2	28.1	8.9	0.0	0.0	0.0	7.9	1550.0	980.0
EE3		HAc (mg L^{-1})					PO_4^{3-}-P (mg L^{-1})			Removal rate	NO_3^--N (mg L^{-1})			NO_2^--N (mg L^{-1})					
Date	Day	feedstock	Ana	Ano	E	feedstock	Ana	Ano	E		Ana	Ano	E	Ana	Ano	E	pH	MLSS&MLVSS (mg L^{-1})	
2018/11/1	0	246.1	123.1	0.0	0.0	12.4	10.2	21.6	7.4	27.5%	1.3	0.0	0.0	4.8	46.4	12.0		637.5	532.5
2018/11/4	3	254.3	127.2	37.6	0.0	12.7	10.3	19.9	8.3	19.3%	1.5	0.0	0.1	10.3	46.4	16.1			
2018/11/9	8	251.0	125.5	18.3	0.0	11.7	9.8	22.0	8.9	9.5%	1.6	0.0	0.0	10.8	46.2	21.4	8.0	530.0	430.0
2018/11/12	11	237.8	118.9	15.3	0.0	13.4	11.1	20.8	9.5	14.9%	1.5	0.0	0.0	11.5	46.6	22.9	7.8	270.0	230.0
2018/11/15	14	224.8	112.4	21.3	0.0	11.6	9.7	22.3	7.8	20.4%	2.2	0.0	0.0	7.7	47.2	15.1	8.0	380.0	320.0
2018/11/19	18	227.2	113.6	0.0	0.0	12.2	7.9	26.6	6.4	19.2%	2.1	0.0	0.4	5.4	46.6	13.3	7.7	450.0	340.0
2018/11/23	22	243.2	121.6	0.0	0.0	12.7	7.5	36.3	3.8	50.2%	2.1	0.0	0.0	4.7	46.6	8.0	7.9	560.0	430.0
2018/11/26	25	231.7	115.9	0.0	0.0	12.5	8.7	31.1	3.5	59.1%	2.2	0.0	0.0	8.7	47.3	12.7	7.7		
2018/11/29	28	240.7	120.4	0.0	0.0	11.5	8.5	34.9	3.1	63.9%	2.0	0.0	3.3	7.6	47.2	9.3	7.8	480	370
2018/12/5	34	247.3	123.6	0.0	0.0	11.9	6.2	40.0	4.2	32.7%	2.1	0.0	0.0	2.8	46.9	8.4	7.9	640.0	500.0
2018/12/11	40	241.1	120.6	0.0	0.0	13.0	8.9	37.4	2.7	69.2%	2.1	0.0	0.0	7.6	46.9	8.3	7.9		
2018/12/14	43	247.5	123.7	0.0	0.0	12.8	6.3	51.5	0.3	95.1%	2.1	0.0	0.0	0.3	47.0	0.1	7.8	1830.0	1380.0
2018/12/17	46	261.5	130.7	0.0	0.0	12.5	6.4	49.7	0.5	91.5%	2.2	0.0	0.1	2.0	47.1	5.6	7.8	1390.0	1100.0
2018/12/21	50	247.8	123.9	0.0	0.0	12.3	6.1	50.6	0.7	88.2%	2.0	0.0	0.1	1.5	47.0	4.9	8.1	1200.0	810.0
2018/12/25	54	242.8	121.4	0.0	0.0	11.8	6.3	51.8	0.8	87.0%	2.0	0.0	0.1	1.6	47.0	7.9		1370.0	920.0
2019/1/1	61	250.0	125.0	0.0	0.0	13.8	6.5	53.2	0.1	98.4%	2.3	0.0	0.1	4.4	47.3	6.4		1310.0	810.0
2019/1/4	64	234.4	117.2	0.0	0.0	12.7	6.4	58.5	0.1	98.5%	2.3	0.0	0.0	3.3	47.5	8.7	7.7		
2019/1/8	68	245.3	122.7	0.0	0.0	13.5	6.8	59.0	0.0	100.0%	2.4	0.0	0.1	0.9	47.4	4.0		1600.0	1030.0
2019/1/11	71	238.0	119.0	0.0	0.0	13.4	6.7	58.2	0.1	98.4%	2.3	0.0	0.1	2.5	47.6	7.0	8.3	1530.0	920.0
2019/1/15	75	235.1	117.5	0.0	0.0	13.8	6.9	59.7	0.2	96.7%	2.6	0.0	0.0	2.2	47.7	5.0	7.8	1410.0	860.0
EE4		HAc (mg L^{-1})					PO_4^{3-}-P (mg L^{-1})				NO_3^--N (mg L^{-1})			NO_2^--N (mg L^{-1})					

Appendix A

Date	Day	feedstock	Ana	Ano	E	feedstock	Ana	Ano	E	Removal rate	Ana	Ano	E	Ana	Ano	E	pH	MLSS&MLVSS (mg L^{-1})	
2018/11/1	0	246.1	123.1	38.7	0.0	12.4	14.6	20.2	11.8	19.4%	1.3	0.0	0.0	2.7	47.9	3.8		637.5	532.5
2018/11/4	3	254.3	127.2	48.3	0.0	12.7	10.8	19.4	6.4	41.2%	1.5	0.0	0.1	7.3	47.9	9.1			
2018/11/9	8	251.0	125.5	8.7	0.0	13.2	9.8	26.2	8.2	16.8%	1.6	0.0	0.0	10.8	47.2	20.9	7.7	660.0	530.0
2018/11/12	11	237.8	118.9	14.5	0.0	13.4	11.7	27.2	8.5	27.2%	1.5	0.0	0.0	10.0	47.7	19.4	7.8	530.0	430.0
2018/11/15	14	224.8	112.4	17.7	0.0	11.6	9.3	28.4	6.3	31.6%	2.2	0.0	0.0	7.0	48.0	13.8	7.9	460.0	380.0
2018/11/19	18	227.2	113.6	0.0	0.0	12.2	10.2	26.7	8.9	12.7%	2.1	0.0	0.0	6.1	47.4	14.4	7.8	240.0	150.0
2018/11/23	22	243.2	121.6	0.0	0.0	12.7	9.1	37.4	4.3	52.9%	2.1	0.0	0.0	5.5	47.1	8.8	7.8	570.0	430.0
2018/11/26	25	231.7	115.9	0.0	0.0	12.5	8.9	36.8	1.7	80.6%	2.1	0.0	0.0	7.6	47.7	9.7	7.8		
2018/11/29	28	240.7	120.4	0.0	0.0	11.5	9.1	37.5	1.9	78.7%	2.0	0.0	0.2	5.7	47.7	6.9	7.9	600	470
2018/12/5	34	247.3	123.6	0.0	0.0	11.9	7.4	39.3	2.6	64.9%	2.1	0.0	0.0	3.2	47.4	6.3	7.9	530.0	400.0
2018/12/11	40	241.1	120.6	0.0	0.0	13.0	8.8	47.6	2.7	69.5%	2.1	0.0	0.0	5.3	47.2	4.8	7.7		
2018/12/14	43	247.5	123.7	0.0	0.0	12.8	7.2	53.0	0.0	100.0%	2.1	0.0	0.0	1.4	47.1	1.8	7.9	1800.0	1120.0
2018/12/17	46	261.5	130.7	0.0	0.0	12.5	7.8	55.1	1.2	84.8%	2.1	0.0	0.1	1.8	47.4	3.1	7.7	1650.0	1250.0
2018/12/21	50	247.8	123.9	0.0	0.0	12.3	6.0	48.2	3.0	50.0%	2.0	0.0	0.1	0.1	47.3	5.0	7.7	1390.0	940.0
2018/12/25	54	242.8	121.4	0.0	0.0	11.8	6.1	48.6	5.5	9.2%	2.0	0.0	0.1	1.4	47.3	9.5		1400.0	1040.0
2019/1/1	61	250.0	125.0	0.0	0.0	13.8	12.6	40.4	0.0	99.9%	2.3	0.0	0.0	10.0	47.7	0.0		1210.0	870.0
2019/1/4	64	234.4	117.2	0.0	0.0	12.7	9.7	59.9	1.4	85.7%	2.3	0.0	0.0	3.0	47.5	6.1	7.9		
2019/1/8	68	245.3	122.7	0.0	0.0	13.5	9.2	52.0	0.0	100.0%	2.4	0.0	0.0	4.4	47.3	10.4		1120.0	760.0
2019/1/11	71	238.0	119.0	0.0	0.0	13.4	6.7	48.0	0.0	100.0%	2.2	0.0	0.1	0.3	47.2	2.1	8.0	1180.0	830.0
2019/1/15	75	235.1	117.5	0.0	0.0	13.8	6.9	49.4	2.3	67.1%	2.6	0.0	0.1	2.0	47.3	4.5	7.7	1080.0	730.0
EE5		HAc (mg L^{-1})					PO_4^{3-}-P (mg L^{-1})			Removal rate	NO_3^--N (mg L^{-1})			NO_2^--N (mg L^{-1})					
Date	Day	feedstock	Ana	Ano	E	feedstock	Ana	Ano	E		Ana	Ano	E	Ana	Ano	E	pH	MLSS&MLVSS (mg L^{-1})	
2018/11/1	0	226.5	113.3	14.4	0.0	12.3	12.4	18.5	10.5	15.5%	1.4	0.0	0.1	4.7	46.8	10.1		877.5	747.5
2018/11/4	3	241.0	120.5	35.9	0.0	12.7	10.5	18.7	8.5	19.1%	1.5	0.0	0.1	8.0	46.8	13.7			
2018/11/9	8	245.7	122.9	9.6	0.0	13.4	11.9	23.3	9.6	18.8%	1.6	0.0	0.0	9.6	46.4	18.6	7.9	550.0	430.0
2018/11/12	11	235.1	117.5	0.0	0.0	12.8	10.7	23.6	9.5	11.2%	1.5	0.0	0.1	9.7	46.9	19.0	7.8	550.0	470.0

Appendix A

2018/11/15	14	215.8	107.9	0.0	0.0	12.2	11.2	25.5	8.7	22.6%	2.2	0.0	0.0	6.1	47.2	11.8	7.9	390.0	330.0
2018/11/19	18	213.8	106.9	0.0	0.0	11.3	7.5	29.7	5.0	32.6%	2.1	0.0	0.5	3.6	46.5	9.7	7.7	530.0	380.0
2018/11/23	22	247.1	123.6	0.0	0.0	12.5	7.0	43.2	1.7	75.6%	2.1	0.0	0.0	3.5	45.5	4.4	7.9	650.0	460.0
2018/11/26	25	227.3	113.7	0.0	0.0	11.8	7.1	39.6	0.4	94.4%	2.2	0.0	0.2	6.6	46.4	8.0	8.0		
2018/11/29	28	221.8	110.9	0.0	0.0	10.5	12.7	41.5	4.4	65.7%	2.0	0.0	0.0	6.4	46.7	5.4	7.9	620	480
2018/12/5	34	262.3	131.2	0.0	0.0	11.5	7.9	48.4	0.1	99.0%	2.1	0.0	0.0	1.3	45.8	1.5	7.7	850.0	640.0
2018/12/11	40	236.3	118.1	0.0	0.0	13.2	11.2	53.8	0.4	96.0%	2.1	0.0	0.0	4.5	46.0	1.0	7.8		
2018/12/14	43	237.1	118.5	0.0	0.0	12.5	7.8	50.9	0.0	100.0%	2.1	0.0	0.0	0.0	45.6	0.0	7.9	1940.0	1250.0
2018/12/17	46	238.2	119.1	0.0	0.0	12.4	9.1	55.8	0.5	94.5%	2.1	0.0	0.1	1.6	45.2	0.1	7.7	1770.0	1280.0
2018/12/21	50	238.9	119.5	0.0	0.0	12.0	7.8	57.5	0.0	100.0%	2.0	0.0	0.1	0.9	45.1	0.0	7.7	1500.0	970.0
2018/12/25	54	233.9	117.0	0.0	0.0	12.3	6.1	54.8	0.2	97.0%	2.0	0.0	0.1	1.5	45.1	0.2		1520.0	1050.0
2019/1/1	61	250.0	125.0	0.0	0.0	13.4	6.5	42.5	0.3	95.6%	2.3	0.0	0.1	0.6	47.3	1.2	7.0	1180.0	800.0
2019/1/4	64	233.3	116.6	0.0	0.0	13.3	9.1	41.2	0.7	92.7%	2.3	0.0	0.1	3.4	41.5	7.2	7.2		
2019/1/8	68	242.9	121.5	0.0	0.0	13.4	7.0	51.2	1.6	77.7%	2.5	0.0	0.1	5.3	45.9	11.5		1060.0	700.0
2019/1/11	71	238.4	119.2	0.0	0.0	13.4	9.0	38.6	7.9	12.1%	2.3	0.0	0.1	5.5	46.3	12.7	7.1	1000.0	710.0
2019/1/15	75	239.9	120.0	0.0	0.0	13.8	9.4	37.2	10.9	-15.2%	2.6	0.0	0.1	4.7	46.0	15.3	7.2	920.0	660.0
EE6		HAc (mg L^{-1})					PO_4^{3-}-P (mg L^{-1})			Removal rate	NO_3^--N (mg L^{-1})			NO_2^--N (mg L^{-1})					
Date	Day	feedstock	Ana	Ano	E	feedstock	Ana	Ano	E		Ana	Ano	E	Ana	Ano	E	pH	MLSS&MLVSS (mg L^{-1})	
2018/11/1	0	226.5	113.3	30.4	0.0	12.3	11.9	18.6	10.4	12.3%	1.4	0.0	0.2	1.4	44.8	5.5		877.5	747.5
2018/11/4	3	241.0	120.5	43.7	0.0	12.7	10.4	19.3	8.2	20.9%	1.5	0.0	0.1	6.3	44.8	9.2			
2018/11/9	8	245.7	122.9	0.0	0.0	13.4	10.7	28.7	6.8	36.4%	1.6	0.0	0.0	6.1	44.5	12.9	7.9	740.0	600.0
2018/11/12	11	235.1	117.5	0.0	0.0	12.8	9.4	32.9	6.8	27.0%	1.5	0.0	0.1	7.7	45.1	14.3	7.9	650.0	500.0
2018/11/15	14	215.8	107.9	0.0	0.0	12.2	9.1	35.0	6.1	32.8%	2.2	0.0	0.0	4.0	45.1	7.5	7.8	550.0	440.0
2018/11/19	18	213.8	106.9	0.0	0.0	11.3	9.0	41.6	5.3	41.0%	2.1	0.0	0.0	2.3	44.6	5.2	8.0	590.0	410.0
2018/11/23	22	247.1	123.6	0.0	0.0	12.5	7.5	49.1	3.5	53.4%	2.1	0.0	0.0	2.8	44.6	3.3	7.9	550.0	360.0
2018/11/26	25	227.3	113.7	0.0	0.0	11.8	9.9	43.2	2.5	74.5%	2.2	0.0	0.1	5.2	45.3	10.1	7.8		
2018/11/29	28	221.8	110.9	0.0	0.0	10.5	9.7	42.1	1.2	87.3%	2.0	0.0	0.4	6.2	45.5	7.9	7.8	320	250
2018/12/5	34	262.3	131.2	0.0	0.0	11.5	9.7	47.4	0.7	93.1%	2.1	0.0	0.0	2.9	45.2	7.8	7.9	290.0	230.0

Appendix A

2018/12/11	40	236.3	118.1	0.0	0.0	13.2	8.8	55.2	0.4	95.6%	2.2	0.0	0.0	3.5	45.5	3.3	8.2		
2018/12/14	43	237.1	118.5	0.0	0.0	12.5	7.0	53.9	0.0	100.0%	2.1	0.0	0.0	0.0	45.3	0.0	7.8	1820.0	1350.0
2018/12/17	46	238.2	119.1	0.0	0.0	12.4	7.1	58.4	1.7	76.5%	2.1	0.0	0.1	0.9	45.6	1.6	7.7	1980.0	1480.0
2018/12/21	50	238.9	119.5	0.0	0.0	12.0	6.4	56.7	1.4	77.8%	1.9	0.0	0.0	0.0	45.5	0.1	7.7	1670.0	1130.0
2018/12/25	54	233.9	117.0	0.0	0.0	12.3	6.6	64.3	2.1	68.6%	2.0	0.0	0.2	0.0	45.5	0.1		1550.0	1020.0
2019/1/1	61	250.0	125.0	0.0	0.0	13.4	6.6	58.0	0.3	95.3%	2.3	0.0	0.1	1.5	47.7	1.1		1490.0	940.0
2019/1/4	64	233.3	116.6	0.0	0.0	13.3	7.2	59.7	1.0	86.1%	2.3	0.0	0.0	1.7	45.7	2.8	8.1		
2019/1/8	68	242.9	121.5	0.0	0.0	13.4	7.4	64.5	1.2	83.6%	2.4	0.0	0.1	0.7	46.1	3.1		1340.0	810.0
2019/1/11	71	238.4	119.2	0.0	0.0	13.4	7.9	65.2	1.3	83.9%	2.2	0.0	0.1	0.7	45.8	1.4	8.1	1610.0	940.0
2019/1/15	75	239.9	120.0	0.0	0.0	13.8	11.1	71.7	0.9	92.2%	2.5	0.0	0.1	2.9	47.3	4.1	8.1	1550.0	940.0
EE7		HAc (mg L^{-1})					PO_4^{3-}-P (mg L^{-1})			Removal rate	NO_3^--N (mg L^{-1})			NO_2^--N (mg L^{-1})					
Date	Day	feedstock	Ana	Ano	E	feedstock	Ana	Ano	E		Ana	Ano	E	Ana	Ano	E	pH	MLSS&MLVSS (mg L^{-1})	
2018/11/1	0	252.7	126.3	0.0	0.0	12.8	10.7	32.5	11.0	-2.5%	4.3	30.2	7.4	0.1	0.0	0.1		877.5	747.5
2018/11/4	3	255.0	127.5	14.1	0.0	13.2	10.7	28.8	9.1	15.3%	5.1	30.2	6.2	0.0	0.0	0.1			
2018/11/9	8	250.0	125.0	0.0	0.0	13.6	11.6	31.0	9.9	15.1%	5.2	27.4	6.7	0.0	0.0	0.0	7.9	500.0	400.0
2018/11/12	11	246.1	123.1	25.2	0.0	14.1	13.2	24.3	14.6	-10.9%	4.4	27.6	6.2	0.0	0.0	0.0	7.8	160.0	120.0
2018/11/15	14	222.5	111.3	12.8	0.0	11.5	11.5	22.6	11.8	-3.2%	5.1	28.0	7.4	0.0	0.0	0.0	7.9	390.0	350.0
2018/11/19	18	242.1	121.0	0.0	0.0	12.3	10.3	24.3	11.1	-7.6%	3.9	27.6	5.8	0.0	0.0	0.1	8.0	480.0	380.0
2018/11/23	22	257.3	128.7	0.0	0.0	13.3	10.6	30.8	10.2	4.5%	3.8	27.5	3.3	0.0	0.0	0.1	8.0	750.0	620.0
2018/11/26	25	240.7	120.4	0.0	0.0	12.8	10.1	29.1	5.6	44.4%	5.9	27.8	5.2	0.1	0.0	0.1	8.0		
2018/11/29	28	243.1	121.5	0.0	0.0	11.9	10.1	32.4	5.9	41.7%	5.5	27.9	4.1	0.1	0.0	0.3	8.1	760	630
2018/12/5	34	248.0	124.0	0.0	0.0	11.5	8.3	40.2	8.0	3.4%	3.4	27.9	4.9	0.0	0.0	0.1	8.1	1000.0	780.0
2018/12/11	40	254.3	127.1	0.0	0.0	13.4	10.4	42.6	5.2	50.0%	4.4	27.8	2.8	0.0	0.0	0.1	8.3		
2018/12/14	43	265.2	132.6	0.0	0.0	13.3	9.5	48.0	7.1	25.3%	3.7	27.8	4.2	0.0	0.0	0.1	7.8	1890.0	1560.0
2018/12/17	46	257.7	128.9	0.0	0.0	12.2	8.3	48.7	6.4	23.6%	4.0	28.0	5.0	0.0	0.0	0.1	7.9	1790.0	1400.0
2018/12/21	50	260.0	130.0	0.0	0.0	12.7	8.0	51.5	7.7	3.4%	3.2	27.9	4.4	0.1	0.0	0.1	7.8	1430.0	1120.0
2018/12/25	54	253.6	126.8	0.0	0.0	12.5	7.6	56.2	14.2	-87.0%	2.8	27.9	2.9	0.0	0.0	0.1		1600.0	1210.0
2019/1/1	61	250.0	125.0	0.0	0.0	14.0	10.0	51.3	4.4	55.5%	5.4	27.3	3.6	0.0	0.0	0.1		1240.0	910.0

Appendix A

2019/1/4	64	235.1	117.5	0.0	0.0	13.1	9.9	53.8	7.1	28.3%	5.5	28.7	6.7	0.0	0.0	0.0	8.0		
2019/1/8	68	250.3	125.1	0.0	0.0	14.2	8.3	54.4	10.6	-27.4%	4.4	28.5	7.9	0.0	0.0	0.0		1430.0	1030.0
2019/1/11	71	240.6	120.3	0.0	0.0	13.7	9.3	54.3	5.8	37.0%	4.7	28.5	5.9	0.0	0.0	0.1	8.1	1500.0	1090.0
2019/1/15	75	232.6	116.3	0.0	0.0	14.0	10.8	56.0	11.1	-2.9%	4.5	28.5	8.5	0.0	0.0	0.0	7.8	1400.0	1010.0
EE8		HAc (mg L^{-1})					PO_4^{3-}-P (mg L^{-1})			Removal rate	NO_3^--N (mg L^{-1})			NO_2^--N (mg L^{-1})					
Date	Day	feedstock	Ana	Ano	E	feedstock	Ana	Ano	E		Ana	Ano	E	Ana	Ano	E	pH	MLSS&MLVSS (mg L^{-1})	
2018/11/1	0	252.7	126.3	34.5	0.0	12.8	12.5	27.3	13.1	-4.7%	1.4	24.4	0.5	0.0	0.0	0.1		877.5	747.5
2018/11/4	3	255.0	127.5	46.7	0.0	13.2	11.7	24.2	12.4	-6.3%	2.4	24.4	1.2	0.0	0.0	0.1			
2018/11/9	8	250.0	125.0	46.6	0.0	13.6	12.1	19.5	11.6	4.5%	1.7	26.8	0.1	0.0	0.0	0.1	7.7	550.0	490.0
2018/11/12	11	246.1	123.1	37.2	0.0	14.1	11.8	22.1	11.3	3.8%	3.0	27.2	3.5	0.0	0.0	0.0	7.9	540.0	470.0
2018/11/15	14	222.5	111.3	26.0	0.0	11.5	11.1	23.0	10.7	3.9%	3.7	25.7	3.9	0.0	0.0	0.0	7.9	470.0	440.0
2018/11/19	18	242.1	121.0	0.0	0.0	12.3	10.7	24.4	10.5	1.3%	2.7	25.0	3.3	0.0	0.0	0.0	7.9	500.0	410.0
2018/11/23	22	257.3	128.7	0.0	0.0	13.3	11.1	28.8	9.4	15.1%	2.9	25.3	2.1	0.0	0.0	0.1	7.9	580.0	460.0
2018/11/26	25	240.7	120.4	0.0	0.0	12.8	10.1	27.7	7.5	26.4%	4.0	26.4	3.3	0.0	0.0	0.0	7.9		
2018/11/29	28	243.1	121.5	0.0	0.0	11.9	10.8	28.1	9.3	13.9%	3.5	26.6	1.8	0.0	0.0	0.1	7.9	530.0	440.0
2018/12/5	34	248.0	124.0	0.0	0.0	11.5	11.3	27.5	11.9	-4.8%	2.5	26.0	2.3	0.0	0.0	0.1	7.9	390.0	320.0
2018/12/11	40	254.3	127.1	0.0	0.0	13.4	8.9	24.6	7.9	11.6%	2.1	27.3	0.1	0.0	0.0	0.0	8.1		
2018/12/14	43	265.2	132.6	0.0	0.0	13.3	7.7	33.2	1.8	76.3%	2.1	26.8	0.6	0.0	0.0	0.0	7.7	1420	1250
2018/12/17	46	257.7	128.9	0.0	0.0	12.2	8.7	44.5	5.4	38.5%	2.3	26.9	1.1	0.0	0.0	0.1	7.9	1070.0	840.0
2018/12/21	50	260.0	130.0	0.0	0.0	12.7	9.8	55.1	4.4	55.2%	2.0	26.4	0.0	0.0	0.0	0.0	7.8	2130.0	1660.0
2018/12/25	54	253.6	126.8	0.0	0.0	12.5	8.4	61.7	2.8	66.7%	2.0	26.4	0.2	0.0	0.0	0.0		1410.0	1020.0
2019/1/1	61	250.0	125.0	0.0	0.0	14.0	8.2	61.4	2.1	73.9%	3.8	27.7	1.2	0.0	0.0	0.0		1580.0	1010.0
2019/1/4	64	235.1	117.5	0.0	0.0	13.1	8.7	65.3	3.3	62.2%	3.4	27.1	2.6	0.0	0.0	0.0	7.9		
2019/1/8	68	250.3	125.1	0.0	0.0	14.2	8.4	65.6	3.6	56.5%	3.0	27.0	3.1	0.0	0.0	0.0		1570.0	1000.0
2019/1/11	71	240.6	120.3	0.0	0.0	13.7	8.7	66.3	4.2	52.2%	2.9	26.6	2.2	0.0	0.0	0.0	8.0	1840.0	1160.0
2019/1/15	75	232.6	116.3	0.0	0.0	14.0	10.8	68.0	6.9	35.8%	2.8	26.1	2.4	0.0	0.0	0.0	7.9	1390.0	900.0

d. Performance of dosing strategies and pH

H1		HAc (mg L^{-1})					PO_4^{3-}-P (mg L^{-1})			Removal rate	NO_3^--N (mg L^{-1})			NO_2^--N (mg L^{-1})					
Date	Day	feedstock	Ana	Ano	E	feedstock	Ana	Ano	E		Ana	Ano	E	Ana	Ano	E	pH	MLSS&MLVSS (mg L^{-1})	
2018/12/5	0	262.3	131.2	0.0	0.0	11.5	7.9	48.4	0.1	99.0%	2.1	0.0	0.0	1.3	45.8	1.5	7.7	850.0	640.0
2018/12/11	6	236.3	118.1	0.0	0.0	13.2	11.2	53.8	0.4	96.0%	2.1	0.0	0.0	4.5	46.0	1.0	7.8		
2018/12/14	9	237.1	118.5	0.0	0.0	12.5	7.8	50.9	0.0	100.0%	2.1	0.0	0.0	0.0	45.6	0.0	7.9	1940.0	1250.0
2018/12/17	12	238.2	119.1	0.0	0.0	12.4	9.1	55.8	0.5	94.5%	2.1	0.0	0.1	1.6	45.2	0.1	7.7	1770.0	1280.0
2018/12/21	16	238.9	119.5	0.0	0.0	12.0	7.8	57.5	0.0	100.0%	2.0	0.0	0.1	0.9	45.1	0.0	7.7	1500.0	970.0
2018/12/25	20	233.9	117.0	0.0	0.0	12.3	6.1	54.8	0.2	97.0%	2.0	0.0	0.1	1.5	45.1	0.2		1520.0	1050.0
2019/1/1	27	250.0	125.0	0.0	0.0	13.4	6.5	42.5	0.3	95.6%	2.3	0.0	0.1	0.6	47.3	1.2	7.0	1180.0	800.0
2019/1/4	30	233.3	116.6	0.0	0.0	13.3	9.1	41.2	0.7	92.7%	2.3	0.0	0.1	3.4	41.5	7.2	7.2		
2019/1/8	34	242.9	121.5	0.0	0.0	13.4	7.0	51.2	1.6	77.7%	2.5	0.0	0.1	5.3	45.9	11.5		1060.0	700.0
2019/1/11	37	238.4	119.2	0.0	0.0	13.4	9.0	38.6	7.9	12.1%	2.3	0.0	0.1	5.5	46.3	12.7	7.1	1000.0	710.0
2019/1/15	41	239.9	120.0	0.0	0.0	13.8	9.4	37.2	10.9	-15.2%	2.6	0.0	0.1	4.7	46.0	15.3	7.2	920.0	660.0
2019/1/16	42	227.5	113.7	0.0	0.0	12.5	7.6	34.5	11.2	-47.7%	2.4	0.0	0.1	4.3	45.3	13.5			
2019/1/18	44	253.6	126.8	0.0	0.0	12.6	9.2	29.3	6.8	26.7%	2.6	0.0	0.0	5.4	44.6	11.6	back to 7.5-8.0	950.0	690.0
2019/1/22	48	251.7	125.8	0.0	0.0	13.2	6.6	35.6	1.4	79.0%	2.5	0.0	0.1	2.1	44.6	8.3		900.0	660.0

2019/1/25	51	245.0	122.5	0.0	0.0	13.1	7.4	40.1	1.0	86.5%	2.3	0.0	0.1	7.2	46.7	14.6		690.0	470.0
2019/1/30	56	229.5	114.7	0.0	0.0	11.8	6.4	40.5	2.2	65.5%	2.4	0.0	0.4	5.0	46.0	12.9			
2019/2/1	58	234.3	117.2	0.0	0.0	12.4	6.8	36.9	4.0	41.6%	2.3	0.0	0.1	6.7	45.0	15.1		680.0	410.0
2019/2/7	64	226.3	113.1	0.0	0.0	11.9	12.2	52.1	1.5	87.3%	2.3	0.0	0.1	4.7	45.9	7.0		970.0	690.0
2019/2/12	69	235.8	117.9	0.0	0.0	11.7	10.0	51.1	0.3	96.9%	2.0	0.0	0.1	6.4	45.4	3.4		980.0	650.0
2019/2/15	72	239.2	119.6	0.0	0.0	12.5	6.3	47.7	0.0	100.0%	2.3	0.0	0.0	4.3	45.0	6.9			
2019/2/19	76	235.3	117.6	0.0	0.0	12.6	7.5	51.8	0.0	100.0%	2.7	0.0	0.1	4.0	45.7	2.8		1210.0	760.0
2019/2/22	79	231.6	115.8	0.0	0.0	12.8	6.4	52.4	4.6	27.0%	2.5	0.0	0.1	0.3	45.6	7.2		1230.0	800.0
2019/2/26	83	239.3	119.6	0.0	0.0	12.4	6.3	48.8	0.1	99.2%	2.5	0.0	0.0	2.2	44.5	0.0			
2019/2/28	85	243.0	121.5	0.0	0.0	11.4	5.7	46.9	0.0	100.0%	2.6	0.0	0.0	3.2	44.5	5.4			
2019/3/5	90	250.0	125.0	0.0	0.0	12.0	6.0	54.9	0.1	98.3%	2.6	0.0	0.2	2.6	45.0	3.0			
2019/3/7	92	250.0	125.0	0.0	0.0	11.6	6.5	63.7	0.5	92.9%	2.5	0.0	0.0	0.4	45.0	2.7			

e. Performance at different temperature (T1-T4)

T1		HAc (mg L^{-1})					PO_4^{3-}-P (mg L^{-1})			Removal rate	NO_3^--N (mg L^{-1})			NO_2^--N (mg L^{-1})					
Date	Day	feedstock	Ana	Ano	E	feedstock	Ana	Ano	E		Ana	Ano	E	Ana	Ano	E	pH	MLSS&MLVSS (mg L^{-1})	
2018/11/1	0	246.4	123.2	0.0	0.0	12.7	9.6	32.0	9.5	1.9%	5.3	27.6	8.9	0.0	0.0	0.0		637.5	532.5
2018/11/4	3	232.0	116.0	0.0	0.0	12.8	9.4	27.3	6.6	29.6%	6.1	27.6	8.4	0.0	0.0	0.1			
2018/11/9	8	244.7	122.3	0.0	0.0	13.2	10.1	35.1	6.1	39.0%	5.8	27.6	8.5	0.0	0.0	0.0	7.8	830.0	690.0
2018/11/12	11	240.1	120.0	0.0	0.0	13.3	9.4	37.2	5.9	37.6%	5.3	27.9	8.2	0.0	0.0	0.0	7.9	950.0	780.0

2018/11/15	14	233.6	116.8	0.0	0.0	12.8	8.5	41.9	3.3	61.1%	6.5	28.0	9.3	0.0	0.0	0.1	8.0	1040.0	830.0
2018/11/19	18	228.4	114.2	0.0	0.0	11.5	6.4	45.8	4.3	32.1%	5.0	27.9	8.1	0.0	0.0	0.1	8.0	1020.0	730.0
2018/11/23	22	249.1	124.5	0.0	0.0	12.9	8.6	45.9	3.6	58.7%	6.0	27.8	6.5	0.0	0.0	0.0	8.0	1000.0	740.0
2018/11/26	25	237.2	118.6	0.0	0.0	12.3	8.0	37.1	0.8	90.5%	7.1	28.0	8.6	0.1	0.0	0.0	8.1		
2018/11/29	28	216.5	108.2	0.0	0.0	11.4	10.4	40.8	2.3	77.7%	6.6	27.9	5.8	0.1	0.0	0.3	8.1	900.0	670.0
2018/12/5	34	242.4	121.2	0.0	0.0	11.6	6.4	47.0	3.6	43.6%	3.9	27.5	5.7	0.0	0.0	0.1	8.2	990.0	700.0
2018/12/11	40	250.0	125.0	0.0	0.0	13.3	8.9	51.9	1.0	88.4%	5.4	27.3	3.4	0.0	0.0	0.0	8.4		
2018/12/14	43	239.2	119.6	0.0	0.0	12.6	7.3	54.9	0.4	94.6%	3.9	27.2	3.3	0.0	0.0	0.0	7.8	1530.0	1070.0
2018/12/17	46	249.9	124.9	0.0	0.0	12.3	7.1	54.3	1.1	83.9%	4.0	27.5	4.3	0.0	0.0	0.0	8.0	1400.0	1030.0
2018/12/21	50	261.6	130.8	0.0	0.0	12.5	7.3	52.5	3.0	58.8%	3.6	27.3	4.9	0.0	0.0	0.0	7.9	1140.0	760.0
2018/12/25	54	238.2	119.1	0.0	0.0	11.9	7.0	51.6	3.1	55.8%	4.5	27.3	6.7	0.0	0.0	0.1		1160.0	780.0
2019/1/1	61	250.0	125.0	0.0	0.0	13.5	9.4	48.6	2.7	71.6%	2.3	27.3	2.2	0.0	0.0	0.0		960.0	640.0
2019/1/4	64	247.8	123.9	0.0	0.0	13.4	7.6	45.6	1.4	81.2%	6.5	27.6	7.6	0.0	0.0	0.0	7.9		
2019/1/8	68	244.0	122.0	0.0	0.0	14.0	7.5	46.6	2.8	62.1%	5.8	28.3	8.8	0.0	0.0	0.0		940.0	620.0
2019/1/11	71	241.0	120.5	0.0	0.0	13.4	7.9	46.8	1.9	76.5%	6.2	27.3	8.1	0.0	0.0	0.0	8.2	1080.0	720.0
2019/1/15	75	244.6	122.3	0.0	0.0	13.7	8.3	47.6	3.6	56.6%	6.4	27.2	9.6	0.0	0.0	0.0	8.0	920.0	620.0
2019/1/16	76	224.4	112.2	0.0	0.0	14.2	7.8	46.4	2.0	74.6%	6.3	27.2	6.9	0.0	0.0	0.1			
2019/1/18	78	247.7	123.9	0.0	0.0	12.4	8.2	48.0	4.4	46.7%	6.4	26.9	8.0	0.0	0.0	0.1		1030.0	670.0
2019/1/22	82	242.4	121.2	0.0	0.0	13.3	8.6	49.7	4.9	43.3%	6.8	27.5	9.0	0.0	0.0	0.0		1120.0	760.0
2019/1/25	85	246.2	123.1	0.0	0.0	13.2	9.1	49.4	3.1	65.6%	6.3	26.9	7.8	0.1	0.0	0.0		1080.0	700.0
2019/1/30	90	227.3	113.7	0.0	0.0	13.5	9.8	60.1	4.7	52.3%	6.1	27.6	7.7	0.1	0.0	0.4			
2019/2/1	92	236.0	118.0	0.0	0.0	12.5	8.3	55.9	3.8	54.9%	5.6	27.7	6.6	0.1	0.0	0.1		1160.0	800.0
2019/2/7	98	238.2	119.1	0.0	0.0	12.6	9.0	59.6	6.0	33.1%	5.8	27.9	6.4	0.0	0.0	0.1		1110.0	760.0
2019/2/12	103	229.2	114.6	0.0	0.0	12.0	8.0	56.9	2.9	63.5%	5.1	28.1	6.3	0.0	0.0	0.0		1030.0	730.0
2019/2/15	106	223.7	111.8	0.0	0.0	12.3	9.9	56.4	5.3	46.7%	6.1	28.5	6.4	0.0	0.0	0.1			
2019/2/19	110	229.3	114.6	0.0	0.0	12.4	9.1	56.0	3.9	57.3%	5.9	28.2	6.3	0.0	0.0	0.1		1070.0	750.0
2019/2/22	113	227.9	114.0	0.0	0.0	12.7	8.6	58.6	4.0	53.8%	5.4	28.6	6.6	0.0	0.0	0.1		1010.0	730.0
2019/2/26	117	254.7	127.3	0.0	0.0	12.2	9.6	54.5	5.1	46.5%	6.4	28.4	7.4	0.0	0.0	0.1			

Appendix A

2019/2/28	119	230.7	115.3	0.0	0.0	11.5	8.5	52.7	2.9	66.3%	6.6	28.4	8.0	0.0	0.0	0.1			
2019/3/5	124	250.0	125.0	0.0	0.0	12.3	9.3	53.0	3.6	61.1%	6.4	28.0	8.3	0.0	0.0	0.0			
2019/3/7	126	250.0	125.0	0.0	0.0	12.3	9.0	51.2	5.1	43.9%	6.3	28.0	8.6	0.0	0.0	0.0			
T2		HAc (mg L^{-1})					PO_4^{3-}-P (mg L^{-1})			Removal rate	NO_3^--N (mg L^{-1})			NO_2^--N (mg L^{-1})					
Date	Day	feedstock	Ana	Ano	E	feedstock	Ana	Ano	E		Ana	Ano	E	Ana	Ano	E	pH	MLSS&MLVSS (mg L^{-1})	
2018/11/1	0	246.4	123.2	0.0	0.0	12.7	11.6	31.2	11.4	1.8%	4.9	27.6	6.1	2.7	0.0	0.1		637.5	532.5
2018/11/4	3	232.7	116.4	15.4	0.0	12.8	9.7	27.7	8.0	17.8%	4.2	27.6	5.1	0.1	0.0	0.1			
2018/11/9	8	244.7	122.3	0.0	0.0	13.2	10.9	35.2	8.6	21.3%	4.9	27.3	6.6	0.0	0.0	0.1	7.8	870.0	720.0
2018/11/12	11	240.1	120.0	0.0	0.0	13.3	8.5	38.4	6.9	19.3%	3.8	27.6	5.4	0.0	0.0	0.0	7.9	320.0	260.0
2018/11/15	14	233.6	116.8	0.0	0.0	12.8	7.5	44.8	4.5	39.7%	4.0	27.7	5.0	0.0	0.0	0.0	8.0	1140.0	910.0
2018/11/19	18	228.4	114.2	0.0	0.0	11.5	6.0	49.1	3.5	41.5%	2.3	27.5	3.3	0.0	0.0	0.0	8.2	1200.0	880.0
2018/11/23	22	249.1	124.5	0.0	0.0	12.9	6.4	48.4	3.0	53.8%	3.8	27.5	3.8	0.0	0.0	0.1	7.9	1250.0	910.0
2018/11/26	25	237.2	118.6	0.0	0.0	12.3	7.2	40.6	1.3	81.8%	6.2	27.8	5.9	0.0	0.0	0.0	8.1		
2018/11/29	28	216.5	108.2	0.0	0.0	11.4	9.3	43.3	2.4	74.6%	5.4	27.9	3.3	0.1	0.0	0.5	8.1	1110	850
2018/12/5	34	242.4	121.2	0.0	0.0	11.6	6.2	44.8	5.1	17.4%	4.2	27.6	5.6	0.0	0.0	0.1	7.9	1160.0	870.0
2018/12/11	40	250.0	125.0	0.0	0.0	13.3	9.9	44.6	2.5	74.9%	5.9	27.6	4.4	0.0	0.0	0.1	8.2		
2018/12/14	43	239.2	119.6	0.0	0.0	12.6	7.7	50.4	2.3	69.9%	3.6	27.6	2.6	0.0	0.0	0.0	7.7	1540.0	1140.0
2018/12/17	46	249.9	124.9	0.0	0.0	12.3	6.9	49.2	2.4	65.1%	4.7	27.8	4.3	0.0	0.0	0.1	8.0	1280.0	1000.0
2018/12/21	50	261.6	130.8	0.0	0.0	12.5	6.9	47.4	2.4	64.9%	4.2	27.7	5.9	0.0	0.0	0.0	7.8	1120.0	780.0
2018/12/25	54	238.2	119.1	0.0	0.0	11.9	7.2	51.2	4.3	40.0%	4.4	27.7	6.0	0.0	0.0	0.0		1400.0	940.0
2019/1/1	61	250.0	125.0	0.0	0.0	13.5	7.3	46.4	0.1	98.3%	6.6	27.7	5.3	0.0	0.0	0.0		1420.0	910.0
2019/1/4	64	247.8	123.9	0.0	0.0	13.4	7.7	47.2	0.1	99.2%	6.2	27.9	8.4	0.0	0.0	0.0	7.9		
2019/1/8	68	244.0	122.0	0.0	0.0	14.0	7.4	52.6	2.1	71.1%	5.3	27.9	7.8	0.0	0.0	0.0		1520.0	960.0
2019/1/11	71	241.0	120.5	0.0	0.0	13.4	7.8	49.6	1.0	87.1%	6.0	27.9	7.4	0.0	0.0	0.0	8.2	1540.0	990.0
2019/1/15	75	244.6	122.3	0.0	0.0	13.7	8.0	49.4	2.3	71.6%	6.2	28.1	8.9	0.0	0.0	0.0	7.9	1550.0	980.0
2019/1/16	76	224.4	112.2	0.0	0.0	14.2	7.9	52.0	1.9	76.3%	5.7	27.9	5.5	0.0	0.0	0.1		1530.0	960.0
2019/1/18	78	247.7	123.9	0.0	0.0	12.4	9.8	51.0	8.7	11.1%	5.5	27.8	7.1	0.0	0.0	0.1			

Appendix A

2019/1/22	82	242.4	121.2	0.0	0.0	13.3	9.6	51.7	6.9	28.4%	6.0	28.3	7.4	0.0	0.0	0.0		1300.0	900.0
2019/1/25	85	246.2	123.1	0.0	0.0	13.2	9.0	48.4	2.2	75.9%	5.9	28.0	7.0	0.0	0.0	0.1		1200.0	770.0
2019/1/30	90	227.3	113.7	0.0	0.0	13.5	8.8	57.5	1.4	84.4%	5.6	27.8	5.5	0.0	0.0	0.2			
2019/2/1	92	236.0	118.0	0.0	0.0	12.5	7.3	49.5	1.5	79.1%	5.2	27.9	5.7	0.0	0.0	0.1		1200.0	780.0
2019/2/7	98	238.2	119.1	0.0	0.0	12.6	8.7	58.9	5.4	38.2%	4.9	28.1	4.8	0.0	0.0	0.1		1230.0	790.0
2019/2/12	103	229.2	114.6	0.0	0.0	12.0	9.7	56.6	9.1	6.3%	5.2	28.2	5.7	0.0	0.0	0.1		1120.0	850.0
2019/2/15	106	223.7	111.8	0.0	0.0	12.3	9.3	49.7	7.4	20.5%	5.3	28.3	4.7	0.0	0.0	0.1			
2019/2/19	110	229.3	114.6	0.0	0.0	12.4	8.7	49.4	3.4	61.3%	5.3	28.5	5.0	0.0	0.0	0.1		1020.0	770.0
2019/2/22	113	227.9	114.0	0.0	0.0	12.7	7.9	46.9	2.5	68.4%	5.8	28.7	6.4	0.0	0.0	0.1		860.0	650.0
2019/2/26	117	254.7	127.3	0.0	0.0	12.2	9.3	46.1	2.6	72.2%	6.6	28.7	7.7	0.0	0.0	0.1			
2019/2/28	119	230.7	115.3	0.0	0.0	11.5	7.2	43.8	0.0	100.0%	7.2	28.7	8.3	0.0	0.0	0.1			
2019/3/5	124	250.0	125.0	0.0	0.0	12.3	7.9	41.5	0.7	91.4%	8.2	28.7	10.0	0.1	0.0	0.1			
2019/3/7	126	250.0	125.0	0.0	0.0	12.3	7.8	43.2	1.6	79.7%	7.8	28.7	9.7	0.0	0.0	0.0			
T3		HAc (mg L^{-1})					PO_4^{3-}-P (mg L^{-1})			Removal rate	NO_3^--N (mg L^{-1})			NO_2^--N (mg L^{-1})					
Date	Day	feedstock	Ana	Ano	E	feedstock	Ana	Ano	E		Ana	Ano	E	Ana	Ano	E	pH	MLSS&MLVSS (mg L^{-1})	
2018/11/1	0	246.1	123.1	0.0	0.0	12.4	10.2	21.6	7.4	27.5%	1.3	0.0	0.0	4.8	46.4	12.0		637.5	532.5
2018/11/4	3	254.3	127.2	37.6	0.0	12.7	10.3	19.9	8.3	19.3%	1.5	0.0	0.1	10.3	46.4	16.1			
2018/11/9	8	251.0	125.5	18.3	0.0	11.7	9.8	22.0	8.9	9.5%	1.6	0.0	0.0	10.8	46.2	21.4	8.0	530.0	430.0
2018/11/12	11	237.8	118.9	15.3	0.0	13.4	11.1	20.8	9.5	14.9%	1.5	0.0	0.0	11.5	46.6	22.9	7.8	270.0	230.0
2018/11/15	14	224.8	112.4	21.3	0.0	11.6	9.7	22.3	7.8	20.4%	2.2	0.0	0.0	7.7	47.2	15.1	8.0	380.0	320.0
2018/11/19	18	227.2	113.6	0.0	0.0	12.2	7.9	26.6	6.4	19.2%	2.1	0.0	0.4	5.4	46.6	13.3	7.7	450.0	340.0
2018/11/23	22	243.2	121.6	0.0	0.0	12.7	7.5	36.3	3.8	50.2%	2.1	0.0	0.0	4.7	46.6	8.0	7.9	560.0	430.0
2018/11/26	25	231.7	115.9	0.0	0.0	12.5	8.7	31.1	3.5	59.1%	2.2	0.0	0.0	8.7	47.3	12.7	7.7		
2018/11/29	28	240.7	120.4	0.0	0.0	11.5	8.5	34.9	3.1	63.9%	2.0	0.0	3.3	7.6	47.2	9.3	7.8	480	370
2018/12/5	34	247.3	123.6	0.0	0.0	11.9	6.2	40.0	4.2	32.7%	2.1	0.0	0.0	2.8	46.9	8.4	7.9	640.0	500.0
2018/12/11	40	241.1	120.6	0.0	0.0	13.0	8.9	37.4	2.7	69.2%	2.1	0.0	0.0	7.6	46.9	8.3	7.9		
2018/12/14	43	247.5	123.7	0.0	0.0	12.8	6.3	51.5	0.3	95.1%	2.1	0.0	0.0	0.3	47.0	0.1	7.8	1830.0	1380.0

Appendix A

2018/12/17	46	261.5	130.7	0.0	0.0	12.5	6.4	49.7	0.5	91.5%	2.2	0.0	0.1	2.0	47.1	5.6	7.8	1390.0	1100.0
2018/12/21	50	247.8	123.9	0.0	0.0	12.3	6.1	50.6	0.7	88.2%	2.0	0.0	0.1	1.5	47.0	4.9	8.1	1200.0	810.0
2018/12/25	54	242.8	121.4	0.0	0.0	11.8	6.3	51.8	0.8	87.0%	2.0	0.0	0.1	1.6	47.0	7.9		1370.0	920.0
2019/1/1	61	250.0	125.0	0.0	0.0	13.8	6.5	53.2	0.1	98.4%	2.3	0.0	0.1	4.4	47.3	6.4		1310.0	810.0
2019/1/4	64	234.4	117.2	0.0	0.0	12.7	6.4	58.5	0.1	98.5%	2.3	0.0	0.0	3.3	47.5	8.7	7.7		
2019/1/8	68	245.3	122.7	0.0	0.0	13.5	6.8	59.0	0.0	100.0%	2.4	0.0	0.1	0.9	47.4	4.0		1600.0	1030.0
2019/1/11	71	238.0	119.0	0.0	0.0	13.4	6.7	58.2	0.1	98.4%	2.3	0.0	0.1	2.5	47.6	7.0	8.3	1530.0	920.0
2019/1/15	75	235.1	117.5	0.0	0.0	13.8	6.9	59.7	0.2	96.7%	2.6	0.0	0.0	2.2	47.7	5.0	7.8	1410.0	860.0
2019/1/16	76	226.9	113.4	0.0	0.0	14.0	7.0	60.9	1.7	75.7%	2.3	0.0	0.1	1.8	47.4	2.4		1280.0	840.0
2019/1/18	78	254.0	127.0	0.0	0.0	12.7	10.9	65.3	24.5	-124.7%	2.5	0.0	0.1	0.0	47.3	6.5			
2019/1/22	82	247.8	123.9	0.0	0.0	13.0	9.0	58.1	19.8	-120.4%	2.4	0.0	0.1	0.6	48.0	9.4		1030.0	860.0
2019/1/25	85	243.1	121.5	0.0	0.0	13.3	13.1	16.6	13.4	-1.8%	2.3	0.0	0.1	7.9	47.6	16.9		770.0	690.0
2019/1/30	90	236.7	118.4	16.2	0.0	12.9	11.8	18.0	12.0	-1.4%	2.3	0.0	0.4	5.8	47.3	14.2			
2019/2/1	92	210.8	105.4	21.1	0.0	12.4	10.4	15.5	9.7	7.3%	2.3	0.0	0.1	5.7	47.8	15.3		760.0	640.0
2019/2/7	98	217.2	108.6	22.9	0.0	12.4	11.4	22.4	8.8	23.2%	2.3	0.0	0.1	10.4	47.9	18.4		750.0	670.0
2019/2/12	103	246.3	123.2	46.0	0.0	12.1	11.4	25.0	7.1	38.1%	2.1	0.0	0.1	7.6	48.5	11.8		770.0	700.0
2019/2/15	106	235.4	117.7	11.1	0.0	12.7	9.1	31.1	7.6	16.6%	2.3	0.0	0.1	5.4	48.8	11.3			
2019/2/19	110	242.7	121.4	25.4	0.0	12.4	12.3	32.9	6.0	51.6%	2.6	0.0	0.0	5.2	48.4	6.3		820.0	690.0
2019/2/22	113	248.6	124.3	53.1	0.0	12.3	10.7	26.7	9.9	7.5%	2.5	0.0	0.1	5.1	48.8	8.7		810.0	710.0
2019/2/26	117	249.6	124.8	34.0	0.0	11.5	9.3	28.8	7.4	19.9%	2.6	0.0	0.1	3.6	45.6	6.7			
2019/2/28	119	245.6	122.8	29.5	0.0	11.7	10.5	29.9	3.7	65.1%	2.5	0.0	0.0	4.2	45.6	5.3			
2019/3/5	124	250.0	125.0	30.9	0.0	11.9	10.5	38.8	2.9	72.2%	2.6	0.0	0.1	2.2	45.0	0.6			
2019/3/7	126	250.0	125.0	30.0	0.0	12.9	10.4	38.4	3.6	65.1%	2.5	0.0	0.1	1.6	45.0	0.9			
T4		HAc (mg L^{-1})					PO_4^{3-}-P (mg L^{-1})			Removal rate	NO_3^--N (mg L^{-1})			NO_2^--N (mg L^{-1})					
Date	Day	feedstock	Ana	Ano	E	feedstock	Ana	Ano	E		Ana	Ano	E	Ana	Ano	E	pH	MLSS&MLVSS (mg L^{-1})	
2018/11/1	0	246.1	123.1	38.7	0.0	12.4	14.6	20.2	11.8	19.4%	1.3	0.0	0.0	2.7	47.9	3.8		637.5	532.5
2018/11/4	3	254.3	127.2	48.3	0.0	12.7	10.8	19.4	6.4	41.2%	1.5	0.0	0.1	7.3	47.9	9.1			

2018/11/9	8	251.0	125.5	8.7	0.0	13.2	9.8	26.2	8.2	16.8%	1.6	0.0	0.0	10.8	47.2	20.9	7.7	660.0	530.0
2018/11/12	11	237.8	118.9	14.5	0.0	13.4	11.7	27.2	8.5	27.2%	1.5	0.0	0.0	10.0	47.7	19.4	7.8	530.0	430.0
2018/11/15	14	224.8	112.4	17.7	0.0	11.6	9.3	28.4	6.3	31.6%	2.2	0.0	0.0	7.0	48.0	13.8	7.9	460.0	380.0
2018/11/19	18	227.2	113.6	0.0	0.0	12.2	10.2	26.7	8.9	12.7%	2.1	0.0	0.0	6.1	47.4	14.4	7.8	240.0	150.0
2018/11/23	22	243.2	121.6	0.0	0.0	12.7	9.1	37.4	4.3	52.9%	2.1	0.0	0.0	5.5	47.1	8.8	7.8	570.0	430.0
2018/11/26	25	231.7	115.9	0.0	0.0	12.5	8.9	36.8	1.7	80.6%	2.1	0.0	0.0	7.6	47.7	9.7	7.8		
2018/11/29	28	240.7	120.4	0.0	0.0	11.5	9.1	37.5	1.9	78.7%	2.0	0.0	0.2	5.7	47.7	6.9	7.9	600	470
2018/12/5	34	247.3	123.6	0.0	0.0	11.9	7.4	39.3	2.6	64.9%	2.1	0.0	0.0	3.2	47.4	6.3	7.9	530.0	400.0
2018/12/11	40	241.1	120.6	0.0	0.0	13.0	8.8	47.6	2.7	69.5%	2.1	0.0	0.0	5.3	47.2	4.8	7.7		
2018/12/14	43	247.5	123.7	0.0	0.0	12.8	7.2	53.0	0.0	100.0%	2.1	0.0	0.0	1.4	47.1	1.8	7.9	1800.0	1120.0
2018/12/17	46	261.5	130.7	0.0	0.0	12.5	7.8	55.1	1.2	84.8%	2.1	0.0	0.1	1.8	47.4	3.1	7.7	1650.0	1250.0
2018/12/21	50	247.8	123.9	0.0	0.0	12.3	6.0	48.2	3.0	50.0%	2.0	0.0	0.1	0.1	47.3	5.0	7.7	1390.0	940.0
2018/12/25	54	242.8	121.4	0.0	0.0	11.8	6.1	48.6	5.5	9.2%	2.0	0.0	0.1	1.4	47.3	9.5		1400.0	1040.0
2019/1/1	61	250.0	125.0	0.0	0.0	13.8	12.6	40.4	0.0	99.9%	2.3	0.0	0.0	10.0	47.7	0.0		1210.0	870.0
2019/1/4	64	234.4	117.2	0.0	0.0	12.7	9.7	59.9	1.4	85.7%	2.3	0.0	0.0	3.0	47.5	6.1	7.9		
2019/1/8	68	245.3	122.7	0.0	0.0	13.5	9.2	52.0	0.0	100.0%	2.4	0.0	0.0	4.4	47.3	10.4		1120.0	760.0
2019/1/11	71	238.0	119.0	0.0	0.0	13.4	6.7	48.0	0.0	100.0%	2.2	0.0	0.1	0.3	47.2	2.1	8.0	1180.0	830.0
2019/1/15	75	235.1	117.5	0.0	0.0	13.8	6.9	49.4	2.3	67.1%	2.6	0.0	0.1	2.0	47.3	4.5	7.7	1080.0	730.0
2019/1/16	76	226.9	113.4	0.0	0.0	14.0	7.0	51.9	0.1	98.8%	2.4	0.0	0.1	2.0	46.7	2.0		1090.0	740.0
2019/1/18	78	254.0	127.0	0.0	0.0	12.7	6.8	54.6	6.3	7.5%	2.5	0.0	0.1	0.0	46.9	2.4			
2019/1/22	82	247.8	123.9	0.0	0.0	13.0	8.6	61.0	26.8	-212.5%	2.3	0.0	0.1	0.0	47.3	13.2		1170.0	650.0
2019/1/25	85	243.1	121.5	0.0	0.0	13.3	13.4	18.1	12.4	7.5%	2.3	0.0	0.1	7.3	46.9	13.3		780.0	690.0
2019/1/30	90	236.7	118.4	15.1	0.0	12.9	11.4	21.6	12.0	-5.6%	2.3	0.0	0.3	6.2	47.1	15.3			
2019/2/1	92	210.8	105.4	15.5	0.0	12.4	10.6	15.7	9.7	7.9%	2.4	0.0	0.1	7.1	47.2	15.2		830.0	710.0
2019/2/7	98	217.2	108.6	0.0	0.0	12.4	11.6	26.6	7.4	36.6%	2.3	0.0	0.0	9.3	47.7	15.5		770.0	690.0
2019/2/12	103	225.7	112.9	18.0	0.0	12.8	11.8	21.1	8.3	29.4%	2.0	0.0	0.1	9.3	48.1	15.5		740.0	670.0
2019/2/15	106	216.7	108.3	0.0	0.0	12.1	10.8	25.2	9.6	11.6%	2.3	0.0	0.1	10.8	47.9	19.4			
2019/2/19	110	233.8	116.9	4.2	0.0	13.4	11.3	28.1	9.8	13.6%	2.6	0.0	0.3	8.7	48.3	14.4		840.0	730.0

2019/2/22	113	233.4	116.7	23.6	0.0	14.0	11.9	22.3	11.3	4.9%	2.4	0.0	0.1	10.4	48.8	20.0		810.0	740.0
2019/2/26	117	228.3	114.2	6.1	0.0	12.8	11.7	26.5	9.4	19.6%	2.5	0.0	0.1	9.9	45.5	17.8			
2019/2/28	119	219.7	109.8	0.0	0.0	11.0	9.7	30.7	4.7	51.2%	2.5	0.0	0.1	8.5	45.5	15.3			
2019/3/5	124	250.0	125.0	17.0	0.0	13.6	9.3	43.1	7.7	17.2%	2.6	0.0	0.1	5.2	45.0	11.1			
2019/3/7	126	240.0	120.0	15.0	0.0	12.8	10.5	43.4	4.1	60.8%	2.5	0.0	0.0	5.7	45.0	8.2			

f. NO_x^--N dosing record

Preliminary experiments																		
Weight (g)	1	2	3	4	5	6	mg N/L	1		2		3		4		5		6
Empty flasks	174	154.3	168	195	153.1	172.2	NO_3^--N	NO_2^--N	NO_3^--N	NO_2^--N	NO_3^--N	NO_2^--N	NO_3^--N	NO_2^--N	NO_3^--N	NO_2^--N	NO_3^--N	NO_2^--N
Start	652	639.7	656	677	640	650.7	41.2	0	41.1	0	30.9	10.2	30.9	10	20.7	20.3	20.7	20.4
17/08/2017	618	611.3	628	648	613.7	618.7	41.0	0.0	39.7	0.0	30.9	10.2	29.9	9.7	20.2	19.8	21.4	21.1
18/08/2017	599	595.9	612	632	599.2	601	22.4	0.0	22.3	0.0	17.3	5.7	16.6	5.4	11.1	10.9	11.8	11.6
19/08/2017	581.4	581.0	596.8	616.5	585.3	584.2	21.6	0.0	21.3	0.0	16.6	5.5	16.0	5.2	10.7	10.5	11.3	11.1
20/08/2017	564	566	582	601	571.4	567.3	21.6	0.0	21.3	0.0	16.6	5.5	16.0	5.2	10.7	10.5	11.3	11.1

21/08/2017	546	551.2	567	586	557.6	550.5	21.3	0.0	21.1	0.0	16.4	5.4	15.8	5.1	10.6	10.4	11.2	11.1
22/08/2017	531	538.8	555	573	546.2	536.6	17.7	0.0	17.4	0.0	13.6	4.5	13.1	4.2	8.7	8.6	9.3	9.1
23/08/2017	516	526	542	560	534.2	522.2	18.5	0.0	18.3	0.0	14.2	4.7	13.7	4.4	9.2	9.0	9.6	9.5
24/08/2017	498	510.9	527	544	520.1	505.2	21.6	0.0	21.1	0.0	16.4	5.4	16.1	5.2	10.8	10.6	11.4	11.2
25/08/2017	481	496.4	512	529	506.6	488.9	21.1	0.0	20.6	0.0	16.0	5.3	15.5	5.0	10.4	10.2	10.9	10.7
26/08/2017	464	482.1	498	514	493.4	472.9	20.5	0.0	20.4	0.0	15.9	5.2	15.2	4.9	10.1	9.9	10.7	10.5
27/08/2017	446.7	467.6	483.4	499.3	480.1	456.6	20.9	0.0	20.6	0.0	16.0	5.3	15.5	5.0	10.2	10.0	10.9	10.8
28/08/2017	429	453.1	469	484	466.7	440.2	20.9	0.0	20.6	0.0	16.0	5.3	15.4	5.0	10.2	10.0	10.9	10.8
29/08/2017	413	439	455	470	453.4	424.5	20.1	0.0	19.8	0.0	15.5	5.1	15.0	4.9	10.2	10.0	10.5	10.3
30/08/2017	396	424.3	440	455	439.9	408	21.0	0.0	21.0	0.0	16.3	5.4	15.7	5.1	10.4	10.2	11.0	10.9
31/08/2017	378	409.8	426	439	426.4	391.6	21.0	0.0	20.6	0.0	16.0	5.3	15.6	5.0	10.4	10.2	11.0	10.8
01/09/2017	344	381	397	410	399.7	359.5	41.0	0.0	40.8	0.0	31.8	10.5	30.6	9.9	20.5	20.1	21.4	21.1
02/09/2017	310	351.9	368	380	372.8	326.9	41.6	0.0	41.0	0.0	31.9	10.5	31.0	10.0	20.7	20.3	21.8	21.5
03/09/2017	276	322.8	339	350	345.8	294.3	41.6	0.0	41.0	0.0	31.9	10.5	31.0	10.0	20.7	20.3	21.8	21.5
04/09/2017	242	294	310	320	319.2	261.9	41.1	0.0	40.7	0.0	31.7	10.5	30.6	9.9	20.4	20.0	21.6	21.3
05/09/2017	207	264.7	281	290	292.3	229.3	41.8	0.0	41.5	0.0	32.3	10.7	31.2	10.1	20.6	20.2	21.8	21.5
Start	680	662.2	675	702	661.1	678.6	41.2	0.0	41.1	0.0	30.8	10.3	30.9	10.0	20.7	20.3	20.7	20.5
06/09/2017	646	633.3	646	672	634.2	646.2	41.4	0.0	41.1	0.0	31.9	10.7	30.9	10.0	20.6	20.2	21.6	21.4
07/09/2017	611	604.2	617	642	607.2	613.6	41.4	0.0	40.8	0.0	31.7	10.6	31.0	10.0	20.7	20.3	21.8	21.6

08/09/2017	577	575.2	589	612	580.5	581.1	41.4	0.0	40.7	0.0	31.6	10.6	30.7	9.9	20.5	20.1	21.7	21.5
09/09/2017	544	546.4	560	582	554.7	548.3	40.8	0.0	40.7	0.0	31.6	10.6	30.7	9.9	19.8	19.4	21.9	21.7
10/09/2017	518	524.6	538	560	523.8	534.5	31.0	0.0	30.6	0.0	23.8	7.9	23.1	7.5	23.7	23.2	9.2	9.1
11/09/2017	492	502.9	517	537	503.7	510.2	31.1	0.0	30.8	0.0	23.9	8.0	23.2	7.5	15.4	15.1	16.2	16.1
12/09/2017	467	481.1	495	515	483.6	486	30.8	0.0	30.8	0.0	23.9	8.0	23.2	7.5	15.4	15.1	16.2	16.0
13/09/2017	441	459.2	473	492	463.5	461.7	31.1	0.0	30.8	0.0	23.9	8.0	23.1	7.5	15.4	15.1	16.2	16.1
14/09/2017	391	416.8	431	448	424.3	414.1	20.2	0.0	20.0	0.0	15.5	5.2	15.1	4.9	10.0	9.8	10.6	10.5
15/09/2017	344	376.5	391	407	386.9	368.8	19.1	0.0	19.1	0.0	14.8	4.9	14.4	4.7	9.6	9.4	10.1	10.0
16/09/2017	296	336.2	350	365	349.5	323.5	19.1	0.0	19.1	0.0	14.8	4.9	14.4	4.7	9.6	9.4	10.1	10.0
17/09/2017	249	296.2	310	323	312.6	278.6	19.0	0.0	18.8	0.0	14.6	4.9	14.2	4.6	9.4	9.2	10.0	9.9
18/09/2017	200	254.7	269	280	274.1	232	19.8	0.0	19.7	0.0	15.3	5.1	14.8	4.8	9.8	9.6	10.4	10.3
Start	706	760.9	771	750	749.8	737.5												
19/09/2017	656	718.7	729	706	710.8	690.7	20.1	0.0	19.9	0.0	15.5	5.2	15.0	4.9	10.0	9.8	10.4	10.3
20/09/2017	607	677.1	687	663	672.5	644	19.8	0.0	19.7	0.0	15.3	5.1	14.8	4.8	9.8	9.6	10.4	10.3
22/09/2017	560	637.4	648	622	636	599.6	18.8	0.0	18.7	0.0	14.5	4.9	14.1	4.6	9.3	9.1	9.9	9.8
23/09/2017	511	595.7	606	579	597.7	553.2	19.7	0.0	19.6	0.0	15.2	5.1	14.8	4.8	9.8	9.6	10.3	10.2
24/09/2017	464	555.7	566	538	560.8	508.4	19.0	0.0	18.9	0.0	14.7	4.9	14.2	4.6	9.4	9.2	10.0	9.9
25/09/2017	416	514.1	525	495	522.6	462.1	19.7	0.0	19.6	0.0	15.2	5.1	14.8	4.8	9.8	9.6	10.3	10.2
26/09/2017	367	472.6	483	452	484.5	415.7	19.7	0.0	19.6	0.0	15.2	5.1	14.8	4.8	9.7	9.5	10.3	10.2

27/09/2017	318	430.9	442	409	446.3	369.3	19.7	0.0	19.6	0.0	15.2	5.1	14.8	4.8	9.8	9.6	10.3	10.2
28/09/2017	269	389.3	400	365	408.2	322.7	19.7	0.0	19.7	0.0	15.3	5.1	14.8	4.8	9.7	9.5	10.4	10.3
Start	483	647.5	656	615	687.6	550.6												
05/10/2017	434	606	615	572	649.5	504.5	19.6	0.0	19.6	0.0	15.2	5.1	14.7	4.8	9.7	9.5	10.3	10.2
06/10/2017	386	564.8	574	529	611.9	458.7	19.4	0.0	19.5	0.0	15.1	5.1	14.6	4.7	9.6	9.4	10.2	10.1
07/10/2017	338	523.5	532	487	574.2	412.9	19.4	0.0	19.5	0.0	15.1	5.1	14.6	4.7	9.6	9.4	10.2	10.1
	699	399.4	408	359	460.8	275.3												
11/10/2017	651	358.9	367	317	423.9	230	19.4	0.0	19.3	0.0	15.0	5.0	14.5	4.7	9.4	9.2	10.1	10.0
Enrichment 1																		
Weight (g)	1	2	3	4	5	6	mg N/L	1		2		3		4		5		6
Empty flasks	174	154.3	168	195	153.1	172.2	NO_3^--N	NO_2^--N	NO_3^--N	NO_2^--N	NO_3^--N	NO_2^--N	NO_3^--N	NO_2^--N	NO_3^--N	NO_2^--N	NO_3^--N	NO_2^--N
	654	639.6	652	678	650.9	653.2												
23/01/2018	646	632.4	645	671	644.3	645.3	9.9	0.0	10.2	0.0	8.6	1.2	8.8	1.3	7.3	2.5	7.4	2.5
23/01/2018	639	626.3	639	664	638.8	638.6	8.5	0.0	8.6	0.0	7.6	1.1	7.5	1.1	6.1	2.1	6.3	2.1
24/01/2018	632	620.2	633	658	633.3	631.9	8.5	0.0	8.6	0.0	7.6	1.1	7.5	1.1	6.1	2.1	6.3	2.1
24/01/2018	627	616	629	654	629.5	627.3	5.7	0.0	6.0	0.0	5.0	0.7	5.0	0.7	4.2	1.4	4.3	1.5
24/01/2018	620.7	610.1	622.6	647.4	624.2	620.8	8.2	0.0	8.4	0.0	7.3	1.0	7.3	1.0	5.9	2.0	6.1	2.1
25/01/2018	614	604.2	617	641	618.8	614.2	8.2	0.0	8.4	0.0	7.3	1.0	7.3	1.0	5.9	2.0	6.1	2.1
25/01/2018	606	597.1	609	634	612.4	606.4	9.8	0.0	10.1	0.0	8.7	1.2	8.7	1.2	7.1	2.4	7.3	2.5
25/01/2018	599	591.3	603	628	607.1	600	8.2	0.0	8.3	0.0	7.2	1.0	7.2	1.0	5.9	2.0	6.0	2.0

26/01/2018	592	585.4	598	622	601.7	593.5	8.2	0.0	8.3	0.0	7.2	1.0	7.2	1.0	5.9	2.0	6.0	2.0
26/01/2018	584	578.4	590	614	595.3	585.7	9.7	0.0	9.9	0.0	8.7	1.2	8.5	1.2	7.1	2.4	7.3	2.5
26/01/2018	577.4	572.5	584.3	608.0	589.9	579.2	8.3	0.0	8.4	0.0	7.3	1.0	7.3	1.0	6.0	2.0	6.1	2.1
27/01/2018	571	566.5	578	602	584.5	572.6	8.3	0.0	8.4	0.0	7.3	1.0	7.3	1.0	6.0	2.0	6.1	2.1
29/01/2018	532	533.1	544	567	554.2	535.6												
29/01/2018	526	528	539	561	549.5	529.9	7.1	0.0	7.2	0.0	6.3	0.9	6.3	0.9	5.2	1.8	5.3	1.8
29/01/2018	520	522.1	533	555	544.2	523.4	8.3	0.0	8.4	0.0	7.3	1.0	7.3	1.0	5.9	2.0	6.1	2.1
30/01/2018	513	516.1	527	549	538.8	516.9	8.3	0.0	8.4	0.0	7.3	1.0	7.3	1.0	5.9	2.0	6.1	2.1
30/01/2018	507	510.7	522	543	533.9	510.9	7.5	0.0	7.7	0.0	6.5	0.9	6.6	0.9	5.4	1.8	5.6	1.9
30/01/2018	500	504.8	516	537	528.6	504.5	8.2	0.0	8.4	0.0	7.3	1.0	7.2	1.0	5.9	2.0	6.0	2.0
31/01/2018	493	498.9	510	531	523.3	498	8.2	0.0	8.4	0.0	7.3	1.0	7.2	1.0	5.9	2.0	6.0	2.0
31/01/2018	487	493.9	505	526	518.7	492.4	6.9	0.0	7.1	0.0	6.2	0.9	6.1	0.9	5.1	1.7	5.3	1.8
31/01/2018	472	480.8	491	512	506.8	477.9	18.3	0.0	18.6	0.0	16.3	2.3	16.1	2.3	13.3	4.5	13.6	4.6
01/02/2018	457	467.6	478	498	494.8	463.4	18.3	0.0	18.6	0.0	16.3	2.3	16.1	2.3	13.3	4.5	13.6	4.6
01/02/2018	442	454.7	465	485	483	449	17.9	0.0	18.3	0.0	15.7	2.2	15.9	2.3	13.1	4.4	13.5	4.5
01/02/2018	427	441.6	451	471	471.1	434.6	18.2	0.0	18.6	0.0	16.2	2.3	16.0	2.3	13.2	4.5	13.5	4.6
02/02/2018	412	428.5	438	457	459.2	420.1	18.2	0.0	18.6	0.0	16.2	2.3	16.0	2.3	13.2	4.5	13.5	4.6
02/02/2018	398	415.6	425	444	447.6	405.9	17.8	0.0	18.3	0.0	15.9	2.3	15.7	2.2	12.9	4.3	13.3	4.5
02/02/2018	383	402.7	412	430	435.8	391.6	18.1	0.0	18.4	0.0	16.0	2.3	15.9	2.3	13.2	4.4	13.5	4.5

03/02/2018	368	389.7	398	417	423.9	377.2	18.1	0.0	18.4	0.0	16.0	2.3	15.9	2.3	13.2	4.4	13.5	4.5
05/02/2018	292	323.3	331	347	363.8	304	18.4	0.0	94.1	0.0	16.3	2.3	16.2	2.3	13.4	4.5	13.7	4.6
05/02/2018	277	310.4	318	334	352.1	289.7	18.1	0.0	18.4	0.0	16.0	2.3	15.9	2.3	13.1	4.4	13.5	4.5
06/02/2018	262	297.4	305	320	340.3	275.3	18.1	0.0	18.4	0.0	16.0	2.3	15.9	2.3	13.1	4.4	13.5	4.5
06/02/2018	247	284	291	306	328.2	260.5	18.5	0.0	19.0	0.0	16.5	2.3	16.3	2.3	13.4	4.5	13.9	4.7
06/02/2018	225	270.7	277	292	316.1	245.8	18.6	0.0	18.9	0.0	16.5	2.3	16.4	2.3	13.5	4.5	13.8	4.7
07/02/2018	210	257.3	264	278	303.9	231	18.6	0.0	18.9	0.0	16.5	2.3	16.4	2.3	13.5	4.5	13.8	4.7
07/02/2018	195	244.1	250	265	291.9	216.4	18.3	0.0	18.7	0.0	16.2	2.3	16.1	2.3	13.3	4.5	13.7	4.6
07/02/2018	262	229.3	239	251	279.8	252.3	7.6	0.0	21.0	0.0	13.4	1.9	16.4	2.3	13.5	4.5	12.3	4.2
08/02/2018	256	214.4	228	237	267.6	239.1	7.6	0.0	21.0	0.0	13.4	1.9	16.4	2.3	13.5	4.5	12.3	4.2
13/02/2018	585	581.5	599	618	600.5	604												
13/02/2018	569	567.3	585	603	587.7	586.5	19.6	0.0	20.1	0.0	17.4	2.5	17.2	2.4	14.2	4.8	16.4	5.5
14/02/2018	539	541.3	559	576	564.5	554.4												
14/02/2018	520	524.4	542	559	549.7	531.9	23.3	0.0	24.0	0.0	20.6	2.9	20.4	2.9	16.4	5.5	21.1	7.1
20/02/2018	309	339.7	355	368	384.6	310.4												
20/02/2018	294	326.3	342	354	372.7	294.8	18.3	0.0	19.0	0.0	16.3	2.3	16.3	2.3	13.2	4.5	14.6	4.9
20/02/2018	280	313.4	329	340	361.2	279.7	17.9	0.0	18.3	0.0	15.8	2.3	15.6	2.2	12.8	4.3	14.2	4.8
21/02/2018	265	300.5	316	327	349.7	264.5	17.9	0.0	18.3	0.0	15.8	2.2	15.6	2.2	12.8	4.3	14.2	4.8
21/02/2018	250	289.2	302	313	337.7	248.8	18.4	0.0	16.0	0.0	16.3	2.3	16.3	2.3	13.3	4.5	14.7	5.0

21/02/2018	235	275.2	289	300	326.2	233.6	17.9	0.0	19.8	0.0	15.9	2.3	15.7	2.2	12.8	4.3	14.3	4.8
22/02/2018	220	261.2	276	286	314.6	218.3	17.9	0.0	19.8	0.0	15.9	2.3	15.7	2.2	12.8	4.3	14.3	4.8
22/02/2018	204	247.1	262	272	302	201.6	19.4	0.0	20.0	0.0	17.2	2.4	17.1	2.4	14.0	4.7	15.7	5.3
22/02/2018	711	756	770	749	763.4	708.9												
22/02/2018	695	742.3	756	734	750.8	692.7	19.0	0.0	19.4	0.0	16.9	2.4	17.0	2.4	14.0	4.7	15.2	5.1
23/02/2018	681	730.1	744	722	739.9	678.7	16.7	0.0	17.3	0.0	14.8	2.1	14.7	2.1	12.1	4.1	13.1	4.4
23/02/2018	665	715.9	729	707	727.3	662.8	19.5	0.0	20.1	0.0	17.3	2.5	17.1	2.4	14.0	4.7	14.9	5.0
26/02/2018	545	610.8	623	598	633.2	539.3												
26/02/2018	530	596.9	609	584	620.7	523	19.3	0.0	19.7	0.0	16.9	2.4	16.7	2.4	13.9	4.7	15.3	5.1
26/02/2018	515	583.8	595	570	609	507.6	18.2	0.0	18.6	0.0	16.2	2.3	16.0	2.3	13.1	4.4	14.5	4.9
27/02/2018	500	570.6	582	556	597.2	492.1	18.2	0.0	18.6	0.0	16.2	2.3	16.0	2.3	13.1	4.4	14.5	4.9
28/02/2018	455	531.9	543	516	562.7	447.3	17.8	0.0	54.8	0.0	15.8	2.2	15.7	2.2	12.8	4.3	14.0	4.7
01/03/2018	407	489.4	500	472	524.8	450.8	19.7	0.0	20.1	0.0	17.4	2.5	17.2	2.5	14.0	4.7		
05/03/2018	619	660	676	650	619	602.7												
05/03/2018	603	645.6	662	635	606.5	582.9	19.63	0	20.41	0	17.43	2.483	17.3	2.47	13.89	4.68	18.6	6.25
06/03/2018	573	619.2	635	608	583.2	547.7	18.06	0	18.71	0	16.1	2.293	15.9	2.27	12.94	4.36	16.5	5.55
09/03/2018	414	478.8	494	463	459.6	360.3												
09/03/2018	391	458.4	473	442	441.6	332.9	27.99	0	28.91	0	24.93	3.552	24.7	3.52	20	6.73	25.7	8.65
13/03/2018	594	586.9	598	622	604.1	573.4												

14/03/2018	525	526.1	537	559	550.5	492.9	27.83	0	28.72	0	24.81	3.534	24.6	3.5	19.85	6.68	25.2	8.47
15/03/2018	456	465.2	475	496	496.9	412.7	27.91	0	28.77	0	24.93	3.552	24.6	3.51	19.85	6.68	25.1	8.44
19/03/2018	689	733.1	737	752	766.6	609.1												
20/03/2018	620	672.5	676	689	712.8	528	27.71	0	28.63	0	24.81	3.534	24.6	3.51	19.93	6.71	25.3	8.53
21/03/2018	552	612.7	615	627	660	447.9	27.35	0	28.25	0	24.57	3.5	24.3	3.46	19.56	6.58	25	8.43
22/03/2018	487	553	554	565	607.5	368.9	26.5	0	28.2	0	24.49	3.489	24.2	3.45	19.44	6.55	24.7	8.31
23/03/2018	411	488.3	489	498	550.9	282.7	30.42	0	30.57	0	26.43	3.764	26.2	3.73	20.96	7.06	26.9	9.07
24/03/2018	343	427.8	427	435	497.7	203.5	27.71	0	28.58	0	24.85	3.54	24.6	3.5	19.7	6.63	24.8	8.33
26/03/2018	713	307	304	309	391.4	555.1												
27/03/2018	638	240.2	236	240	332.5	469.6	30.62	0	31.56	0	27.43	3.908	27.1	3.86	21.81	7.34	26.7	9
28/03/2018	560	192.3	675	676	272.7	382.6	31.26	0	33.94	0	28.08	4	27.8	3.97	22.15	7.46	27.2	9.15
		680.9							29.05	0								
29/03/2018	493	620.8	614	614	219.9	311.4	27.35	0	28.39	0	24.65	3.511	24.5	3.48	19.56	6.58	22.3	7.49
30/03/2018	424	560.4	553	551	169.3	238.5	27.55	0	28.53	0	24.77	3.529	24.5	3.49	18.74	6.31	22.8	7.67
31/03/2018	356	499.7	491	487	624.4	669.8	27.67	0	28.68	0	24.85	3.54	24.7	3.52	19.93	6.71	23.3	7.85
01/04/2018	289	440	430	425	572	596.7	27.14	0	28.2	0	24.61	3.506	24.3	3.46	19.41	6.53	20.3	6.7
02/04/2018	221	380.1	369	363	519.2	524	27.39	0	28.3	0	24.65	3.511	24.3	3.47	19.56	6.58	20.2	6.66
03/04/2018	660	320	308	300	466.4	451.4	27.47	0	28.39	0	24.65	3.511	24.4	3.48	19.56	6.58	20.2	6.66
04/04/2018	592	260.1	247	238	413.9	379.2	27.35	0	28.3	0	24.53	3.494	24.3	3.46	19.44	6.55	20.1	6.62

05/04/2018	524	200.4	187	203	361.5	306.9	27.43	0	28.2	0	24.53	3.494	13.4	1.91	19.41	6.53	20.1	6.63
09/04/2018	761	471.4	677	703	679.4	678												
10/04/2018	693	411.5	616	641	626.3	605.1	29.88	0	29.76	0	26.19	3.758	26.2	3.73	22.29	7.33	20.3	6.68
09/05/2018	705	721.2	646	654	645.5	663.5												
10/05/2018	637	660.6	585	591	592.8	590.7	30.14	0	30.11	0	26.14	3.752	26.1	3.71	22.12	7.28	20.2	6.67
11/05/2018	568	600	523	529	540.3	518	30.23	0	30.11	0	26.23	3.764	26.2	3.73	22.04	7.25	20.2	6.66
15/05/2018	698	691.2	672	704	681.6	685.9												
16/05/2018	629	630.5	611	641	628.9	612	30.23	0	30.16	0	26.23	3.764	26.2	3.73	22.12	7.28	20.5	6.77
21/05/2018	411	471.8	640	466	747.2	660.8												
22/05/2018	343	411.1	578	403	694.1	586.9	30.14	0	30.16	0	26.27	3.77	26.1	3.72	22.29	7.33	20.5	6.77
25/05/2018	636	618.7	673	678	531.9	703.9												
26/05/2018	567	557	611	615	478.5	628.9	30.53	0	30.66	0	26.53	3.807	26.4	3.76	22.42	7.37	20.8	6.88
29/05/2018	359	374.3	427	426	319.6	406.3												
30/05/2018	285	309.1	362	358	263	337.4	32.42	0	32.4	0	28.16	4.041	28.3	4.04	23.76	7.82	19.1	6.32
01/06/2018	584	634.4	609	592	441	592												
02/06/2018	509	568.5	543	523	383.9	513	32.86	0	32.75	0	28.41	4.077	28.6	4.08	23.97	7.88	21.9	7.24
08/06/2018	693	370.1	529	324	577.3	331												
09/06/2018	624	309.9	469	261	525	259	30.01	0	29.91	0	25.93	3.721	26.1	3.71	21.96	7.22	20	6.6
12/06/2018	415	452.4	482	481	365.2	495.5												

Appendix A

13/06/2018	346	391.5	421	418	312.8	422.7	30.31	0	30.26	0	26.14	3.752	26.3	3.75	22	7.24	20.2	6.67
04/07/2018	562	608.9	426	390	223	482.9												
05/07/2018	490	547.2	364	325	173.8	409.1	31.81	0	30.66	0	26.53	3.807	27.1	3.86	20.65	6.79	20.5	6.77
14/07/2018	410	430.1	443	459	481	401.8												
15/07/2018	337	367.8	380	393	429.5	328.3	31.9	0	30.96	0	26.79	3.844	27.2	3.88	21.62	7.11	20.4	6.74
18/07/2018	266	306	318	329	378.4	255.3	31.59	0	30.71	0	26.57	3.813	27	3.85	21.45	7.06	20.3	6.69
19/07/2018	447	497.8	257	265	327.8	437.3												
20/07/2018	375	435.5	195	199	276.3	363.9	31.76	0	30.96	0	26.61	3.819	27.2	3.88	21.62	7.11	20.4	6.73
07/08/2018	470	604.1	593	578	539.4	464.8												
08/08/2018	398	543	531	513	488.3	391.9	29.7	0	29.48	0	26.21	3.744	26.2	3.75	22.31	7.44	22.4	7.45
21/08/2018	745	711.1	721	688	744	763.7												
23/08/2018	598	585.8	595	554	640.3	613.8	30.4	0	30.23	0	26.67	3.81	27	3.85	22.64	7.55	23	7.66
26/09/2018	299	343.4	368	324	196.9	310.5												
	275	323.2	347	303	181.6	286.6	29.41	0	29.24	0	25.74	3.678	25.9	3.7	20.04	6.68	22	7.33

Enrichment 2 and tests																										
Weight (g)	1	2	3	4	5	6	7	8	1	2	3	4	5	6	7	8	1	2	3	4	5	6	7	8		
									NO_3^--N	NO_3^--N	NO_2^--N	NO_2^--N	NO_2^--N	NO_2^--N	NO_3^--N	NO_3^--N										
16/10/2018	673	757.9	641	561	415.4	304	416.4	560.1																		
	615	707.9	594	512	373.9	254.8	374.2	523.2	30.69	31.25	46.58	47.76	47.2	52.7	32.97	28.8	57.7	50	47.2	48.4	41.5	49.2	42.2	36.9		
19/10/2018	657	312.9	737	632	537.4	369.6	618.8	658.8																		

	600	264	690	584	496.2	320.6	576.8	622.6	30.43	30.56	46.18	47.27	46.8	44.8	32.81	28.3	57.2	48.9	46.8	47.9	41.2	49	42	36.2
23/10/2018	474	730.9	682	567	556.6	763.4	620.9	732.3																
	417	681.8	635	519	515.5	713.8	578.9	696.2	30.53	30.69	46.09	46.97	46.7	45.4	32.81	28.2	57.4	49.1	46.7	47.6	41.1	49.6	42	36.1
29/10/2018	392	269.8	304	713	325.3	420.1	240.2	566.1																
	334	220.8	257	665	284.1	371.1	197.2	531.4	27.62	27.56	46.38	47.86	46.8	44.8	30.23	24.4	57.7	49	47	48.5	41.2	49	43	34.7
31/10/2018	559	488.7	449	434	555.5	635.1	496.8	367																
	501	439.9	402	386	514.4	586.1	454.2	332.9	27.67	27.45	46.38	47.66	46.7	44.8	29.95	24	57.8	48.8	47	48.3	41.1	49	42.6	34.1
06/11/2018	517	619.3	754	440	324.2	262.8	477.5	521.9																
	459	570.7	707	392	283.5	213.5	435	488.9	27.53	27.34	46.48	47.07	46.3	45.1	29.88	23.2	57.5	48.6	47.1	47.7	40.7	49.3	42.5	33
08/11/2018	672	328.2	473	657	579.3	472.5	658.5	668.6																
	614	279.7	426	609	538.5	423.9	615.9	635.9	27.62	27.28	46.18	47.17	46.4	44.5	27.39	26.8	57.7	48.5	46.8	47.8	40.8	48.6	42.6	32.7
12/11/2018	480	248	392	618	581.7	393.4	651.5	281.7																
	422	198.9	345	569	540.4	344.1	608.5	248.5	27.91	27.62	46.58	47.66	46.9	45.1	27.64	27.2	58.3	49.1	47.2	48.3	41.3	49.3	43	33.2
15/11/2018	459	309.5	482	725	718.7	455.4	267.5	488.7																
	400	260.3	434	676	677.2	406.1	224	457.3	28.01	27.68	47.17	47.96	47.2	45.1	27.96	25.7	58.5	49.2	47.8	48.6	41.5	49.3	43.5	31.4
19/11/2018	764	727.4	422	646	734.2	371.6	757.8	615.3																
	705	678.5	375	598	693.3	322.8	714.9	584.8	27.91	27.51	46.58	47.37	46.5	44.6	27.58	25	58.3	48.9	47.2	48	40.9	48.8	42.9	30.5
20/11/2018	590	581.6	762	526	612.5	726.8	629.8	524.8																
	531	532.6	714	478	571.7	677.5	586.8	494.6	27.91	27.56	47.27	47.37	46.4	45.1	27.64	24.7	58.3	49	47.9	48	40.8	49.3	43	30.2

21/11/2018	416	436.1	620	383	491.3	580.3	501.9	435.5															
	358	387.1	572	336	450.7	531.2	458.9	405.5	27.96	27.56	46.97	47.27	46.1	44.9	27.64	24.5	58.4	49	47.6	47.9	40.6	49.1	43	30
23/11/2018	570	646.1	439	499	251.1	288.4	246.4	256.4															
	512	597.2	392	452	211.1	239.6	203.7	225.5	27.77	27.51	46.58	47.07	45.5	44.6	27.45	25.3	58	48.9	47.2	47.7	40	48.8	42.7	30.9
26/11/2018	550	656.9	507	583	391.4	351.2	364.1	435.9															
	492	607.5	459	535	350.6	301.7	320.9	406.6	27.96	27.79	47.27	47.66	46.4	45.3	27.77	26.4	58.4	49.4	47.9	48.3	40.8	49.5	43.2	29.3
29/11/2018	530	718	388	348	531.1	411.7	480.1	680.2															
	472	668.4	340	300	490	362	436.7	650.7	27.86	27.9	47.17	47.66	46.7	45.5	27.9	26.6	58.2	49.6	47.8	48.3	41.1	49.7	43.4	29.5
04/12/2018	270	480.8	435	380	425	669.2	335.5	248.1															
	213	431.6	387	332	375.6	628.5	292.5	220.1	27.38	27.68	46.68	47.17	56.1	37.2	27.64	25.2	57.2	49.2	47.3	47.8	49.4	40.7	43	28
05/12/2018	600	334.1	516	518	295.5	530.4	709.5	667.8															
	542	285	468	470	255.2	481	666.1	638.9	27.48	27.62	46.88	47.37	45.8	45.2	27.9	26	57.4	49.1	47.5	48	40.3	49.4	43.4	28.9
11/12/2018	577	458.4	561	269	576.3	647.5	465.8	616.1															
	520	409.3	514	221	535.8	597.7	422.6	588.5	27.34	27.62	46.88	47.17	46	45.5	27.77	27.3	57.1	49.1	47.5	47.8	40.5	49.8	43.2	27.6
14/12/2018	568	511.4	578	406	711.6	454.7	579.6	371															
	511	462.3	531	358	671.5	405.2	536.4	343.9	27.24	27.62	46.97	47.07	45.6	45.3	27.77	26.8	56.9	49.1	47.6	47.7	40.1	49.5	43.2	27.1
17/12/2018	557	571.1	577	556	353.3	515.3	692.8	631.8															
	499	521.7	529	508	313.5	465.4	649.3	604.6	27.48	27.79	47.07	47.37	45.2	45.6	27.96	26.9	57.4	49.4	47.7	48	39.8	49.9	43.5	27.2
21/12/2018	375	483.3	554	443	378	422.8	677.2	306.1															

	318	434.1	506	395	338.3	373.1	633.8	279.4	27.29	27.68	46.97	47.27	45.1	45.5	27.9	26.4	57	49.2	47.6	47.9	39.7	49.7	43.4	26.7
04/11/2019	749	419.8	404	603	482.6	341.1	373.6	702.2																
	691	370.3	355	555	443.1	291.1	330.1	675.9	27.61	27.88	47.48	47.48	41.5	45.7	28.66	27.1	57.7	49.5	48.2	48.2	39.5	50	43.5	26.3
08/01/2019	568	329.2	310	556	432.1	748.8	357.4	386.8																
	509	279.6	262	508	392.8	698.3	314.1	360.6	28.33	27.94	47.38	47.28	45.9	46.1	28.53	27	59.2	49.6	48.1	48	39.3	50.5	43.3	26.2
11/01/2019	558	386.7	456	556	586.5	298.3	471.7	660.8																
	501	337.2	408	508	546.8	248.1	428.5	635	27.32	27.88	47.58	47.18	46.3	45.8	28.46	27.6	57.1	49.5	48.3	47.9	39.7	50.2	43.2	25.8
15/01/2019	393	294	334	532	620.4	700.5	472.5	352.3																
	336	244.2	286	484	581	650.1	429.3	327.9	27.18	28.05	47.68	47.28	46	47.3	28.46	26.1	56.8	49.8	48.4	48	39.4	50.4	43.2	24.4
16/01/2019	724	646.5	575	506	502.9	550.1	343.6	275.8																
	553	498.1	431	364	386.4	400.2	214.9	199.6	27.21	27.86	47.38	46.66	45.3	46.9	28.26	28.2	56.9	49.5	48.1	47.367	38.83	49.97	42.9	25.4
18/01/2019	383	350.4	314	699	271.4	676.5	587.4	593.7																
	327	301	266	651	233.2	626.1	544.4	568.1	26.94	27.83	47.28	46.89	44.6	47.3	28.33	27.4	56.3	49.4	48	47.6	38.2	50.4	43	25.6
22/01/2019	708	759.2	676	699	312.6	577.9	573.2	289.1																
	650	708.9	627	651	274.4	527.3	529.8	264.6	27.46	28.33	47.97	47.28	44.6	47.5	28.59	26.2	57.4	50.3	48.7	48	38.2	50.6	43.4	24.5
25/01/2019	451	313.3	699	320	499.2	681.6	689.1	568.7																
	395	263.6	650	272	459.2	629.4	646.2	542.7	27.91	28	47.58	46.89	46.7	49	28.26	28.9	56.3	49.7	48.3	47.6	40	52.2	42.9	26
30/01/2019	365	571	481	602			303	697																
	309	521.7	433	555			260.3	671.8	27.56	27.77	47.28	47.09	0	0	28.13	28	55.6	49.3	48	47.8	0	0	42.7	25.2

01/02/2019	280	274.7	443	316	244	396.9	297.6	546.1															
	224	225.1	395	268	205.4	345	254.7	521.3	27.71	27.94	47.78	47.18	45	48.7	28.26	27.6	55.9	49.6	48.5	47.9	38.6	51.9	42.9	24.8
07/02/2019	339	356.7	379	407	432.1	365	573.5	623.9															
	282	306.8	330	358	392.8	313.2	530.6	598.1	27.86	28.11	47.87	47.68	45.9	48.6	28.26	28.7	56.2	49.9	48.6	48.4	39.3	51.8	42.9	25.8
12/02/2019	747	609.4	611	724	349.5	590.8	433.5	241.6															
	691	559.3	562	675	310.6	538.6	390.9	216.8	28.11	28.22	48.47	48.07	45.4	49	28.07	27.6	56.7	50.1	49.2	48.8	38.9	52.2	42.6	24.8
15/02/2019	740	660.4	671	285	503.3		551.2	521.7															
	683	610.1	622	237	464.7		508.5	497.2	28.46	28.33	48.76	47.87	45	0	28.13	27.2	57.4	50.3	49.5	48.6	38.6	0	42.7	24.5
19/02/2019	561	560.5	499	294	543	338	291.2	734.5															
	504	509.9	450	245	503.8	285	248.4	709	28.21	28.5	48.37	48.27	45.7	49.7	28.2	28.4	56.9	50.6	49.1	49	39.2	53	42.8	25.5
22/02/2019	550	609.3	639	277	690.3	420.8	408.4	508															
	493	558.4	589	228	651.2	367.3	365.2	483	28.56	28.67	48.76	48.76	45.6	50.2	28.46	27.8	57.6	50.9	49.5	49.5	39.1	53.5	43.2	25
26/02/2019	428	556.1	501	342	268.4		473.2	740.3															
	371	505.1	451	292	230.3		430	714.6	28.41	28.73	45.61	45.51	44.5		28.46	28.6	57.3	51	49.4	49.3	38.1		43.2	25.7

g. MLSS and MLVSS results

Preliminary experiments								
08/08/2017	R1	R2	R3	R4	R5	R6	R7	R8
V sample (ml)	15	15	15	15	15	15	15	15
Empty	1.2067	1.1894	1.1922	1.2117	1.2076	1.2013	1.1952	1.209
With dry sludge	1.2338	1.2201	1.223	1.2378	1.2343	1.2312	1.2286	1.2458
With ash	1.2092	1.1928	1.1958	1.2143	1.2101	1.2045	1.2012	1.2161
MLSS (mg/l)	1806.6667	2046.6667	2053.3333	1740	1780	1993.3333	2226.6667	2453.3333

MLVSS (mg/l)	1640	1820	1813.3333	1566.6667	1613.3333	1780	1826.6667	1980
12/08/2017	R1	R2	R3	R4	R5	R6	R7	R8
V sample (ml)	15	15	15	15	15	15	15	15
Empty	1.1995	1.1826	1.1835	1.2097	1.2063	1.1929	1.1888	1.2028
With dry sludge	1.2254	1.208	1.2085	1.2314	1.2298	1.2183	1.2182	1.2343
With ash	1.2052	1.1886	1.1909	1.2128	1.21	1.1992	1.199	1.2158
MLSS (mg/l)	1726.6667	1693.3333	1666.6667	1446.6667	1566.6667	1693.3333	1960	2100
MLVSS (mg/l)	1346.6667	1293.3333	1173.3333	1240	1320	1273.3333	1280	1233.3333
18/08/2017	R1	R2	R3	R4	R5	R6	R7	R8
V sample (ml)	15	15	15	15	15	15	15	15
Empty	1.2091	1.1864	1.1931	1.2112	1.206	1.2017	1.1935	1.2098
With dry sludge	1.2316	1.2089	1.2163	1.2331	1.2304	1.2276	1.2219	1.2369
With ash	1.2113	1.1889	1.1959	1.214	1.2101	1.2055	1.202	1.2176
MLSS (mg/l)	1500	1500	1546.6667	1460	1626.6667	1726.6667	1893.3333	1806.6667
MLVSS (mg/l)	1353.3333	1333.3333	1360	1273.3333	1353.3333	1473.3333	1326.6667	1286.6667
25/08/2017	R1	R2	R3	R4	R5	R6	R7	R8
V sample (ml)	15	15	15	15	15	15	15	15
Empty	1.2045	1.1906	1.1984	1.2137	1.1711	1.1645	1.1935	1.2066
With dry sludge	1.2302	1.2156	1.2249	1.2372	1.1968	1.2044	1.2209	1.2384
With ash	1.2071	1.1933	1.2018	1.216	1.1774	1.1751	1.2016	1.2164
MLSS (mg/l)	1713.3333	1666.6667	1766.6667	1566.6667	1713.3333	2660	1826.6667	2120
MLVSS (mg/l)	1540	1486.6667	1540	1413.3333	1293.3333	1953.3333	1286.6667	1466.6667
31/08/2017	R1	R2	R3	R4	R5	R6	R7	R8
V sample (ml)	15	15	15	15	15	15	15	15
Empty	1.195	1.1816	1.1935	1.2039	1.2178	1.2042	1.2037	1.1984
With dry sludge	1.2195	1.2077	1.2165	1.2288	1.2377	1.2214	1.2129	1.2133
With ash	1.1961	1.1834	1.195	1.2057	1.2192	1.2054	1.2043	1.1997
MLSS (mg/l)	1633.3333	1740	1533.3333	1660	1326.6667	1146.6667	613.33333	993.33333
MLVSS (mg/l)	1560	1620	1433.3333	1540	1233.3333	1066.6667	573.33333	906.66667
04/09/2017	R1	R2	R3	R4	R5	R6	R7	R8
V sample (ml)	15	15	15	15	15	15	15	15
Empty	1.1975	1.1826	1.1943	1.2066	1.2163	1.2046	1.201	1.1991
With dry sludge	1.2174	1.2013	1.2095	1.2207	1.2283	1.2148	1.2078	1.2079

With ash	1.1986	1.1836	1.1945	1.2068	1.2166	1.205	1.2014	1.1994
MLSS (mg/l)	1326.6667	1246.6667	1013.3333	940	800	680	453.33333	586.66667
MLVSS (mg/l)	1253.3333	1180	1000	926.66667	780	653.33333	426.66667	566.66667
07/09/2017	R1	R2	R3	R4	R5	R6	R7	R8
V sample (ml)	15	15	15	15	15	15	15	15
Empty	1.1943	1.1807	1.195	1.2044	1.2183	1.2082	1.2048	1.1986
With dry sludge	1.2172	1.2031	1.215	1.2243	1.234	1.2229	1.2132	1.2072
With ash	1.1961	1.1824	1.1963	1.2054	1.2197	1.2095	1.2051	1.1989
MLSS (mg/l)	1526.6667	1493.3333	1333.3333	1326.6667	1046.6667	980	560	573.33333
MLVSS (mg/l)	1406.6667	1380	1246.6667	1260	953.33333	893.33333	540	553.33333
11/09/2017	R1	R2	R3	R4	R5	R6	R7	R8
V sample (ml)	20	20	20	20	20	20	30	30
Empty	1.1979	1.1833	1.1946	1.2053	1.2168	1.2054	1.2031	1.1967
With dry sludge	1.2278	1.2127	1.2218	1.2314	1.2375	1.2263	1.2139	1.2089
With ash	1.1999	1.1854	1.1963	1.2074	1.2197	1.2095	1.2051	1.1989
MLSS (mg/l)	1495	1470	1360	1305	1035	1045	360	406.66667
MLVSS (mg/l)	1395	1365	1275	1200	890	840	293.33333	333.33333
16/09/2017	R1	R2	R3	R4	R5	R6	R7	R8
V sample (ml)	20	20	20	20	20	20	20	20
Empty	1.2085	1.203	1.2035	1.2059	1.2064	1.2048	1.2021	1.2084
With dry sludge	1.2421	1.232	1.2338	1.2285	1.2398	1.2379	1.2312	1.2416
With ash	1.2132	1.2068	1.2079	1.2084	1.2102	1.2087	1.2048	1.2118
MLSS (mg/l)	1680	1450	1515	1130	1670	1655	1455	1660
MLVSS (mg/l)	1445	1260	1295	1005	1480	1460	1320	1490
23/09/2017	R1	R2	R3	R4	R5	R6	R7	R8
V sample (ml)	15	15	15	15	15	15	15	15
Empty	1.2062	1.2057	1.2041	1.2112	1.2045	1.2088	1.2006	1.2092
With dry sludge	1.2597	1.2579	1.2589	1.2661	1.2684	1.2709	1.2537	1.2614
With ash	1.2197	1.2188	1.2195	1.2276	1.2225	1.2261	1.2122	1.2205
MLSS (mg/l)	3566.6667	3480	3653.3333	3660	4260	4140	3540	3480
MLVSS (mg/l)	2666.6667	2606.6667	2626.6667	2566.6667	3060	2986.6667	2766.6667	2726.6667
27/09/2017	R1	R2	R3	R4	R5	R6	R7	R8
V sample (ml)	15	15	15	15	15	15	15	15

Empty	1.2114	1.2057	1.2067	1.2083	1.2067	1.2076	1.2025	1.2079
With dry sludge	1.2495	1.2423	1.2523	1.2527	1.261	1.2582	1.2497	1.2467
With ash	1.2178	1.2116	1.2171	1.2187	1.2192	1.2192	1.2104	1.2129
MLSS (mg/l)	2540	2440	3040	2960	3620	3373.3333	3146.6667	2586.6667
MLVSS (mg/l)	1585	1535	1760	1700	2090	1950	1965	1690
03/10/2017	R1	R2	R3	R4	R5	R6	R7	R8
V sample (ml)	15	15	15	15	15	15	15	15
Empty	1.191	1.2067	1.1967	1.2102	1.1924	1.2124	1.2126	1.2102
With dry sludge	1.2213	1.2333	1.228	1.2386	1.2258	1.2471	1.2436	1.2395
With ash	1.1919	1.2071	1.1985	1.2113	1.1951	1.2155	1.2151	1.2112
MLSS (mg/l)	2020	1773.3333	2086.6667	1893.3333	2226.6667	2313.3333	2066.6667	1953.3333
MLVSS (mg/l)	1470	1310	1475	1365	1535	1580	1425	1415
09/10/2017	R1	R2	R3	R4	R5	R6	R7	R8
V sample (ml)	15	15	15	15	15	15	15	15
Empty	1.1885	1.2058	1.1983	1.2076	1.1934	1.2104	1.2125	1.1683
With dry sludge	1.2159	1.2296	1.2253	1.2334	1.2236	1.2436	1.2371	1.1889
With ash	1.1894	1.2062	1.1992	1.2084	1.1952	1.2128	1.2133	1.1709
MLSS (mg/l)	1826.6667	1586.6667	1800	1720	2013.3333	2213.3333	1640	1373.3333
MLVSS (mg/l)	1325	1170	1305	1250	1420	1540	1190	900
20/10/2017	R1	R2	R3	R4	R5	R6	R7	R8
V sample (ml)	15	15	15	15	15	15	15	15
Empty	1.1484	1.1442	1.1627	1.1661	1.1689	1.1544	1.1485	1.1662
With dry sludge	1.1732	1.1695	1.1866	1.1867	1.1924	1.1827	1.1728	1.1845
With ash	1.1502	1.1461	1.1647	1.1676	1.1708	1.1573	1.1519	1.1675
MLSS (mg/l)	1653.3333	1686.6667	1593.3333	1373.3333	1566.6667	1886.6667	1620	1220
MLVSS (mg/l)	1150	1170	1095	955	1080	1270	1045	850
07/11/2017	R1	R2	R3	R4	R5	R6	R7	R8
V sample (ml)	15	15	15	15	15	15	15	15
Empty	1.1482	1.1461	1.1626	1.1677	1.169	1.1552	1.1489	1.1626
With dry sludge	1.1689	1.1657	1.1819	1.1878	1.1955	1.1811	1.1716	1.1774
With ash	1.1501	1.148	1.1647	1.1696	1.1721	1.1586	1.1539	1.165
MLSS (mg/l)	1380	1306.6667	1286.6667	1340	1766.6667	1726.6667	1513.3333	986.66667
MLVSS (mg/l)	1253.3333	1180	1146.6667	1213.3333	1560	1500	1180	826.66667

09/12/2017	R1	R2	R3	R4	R5	R6	R7	R8
V sample (ml)	15	15	15	15	15	15	15	15
Empty	1.4262	1.4233	1.425	1.4225	1.1033	1.12	1.1161	1.1388
With dry sludge	1.4603	1.4571	1.4601	1.4585	1.1381	1.155	1.1474	1.1698
With ash	1.4295	1.4274	1.4291	1.4265	1.1081	1.1244	1.1207	1.1433
MLSS (mg/l)	2273.3333	2253.3333	2340	2400	2320	2333.3333	2086.6667	2066.6667
MLVSS (mg/l)	2053.3333	1980	2066.6667	2133.3333	2000	2040	1780	1766.6667
Enrichment 1								
09/12/2017	R1	R2	R3	R4	R5	R6	R7	R8
V sample (ml)	15	15	15	15	15	15	15	15
Empty	1.4262	1.4233	1.425	1.4225	1.1033	1.12	1.1161	1.1388
With dry sludge	1.4603	1.4571	1.4601	1.4585	1.1381	1.155	1.1474	1.1698
With ash	1.4295	1.4274	1.4291	1.4265	1.1081	1.1244	1.1207	1.1433
MLSS (mg/l)	2273.3333	2253.3333	2340	2400	2320	2333.3333	2086.6667	2066.6667
MLVSS (mg/l)	2053.3333	1980	2066.6667	2133.3333	2000	2040	1780	1766.6667
20/12/2017	R1	R2	R3	R4	R5	R6	R7	R8
V sample (ml)	15	15	15	15	15	15	15	15
Empty	1.4277	1.4205	1.425	1.4236	1.104	1.1106	1.1157	1.1396
With dry sludge	1.4577	1.4517	1.4548	1.4545	1.1351	1.14	1.1414	1.167
With ash	1.4295	1.4255	1.4287	1.4285	1.1068	1.1116	1.118	1.142
MLSS (mg/l)	2000	2080	1986.6667	2060	2073.3333	1960	1713.3333	1826.6667
MLVSS (mg/l)	1880	1746.6667	1740	1733.3333	1886.6667	1893.3333	1560	1666.6667
07/01/2018	R1	R2	R3	R4	R5	R6	R7	R8
V sample (ml)	15	15	15	15	15	15	15	15
Empty	1.4253	1.4235	1.4248	1.4242	1.1045	1.1222	1.1637	1.1392
With dry sludge	1.4533	1.4518	1.455	1.4489	1.1325	1.1509	1.1928	1.164
With ash	1.4278	1.4259	1.4275	1.4258	1.1072	1.1246	1.1651	1.1414
MLSS (mg/l)	1866.6667	1886.6667	2013.3333	1646.6667	1866.6667	1913.3333	1940	1653.3333
MLVSS (mg/l)	1700	1726.6667	1833.3333	1540	1686.6667	1753.3333	1846.6667	1506.6667
17/01/2018	R1	R2	R3	R4	R5	R6	R7	R8
V sample (ml)	20	20	20	20	20	20	20	20
Empty	1.4228	1.4198	1.4213	1.4207	1.1008	1.1175	1.1136	1.1407
With dry sludge	1.4464	1.4407	1.4427	1.4393	1.1236	1.1391	1.1286	1.1556

With ash	1.4247	1.4215	1.4228	1.4218	1.1025	1.1189	1.1147	1.1419
MLSS (mg/l)	1180	1045	1070	930	1140	1080	750	745
MLVSS (mg/l)	1085	960	995	875	1055	1010	695	685
24/01/2018	R1	R2	R3	R4	R5	R6	R7	R8
V sample (ml)	15	15	15	15	15	15	15	15
Empty	1.4243	1.4204	1.4212	1.4208	1.1012	1.119	1.1135	1.1364
With dry sludge	1.4771	1.4685	1.4705	1.47	1.1479	1.1677	1.1594	1.1835
With ash	1.4309	1.4265	1.4276	1.4269	1.1072	1.1252	1.1206	1.1433
MLSS (mg/l)	3520	3206.6667	3286.6667	3280	3113.3333	3246.6667	3060	3140
MLVSS (mg/l)	3080	2800	2860	2873.3333	2713.3333	2833.3333	2586.6667	2680
27/01/2018	R1	R2	R3	R4	R5	R6	R7	R8
V sample (ml)	15	15	15	15	15	15	15	15
Empty	1.4238	1.4239	1.425	1.4188	1.1027	1.1197	1.1161	1.1377
With dry sludge	1.452	1.4506	1.4516	1.4418	1.128	1.1449	1.145	1.1635
With ash	1.4265	1.4263	1.4272	1.4205	1.1051	1.1219	1.12	1.1414
MLSS (mg/l)	1880	1780	1773.3333	1533.3333	1686.6667	1680	1926.6667	1720
MLVSS (mg/l)	1700	1620	1626.6667	1420	1526.6667	1533.3333	1666.6667	1473.3333
01/02/2018	R1	R2	R3	R4	R5	R6	R7	R8
V sample (ml)	15	15	15	15	15	15	15	15
Empty	1.4239	1.4215	1.4226	1.422	1.1024	1.1195	1.1139	1.1381
With dry sludge	1.4423	1.4405	1.4427	1.4389	1.1234	1.1373	1.1341	1.1599
With ash	1.4252	1.423	1.4241	1.423	1.1042	1.1207	1.1168	1.1415
MLSS (mg/l)	1226.6667	1266.6667	1340	1126.6667	1400	1186.6667	1346.6667	1453.3333
MLVSS (mg/l)	1140	1166.6667	1240	1060	1280	1106.6667	1153.3333	1226.6667
07/02/2018	R1	R2	R3	R4	R5	R6	R7	R8
V sample (ml)	20	20	20	20	20	20	20	20
Empty	1.4237	1.4231	1.4244	1.4217	1.1031	1.12	1.114	1.1381
With dry sludge	1.4442	1.4463	1.4429	1.4433	1.1268	1.1414	1.1341	1.1626
With ash	1.4256	1.425	1.4258	1.4234	1.1055	1.1222	1.1173	1.1426
MLSS (mg/l)	1025	1160	925	1080	1185	1070	1005	1225
MLVSS (mg/l)	930	1065	855	995	1065	960	840	1000
13/02/2018	R1	R2	R3	R4	R5	R6	R7	R8
V sample (ml)	20	20	20	15	20	20	20	20

Empty	1.4229	1.4212	1.4228	1.4209	1.1009	1.1196	1.1152	1.1394
With dry sludge	1.4417	1.4433	1.4444	1.4366	1.1195	1.1363	1.1319	1.1601
With ash	1.424	1.4232	1.4246	1.4221	1.1026	1.1211	1.1181	1.1434
MLSS (mg/l)	940	1105	1080	1046.7	930	835	835	1035
MLVSS (mg/l)	885	1005	990	966.7	845	760	690	835
20/02/2018	R1	R2	R3	R4	R5	R6	R7	R8
V sample (ml)	20	20	20	20	20	20	20	20
Empty	1.4234	1.4207	1.4248	1.4225	1.1008	1.118	1.1147	1.1385
With dry sludge	1.4426	1.44	1.4437	1.4422	1.1129	1.1336	1.1327	1.1574
With ash	1.4248	1.4222	1.4268	1.4242	1.1015	1.1194	1.1188	1.1432
MLSS (mg/l)	960	965	945	985.0	605	780	900	945
MLVSS (mg/l)	890	890	845	900.0	570	710	695	710
27/02/2018	R1	R2	R3	R4	R5	R6	R7	R8
V sample (ml)	20	20	20	20	20	20	20	20
Empty	1.4248	1.4234	1.4235	1.4214	1.102	1.119	1.1143	1.1383
With dry sludge	1.4453	1.4426	1.4397	1.4392	1.1141	1.1332	1.1314	1.1473
With ash	1.4256	1.4243	1.4241	1.4222	1.1025	1.1198	1.1188	1.1396
MLSS (mg/l)	1025	960	810	890.0	605	710	855	450
MLVSS (mg/l)	985	915	780	850.0	580	670	630	385
07/03/2018	R1	R2	R3	R4	R5	R6	R7	R8
V sample (ml)	20	20	20	20	20	20	20	20
Empty	1.4237	1.4209	1.4232	1.4228	1.1022	1.1177	1.1153	1.1384
With dry sludge	1.4448	1.4379	1.4412	1.4366	1.1156	1.1284	1.1391	1.152
With ash	1.4245	1.4215	1.4247	1.4231	1.1025	1.1178	1.1235	1.1402
MLSS (mg/l)	1055	850	900	690.0	670	535	1190	680
MLVSS (mg/l)	1015	820	825	675.0	655	530	780	590
10/03/2018	R1	R2	R3	R4	R5	R6	R7	R8
V sample (ml)	20	20	20	20	20	20	20	20
Empty	1.4233	1.4215	1.4231	1.4233	1.103	1.1183	1.1143	1.1382
With dry sludge	1.4393	1.4387	1.4367	1.4362	1.1128	1.1291	1.1332	1.1608
With ash	1.4237	1.4222	1.4237	1.4239	1.1031	1.1185	1.1205	1.1456
MLSS (mg/l)	800	860	680	645.0	490	540	945	1130
MLVSS (mg/l)	780	825	650	615.0	485	530	635	760

Appendix A

13/03/2018	R1	R2	R3	R4	R5	R6	R7	R8
V sample (ml)	20	20	20	20	20	20	20	20
Empty	1.4233	1.4231	1.4226	1.4216	1.1014	1.119	1.115	1.1391
With dry sludge	1.4379	1.4368	1.4346	1.4329	1.1125	1.128	1.135	1.1551
With ash	1.4238	1.4237	1.4232	1.4221	1.1017	1.1192	1.1217	1.1437
MLSS (mg/l)	730	685	600	565.0	555	450	1000	800
MLVSS (mg/l)	705	655	570	540.0	540	440	665	570
16/03/2018	R1	R2	R3	R4	R5	R6	R7	R8
V sample (ml)	20	20	20	20	20	20	20	20
Empty	1.4241	1.4232	1.424	1.4236	1.1032	1.1213	1.1168	1.1385
With dry sludge	1.4363	1.4373	1.4393	1.4368	1.1144	1.1314	1.1325	1.1555
With ash	1.4243	1.4236	1.4247	1.424	1.1034	1.1216	1.1222	1.1445
MLSS (mg/l)	610	705	765	660.0	560	505	785	850
MLVSS (mg/l)	600	685	730	640.0	550	490	515	550
19/03/2018	R1	R2	R3	R4	R5	R6	R7	R8
V sample (ml)	20	20	20	20	20	20	20	20
Empty	1.4259	1.4221	1.4219	1.4203	1.102	1.1184	1.114	1.1383
With dry sludge	1.4406	1.4381	1.4377	1.4374	1.1141	1.1293	1.138	1.1641
With ash	1.4265	1.4228	1.4226	1.421	1.1022	1.1186	1.1238	1.1488
MLSS (mg/l)	735	800	790	855.0	605	545	1200	1290
MLVSS (mg/l)	705	765	755	820.0	595	535	710	765
22/03/2018	R1	R2	R3	R4	R5	R6	R7	R8
V sample (ml)	20	20	20	20	20	20	20	20
Empty	1.428	1.4244	1.4271	1.4248	1.1063	1.1231	1.1179	1.1436
With dry sludge	1.4437	1.4418	1.4457	1.4461	1.1206	1.1342	1.1448	1.1711
With ash	1.4282	1.4249	1.4278	1.4256	1.1065	1.1232	1.1289	1.1547
MLSS (mg/l)	785	870	930	1065.0	715	555	1345	1375
MLVSS (mg/l)	775	845	895	1025.0	705	550	795	820
27/03/2018	R1	R2	R3	R4	R5	R6	R7	R8
V sample (ml)	20	20	20	20	20	20	20	20
Empty	1.4278	1.4258	1.4272	1.4253	1.1068	1.1214	1.1156	1.1414
With dry sludge	1.439	1.4353	1.4365	1.4365	1.1165	1.1307	1.1334	1.1569
With ash	1.4281	1.4262	1.4275	1.4259	1.1069	1.1222	1.1236	1.1475

MLSS (mg/l)	560	475	465	560.0	485	465	890	775
MLVSS (mg/l)	545	455	450	530.0	480	425	490	470
30/03/2018	R1	R2	R3	R4	R5	R6	R7	R8
V sample (ml)	20	20	20	20	20	20	20	20
Empty	1.4273	1.4257	1.4275	1.4244	1.1049	1.1237	1.1169	1.1407
With dry sludge	1.44	1.4387	1.4394	1.4372	1.117	1.1346	1.138	1.1601
With ash	1.429	1.4277	1.4292	1.4262	1.1061	1.1245	1.1263	1.1499
MLSS (mg/l)	635	650	595	640.0	605	545	1055	970
MLVSS (mg/l)	550	550	510	550.0	545	505	585	510
03/04/2018	R1	R2	R3	R4	R5	R6	R7	R8
V sample (ml)	20	20	20	20	20	20	20	20
Empty	1.4252	1.4256	1.427	1.4238	1.1045	1.1223	1.1186	1.1399
With dry sludge	1.4391	1.4413	1.4405	1.4374	1.1169	1.1382	1.1433	1.1676
With ash	1.4265	1.4277	1.4291	1.4258	1.1057	1.1239	1.1301	1.153
MLSS (mg/l)	695	785	675	680.0	620	795	1235	1385
MLVSS (mg/l)	630	680	570	580.0	560	715	660	730
06/04/2018	R1	R2	R3	R4	R5	R6	R7	R8
V sample (ml)	20	20	20	20	20	20	20	20
Empty	1.4239	1.4241	1.4267	1.4239	1.1036	1.1212	1.1168	1.14
With dry sludge	1.4392	1.44	1.4389	1.4368	1.1155	1.1414	1.1432	1.1636
With ash	1.4257	1.426	1.4282	1.4252	1.1048	1.1231	1.1288	1.1512
MLSS (mg/l)	765	795	610	645.0	595	1010	1320	1180
MLVSS (mg/l)	675	700	535	580.0	535	915	720	620
07/05/2018	R1	R2	R3	R4	R5	R6	R7	R8
V sample (ml)	20	20	20	20	20	20	20	20
Empty	1.4255	1.4258	1.426	1.4261	1.1053	1.123	1.1167	1.1404
With dry sludge	1.4385	1.4379	1.4368	1.4346	1.1135	1.1337	1.1436	1.1663
With ash	1.4269	1.4268	1.4272	1.4265	1.1057	1.1238	1.1285	1.1485
MLSS (mg/l)	650	605	540	425.0	410	535	1345	1295
MLVSS (mg/l)	580	555	480	405.0	390	495	755	890
23/05/2018	R1	R2	R3	R4	R5	R6	R7	R8
V sample (ml)	20	20	20	20	20	20	20	20
Empty	1.426	1.4223	1.4233	1.4236	1.1032	1.1209	1.1168	1.1391

With dry sludge	1.4454	1.4401	1.4386	1.4413	1.1128	1.1342	1.14	1.1706
With ash	1.4317	1.4271	1.4267	1.4269	1.1046	1.1232	1.124	1.1528
MLSS (mg/l)	970	890	765	885.0	480	665	1160	1575
MLVSS (mg/l)	685	650	595	720.0	410	550	800	890
29/05/2018	R1	R2	R3	R4	R5	R6	R7	R8
V sample (ml)	20	20	20	20	20	20	20	20
Empty	1.4254	1.425	1.4248	1.4237	1.1038	1.1214	1.1148	1.1415
With dry sludge	1.4437	1.444	1.4399	1.441	1.1142	1.1353	1.1453	1.1647
With ash	1.4303	1.4297	1.428	1.4275	1.1056	1.1237	1.1272	1.1491
MLSS (mg/l)	915	950	755	865.0	520	695	1525	1160
MLVSS (mg/l)	670	715	595	675.0	430	580	905	780
06/06/2018	R1	R2	R3	R4	R5	R6	R7	R8
V sample (ml)	10	10	10	10	10	10	10	10
Empty	1.4274	1.428	1.4277	1.4242	1.1041	1.1256	1.1195	1.1428
With dry sludge	1.4383	1.4393	1.4352	1.4325	1.1107	1.134	1.1318	1.1524
With ash	1.4302	1.4307	1.4295	1.4263	1.1052	1.1271	1.123	1.1451
MLSS (mg/l)	1090	1130	750	830.0	660	840	1230	960
MLVSS (mg/l)	810	860	570	620.0	550	690	880	730
08/06/2018	R1	R2	R3	R4	R5	R6	R7	R8
V sample (ml)	10	10	10	10	10	10	10	10
Empty	1.4268	1.428	1.4275	1.4223	1.1055	1.1238	1.1173	1.142
With dry sludge	1.438	1.4391	1.4354	1.4303	1.1128	1.1332	1.1316	1.1534
With ash	1.4297	1.4305	1.4295	1.424	1.1066	1.1257	1.1215	1.1448
MLSS (mg/l)	1120	1110	790	800.0	730	940	1430	1140
MLVSS (mg/l)	830	860	590	630.0	620	750	1010	860
28/06/2018	R1	R2	R3	R4	R5	R6	R7	R8
V sample (ml)	10	10	10	10	10	10	10	10
Empty	1.424	1.4258	1.422	1.4209	1.1033	1.1175	1.1219	1.14
With dry sludge	1.4331	1.436	1.4313	1.4316	1.1132	1.1265	1.1356	1.1516
With ash	1.4258	1.4278	1.4243	1.4244	1.1055	1.1195	1.1258	1.1433
MLSS (mg/l)	910	1020	930	1070.0	990	900	1370	1160
MLVSS (mg/l)	730	820	700	720.0	770	700	980	830
14/07/2018	R1	R2	R3	R4	R5	R6	R7	R8

V sample (ml)	9.8	9.8	9.8	9.8	9.8	9.8	9.8	9.8
Empty	1.4256	1.4262	1.425	1.4226	1.1174	1.1052	1.1221	1.1404
With dry sludge	1.4317	1.4327	1.4338	1.4297	1.1244	1.1116	1.1349	1.1521
With ash	1.4262	1.4268	1.4265	1.4235	1.1189	1.1062	1.1257	1.1423
MLSS (mg/l)	622.44898	663.26531	897.95918	724.5	714.28571	653.06122	1306.1224	1193.8776
MLVSS (mg/l)	561.22449	602.04082	744.89796	632.7	561.22449	551.02041	938.77551	1000
19/07/2018	R1	R2	R3	R4	R5	R6	R7	R8
V sample (ml)	10	10	10	10	10	10	10	10
Empty	1.4236	1.4271	1.426	1.4233	1.1023	1.1217	1.1172	1.1404
With dry sludge	1.4315	1.4335	1.4358	1.4311	1.1114	1.1294	1.1303	1.1538
With ash	1.4247	1.4284	1.4284	1.4251	1.1046	1.1235	1.1214	1.1428
MLSS (mg/l)	790	640	980	780.0	910	770	1310	1340
MLVSS (mg/l)	680	510	740	600.0	680	590	890	1100
31/07/2018	R1	R2	R3	R4	R5	R6	R7	R8
V sample (ml)	10	10	10	10	10	10	10	10
Empty	1.3386	1.3379	1.3382	1.3367	1.0174	1.0345	1.0303	1.054
With dry sludge	1.3516	1.35	1.3524	1.348	1.0328	1.0485	1.042	1.0693
With ash	1.3435	1.3425	1.3439	1.3414	1.0224	1.0397	1.0345	1.0579
MLSS (mg/l)	1300	1210	1420	1130	1540	1400	1170	1530
MLVSS (mg/l)	810	750	850	660	1040	880	750	1140
07/08/2018	R1	R2	R3	R4	R5	R6	R7	R8
V sample (ml)	10	10	10	10	10	10	10	10
Empty	1.1592	1.1558	1.1567	1.1518	1.1562	1.162	1.1608	1.1487
With dry sludge	1.1685	1.1638	1.1651	1.1569	1.1669	1.1731	1.1757	1.161
With ash	1.1612	1.1573	1.1586	1.1531	1.1587	1.1647	1.1657	1.1501
MLSS (mg/l)	930	800	840	510	1070	1110	1490	1230
MLVSS (mg/l)	730	650	650	380	820	840	1000	1090
15/08/2018	R1	R2	R3	R4	R5	R6	R7	R8
V sample (ml)	10	10	10	10	10	10	10	10
Empty	1.1595	1.1555	1.1559	1.149	1.1542	1.1601	1.1611	1.1457
With dry sludge	1.1706	1.1659	1.1653	1.1544	1.1664	1.1741	1.174	1.1546
With ash	1.1622	1.1583	1.1588	1.1509	1.1583	1.1649	1.1657	1.1479
MLSS (mg/l)	1110	1040	940	540	1220	1400	1290	890

MLVSS (mg/l)	840	760	650	350	810	920	830	670
21/08/2018	R1	R2	R3	R4	R5	R6	R7	R8
V sample (ml)	10	10	10	10	10	10	10	10
Empty	1.1611	1.1573	1.1589	1.1509	1.1553	1.1625	1.1604	1.1485
With dry sludge	1.171	1.1687	1.1682	1.1572	1.1674	1.1791	1.1756	1.1549
With ash	1.1633	1.1605	1.1613	1.1527	1.1593	1.168	1.1664	1.15
MLSS (mg/l)	990	1140	930	630	1210	1660	1520	640
MLVSS (mg/l)	770	820	690	450	810	1110	920	490
06/09/2018	R1	R2	R3	R4	R5	R6	R7	R8
V sample (ml)	10	10	10	10	10	10	10	10
Empty	1.1623	1.1566	1.1585	1.1499	1.155	1.1629	1.1489	1.1605
With dry sludge	1.173	1.1673	1.1684	1.1577	1.1667	1.1737	1.1625	1.1729
With ash	1.1649	1.1598	1.1613	1.152	1.1583	1.166	1.1547	1.1644
MLSS (mg/l)	1070	1070	990	780	1170	1080	1360	1240
MLVSS (mg/l)	810	750	710	570	840	770	780	850
25/09/2018	R1	R2	R3	R4	R5	R6	R7	R8
V sample (ml)	10	10	10	10	10	10	10	10
Empty	1.1608	1.1586	1.1581	1.1502	1.157	1.1622	1.1485	1.1613
With dry sludge	1.1732	1.1693	1.1654	1.1604	1.168	1.1719	1.163	1.1718
With ash	1.1641	1.1619	1.1601	1.1522	1.1598	1.1637	1.1545	1.1644
MLSS (mg/l)	1240	1070	730	1020	1100	970	1450	1050
MLVSS (mg/l)	910	740	530	820	820	820	850	740
05/10/2018	R1	R2	R3	R4	R5	R6	R7	R8
V sample (ml)	10	10	10	10	10	10	10	10
Empty	1.1589	1.1561	1.1571	1.1563	1.1611	1.1643	1.1478	1.1608
With dry sludge	1.172	1.1674	1.1658	1.1708	1.1721	1.1717	1.1612	1.1715
With ash	1.163	1.1592	1.1597	1.1601	1.1642	1.1664	1.1538	1.1647
MLSS (mg/l)	1310	1130	870	1450	1100	740	1340	1070
MLVSS (mg/l)	900	820	610	1070	790	530	740	680
16/10/2018	R1	R2	R3	R4	R5	R6	R7	R8
V sample (ml)	10	10	10	10	10	10	10	10
Empty	1.2829	1.2922	1.278	1.2765	1.2625	1.2652	1.3078	1.2682
With dry sludge	1.2928	1.3024	1.2848	1.2851	1.2742	1.2866	1.3249	1.2841

With ash	1.2847	1.2934	1.2787	1.2775	1.264	1.2694	1.309	1.2691
MLSS (mg/l)	990	1020	680	860	1170	2140	1710	1590
MLVSS (mg/l)	810	900	610	760	1020	1720	1590	1500
Enrichment 2 and trials								
05/10/2018	R1	R2	R3	R4	R5	R6	R7	R8
V sample (ml)	10	10	10	10	10	10	10	10
Empty	1.1589	1.1561	1.1571	1.1563	1.1611	1.1643	1.1478	1.1608
With dry sludge	1.172	1.1674	1.1658	1.1708	1.1721	1.1717	1.1612	1.1715
With ash	1.163	1.1592	1.1597	1.1601	1.1642	1.1664	1.1538	1.1647
MLSS (mg/l)	1310	1130	870	1450	1100	740	1340	1070
MLVSS (mg/l)	900	820	610	1070	790	530	740	680
16/10/2018	R1	R2	R3	R4	R5	R6	R7	R8
V sample (ml)	10	10	10	10	10	10	10	10
Empty	1.2829	1.2922	1.278	1.2765	1.2625	1.2652	1.3078	1.2682
With dry sludge	1.2928	1.3024	1.2848	1.2851	1.2742	1.2866	1.3249	1.2841
With ash	1.2847	1.2934	1.2787	1.2775	1.264	1.2694	1.309	1.2691
MLSS (mg/l)	990	1020	680	860	1170	2140	1710	1590
MLVSS (mg/l)	810	900	610	760	1020	1720	1590	1500
19/10/2018	R1	R2	R3	R4	R5	R6	R7	R8
V sample (ml)	10	10	10	10	10	10	10	10
Empty	1.286	1.2911	1.2786	1.2821	1.2635	1.2683	1.3059	1.2643
With dry sludge	1.2947	1.3009	1.2844	1.2921	1.2746	1.2858	1.3196	1.2784
With ash	1.2882	1.2939	1.2804	1.2843	1.2664	1.2732	1.3079	1.2662
MLSS (mg/l)	870	980	580	1000	1110	1750	1370	1410
MLVSS (mg/l)	650	700	400	780	820	1260	1170	1220
30/10/2018	R1	R2	R3	R4	R5	R6	R7	R8
V sample (ml)	10	10	10	10	10	10	10	10
Empty	1.2865	1.2917	1.2812	1.2755	1.263	1.2682	1.3024	1.2657
With dry sludge	1.2972	1.3007	1.284	1.2785	1.2707	1.2765	1.3114	1.2758
With ash	1.2882	1.2931	1.2817	1.2761	1.2641	1.2694	1.3039	1.2671
MLSS (mg/l)	1070	900	280	300	770	830	900	1010
MLVSS (mg/l)	900	760	230	240	660	710	750	870

Appendix A

08/11/2018	R1	R2	R3	R4	R5	R6	R7	R8
V sample (ml)	10	10	10	10	10	10	10	10
Empty	1.2825	1.2933	1.2774	1.2787	1.2619	1.2662	1.3083	1.2701
With dry sludge	1.2908	1.302	1.2827	1.2853	1.2674	1.2736	1.3133	1.2756
With ash	1.2839	1.2948	1.2784	1.28	1.2631	1.2676	1.3093	1.2707
MLSS (mg/l)	830	870	530	660	550	740	500	550
MLVSS (mg/l)	690	720	430	530	430	600	400	490
12/11/2018	R1	R2	R3	R4	R5	R6	R7	R8
V sample (ml)	10	10	10	10	10	10	10	10
Empty	1.2826	1.294	1.2794	1.2791	1.2669	1.2709	1.3059	1.2653
With dry sludge	1.2921	1.2972	1.2821	1.2844	1.2724	1.2774	1.3075	1.2707
With ash	1.2843	1.2946	1.2798	1.2801	1.2677	1.2724	1.3063	1.266
MLSS (mg/l)	950	320	270	530	550	650	160	540
MLVSS (mg/l)	780	260	230	430	470	500	120	470
15/11/2018	R1	R2	R3	R4	R5	R6	R7	R8
V sample (ml)	10	10	10	10	10	10	10	10
Empty	1.2832	1.2937	1.2778	1.28	1.2678	1.2633	1.3054	1.2654
With dry sludge	1.2936	1.3051	1.2816	1.2846	1.2717	1.2688	1.3093	1.2701
With ash	1.2853	1.296	1.2784	1.2808	1.2684	1.2644	1.3058	1.2657
MLSS (mg/l)	1040	1140	380	460	390	550	390	470
MLVSS (mg/l)	830	910	320	380	330	440	350	440
19/11/2018	R1	R2	R3	R4	R5	R6	R7	R8
V sample (ml)	10	10	10	10	10	10	10	10
Empty	1.281	1.2932	1.2792	1.2786	1.2639	1.2672	1.3046	1.2642
With dry sludge	1.2912	1.3052	1.2837	1.281	1.2692	1.2731	1.3094	1.2692
With ash	1.2839	1.2964	1.2803	1.2795	1.2654	1.269	1.3056	1.2651
MLSS (mg/l)	1020	1200	450	240	530	590	480	500
MLVSS (mg/l)	730	880	340	150	380	410	380	410
23/11/2018	R1	R2	R3	R4	R5	R6	R7	R8
V sample (ml)	10	10	10	10	10	10	10	10
Empty	1.2848	1.2905	1.2817	1.2788	1.2643	1.2675	1.3047	1.2645
With dry sludge	1.2948	1.303	1.2873	1.2845	1.2708	1.273	1.3122	1.2703
With ash	1.2874	1.2939	1.283	1.2802	1.2662	1.2694	1.306	1.2657

MLSS (mg/l)	1000	1250	560	570	650	550	750	580
MLVSS (mg/l)	740	910	430	430	460	360	620	460
29/11/2018	R1	R2	R3	R4	R5	R6	R7	R8
V sample (ml)	10	10	10	10	10	10	10	10
Empty	1.2831	1.294	1.2786	1.2795	1.2634	1.2665	1.3048	1.2666
With dry sludge	1.2921	1.3051	1.2834	1.2855	1.2696	1.2697	1.3124	1.2719
With ash	1.2854	1.2966	1.2797	1.2808	1.2648	1.2672	1.3061	1.2675
MLSS (mg/l)	900	1110	480	600	620	320	760	530
MLVSS (mg/l)	670	850	370	470	480	250	630	440
04/12/2018	R1	R2	R3	R4	R5	R6	R7	R8
V sample (ml)	10	10	10	10	10	10	10	10
Empty	1.2831	1.2931	1.278	1.2799	1.2632	1.2657	1.3071	1.2667
With dry sludge	1.293	1.3047	1.2844	1.2852	1.2717	1.2686	1.3171	1.2706
With ash	1.286	1.296	1.2794	1.2812	1.2653	1.2663	1.3093	1.2674
MLSS (mg/l)	990	1160	640	530	850	290	1000	390
MLVSS (mg/l)	700	870	500	400	640	230	780	320
14/12/2018	R1	R2	R3	R4	R5	R6	R7	R8
V sample (ml)	10	10	10	10	10	10	10	10
Empty	1.2841	1.295	1.2792	1.2805	1.2656	1.2687	1.3068	1.2669
With dry sludge	1.2994	1.3104	1.2995	1.3015	1.285	1.2949	1.3257	1.2811
With ash	1.2887	1.299	1.2837	1.2853	1.2705	1.2744	1.3101	1.2686
MLSS (mg/l)	1530	1540	2030	2100	1940	2620	1890	1420
MLVSS (mg/l)	1070	1140	1580	1620	1450	2050	1560	1250
17/12/2018	R1	R2	R3	R4	R5	R6	R7	R8
V sample (ml)	10	10	10	10	10	10	10	10
Empty	1.2871	1.2959	1.2815	1.2821	1.2655	1.2694	1.3068	1.2674
With dry sludge	1.3011	1.3087	1.2954	1.2986	1.2832	1.2892	1.3247	1.2781
With ash	1.2908	1.2987	1.2844	1.2861	1.2704	1.2744	1.3107	1.2697
MLSS (mg/l)	1400	1280	1390	1650	1770	1980	1790	1070
MLVSS (mg/l)	1030	1000	1100	1250	1280	1480	1400	840
21/12/2018	R1	R2	R3	R4	R5	R6	R7	R8
V sample (ml)	10	10	10	10	10	10	10	10
Empty	1.2852	1.2953	1.2796	1.2816	1.2668	1.2683	1.3066	1.2666

With dry sludge	1.2966	1.3065	1.2916	1.2955	1.2818	1.285	1.3209	1.2879
With ash	1.289	1.2987	1.2835	1.2861	1.2721	1.2737	1.3097	1.2713
MLSS (mg/l)	1140	1120	1200	1390	1500	1670	1430	2130
MLVSS (mg/l)	760	780	810	940	970	1130	1120	1660
23/12/2018	R1	R2	R3	R4	R5	R6	R7	R8
V sample (ml)	10	10	10	10	10	10	10	10
Empty	1.2668	1.2712	1.2554	1.2552	1.2734	1.2593	1.2587	1.2792
With dry sludge	1.2757	1.2801	1.2645	1.2582	1.2859	1.2748	1.27	1.2937
With ash	1.2682	1.2722	1.2567	1.2554	1.2756	1.2626	1.2598	1.2799
MLSS (mg/l)	890	890	910	300	1250	1550	1130	1450
MLVSS (mg/l)	750	790	780	280	1030	1220	1020	1380
25/12/2018	R1	R2	R3	R4	R5	R6	R7	R8
V sample (ml)	10	10	10	10	10	10	10	10
Empty	1.2859	1.296	1.2808	1.2807	1.2668	1.2687	1.3069	1.2681
With dry sludge	1.2975	1.31	1.2945	1.2947	1.282	1.2842	1.3229	1.2822
With ash	1.2897	1.3006	1.2853	1.2843	1.2715	1.274	1.3108	1.272
MLSS (mg/l)	1160	1400	1370	1400	1520	1550	1600	1410
MLVSS (mg/l)	780	940	920	1040	1050	1020	1210	1020
31/12/2018	R1	R2	R3	R4	R5	R6	R7	R8
V sample (ml)	10	10	10	10	10	10	10	10
Empty	1.285	1.2936	1.2803	1.282	1.266	1.2694	1.3079	1.2687
With dry sludge	1.2946	1.3078	1.2934	1.2941	1.2778	1.2843	1.3203	1.2845
With ash	1.2882	1.2987	1.2853	1.2854	1.2698	1.2749	1.3112	1.2744
MLSS (mg/l)	960	1420	1310	1210	1180	1490	1240	1580
MLVSS (mg/l)	640	910	810	870	800	940	910	1010
08/01/2019	R1	R2	R3	R4	R5	R6	R7	R8
V sample (ml)	10	10	10	10	10	10	10	10
Empty	1.2856	1.2962	1.2802	1.2816	1.2661	1.2696	1.308	1.2675
With dry sludge	1.295	1.3114	1.2962	1.2928	1.2767	1.283	1.3223	1.2832
With ash	1.2888	1.3018	1.2859	1.2852	1.2697	1.2749	1.312	1.2732
MLSS (mg/l)	940	1520	1600	1120	1060	1340	1430	1570
MLVSS (mg/l)	620	960	1030	760	700	810	1030	1000
11/01/2019	R1	R2	R3	R4	R5	R6	R7	R8

V sample (ml)	10	10	10	10	10	10	10	10
Empty	1.285	1.2951	1.2818	1.2832	1.2661	1.2686	1.3076	1.2682
With dry sludge	1.2958	1.3105	1.2971	1.295	1.2761	1.2847	1.3226	1.2866
With ash	1.2886	1.3006	1.2879	1.2867	1.269	1.2753	1.3117	1.275
MLSS (mg/l)	1080	1540	1530	1180	1000	1610	1500	1840
MLVSS (mg/l)	720	990	920	830	710	940	1090	1160
15/01/2019	R1	R2	R3	R4	R5	R6	R7	R8
V sample (ml)	10	10	10	10	10	10	10	10
Empty	1.2668	1.2711	1.2575	1.2564	1.2699	1.2584	1.2595	1.281
With dry sludge	1.276	1.2866	1.2716	1.2672	1.2791	1.2739	1.2735	1.2949
With ash	1.2698	1.2768	1.263	1.2599	1.2725	1.2645	1.2634	1.2859
MLSS (mg/l)	920	1550	1410	1080	920	1550	1400	1390
MLVSS (mg/l)	620	980	860	730	660	940	1010	900
18/01/2019	R1	R2	R3	R4	R5	R6	R7	R8
V sample (ml)	10	10	10	10	10	10	10	10
Empty	1.2668	1.2704	1.2572	1.2557	1.2733	1.2596	1.2596	1.2824
With dry sludge	1.2771	1.2857	1.27	1.2666	1.2828	1.2741	1.274	1.2935
With ash	1.2704	1.2761	1.2616	1.2592	1.2759	1.2651	1.264	1.2865
MLSS (mg/l)	1030	1530	1280	1090	950	1450	1440	1110
MLVSS (mg/l)	670	960	840	740	690	900	1000	700
22/01/2019	R1	R2	R3	R4	R5	R6	R7	R8
V sample (ml)	10	10	10	10	10	10	10	10
Empty	1.2678	1.2714	1.2579	1.2555	1.2729	1.2587	1.2607	1.2801
With dry sludge	1.279	1.2844	1.2682	1.2672	1.2819	1.2723	1.2761	1.2929
With ash	1.2714	1.2754	1.2596	1.2607	1.2753	1.2638	1.2652	1.2847
MLSS (mg/l)	1120	1300	1030	1170	900	1360	1540	1280
MLVSS (mg/l)	760	900	860	650	660	850	1090	820
25/01/2019	R1	R2	R3	R4	R5	R6	R7	R8
V sample (ml)	10	10	10	10	10	10	10	10
Empty	1.2673	1.2706	1.2582	1.2568	1.2723	1.2589	1.2616	1.2811
With dry sludge	1.2781	1.2826	1.2659	1.2646	1.2792	1.2713	1.2766	1.2936
With ash	1.2711	1.2749	1.259	1.2577	1.2745	1.264	1.2663	1.2857
MLSS (mg/l)	1080	1200	770	780	690	1240	1500	1250

MLVSS (mg/l)	700	770	690	690	470	730	1030	790
01/02/2019	R1	R2	R3	R4	R5	R6	R7	R8
V sample (ml)	10	10	10	10	10	10	10	10
Empty	1.2666	1.2704	1.2573	1.2558	1.2718	1.2598	1.2612	1.2794
With dry sludge	1.2782	1.2824	1.2649	1.2641	1.2786	1.2748	1.276	1.2935
With ash	1.2702	1.2746	1.2585	1.257	1.2745	1.2658	1.266	1.2841
MLSS (mg/l)	1160	1200	760	830	680	1500	1480	1410
MLVSS (mg/l)	800	780	640	710	410	900	1000	940
07/02/2019	R1	R2	R3	R4	R5	R6	R7	R8
V sample (ml)	10	10	10	10	10	10	10	10
Empty	1.2679	1.2716	1.2583	1.2572	1.2727	1.2606	1.2627	1.2824
With dry sludge	1.279	1.2839	1.2658	1.2649	1.2824	1.2726	1.2764	1.2947
With ash	1.2714	1.276	1.2591	1.258	1.2755	1.2647	1.2664	1.2854
MLSS (mg/l)	1110	1230	750	770	970	1200	1370	1230
MLVSS (mg/l)	760	790	670	690	690	790	1000	930
12/02/2019	R1	R2	R3	R4	R5	R6	R7	R8
V sample (ml)	10	10	10	10	10	10	10	10
Empty	1.2689	1.273	1.2595	1.2591	1.275	1.2611	1.2626	1.2832
With dry sludge	1.2792	1.2842	1.2672	1.2665	1.2848	1.2747	1.276	1.293
With ash	1.2719	1.2757	1.2602	1.2598	1.2783	1.266	1.2662	1.2856
MLSS (mg/l)	1030	1120	770	740	980	1360	1340	980
MLVSS (mg/l)	730	850	700	670	650	870	980	740
19/02/2019	R1	R2	R3	R4	R5	R6	R7	R8
V sample (ml)	10	10	10	10	10	10	10	10
Empty	1.2685	1.2717	1.256	1.2561	1.274	1.2634	1.2621	1.2825
With dry sludge	1.2792	1.2819	1.2642	1.2645	1.2861	1.2783	1.2737	1.289
With ash	1.2717	1.2742	1.2573	1.2572	1.2785	1.2693	1.2653	1.2838
MLSS (mg/l)	1070	1020	820	840	1210	1490	1160	650
MLVSS (mg/l)	750	770	690	730	760	900	840	520
22/02/2019	R1	R2	R3	R4	R5	R6	R7	R8
V sample (ml)	10	10	10	10	10	10	10	10
Empty	1.2704	1.2725	1.2593	1.258	1.2749	1.2626	1.2641	1.2833
With dry sludge	1.2805	1.2811	1.2674	1.2661	1.2872	1.2758	1.276	1.2916

With ash	1.2732	1.2746	1.2603	1.2587	1.2792	1.2672	1.2672	1.2849
MLSS (mg/l)	1010	860	810	810	1230	1320	1190	830
MLVSS (mg/l)	730	650	710	740	800	860	880	670
07/03/2019	R1	R2	R3	R4	R5	R6	R7	R8
V sample (ml)	10	10	10	10	10	10	10	10
Empty	1.2685	1.2737	1.2588	1.2593	1.2744	1.2612	1.2626	1.2838
With dry sludge								
With ash								
MLSS (mg/l)	-126850	-127370	-125880	-125930	-127440	-126120	-126260	-128380
MLVSS (mg/l)	0	0	0	0	0	0	0	0

h. kinetics data

Enrichment I

NO_2^--N based tests

	NO_2^--N based anoxic P uptake tests without pH adjustment					
	PO_4^{3-}-P	NO_2^--N	pH	P uptake	N consumption	P/N
0.0	55.0	0.0	7.2			
1.0	41.2	0.5	7.4	13.8	7.5	1.8
2.0	30.5	0.5	7.8	10.7	7.9	1.3
3.0	21.2	1.1	8.4	9.2	7.4	1.2
4.0	15.0	2.1	8.8	6.2	7.0	0.9
5.0	11.9	3.5	9.0	3.1	6.5	0.5

	NO_2^--N based anoxic P uptake tests with pH adjustment					
		40				
	PO_4^{3-}-P	NO_2^--N	pH	P uptake	N consumption	P/N

0.0	52.8	0.0				
1.0	38.5	0.0		14.4	8.0	1.8
2.0	29.7	0.1		8.7	7.9	1.1
3.0	20.2	0.1	8.0	9.5	8.1	1.2
4.0	9.6	0.7	8.0	10.6	7.4	1.4
5.0	2.2	1.4	8.1	7.4	7.3	1.0
	NO_3^--N based anoxic P uptake tests with pH adjustment					
		40				
	PO_4^{3-}-P	NO_3^--N	pH	P uptake	N consumption	P/N
0.0	54.5	0.0	7.1			
1.0	41.9	1.1	7.2	12.6	6.9	1.8
2.0	28.0	2.8	7.4	13.9	6.4	2.2
3.0	15.4	4.4	7.8	12.6	6.3	2.0
4.0	5.7	6.3	8.2	9.7	6.1	1.6
5.0	0.6	8.8	8.3	5.1	5.5	0.9

Stable period:

t	PO_4^{3-}-P	NO_3^--N	NO_2^--N	t	PO_4^{3-}-P	NO_3^--N	NO_2^--N
0.0	8.5	4.7	0.0	0.0	8.9	4.6	0.0
0.5	31.1	0.0	0.0	0.5	24.8	0.0	0.0
1.0	46.3	0.0	0.0	1.0	39.9	0.1	0.0
1.5	51.8	0.0	0.0	1.5	49.9	0.0	0.0
2.0	52.2	0.1	0.0	2.0	53.6	0.0	0.0
2.5	44.1	14.7	0.1	2.5	46.5	12.0	0.2
3.0	34.3	24.7	0.0	3.0	37.4	22.6	0.0
3.5	28.6	22.1	0.0	3.5	30.5	19.9	0.0
4.0	23.2	19.6	0.0	4.0	24.1	17.4	0.0
4.5	17.4	16.9	0.0	4.5	18.5	15.0	0.0
5.0	13.9	14.9	0.0	5.0	14.0	12.8	0.0
5.5	10.6	12.9	0.0	5.5	10.6	10.7	0.0
6.0	8.2	11.4	0.0	6.0	8.0	9.1	0.0
6.5	6.5	9.9	0.0	6.5	6.3	7.7	0.0

7.0	5.6	8.9	0.0	7.0	5.3	7.0	0.0

Enrichment II and dosing tests

NO_2^--N based anoxic P uptake tests in early period			
	PO_4^{3-}-P	NO_2^--N	
0	26.6	0.0	
0.5	28.5	0.0	5.6
1	28.5	0.3	5.3
1.5	25.2	4.9	1.1
2	21.9	7.7	2.8
2.5	20.0	10.5	2.8
3	17.1	13.4	2.7
3.5	14.0	16.5	2.5
4	11.2	18.1	4.0
4.5	9.9	17.0	1.1
5	7.3	13.8	3.2
	21.2	31.2	0.7

NO_3^--N based anoxic P uptake tests in stable period							
	PO_4^{3-}-P	NO_3^--N	pH	Acetate	P uptake	N consumption	P/N
0	6.6	6.5	7.1	124.5			
0.5	33.3	0.0	7.6	0.0			
1	46.4	0.0	7.6	0.0			
1.5	47.5	0.1	7.6	0.0			
2	47.2	0.0	7.6	0.0			
2.5	41.0	0.6	7.6	0.0	6.2	2.9	2.1
3	33.5	1.2	7.7	0.0	7.5	2.9	2.6
3.5	26.8	1.9	7.8	0.0	6.7	2.7	2.4

4	20.8	2.8	7.9	0.0	6.0	2.6	2.3
4.5	15.1	4.1	8.0	0.0	5.7	2.2	2.6
5	10.5	5.8	7.8	0.0	4.6	1.8	2.6
5.5	6.0	7.7	7.9	0.0	4.5	1.7	2.7
6	2.5	9.9	7.9	0.0	3.4	1.2	2.8
6.5	0.3	9.1	7.9	0.0	2.2	0.8	2.8
7	0.1	8.4	7.9	0.0	0.2	0.7	0.3

NO_2^--N based anoxic P uptake tests in stable period							
	PO_4^{3-}-P	NO_2^--N	pH	Acetate	P uptake	N consumption	P/N
0	6.4	3.3	7.2	117.7			
0.5	35.0	0.0	7.6	0.0			
1	57.7	0.0	7.5	0.0			
1.5	57.9	0.0	7.5	0.0			
2	58.5	0.0	7.7	0.0			
2.5	51.4	0.8	7.7	0.0	7.1	5.1	1.4
3	41.8	1.1	7.9	0.0	9.6	5.6	1.7
3.5	32.5	1.3	8.0	0.0	9.3	5.7	1.6
4	23.6	1.8	8.0	0.0	8.9	5.4	1.7
4.5	15.7	3.0	7.9	0.0	8.0	4.8	1.7
5	10.1	5.4	7.8	0.0	5.6	3.6	1.5
5.5	5.4	8.4	7.7	0.0	4.7	2.9	1.6
6	2.7	12.3	7.5	0.0	2.7	2.0	1.3
6.5	1.3	10.2	7.7	0.0	1.4	2.1	0.7
7	0.1	8.7	7.7	0.0	1.2	1.5	0.8

5-hour		PO_4^{3-}-P	NO_2^--N		P uptake	N consumption	P/N
	0	9.9	0.0				

	0.5	33.5	0.0				
	1	50.6	0.0				
	1.5	53.3	0.0				
	2	52.7	0.0		P uptake	N consumption	P/N
	2.5	48.5	0.0	2.0~2.5	4.2	4.5	0.9
	3	41.8	0.2	2.5~3.0	6.7	4.4	1.5
	3.5	34.4	0.1	3.0~3.5	7.5	4.6	1.6
	4	27.7	0.3	3.5~4.0	6.6	4.3	1.5
	4.5	23.4	0.6	4.0~4.5	4.3	4.2	1.0
	5	17.6	1.2	4.5~5.0	5.9	3.9	1.5
	5.5	12.8	2.3	5.0~5.5	4.7	3.3	1.4
	6	8.0	3.3	5.5~6.0	4.8	3.5	1.4
	6.5	3.7	5.1	6.0~6.5	4.3	2.7	1.6
	7	1.0	7.4	6.5~7.0	2.7	2.2	1.2
4-hour		PO_4^{3-}-P	NO_2^--N		P uptake	N consumption	P/N
	0	6.4	3.3				
	0.5	35.0	0.0				
	1	57.7	0.0				
	1.5	57.9	0.0				
	2	58.5	0.0				
	2.5	51.4	0.8		2.0~2.5	7.1	5.1
	3	41.8	1.1		2.5~3.0	9.6	5.6
	3.5	32.5	1.3		3.0~3.5	9.3	5.7
	4	23.6	1.8		3.5~4.0	8.9	5.4
	4.5	15.7	3.0		4.0~4.5	8.0	4.8
	5	10.1	5.4		4.5~5.0	5.6	3.6
	5.5	5.4	8.4		5.0~5.5	4.7	2.9
	6	2.7	12.3		5.5~6.0	2.7	2.0
	6.5	1.3	10.2		6.0~6.5	1.4	2.1
	7	0.1	8.7		6.5~7.0	1.2	1.5

3-hour	a	PO_4^{3-}-P	NO_2^--N			Δ-PO_4^{3-}-P	Δ-NO_2^--N	
	6.4	4.0						6.4

	39.3	0.0	4.0					39.3
	52.7	0.0	0.0					52.7
	53.5	0.0	0.0					53.5
	53.2	0.0	0.0					53.2
	47.0	1.4	7.2	2.0~2.5	6.3	7.2	0.9	47.0
	35.9	2.2	7.8	2.5~3.0	11.1	7.8	1.4	35.9
	26.4	3.4	7.4	3.0~3.5	9.5	7.4	1.3	26.4
	17.0	5.4	6.7	3.5~4.0	9.4	6.7	1.4	17.0
	11.0	9.4	4.6	4.0~4.5	6.0	4.6	1.3	11.0
	6.5	14.9	3.1	4.5~5.0	4.5	3.1	1.4	6.5
	4.8	12.5	2.4	5.0~5.5	1.7	2.4	0.7	4.8
	4.0	10.2	2.3	5.5~6.0	0.8	2.3	0.4	4.0
	3.6	8.6	1.6	6.0~6.5	0.4	1.6	0.3	3.6
	3.4	7.2	1.4	6.5~7.0	0.2	1.4	0.1	3.4
	b	PO_4^{3-}-P	NO_2^--N			Δ-PO_4^{3-}-P	Δ-NO_2^--N	
	0	6.9	3.3					
	0.5	43.2	0.0	3.3				
	1	57.8	0.0	0.0				
	1.5	61.0	0.0	0.0				
	2	60.5	0.0	0.0				
	2.5	53.1	1.2	7.4	2.0~2.5	7.3	7.4	1.0
	3	42.3	1.9	8.0	2.5~3.0	10.8	8.0	1.4
	3.5	32.2	3.0	7.5	3.0~3.5	10.1	7.5	1.3
	4	22.5	5.2	6.4	3.5~4.0	9.7	6.4	1.5
	4.5	15.1	8.8	5.0	4.0~4.5	7.4	5.0	1.5
	5	9.7	13.9	3.5	4.5~5.0	5.4	3.5	1.5
	5.5	6.2	11.0	2.9	5.0~5.5	3.5	2.9	1.2
	6	4.9	8.9	2.1	5.5~6.0	1.3	2.1	0.6
	6.5	3.7	6.9	2.0	6.0~6.5	1.1	2.0	0.6
	7	3.3	5.4	1.6	6.5~7.0	0.4	1.6	0.3
2-hour		PO_4^{3-}-P	NO_2^--N			P uptake	N consumption	P/N
	0	6.0	1.9					

	0.5	47.9	0.0	1.9				
	1	57.6	0.0	0.0				
	1.5	56.6	0.0	0.0				
	2	57.4	0.0	0.0				
	2.5	48.2	2.1	9.9	2.0~2.5	9.2	9.9	0.9
	3	35.2	4.4	9.7	2.5~3.0	13.0	9.8	1.3
	3.5	24.5	7.9	8.6	3.0~3.5	10.8	8.6	1.2
	4	13.2	13.0	6.9	3.5~4.0	11.3	7.0	1.6
	4.5	5.0	6.8	6.2	4.0~4.5	8.2	6.0	1.4
	5	1.2	2.7	4.1	4.5~5.0	3.7	4.0	0.9
	5.5	0.0	0.1	2.6	5.0~5.5	1.2	2.5	0.5
	6	0.1	0.0	0.1	5.5~6.0	0.0	0.1	0.0
	6.5	0.2	0.0	0.0	6.0~6.5	0.0	0.0	0.0
	7	6.0	1.9		6.5~7.0	0.0	0.0	0.0
1-hour	R6	PO_4^{3-}-P	NO_2^--N			P uptake	N consumption	P/N
	0	8.0	1.1					
	0.5	49.4	0.0	1.1				
	1	61.4	0.0	0.0				
	1.5	65.3	0.0	0.0				
	2	64.8	0.0	0.0				
	2.5	51.9	9.9	14.1	2.0~2.5	12.9	14.1	0.9
	3	39.9	26.5	7.4	2.5~3.0	12.0	7.4	1.6
	3.5	36.3	20.7	5.8	3.0~3.5	3.5	5.8	0.6
	4	32.0	16.4	4.3	3.5~4.0	4.4	4.3	1.0
	4.5	28.9	12.9	3.5	4.0~4.5	3.0	3.5	0.9
	5	26.0	9.7	3.2	4.5~5.0	2.9	3.2	0.9
	5.5	24.9	7.0	2.7	5.0~5.5	1.1	2.7	0.4
	6	21.2	4.4	2.6	5.5~6.0	3.8	2.6	1.4
	6.5	18.4	1.9	2.5	6.0~6.5	2.8	2.5	1.1
	7	15.0	0.0	1.9	6.5~7.0	3.4	1.9	1.8

Performance without pH control

Appendix A

	PO_4^{3-}-P	NO_2^--N	pH
0	9.1	0.0	6.9
0.5	35.8	0.0	7.2
1	52.1	0.0	7.2
1.5	53.4	0.0	7.2
2	54.9	0.0	7.2
2.5	49.8	0.1	7.3
3	43.6	0.1	7.5
3.5	36.2	0.2	7.8
4	30.1	0.5	8.3
4.5	25.6	1.0	8.7
5	22.6	2.5	9.1
5.5	19.9	4.2	9.3
6	18.2	6.3	9.3
6.5	17.6	9.4	9.5
7	17.5	12.2	9.5

i. P/HAc

Preliminary experiments

	R1	R2	R3	R4	R5	R6	R7	R8
1	0.10	0.09	0.03	0.08	0.11	0.07	0.09	0.18
8	0.01	0.02	-0.01	-0.02	-0.01	0.01	0.01	-0.01
16	0.05	0.05	0.02	0.01	0.00	-0.01	0.02	0.01
20	0.09	0.06	0.03	0.03	0.02	0.02	0.05	0.07
21	0.06	0.04	0.07	0.07	0.09	0.08	0.07	0.10
28	0.06	0.01	0.02	0.03	0.06	0.05	0.10	0.11
33	0.07	0.06	0.04	0.01	0.09	0.07	0.12	0.15
37	0.11	0.07	0.05	0.04	0.01	0.01	0.06	0.04

40	0.12	0.10	0.06	0.08	0.01	0.01	0.02	0.01
47	-0.04	-0.06	-0.08	-0.09	-0.09	-0.14	0.00	0.00
48	0.01	0.01	0.01	0.01	0.01	0.01	0.03	0.02
50	0.00	0.02	-0.04	-0.05	-0.11	-0.08	0.04	0.04
52	0.04	0.07	0.00	0.04	0.16	0.00	0.20	0.19
54	0.18	0.16	0.20	0.26	0.43	0.35	0.16	0.17
56	0.12	0.11	0.27	0.32	0.50	0.36	0.11	0.14
68	0.00	0.00	0.00	0.00	0.00	0.00	0.00	0.00
72	0.03	0.05	0.04	0.02	0.00	0.01	0.16	0.12
77	0.00	0.00	0.02	0.01	0.01	0.00	0.26	0.25
84	0.02	0.01	0.00	0.02	0.01	0.04	0.44	0.17
85	0.14	0.08	0.05	0.04	0.03	0.03	0.36	0.11
96	0.00	0.00	0.00	0.00	0.00	0.00	0.18	0.18
97	0.00	0.00	0.00	0.00	0.00	0.00	0.24	0.24
98	0.00	0.00	0.00	0.00	0.00	-0.01	0.17	0.14
99	0.01	0.01	0.00	0.01	0.01	0.01	0.15	0.13
100	0.01	0.00	0.00	0.00	0.00	0.00	0.18	0.16
101	0.01	0.04	0.02	0.01	0.08	0.03	0.00	0.00
127	0.00	0.00	0.00	0.03	0.05	0.05	0.06	0.06
129	0.00	0.04	0.04	0.05	0.04	0.02	0.10	0.07
134	0.02	0.02	0.06	0.05	0.00	0.04	0.04	0.04
137	0.01	0.02	0.05	0.05	0.00	0.03	0.04	0.04

Enrichment I

	E1	E2	E3	E4	E5	E6	E7	E8
13	0.0	0.0	0.0	0.0	0.0	0.0	0.2	0.3
14	0.0	0.0	0.0	0.0	0.0	0.0	0.2	0.3
22	0.0	0.0	0.0	0.0	0.0	0.0	0.2	0.4
27	0.0	0.0	0.0	0.0	0.0	0.0	0.3	0.1
33	0.0	0.0	0.0	0.0	0.0	0.0	0.3	0.1
38	0.0	0.0	0.0	0.0	0.0	0.0	0.3	0.3
40	0.0	0.0	0.0	0.0	0.0	0.0	0.3	0.3
45	0.0	0.0	0.0	0.0	0.0	0.0	0.7	0.3

47	0.0	0.0	0.0	0.1	0.0	0.0	0.4	0.4
53	0.1	0.1	0.1	0.1	0.0	0.0	0.3	0.3
69	0.1	0.1	0.1	0.1	0.1	0.1	0.4	0.4
74	0.1	0.1	0.1	0.1	0.0	0.1	0.4	0.3
82	0.2	0.1	0.2	0.1	0.1	0.1	0.4	0.3
85	0.2	0.1	0.2	0.2	0.1	0.1	0.4	0.4
88	0.1	0.1	0.2	0.2	0.1	0.1	0.4	0.3
92	0.3	0.2	0.2	0.2	0.1	0.2	0.4	0.3
96	0.5	0.3	0.3	0.3	0.2	0.2	0.4	0.3
99	0.3	0.3	0.3	0.3	0.2	0.3	0.4	0.3
106	0.3	0.3	0.4	0.5	0.3	0.4	0.4	0.3
110	0.3	0.3	0.5	0.5	0.3	0.4	0.5	0.4
123	0.2	0.3	0.4	0.4	0.4	0.4	0.4	0.4
142	0.1	0.1	0.3	0.3	0.3	0.3	0.3	0.3
145	0.1	0.1	0.4	0.3	0.3	0.3	0.4	0.2
147	0.1	0.1	0.4	0.3	0.3	0.3	0.4	0.3
159	0.2	0.2	0.4	0.3	0.3	0.4	0.3	0.2
166	0.2	0.2	0.4	0.4	0.4	0.4	0.4	0.2
174	0.3	0.2	0.4	0.4	0.4	0.4	0.4	0.2
180	0.2	0.2	0.4	0.4	0.3	0.4	0.4	0.2
187	0.2	0.2	0.4	0.4	0.4	0.4	0.4	0.2
194	0.3	0.3	0.4	0.3	0.4	0.4	0.4	0.2
204	0.2	0.2	0.3	0.4	0.3	0.3	0.4	0.2
209	0.3	0.3	0.4	0.3	0.4	0.3	0.4	0.3
211	0.3	0.2	0.4	0.3	0.4	0.3	0.3	0.2
216	0.2	0.2	0.3	0.3	0.3	0.2	0.4	0.3

Enrichment II

	1	2	3	4	5	6	7	8
0	0.2	0.2	0.1	0.1	0.1	0.1	0.2	0.2
3	0.2	0.2	0.1	0.1	0.1	0.1	0.2	0.2
8	0.2	0.2	0.1	0.2	0.1	0.2	0.2	0.1
11	0.3	0.3	0.1	0.2	0.1	0.2	0.1	0.1

14	0.3	0.4	0.2	0.2	0.2	0.3	0.1	0.2
18	0.4	0.4	0.2	0.2	0.2	0.3	0.1	0.1
22	0.3	0.4	0.3	0.3	0.3	0.4	0.2	0.1
25	0.3	0.3	0.2	0.3	0.3	0.3	0.2	0.2
28	0.3	0.4	0.3	0.3	0.3	0.3	0.2	0.2
34	0.4	0.4	0.3	0.3	0.3	0.3	0.3	0.1
40	0.4	0.3	0.3	0.4	0.4	0.4	0.3	0.1
43	0.4	0.4	0.4	0.4	0.4	0.4	0.3	0.2
46	0.4	0.4	0.4	0.4	0.4	0.5	0.3	0.3
50	0.4	0.3	0.4	0.4	0.4	0.4	0.4	0.4
54	0.4	0.4	0.4	0.4	0.4	0.5	0.4	0.4
61	0.3	0.4	0.4	0.3	0.3	0.4	0.4	0.5
64	0.4	0.4	0.5	0.5	0.3	0.5	0.4	0.5
68	0.4	0.4	0.5	0.4	0.4	0.5	0.4	0.5
71	0.4	0.4	0.5	0.4	0.3	0.5	0.4	0.5
75	0.4	0.4	0.5	0.4	0.3	0.6	0.4	0.5

Different temperature

	1	2	3	4
0	0.2	0.2	0.1	0.1
3	0.2	0.2	0.1	0.1
8	0.2	0.2	0.1	0.2
11	0.3	0.3	0.1	0.2
14	0.3	0.3	0.2	0.2
18	0.4	0.4	0.2	0.2
22	0.3	0.3	0.2	0.2
25	0.3	0.3	0.2	0.3
28	0.3	0.3	0.2	0.3

34	0.3	0.3	0.3	0.3
40	0.4	0.3	0.3	0.3
43	0.4	0.4	0.4	0.4
46	0.4	0.4	0.3	0.4
50	0.4	0.3	0.4	0.3
54	0.4	0.4	0.4	0.4
61	0.3	0.4	0.4	0.3
64	0.3	0.3	0.4	0.4
68	0.4	0.4	0.4	0.4
71	0.4	0.4	0.5	0.4
75	0.4	0.4	0.5	0.4
76	0.4	0.4	0.5	0.4
78	0.4	0.4	0.4	0.4
82	0.4	0.4	0.4	0.4
85	0.4	0.4	0.0	0.0
90	0.5	0.5	0.1	0.1
92	0.5	0.4	0.1	0.1
98	0.5	0.5	0.2	0.2
103	0.5	0.5	0.2	0.1
106	0.5	0.4	0.2	0.2
110	0.5	0.4	0.3	0.2
113	0.5	0.4	0.3	0.1
117	0.4	0.3	0.2	0.2
119	0.5	0.4	0.2	0.2
124	0.4	0.3	0.3	0.4

126	0.4	0.3	0.3	0.4

pH

	1	2
0	0.3	0.2
6	0.4	0.3
9	0.4	0.4
12	0.4	0.4
16	0.4	0.4
20	0.4	0.5
27	0.3	0.4
30	0.3	0.4
34	0.4	0.5
37	0.3	0.5
41	0.2	0.5
42	0.3	0.4
44	0.2	0.3
48	0.2	0.4
51	0.3	0.4
56	0.3	0.5
58	0.3	0.5
64	0.4	0.5
69	0.4	0.4

72	0.4	0.4
76	0.4	0.4
79	0.4	0.4
83	0.4	0.4
85	0.4	0.4
90	0.4	0.4
92	0.5	0.5

j. P/N

Preliminary experiment

	R1	R2	R3	R4	R5	R6
16	0.5	0.5	0.3	1.0	0.2	0.2
20	0.3	0.2	0.1	0.1	0.1	0.1
21	0.2	0.1	0.1	0.1	0.1	0.1
28	0.3	0.1	0.1	0.1	0.1	0.1
33	0.8	0.8	0.1	0.1	0.0	0.0
37	2.6	1.2	0.4	0.5	0.1	0.1
48	0.0	0.1	0.0	0.0	0.0	0.0

50	0.2	0.3	0.2	0.2	0.2	0.2
52	0.1	0.1	0.0	0.0	0.1	0.0
77	0.4	0.2	0.2	0.2	0.0	0.1
84	0.0	0.2	0.0	0.0	0.0	0.1
85	0.3	0.2	0.1	0.1	0.1	0.1
96	-0.1	-0.1	-0.2	-0.2	-0.1	-1.0
101	0.1	0.7	0.0	0.0	0.1	0.0
127	0.1	0.2	0.1	0.1	0.1	0.2
129	0.0	0.0	0.0	0.1	0.1	0.1
134	0.0	0.1	0.1	0.1	0.1	0.0
137	0.1	0.1	0.0	0.1	0.0	0.0

Enrichment I

	E1	E2	E3	E4	E5	E6
1	0.1	0.0	0.0	0.0	0.0	0.0
7	0.2	0.2	0.2	0.1	0.1	0.1
13	0.0	0.1	0.1	0.1	0.1	0.1
14	0.1	0.1	0.1	0.1	0.1	0.2
22	0.1	0.1	0.0	0.1	0.0	0.0
27	0.0	0.0	0.0	0.0	0.0	0.0
33	0.1	0.0	0.0	0.0	0.0	0.0
38	0.1	0.1	0.0	0.0	0.0	0.0
40	0.1	0.1	0.1	0.0	0.0	0.1
45	0.2	0.2	0.2	0.1	0.1	0.1
47	0.2	0.3	0.2	0.2	0.1	0.1

53	0.4	0.4	0.4	0.5	0.2	0.2
69	1.1	1.0	1.1	0.8	0.6	0.3
74	0.9	0.7	0.9	0.6	0.3	0.3
82	1.4	1.2	1.2	1.0	0.5	0.6
85	1.4	1.2	1.1	1.0	0.5	0.6
88	1.6	1.5	1.5	1.3	0.7	0.8
92	1.8	1.7	1.5	1.6	0.9	1.0
96	2.2	2.3	1.8	1.9	1.1	1.2
99	2.3	2.3	2.0	2.1	1.4	1.5
106	2.1	2.1	1.8	2.0	1.4	1.8
110	2.1	2.1	2.0	1.9	1.7	1.9
123	1.9	2.1	1.7	1.9	1.5	1.6
142	1.2	1.5	2.1	1.4	1.5	1.5
145	1.4	1.5	2.3	1.6	1.7	1.8
147	1.4	1.3	2.3	1.7	1.7	1.6
159	1.6	1.4	2.3	1.8	1.6	1.8
166	1.8	1.7	2.4	1.9	1.7	1.9
174	1.9	1.8	2.4	1.9	2.0	1.8
180	1.8	1.6	2.4	2.0	1.9	1.9
187	1.8	1.9	2.0	1.8	1.8	1.7
194	2.2	2.4	2.1	1.9	2.0	1.8
204	2.3	1.2	1.7	1.8	2.0	1.6
209	2.3	2.1	1.9	1.6	2.0	1.7
211	1.7	1.4	1.8	1.3	1.6	1.4
216	1.7	1.6	1.7	1.7	1.7	1.3

Enrichment II

	1	2	3	4	5	6	7	8
0	1.2	0.9	0.4	0.2	0.2	0.2	0.9	0.6
3	1.1	0.9	0.4	0.3	0.3	0.3	0.8	0.5
8	1.5	1.3	0.5	0.7	0.5	0.7	1.0	0.3
11	1.6	1.4	0.5	0.7	0.5	0.9	0.5	0.5
14	2.1	1.8	0.5	0.6	0.5	0.8	0.5	0.6
18	2.1	1.9	0.6	0.5	0.7	0.9	0.6	0.6
22	2.0	1.9	0.8	0.9	1.0	1.1	0.9	0.8
25	1.9	1.8	0.8	0.9	1.0	1.2	1.0	0.9
28	1.8	1.7	0.9	0.9	0.9	1.1	1.1	0.8
34	2.0	1.8	0.9	0.9	1.1	1.3	1.4	0.7
40	2.1	1.8	0.9	1.1	1.2	1.3	1.5	0.6
43	2.3	1.9	1.1	1.2	1.1	1.2	1.7	1.2
54	2.3	2.0	1.2	1.2	1.2	1.3	1.8	1.5
61	2.2	2.1	1.2	1.1	1.3	1.2	1.9	1.9
64	2.4	2.2	1.3	1.1	1.2	1.4	1.7	2.2
68	1.8	2.1	1.3	0.8	0.9	1.2	2.0	2.2
71	2.2	2.4	1.5	1.4	1.2	1.4	2.1	2.5
75	2.2	2.5	1.4	1.4	1.4	1.5	2.1	2.6

Different temperature

	1	2	3	4
0	1.2	0.9	0.4	0.2

3	1.1	0.9	0.4	0.3
8	1.5	1.3	0.5	0.7
11	1.6	1.4	0.5	0.7
14	2.1	1.8	0.5	0.6
18	2.1	1.9	0.6	0.5
22	2.0	1.9	0.8	0.9
25	1.9	1.8	0.8	0.9
28	1.8	1.7	0.9	0.9
34	2.0	1.8	0.9	0.9
40	2.1	1.8	0.9	1.1
43	2.3	1.9	1.1	1.2
46	2.3	2.0	1.2	1.2
50	2.2	2.1	1.2	1.1
54	2.4	2.2	1.3	1.1
61	1.8	2.1	1.3	0.8
64	2.2	2.4	1.5	1.4
68	2.2	2.5	1.4	1.4
71	2.3	2.4	1.4	1.1
75	2.5	2.5	1.4	1.1
76	2.2	2.2	1.3	1.2
78	2.3	2.1	1.0	1.1
82	2.4	2.1	1.0	1.0
85	2.4	2.2	0.1	0.2
90	2.8	2.5	0.2	0.3

92	2.5	2.2	0.2	0.2
98	2.5	2.3	0.5	0.6
103	2.5	2.1	0.5	0.4
106	2.3	1.8	0.6	0.5
110	2.4	2.0	0.6	0.5
113	2.5	2.0	0.4	0.4
117	2.4	2.1	0.5	0.6
119	2.5	2.2	0.7	0.9
124	2.5	2.2	0.8	1.1
126	2.4	2.2	0.8	1.1

pH

	1	2
0	1.1	1.3
6	1.2	1.3
9	1.1	1.2
12	1.2	1.3
16	1.3	1.2
20	1.2	1.4
27	0.9	1.2
30	1.2	1.4
34	1.4	1.5

37	0.9	1.4
41	0.9	1.6
42	0.7	1.7
44	0.7	1.1
48	0.9	1.3
51	1.2	1.3
56	1.2	1.2
58	1.1	1.5
64	1.3	1.3
69	1.2	1.1
72	1.3	1.1
76	1.2	1.2
79	1.2	1.1
83	1.1	1.0
85	1.2	1.0
90	1.3	1.2
92	1.5	1.3

k. e^-/P

Appendix A

Enrichment I

	E1	E2	E3	E4	E5	E6
1	200.6	260.9	369.2	287.0	583.5	740.9
7	54.3	51.9	54.5	76.7	111.0	106.9
13	286.0	146.7	96.2	115.2	134.8	175.8
14	128.1	124.0	131.1	142.6	70.9	52.7
22	139.8	93.5	352.5	165.4	534.4	418.3
27	387.4	397.2	293.9	395.2	587.2	474.0
33	198.2	841.0	3106.6	-1434.9	4581.0	491.0
38	150.5	115.4	683.0	430.7	304.4	486.0
40	83.6	78.6	169.7	563.7	517.6	115.5
45	48.1	46.2	62.8	76.6	126.4	77.8
47	46.8	41.3	69.1	50.0	160.0	104.7
53	26.5	27.1	28.1	22.4	48.4	47.6
69	11.9	12.8	10.6	13.8	18.2	29.4
74	12.3	16.3	12.1	17.1	32.9	29.7
82	7.7	9.6	8.4	10.2	18.6	16.0
85	8.0	9.5	9.4	10.6	17.8	15.9
88	6.9	7.4	6.8	7.7	13.2	12.4
92	6.3	6.5	6.7	6.5	11.0	10.3
96	4.9	4.8	5.8	5.5	8.3	8.4
99	4.8	4.7	5.2	5.0	6.5	6.7
106	5.3	5.4	5.7	5.3	6.8	5.7
110	5.4	5.2	5.3	5.6	5.9	5.3
123	5.8	5.3	6.4	5.4	6.5	6.4

142	9.0	7.6	5.3	7.4	6.5	6.6
145	8.1	7.3	4.7	6.4	5.8	5.5
147	7.8	8.3	4.8	6.1	6.0	6.4
159	6.9	7.7	4.8	5.9	6.3	5.4
166	6.3	6.5	4.7	5.5	5.7	5.3
174	5.9	6.2	4.7	5.5	5.0	5.4
180	6.2	7.1	4.6	5.3	5.1	5.2
187	6.3	5.8	5.1	5.9	5.5	5.9
194	5.1	4.6	4.9	5.5	4.9	5.6
204	4.8	9.1	6.4	5.9	4.8	6.2
209	4.9	5.3	5.5	6.7	4.9	5.8
211	6.4	7.7	6.0	8.2	6.3	7.3
216	6.7	6.9	6.0	6.3	5.9	7.8

Enrichment II

	1	2	3	4	5	6	7	8
0	9.2	11.9	16.1	34.8	30.2	31.9	11.7	18.6
3	10.3	12.6	17.2	19.8	21.6	21.2	13.5	21.8
8	7.3	8.6	12.6	9.7	13.5	9.6	10.8	36.9
11	7.0	7.8	13.9	10.0	13.1	7.8	24.5	24.2
14	5.4	6.2	14.6	10.3	13.9	8.6	21.1	19.6
18	5.3	5.9	10.7	12.3	9.7	7.2	18.2	17.2
22	5.6	5.8	7.9	7.7	6.6	6.0	12.9	13.2
25	5.9	6.2	8.3	7.2	6.5	5.7	10.6	12.6

28	6.3	6.6	6.8	7.6	7.4	6.0	9.9	14.5
34	5.6	6.1	7.1	7.4	6.1	5.3	7.9	16.7
40	5.2	6.1	7.4	6.3	5.6	5.1	7.4	18.0
43	4.9	5.8	6.1	5.7	5.9	5.6	6.4	9.2
46	4.8	5.6	5.6	5.4	5.4	5.1	6.0	7.3
50	5.0	5.4	5.6	6.2	5.2	5.5	5.9	5.8
54	4.7	5.1	5.1	5.8	5.4	4.8	6.6	4.9
61	6.0	5.4	5.1	7.8	7.2	5.3	5.6	4.9
64	5.0	4.6	4.4	4.7	5.6	4.8	5.2	4.4
68	4.9	4.4	4.9	4.7	4.6	4.5	5.2	4.3
71	4.7	4.7	4.6	6.2	7.3	4.6	5.2	4.3
75	4.4	4.5	4.8	6.0	7.7	4.0	4.9	4.3

Temperature

	1	2	3	4
0	9.2	11.9	16.1	34.8

3	10.3	12.6	17.2	19.8
8	7.3	8.6	12.6	9.7
11	7.0	7.8	13.9	10.0
14	5.4	6.2	14.6	10.3
18	5.3	5.9	10.7	12.3
22	5.6	5.8	7.9	7.7
25	5.9	6.2	8.3	7.2
28	6.3	6.6	6.8	7.6
34	5.6	6.1	7.1	7.4
40	5.2	6.1	7.4	6.3
43	4.9	5.8	6.1	5.7
46	4.8	5.6	5.6	5.4
50	5.0	5.4	5.6	6.2
54	4.7	5.1	5.1	5.8
61	6.0	5.4	5.1	7.8
64	5.0	4.6	4.4	4.7
68	4.9	4.4	4.9	4.7
71	4.7	4.7	4.6	6.2
75	4.4	4.5	4.8	6.0
76	5.1	4.9	5.0	5.7
78	4.8	5.4	6.6	6.1
82	4.6	5.2	6.7	6.6
85	4.6	5.0	64.0	38.5
90	3.9	4.4	35.6	21.8
92	4.5	5.1	36.8	35.7

98	4.4	4.8	14.3	11.1
103	4.5	5.2	13.5	16.9
106	4.8	6.2	10.5	12.1
110	4.6	5.6	10.3	12.1
113	4.4	5.5	15.8	17.2
117	4.7	5.3	12.1	10.7
119	4.5	5.1	10.2	7.7
124	4.4	5.1	8.2	6.3
126	4.7	5.1	8.4	6.2

pH

	1	2
0	6.1	5.3
6	5.6	5.1
9	5.9	5.6
12	5.4	5.1
16	5.2	5.5
20	5.4	4.8
27	7.2	5.3
30	5.6	4.8
34	4.6	4.5
37	7.3	4.6
41	7.7	4.0

42	9.0	4.0
44	9.7	5.9
48	7.0	5.1
51	5.4	5.0
56	5.6	5.6
58	6.0	4.4
64	5.1	5.1
69	5.5	5.9
72	5.3	6.0
76	5.5	5.6
79	5.3	5.8
83	6.0	6.5
85	5.5	6.5
90	5.1	5.6
92	4.4	5.0

Appendix B: Simulation of A_2N process operation

Exchange rate of 80%

80% exchange of liquid				Influe	8 mg P L	75 mg N L-1																					
		Cycle		1	2	3	4	5	6	7	8	9	10	11	12	13	14	15	16	17	18	19	20	21	22	23	24
		time	h	0.5	8.5	16.5	24.5	32.5	40.5	48.5	56.5	64.5	72.5	80.5	88.5	96.5	105	113	121	128.5	137	145	153	160.5	168.5	176.5	184.5
Influent		concentration	P	6	6	6	6	6	6	6	6	6	6	6	6	6	6	6	6	6	6	6	6	6	6	6	6
			NH4	60	62.4	62.496	62.5	62.5	62.5	62.5	62.5	62.5	62.5	62.5	62.5	62.5	62.5	62.5	62.5	62.5	62.5	62.5	62.5	62.5	62.5	62.5	62.5
			NO2	0	0	0	0	0	0	0	0	0	0	0	0	0	0	0	0	0	0	0	0	0	0	0	0
	A2 SBR	V	v	4	4	4	4	4	4	4	4	4	4	4	4	4	4	4	4	4	4	4	4	4	4	4	4
		concentration	P	0	41.12	49.344	50.99	51.3	51.4	51.4	51.4	51.4	51.4	51.4	51.4	51.4	51.4	51.4	51.4	51.4	51.4	51.4	51.4	51.4	51.4	51.4	51.4
			NH4	0	0	0	0	0	0	0	0	0	0	0	0	0	0	0	0	0	0	0	0	0	0	0	0
			NO2	0	48	59.52	61.9	62.4	62.5	62.5	62.5	62.5	62.5	62.5	62.5	62.5	62.5	62.5	62.5	62.5	62.5	62.5	62.5	62.5	62.5	62.5	62.5
	N SBR	V	v	0.8	0.8	0.8	0.8	0.8	0.8	0.8	0.8	0.8	0.8	0.8	0.8	0.8	0.8	0.8	0.8	0.8	0.8	0.8	0.8	0.8	0.8	0.8	0.8
		time		1.5	9.5	17.5	25.5	33.5	41.5	49.5	57.5	65.5	73.5	81.5	89.5	97.5	106	114	122	129.5	138	146	154	161.5	169.5	177.5	185.5
P release		concentration	P	51.4	51.4	51.4	51.4	51.4	51.4	51.4	51.4	51.4	51.4	51.4	51.4	51.4	51.4	51.4	51.4	51.4	51.4	51.4	51.4	51.4	51.4	51.4	51.4
			NH4	60	62.4	62.496	62.5	62.5	62.5	62.5	62.5	62.5	62.5	62.5	62.5	62.5	62.5	62.5	62.5	62.5	62.5	62.5	62.5	62.5	62.5	62.5	62.5
			NO2	0	0	0	0	0	0	0	0	0	0	0	0	0	0	0	0	0	0	0	0	0	0	0	0
	A2 SBR	V	v	4	4	4	4	4	4	4	4	4	4	4	4	4	4	4	4	4	4	4	4	4	4	4	4
		concentration	P	0	41.12	49.344	50.99	51.3	51.4	51.4	51.4	51.4	51.4	51.4	51.4	51.4	51.4	51.4	51.4	51.4	51.4	51.4	51.4	51.4	51.4	51.4	51.4
			NH4	0	0	0	0	0	0	0	0	0	0	0	0	0	0	0	0	0	0	0	0	0	0	0	0
			NO2	0	48	59.52	61.9	62.4	62.5	62.5	62.5	62.5	62.5	62.5	62.5	62.5	62.5	62.5	62.5	62.5	62.5	62.5	62.5	62.5	62.5	62.5	62.5
	N SBR	V	v	0.8	0.8	0.8	0.8	0.8	0.8	0.8	0.8	0.8	0.8	0.8	0.8	0.8	0.8	0.8	0.8	0.8	0.8	0.8	0.8	0.8	0.8	0.8	0.8

Appendix B

		time		2.5	10.5	18.5	26.5	34.5	42.5	50.5	58.5	66.5	74.5	82.5	90.5	98.5	107	115	123	130.5	139	147	155	162.5	170.5	178.5	186.5
From A2 to N SBR			P	51.4	51.4	51.4	51.4	51.4	51.4	51.4	51.4	51.4	51.4	51.4	51.4	51.4	51.4	51.4	51.4	51.4	51.4	51.4	51.4	51.4	51.4	51.4
		concentration	NH4	60	62.4	62.496	62.5	62.5	62.5	62.5	62.5	62.5	62.5	62.5	62.5	62.5	62.5	62.5	62.5	62.5	62.5	62.5	62.5	62.5	62.5	62.5
			NO2	0	0	0	0	0	0	0	0	0	0	0	0	0	0	0	0	0	0	0	0	0	0	0	0
	A2 SBR	V	v	0.8	0.8	0.8	0.8	0.8	0.8	0.8	0.8	0.8	0.8	0.8	0.8	0.8	0.8	0.8	0.8	0.8	0.8	0.8	0.8	0.8	0.8	0.8	0.8
			P	41.1	49.34	50.989	51.32	51.4	51.4	51.4	51.4	51.4	51.4	51.4	51.4	51.4	51.4	51.4	51.4	51.4	51.4	51.4	51.4	51.4	51.4	51.4	51.4
		concentration	NH4	48	49.92	49.997	50	50	50	50	50	50	50	50	50	50	50	50	50	50	50	50	50	50	50	50	50
			NO2	0	9.6	11.904	12.38	12.5	12.5	12.5	12.5	12.5	12.5	12.5	12.5	12.5	12.5	12.5	12.5	12.5	12.5	12.5	12.5	12.5	12.5	12.5	12.5
	N SBR	V	v	4	4	4	4	4	4	4	4	4	4	4	4	4	4	4	4	4	4	4	4	4	4	4	4
		time		3.5	11.5	19.5	27.5	35.5	43.5	51.5	59.5	67.5	75.5	83.5	91.5	99.5	108	116	124	131.5	140	148	156	163.5	171.5	179.5	187.5
			P	51.4	51.4	51.4	51.4	51.4	51.4	51.4	51.4	51.4	51.4	51.4	51.4	51.4	51.4	51.4	51.4	51.4	51.4	51.4	51.4	51.4	51.4	51.4	51.4
		concentration	NH4	60	62.4	62.496	62.5	62.5	62.5	62.5	62.5	62.5	62.5	62.5	62.5	62.5	62.5	62.5	62.5	62.5	62.5	62.5	62.5	62.5	62.5	62.5	62.5
			NO2	0	0	0	0	0	0	0	0	0	0	0	0	0	0	0	0	0	0	0	0	0	0	0	0
	A2 SBR	V	v	0.8	0.8	0.8	0.8	0.8	0.8	0.8	0.8	0.8	0.8	0.8	0.8	0.8	0.8	0.8	0.8	0.8	0.8	0.8	0.8	0.8	0.8	0.8	0.8
Aerobic			P	41.1	49.34	50.989	51.32	51.4	51.4	51.4	51.4	51.4	51.4	51.4	51.4	51.4	51.4	51.4	51.4	51.4	51.4	51.4	51.4	51.4	51.4	51.4	51.4
		concentration	NH4	0	0	0	0	0	0	0	0	0	0	0	0	0	0	0	0	0	0	0	0	0	0	0	0
			NO2	48	59.52	61.901	62.38	62.5	62.5	62.5	62.5	62.5	62.5	62.5	62.5	62.5	62.5	62.5	62.5	62.5	62.5	62.5	62.5	62.5	62.5	62.5	62.5
	N SBR	V	v	4	4	4	4	4	4	4	4	4	4	4	4	4	4	4	4	4	4	4	4	4	4	4	4

Appendix B

		time		5.5	13.5	21.5	29.5	37.5	45.5	53.5	61.5	69.5	77.5	85.5	93.5	102	110	118	126	133.5	142	150	158	165.5	173.5	181.5	189.5
From N to A2 SBR	A2 SBR	concentration	P	43.2	49.76	51.071	51.33	51.4	51.4	51.4	51.4	51.4	51.4	51.4	51.4	51.4	51.4	51.4	51.4	51.4	51.4	51.4	51.4	51.4	51.4	51.4	51.4
			NH4	12	12.48	12.499	12.5	12.5	12.5	12.5	12.5	12.5	12.5	12.5	12.5	12.5	12.5	12.5	12.5	12.5	12.5	12.5	12.5	12.5	12.5	12.5	12.5
			NO2	38.4	47.62	49.521	49.9	50	50	50	50	50	50	50	50	50	50	50	50	50	50	50	50	50	50	50	50	50
		V	v	4	4	4	4	4	4	4	4	4	4	4	4	4	4	4	4	4	4	4	4	4	4	4	4
		P/N		1.1	1.045	1.031	1.029	1	1	1.03	1.03	1.03	1.03	1	1.03	1.03	1.03	1	1.03	1.03	1.03	1.03	1.03	1.03	1.03	1.03	1.03
	N SBR	concentration	P	41.1	49.34	50.989	51.32	51.4	51.4	51.4	51.4	51.4	51.4	51.4	51.4	51.4	51.4	51.4	51.4	51.4	51.4	51.4	51.4	51.4	51.4	51.4	51.4
			NH4	0	0	0	0	0	0	0	0	0	0	0	0	0	0	0	0	0	0	0	0	0	0	0	0
			NO2	48	59.52	61.901	62.38	62.5	62.5	62.5	62.5	62.5	62.5	62.5	62.5	62.5	62.5	62.5	62.5	62.5	62.5	62.5	62.5	62.5	62.5	62.5	62.5
		V	v	0.8	0.8	0.8	0.8	0.8	0.8	0.8	0.8	0.8	0.8	0.8	0.8	0.8	0.8	0.8	0.8	0.8	0.8	0.8	0.8	0.8	0.8	0.8	0.8
		time		7	15	23	31	39	47	55	63	71	79	87	95	103	111	119	127	135	143	151	159	167	175	183	191
P uptake		concentration	P	0	0	0	0	0	0	0	0	0	0	0	0	0	0	0	0	0	0	0	0	0	0	0	0
			NH4	12	12.48	12.499	12.5	12.5	12.5	12.5	12.5	12.5	12.5	12.5	12.5	12.5	12.5	12.5	12.5	12.5	12.5	12.5	12.5	12.5	12.5	12.5	12.5
			NO2	0	0	0	0	0	0	0	0	0	0	0	0	0	0	0	0	0	0	0	0	0	0	0	0
	A2 SBR	V	v	4	4	4	4	4	4	4	4	4	4	4	4	4	4	4	4	4	4	4	4	4	4	4	4
		concentration	P	41.1	49.34	50.989	51.32	51.4	51.4	51.4	51.4	51.4	51.4	51.4	51.4	51.4	51.4	51.4	51.4	51.4	51.4	51.4	51.4	51.4	51.4	51.4	51.4
			NH4	0	0	0	0	0	0	0	0	0	0	0	0	0	0	0	0	0	0	0	0	0	0	0	0
			NO2	48	59.52	61.901	62.38	62.5	62.5	62.5	62.5	62.5	62.5	62.5	62.5	62.5	62.5	62.5	62.5	62.5	62.5	62.5	62.5	62.5	62.5	62.5	62.5
	N SBR	V	v	0.8	0.8	0.8	0.8	0.8	0.8	0.8	0.8	0.8	0.8	0.8	0.8	0.8	0.8	0.8	0.8	0.8	0.8	0.8	0.8	0.8	0.8	0.8	0.8

Appendix B

		time		8	16	24	32	40	48	56	64	72	80	88	96	104	112	120	128	136	144	152	160	168	176	184	192
Effluent			P	0	0	0	0	0	0	0	0	0	0	0	0	0	0	0	0	0	0	0	0	0	0	0	0
		concentration	NH4	12	12.48	12.499	12.5	12.5	12.5	12.5	12.5	12.5	12.5	12.5	12.5	12.5	12.5	12.5	12.5	12.5	12.5	12.5	12.5	12.5	12.5	12.5
			NO2	0	0	0	0	0	0	0	0	0	0	0	0	0	0	0	0	0	0	0	0	0	0	0	0
	A2 SBR	V	v	0.8	0.8	0.8	0.8	0.8	0.8	0.8	0.8	0.8	0.8	0.8	0.8	0.8	0.8	0.8	0.8	0.8	0.8	0.8	0.8	0.8	0.8	0.8	0.8
			P	41.1	49.34	50.989	51.32	51.4	51.4	51.4	51.4	51.4	51.4	51.4	51.4	51.4	51.4	51.4	51.4	51.4	51.4	51.4	51.4	51.4	51.4	51.4	51.4
		concentration	NH4	0	0	0	0	0	0	0	0	0	0	0	0	0	0	0	0	0	0	0	0	0	0	0	0
			NO2	48	59.52	61.901	62.38	62.5	62.5	62.5	62.5	62.5	62.5	62.5	62.5	62.5	62.5	62.5	62.5	62.5	62.5	62.5	62.5	62.5	62.5	62.5	62.5
	N SBR	V	v	0.8	0.8	0.8	0.8	0.8	0.8	0.8	0.8	0.8	0.8	0.8	0.8	0.8	0.8	0.8	0.8	0.8	0.8	0.8	0.8	0.8	0.8	0.8	0.8

Appendix B

Exchange rate of 50%

50% exchange of liquid				Influer 8 mg P L- 75 mg N L-1																						
		Cycle		1	2	3	4	5	6	7	8	9	10	11	12	13	14	15	16	17	18	19	20	21	22	23	24
		time		0.5	8.5	16.5	24.5	32.5	40.5	48.5	56.5	64.5	72.5	80.5	88.5	96.5	104.5	112.5	120.5	128.5	136.5	144.5	152.5	160.5	168.5	177	184.5
Influent			P	4	4	4	4	4	4	4	4	4	4	4	4	4	4	4	4	4	4	4	4	4	4	4	4
		concen	NH4	37.5	46.875	49.219	49.8	50	50	50	50	50	50	50	50	50	50	50	50	50	50	50	50	50	50	50	50
		tration	NO2	0	0	0	0	0	0	0	0	0	0	0	0	0	0	0	0	0	0	0	0	0	0	0	0
	A2 SBR	V	v	4	4	4	4	4	4	4	4	4	4	4	4	4	4	4	4	4	4	4	4	4	4	4	4
			P	0	41.12	24.7	24.7	24.7	24.7	24.7	24.7	24.7	24.7	24.7	24.7	24.7	24.7	24.7	24.7	24.7	24.7	24.7	24.7	24.7	24.7	24.7	24.7
		concen	NH4	0	0	0	0	0	0	0	0	0	0	0	0	0	0	0	0	0	0	0	0	0	0	0	0
		tration	NO2	0	48	47.438	48.3	49.1	49.5	49.75	49.9	49.9	50	50	50	50	50	50	50	50	50	50	50	50	50	50	50	50
	N SBR	V	v	2	2	2	2	2	2	2	2	2	2	2	2	2	2	2	2	2	2	2	2	2	2	2	2
		time		1.5	9.5	17.5	25.5	33.5	41.5	49.5	57.5	65.5	73.5	81.5	89.5	97.5	105.5	113.5	121.5	129.5	137.5	145.5	153.5	161.5	169.5	178	185.5
P release			P	49.4	49.4	49.4	49.4	49.4	49.4	49.4	49.4	49.4	49.4	49.4	49.4	49.4	49.4	49.4	49.4	49.4	49.4	49.4	49.4	49.4	49.4	49.4	49.4
		concen	NH4	37.5	46.875	49.219	49.8	50	50	50	50	50	50	50	50	50	50	50	50	50	50	50	50	50	50	50	50
		tration	NO2	0	0	0	0	0	0	0	0	0	0	0	0	0	0	0	0	0	0	0	0	0	0	0	0
	A2 SBR	V	v	4	4	4	4	4	4	4	4	4	4	4	4	4	4	4	4	4	4	4	4	4	4	4	4
			P	0	41.12	24.7	24.7	24.7	24.7	24.7	24.7	24.7	24.7	24.7	24.7	24.7	24.7	24.7	24.7	24.7	24.7	24.7	24.7	24.7	24.7	24.7	24.7
		concen	NH4	0	0	0	0	0	0	0	0	0	0	0	0	0	0	0	0	0	0	0	0	0	0	0	0
		tration	NO2	0	48	47.438	48.3	49.1	49.5	49.75	49.9	49.9	50	50	50	50	50	50	50	50	50	50	50	50	50	50	50	50
	N SBR	V	v	2	2	2	2	2	2	2	2	2	2	2	2	2	2	2	2	2	2	2	2	2	2	2	2

Appendix B

		time		2.5	10.5	18.5	26.5	34.5	42.5	50.5	58.5	66.5	74.5	82.5	90.5	98.5	106.5	114.5	122.5	130.5	138.5	146.5	154.5	162.5	170.5	179	186.5
From A2 to N SBR			P	49.4	49.4	49.4	49.4	49.4	49.4	49.4	49.4	49.4	49.4	49.4	49.4	49.4	49.4	49.4	49.4	49.4	49.4	49.4	49.4	49.4	49.4	49.4	49.4
		concen	NH4	37.5	46.875	49.219	49.8	50	50	50	50	50	50	50	50	50	50	50	50	50	50	50	50	50	50	50	50
		tration	NO2	0	0	0	0	0	0	0	0	0	0	0	0	0	0	0	0	0	0	0	0	0	0	0	0
	A2 SBR	V	v	2	2	2	2	2	2	2	2	2	2	2	2	2	2	2	2	2	2	2	2	2	2	2	2
			P	24.7	24.7	24.7	24.7	24.7	24.7	24.7	24.7	24.7	24.7	24.7	24.7	24.7	24.7	24.7	24.7	24.7	24.7	24.7	24.7	24.7	24.7	24.7	24.7
		concen	NH4	18.8	23.438	24.609	24.9	25	25	25	25	25	25	25	25	25	25	25	25	25	25	25	25	25	25	25	25
		tration	NO2	0	24	23.719	24.2	24.5	24.8	24.87	24.9	25	25	25	25	25	25	25	25	25	25	25	25	25	25	25	25
	N SBR	V	v	4	4	4	4	4	4	4	4	4	4	4	4	4	4	4	4	4	4	4	4	4	4	4	4
		time		3.5	11.5	19.5	27.5	35.5	43.5	51.5	59.5	67.5	75.5	83.5	91.5	99.5	107.5	115.5	123.5	131.5	139.5	147.5	155.5	163.5	171.5	180	187.5
			P	49.4	49.4	49.4	51.4	49.4	49.4	49.4	49.4	49.4	49.4	49.4	49.4	49.4	49.4	49.4	49.4	49.4	49.4	49.4	49.4	49.4	49.4	49.4	49.4
		concen	NH4	37.5	46.875	49.219	49.8	50	50	50	50	50	50	50	50	50	50	50	50	50	50	50	50	50	50	50	50
		tration	NO2	0	0	0	0	0	0	0	0	0	0	0	0	0	0	0	0	0	0	0	0	0	0	0	0
	A2 SBR	V	v	2	2	2	2	2	2	2	2	2	2	2	2	2	2	2	2	2	2	2	2	2	2	2	2
Aerobic			P	24.7	24.7	24.7	24.7	24.7	24.7	24.7	24.7	24.7	24.7	24.7	24.7	24.7	24.7	24.7	24.7	24.7	24.7	24.7	24.7	24.7	24.7	24.7	24.7
		concen	NH4	0	0	0	0	0	0	0	0	0	0	0	0	0	0	0	0	0	0	0	0	0	0	0	0
		tration	NO2	18.8	47.438	48.328	49.1	49.5	49.7	49.87	49.9	50	50	50	50	50	50	50	50	50	50	50	50	50	50	50	50
	N SBR	V	v	4	4	4	4	4	4	4	4	4	4	4	4	4	4	4	4	4	4	4	4	4	4	4	4
		time		5.5	13.5	21.5	29.5	37.5	45.5	53.5	61.5	69.5	77.5	85.5	93.5	102	109.5	117.5	125.5	133.5	141.5	149.5	157.5	165.5	173.5	182	189.5
From N to A2 SBR			P	37.1	37.05	37.05	38.1	37.1	37.1	37.05	37.1	37.1	37.1	37.1	37.1	37.1	37.05	37.05	37.05	37.05	37.05	37.05	37.05	37.05	37.05	37.1	37.05
		concen	NH4	18.8	23.438	24.609	24.9	25	25	25	25	25	25	25	25	25	25	25	25	25	25	25	25	25	25	25	25
		tration	NO2	9.38	23.719	24.164	24.5	24.8	24.9	24.94	25	25	25	25	25	25	25	25	25	25	25	25	25	25	25	25	25
	A2 SBR	V	v	4	4	4	4	4	4	4	4	4	4	4	4	4	4	4	4	4	4	4	4	4	4	4	4
		P/N		3.95	1.562	1.533	1.55	1.5	1.49	1.49	1.5	1.5	1.5	1.48	1.5	1.5	1.48	1.48	1.48	1.482	1.482	1.482	1.48	1.48	1.48	1.48	1.48
			P	24.7	24.7	24.7	24.7	24.7	24.7	24.7	24.7	24.7	24.7	24.7	24.7	24.7	24.7	24.7	24.7	24.7	24.7	24.7	24.7	24.7	24.7	24.7	24.7
		concen	NH4	0	0	0	0	0	0	0	0	0	0	0	0	0	0	0	0	0	0	0	0	0	0	0	0
		tration	NO2	18.8	47.438	48.328	49.1	49.5	49.7	49.87	49.9	50	50	50	50	50	50	50	50	50	50	50	50	50	50	50	50
	N SBR	V	v	2	2	2	2	2	2	2	2	2	2	2	2	2	2	2	2	2	2	2	2	2	2	2	2

Appendix B

		time		7	15	23	31	39	47	55	63	71	79	87	95	103	111	119	127	135	143	151	159	167	175	183	191
P uptake			P	26.7	10.959	10.47	11.1	9.82	9.69	9.62	9.59	9.57	9.56	9.55	9.55	9.55	9.551	9.55	9.55	9.5501	9.55	9.55	9.55	9.55	9.55	9.55	9.55
		concen	NH4	18.8	23.438	24.609	24.9	25	25	25	25	25	25	25	25	25	25	25	25	25	25	25	25	25	25	25	25
		tration	NO2	0	0	0	0	0	0	0	0	0	0	0	0	0	0	0	0	0	0	0	0	0	0	0	0
	A2 SBR	V	v	4	4	4	4	4	4	4	4	4	4	4	4	4	4	4	4	4	4	4	4	4	4	4	4
			P	24.7	24.7	24.7	24.7	24.7	24.7	24.7	24.7	24.7	24.7	24.7	24.7	24.7	24.7	24.7	24.7	24.7	24.7	24.7	24.7	24.7	24.7	24.7	24.7
		concen	NH4	0	0	0	0	0	0	0	0	0	0	0	0	0	0	0	0	0	0	0	0	0	0	0	0
		tration	NO2	18.8	47.438	48.328	49.1	49.5	49.7	49.87	49.9	50	50	50	50	50	50	50	50	50	50	50	50	50	50	50	50
	N SBR	V	v	2	2	2	2	2	2	2	2	2	2	2	2	2	2	2	2	2	2	2	2	2	2	2	2
		time		8	16	24	32	40	48	56	64	72	80	88	96	104	112	120	128	136	144	152	160	168	176	184	192
Effluent			P	26.7	10.959	10.47	11.1	9.82	9.69	9.62	9.59	9.57	9.56	9.55	9.55	9.55	9.551	9.55	9.55	9.5501	9.55	9.55	9.55	9.55	9.55	9.55	9.55
		concen	NH4	18.8	23.438	24.609	24.9	25	25	25	25	25	25	25	25	25	25	25	25	25	25	25	25	25	25	25	25
		tration	NO2	0	0	0	0	0	0	0	0	0	0	0	0	0	0	0	0	0	0	0	0	0	0	0	0
	A2 SBR	V	v	2	2	2	2	2	2	2	2	2	2	2	2	2	2	2	2	2	2	2	2	2	2	2	2
			P	24.7	24.7	24.7	24.7	24.7	24.7	24.7	24.7	24.7	24.7	24.7	24.7	24.7	24.7	24.7	24.7	24.7	24.7	24.7	24.7	24.7	24.7	24.7	24.7
		concen	NH4	0	0	0	0	0	0	0	0	0	0	0	0	0	0	0	0	0	0	0	0	0	0	0	0
		tration	NO2	18.8	47.438	48.328	49.1	49.5	49.7	49.87	49.9	50	50	50	50	50	50	50	50	50	50	50	50	50	50	50	50
	N SBR	V	v	2	2	2	2	2	2	2	2	2	2	2	2	2	2	2	2	2	2	2	2	2	2	2	2

Appendix C: Kinetics and stoichiometric parameters applied in the model development

Parameter	Definition	Value	Unit	Source in this study
Y_{HAc}^{PHB}	Yield coefficient (PHB/HAc in anaerobic phase)	1.05	mmol C/mmol C	Experiment results
$Y_{HAc}^{PO_4}$	Yield coefficient (PO_4^{3-}-P/HAc in anaerobic phase)	0.43	mmol P/mmol C	Experiment results
Y_{HAc}^{Gly}	Yield coefficient (Glycogen/HAc in anaerobic phase)	0.38	mmol C/mmol C	Experiment results
$Y_{NO_2}^{PO_4}$	Yield coefficient (PO_4^{3-}-P/NO_2^--N in anoxic phase)	0.50	mmol P/mmol N	Experiment results
$Y_{NO_2}^{PHB}$	Yield coefficient (PHB/NO_2^--N in anoxic phase)	1.15	mmol C/mmol N	Experiment results
$Y_{NO_2}^{Gly}$	Yield coefficient (Glycogen/NO_2^--N in anoxic phase)	0.32	mmol C/mmol N	Experiment results
$Y_{NO_2}^{Biomass}$	Yield coefficient (Biomass/NO_2^--N in anoxic phase)	0.32	mmol C/mmol N	Experiment results
$Y_{NO_2}^{PP}$	Yield coefficient (PolyP/NO_2^--N in anoxic phase)	0.50	mmol P/mmol N	Experiment results
k_{HAc}	HAc consumption constant	5.3	h^{-1}	Experiment results
r_{Pmax}	Maximum of PO_4^{3-}-P consumption rate	25.4	h^{-1}	Experiment results

r_{Nmax}	Maximum of NO_2^--N consumption rate	28.6	h^{-1}	Experiment results
K_{P-PO_4}	Saturation coefficient of PO_4^{3-}-P for P uptake	8.5	mg P L^{-1}	Experiment results
K_{P-NO_2}	Saturation coefficient of PO_4^{3-}-P for N consumption	21.0	mg P L^{-1}	Experiment results
K_{N-PO_4}	Saturation coefficient of NO_2^--N for P uptake	2.0	mg N L^{-1}	Experiment results
K_{N-NO_2}	Saturation coefficient of NO_2^--N for N consumption	7.0	mg P L^{-1}	Experiment results
K_{PHB}	Saturation coefficient of PHB	5.6	mg C g^{-1}MLSS	Henze *et al*., 1999
K_{PI}	Inhibition coefficient of NO_2^--N for P uptake	5.0	mg N L^{-1}	Experiment results
K_{NI}	Inhibition coefficient of NO_2^--N for N consumption	6.5	mg N L^{-1}	Experiment results